

**Extreme wind statistics for the
Hydraulic Boundary Conditions
for the Dutch primary water
defences**

**SBW-Belastingen: Phase 2 of subproject "Wind
Modelling"**



Extreme wind statistics for the Hydraulic Boundary Conditions for the Dutch primary water defences

SBW-Belastingen: Phase 2 of subproject "Wind Modelling"

Sofia Caires

Title

Extreme wind statistics for the Hydraulic Boundary Conditions for the Dutch primary water defences

Client

Rijkswaterstaat - Centre for Water Management

Project

1200264-005

Pages

314

Keywords

Potential wind speed, extreme climate, hydraulic boundary conditions, Netherlands, WTI

Abstract (see the Executive summary for a non-technical description)

Updated extreme potential wind statistics were computed for 21 KNMI wind stations with long time series available. The updated wind statistics are to be made available for the inference of the Hydraulic Boundary Conditions for the Dutch primary water defences by the WTI team.

The period of data considered in the analysis was the 1970-2008 period. Both omni-directional and directional estimates were obtained. The sensitivity of the results to different periods was also analysed and found to be reasonable. I.e. the found differences do not exceed the uncertainty associated with the estimates.


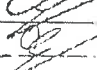
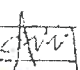


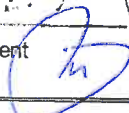
The data was analysed using the standard AM/GEV and a POT/GPD approaches. The hypothesis of a type I tail for the potential wind data was extensively tested. Power 2 and power k , with k being the shape parameter of the Weibull fit to the whole dataset, data transformations were considered in order to accelerate the convergence to a type I tail. However, in the cases considered, the transformations do not appear to improve the convergence to a type I tail, nor do they seem to be needed. The assumption of a type I tail seems to be valid for the considered potential wind data. Furthermore, the estimates obtained from exponential fits to the POT data were found to be realistic and reliable and are given as final/best estimates.

Mainly due to the type I tail assumption, the curvature problem does not seem to strongly affect the computed estimates. Furthermore, these new estimates do not differ much from the currently used estimates of Wieringa and Rijkoort (1983). More precisely, the 10,000 yr return value estimates of this study differ by less than 3% from those of Wieringa and Rijkoort (1983) in 10 of the 13 stations considered by them. The two stations for which the differences are larger—about 10%—the estimates were adjusted 'by hand' by Wieringa and Rijkoort (1983) and discrepancies would even be larger if they had not been adjusted.

A number of caveats apply to the given estimates: the confidence intervals given are underestimated and long term trends and inhomogeneities in the data were ignored.

References

Projectplan SBW Belastingen 2009, Deltares (A. van der Westhuisen)

Version	Date	Author	Initials	Review	Initials	Approval	Initials
1	2009-07-21	Sofia Caires		Chris Geerse			
2	2009-07-31	Sofia Caires		Chris Geerse		Marcel van Gent	
3	2009-09-30 (after the RWS-CWM review)	Sofia Caires		Chris Geerse		Marcel van Gent	

State
final

Title

Extreme wind statistics for the Hydraulic Boundary Conditions for the Dutch primary water defences SBW-Belastingen: Phase 2 of subproject "Wind Modelling"

Executive summary

General

According to the Dutch Water Defence Act ("Wet op de Waterkering, 1996") the strength of the Dutch primary water defences must be checked every five years (1996, 2001, 2006, 2011, etc.) for the required of protection from loads with return periods varying from 250 to 10,000 years, depending on the area protected by the water defence. These loads are determined on the basis of Hydraulic Boundary Conditions (HBC) and must also be derived anew and approved by the Dutch Ministry of Transport, Public Works and Water Management (VenW) every five years.

With the aim of filling knowledge gaps in the determination of the strengths and loads of the water defences, Rijkswaterstaat - Centre for Water Management in The Netherlands is funding the long-term research project "Strengths and loads of water defences" (in Dutch: "Sterkte en Belastingen Waterkeringen"; in short: SBW).

In 2008 a number of no-regret actions were defined in the framework of the SBW-Belastingen project; the present document reports on a part of one of those actions within the sub-project SBW-Wind. The no-regret actions were undertaken to gain insight into methods, models and techniques that are relevant for the short-term project WTI (Wettelijk Toets Instrumentarium; in English: Legal Assessment Instruments). WTI is based on the HBC and on the Safety Assessment Regulation (VTV: Voorschrift Toetsen op Veiligheid). Given that the presently available extreme wind statistics have not yet been updated and are based on a small data set (1962-1976; see Wieringa and Rijkooort 1983), the current no-regret action is an attempt to update such statistics and make them available for WTI 2011.

Problem statement

For the assessment of the HBC, information on wind conditions over open water areas pertaining to return periods up to thousands of years is required. This information needs to be derived from the KNMI-stations data. Two aspects are relevant here:

- The KNMI-data cover only some decades, which means that statistical extrapolation is required.
- The KNMI-measuring stations are located on land, typically several tens of kilometers away from the centre of the open water areas considered (such as Lake IJssel and the Wadden Sea). This means that spatial interpolation of wind information, taking account of transitions from land to water and vice versa, is required.

Wieringa and Rijkooort (1983) developed a wind modelling concept to provide adequate estimates of extreme wind statistics. This modelling concept is based on wind measurement data at KNMI stations and relies on some assumptions pertaining to the physics and the statistics of wind over the Netherlands. *Potential wind speed* is the measure used to describe the wind and represents the wind speed 1 hour average at 10 metres height after correction for nearby sheltering, so that it is representative for an open grass area with a so-called roughness length of 3 cm.

About five years ago it was noticed that for storms, it was not possible to translate KNMI-winds to open water (and vice versa) without significant (greater than 10-20%) violation of either broadly accepted theories or broadly accepted measurements. In some cases,

Title

Extreme wind statistics for the Hydraulic Boundary Conditions for the Dutch primary water defences SBW-Belastingen: Phase 2 of subproject "Wind Modelling"

statistically extrapolated wind extremes (or even observed wind extremes) over land were as large as those over open water, which is physically implausible. Also, the observed extreme value distributions of open water wind differed in shape (curvature) from the distribution of land-based wind observations. Hence, the above-mentioned situation was described as the curvature problem. It was clear that the curvature problem needed to be solved in order to derive reliable estimates for the required wind information (for the assessment of the HBC).

Within the framework of the 'SBW Belastingen' project, a project was set up to derive (update) the required wind information for the assessment of the HBC, SBW-Wind, which consists of three phases. In Phase 2, the current study, the new potential wind series are subjected to statistical analyses in order to update the wind statistics at the KNMI stations. The results of the present study should be interpreted with care, given the fact that the other phases of SBW-Wind (as described below) indicated that no simple solution for the curvature problem is in sight.

The other phases of SBW-Wind all relate to the translation of (observed or statistically extrapolated) KNMI-winds to open water locations. Phase 1 of SBW-wind attempted to solve the curvature problem by improving the exposure corrections that are needed to convert measured KNMI-winds to standardised potential wind speeds. It provided improved exposure corrections, but the effect on wind speeds was often less than 5%, so that the curvature problem was only slightly mitigated. Given this result, a Phase 1b was added to the project, aiming at gaining further insight into the curvature problem. It was then concluded that the curvature problem has not got a single cause but is, to a large extent, caused by a number of fundamental aspects of both the available data and the present wind modelling concept. Phase 3 will focus on the spatial interpolation of the wind statistics and on the spatial and temporal schematisation of extreme wind events in order to determine the input for the water level and wave models.

Study aim

The primary objective of this study is to determine updated extreme potential wind statistics for the KNMI wind stations for which long time series are available. These should be computed based on data over a period longer than the original period of 1962-1976 (15 years) used, and at more stations than the original 13 considered, by Wieringa and Rijkooft (1983). They also include distributions per wind direction sector. The updated wind statistics are to be made available for the inference of HBC for the Dutch primary water defences by the WTI team. The decision of whether to replace the 1983 statistics by those being determined here is to be taken by the WTI 2011 project team.

Approach

The data considered in the analysis are from the 1970-2008 period (39 years) and as much as 21 stations with almost no data gaps can be considered in this period. The considered stations are: IJmuiden, Texelhors, De Kooy, Schiphol, De Bilt, Soesterberg, Leeuwarden, Deelen, Lauwersoog, Eelde, Twenthe, Cadzand, Vlissingen, L. E. Goeree, Hoek van Holland, Zestienhoven, Gilze-Rijen, Herwijnen, Eindhoven, Volkel and Beek. The data were analysed using the standard extreme value approaches based on annual maxima and storm maxima data. The hypothesis of a so-called type I tail in the extreme value distribution was extensively tested. This corresponds to an exponential distribution if the underlying data consist of storm maxima and a Gumbel distribution if the data are annual maxima for the potential wind data.

Title

Extreme wind statistics for the Hydraulic Boundary Conditions for the Dutch primary water defences SBW-Belastingen: Phase 2 of subproject "Wind Modelling"

Furthermore, data transformations were considered to try to accelerate the convergence to a type I tail. Hence, not only the wind speeds U were analysed but also squared wind speed (U^2) and U^k , k being the shape parameter of the Weibull fit to the whole data). Both omnidirectional and directional estimates were obtained. The sensitivity of the results to the use of data from different periods was also assessed.

Conclusions

The conclusions of this study were as follows:

- A significant result in WTI context is the observation that the new estimates of KNMI wind extremes do not differ much from the currently used estimates of Wieringa and Rijkoort (1983). More precisely, the omnidirectional 10,000 yr return value estimates of this study differ by less than 3% from those of Wieringa and Rijkoort (1983) in 10 of the 13 stations considered by them. Only the Deelen and Leeuwarden stations have differences larger than 10%. However, the estimates for those stations were adjusted 'by hand' by Wieringa and Rijkoort (1983) and discrepancies would even be larger if they had not been adjusted.
- The estimates obtained from exponential fits to the storm maxima data were found to be realistic and reliable and are given as final/best estimates, compared to the alternative of Gumbel fits to observed yearly maxima.
- The sensitivity of the results to different periods was also analysed and found to be reasonable. I.e. the found differences do not exceed the uncertainty associated with the estimates.
- The assumption of a type I tail seems to be valid for the potential wind data considered. Applying the extreme value analysis on transformed (i.e. U^2 or U^k) data does not appear to improve the convergence to a type I tail, nor do they seem to be needed. In fact this might even cause some bias in the results.

Recommendations

This study suggests that for KNMI-stations, sound estimates of extreme wind speeds may be obtained through statistical extrapolation. However, the translation of (extreme) KNMI-winds to open water remains an issue that needs further investigation. Even though the curvature problem seems to have been partly circumvented in this study (thanks to the assumption of a type I tail, especially in the statistics for Hoek van Holland), it is paramount that the curvature problem be fully understood. The quantification of its main components and the determination of corrections eventually needed in the potential wind time series may allow the estimation of extreme values without constraints on the tail type, and for spatial wind transformation methods that are consistent with both theory and observations. This would require a follow-up to the Phase 1b of SBW-Wind that was described above.

In the next phase of this project, Phase 3, the point estimates computed here will be used to interpolate the estimates in space. Preliminary results of this phase indicate that assumptions of simultaneous occurrence of a certain return value with the same return period at distant stations should be treated with care.

Finally, the potential wind data considered here were found to show some unexplained inhomogeneities. It would be useful to investigate the origin of such inhomogeneities and remove them from the data.

Contents

1	Introduction	1
1.1	Framework	1
1.2	Background and motivation	1
1.3	Objectives	3
1.4	Approach	3
1.5	Project team	4
1.6	Outline of this report	5
2	Statistical methods	7
2.1	Introduction	7
2.2	Extreme value theory	7
2.2.1	Block maxima	7
2.2.2	Peaks Over Threshold	8
2.3	Other approaches	10
2.3.1	Choice of distribution	10
2.3.2	Data transformation	10
2.4	Estimation and diagnosis	11
2.5	Climate change	13
2.6	Hypothesis testing	14
3	Data description	15
3.1	Choice of stations	15
3.2	1970-2008 mean climate	17
3.3	Known features contributing to the curvature problem	18
4	Data analysis	21
4.1	AM/GEV analysis	22
4.2	POT/GPD analysis	30
4.2.1	Choice of threshold	30
4.2.2	Analysis	31
4.2.3	Seasonal variability	37
4.3	Climate change and sampling variability	39
4.3.1	Trends	39
4.3.2	Sampling variability	40
5	Directional extreme climate	43
5.1	Model description	43
5.2	10,000-yr return value estimates	43
5.3	Comparison with the presently used estimates	55
6	Concluding remarks	59
6.1	Overview	59
6.2	Caveats	59
6.3	Recommendations	60
	References	61

Deltares

Appendices

A Report review	63
A.1 Review report	63
A.2 Acknowledgment of the review	79
B Tables	81
C Figures	101

1 Introduction

1.1 Framework

According to the Dutch Water Defence Act (“Wet op de Waterkering, 1996”) the strength of the Dutch primary water defences must be checked every five years (1996, 2001, 2006, 2011, etc.) for the required level of protection, which, depending on the area protected by the water defence, may vary from the 250 to 10,000 year loads. These loads are determined on the basis of Hydraulic Boundary Conditions (HBC) and must also be derived anew and approved by the Dutch Ministry of Transport, Public Works and Water Management (VenW) every five years.

With the aim of filling knowledge gaps in the determination of the strengths and loads of the water defences, Rijkswaterstaat - Centre for Water Management (to be called RWS-CWM in the remainder of this report; in Dutch: “Waterdienst”) in The Netherlands is funding the long-term research project “Strengths and loads of water defences” (in Dutch: “Sterkte en Belastingen Waterkeringen”; in short: SBW).

The SBW program presently comprises nine projects, of which seven are related to the strengths and two to the loads of water defences: SBW-Waddenzee and SBW-Belastingen¹. They aim at determining the quality of models and methods and improving them where needed, in order that in 2011 and onwards more accurate HBC can be determined.

In 2008 a number of no-regret actions were defined in the framework of the SBW-Belastingen project; the present document reports on a part of one of those. The no-regret actions were undertaken to gain insight into methods, models and techniques that are relevant for the short-term project WTI (Wettelijk Toets Instrumentarium; in English: Legal Assessment Instruments). WTI is based on the HBC and on the Safety Assessment Regulation (VTV: Voorschrift Toetsen op Veiligheid). Given that the presently available extreme wind statistics were defined in 1983, the current no-regret action is an attempt to update such statistics and make them available for WTI 2011. The decision of whether to replace the 1983 statistics for those being determined here is for the WTI 2011 project team.

1.2 Background and motivation

An important component in the determination of the HBC for the water defences is the statistical analysis of the natural variables that, directly or indirectly, may cause the water defences to fail. One such natural variables is the wind.

The software package used for the verification of the required level of protection of the Dutch primary water defences is called the HYDRA-family or the probabilistic HYDRA models (Beckers et al., 2009). The current HYDRA software uses extreme *potential wind speed* statistics that were determined 25 years ago (Wieringa and Rijkoort, 1983). Potential wind speed is the measure used in this context to describe the wind and represents the wind speed 1 hour average at 10 metres height in a location with a local roughness of 3 cm. The Wieringa and Rijkoort, (1983) statistics are not only used directly in the HYDRA package, but

1. *Dutch for loads.*

also indirectly, as the available wind extreme statistics are used to force the hydrodynamic models. The latter providing the wave and water level loads on the water defences.

In an attempt to update the wind statistics, by extending the time series used in the estimation and improving the estimation methodology, the KNMI-Hydra project (not to be confused with the software package) was carried out from 1998 to 2005 (see <http://www.knmi.nl/samenw/hydra>). The project was a joint project between Rijkswaterstaat (the former Institute for Inland Water Management, RIZA, and the former National Institute for Coastal and Marine Management, RIKZ) and the Royal Netherlands Meteorological Institute (KNMI). The KNMI-Hydra project was very important for the consolidation and improvement of the wind modelling knowledge, as the several documents available at the KNMI-Hydra project webpage (see above) indicate. The knowledge acquired in the KNMI-Hydra project is seen as one of the building blocks of the current project. Nevertheless, the KNMI-Hydra project failed at updating the available wind statistics because unexplainable differences according to the developed wind modelling concept were found in the tails of the potential wind data from stations near the coast and stations further inland. The latter problem has been named the “*curvature problem*”. More precisely, when comparing omni-directional extreme potential wind velocities from coastal and inland stations, the higher potential wind velocity peaks for the inland stations exceed those for the coastal stations. When fitting through the data, the return value lines cross each other and for longer return periods the estimates for inland stations are higher than for the coastal stations. This is considered implausible because the surface roughness over land is generally much higher than over open water, while the intensity of storm depressions over land is generally less. The stations used to illustrate the problem were the Hoek van Holland and the Soesterberg stations (see Wever and Groen, 2009, Fig. 1.2.1). In order to update the 1983 wind statistics (at the wind stations) and to create wind fields above land and open water from the point statistics, it is imperative that the curvature problem be solved or dealt with in the modelling.

After an initial reconnaissance study by the KNMI in the 2nd half of 2007, where it was concluded that the curvature problem is not (or to a lesser extent) present in the raw wind measurements, i.e. before they are transformed into potential wind, it was postulated that the problem should probably be in the factors used to compute the potential wind from the raw wind, the exposure correction factors (ECF). Reasons for the faulty ECF were that wind variations at a time scale of 1 hour are not solely due to the surface roughness, but also due to thermal effects. In 2008, KNMI and Deltares started a joint venture project. The project was divided in three phases (see KNMI and Deltares wind modelling team, 2008). The goals of phases 1, 2, and 3 were to correct the ECF, to compute extreme statistics using the (since 1983) extended time series per point (wind station) and to spatially interpolate the point statistics, respectively.

In Phase 1 of the project, the algorithm to calculate the ECFs was improved, by making use of measurements of the 10 minute wind standard deviation to relate ECFs based on 1 hour gustiness analysis to ECFs based on 10 minute wind standard deviation (see Wever and Groen, 2009).

There are indications that the curvature problem is slightly mitigated in the newly derived data. The correction typically led to a 1 to 5% downward revision of the ECFs over land. Nevertheless, Wever and Groen (2009), based on Gumbel fits to U^2 annual maxima from the period 1993-2007, report that the crossing point has moved towards longer return periods. However, a thorough study on the extent of the curvature problem in the newly derived data has not yet been carried out. It was also suggested that the curvature problem is to a certain

extent present in the raw data (Bottema and Van Vledder, 2009). This may imply that the curvature problem is (to a greater extent) related to real physics, which are probably not well described by the used wind modelling concept. Another hint in this direction is the 10-30% difference between measurement data and expectations based on the presently used wind modelling concept as reported by Bottema (2007, p. 184) and Taminiau (2004).

Preliminary rough potential wind speed return value estimates computed by Wever and Groen (2009) compare well with the estimates from the Rijkooort-Weibull model in a qualitative sense. I.e., the spatial patterns obtained with both approaches are similar. However, in general the Wever and Groen (2009) estimates are 10 to 40% lower than the Rijkooort-Weibull model estimates, which if confirmed is a difference of consequence in practical applications. Nevertheless, the results from Wever and Groen (2009) suggest that the newly obtained wind speed return value estimates can be considered as a refinement of Wieringa and Rijkooort (1983), giving the possibility to make use of the longer measurement period and new wind measurement sites currently available. Definite potential wind statistics still need to be derived from the newly-derived data.

Since the curvature problem is in principle still present in the newly-derived potential wind series (Wever and Groen, 2009), it was decided to add a sub phase, Phase 1b, to the original SBW plans (KNMI and Deltares wind modelling team, 2008) to gain more insight in the curvature problem. To that end, some basic tests were carried out on the data produced by Wever and Groen (2009). The main conclusions put forward a number of causes (cf. Section 3.3), among which that differences in stability between land and sea regions and storm dynamics might partially explain the curvature problem. Furthermore, that no further improvement of newly-derived potential wind series can be envisaged on short term. No attempt to solve the curvature problem will therefore be made in the current study, which concentrates on the extreme value analysis of the newly-derived data.

1.3 Objectives

The primary objective of this study is to determine, for the KNMI wind stations for which long time series are available, updated extreme potential wind statistics for several directional sectors. These should be computed based on data over a period longer than the original period of 1962-1976 used by Wieringa and Rijkooort (1983). Associated uncertainties are also to be studied. The updated wind statistics are to be made available for the inference of HBC for the Dutch primary water defences by the WTI team.

1.4 Approach

The currently available extreme wind statistics have been determined using the so-called Rijkooort-Weibull model (Rijkooort, 1983), which is a rather intricate model. Estimates were provided separately for 12 wind measuring stations in the Netherlands (Schiphol, Eelde, Soesterberg, De Bilt, Deelen, Vlissingen, Gilze Rijen, Eindhoven, Beek, Leeuwarden, L.V. Texel and Zestienhoven). Hourly averaged potential wind speed data from 1962-1976 were used for the estimation. The model is described in Geerse (1999) and Smits (2001) and further summarized in Diermanse et al. (2007).

The Rijkooort-Weibull model is based on fits to the whole dataset (not only storm peaks) and extrapolating from it. However, due to dependence and non-stationarity, wind speed series violate the assumptions of independence and identity in distribution. Also, there is no

scientific justification for using one particular distribution to fit the data. In contrast, if for example one concentrates on averages, maximum values, or excesses over a high threshold of very general variables, statistical theory provides a scientific basis for the use of, respectively, the normal, Generalized Extreme Value (GEV) and Generalized Pareto Distributions (GPD).

In the KNMI-Hydra project it was attempted to improve or find alternatives for the Rijkooort-Weibull methodology used for return value estimation (see <http://www.knmi.nl/samenw/hydra/documents/storms/storms.htm>), but such attempts failed because, due to the curvature problem, no available data could be used with confidence to assess different statistical approaches.

For WTI 2011 is however paramount that reproducible extreme wind statistics are computed from the newly available data using more stations and longer time series than in the Rijkooort-Weibull model. The objectives of Phase 2 of this project is therefore to compute for several measurement locations extreme value statistics and associated uncertainties from the new potential wind time series. Not only omni-directional estimates are to be computed, but also directional (per wind sector). The directional estimates are those needed by WTI to infer the HBC for the Dutch primary water defences.

The following procedure will be applied in this study:

- 1 The approaches used in the extreme value analyses are the standard AM/GEV and POT/GPD analyses (see e.g. Caires et al., 2007).
- 2 Although not without controversy, it is common practice to assume that wind data have a type I tail. This assumption is also investigated in this study.
- 3 Furthermore, according to Galambos (1987) the rate of convergence at which the tail of the distribution function of observations can be approximated by the tail of the GPD or the GEV distribution in the case of distributions such as the normal, which are rather concentrated around the mean, can be very slow, demanding comparatively high thresholds/large sample sizes. However, applying a, say, a power of 2 to the data will make the data more skewed and “nonnormal” and hence improve convergence. The suitability of applying such transformations to the wind data is therefore also considered.
- 4 The results of this study are compared to the estimates provided by Wieringa and Rijkooort (1983) and the spatial consistency of the results to be judged in a qualitative way.
- 5 Furthermore, we look at the effect of considering different periods of data in the extreme value analyses.

This study should form the basis for the WTI project to decide whether the estimates of Wieringa and Rijkooort should again be used or these newly derived estimates.

1.5 Project team

The project team consists of KNMI and Deltares employees with expertise in wind modelling and extreme value analysis. The team is referred to as the wind modelling team and includes: Jules Beersma (KNMI), Sofia Caires (Deltares), Hans de Waal (Deltares), Douwe Dillingh (Deltares), Geert Groen (KNMI), Jacco Groeneweg (Deltares) and Nander Wever (KNMI).

The analysis and reporting presented here was carried out by Sofia Caires with critical advice and help from all the involved.

There were a number of discussions on the analysis and results presented here with the participation of the wind modelling team, the Phase 2 project reviewer, Chris Geerse, from HKV, and the RWS-CWM project leader, Marcel Bottema. Chris Geerse and Marcel Bottema have provided valuable and constructive input also outside such meetings.

1.6 Outline of this report

Chapter 2 of this report presents the basic elements of extreme value theory. Chapter 3 describes the data considered and outlines the conclusions of Phase 1b of this project. Chapter 4 describes the data analysis including the sensitivity of the results to different choices and data periods. Chapter 5 describes the presently obtained statistics and compares them with those used for WTI 2006. The report ends in Chapter 6 with conclusions, important caveats to the results presented here and recommendations for further work. For completeness, the appendices contain the report review and several analysis results figures and tables, only a few examples are given as illustration in the text.

2 Statistical methods

2.1 Introduction

This chapter briefly introduces the principles of extreme value theory and describes the methods used in extreme value analysis (EVA) and other statistical analysis.

2.2 Extreme value theory

2.2.1 Block maxima

In order to explain the basic ideas of the extreme value theory, let us define $M_n = \max\{X_1, \dots, X_n\}$, where X_1, X_2, \dots is a sequence of independent random variables having a common distribution function F . In its simplest form, the *extremal types theorem* states the following: If there exist sequences of constants $\{\sigma_n > 0\}$ and $\{\mu_n\}$ such that $P\{\sigma_n M_n + \mu_n \leq z\} \rightarrow G(z)$ as $n \rightarrow \infty$, where G is a *non-degenerate distribution function*², then G must be a Generalized Extreme Value (GEV) distribution, which is given by

$$G(z) = \begin{cases} \exp\left\{-\left[1 + \xi\left(\frac{z - \mu}{\sigma}\right)\right]^{-1/\xi}\right\}, & \text{for } \xi \neq 0 \\ \exp\left\{-\exp\left[-\left(\frac{z - \mu}{\sigma}\right)\right]\right\}, & \text{for } \xi = 0, \end{cases} \quad (2.1)$$

where z takes values in three different sets according to the sign of the shape parameter ξ : $z > \mu - \sigma/\xi$ if $\xi > 0$ (the domain of z has a lower bound), $z < \mu - \sigma/\xi$ if $\xi < 0$ (the domain of z has an upper bound), and $-\infty < z < \infty$ if $\xi = 0$.

In other words, if the distribution function of (a normalization of) the maximum value in a random sample of size n converges to a distribution function as n tends to infinity, then that distribution function must be a GEV distribution. Moreover, this and other results of extreme value theory *hold true even under general dependence conditions* (see Chapter 5 of Coles, 2001).

In Eq. (2.1) the parameters μ , σ and ξ are called the location, scale, and shape parameters and satisfy $-\infty < \mu < \infty$, $\sigma > 0$ and $-\infty < \xi < \infty$. For $\xi = 0$ the GEV is the *Gumbel distribution*, for $\xi > 0$ it is the *Fréchet distribution*, and for $\xi < 0$ it is the (*reverse*) *Weibull distribution*. For $\xi > 0$ the tail of the GEV is “heavier” (i.e., decreases more slowly) than the tail of the Gumbel distribution, and for $\xi < 0$ it is “lighter” (decreases more quickly and actually reaches 0) than that of the Gumbel distribution. The GEV is said to have a *type II tail* when the shape parameter is positive ($\xi > 0$) and a *type III tail* when the shape parameter is

2. A distribution function is said to be degenerate if it allocates probability 1 to a single point.

negative ($\xi < 0$, the domain of z has an upper bound)³. The tail of the Gumbel distribution ($\xi = 0$) is called a *type I tail*.

The extremal types theorem gives rise to the *annual maxima* (AM) method of modelling extremes, in which the GEV distribution is fitted to a sample of block maxima (e.g. to annual maxima, though biannual, monthly or even daily maxima can of course be used as well).

One of the main applications of extreme value theory is the estimation of the *once per m year* (*m-yr*) *return value*, the value which is exceeded on average once every m years. The m -yr return value (for $m > 1$) based on the AM method/GEV distribution, z_m , is given by⁴

$$z_m = \begin{cases} \mu - \frac{\sigma}{\xi} \left(1 - \left\{ -\ln \left(1 - \frac{1}{m} \right) \right\}^{-\xi} \right), & \text{for } \xi \neq 0 \\ \mu - \sigma \log \left\{ -\ln \left(1 - \frac{1}{m} \right) \right\}, & \text{for } \xi = 0. \end{cases} \quad (2.2)$$

The sample sizes of annual maxima data are usually small, so that model estimates, especially return values, have large uncertainties. This has motivated the development of more sophisticated methods that enable the modelling of more data than just block maxima. These methods are based on two well-known characterizations of extreme value distributions: one based on exceedances of a threshold, and the other based on the behaviour of the r largest, for small values of r , observations within a block. The first method is considered here and described in the following section.

2.2.2 Peaks Over Threshold

The approach based on the exceedances of a high threshold, hereafter referred to as the *Peaks Over Threshold* (POT) method, consists of fitting the generalized Pareto distribution (GPD) to the peaks of clustered excesses over a threshold, the excesses being the observations in a cluster minus the threshold, and calculating return values by taking into account the rate of occurrence of clusters (see Pickands, 1971 and 1975, and Davidson and Smith, 1990). Under very general conditions this procedure ensures that the data can have only three possible, albeit asymptotic, distributions (the three forms of the GPD given below) and, moreover, that observations belonging to different peak clusters are (approximately) independent. In the POT method, the peak excesses over a high threshold u of a time series are assumed to occur in time according to a Poisson process with rate λ_u and to be independently distributed with a GPD, whose distribution function is given by

$$F_u(y) = \begin{cases} 1 - \left(1 + \xi \frac{y}{\tilde{\sigma}} \right)^{-1/\xi}, & \text{for } \xi \neq 0 \\ 1 - \exp \left(-\frac{y}{\tilde{\sigma}} \right), & \text{for } \xi = 0, \end{cases} \quad (2.3)$$

3. Please note that some articles (e.g. Hosking and Wallis, 1987) use another convention for the signal of the shape parameter: a negative shape parameter in those references corresponds to a type II distribution.

4. In this report the natural logarithm of x is written as $\ln(x)$.

where, $y > 0$, $\tilde{\sigma} > 0$ and $(1 + \xi(y/\tilde{\sigma})) > 0$. The two parameters of the GPD are called the scale ($\tilde{\sigma}$) and shape (ξ) parameters. When $\xi = 0$ the GPD is said to have a type I tail and amounts to the exponential distribution with mean $\tilde{\sigma}$; when $\xi > 0$ it has a type II tail and it is the Pareto distribution; and when $\xi < 0$ it has a type III tail and it is a special case of the beta distribution. If $\xi < 0$, just as with the GEV, the support of the GPD was an upper bound, $-\tilde{\sigma}/\xi$, which is called the *upper end-point* of the GPD and is to be thought of as the *upper-limit of the variable of interest*, the upper limit being then $u - \tilde{\sigma}/\xi$.

The m-yr return value based on a POT/GPD analysis, z_m , is given by

$$z_m = \begin{cases} u + \frac{\tilde{\sigma}}{\xi} \{ (\lambda_u m)^\xi - 1 \}, & \text{for } \xi \neq 0 \\ u + \tilde{\sigma} \ln(\lambda_u m), & \text{for } \xi = 0. \end{cases} \quad (2.4)$$

Just as block maxima have the GEV as their approximate distribution, the threshold excesses have a corresponding approximate distribution within the GPD. Moreover, the parameters of the GPD of threshold excesses are uniquely determined by those of the associated GEV distribution of block maxima. In particular, the shape parameter is the same, and the scale parameters of the two distributions are related by $\tilde{\sigma} = \sigma + \xi(u - \mu)$.

The sample to be used in the POT method has to be extracted from the original time series in such a way that the data can be modelled as independent observations. This is done by a process of declustering in which only the peak (highest) observations in clusters of successive exceedances of a specified threshold are retained and, of these, only those which in some sense are sufficiently apart (so that they belong to more or less 'independent storms') are considered as belonging to the collection of POT points. Specifically, in the present applications we have treated cluster maxima at a distance of less than 96 h apart as belonging to the same cluster (storm). The 4 days period considered is a bit longer than the usually considered 2 to 3 days period, but recent research has shown that storm durations are maybe longer than previously thought. In any case, analysis results are not very sensitive to whether 2 or 4 days are used.

The choice of threshold (analogous to the choice of block size in the block maxima approach) represents a trade off between bias and variance: too low a threshold is likely to violate the asymptotic basis of the model, leading to bias; too high a threshold will generate fewer excesses with which to estimate the model, leading to high variance. An important property of the POT/GPD approach is the threshold stability property: if a GPD is a reasonable model for excesses of a threshold u_0 , then for a higher threshold u a GPD should also apply; the two GPD's have identical shape parameter and their scale parameters are related by $\tilde{\sigma}_u = \tilde{\sigma}_{u_0} + \xi(u - u_0)$, which can be reparameterized as:

$$\sigma^* = \tilde{\sigma}_u + \xi\mu \quad (2.5)$$

Consequently, if μ_0 is a valid threshold for excesses to follow the GPD then estimates of both σ^* and ξ should remain nearly constant above μ_0 . This property of the GPD can also be used to find the minimum threshold at which a GPD model applies to the data.

2.3 Other approaches

2.3.1 Choice of distribution

The choice of distribution with which to fit AM and POT data is limited by the extreme value theory as mentioned above. However, mostly for historical reasons, in many studies the Weibull distribution is fitted instead of the GPD to POT data.

This Weibull distribution is not the (reverse) Weibull distribution of maxima referred to in Section 2.2.1, but the Weibull distribution of minima (a form of the GEV distribution for minima). In particular, while the latter has a type III upper tail, the former has a type I (exponential) upper tail. It was introduced by Weibull in connection with failure data because it is the approximate distribution of the minimum of many variables, which could be seen as the weakest link among many links that can be broken in a structure. Popularized by reliability engineers, its use has spread to other areas, in particular to ocean engineering. Its distribution function is given by

$$F_u(y) = 1 - \exp\left(-\left(\frac{y}{s}\right)^k\right). \quad (2.6)$$

Although it is not generally recommended, fitting a Weibull distribution to the peak excesses in place of the GPD model makes sense in certain situations. Indeed, suppose that the data really follow a type I tail, or at least that this has been convincingly demonstrated on the basis of some statistical analyses. Then the asymptotic distribution of the excesses is exponential. Since the exponential is a special case of the Weibull distribution, one might think that there would be no harm in fitting a Weibull rather than an exponential distribution to the data. Now, if the data are truly exponential, this would actually entail more uncertainty in parameter estimates, which would be undesirable (intuitively, to know that the data are exactly exponential amounts to more information than knowing that they are Weibull). However, it may happen that, because the exponential is only valid asymptotically, the Weibull distribution will provide a better approximation to the data (since it has one more parameter and hence more flexibility), and in that case fitting the latter would provide better results than fitting the former. In any case, if one is to step outside the GPD domain one should do so on the basis of some justification.

When there are indications that the asymptotic distribution is of a certain type (for instance of type I) but the rate of convergence to this asymptotic distribution is slow, data transformations are often used to accelerate convergence.

2.3.2 Data transformation

As mentioned before, the rate at which the tail of the distribution function of the observations converges to the tail of the GPD or the GEV distribution in the case of type I tail distributions such as the normal, which is rather concentrated around the mean, can be very slow, demanding comparatively high thresholds/large sample sizes. In such cases, a data transformation can help accelerating convergence and hence improving the fit of the observed by the asymptotic tail (Galambos, 1987). For instance, although the convergence required by the POT method is slow in the case of standard normal random variables, it will be rather fast with their squares, which are essentially chi-square variables.

Although not without controversy, it has been common practice since the landmark work of Cook (1982) to assume that wind data have a type I tail. Furthermore, it is known that in the case of wind data the convergence to the relevant asymptotic distribution is slow and can be accelerated by data transformations such as taking a power of two, U^2 , or, as also suggested by Cook (1982), or taking power equal to the shape parameter of the Weibull distribution fitted to the whole data set (i.e. not only to the extremes), U^k . However, in the case of the data considered by Cook (1982) the shape parameter k varies between 1.8 and 2.2, and he fixes the power at 2. He advocates thus the use of squared wind speed in place of wind speed, on the grounds that the rate of convergence to the asymptotic distribution improve, and also because engineers are usually more interested in dynamic pressure instead of wind speed. The former being proportional to the squared wind speed. His final argument for using the dynamic pressure rather than wind speed when fitting the Gumbel distribution to extreme value time series rests on the assumption that the parent population from which the extreme speeds are extracted is fitted by a distribution that is, approximately, of the Rayleigh type.

Discussions around such transformations as a means to improve approximations are therefore as old as Cook's paper. Here are some examples:

- Holmes and Moriarty (1999) argue that fitting a type III tail to U is "more appropriate" than fitting a type I tail to U since the data have in principle an upper bound. Cook and Harris (2001) reply pleading for fits of a type I tail to U^k .
- Harris (2004) reply to Holmes's (2003) comment on the article of Cheng and Yeung (2002): Holmes (2003) argues that Cheng and Yeung (2002) find estimates of the shape parameter of the extreme value distribution that are too low and that values closer to -0.1 are more reasonable and yield reasonable (not too low) upper bounds. Harris (2004), however, counter argues that using a type I tail is a better option and that both type I and type II can be obtained by transforming the data using U^k or U^2 , respectively.
- Simiu et al. (2001) argue that it is considerably better to fit the GEV (the resulting fit being then a type III tail) to the (not transformed) wind speed U than to fit a Gumbel distribution to U^2 .

More recently, Smith (2009) argues that "in the case where the true tail is in the domain of attraction of Gumbel, the theory of the "penultimate approximation" shows that in many cases, approximating the tail by GEV gives a faster rate of convergence than if you approximate by the true (Gumbel) limit; the rate of convergence is never worse. Therefore, there is never any reason to restrict to the Gumbel law (or exponential in the case of GPD)." In contrast, Van den Brink and Können (2008) argue that extreme winds should be estimated by fitting a type I (Gumbel) tail extreme value distribution to annual maxima of U^k . In Phase 1 of this study Wever and Groen (2009) fitted the Gumbel distribution to U^2 based on the observation of Wieringa and Rijkooort (1983) that the estimates of k of the Weibull distribution fitted to whole (i.e. containing not only extreme values) sets of the Dutch wind data vary around 2, similarly to Cook's (1982) estimates obtained from British data.

2.4 Estimation and diagnosis

There are several numerical methods available for the estimation of the parameters of extreme value distributions. Most of them, for instance the methods of moments and of probability weighted moments (PWM), give explicit expressions for the parameter estimates. The maximum likelihood (ML) method tends to be the preferred estimation method since it is quite general and more flexible than other methods, especially when the number of

parameters is increased as for instance when extending the extreme value approach to account for non-stationarity (see Section 2.5). However, for the range of tails typically found with wind data (not too heavy-tailed distributions) and for small to moderate sample sizes (15-500) the method of PWM performs better than the ML method in the estimation of the GPD and GEV parameters (for details, see Hosking and Wallis, 1987, and Hosking et al., 1985).

When estimating it is not only important to obtain the (point) estimates, but also the uncertainty in the estimation. There are several methods for computing the confidence intervals (uncertainty) of the estimates (see e.g. Cairns, 2007):

- The standard approach is based on the asymptotic variance of the parameter estimates (the asymptotic covariance matrices of the GPD and GEV parameter estimates based on the ML or the PWM methods are available in Hosking and Wallis, 1987), the *delta method* (see Ferguson, 1996, p. 45)⁵ and assuming that the estimates are asymptotically normal centred at the parameter values. The (symmetric) confidence intervals obtained in such way are known as *asymptotic intervals*.
- The assumption that extreme value estimates are asymptotically normal centred at the parameter values is usually not valid. For the computation of confidence intervals based on maximum likelihood estimates (e.g. Coles, 2001) the *profile likelihood method* is usually preferable. This method is based on the likelihood ratio and is valid under certain regularity conditions (see Coles, 2001, and references therein for more details). The generally asymmetric confidence intervals obtained in such way are known as *profile likelihood intervals*.
- In some cases the delta method cannot be used to find explicit expressions for the variances of the estimators. In such cases, resampling methods like the bootstrap offer a simple and reliable alternative for estimating standard errors of estimators. Furthermore, the bootstrap method also allows one to compute *percentile confidence intervals* (Efron and Tibshirani, 1993) which also work asymptotically and can be asymmetric. However, Tajvidi (2003) investigated the performance of several bootstrap methods for constructing confidence intervals for the parameters and quantiles of the GPD and concluded that none of the bootstrap methods gives satisfactory intervals for small sample sizes (20-200). In addition, Coles and Simiu (2003) state that “it is well known that bootstrap procedures are not consistent for extreme value problems—there is a tendency for the bootstrap sample to generate shorter tails than the true sample distribution”⁶. Coles and Simiu (2003) propose an ad-hoc method to correct/adjust the bootstrap estimates which consists of applying a bias correction to the bootstrap parameter estimates assuring that the bootstrap sample mean coincides with the parameter estimates. We shall refer to such confidence intervals as *adjusted bootstrap*.

Cairns (2007) studied the coverage rate of confidence intervals of extreme value estimates based on the methods above and that concluded the adjusted percentile bootstrap method generally produce the best confidence intervals from the point of view of coverage rates. Furthermore, that the quality of the coverage rate does not depend much on the *bootstrap sample size*—the number of samples randomly generated (using resampling) to obtain the bootstrap estimates; a bootstrap sample size of 1000 seems to be quite adequate for most practical purposes. Adjusted percentile bootstrap confidence intervals are to be given with the estimates presented in this report.

5. The delta method allows the determination of the asymptotic distribution of estimators that are functions of other estimators whose distribution is known, by means of a Taylor expansion.

6. Shorter tails \equiv lighter tails.

Another parameter that needs to be estimated is λ_u , the yearly cluster rate. It can generally be estimated by the average number of clusters/peak excesses per year. However, for yearly series with different numbers of observations (gaps) the estimation of λ_u should account for the gaps in the data (see Ferreira and Guedes Soares, 1998). In order to account for gaps, λ_u is estimated by dividing the total number of peaks by the *actual number* of years of data (the total period of valid data). The gaps in the summer months are not counted for, since the expected number of peaks in the summer months is very small.

2.5 Climate change

In the methods described so far the extreme wind climate is assumed to be stationary. However, it is believed today that climate is not stationary, as the detection of both decadal variability and long term time trends in different climate variables, reported by several authors, indicates (see e.g. Smits et al., 2005). Both the AM/GEV and POT/GPD approach can be extended to the non-stationary situation by making the parameters of the distributions functions of time (see Coles, 2001 and Caires et al., 2006).

The non-stationary analogue of the POT/GPD approach is the non-homogeneous Poisson process (NPP). In the point process approach to modelling extreme values (Smith, 1989), one looks at the times at which “high values” occur and at their magnitude. If t denotes the generic time at which a high value occurs and if x is the corresponding magnitude of the variable of interest, then the point process consists of a collection of points (t, x) in a region of the positive quadrant of the plane. Thus the point process, or rather its “realization”, consists of a collection of points belonging to the plane set $C = \{(t, x) : x > u, 0 \leq t \leq T\}$ where T is the number of years over which observations are available and u denotes the threshold at time t . The NPP model of extremes is specified by the following two properties. Firstly, if A is a subset of C , then the number of points occurring in A , which we denote by $N(A)$, is a random variable with a Poisson probability function with mean $\rho(A)$, where, writing $x_+ = \max(0, x)$ for real x ,

$$\rho(A) = \int_A \lambda(t, x) dt dx, \quad \lambda(t, x) = \frac{1}{\sigma(t)} \left(1 + \xi(t) \frac{x - \mu(t)}{\sigma(t)} \right)_+^{-\frac{1}{\xi(t)-1}} \quad \text{for } (t, x) \in C, \quad (2.7)$$

and $\mu(t)$, $\sigma(t)$ and $\xi(t)$ are respectively the location, scale and shape parameters—or rather “parameter functions”—that may depend on time and need to be specified and estimated in practice.

The m -yr return value, x_m , is determined by solving

$$\int_0^m \left(1 + \xi(t) \frac{x_m - \mu(t)}{\sigma(t)} \right)_+^{-\frac{1}{\xi(t)-1}} dt = 1. \quad (2.8)$$

The above expression incorporates the time variability of the parameter estimates in the particular return value estimate. However, in general one is interested in the yearly variation of return-value estimates because of the time changes in the parameters, that is, in the variation of the return values once the estimates of the parameters for a given time are fixed.

Treating the parameters in (2.8) as constant in t and solving for x_m , we find that the m -year return value based on the NPP parameters at a fixed time t is

$$x_m = \frac{\sigma(t)}{\xi(t)} \left[\left(\frac{1}{m} \right)^{-\xi(t)} - 1 \right] + \mu(t). \quad (2.9)$$

In order to infer the non-stationarity of the POT extremes in the most complete case the following models for its parameters are to be considered with time and time square covariates:

$$\mu(t) = \mu_0 + \mu_1 t + \mu_2 t^2, \quad \sigma(t) = \sigma_0 + \sigma_1 t + \sigma_2 t^2 \quad \text{and} \quad \xi(t) = \xi \quad (2.10)$$

with $t = 1, 2, \dots, T$, μ_1 , μ_2 , etc.

Our assumption is therefore that climate change and variability may be felt in the form of shifts ($\mu_1 \neq 0$ and/or $\mu_2 \neq 0$) and/or changes in spread ($\sigma_1 \neq 0$ and/or $\sigma_2 \neq 0$) in the distribution of extremes, which can be interpreted as increases/decreases in severity and/or variability of extreme the extreme wind, respectively.

The parameters of the NPP model outlined above are estimated by the maximum likelihood (ML) method. In order to assess whether the dependence of the NPP location and scale parameters on the time covariates are statistically significant, we use the likelihood ratio test (Coles, 2001). The models are to be tested hierarchically with the first model considered being a linear trend in the location parameter.

$$\mu(t) = \mu_0 + \mu_1 t, \quad \sigma(t) = \sigma_0 \quad \text{and} \quad \xi(t) = \xi. \quad (2.11)$$

In the case of the NPP model the choice of the threshold is less obvious than in the POT/GPD approach, where some experience and empirical rules exist. We will therefore, in the non-stationary extreme value analysis, use the same threshold defined as in the stationary extreme value analysis.

The data sampling follows the usual POT approach, with the peak exceedances and the times at which they occur being represented by $\{t_{i,j}, x_{i,j}\}$, $j = 1, 2, \dots, n_i$, $i = 1, 2, \dots, T$, where n_i is the number of clusters in the i -th year. They correspond to the peaks of cluster exceedances above the threshold u and the times at which they occur.

2.6 Hypothesis testing

In order to check whether the data have a type I tail, goodness-of-fit tests will be used. When analysing AM data the Anderson-Darling statistic (D'Agostino and Stephens, 1986) will be used for testing the Gumbel versus any other distribution. The null hypothesis will be tested at the standard 5% significance level, for which the critical value is 0.757. The Gomes and Monfort (1986) test of the exponential distribution against the GPD is to be used when analysing POT data. The null hypothesis is to be tested again at the standard 5% significance level and given that the statistic is normally distributed the critical value is 1.96.

3 Data description

3.1 Choice of stations

Hourly time series of potential wind speed, U_p , and direction were delivered by the KNMI to Deltares for the purposes of this study. The potential wind speed data represent hourly means of wind speed at 10 metres height in a location with a local roughness of 3 cm. Wind directions are reported in units of 10 degrees, starting from 10 to 360 degrees. The wind direction is always an average over the last 10 minutes preceding the full hour.

Figure 3.1 shows the stations for which data were received and the periods on which the data are available. The station names and reference numbers are given in the figure. Most of the stations became operational after the 80's. Wieringa and Rijkoort (1983) considered the data from the stations with the name labelled in red in Figure 3.1 in their analysis of data from 1962 until 1976. Rijkoort (1983) considered also data from the station L.S. Texel, but that station stopped operating at the end of the 70's and its data was not considered by Wever and Groen (2009).

For the determination of the extreme value statistics we have tried to find a period of at least 30 years in which data from a maximum number of stations would be available with a good coverage of the period considered. The period chosen was 1970 until 2008 (39 years) and as much as 21 stations can be considered in that period (cf. Figure 3.1). Namely, IJmuiden, Texelhors, De Kooy, Schiphol, De Bilt, Soesterberg, Leeuwarden, Deelen, Lauwersoog, Eelde, Twenthe, Cadzand, Vlissingen, L. E. Goeree, Hoek van Holland, Zestienhoven, Gilze-Rijen, Herwijnen, Eindhoven, Volkel and Beek, see Figure 3.2. The green lines and the pluses in Figure 3.1 indicate the stations considered in this study.

The chosen period does not fully cover the period considered by Wieringa and Rijkoort (1983), namely 1962-1976, because if we were to choose the period 1962-2008 only 13 stations, which have a good data coverage in that period, could have been considered. Namely, IJmuiden, Schiphol, De Bilt, Soesterberg, Leeuwarden, Deelen, Eelde, Vlissingen, Hoek van Holland, Zestienhoven, Gilze-Rijen, Eindhoven and Beek. We shall analyse the sensitivity of the results to the chosen period using the data of these 13 stations.

Note that the present period of 39 years is more than 2.5 times longer than the original period of 15 years.

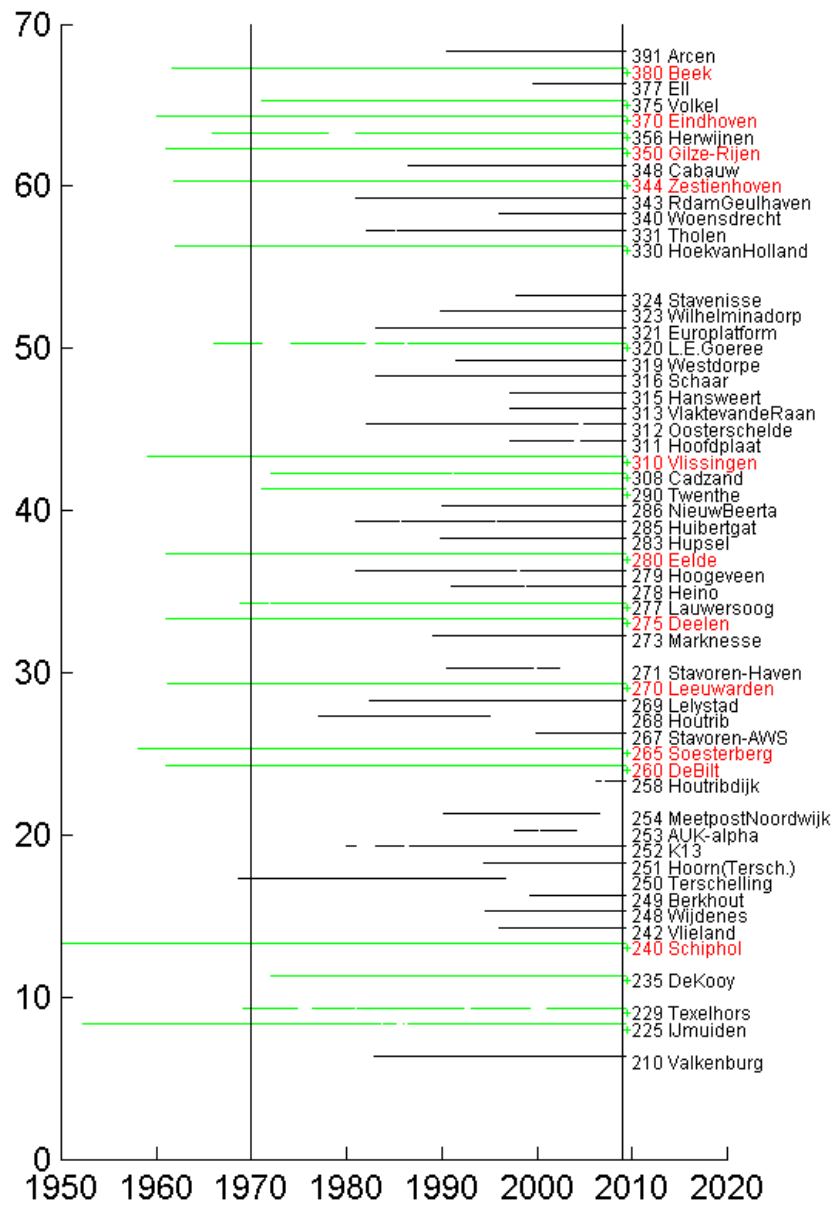


Figure 3.1 Data availability. Stations labelled in red were used in the Rijkooort-Weibull model. The green + before the station reference number indicate the stations considered in this study.

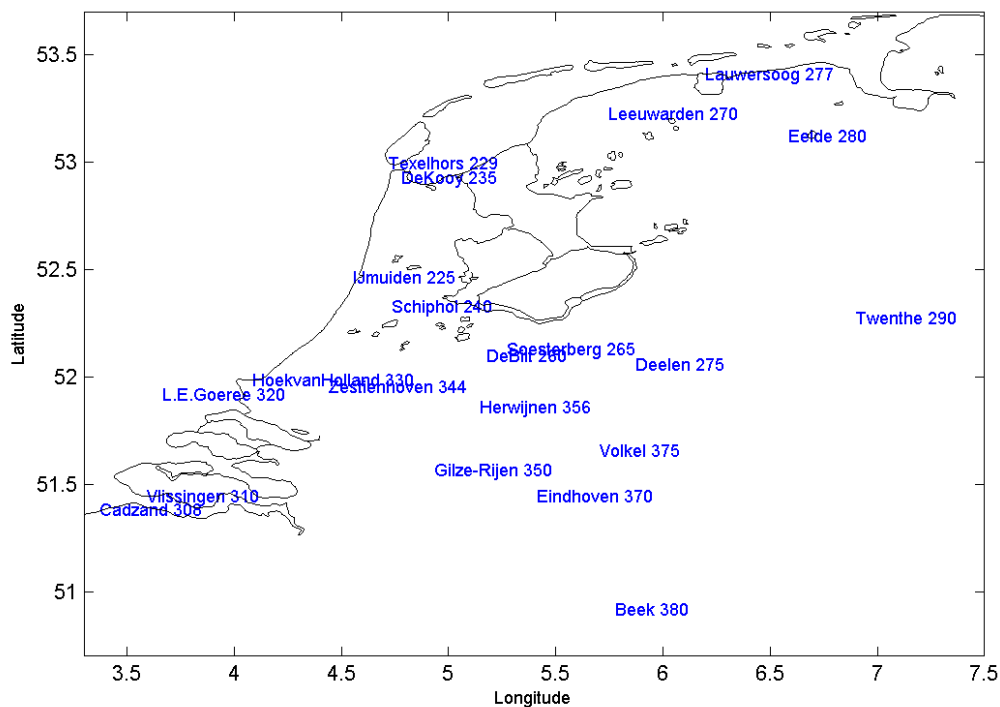


Figure 3.2 Location and reference number of the considered stations.

3.2 1970-2008 mean climate

Figure 3.3 shows the wind roses of the potential wind data from 1970 until 2008 at 18 of the selected 21 stations. The stations for which the roses are not shown are De Kooy, De Bilt and Vlissingen. They have been excluded to improve the readability of the figure.

The figure shows that wind above Beaufort 3 force (5.4 m/s) blows more frequently from the Southwest. Coastal stations are affected by extreme winds from the Southwest to the Northwest sectors, whereas land stations are less affected by Northwesterly extreme winds. The percentage of time with lower wind speeds (below Beaufort 4) is higher in the land stations than in the coastal stations. However, stations like Zestienhoven and Herwijnen seem to be equally affected by extreme conditions as the coastal stations at the same latitude, cf. the red percentage (wind above 24.4 m/s, Beaufort 9) in those and in the Hoek van Holland station.

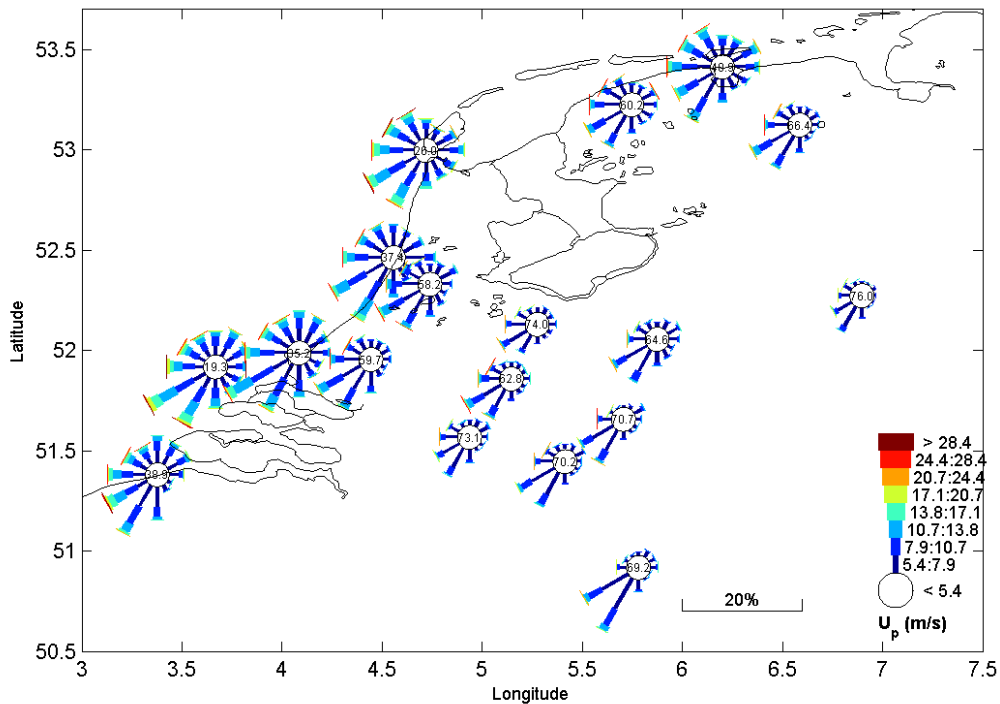


Figure 3.3 Potential wind speed roses for the 1970 – 2008 period. The bar lengths indicate the occurrence percentages. Directions are to the centre of the roses. The numbers in the centre of the roses are the percentage of occurrences in the lowest class.

3.3 Known features contributing to the curvature problem

In Phase 1b of this project a number of causes for the curvature problem have been analysed, see Caires et al. (2009). As also reported by Taminiau (2004) and Bottema (2007), discrepancies have been found between what should be the relation between extremes above water and above land according to the used modelling concept—a simple two-layer model, in which neutral stability and constant geostrophic wind in the region considered is assumed—and the relations inferred from the data. The following major factors have been identified as contributing to the curvature problem:

- *Non-neutral atmospheric stability* : The assumption of a neutral atmospheric stability for all conditions in which the wind speed exceeds 6 m/s appears to be invalid (at sea and coastal stations). This implies that the (shape of the) wind speed profile is not guaranteed "logarithmic and governed by surface roughness only", complicating the use and interpretation of the concept of 'potential wind'.
- *Wind speed dependent water roughness*: The roughness of water increases with increasing wind speed, whereas the roughness at inland sites does not depend on the wind speed. Furthermore, in the homogenisation of the series of measurement data, a "constant" (wind speed independent) exposure correction factor is applied. In case of advection over water, the actual roughness, which the factor is supposed to correct for, does depend on the wind speed. Neglecting the wind speed dependence in water roughness and in the determination of the potential wind series, both enhance the difference in curvature of wind speed statistics at inland sites versus coastal sites.
- *Non-stationary anemometer height*: Certain coastal stations, such as at Hoek van Holland and IJmuiden, are exposed to the sea. It is expected that when high surges accompany extreme sea wind, a rather common situation, that the considered height of

anemometer relatively to the mean sea level is an overestimation of the effective measuring height and the computed potential wind an underestimation.

Further uncertainties have been identified in the data, which influence the quality of the data. The uncertainties may have an influence on the curvature problem.

- The potential wind time series contain inhomogeneities: jumps and trends. Furthermore, a relationship was found between trends in potential wind and trends in exposure correction factors. If this indicates changes in meso-scale roughness, this can have a strong impact in the way potential wind is used in extreme wind statistics.
- The scatter between the turbulence and the land-use maps roughness length estimates is high.

Given that it is not feasible to produce potential wind time series for this project without such discrepancies and given that they are to some extent a true physical feature, the results of the analysis that follows should be interpreted having these aspects in mind.

Furthermore, this list is probably not comprehensive. As recommended in Caires et al. (2009) more research is needed to quantify each of the factors above and remaining uncertainty.

4 Data analysis

Data from 1970 until 2008 at the selected stations were analysed using the AM/GEV and the POT/GPD approach. Most of the stations have hardly any gap in the considered period, but the stations IJmuiden, Texelhors, De Kooy, Twenthe, Cadzand and L.E. Goeree miss some years of data. The data availability per month and per station are given in the tables T.1 of Appendix B. Table 4.1 shows the stations with missing data in the severe storms over the Netherlands identified in the period 1970-2002 in the KNMI-Hydra project (see http://www.knmi.nl/samenw/hydra/cgi-bin/storm_list.cgi).

13-Nov-1972	L.E.Goeree
02-Apr-1973	L.E.Goeree
02-Jan-1976	Texelhors
14-Feb-1979	Herwijnen
01-Feb-1983	—
12-May-1983	—
27-Nov-1983	—
14-Jan-1984	—
16-Oct-1987	Texelhors, L.E.Goeree
25-Jan-1990	—
26-Feb-1990	L.E.Goeree
13-Jan-1993	Texelhors
09-Dec-1993	—
01-Apr-1994	—
03-Mar-1995	—
04-Jan-1998	—
03-Dec-1999	Texelhors
28-May-2000	Texelhors
30-Oct-2000	Texelhors
26-Feb-2002	—
09-Mar-2002	—
27-Oct-2002	—

Table 4.1 List of stations with missing data in the severe storms over the Netherlands identified in the KNMI-Hydra project (see http://www.knmi.nl/samenw/hydra/cgi-bin/storm_list.cgi).

The EVA of the data included omni-directional analyses and directional analyses over 30° sectors. The sectors considered are: 345°N-15°N, 15°N-45°N, ..., 285°N-315°N and 315°N-345°N. Given that wind directions are given in units of 10 degrees, starting from 10 °N, three discrete values of the wind direction are considered per sector. In the omni-directional analysis all data are considered. In the directional analysis only the data falling in the sector of interest are taken into account. The data are stratified into sectors before the EVA is carried out, meaning that a given storm may be considered in more than one sector. The stratification into sectors before the analysis is necessary because we are interested in the return value for the above enumerated fixed sectors. If only storm peaks were to be stratified, the return values obtained for a given sector could have been underestimates.

We will first describe the omni-directional AM/GEV analysis of the data. Subsection 4.2 will present the more sophisticated POT/GPD analysis. The two types of analysis are compatible (can be carried out with different subsets of the same dataset) and are expected to give compatible results (similar estimates of the shape parameter, similar return value estimates, etc.). The POT/GPD analysis is expected to provide more reliable estimates thanks to its

more efficient use of the data. However, given that the AM/GEV analysis is rather simple and fast it is often carried out to get a first idea of the results, and as a global check by comparing its results with those of the POT/GPD.

4.1 AM/GEV analysis

For each station the 1970-2008 period was considered and in each year for which less than 50% of the data were missing the annual maxima was computed. Annual maxima at a distance of less than 96h were treated as belonging to the same storm and occurring at the year of the maximal value. The sample sizes of the time series of annual maxima per station are given in Table 4.2.

The GEV and the Gumbel (GEV with $\xi = 0$) distributions were fitted to the AM samples of U_p , U_p^2 and U_p^k . The value k was estimated by fitting the Weibull distribution to the entire hourly dataset per station, not only to the annual maxima (AM).

Figure 4.1 to Figure 4.3 show the estimates of the GEV shape parameter, ξ , obtained from the fits to annual maxima of U_p , U_p^2 and U_p^k . Estimates between -0.05 and +0.05 are given in green, those above 0.05 in red and those below -0.05 in blue. The estimates of k are given in the Figure 4.4. In the figures it can be seen that the estimates from the fit to annual maxima of U_p vary mostly around zero, the respective Figure 4.1 showing the most green digits. On the other hand, the figure of fit to annual maxima of U_p^2 shows the least green digits and the shape parameter estimates are higher than those of the other fits.

Table 4.3 gives the GEV shape parameter estimates, associated 95% confidence intervals and the results of the Anderson-Darling test, for testing the Gumbel versus any other distribution. The cases for which the null hypothesis was rejected are indicated by 1.

Station	Sample size
IJmuiden	38
Texelhors	34
De Kooy	37
Schiphol	39
De Bilt	39
Soesterberg	39
Leeuwarden	39
Deelen	39
Lauwersoog	39
Eelde	39
Twenthe	38
Cadzand	37
Vlissingen	39
L.E. Goeree	33
Hoek van Holland	39
Zestienhoven	39
Gilze-Rijen	39
Herwijnen	36
Eindhoven	39
Volkel	38
Beek	39

Table 4.2 Sample size of the AM data in the 1970-2008 period.

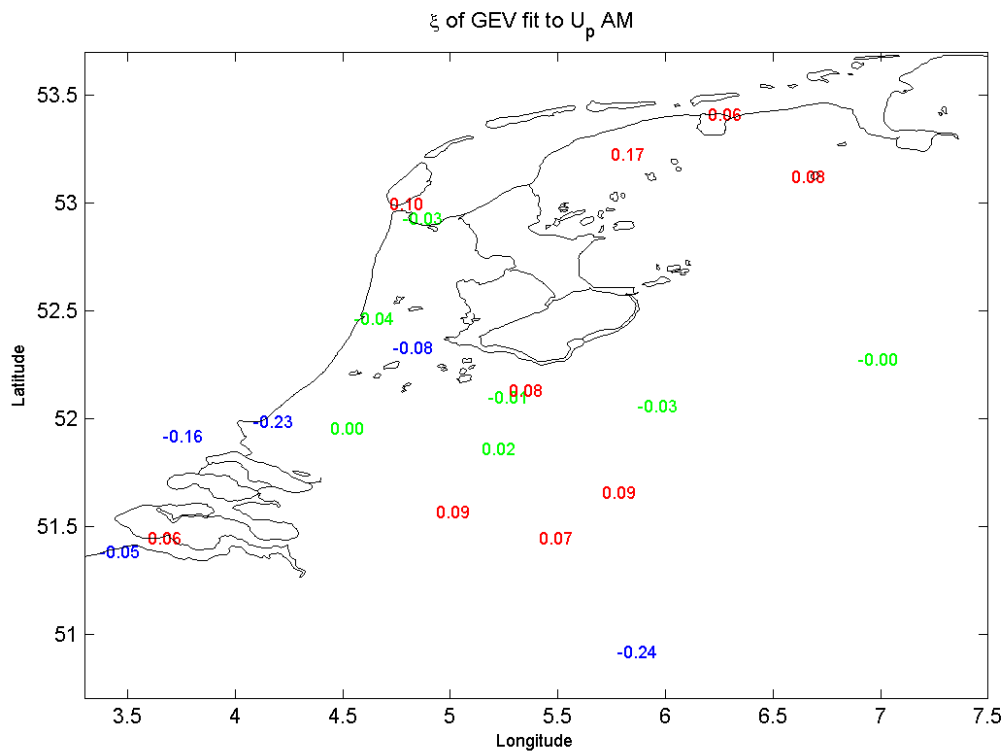


Figure 4.1 Shape parameter estimates of GEV fits to U_p AM.

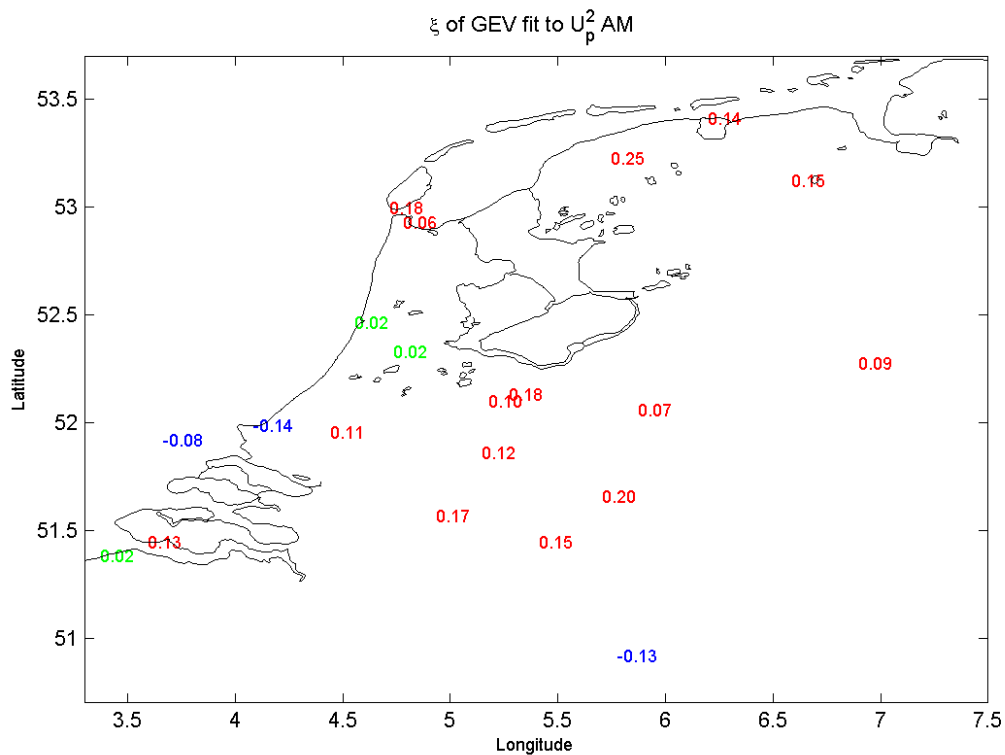


Figure 4.2 Shape parameter estimates of GEV fits to U_p^2 AM.

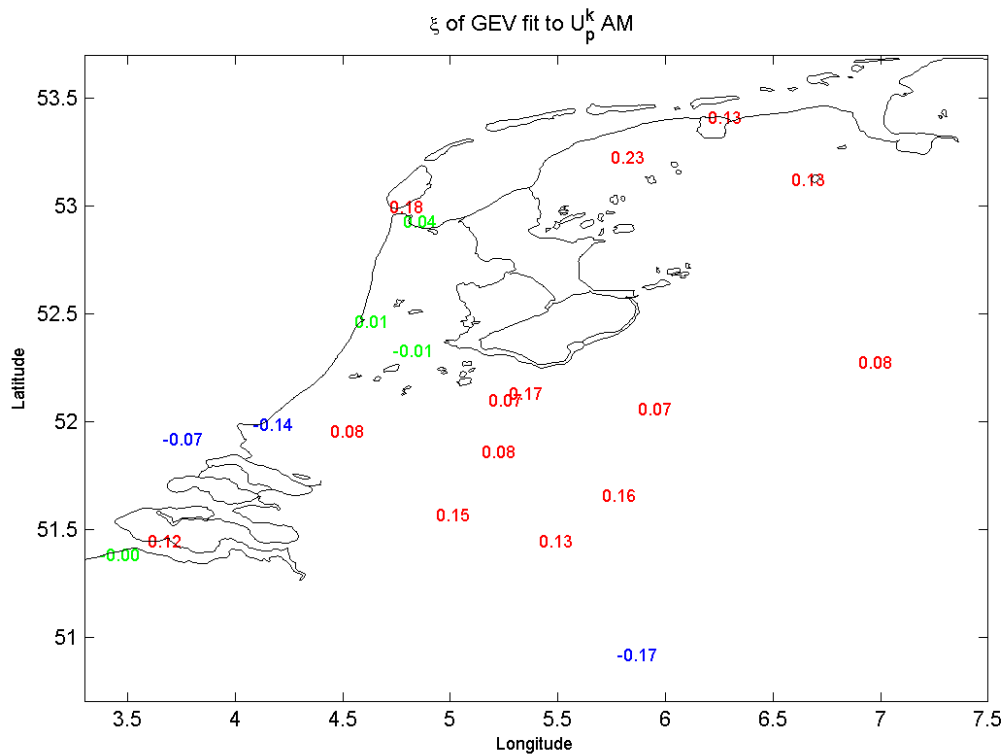


Figure 4.3 Shape parameter estimates of GEV fits to U_p^k AM (with k as given in Figure 4.4).

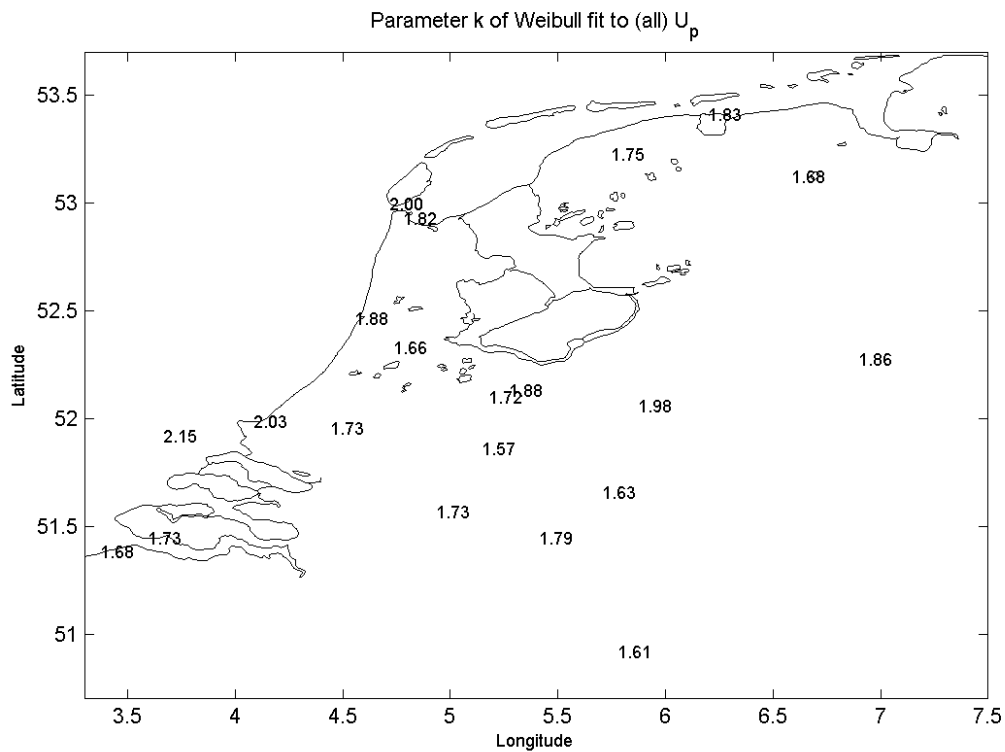


Figure 4.4 Weibull shape parameter k estimates from fits to the whole U_p data.

Recall that we consider the power 2 and power k data transformations to try to accelerate the convergence to a type I tail (in this case Gumbel). Note that the null hypothesis is rejected

only in one station in the U_p and in the U_p^k AM analysis (just below 5% of the cases) and in four stations in the U_p^2 AM analysis (about 19% of the cases). From these results it can be concluded that data transformations do not, in the cases considered, appear to improve the convergence to a type I tail, nor does it seem to be needed, since the type I hypothesis seems to apply to the U_p AM data. Furthermore, when applying a power 2 transformation the tail of the data appears to be closer to the type II domain ($\xi > 0$). Indeed, in general the transformations result in an increase of the shape parameter estimates, the increase being greater when a power 2 transformation is used (cf. Table 4.3). In the review (Appendix A.1, Section 3.4) some comments are made on the basic assumptions underlying the use of the U_p^k analysis.

It is also interesting to note that in some of the cases in which the null hypothesis is rejected by the Anderson-Darling test the confidence intervals for the shape parameter still include zero. This means that an eventual t-test would have been less stringent in terms of rejecting the null hypothesis of a type I tail than the Anderson-Darling test.

	GEV fit to U_p AM		GEV fit to U_p^2 AM		GEV fit to U_p^k AM		
	ξ	AD	ξ	AD	ξ	AD	k
IJmuiden	-0.04 (-0.24, 0.14)	0	0.02 (-0.17, 0.19)	0	0.01 (-0.17, 0.18)	0	1.88
Texelhors	0.10 (-0.11, 0.27)	0	0.18 (-0.05, 0.33)	0	0.18 (-0.05, 0.35)	0	2.00
De Kooy	-0.03 (-0.28, 0.18)	0	0.06 (-0.19, 0.25)	0	0.04 (-0.21, 0.24)	0	1.82
Schiphol	-0.08 (-0.34, 0.15)	0	0.02 (-0.24, 0.25)	0	-0.01 (-0.28, 0.22)	0	1.66
De Bilt	-0.01 (-0.24, 0.22)	0	0.10 (-0.09, 0.31)	0	0.07 (-0.14, 0.27)	0	1.72
Soesterberg	0.08 (-0.18, 0.29)	0	0.18 (-0.11, 0.37)	0	0.17 (-0.10, 0.36)	0	1.88
Leeuwarden	0.17 (-0.02, 0.32)	1	0.25 (0.06, 0.39)	1	0.23 (0.05, 0.37)	1	1.75
Deelen	-0.03 (-0.22, 0.17)	0	0.07 (-0.13, 0.26)	0	0.07 (-0.13, 0.25)	0	1.98
Lauwersoog	0.06 (-0.21, 0.25)	0	0.14 (-0.08, 0.32)	0	0.13 (-0.13, 0.31)	0	1.83
Eelde	0.08 (-0.11, 0.26)	0	0.15 (-0.04, 0.33)	1	0.13 (-0.06, 0.31)	0	1.68
Twenthe	-0.00 (-0.25, 0.21)	0	0.09 (-0.16, 0.29)	0	0.08 (-0.17, 0.28)	0	1.86
Cadzand	-0.05 (-0.30, 0.17)	0	0.02 (-0.21, 0.22)	0	-0.00 (-0.25, 0.21)	0	1.68
Vlissingen	0.06 (-0.13, 0.24)	0	0.13 (-0.04, 0.29)	0	0.12 (-0.07, 0.28)	0	1.73
L.E. Goeree	-0.16 (-0.39, 0.04)	0	-0.08 (-0.28, 0.11)	0	-0.07 (-0.29, 0.12)	0	2.15
Hoek van Holland	-0.23 (-0.53, 0.02)	0	-0.14 (-0.45, 0.10)	0	-0.14 (-0.40, 0.10)	0	2.03
Zestienhoven	0.00 (-0.21, 0.20)	0	0.11 (-0.10, 0.29)	0	0.08 (-0.13, 0.27)	0	1.73
Gilze-Rijen	0.09 (-0.14, 0.27)	0	0.17 (-0.04, 0.35)	1	0.15 (-0.05, 0.34)	0	1.73
Herwijnen	0.02 (-0.19, 0.20)	0	0.12 (-0.09, 0.30)	0	0.08 (-0.11, 0.25)	0	1.57
Eindhoven	0.07 (-0.17, 0.28)	0	0.15 (-0.08, 0.34)	1	0.13 (-0.08, 0.32)	0	1.79
Volkel	0.09 (-0.17, 0.30)	0	0.20 (-0.05, 0.41)	0	0.16 (-0.09, 0.37)	0	1.63
Beek	-0.24 (-0.50, -0.01)	0	-0.13 (-0.38, 0.09)	0	-0.17 (-0.41, 0.05)	0	1.61
Average	0.00		0.09		0.07		1.80

Table 4.3 Estimates of ξ and associated 95% confidence intervals from the fits to omni-directional U_p , U_p^2 and U_p^k AM data. The Anderson-Darling test results are also provided as well as the shape parameter k of the Weibull distribution fitted to the whole U_p data.

The results presented here are only for the omni-directional case. The complete set of the GEV shape parameter estimates and the Anderson-Darling statistics are given in tables T.2 of Appendix B. In addition to the omni-directional analyses, a brief directional analysis has been performed in the review in Appendix A.1, Section 3.3. There it is concluded that the AM analysis in terms of U_p , instead of U_p^k or U_p^2 , seems appropriate not only for the omni-directional case, but also for the directional sectors 225°N-255°N, 255°N-285°N, 285°N-315°N and 315°N-345°N, which are the most important directional sectors with the highest extreme wind speeds. For the other directional sectors however, with less extreme wind speeds, other analyses could be more appropriate, leading probably to lower extremes (cf. Table 4.4). It is

concluded though, that the analysis in terms of U_p seems sufficiently reliable for the determination of the HBC.

Figure 4.5 shows the 10,000-yr return value estimates obtained from the GEV fit to U_p AM. Figure 4.6 to Figure 4.8 show the 10,000-yr return value estimates obtained by a Gumbel fit to U_p , U_p^2 and U_p^k AM data, respectively.

Although the assumption of a type I tail seems to be valid for the considered U_p data, given the large uncertainty associated with the estimates the differences between the GEV and Gumbel estimates based on fits to U_p can be rather large. The GEV estimates are quite noisy and show an unrealistic (in terms of physical arguments, although not statistically significant) spatial variation of the 10,000-yr return value estimates. Especially extremely high 10,000-yr return values at the northern and south-eastern stations, varying between 40 and 60 m/s, and a quite low 10,000-yr return value (and shape parameter estimate) for the Hoek van Holland station. Such noisy (highly uncertain) estimates are not desirable in the further inference of hydraulic boundary conditions. For the inference of the hydraulic boundary conditions, it is desirable that there be some robustness/smoothness in the spatial variation of the estimates since they need to be further interpolated.

Fixing a tail of type I it can be concluded that the 10,000-yr return value estimates obtained by a Gumbel fit to U_p are typically 10-20% larger than the estimates obtained by a Gumbel fit to U_p^2 and to a lesser extent than the estimates obtained by a Gumbel fit to U_p^k AM, cf. Table 4.4. Such differences are to be expected given that the GEV shape parameter estimates for the transformed data are generally greater than zero (cf. Figure 4.1), meaning that when assuming a type I tail the extremes are underestimated. The underestimation being larger the bigger the (positive) shape parameter estimate.

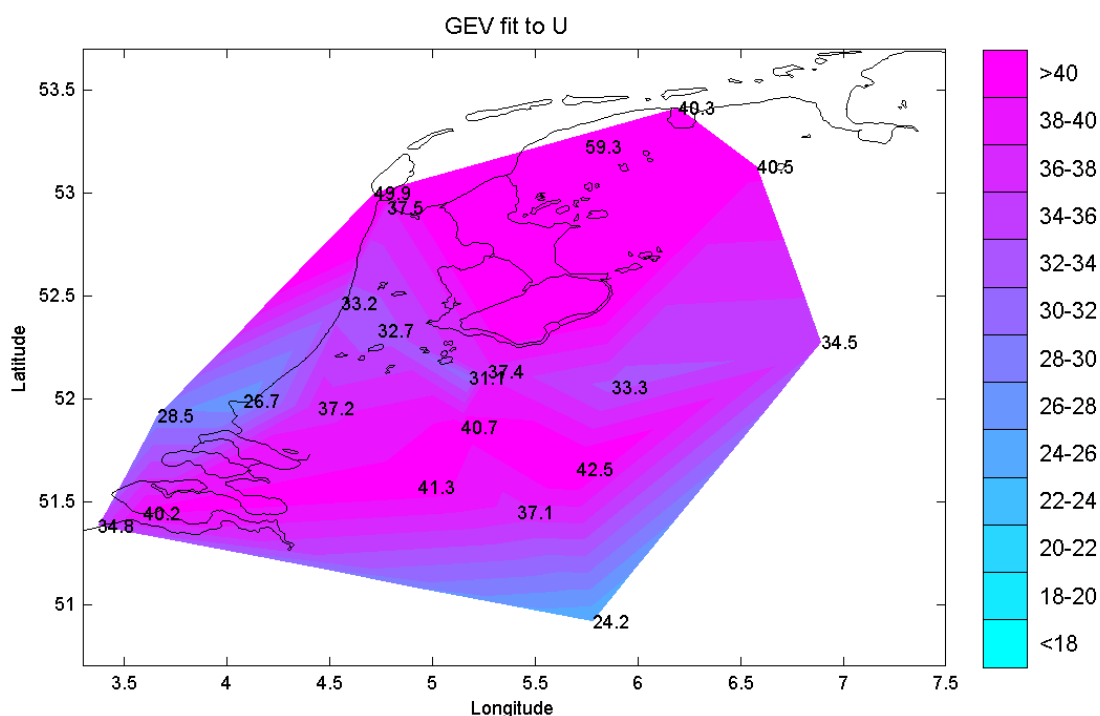


Figure 4.5 10,000-yr return value estimates of the GEV fit to U_p AM data.

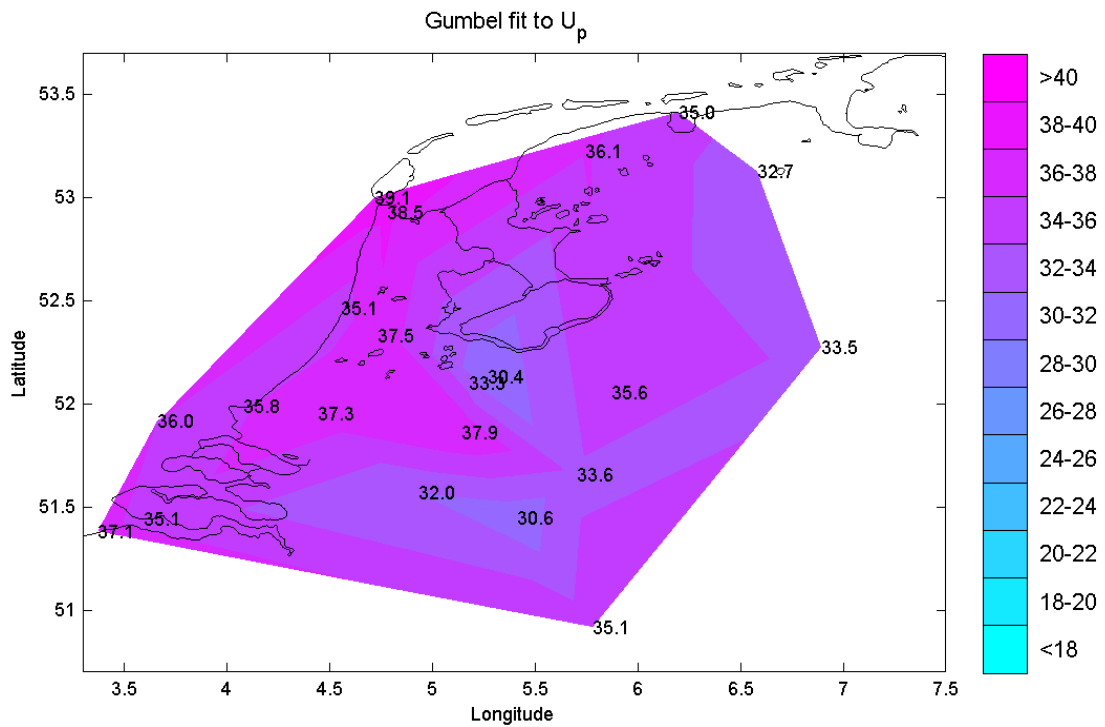


Figure 4.6 10,000-yr return value estimates of Gumbel fits to U_p AM data.

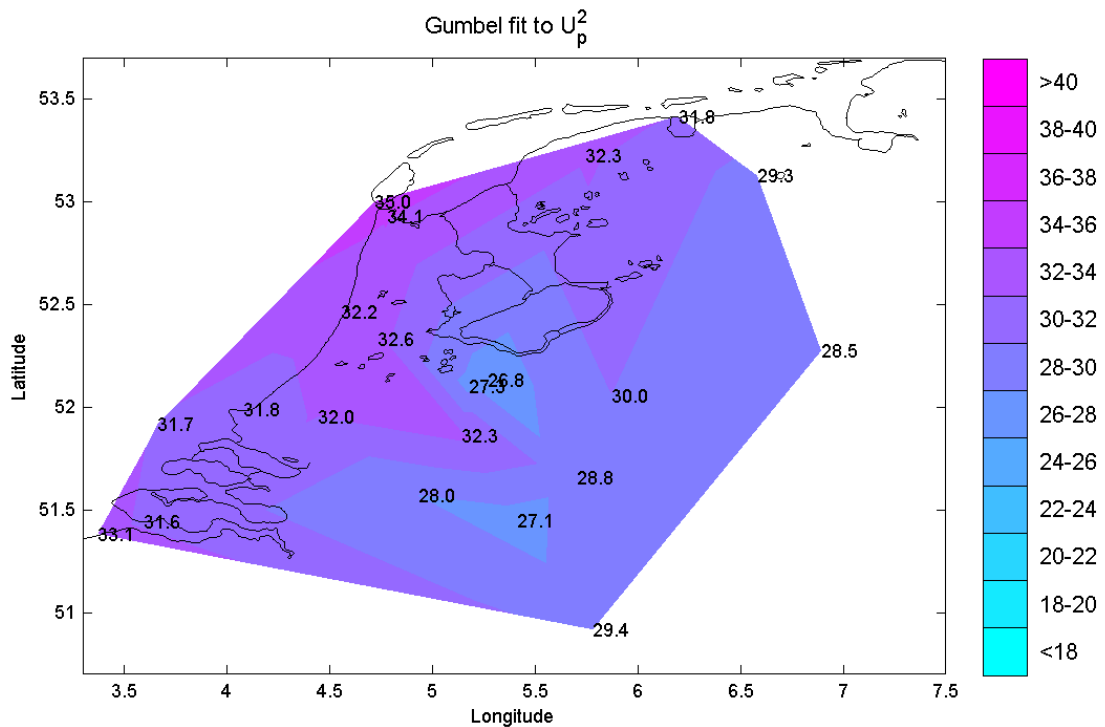


Figure 4.7 10,000-yr return value estimates of Gumbel fits to U_p^2 AM data.

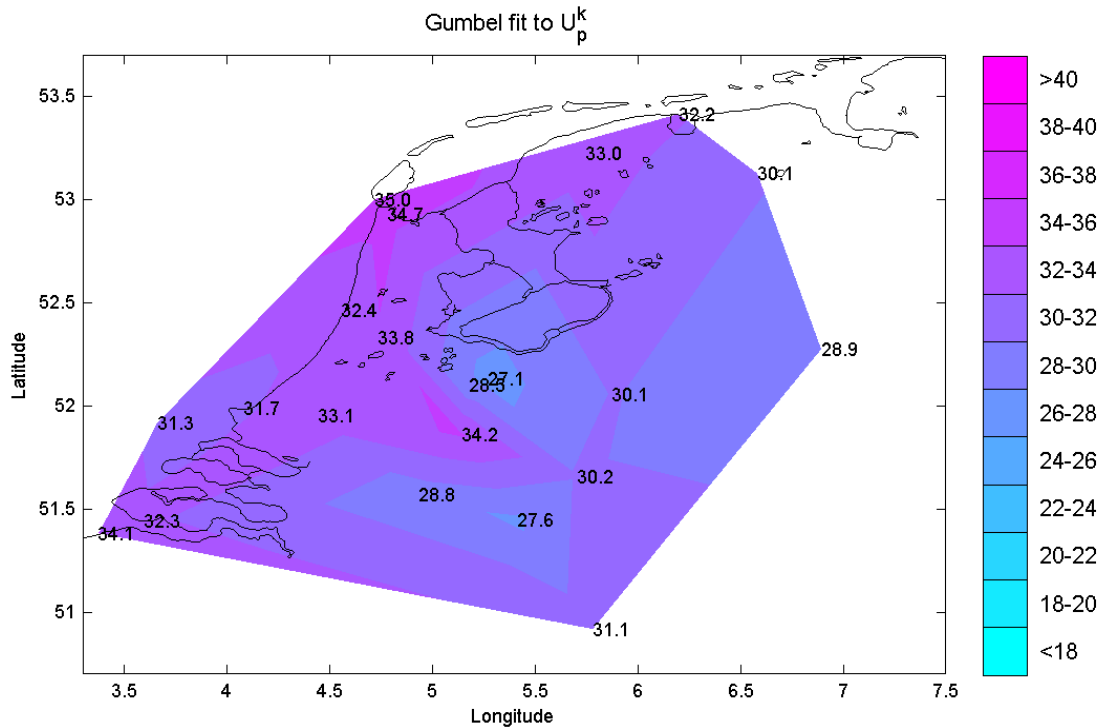


Figure 4.8 10,000-yr return value estimates of Gumbel fits to U_p^k AM data.

	Gumbel fit to U_p AM	Gumbel fit to U_p^2 AM		Gumbel fit to U_p^k AM	
	10,000-yr rv (m/s)	10,000-yr rv (m/s)	Relative differences	10,000-yr rv (m/s)	Relative differences
Ijmuiden	35.1	32.2	-8.3%	32.4	-7.7%
Texelhors	39.1	35.0	-10.5%	35.0	-10.5%
De Kooy	38.5	34.1	-11.4%	34.7	-9.9%
Schiphol	37.5	32.6	-13.1%	33.8	-9.9%
De Bilt	33.3	27.3	-18.0%	28.5	-14.4%
Soesterberg	30.4	26.8	-11.8%	27.1	-10.9%
Leeuwarden	36.1	32.3	-10.5%	33.0	-8.6%
Deelen	35.6	30.0	-15.7%	30.1	-15.4%
Lauwersoog	35.0	31.8	-9.1%	32.2	-8.0%
Eelde	32.7	29.3	-10.4%	30.1	-8.0%
Twenthe	33.5	28.5	-14.9%	28.9	-13.7%
Cadzand	37.1	33.1	-10.8%	34.1	-8.1%
Vlissingen	35.1	31.6	-10.0%	32.3	-8.0%
L.E. Goeree	36.0	31.7	-11.9%	31.3	-13.1%
Hoek van Holland	35.8	31.8	-11.2%	31.7	-11.5%
Zestienhoven	37.3	32.0	-14.2%	33.1	-11.3%
Gilze-Rijen	32.0	28.0	-12.5%	28.8	-10.0%
Herwijnen	37.9	32.3	-14.8%	34.2	-9.8%
Eindhoven	30.6	27.1	-11.4%	27.6	-9.8%
Volkel	33.6	28.8	-14.3%	30.2	-10.1%
Beek	35.1	29.4	-16.2%	31.1	-11.4%
Average			-12.4%		-10.5%

Table 4.4 10,000-yr return value estimates from Gumbel fits to U_p , U_p^2 and U_p^k AM data.

Figure 4.9 presents for four stations (2 coastal stations and 2 inland stations) the omni-directional return value plot of the fits considered. The full lines give the return value estimates and the dashed lines the associated 95% confidence intervals. The horizontal lines when present indicate an eventual upper-limit of the GEV fit. The omni-directional return value plots of all the stations are given in a larger format in figures F.2 in Appendix C.

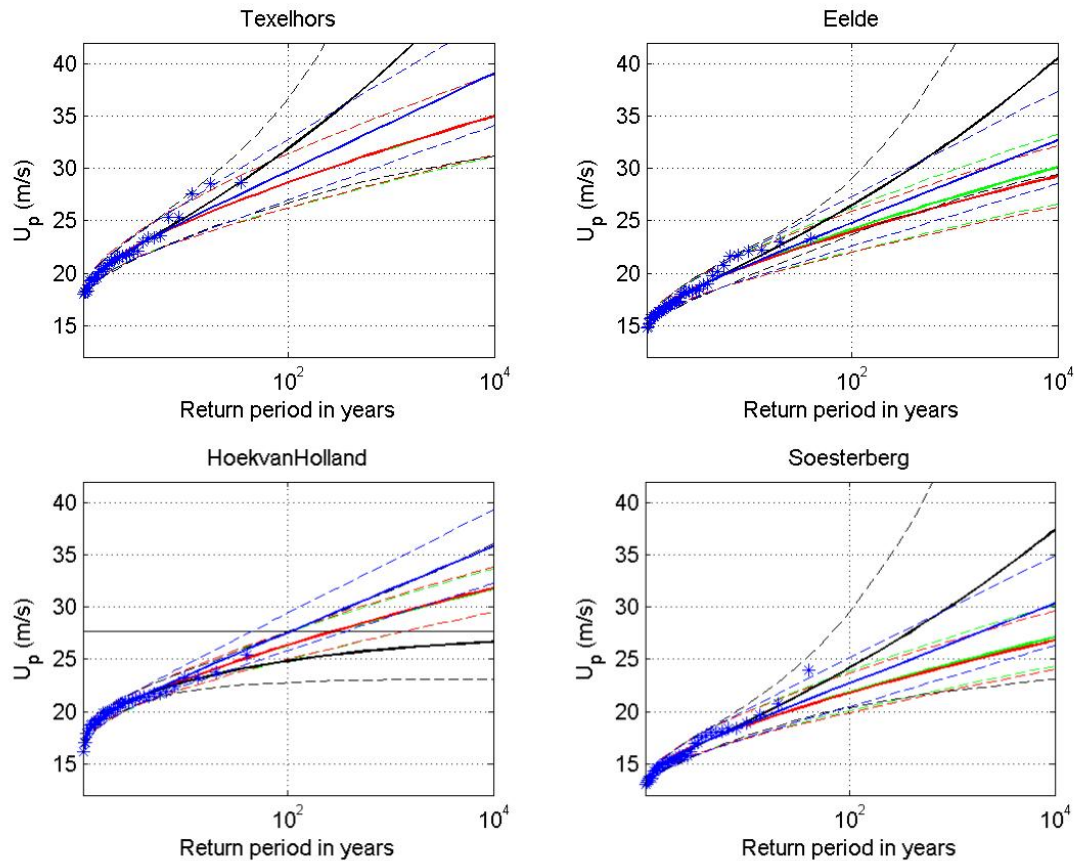


Figure 4.9 Return value plot with Gumbel (blue) and GEV (black) fit to U_p , Gumbel fit to U_p^2 (red) and Gumbel fit to U_p^k (green) AM data. The dashed lines are the associated adjusted bootstrap 95% confidence intervals. The AM data are represented by the asterisks, with plotting positions $\left(x_i, \frac{n+1}{n+1-i}\right)^7$.

In Figure 4.9 it can be seen that, as expected, given the extra parameter, the GEV generally fits the data better. The Gumbel fits to U_p generally follow the data well. The Gumbel fits to U_p^2 and U_p^k do not differ much from each other, only for Eelde, the station for which k deviates more from 2 (cf. Table 4.3), can the red and green full lines be clearly identified. Furthermore, the Gumbel fits to U_p^2 and U_p^k generally underestimate the highest observed storms. Hoek van Holland is the only station for which a type III tail (a GEV with $\xi < 0$) is inferred and the Gumbel fits to U_p^2 and U_p^k seem to follow the data better than the other fits.

Comparing the return values lines in Figure 4.9 of the GEV fits (full black lines) to the Hoek van Holland and Soesterberg U_p AM data, it is clear that the lines cross each other. On the

7. In the review (Appendix A.1, Section 3.3) some remarks are made concerning the plotting positions used.

other hand, if a type I tail is assumed in both stations (full blue lines) that is no longer the case.

4.2 POT/GPD analysis

Having presented the results of the AM/GEV analysis we now present the results of the POT/GPD approach. The results of this approach are in principle more reliable since more storm peaks are considered. Also, as said by De Haan and Zhou (2009); “By choosing the threshold in an intelligent way, either by visual inspection or by using a theoretically justified threshold selection procedure, it is possible to improve the tail estimation substantially. The AM/GEV approach has no room for this improvement since the year is usually the only realistic time period one can consider”.

4.2.1 Choice of threshold

We have used the threshold stability property mentioned in Section 2.2.2 to choose the most appropriate threshold for selecting a sample of peak excesses and fitting the GPD and the exponential distribution to it. More precisely, we have looked for threshold values around which the estimate of the shape parameter shows the least variation (cf. Section 2.2.2). Because we are also interested in choosing a threshold for which the GPD shape parameter is close to zero, we have also looked for a threshold within the stable region that would yield the shape parameter estimate closer to zero. We have tried to automatize such a choice of the threshold using the following procedure:

- 1 POT samples with at least 10 and at most 300 peaks are collected by systematically decreasing the threshold, and for each of these samples GPD fits are obtained. Note that if there is a POT sample with, say, 20 peaks, does not mean that there is also a POT sample with 19 peaks, since different peaks may have the same value and even a small increase of the threshold can eliminate more than one of the peaks collected at a lower threshold.
- 2 For each sample size n , a set of parameter estimates based on sample sizes ranging from $n-l$ to $n+l$ peaks, where l is some fixed value (see below), are obtained, and the standard deviation (v) and the mean of the absolute values (a) of such a set of estimates is computed. In the case of the shape parameter, for example, this procedure yields one standard deviation for each value of n , and each standard deviation quantifies the variability of the parameter estimates around a ‘window’ of $2l+1$ sample sizes ($2l+1=(n+l)-(n-l)+1$).
- 3 The threshold, or sample size n , that is then by this procedure suggested for the inference is the one yielding the smallest $v+a$ value computed in bullet 2.

Several tests were carried out to determine the best choice of the window size on which the standard deviations of the second bullet are computed. $l=10$ turned out to be the best: using about 21 ($2l+1$ for $l=10$) estimates, the automatically determined threshold coincides often with the one that we would have chosen by visual inspection of plots like those in Table 4.5. In most cases the results are resistant against changes in l for l between 10 and 15. With larger values of l the threshold chosen is often too low.

Following this procedure all threshold plots were visually inspected and the threshold was adjusted where deemed necessary.

4.2.2 Analysis

Figure 4.10 shows the threshold plot for the omni-directional POT/GPD analysis of the IJmuiden and Deelen U_p , U_p^2 and U_p^k POT data. The GPD shape parameter estimates based on the U_p data are given in blue, those based on the U_p^2 data are given in red and those based on the U_p^k data given in green. As noted in the AM/GEV analysis, the data transformation results always in an increase of the shape parameter estimate, which not always implies a faster convergence to a shape parameter of zero. In fact, if we look at the Deelen threshold plot in the stable region no shape parameter close to zero can be found in the GPD fits to the U_p^2 and U_p^k POT data. The vertical lines in the figures indicate the threshold suggested by the automatic procedure described above using the U_p POT data.

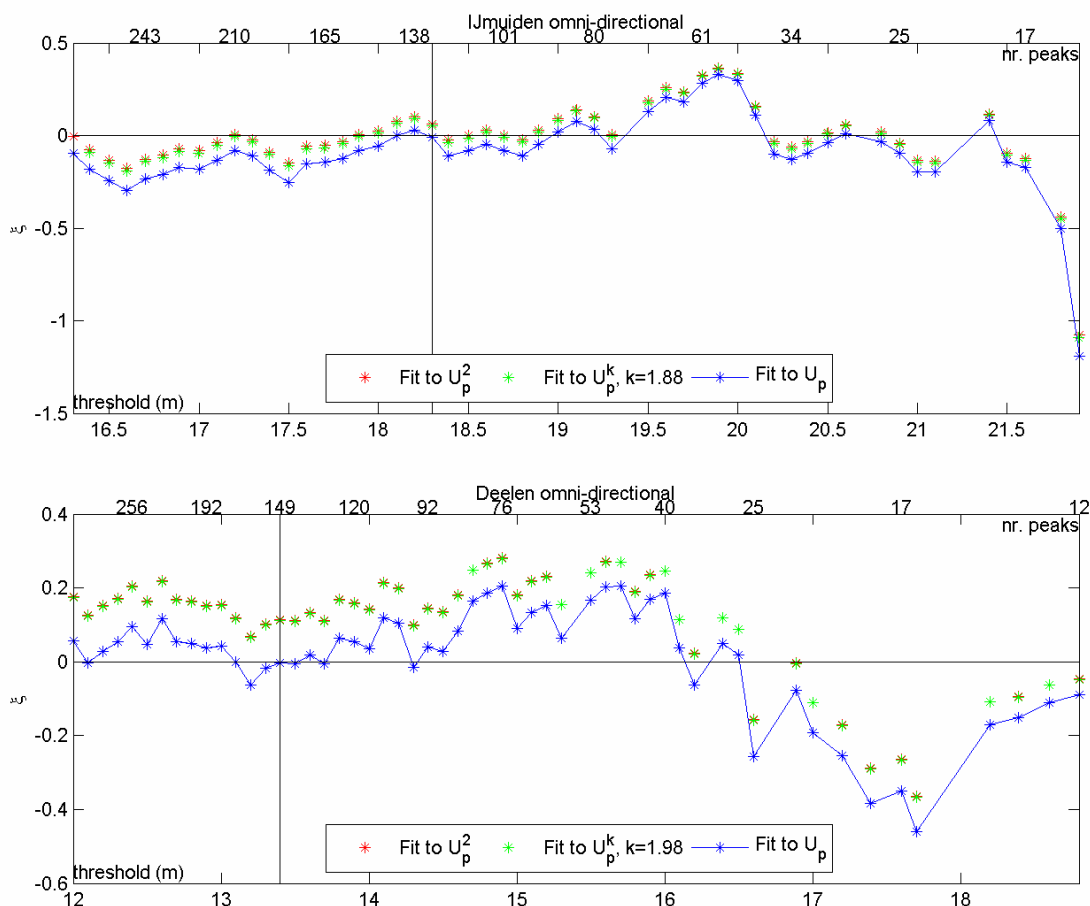


Figure 4.10 Variation of the GPD shape parameter with the threshold for fits to U_p (blue) U_p^2 (red) and U_p^k (green) POT data from IJmuiden (top panel) and Deelen (bottom panel). The vertical line indicates the threshold chosen for further inference.

As was also concluded in the AM/GEV omni-directional analysis the power 2 and power k transformations do not yield the intended accelerated convergence to a type I tail distribution. The power transformations always result in an increase of the GPD shape parameter, independently of the original value. We have therefore decided to fix the threshold solely on the basis of the U_p data analysis. For illustration, the variation of the 10,000-yr return value estimates with the threshold for Exponential and GPD fits to the considered U_p POT data is given in Figure 4.11.

The threshold plots of the IJmuiden and Deelen stations were chosen to be presented here because they provide illustrative examples, the conclusions taken from these plots are general and supported by all the other plots. Figures F.3 in Appendix C present in a larger format all omni-directional threshold plots. When present, the red vertical lines in the plots indicate whether a different threshold was chosen by visual inspection for compiling the final POT sample (there were no different thresholds chosen in the examples presented in Figure 4.10).

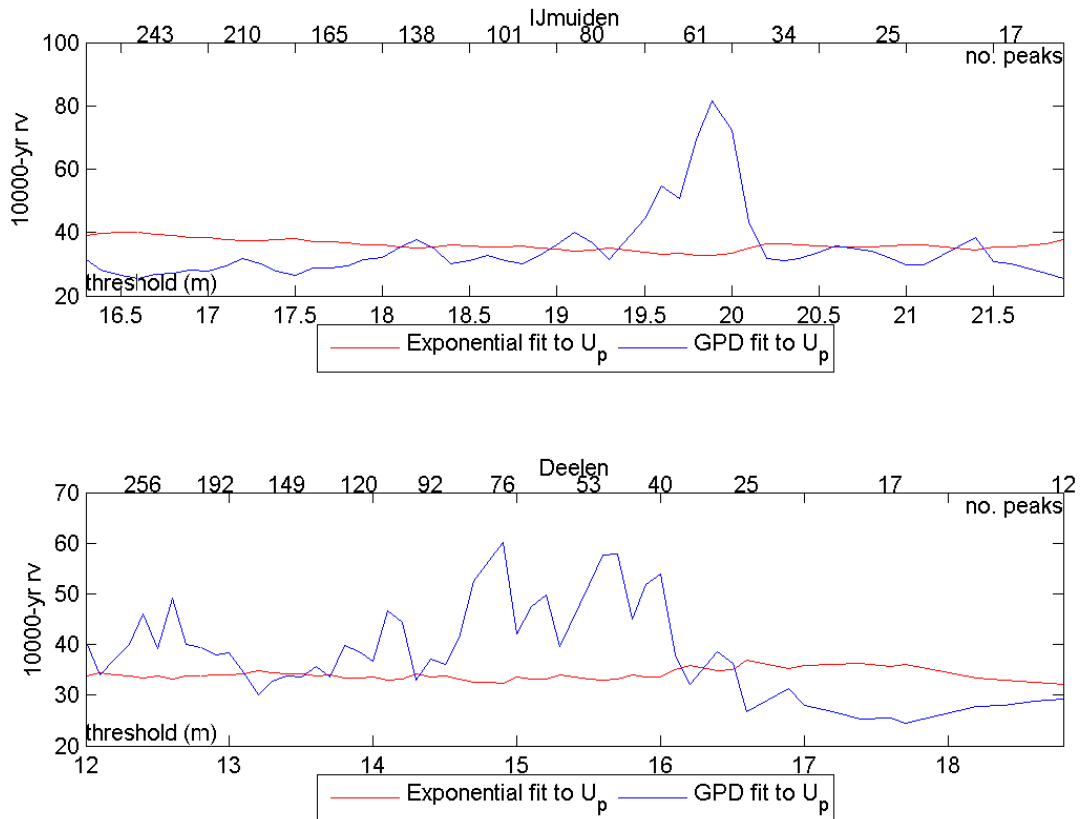


Figure 4.11 Variation of the 10,000-yr return value estimates with the threshold for Exponential (red) and GPD (blue) fits to U_p POT data from IJmuiden (top panel) and Deelen (bottom panel).

Station \ Sector	omni-directional						
IJmuiden	-0.01 (-0.24, 0.18)						
Texelhors	0.01 (-0.21, 0.19)						
De Kooy	-0.00 (-0.20, 0.16)						
Schiphol	-0.01 (-0.27, 0.19)						
De Bilt	0.00 (-0.17, 0.15)						
Soesterberg	-0.02 (-0.17, 0.14)						
Leeuwarden	0.00 (-0.19, 0.16)						
Deelen	-0.00 (-0.18, 0.17)						
Lauwersoog	-0.01 (-0.16, 0.13)						
Eelde	-0.00 (-0.23, 0.18)						
Twenthe	0.00 (-0.21, 0.18)						
Cadzand	-0.02 (-0.20, 0.15)						
Vlissingen	-0.00 (-0.22, 0.18)						
L.E. Goeree	0.02 (-0.17, 0.19)						
Hoek van Holland	-0.05 (-0.27, 0.15)						
Zestienhoven	0.00 (-0.17, 0.15)						
Gilze-Rijen	-0.02 (-0.18, 0.12)						
Herwijnen	-0.00 (-0.23, 0.20)						
Eindhoven	-0.01 (-0.20, 0.16)						
Volkel	0.01 (-0.19, 0.18)						
Beek	0.00 (-0.23, 0.19)						
Station \ Sector	345°N : 15°N	15°N : 45°N	45°N : 75°N	75°N : 105°N	105°N : 135°N	135°N : 165°N	
IJmuiden	0.00 (-0.22, 0.20)	0.02 (-0.18, 0.18)	-0.04 (-0.36, 0.23)	-0.01 (-0.22, 0.16)	0.00 (-0.20, 0.18)	0.01 (-0.14, 0.14)	
Texelhors	-0.06 (-0.41, 0.22)	0.01 (-0.15, 0.15)	0.00 (-0.21, 0.18)	-0.01 (-0.17, 0.13)	0.02 (-0.16, 0.19)	-0.00 (-0.17, 0.16)	
De Kooy	0.01 (-0.23, 0.21)	-0.00 (-0.24, 0.22)	0.01 (-0.20, 0.20)	0.01 (-0.19, 0.18)	0.01 (-0.28, 0.26)	0.06 (-0.22, 0.30)	
Schiphol	-0.00 (-0.15, 0.14)	-0.01 (-0.24, 0.21)	0.02 (-0.15, 0.17)	-0.02 (-0.26, 0.17)	0.01 (-0.15, 0.14)	-0.06 (-0.30, 0.15)	
De Bilt	0.01 (-0.30, 0.27)	0.01 (-0.16, 0.18)	-0.01 (-0.24, 0.18)	-0.04 (-0.21, 0.14)	0.01 (-0.22, 0.20)	-0.00 (-0.23, 0.18)	
Soesterberg	-0.01 (-0.18, 0.13)	0.01 (-0.19, 0.17)	-0.00 (-0.26, 0.20)	-0.06 (-0.34, 0.17)	0.03 (-0.19, 0.22)	-0.05 (-0.25, 0.12)	
Leeuwarden	0.02 (-0.16, 0.16)	-0.00 (-0.21, 0.19)	0.00 (-0.36, 0.30)	-0.01 (-0.24, 0.17)	0.02 (-0.24, 0.23)	0.00 (-0.15, 0.14)	
Deelen	0.00 (-0.24, 0.21)	-0.00 (-0.22, 0.19)	-0.04 (-0.29, 0.18)	0.00 (-0.19, 0.17)	0.01 (-0.35, 0.29)	0.01 (-0.23, 0.19)	
Lauwersoog	-0.01 (-0.19, 0.14)	-0.01 (-0.23, 0.17)	-0.02 (-0.23, 0.17)	-0.02 (-0.33, 0.25)	0.03 (-0.27, 0.26)	0.02 (-0.24, 0.22)	
Eelde	-0.00 (-0.15, 0.14)	0.03 (-0.21, 0.20)	0.02 (-0.19, 0.19)	0.01 (-0.18, 0.17)	-0.04 (-0.30, 0.17)	-0.00 (-0.20, 0.15)	
Twenthe	-0.01 (-0.19, 0.16)	-0.03 (-0.23, 0.16)	0.02 (-0.15, 0.18)	-0.01 (-0.18, 0.16)	-0.01 (-0.17, 0.13)	0.02 (-0.23, 0.21)	
Cadzand	0.02 (-0.29, 0.26)	0.03 (-0.17, 0.19)	-0.04 (-0.26, 0.16)	0.03 (-0.22, 0.24)	0.01 (-0.18, 0.17)	0.00 (-0.16, 0.15)	
Vlissingen	-0.00 (-0.17, 0.14)	-0.03 (-0.37, 0.25)	-0.04 (-0.27, 0.17)	0.01 (-0.17, 0.17)	-0.00 (-0.24, 0.20)	-0.03 (-0.27, 0.17)	
L.E. Goeree	-0.02 (-0.22, 0.17)	-0.03 (-0.29, 0.18)	0.01 (-0.16, 0.15)	0.03 (-0.34, 0.33)	-0.01 (-0.19, 0.16)	-0.03 (-0.29, 0.22)	
Hoek van Holland	-0.02 (-0.33, 0.22)	-0.01 (-0.24, 0.20)	-0.03 (-0.25, 0.16)	-0.03 (-0.24, 0.15)	-0.00 (-0.23, 0.19)	-0.02 (-0.22, 0.16)	
Zestienhoven	-0.04 (-0.24, 0.12)	-0.04 (-0.21, 0.11)	-0.02 (-0.36, 0.24)	-0.01 (-0.21, 0.15)	-0.01 (-0.23, 0.17)	-0.03 (-0.24, 0.14)	
Gilze-Rijen	0.00 (-0.17, 0.16)	0.00 (-0.19, 0.18)	-0.03 (-0.30, 0.21)	-0.04 (-0.24, 0.13)	-0.01 (-0.21, 0.16)	0.02 (-0.15, 0.16)	
Herwijnen	-0.01 (-0.20, 0.16)	-0.02 (-0.20, 0.15)	-0.02 (-0.21, 0.15)	0.02 (-0.20, 0.21)	0.01 (-0.21, 0.19)	0.01 (-0.23, 0.23)	
Eindhoven	0.00 (-0.16, 0.16)	-0.00 (-0.17, 0.14)	-0.01 (-0.21, 0.15)	-0.01 (-0.19, 0.15)	0.06 (-0.24, 0.31)	-0.01 (-0.18, 0.14)	
Volkel	0.02 (-0.16, 0.16)	-0.02 (-0.21, 0.14)	-0.01 (-0.30, 0.24)	0.05 (-0.19, 0.24)	0.01 (-0.39, 0.31)	0.06 (-0.10, 0.19)	
Beek	-0.04 (-0.20, 0.08)	0.04 (-0.11, 0.19)	0.05 (-0.25, 0.25)	-0.04 (-0.22, 0.13)	0.00 (-0.27, 0.22)	-0.02 (-0.17, 0.12)	
Station \ Sector	165°N : 195°N	195°N : 225°N	225°N : 255°N	255°N : 285°N	285°N : 315°N	315°N : 345°N	
IJmuiden	-0.02 (-0.27, 0.19)	-0.01 (-0.22, 0.18)	-0.02 (-0.23, 0.15)	-0.01 (-0.27, 0.18)	-0.00 (-0.31, 0.23)	-0.05 (-0.29, 0.15)	
Texelhors	0.01 (-0.19, 0.18)	-0.01 (-0.19, 0.15)	0.02 (-0.13, 0.15)	-0.03 (-0.21, 0.12)	0.00 (-0.36, 0.27)	0.01 (-0.21, 0.21)	
De Kooy	-0.01 (-0.28, 0.23)	0.01 (-0.44, 0.32)	-0.01 (-0.37, 0.28)	-0.01 (-0.29, 0.20)	-0.01 (-0.48, 0.19)	0.00 (-0.24, 0.21)	
Schiphol	0.00 (-0.23, 0.20)	0.01 (-0.19, 0.18)	-0.01 (-0.30, 0.23)	0.01 (-0.23, 0.20)	-0.11 (-0.44, 0.16)	-0.01 (-0.25, 0.21)	
De Bilt	-0.01 (-0.19, 0.16)	0.02 (-0.22, 0.22)	-0.01 (-0.19, 0.14)	-0.01 (-0.16, 0.13)	-0.00 (-0.31, 0.23)	-0.01 (-0.20, 0.16)	
Soesterberg	-0.04 (-0.30, 0.18)	0.01 (-0.16, 0.16)	-0.01 (-0.26, 0.21)	0.01 (-0.15, 0.15)	0.02 (-0.16, 0.17)	-0.01 (-0.20, 0.15)	
Leeuwarden	0.00 (-0.23, 0.21)	0.01 (-0.23, 0.21)	0.01 (-0.22, 0.20)	-0.01 (-0.28, 0.22)	-0.01 (-0.42, 0.30)	-0.04 (-0.30, 0.18)	
Deelen	-0.00 (-0.16, 0.15)	-0.07 (-0.25, 0.07)	-0.01 (-0.21, 0.16)	-0.02 (-0.17, 0.12)	-0.01 (-0.22, 0.15)	0.01 (-0.24, 0.22)	
Lauwersoog	-0.06 (-0.28, 0.14)	-0.01 (-0.18, 0.14)	0.03 (-0.19, 0.21)	-0.01 (-0.23, 0.19)	0.00 (-0.21, 0.19)	0.01 (-0.25, 0.23)	
Eelde	-0.00 (-0.16, 0.14)	0.01 (-0.19, 0.19)	0.02 (-0.16, 0.20)	0.01 (-0.19, 0.17)	-0.01 (-0.20, 0.15)	-0.01 (-0.21, 0.16)	
Twenthe	-0.01 (-0.22, 0.17)	0.03 (-0.20, 0.20)	0.00 (-0.19, 0.17)	0.00 (-0.17, 0.16)	-0.01 (-0.21, 0.16)	-0.00 (-0.17, 0.13)	
Cadzand	-0.05 (-0.22, 0.11)	-0.01 (-0.27, 0.20)	0.05 (-0.24, 0.28)	-0.01 (-0.25, 0.19)	-0.02 (-0.17, 0.12)	-0.01 (-0.22, 0.16)	
Vlissingen	0.01 (-0.20, 0.19)	-0.01 (-0.22, 0.18)	-0.01 (-0.29, 0.18)	-0.01 (-0.25, 0.19)	-0.01 (-0.26, 0.20)	-0.01 (-0.20, 0.16)	
L.E. Goeree	0.02 (-0.31, 0.30)	0.04 (-0.11, 0.19)	0.01 (-0.19, 0.17)	0.03 (-0.16, 0.21)	-0.13 (-0.40, 0.11)	-0.02 (-0.19, 0.14)	
Hoek van Holland	-0.00 (-0.24, 0.20)	-0.06 (-0.34, 0.16)	-0.02 (-0.31, 0.19)	-0.02 (-0.36, 0.23)	-0.01 (-0.24, 0.17)	-0.02 (-0.37, 0.31)	
Zestienhoven	0.00 (-0.18, 0.15)	-0.04 (-0.30, 0.18)	0.00 (-0.15, 0.15)	-0.01 (-0.22, 0.17)	0.03 (-0.27, 0.25)	0.02 (-0.17, 0.18)	
Gilze-Rijen	-0.03 (-0.20, 0.11)	-0.00 (-0.16, 0.14)	-0.00 (-0.26, 0.20)	0.00 (-0.19, 0.18)	-0.02 (-0.27, 0.20)	-0.02 (-0.19, 0.12)	
Herwijnen	0.00 (-0.17, 0.16)	0.00 (-0.31, 0.24)	0.02 (-0.29, 0.27)	-0.02 (-0.27, 0.18)	-0.01 (-0.24, 0.19)	0.00 (-0.14, 0.14)	
Eindhoven	0.03 (-0.15, 0.20)	-0.09 (-0.27, 0.06)	-0.02 (-0.22, 0.15)	-0.00 (-0.24, 0.20)	-0.05 (-0.32, 0.17)	-0.01 (-0.19, 0.12)	
Volkel	-0.01 (-0.17, 0.13)	0.00 (-0.24, 0.19)	0.00 (-0.15, 0.14)	0.05 (-0.17, 0.24)	-0.02 (-0.21, 0.14)	0.02 (-0.14, 0.16)	
Beek	-0.02 (-0.20, 0.13)	-0.01 (-0.21, 0.17)	-0.07 (-0.37, 0.16)	0.02 (-0.11, 0.14)	-0.00 (-0.19, 0.17)	0.01 (-0.18, 0.19)	

Table 4.5 Estimates of the GPD shape parameter and associated 95% confidence intervals.

Table 4.5 presents the shape parameter estimates of the GPD fits to the U_p POT data. The Gomes and Monfort (1986) exponential-versus-GPD test was used and there were zero rejections of the exponential at a 5% level when applying the test to the U_p POT data. When applying the test to the U_p^k and U_p^2 POT data the hypothesis was rejected for 12 (~4%) and 25 (~9%) of the 273 considered samples (21 stations * (1 omni-directional+12 sectors)),

respectively. The hypothesis is therefore only rejected for more than 5% of the samples in the U_p^2 case. That a type I tail is a good approximation for the U_p POT data is not surprising. First, that was also the case for the U_p AM data. Second, in this analysis we have also tried to chose a threshold that would yield, when possible, a GPD shape parameter estimate close to zero.

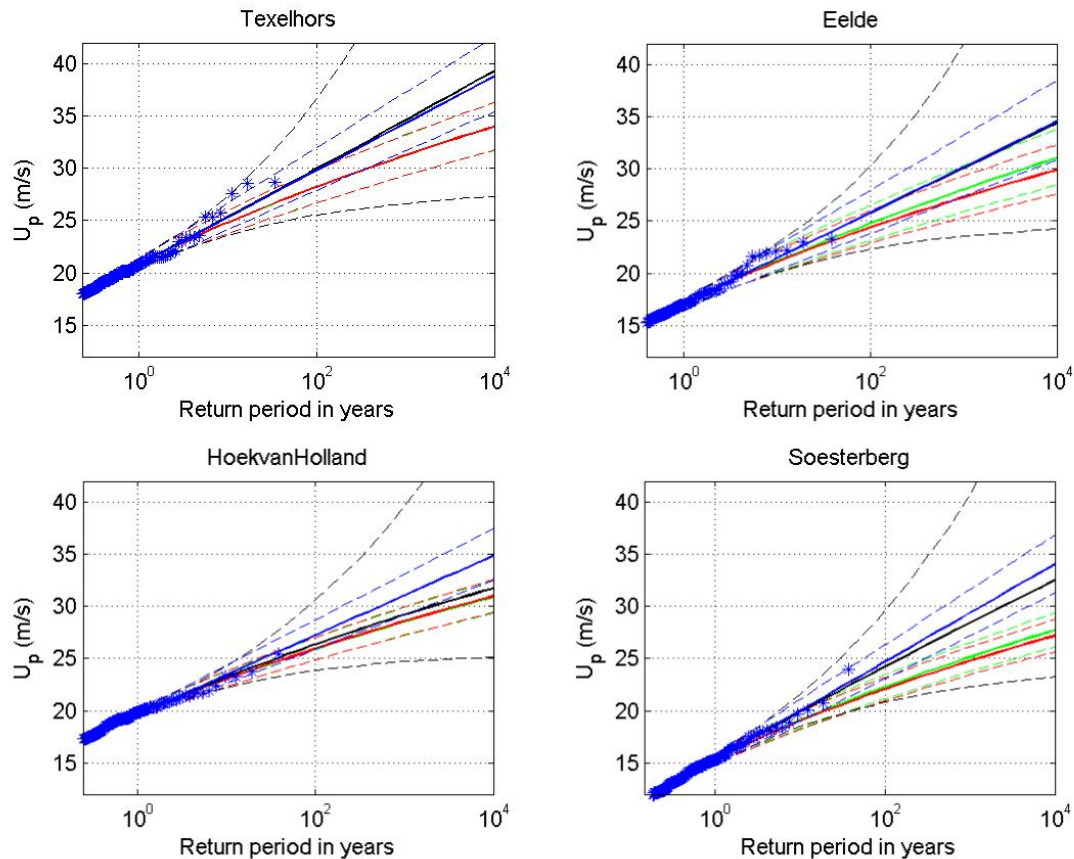


Figure 4.12 Return value plot with Exponential (blue) and GPD (black) fit to U_p , Exponential fit to U_p^2 (red) and Exponential fit to U_p^k (green) POT. The dashed lines are the associated adjusted bootstrap 95% confidence intervals. The POT data are represented by the asterisks, with plotting positions $(x_i, (n+1)/(\lambda(n+1-i)))$.

Figure 4.12 shows, for the same stations shown in Figure 4.9, the return value plot of the considered fits to the POT data. It shows that, as expected, the fit with no constraints to the tail, i.e. the GPD fit, generally follows the data better. The exponential fits to U_p do not differ much from the GPD fits and also depict the data well. The exponential fits to U_p^2 and U_p^k do not differ much from each other and, except for Hoek van Holland, underestimate the highest storms. Again, for Hoek van Holland a type III tail seems to depict the data better.

Comparing the return value lines of the GPD fits to the Hoek van Holland and Soesterberg U_p POT data, the lines do still cross each other, but only at a return value of about 4,000 years. If a type I tail is assumed in both stations the lines do not cross each other.

29 September 2009, final

The return value plots all the stations are given in a larger format in figures F.4 in Appendix C, which also include the fits per directional sector.

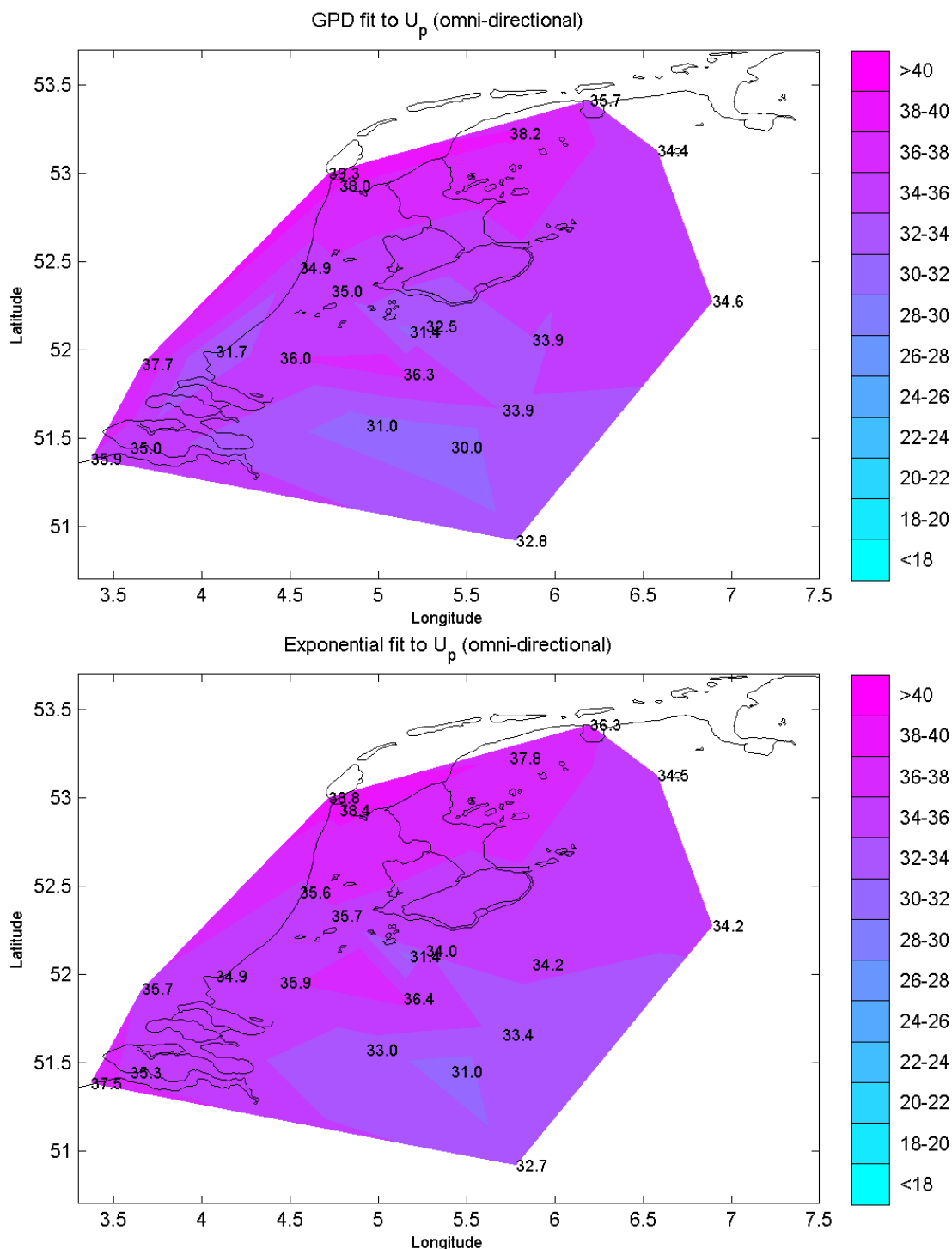


Figure 4.13 Potential wind speed 10,000-yr return value estimates in m/s. GPD (top) and exponential (bottom) fit to omni-directional POT data.

Figures F.5 in Appendix C show comparisons between Schiphol and all other stations GPD and exponential fits to the selected POT data. The empirical distribution of all peaks above 6 m/s are shown in the figures. From comparisons between all stations it can be said that in general when fixing the tail at type I (exponential fits to U_p) there is no crossing of the return

value lines of land and coastal stations for offshore wind. When fitting the GPD, the small deviations of the shape parameter from zero lead to crossings in some cases.

Figure 4.13 shows the 10,000-yr return value estimates obtained by the GPD and by the exponential fit to the U_p POT data. Overall the differences between the exponential and the GPD estimates are not significant (for the omni-directional case the maximal difference between the GPD and the exponential 10,000-yr return value estimates is 9% and the mean difference -1.2%, cf. Table 4.6). The spatial distribution of both estimates is also rather similar. However, the GPD estimate for Hoek van Holland is rather low in comparison with the corresponding estimates for inland stations. The pattern of the exponential estimates looks rather plausible and is quite similar to the pattern defined by Wieringa and Rijkoort (1983) which is based partially on expert judgment. There is a Northwest/Southwest (coast/land) gradient, with a hump in the region of the large rivers. I.e. the 10,000-yr return value estimates for the stations located close to the Rhine and Meuse rivers are close to those of the coast stations.

Table 4.6 compares the omni-directional 10,000-yr return value estimates from Exponential and GPD fits to U_p , POT data and Gumbel fits to U_p AM data. The small differences between the estimates testifies to the compatibility of the different analysis.

	Exponential fit to U_p POT	GPD fit to U_p POT		Gumbel fit to U_p AM	
	10,000-yr rv (m/s)	10,000-yr rv (m/s)	Relative differences	10,000-yr rv (m/s)	Relative differences
IJmuiden	35.6	34.9	-2.0%	35.1	-1.4%
Texelhors	38.8	39.3	1.3%	39.1	0.8%
De Kooy	38.4	38.0	-1.0%	38.5	0.3%
Schiphol	35.7	35.0	-2.0%	37.5	5.0%
De Bilt	31.4	31.4	0.0%	33.3	6.1%
Soesterberg	34.0	32.5	-4.4%	30.4	-10.6%
Leeuwarden	37.8	38.2	1.1%	36.1	-4.5%
Deelen	34.2	33.9	-0.9%	35.6	4.1%
Lauwersoog	36.3	35.7	-1.7%	35.0	-3.6%
Eelde	34.5	34.4	-0.3%	32.7	-5.2%
Twenthe	34.2	34.6	1.2%	33.5	-2.0%
Cadzand	37.5	35.9	-4.3%	37.1	-1.1%
Vlissingen	35.3	35.0	-0.8%	35.1	-0.6%
L.E. Goeree	35.7	37.7	5.6%	36.0	0.8%
Hoek van Holland	34.9	31.7	-9.2%	35.8	2.6%
Zestienhoven	35.9	36.0	0.3%	37.3	3.9%
Gilze-Rijen	33.0	31.0	-6.1%	32.0	-3.0%
Herwijnen	36.4	36.3	-0.3%	37.9	4.1%
Eindhoven	31.0	30.0	-3.2%	30.6	-1.3%
Volkel	33.4	33.9	1.5%	33.6	0.6%
Beek	32.7	32.8	0.3%	35.1	7.3%
Average			-1.2%		0.1%

Table 4.6 10,000-yr return value estimates from Exponential and GPD fits to U_p , POT data and Gumbel fits to U_p AM data.

According to hypothesis tests carried out a type I tail is justified. Furthermore, the spatial coherence and smoothness of the exponential estimates is in line with the expectation of

experts about the spatial variation of wind extremes. For these reasons it was decided to use the POT/exponential estimates as final estimates. Given that the convergence of the U_p data to a type I tail does not seem in need of improvement, it was further decided not to transform the data. The omni-directional and directional final model estimates are described in Chapter 5. The full model parameters are given in tables T.3 in Appendix B.

It is, however, important to note that the given 95% confidence intervals do not account for the uncertainty pertaining to the choice of the exponential instead of the GPD distribution. For the estimates given in Table 4.6 the 95% confidence intervals associated with the exponential estimates have an amplitude of about 20% of the estimate, whereas the 95% confidence intervals associated with the GPD estimates are five times wider. The real uncertainty of the estimates provided here is thought to be somewhere between these two values.

4.2.3 Seasonal variability

The analysis presented so far has been based on the entire yearly period. However, the frequency of storms varies throughout the year, the most extreme months being the winter months. Figure 4.14 shows the distribution of extreme values per month in each of the 21 stations. January is the month with the largest percentage of storms and, as expected, the summer months have the lowest percentage of storms. This shows that the process of exceedences within a year is not homogeneous, and one may wonder to what extent the violation of the homogeneity assumption may affect the results.

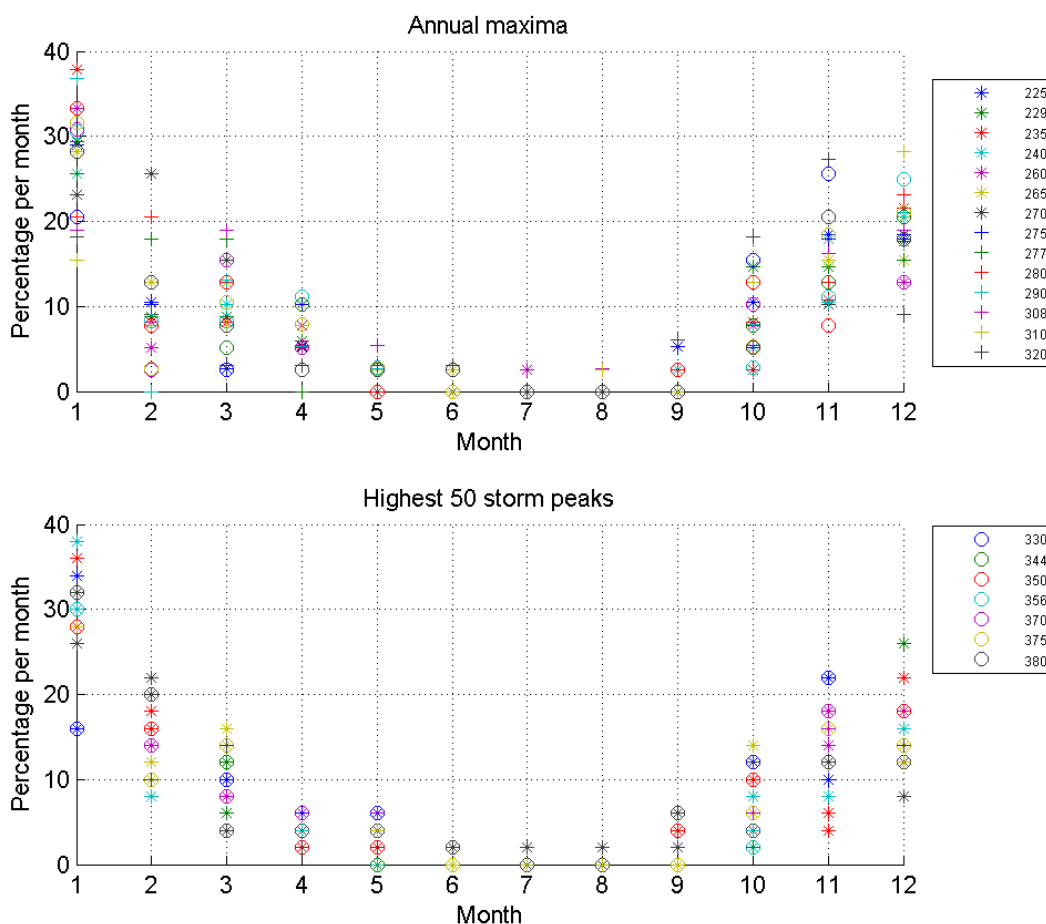


Figure 4.14 Monthly percentage of U_p , AM and highest POT data.

Table 4.7 shows 10,000-yr return value estimates obtained by fitting the exponential distribution to peak excesses of U_p data from two coastal and two land stations. Three

different sets of estimates are shown: one based on the data from the whole year, another based on data from January and February, and a third based on data from November and December. As expected, the largest two-monthly estimates are those from the January-February period. Moreover, these are also slightly larger—and systematically—than the current estimates based on the data from the entire year. However, the differences between taking the entire year and only the more extreme January-February period, being approximately 1 m/s for the two coastal stations and less than 0.5 m/s for the landstations, do not appear to be significant in view of the statistical uncertainty of the estimates.

	Entire year	January to February	November to December
IJmuiden	35.6 (32.9, 38.5)	36.8 (32.5, 41.3)	32.8 (30.0, 36.1)
Texelhors	38.8 (35.4, 42.6)	39.6 (33.5, 46.0)	37.8 (33.6, 43.0)
Schiphol	35.7 (32.4, 39.3)	36.1 (30.8, 42.2)	32.2 (28.4, 36.5)
Soesterberg	34.0 (31.3, 36.9)	34.2 (29.4, 39.7)	33.0 (29.2, 37.0)

Table 4.7 10,000-yr return value estimates from exponential fits to U_p POT data from the whole year, January and February and November and December.

	Entire year		October to May	
	% available data	Actual nr. yrs	% available data	Actual nr. yrs
IJmuiden	95.20%	37.13	95.10%	37.08
Texelhors	85.30%	33.26	85.20%	33.22
De Kooy	93.90%	36.61	94.00%	36.66
Schiphol	97.30%	37.94	97.70%	38.12
De Bilt	96.00%	37.45	96.70%	37.72
Soesterberg	94.80%	36.98	95.20%	37.12
Leeuwarden	98.50%	38.40	98.70%	38.51
Deelen	94.50%	36.85	95.30%	37.15
Lauwersoog	98.50%	38.42	98.50%	38.42
Eelde	96.40%	37.61	97.00%	37.85
Twenthe	92.20%	35.97	93.20%	36.34
Cadzand	92.00%	35.89	91.40%	35.63
Vlissingen	99.40%	38.76	99.50%	38.80
L.E. Goeree	80.00%	31.22	79.20%	30.88
Hoek van Holland	98.50%	38.41	98.50%	38.41
Zestienhoven	95.50%	37.26	96.40%	37.58
Gilze-Rijen	96.90%	37.80	97.30%	37.96
Herwijnen	88.30%	34.42	88.30%	34.42
Eindhoven	96.80%	37.76	97.30%	37.95
Volkel	93.00%	36.26	93.90%	36.60
Beek	97.00%	37.83	97.50%	38.01

Table 4.8 Percentage of available data and actual number of years considering gaps throughout the entire year and only throughout the October-May period.

Contrary to what was done in the AM analysis, data from years with several gaps were also included in the POT analysis, the gaps being accounted for in the yearly cluster rate. Given that gaps in the June-September period will hardly contribute to the POT sample, the gaps in these summer months were ignored. Table 4.8 shows the actual number of years of data available in the 21 stations that results from ignoring and not ignoring the existence of gaps in the summer months. The estimates of λ_u using the corresponding figures for the actual

number of years do not differ critically. The effect of using one λ_u estimate instead of the other in the 10,000-yr return values estimates being less than 0.01 m/s.

4.3 Climate change and sampling variability

4.3.1 Trends

In order to check the stationarity of the data, linear fits were performed to the annual mean and annual maxima time series. The standard Mann-Kendall non-parametric test was used to identify the significant results—namely the existence of trends—at a 5% level. Furthermore, the POT data was modelled using a non-homogeneous Poisson process (NPP) with linear trends in time in the location parameter (cf. Eq. (2.11)) and likelihood ratio test was used to identify the significant results at a 5% level. The identified significant trends are presented in Table 4.9.

Note that the obtained linear trends in the NPP location parameter imply trends in the m -year return values, which are in absolute value independent of m , cf. Eq. (2.9). Therefore the trends given in Table 4.9 can be interpreted as trends in the 1-year return values and directly comparable with the identified trends in the AM data.

In 10 of the considered stations, trends were identified in the extremes. Generally when trends are found they are present in the annual mean, annual maxima and POT data. In all cases, besides for the L.E. Goeree case, the identified trends are negative. The larger trends are found in the AM data and the lower in the annual mean data.

Station		Annual mean		Annual maxima		POT	
		cm/s/yr	%	cm/s/yr	%	cm/s/yr	%
IJmuiden	225	1.0	0.15	—	—	—	—
Texelhors	229	-1.7	-0.25	-12.2	-0.56	-5.4	-0.27
De Kooy	235	-1.0	-0.17	-11.3	-0.54	-6.1	-0.32
Schiphol	240	—	—	—	—	—	—
De Bilt	260	—	—	-11.3	-0.73	-6.6	-0.49
Soesterberg	265	—	—	—	—	—	—
Leeuwarden	270	-1.2	-0.23	-12.2	-0.62	-3.0	-0.17
Deelen	275	-2.6	-0.56	-8.3	-0.48	-4.2	-0.27
Lauwersoog	277	-1.0	-0.15	—	—	—	—
Eelde	280	—	—	—	—	—	—
Twenthe	290	—	—	—	—	—	—
Cadzand	308	-4.0	-0.65	-11.7	-0.57	-6.7	-0.36
Vlissingen	310	—	—	—	—	—	—
L.E. Goeree	320	3.6	0.54	11.9	0.61	11.3	0.62
Hoek van Holland	330	—	—	—	—	—	—
Zestienhoven	344	-1.8	-0.36	—	—	-2.4	-0.15
Gilze-Rijen	350	-1.9	-0.43	-9.8	-0.60	-6.0	-0.43
Herwijnen	356	-1.3	-0.30	—	—	—	—
Eindhoven	370	-2.4	-0.54	-7.1	0.43	-4.7	-0.31
Volkel	375	—	—	—	—	—	—
Beek	380	—	—	—	—	—	—

Table 4.9 Trends in the potential wind annual mean, annual maxima and POT data. Only the trends that were found significant at a 5% level are shown.

For two of these stations, Texelhors and Cadzand, linear trends in the scale parameter of the NPP model were also identified (cf. Eq. (2.10)). Analysing the data from this stations it seems that the considered linear models in time are not good models for the found variations. The data seems to be inhomogeneous due to changes (jumps) in the mean. Figure 4.15 shows the Texelhors and Cadzand AM and the identified trends in the annual maxima. It looks like

that different periods with different means seem to explain better the time variations in the AM data than the identified negative trend in time.

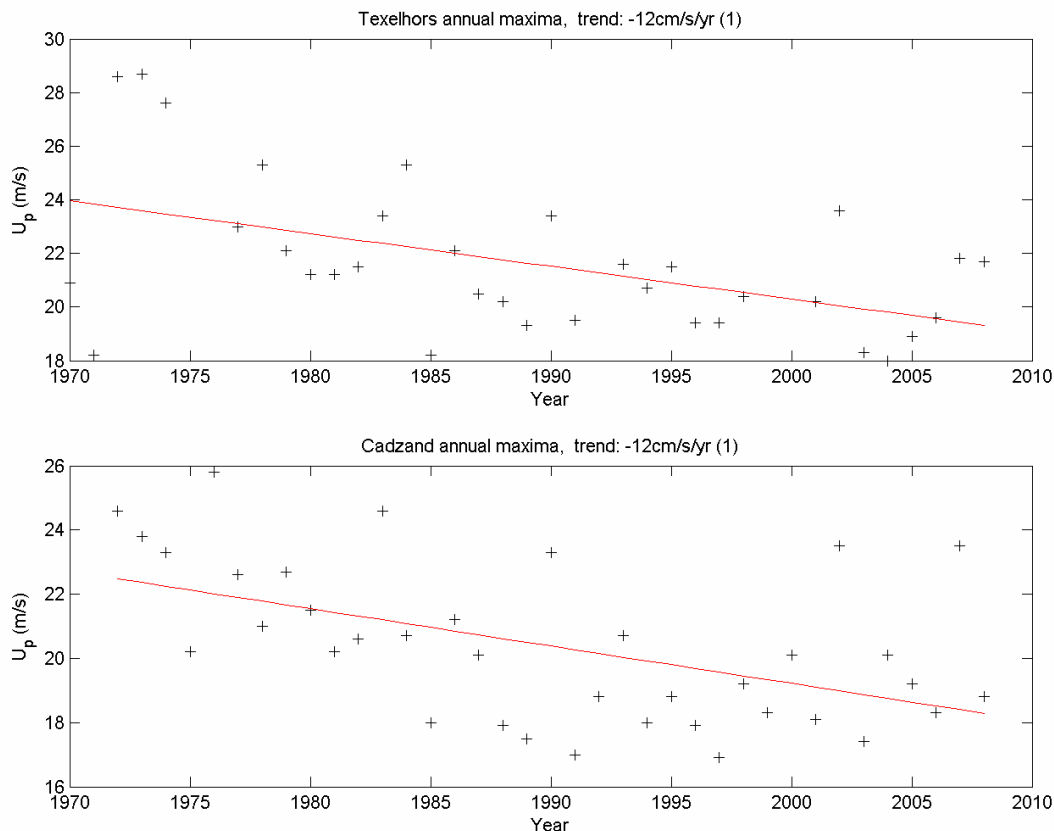


Figure 4.15 Trends in the annual maxima.

Figures F.1 in Appendix C show for completeness plots as those in Figure 4.15 for each station.

We cannot with certainty point out what is the origin of the detected trends. They seem to lack spatial consistence (e.g. significant trends are found in the De Bilt data, but no significant trends are found in the Soesterberg data, cf. Table 4.9). The analysis in Section A.1, however, notes that (although not all significant at a 5% level) they are negative for all stations besides L.E. Goeree. In principle the identified trends can have multiple origins, for instance, they can be due to inhomogeneities as a result of variations in measuring practice, local and meso roughness or climate change. This makes correcting for them rather difficult. Furthermore, it cannot be assumed that these trends will persist, and with the magnitudes identified here, in the future, therefore affecting the considered stationarity of the extreme climate. For these reasons the estimates presented here are not adjusted for these trends.

As noted in the review, it seems that the L.E. Goeree measurements until 1990 suffer from serious systematic errors (cf. Appendix A.1, Section 3.6) and the estimates provided in this report based on that data may not be reliable and should be interpreted with care.

4.3.2 Sampling variability

In order to investigate how the chosen period influences the estimated return values, we have fitted the Gumbel distribution to U_p omni-directional AM from different periods. The periods

considered are the current 1970-2008 period, the period considered in the Wieringa and Rijkoort (1983) study and the extended 1962-2008 period. Only data from 13 stations could be considered for this analysis.

No POT/GPD analysis was carried out, because given the compatibility between the two approaches, such an intensive analysis was deemed unnecessary for these relative comparisons.

Table 4.10 compares the 10,000-yr return value estimates from the different periods. Differences are at most 11.4% when comparing the 1962-2008 with the 1970-2008 period and at most 18.7% when comparing the 1962-1976 with the 1970-2008 period. Given that on average the amplitude of the confidence intervals for the 1970-2008, 1962-2008 and 1962-1976 estimates are 26%, 23% and 37% of the estimates, respectively, the estimates from the different periods are generally compatible. Deelen and Eindhoven are the stations for which the larger differences are found and IJmuiden and Zestienhoven the stations for which the lower differences are found.

Station name	1970-2008		1962-2008			1962-1976		
	<i>n</i>	10,000-yr rv (m/s)	<i>n</i>	10,000-yr rv (m/s)	Relative differences	<i>n</i>	10,000-yr rv (m/s)	Relative differences
IJmuiden	38	35.5	46	34.8	-2.0%	15	35.6	0.3%
Schiphol	39	35.7	47	38.0	6.4%	15	35.1	-1.7%
De Bilt	39	31.4	47	32.2	2.5%	15	28.9	-8.0%
Soesterberg	39	33.9	47	32.0	-5.6%	15	33.1	-2.4%
Leeuwarden	39	37.8	47	34.9	-7.7%	15	36.0	-4.8%
Deelen	39	34.1	47	38.0	11.4%	15	38.6	13.2%
Eelde	39	34.5	47	32.3	-6.4%	15	33.7	-2.3%
Vlissingen	39	35.3	47	34.6	-2.0%	15	35.8	1.4%
Hoek van Holland	39	34.8	47	35.9	3.2%	15	37.3	7.2%
Zestienhoven	39	35.9	47	35.9	0.0%	15	35.8	-0.3%
Gilze-Rijen	39	33.0	47	32.4	-1.8%	15	35.6	7.9%
Eindhoven	39	31.0	47	32.4	4.5%	15	36.8	18.7%
Beek	39	32.7	47	33.9	3.7%	15	35.6	8.9%
Average					0.5%			2.9%

Table 4.10 10,000-yr return value estimates from Gumbel fits to omni-directional U_p AM from different periods

5 Directional extreme climate

5.1 Model description

In the preceding analyses it was decided to estimate the wind speed extremes using an exponential fit to wind speed POT data. The model results are described here in detail.

5.2 10,000-yr return value estimates

Table 5.1 shows for each sector considered the 10,000-yr return value estimates and the associated 95% confidence intervals. Please be aware that the given confidence intervals do not account for uncertainty pertaining to the choice of the exponential instead of the GPD distribution.

Figure 5.1 to Figure 5.12 show for each directional sector the 10,000-yr return value estimates:

- Sector 345°N-15°N – The estimates for this sector are lower than the omni-directional ones (cf. Figure 4.13) and decrease with the distance to the coast.
- Sector 15°N-45°N – The estimates for this sector are along the coast lower than those of the adjacent northern sector.
- Sector 45°N-75°N – The estimates for this sector show a band of higher values south of Lake IJssel.
- Sectors 75°N to 165°N – These sectors are characterized by mild estimates without much spatial variation.
- Sector 165°N-195°N – Higher estimates start to appear in this sector.
- Sector 195°N-225°N – Spatial gradients are smaller than in the previous sector and both southern locations show high values.
- Sectors 225°N to 285°N – Spatial patterns and estimates are quite similar to the omni-directional ones (cf. Figure 4.13). The spatial gradients being rather small.
- 285°N-315°N – The spatial patterns for this sector are similar to the omni-directional ones, but the coast/inland gradients are higher.
- 315°N-345°N – In this sector the coastal stations are those mostly affected by storms. The coast/inland gradients are high.

Figure 5.13 to Figure 5.19 show the directional variation of the 10,000-yr return value estimates per station. The highest return value estimates show an absence of a spatial pattern, for some stations the highest return value estimate is for the 255°N to 285°N sector and for other the 225°N to 255°N sector (cf. Table 5.1). Note that in this study the omni-directional and directional return value estimates were computed independently. In principle, the omni-directional return value estimates should be equal or higher to the highest directional return value estimate. Due to the statistical uncertainty associated with such estimates, in a number of stations the omni-directional estimate is exceeded by directional estimates. The stations for which it occurs are IJmuiden, Texelhors, De Bilt, Vlissingen and Beek (cf. Table 5.1). Only for the case of IJmuiden and De Bilt the differences exceed 0.3 m/s, and are of 1.7 m/s and 1.1 m/s, respectively. It is common practice to adjust in such cases the directional estimates so the omni-directional estimate is the highest (see e.g. Verkaik et al., 2003,

Section 3.5.3). We have chosen not to apply such a procedure because the differences are lower than the associated statistical uncertainty. Furthermore, only directional estimates are needed for the WTI project and, given the in principle uniqueness of the population in a given sector, the directional estimate is in principle more reliable than the omni-directional estimate, which may have been obtained from a mixture of populations. In case omni-directional estimates are needed we advise that, when the omni-directional estimates are exceeded by the sector estimates, that the former be replaced by the higher directional estimate. In the review (Appendix A.1, Section 3.5) it is suggested that, instead of adjusting the directional estimates, the omni-directional estimates should be adjusted using the directional estimates. For example the omni-directional estimate for IJmuiden would be 38.1 m/s and that for De Bilt would be 33.5 m/s. These are, as already predicted in the review, bigger than the maximal directional estimates, which are 37.3 m/s and 32.6 m/s, respectively.

Station \ Sector	omni-directional					
IJmuiden	35.6 (32.9, 38.5)					
Texelhors	38.8 (35.4, 42.6)					
De Kooy	38.4 (35.1, 41.9)					
Schiphol	35.7 (32.4, 39.3)					
De Bilt	31.4 (28.8, 34.1)					
Soesterberg	34.0 (31.3, 36.9)					
Leeuwarden	37.8 (34.4, 41.3)					
Deelen	34.2 (31.2, 37.7)					
Lauwersoog	36.3 (33.9, 38.6)					
Eelde	34.5 (30.9, 38.5)					
Twenthe	34.2 (30.8, 37.9)					
Cadzand	37.5 (34.6, 40.6)					
Vlissingen	35.3 (32.4, 38.4)					
L.E. Goeree	35.7 (33.3, 38.3)					
Hoek van Holland	34.9 (32.5, 37.4)					
Zestienhoven	35.9 (33.3, 38.8)					
Gilze-Rijen	33.0 (30.6, 35.5)					
Herwijnen	36.4 (32.9, 40.5)					
Eindhoven	31.0 (28.4, 33.6)					
Volkel	33.4 (30.0, 36.8)					
Beek	32.7 (29.8, 35.9)					
Station \ Sector	345°N -15°N	15°N -45°N	45°N -75°N	75°N -105°N	105°N -135°N	135°N -165°N
IJmuiden	29.0 (26.5, 32.2)	26.2 (23.9, 28.6)	24.1 (21.5, 26.8)	25.2 (23.1, 27.7)	20.9 (19.2, 22.8)	26.5 (24.2, 29.0)
Texelhors	30.9 (27.5, 34.6)	32.1 (29.4, 35.0)	27.3 (24.4, 30.2)	29.9 (27.4, 32.5)	27.5 (25.1, 30.0)	31.6 (28.5, 34.9)
De Kooy	30.0 (26.2, 34.1)	29.8 (26.2, 33.6)	31.0 (27.9, 34.5)	27.4 (25.0, 30.0)	21.5 (19.2, 24.3)	24.4 (21.5, 27.3)
Schiphol	27.1 (25.0, 29.5)	22.2 (19.9, 24.7)	24.0 (22.0, 26.0)	21.8 (19.8, 24.0)	18.9 (17.5, 20.3)	20.7 (19.0, 22.8)
De Bilt	18.0 (15.9, 20.4)	20.2 (18.4, 22.1)	21.1 (19.0, 23.4)	20.4 (18.7, 22.2)	18.2 (16.5, 20.1)	17.6 (15.8, 19.6)
Soesterberg	19.7 (18.2, 21.3)	18.2 (16.6, 19.8)	16.1 (14.5, 17.7)	18.1 (16.3, 19.9)	15.1 (13.8, 16.4)	16.8 (15.7, 18.1)
Leeuwarden	28.1 (25.5, 30.9)	23.8 (21.5, 25.9)	28.7 (24.5, 33.5)	24.1 (21.7, 26.7)	19.0 (17.3, 20.8)	23.1 (21.3, 25.1)
Deelen	19.8 (17.8, 21.8)	19.9 (18.3, 21.7)	21.0 (18.9, 23.3)	20.3 (18.5, 22.2)	18.0 (15.6, 20.7)	19.7 (17.9, 21.8)
Lauwersoog	31.2 (28.7, 33.6)	26.1 (23.6, 28.8)	26.7 (24.1, 29.2)	24.8 (22.2, 27.5)	20.6 (18.5, 22.8)	22.9 (20.3, 25.7)
Eelde	22.4 (20.8, 24.0)	19.2 (17.5, 20.9)	21.5 (19.4, 23.8)	19.4 (17.7, 21.3)	17.6 (15.6, 19.5)	21.7 (19.8, 23.7)
Twenthe	18.4 (17.0, 20.0)	18.7 (17.1, 20.6)	17.7 (16.4, 19.0)	16.6 (15.3, 18.0)	16.0 (14.9, 17.1)	18.7 (16.7, 20.9)
Cadzand	32.7 (28.6, 36.9)	24.5 (22.5, 26.7)	25.7 (23.1, 28.4)	24.5 (21.6, 27.9)	20.1 (18.2, 22.1)	25.2 (23.0, 27.5)
Vlissingen	23.0 (21.0, 25.1)	19.3 (17.4, 21.5)	22.0 (20.1, 24.1)	22.3 (20.6, 24.1)	22.7 (20.6, 24.8)	24.3 (22.2, 26.6)
L.E. Goeree	30.6 (28.1, 33.2)	26.9 (24.1, 29.7)	29.0 (26.7, 31.2)	25.7 (22.3, 29.9)	25.0 (22.9, 27.3)	24.1 (21.9, 26.2)
Hoek van Holland	28.7 (25.8, 31.7)	28.4 (25.5, 31.8)	25.1 (22.8, 27.5)	22.5 (20.6, 24.4)	22.1 (20.1, 24.2)	24.4 (22.3, 26.4)
Zestienhoven	26.2 (23.7, 28.4)	24.1 (22.1, 26.1)	18.2 (16.4, 20.0)	19.6 (17.9, 21.6)	18.5 (16.8, 20.2)	21.5 (19.8, 23.4)
Gilze-Rijen	21.9 (20.1, 23.8)	20.6 (18.7, 22.5)	20.2 (18.1, 22.3)	21.4 (19.7, 23.2)	17.9 (16.4, 19.5)	18.3 (16.9, 19.8)
Herwijnen	21.7 (19.6, 23.7)	22.1 (20.2, 23.9)	22.9 (20.8, 25.0)	21.9 (19.6, 24.4)	20.2 (18.3, 22.4)	19.7 (17.5, 21.8)
Eindhoven	21.2 (19.4, 22.9)	19.4 (18.1, 20.8)	20.3 (18.6, 22.2)	18.5 (17.1, 20.0)	17.2 (15.1, 19.4)	17.8 (16.3, 19.2)
Volkel	17.4 (16.0, 18.8)	18.0 (16.6, 19.4)	19.1 (17.3, 21.3)	19.5 (17.6, 21.4)	16.1 (14.2, 18.2)	19.0 (17.6, 20.5)
Beek	20.0 (18.5, 21.6)	19.9 (18.5, 21.3)	17.1 (15.3, 19.1)	20.3 (18.6, 22.1)	18.6 (16.1, 21.5)	21.2 (19.4, 23.1)
Station \ Sector	165°N -195°N	195°N -225°N	225°N -255°N	255°N -285°N	285°N -315°N	315°N -345°N
IJmuiden	29.8 (26.9, 32.9)	35.0 (32.6, 37.6)	37.3 (34.4, 40.7)	35.6 (32.3, 39.3)	33.5 (30.3, 36.8)	33.0 (30.1, 36.0)
Texelhors	32.0 (29.2, 35.1)	35.3 (32.8, 37.9)	39.1 (36.1, 42.2)	38.3 (34.9, 41.9)	37.0 (32.7, 42.1)	34.0 (30.7, 37.7)
De Kooy	30.2 (26.8, 33.7)	30.6 (27.2, 34.4)	32.6 (29.1, 36.4)	37.1 (33.1, 42.0)	34.0 (30.6, 38.0)	35.0 (31.3, 38.9)
Schiphol	25.6 (23.2, 28.2)	33.1 (30.2, 36.2)	34.6 (30.6, 39.1)	35.4 (31.7, 39.2)	33.2 (29.3, 37.3)	30.6 (27.0, 34.4)
De Bilt	21.7 (19.7, 23.8)	27.0 (24.6, 29.8)	32.6 (29.4, 35.5)	32.2 (29.4, 35.1)	26.6 (23.3, 30.4)	23.7 (21.5, 26.4)
Soesterberg	20.1 (18.2, 22.3)	25.9 (24.0, 28.0)	33.2 (29.5, 37.0)	32.8 (29.9, 35.9)	28.4 (25.7, 31.1)	23.8 (21.7, 26.2)
Leeuwarden	26.4 (23.9, 29.1)	34.2 (30.4, 38.4)	34.9 (31.4, 38.4)	35.9 (32.4, 39.9)	32.6 (28.3, 37.7)	32.9 (29.4, 36.8)
Deelen	22.7 (20.7, 24.7)	26.5 (24.7, 28.5)	34.0 (31.0, 37.2)	33.7 (30.8, 36.8)	30.5 (27.7, 33.4)	23.0 (20.7, 25.7)
Lauwersoog	29.0 (26.7, 31.5)	35.0 (32.1, 37.8)	35.3 (32.1, 38.8)	35.4 (32.2, 38.7)	34.6 (31.5, 37.9)	31.8 (28.8, 35.1)
Eelde	24.6 (22.6, 26.7)	30.3 (27.3, 33.2)	34.0 (31.1, 36.8)	32.8 (29.9, 35.9)	30.5 (27.7, 33.4)	25.0 (22.8, 27.5)
Twenthe	22.0 (19.9, 24.3)	24.3 (22.3, 26.5)	32.0 (28.3, 35.7)	32.4 (29.3, 35.6)	30.4 (27.5, 33.5)	21.8 (20.0, 23.7)
Cadzand	29.1 (27.1, 31.5)	31.9 (28.7, 35.1)	34.9 (31.5, 38.9)	36.9 (33.7, 40.5)	36.7 (34.0, 39.4)	33.1 (30.3, 36.0)
Vlissingen	28.4 (25.8, 31.2)	29.9 (27.5, 32.6)	35.5 (32.1, 39.2)	35.0 (31.5, 38.7)	30.5 (27.2, 34.1)	26.8 (24.1, 29.5)
L.E. Goeree	25.7 (23.2, 28.2)	33.1 (30.8, 35.4)	35.0 (32.0, 38.2)	35.8 (32.7, 38.8)	34.6 (31.5, 37.8)	35.0 (31.9, 38.1)
Hoek van Holland	27.9 (25.5, 30.6)	28.4 (26.1, 30.8)	33.9 (30.7, 37.4)	34.8 (31.1, 38.7)	34.6 (31.7, 37.8)	29.9 (26.3, 34.0)
Zestienhoven	25.1 (23.4, 27.1)	28.1 (25.7, 30.6)	35.2 (32.5, 37.8)	35.8 (32.6, 39.3)	34.9 (30.4, 39.8)	31.8 (28.9, 34.8)
Gilze-Rijen	25.4 (23.0, 27.9)	28.3 (26.3, 30.5)	33.1 (29.3, 37.5)	33.0 (30.1, 35.9)	30.9 (27.7, 34.4)	22.5 (20.9, 24.4)
Herwijnen	24.9 (22.9, 27.0)	27.0 (23.9, 30.0)	34.9 (30.8, 38.9)	36.2 (31.5, 40.9)	34.0 (30.1, 38.0)	27.1 (25.0, 29.3)
Eindhoven	21.8 (20.0, 23.7)	27.8 (26.0, 29.7)	30.8 (28.2, 33.5)	30.1 (26.8, 33.7)	29.4 (26.1, 33.2)	23.7 (21.7, 25.8)
Volkel	23.4 (21.7, 25.3)	27.7 (25.2, 30.4)	32.9 (30.3, 35.5)	33.1 (29.2, 37.3)	29.2 (26.2, 32.4)	20.4 (18.5, 22.1)
Beek	25.1 (23.0, 27.4)	27.4 (25.6, 29.4)	30.5 (26.9, 34.1)	33.0 (30.1, 36.1)	27.0 (24.2, 30.0)	21.2 (19.2, 23.5)

Table 5.1 10,000-yr return value estimates in m/s based on all-year data.

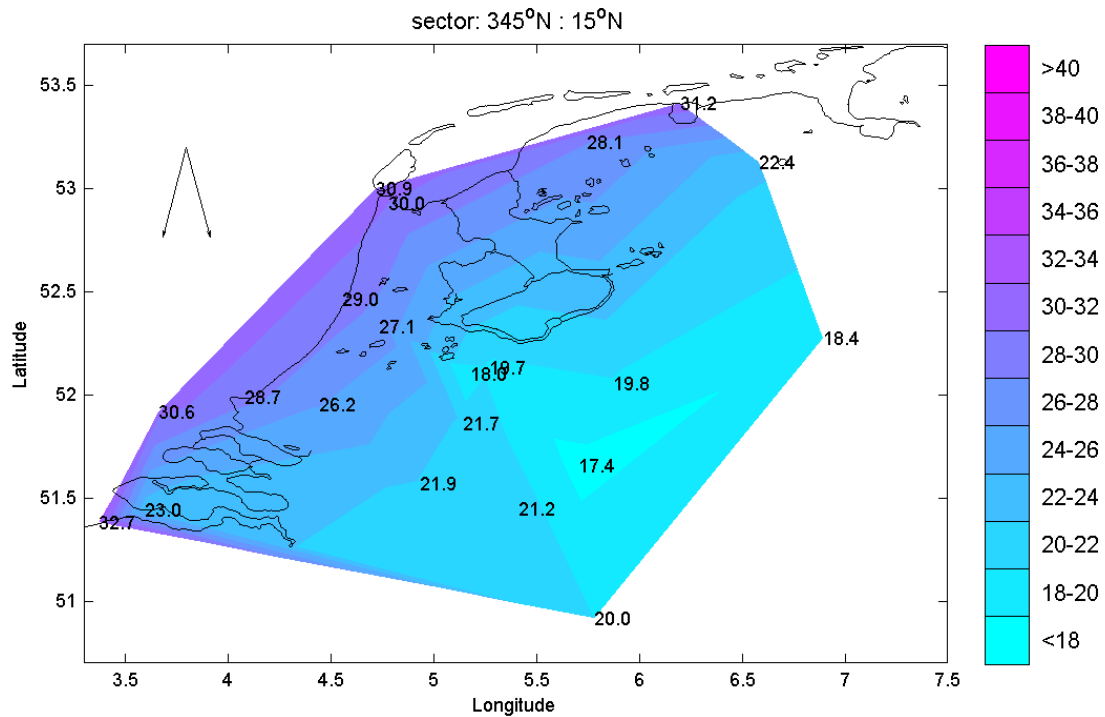


Figure 5.1 Potential wind speed 10,000-yr return value estimates in m/s. Exponential fit to POT data to the specified sector.

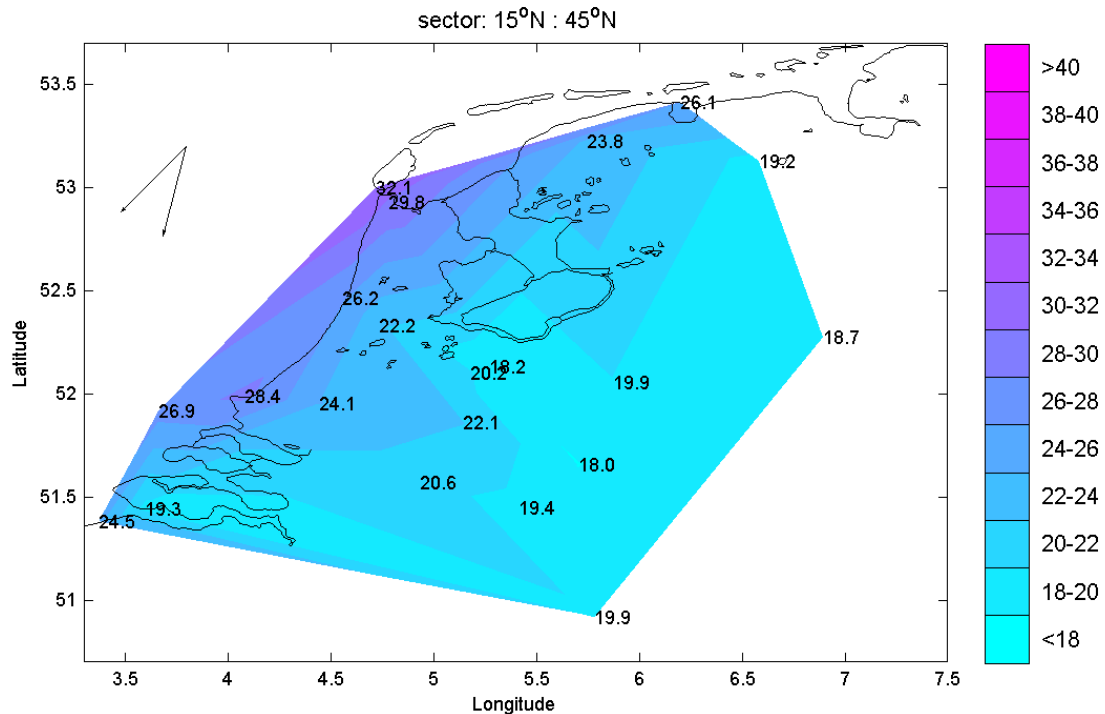


Figure 5.2 Potential wind speed 10,000-yr return value estimates in m/s. Exponential fit to POT data to the specified sector.

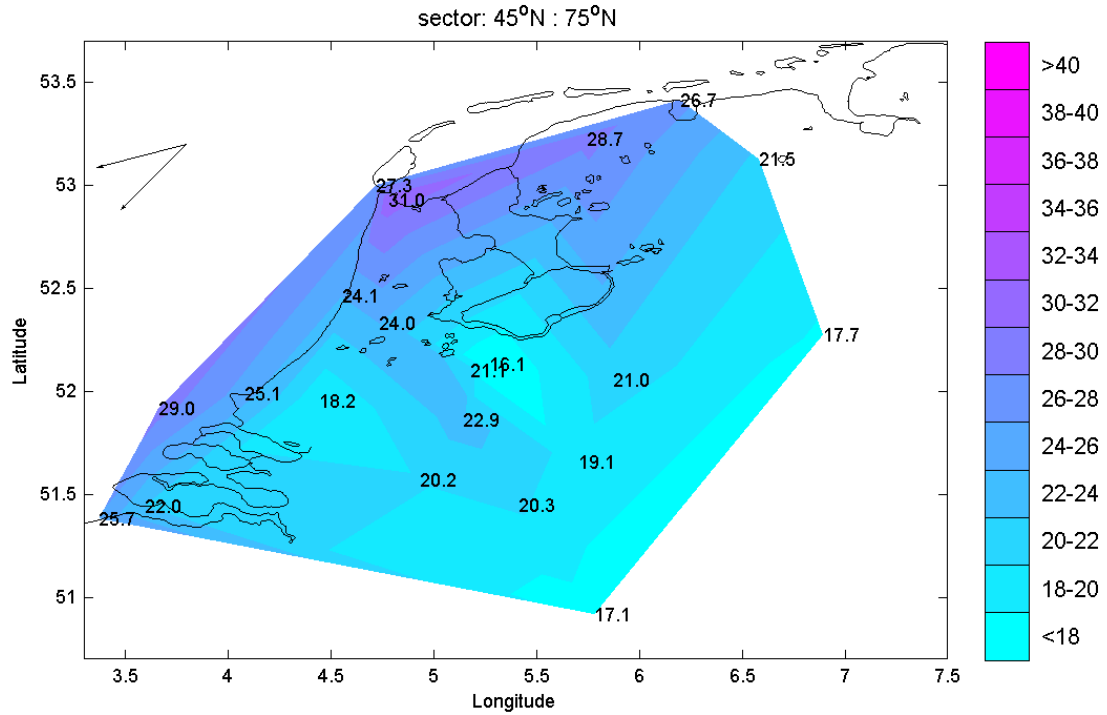


Figure 5.3 Potential wind speed 10,000-yr return value estimates in m/s. Exponential fit to POT data to the specified sector.

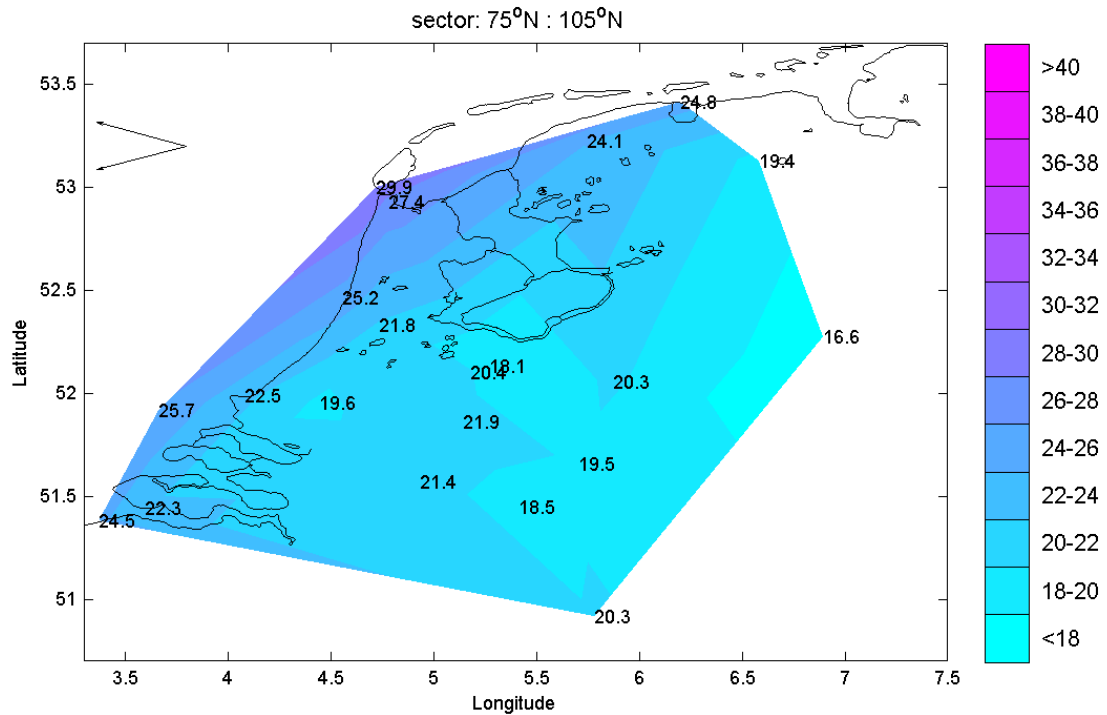


Figure 5.4 Potential wind speed 10,000-yr return value estimates in m/s. Exponential fit to POT data to the specified sector.

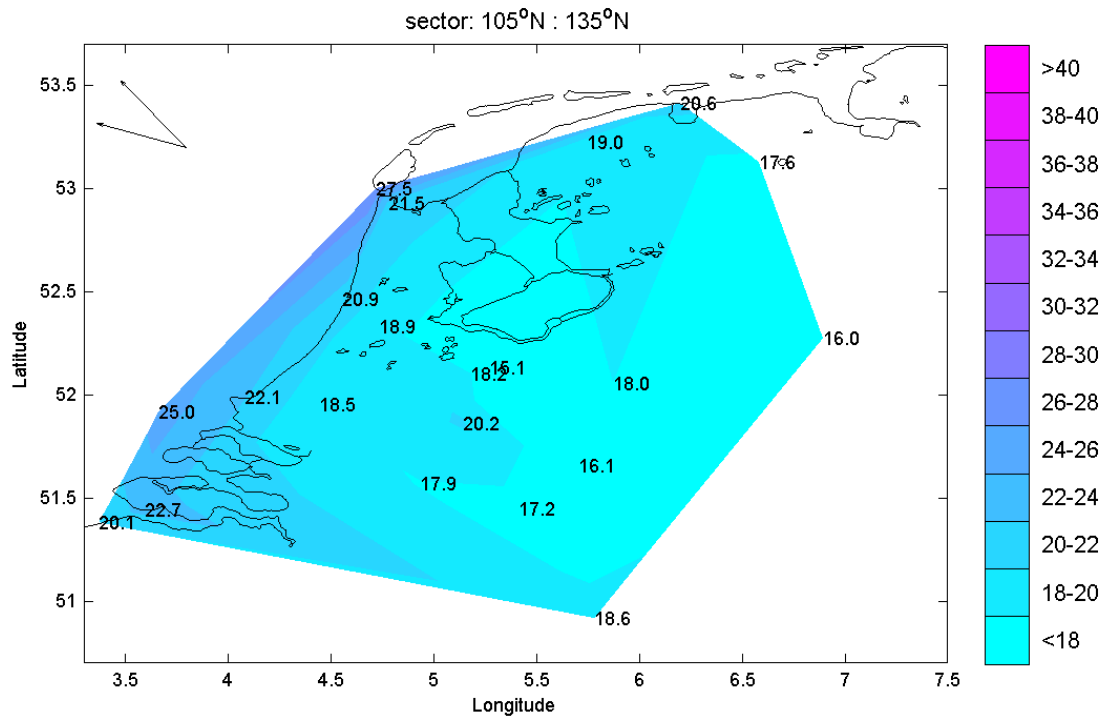


Figure 5.5 Potential wind speed 10,000-yr return value estimates in m/s. Exponential fit to POT data to the specified sector.

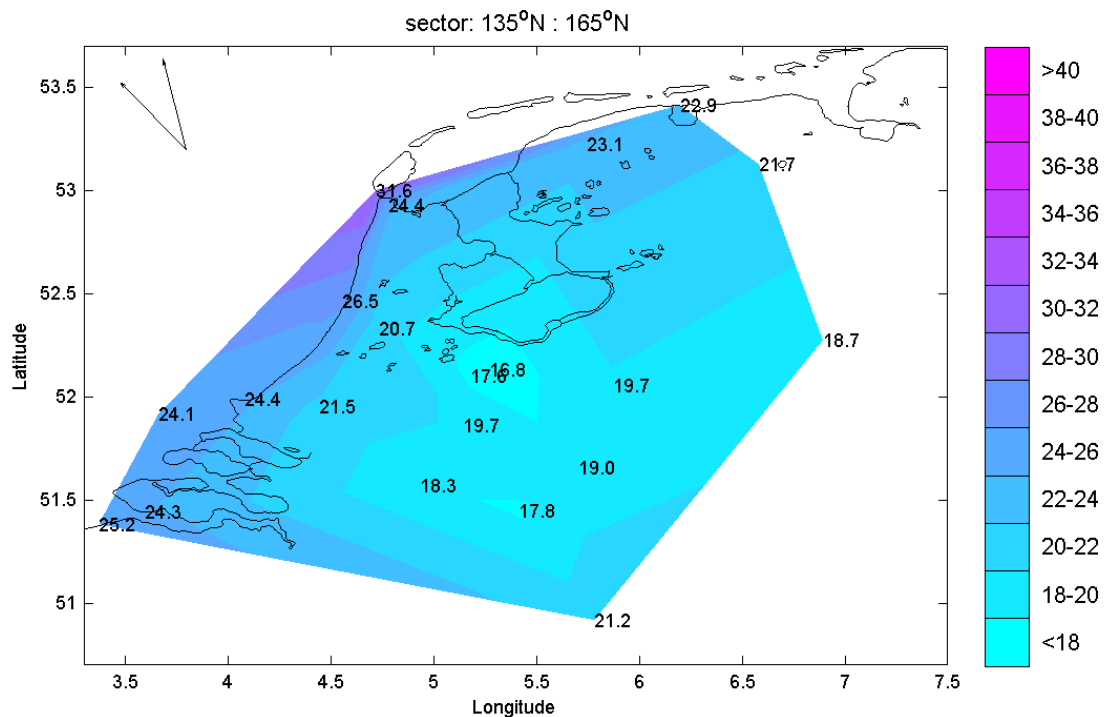


Figure 5.6 Potential wind speed 10,000-yr return value estimates in m/s. Exponential fit to POT data to the specified sector.

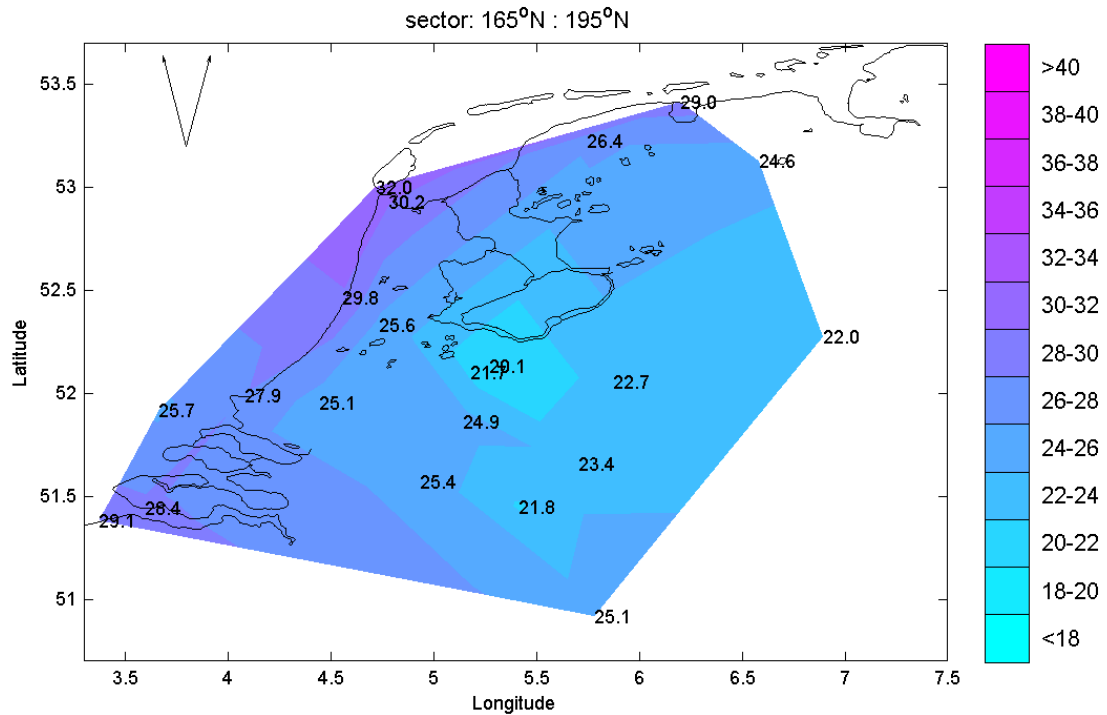


Figure 5.7 Potential wind speed 10,000-yr return value estimates in m/s. Exponential fit to POT data to the specified sector.

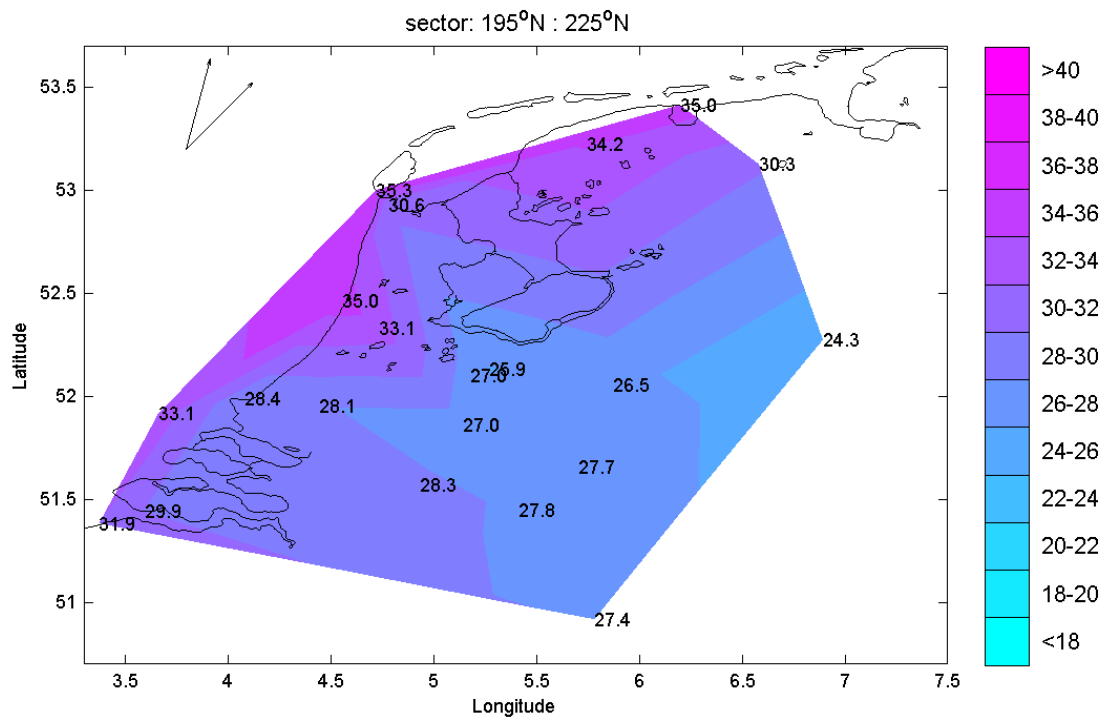


Figure 5.8 Potential wind speed 10,000-yr return value estimates in m/s. Exponential fit to POT data to the specified sector.

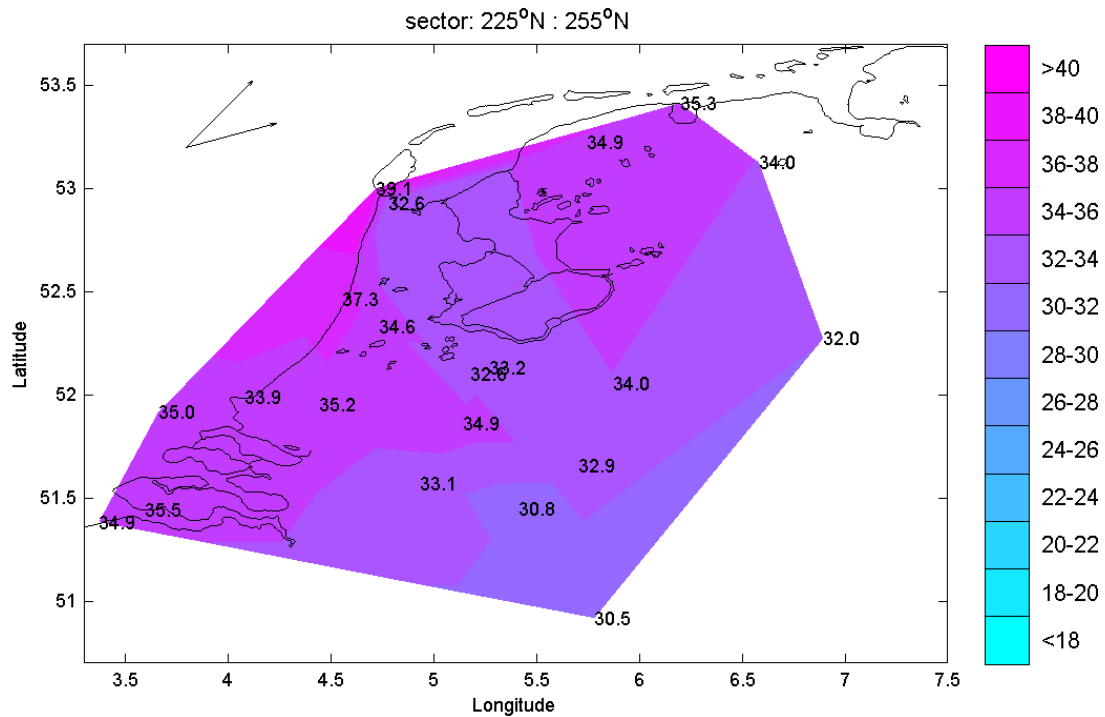


Figure 5.9 Potential wind speed 10,000-yr return value estimates in m/s. Exponential fit to POT data to the specified sector.

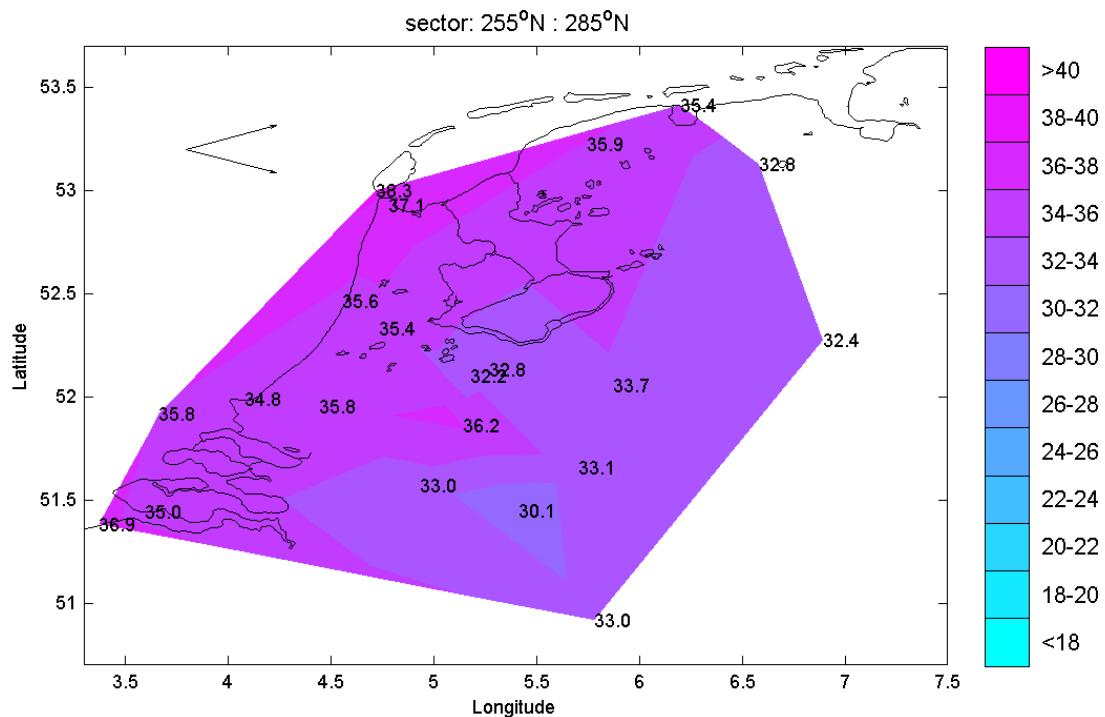


Figure 5.10 Potential wind speed 10,000-yr return value estimates in m/s. Exponential fit to POT data to the specified sector.

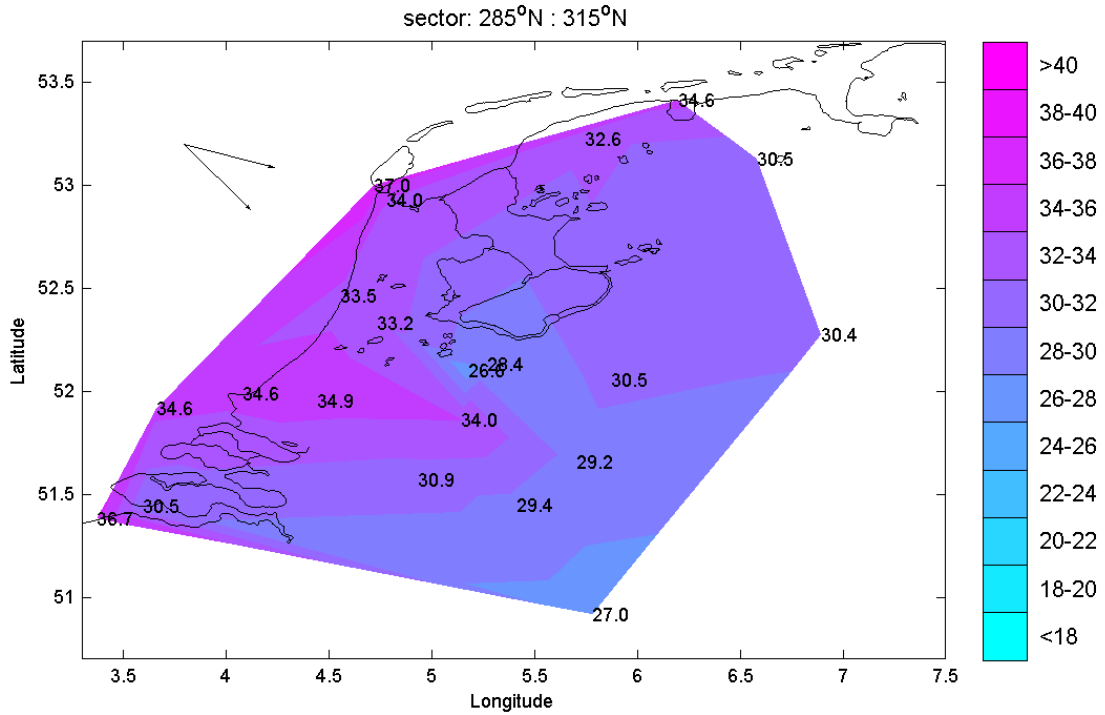


Figure 5.11 Potential wind speed 10,000-yr return value estimates in m/s. Exponential fit to POT data to the specified sector.

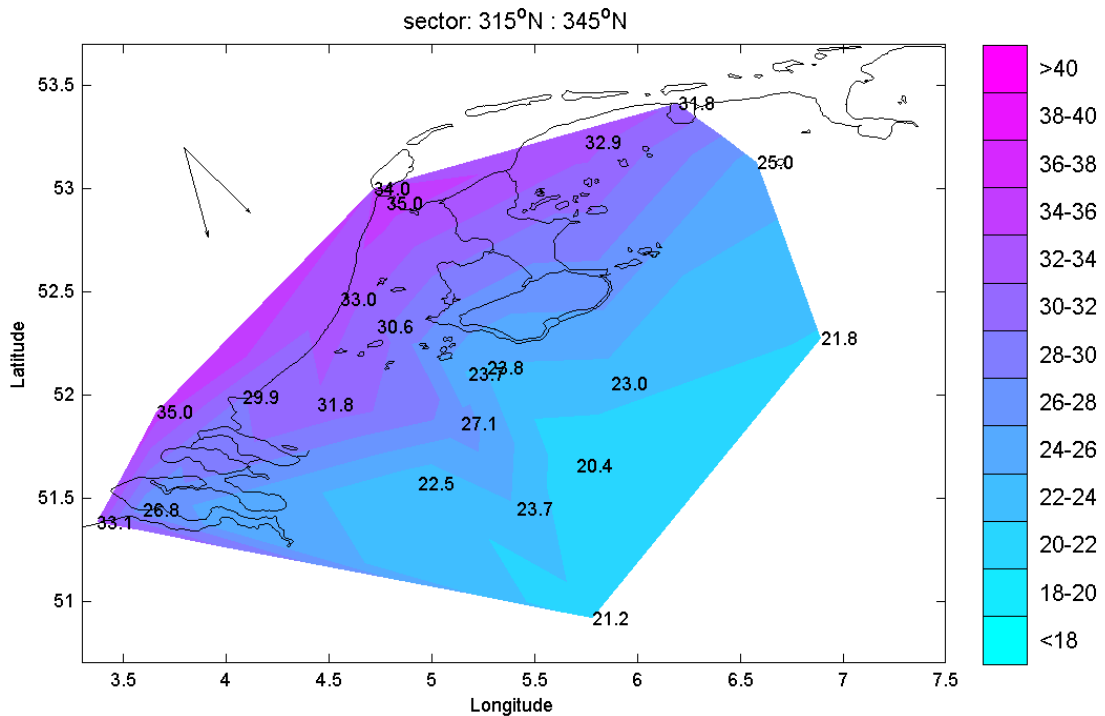


Figure 5.12 Potential wind speed 10,000-yr return value estimates in m/s. Exponential fit to POT data to the specified sector.

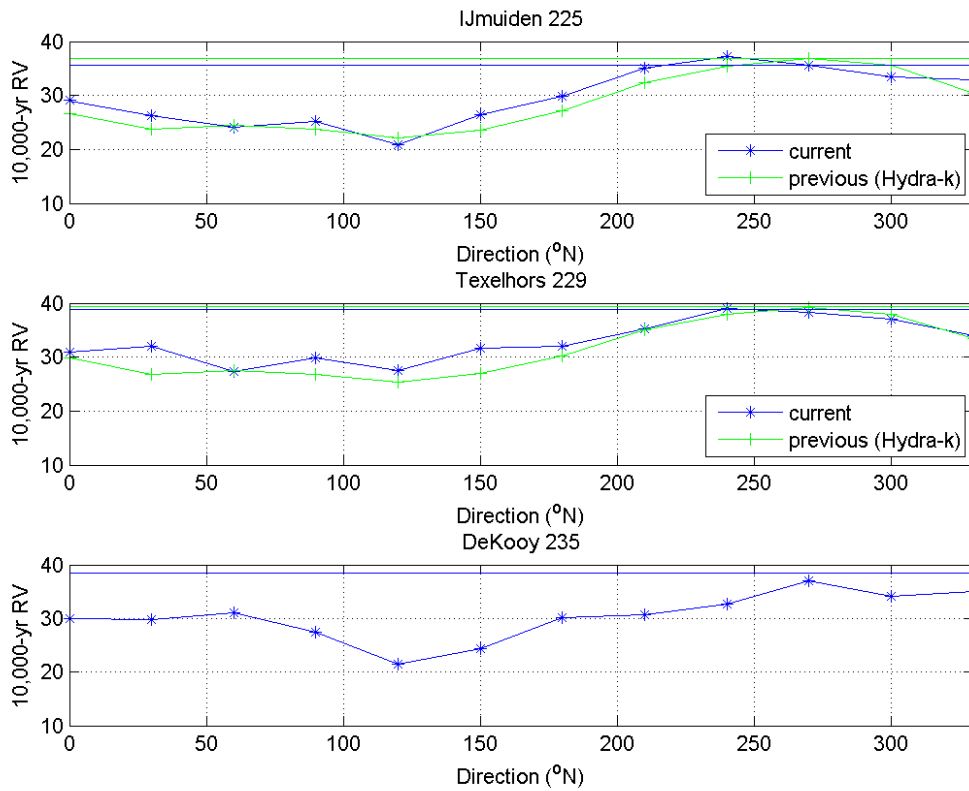


Figure 5.13 Potential wind speed 10,000-yr return value estimates in m/s. Exponential fit to POT data to the specified station. The horizontal line indicates the omni-directional estimate.

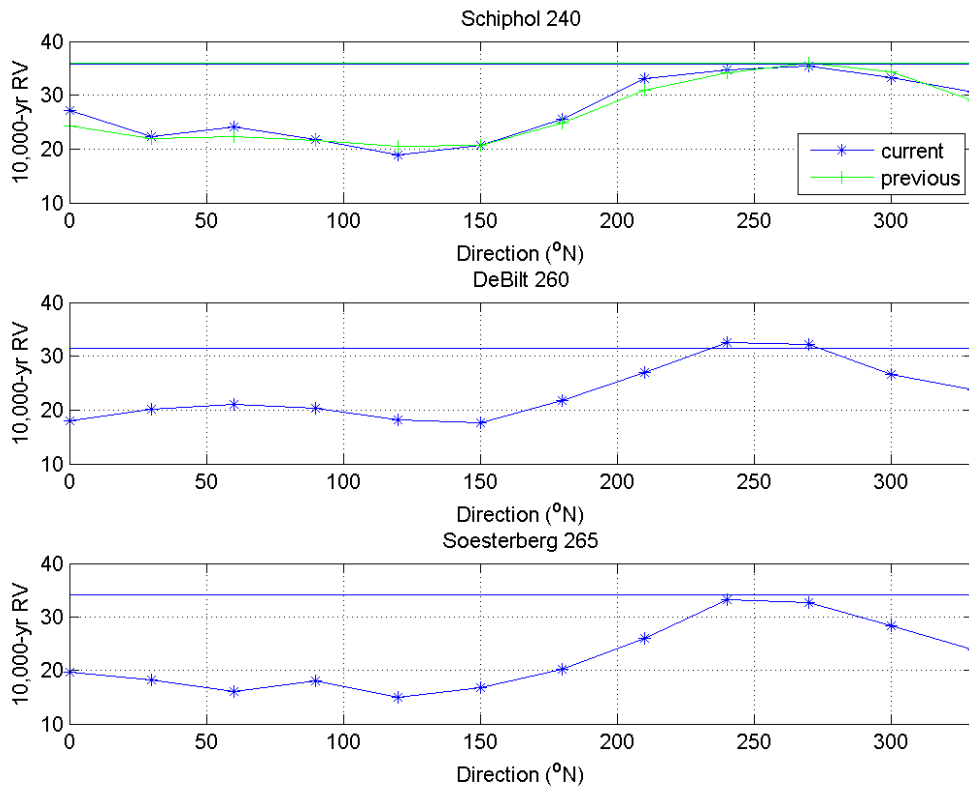


Figure 5.14 Potential wind speed 10,000-yr return value estimates in m/s. Exponential fit to POT data to the specified station. The horizontal line indicates the omni-directional estimate.

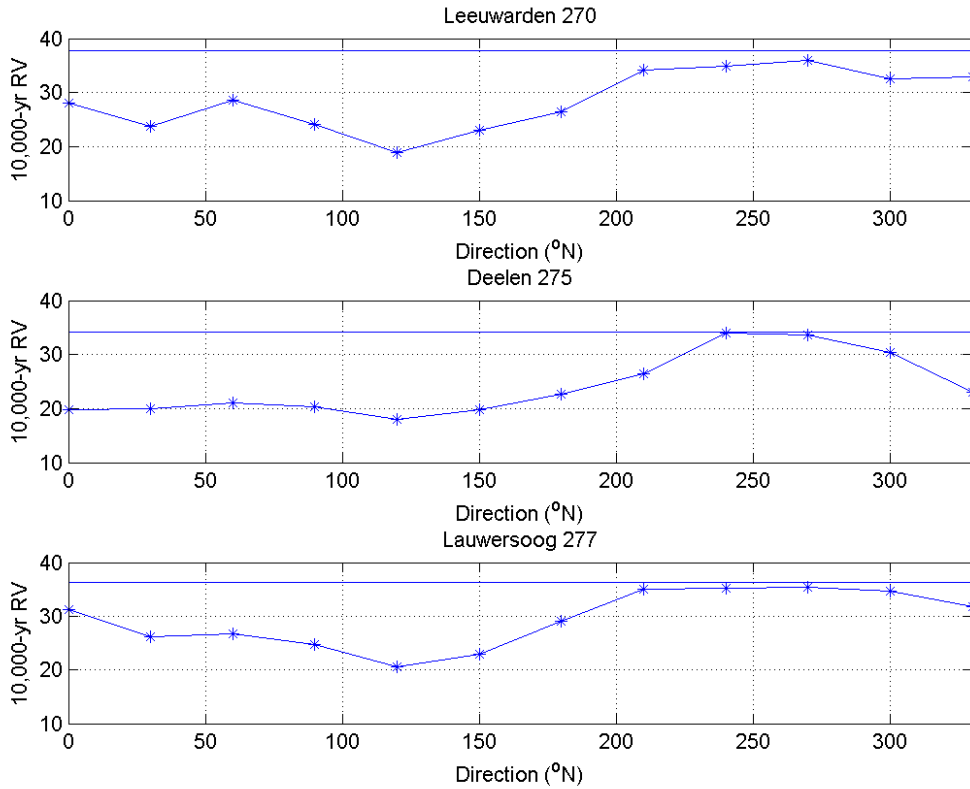


Figure 5.15 Potential wind speed 10,000-yr return value estimates in m/s. Exponential fit to POT data to the specified station. The horizontal line indicates the omni-directional estimate.

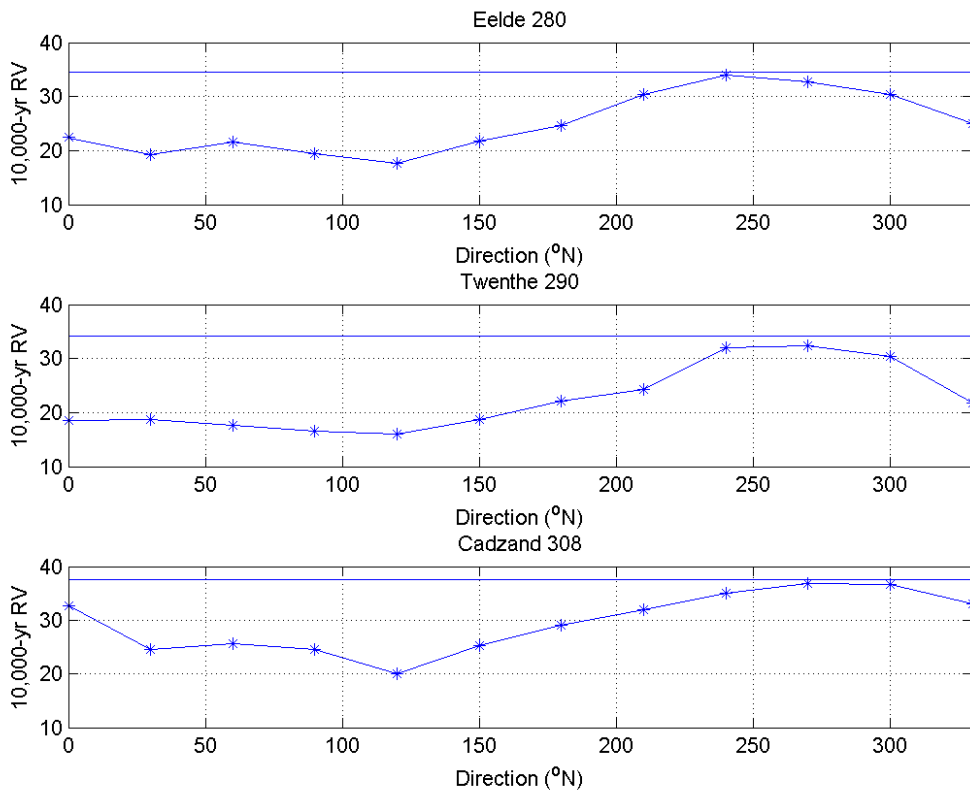


Figure 5.16 Potential wind speed 10,000-yr return value estimates in m/s. Exponential fit to POT data to the specified station. The horizontal line indicates the omni-directional estimate.

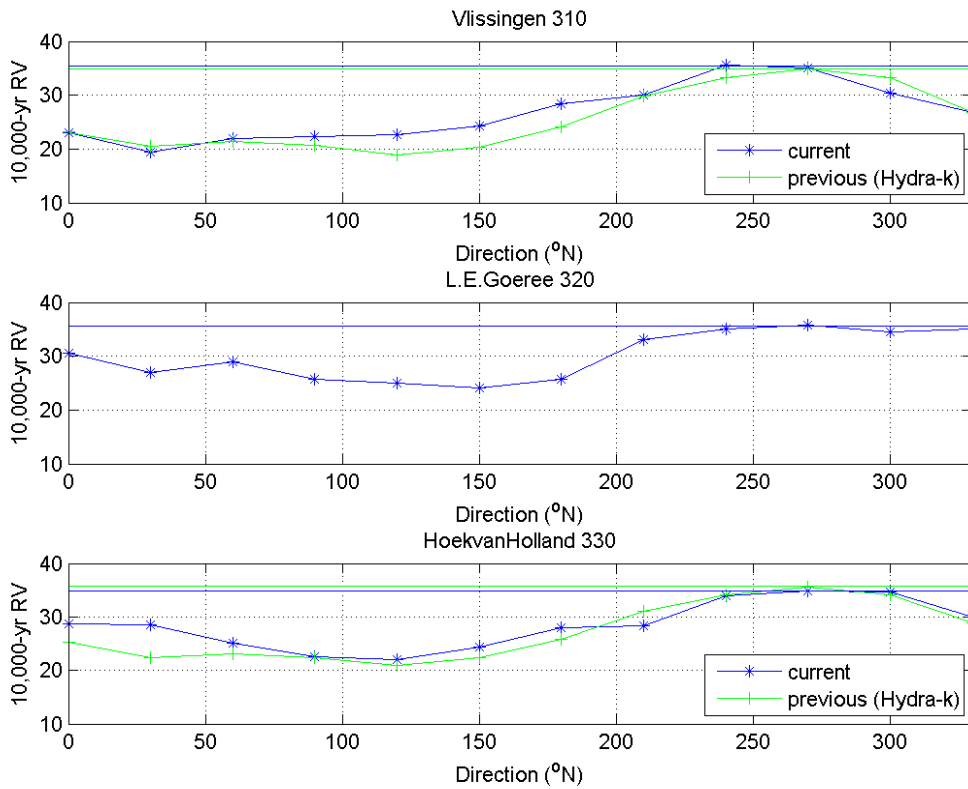


Figure 5.17 Potential wind speed 10,000-yr return value estimates in m/s. Exponential fit to POT data to the specified station. The horizontal line indicates the omni-directional estimate.

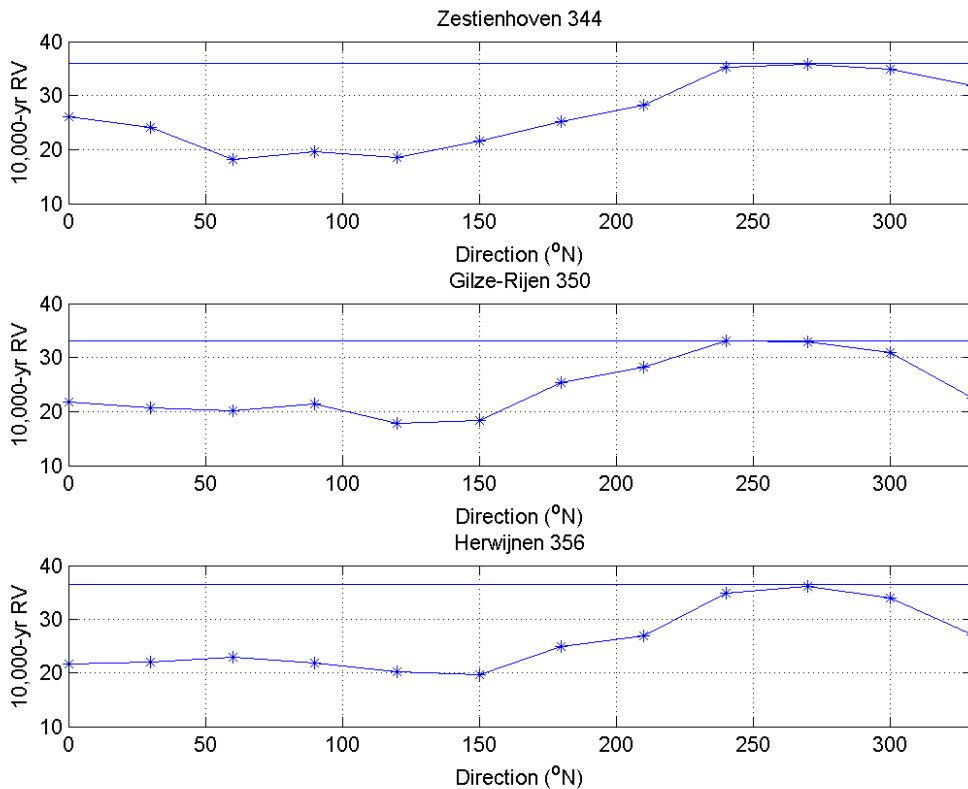


Figure 5.18 Potential wind speed 10,000-yr return value estimates in m/s. Exponential fit to POT data to the specified station. The horizontal line indicates the omni-directional estimate.

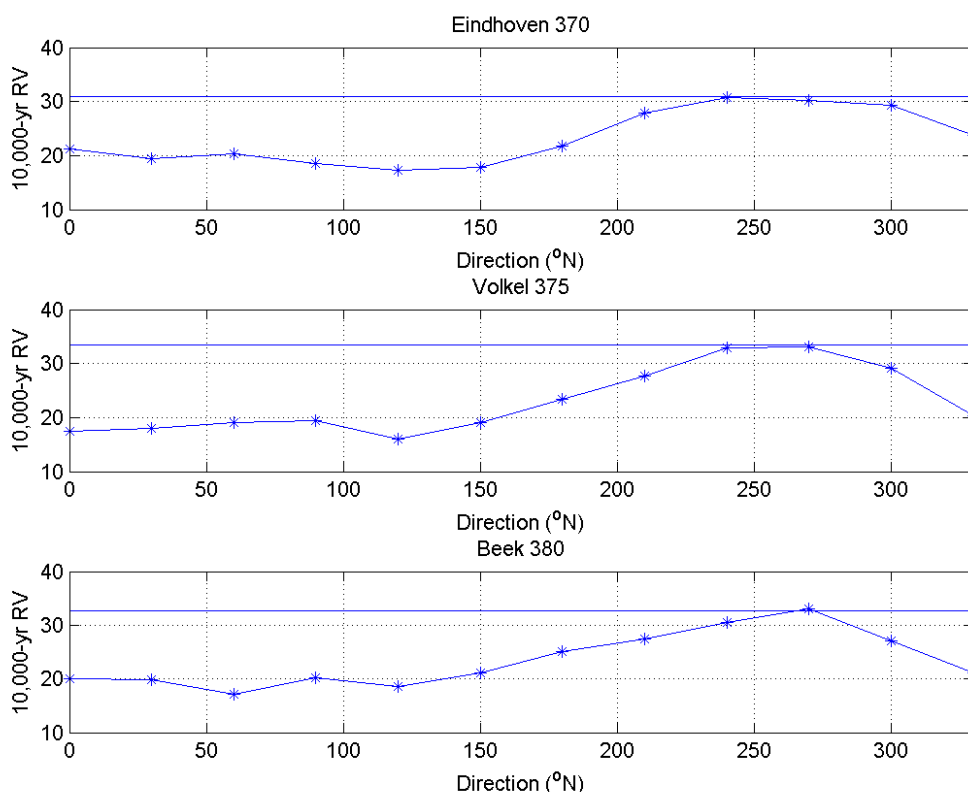


Figure 5.19 Potential wind speed 10,000-yr return value estimates in m/s. Exponential fit to POT data to the specified station. The horizontal line indicates the omni-directional estimate.

5.3 Comparison with the presently used estimates

Table 5.2 compares the values obtain by Wieringa and Rijkoort (1983) and those from this study. Please note that the values presented in Table 5.2 are not the direct Rijkoort-Weibull model results for stations Leeuwarden, Deelen and Eelde, since they were adjusted by hand by Wieringa and Rijkoort (1983). They were previously 31.7 m/s, 43.6 m/s and 31.1 m/s, respectively (cf. Rijkoort, 1983). For a number of stations, namely Leeuwarden and Deelen the discrepancy between the estimates of this study and those of Rijkoort (1983) are significant. These are however stations for which the Rijkoort (1983) were adjusted by Wieringa and Rijkoort (1983) and for which the discrepancies would even be larger if they were not adjusted. In the remaining stations the discrepancies are less than 3%, with the exception of Eindhoven, and they all are well within the uncertainty of the estimates.

	Rijkoort (1983)	This study	Relative bias (%)
L.S. Texel /Texelhors	39.5	38.8 (35.4, 42.6)	-1.8%
Schiphol	36.2	35.7 (32.4, 39.3)	-1.4%
De Bilt	32.3	31.4 (28.8, 34.1)	-2.8%
Soesterberg	33.6	34.0 (31.3, 36.9)	1.2%
Leeuwarden	34.2	37.8 (34.4, 41.3)	10.5%
Deelen	38.0	34.2 (31.2, 37.7)	-10.0%
Eelde	33.8	34.5 (30.9, 38.5)	2.1%
Vlissingen	35.0	35.3 (32.4, 38.4)	0.9%
Zestienhoven	35.6	35.9 (33.3, 38.8)	0.8%
Gilze-Rijen	32.2	33.0 (30.6, 35.5)	2.5%
Eindhoven	33.4	31.0 (28.4, 33.6)	-7.2%
Beek	32.3	32.7 (29.8, 35.9)	1.2%

Table 5.2 Comparison between the Wieringa and Rijkoort (1983, taken from Smits, 2003, Table 3.3) and the current 10,000-yr return value estimates.

Table 5.3 shows a comparison between HYDRA-K (a program of the HYDRA-family dedicated to the determining the coastal HBC) and the current 10,000-yr return value estimates. The HYDRA-K values are also plotted in Figure 5.13 and Figure 5.17. The values and directional variation of the HYDRA-K data compare rather well with the present estimates with the average relative bias being of less than 5%.

Sector	IJmuiden		Texelhors		L.S. Texel		Vlissingen		Hoek van Holland	
	This study	HYDRA-K	This study	HYDRA-K	This study	HYDRA-K	This study	HYDRA-K	This study	HYDRA-K
Omni-directional	35.6 (32.9, 38.5)	36.9	38.8 (35.4, 42.6)	39.4	35.3 (32.4, 38.4)	34.9	34.9 (32.5, 37.4)	35.8		
345°N -15°N	29.0 (26.5, 32.2)	26.6	30.9 (27.5, 34.6)	29.8	23.0 (21.0, 25.1)	23.1	28.7 (25.8, 31.7)	25.2		
15°N -45°N	26.2 (23.9, 28.6)	23.7	32.1 (29.4, 35.0)	26.8	19.3 (17.4, 21.5)	20.5	28.4 (25.5, 31.8)	22.4		
45°N -75°N	24.1 (21.5, 26.8)	24.4	27.3 (24.4, 30.2)	27.6	22.0 (20.1, 24.1)	21.4	25.1 (22.8, 27.5)	23.2		
75°N -105°N	25.2 (23.1, 27.7)	23.7	29.9 (27.4, 32.5)	26.7	22.3 (20.6, 24.1)	20.6	22.5 (20.6, 24.4)	22.4		
105°N -135°N	20.9 (19.2, 22.8)	22.2	27.5 (25.1, 30.0)	25.3	22.7 (20.6, 24.8)	19.0	22.1 (20.1, 24.2)	20.9		
135°N -165°N	26.5 (24.2, 29.0)	23.6	31.6 (28.5, 34.9)	26.9	24.3 (22.2, 26.6)	20.4	24.4 (22.3, 26.4)	22.4		
165°N -195°N	29.8 (26.9, 32.9)	27.2	32.0 (29.2, 35.1)	30.3	28.4 (25.8, 31.2)	24.2	27.9 (25.5, 30.6)	25.9		
195°N -225°N	35.0 (32.6, 37.6)	32.3	35.3 (32.8, 37.9)	35.0	29.9 (27.5, 32.6)	29.9	28.4 (26.1, 30.8)	31.1		
225°N -255°N	37.3 (34.4, 40.7)	35.5	39.1 (36.1, 42.2)	37.9	35.5 (32.1, 39.2)	33.3	33.9 (30.7, 37.4)	34.1		
255°N -285°N	35.6 (32.3, 39.3)	36.9	38.3 (34.9, 41.9)	39.2	35.0 (31.5, 38.7)	34.9	34.8 (31.1, 38.7)	35.6		
285°N -315°N	33.5 (30.3, 36.8)	35.7	37.0 (32.7, 42.1)	38.0	30.5 (27.2, 34.1)	33.2	34.6 (31.7, 37.8)	34.1		
315°N -345°N	33.0 (30.1, 36.0)	30.4	34.0 (30.7, 37.7)	33.4	26.8 (24.1, 29.5)	26.8	29.9 (26.3, 34.0)	28.9		

Table 5.3 Comparison between the HYDRA-K and the current 10,000-yr return value estimates.

Figure 5.14 shows the comparison between the currently used 10,000-yr return value estimates for Schiphol (Van Twuiver and Geerse, 1999, Figure A.1) and those from this study. Again, the comparison with the present estimates is rather good, the average relative bias being of less than 2%.

Name	KNMI-Hydra (2005)	This study	Relative bias (%)	Maximal U_p storm peak
IJmuiden	30.2	35.6	17.9%	25.7
Texelhors	38.5	38.8	0.8%	28.7
De Kooy	35.5	38.4	8.2%	27.6
Schiphol	34.1	35.7	4.7%	27.0
De Bilt	27.9	31.4	12.5%	20.5
Soesterberg	30.3	34.0	12.2%	24.0
Leeuwarden	39.5	37.8	-4.3%	26.8
Deelen	32.0	34.2	6.9%	22.6
Lauwersoog	37.7	36.3	-3.7%	26.6
Eelde	33.1	34.5	4.2%	23.3
Twenthe	36.1	34.2	-5.3%	22.3
Cadzand	29.9	37.5	25.4%	25.8
Vlissingen	29.4	35.3	20.1%	25.6
L.E. Goeree	30.2	35.7	18.2%	24.4
Hoek van Holland	27.3	34.9	27.8%	25.4
Zestienhoven	32.1	35.9	11.8%	26.0
Gilze-Rijen	29.0	33.0	13.8%	22.2
Herwijnen	32.7	36.4	11.3%	25.3
Eindhoven	31.2	31.0	-0.6%	22.0
Volkel	35.7	33.4	-6.4%	25.7
Beek	27.5	32.7	18.9%	21.9

Table 5.4 Comparison between the KNMI-Hydra project (<http://www.knmi.nl/samenw/hydra/cgi-bin/phase14.cgi>) and the current 10,000-yr return value estimates (m/s).

Although it is outside the scope of this study to analyse differences between the estimates obtained here and those obtained in the KNMI-Hydra project, in order to make the

comparison with previous results complete we have also quantitatively compared the current 10,000-yr return value estimates with those from the KNMI-Hydra project (<http://www.knmi.nl/samenw/hydra/cgi-bin/phase14.cgi>). The comparisons are shown in Table 5.4. The maximal U_p per station are also presented in the table. Without going into details, it can be observed that the estimates of this study are on average 9% higher. The higher differences are for the Hoek van Holland estimates. The value obtained here is 27.8% higher than that obtained in the KNMI-Hydra study, the latter being only 1.9 m/s greater than the maximal Hoek van Holland U_p storm peak.

As reported in the Section 1.2 the 1,000-yr return value estimates obtained by Wever and Groen (2009) based on Gumbel fits to U_p^2 annual maxima from the period 1993-2007 are 10 to 40% lower than the Rijkooort-Weibull model estimates when considering also locations where estimates were obtained using a subjective spatial interpolation method. At the 13 stations for which an extreme value analysis was carried out by Wieringa and Rijkooort (1983) the Wever and Groen (2009) estimates are about 20% smaller than the Rijkooort-Weibull model estimates. Such difference can probably be explained by sampling variability (cf. Table 4.10, and its discussion) and chosen EVA method (cf. Table 4.4). A detailed analysis of the Wever and Groen (2009) estimates is however outside the scope of this study.

6 Concluding remarks

6.1 Overview

Updated extreme potential wind statistics were computed for 21 KNMI wind stations with long time series available. The updated wind statistics are to be made available for the inference of HBC for the Dutch primary water defences within the WTI project.

The period of data considered in the analysis was the 1970-2008 period. Both omnidirectional and directional estimates were obtained. The sensitivity of the results to different periods was also analysed and found to be reasonable. I.e. the found differences do not exceed the uncertainty associated with the estimates.

The data was analysed using the standard AM/GEV and a POT/GPD approaches. The hypothesis of a type I tail for the potential wind data was extensively tested. Power 2 and power k (k being the shape parameter of the Weibull fit to the whole data) data transformations were considered to try to accelerate the convergence to a type I tail. However, in the cases considered, the transformations do not appear to improve the convergence to a type I tail, nor do they seem to be needed. In general the transformations result in an increase of the extreme value distributions shape parameter estimates, the increase being greater when a power 2 transformation is used. The assumption of a type I tail seems to be valid for the considered U_p AM and POT data. Furthermore, the estimates obtained from exponential fits to the POT data were found to be realistic and reliable and are given as final/best estimates.

Mainly due to the type I tail assumption, the curvature problem does not seem to strongly affect the computed estimates. Furthermore, these new estimates do not differ much from the currently used estimates of Wieringa and Rijkooort (1983). More precisely, the omnidirectional 10,000 yr return value estimates of this study differ by less than 3% from those of Wieringa and Rijkooort (1983) in 10 of the 13 stations considered by them. The two stations for which the differences are the largest—about 10%—are the Leeuwarden and Deelen stations. However, the estimates for those stations were adjusted ‘by hand’ by Wieringa and Rijkooort (1983) and discrepancies would even be larger if they had not been adjusted.

6.2 Caveats

The following caveats apply to the estimates provided here:

- A type I tail is assumed in the estimation. Although this assumption is here extensively motivated, it remains an approximation. The presented confidence intervals, with amplitudes of about 20% of the respective estimates, do not account for such choice and its amplitudes are therefore underestimated.
- Trends, mostly decreases in time, have been identified as significant, but not accounted for in the return value estimates provided. The main reason for ignoring the trends was that they lack spatial consistence and may have multiple origins as inhomogeneities due to variations in measuring practice, local and meso roughness or climate change. This makes correcting for them rather difficult. Furthermore, it cannot be assumed that the trends that will continue in the future and thus affect the considered stationarity of the extreme climate.
- The omnidirectional and directional return value estimates were computed independently. In principle the omnidirectional return value estimates should be equal or higher to the highest directional return value estimate. Due to the statistical

uncertainty associated with such estimates, in 24% of the stations the omni-directional estimate is—by at most 5%—exceeded by directional estimates. It is common practice to adjust in such cases the directional estimates so that the omni-directional estimate is the highest (see e.g. Verkaik et al., 2003). We have chosen not to apply such a procedure for two reasons. Firstly, because only directional estimates are needed for the WTI. Secondly, given the in principle uniqueness of the population in a given sector, the directional estimate is in principle more reliable than the omni-directional estimate that may have been obtained from a mixture of populations. In case omni-directional estimates are needed we advise that, when the omni-directional estimates are exceeded by the sector estimates, that the former be replaced by the higher directional estimate.

6.3 Recommendations

The curvature problem (see Caires et al., 2009) seems to have been partly circumvented in this study (especially in the statistics for Hoek van Holland), thanks to the assumption of a type I tail. It is, however, paramount that the curvature problem be fully understood. The quantification of its main components and the determination of corrections eventually needed in the potential wind time series may allow the estimation of extreme values without constraints on the tail type.

In the next phase of this project, the point estimates computed here will be used to interpolate the estimates in space. Assumptions of simultaneous occurrence of a certain return value with the same return period at distant stations should be treated with care.

The potential wind data considered here shows some inhomogeneities. It would be useful to investigate the origin of such inhomogeneities and remove them from the data.

References

- Beckers, J., C.P.M. Geerse, N.L. Kramer, R. Nicolai and K. Wojciechowska, 2009: *Uncertainties of the Hydra models. SBW Belastingen*. Deltares Report H5098.20 (with contributions from HKV consultants), March 2009.
- Bottema, M., 2007: *Measured wind-wave climatology Lake IJssel (NL). Main results for the period 1997-2006*. Report RWS RIZA 2007.020, July 2007.
- Caires, S., 2007: *Extreme wave statistics. Confidence Intervals*. WL | Delft Hydraulics Report H4803.30.
- Caires, S., F. Diermanse, D. Dillingh, and R. de Graaff, 2007: Extreme still water levels. Proc. of the 10th int. workshop on wave hindcasting and forecasting, Hawaii, U.S.A, 11-16 November 2007 (available at www.waveworkshop.org/10thWaves/Papers/10thWW_CDDG_article_final.pdf).
- Caires, S., V. Swail and X. L. Wang, 2006: Projection and Analysis of Extreme Wave Climate. *J. Climate*, 19(21), 5581-5605.
- Caires, S., H. de Waal, G. Groen, N. Wever and C. Geerse, 2009: *Preliminary investigations into the curvature problem in extreme wind statistics. SBW Belastingen: Phase 1b of subproject "Wind modelling"*. Deltares Report 12000264-005 (Phase 1b).
- Cheng, E. D. H. and C. Yeung, 2002: Generalized extreme gust wind speeds distributions. *J. Wind Eng. Ind. Aerodyn.*, 90, 1657-1669.
- Coles, S., 2001: *An Introduction to the Statistical Modelling of Extreme Values*. Springer Texts in Statistics, Springer-Verlag: London.
- Coles, S., and E. Simiu, 2003: Estimating uncertainty in the extreme value analysis of data generated by a hurricane simulation model. *J. Engrg. Mech.*, 129 (11), 1288-1294.
- Cook, N. J., 1982: Towards better estimates of extreme winds. *J. Wind Eng. Ind. Aerodyn.*, 9, 295–323.
- Cook, N.J. and R.I. Harris, 2001: Discussion on ‘‘Application of the generalised Pareto distribution to extreme value analysis in wind engineering’’ by Holmes, J.D., Moriarty, W.W. *J. Wind Eng. Ind. Aerodyn.*, 89, 215–224.
- D'Agostino, R. B. and M. A. Stephens, 1986: *Goodness-of-Fit Techniques*, Marcel Dekker, Inc., New York.
- Davison, A. C., and R. L. Smith, 1990: Models for exceedances over high thresholds (with discussion). *J. Roy. Stat. Soc.*, 52B, 393–442.
- De Haan, L. and C. Zhou, 2009: Notes for the discussion Deltares 15/10/08. *Evaluation of the statistical methods currently used to determine boundary conditions: Workshop proceedings* (Deltares Report H5098.70, Eds. S. Caires and D. Dillingh), 38-40.
- Diermanse, F.L.M. , H. van der Klis, C.P.M. Geerse, J. van Noortwijk, H. Gerritsen en J. Groeneweg, 2007: *SBW - Statistiek basisvariabelen* (In Dutch). WL | Delft Hydraulics and HKV Report Q4228.
- Efron, B. and R.J. Tibshirani, 1993: *An Introduction to the Bootstrap*. Monographs on Statistics & Applied Probability 57, Chapman and Hall/CRC, 436p.
- Ferguson, T. S., 1996: *A Course in Large Sample Theory*, Chapman and Hall, New York.
- Ferreira, J.A., and C. Guedes Soares, 1998: An application of the peaks over threshold method to predict extremes of significant wave height. *J. Offshore Mech. Arct. Eng.*, 120, 165–176.
- Galambos, J., 1987: *The Asymptotic Theory of Extreme Order Statistics*. 2d ed. Krieger, 414 pp.
- Geerse, C.P.M., 1999: *De interpretatie van het Rijksoort Weibull model*. RIZA-rapport 99.048 (In Dutch).
- Gomes, M. Y., and M. A. J. van Montfort, 1986: Exponentiality versus Generalized Pareto, quick tests. *Third Int. Conf. On Statistical Climatology*, Vienna, Austria.
- Harris, R.I., 2004: Comment on ‘‘Discussion on ‘‘Generalized extreme gust wind speeds distributions by E. Cheng, C. Yeung’’ by J.D. Holmes’’ [J. Wind Eng. Ind. Aerodyn. 91 (2003) 965–967]. *J. Wind Eng. Ind. Aerodyn.*, 92, 79–81
- Holmes, J.D., 2003: Discussion on Generalized extreme gust wind speeds distributions by E. Cheng, C. Yeung. *J. Wind Eng. Ind. Aerodyn.*, 91, 965–967.
- Holmes, J.D. and W.W. Moriarty, 1999: Application of the generalised Pareto distribution to extreme value analysis in wind engineering. *J. Wind Eng. Ind. Aerodyn.*, 83, 1–10.
- Hosking, J.R.M. and J.R. Wallis, 1987: Parameter and quantile estimation for the Generalized Pareto Distribution. *Technometrics*, 29, 339–349.

- Hosking, J.R.M., J.R. Wallis, and E.F. Wood, 1985: Estimation of the generalized extreme-value distribution by the method of probability-weighted moments. *Technometrics*, 27, 251-261.
- Pickands, J., 1971: The two-dimensional Poisson process and extremal processes. *Journal of Applied Probability*, 8, 745-756.
- Pickands, J., 1975: Statistical inference using extreme order statistics. *Annals of Statistics*, 3, 119-131.
- Rijkoort, P. J., 1983. *A compound Weibull model for the description of surface wind velocity distributions*. Scientific Report, WR 83-13, Royal Netherlands Meteorological Institute (KNMI).
- Simiu, E., N. A. Heckert, J. J. Filliben, and S. K. Johnson, 2001: Extreme wind load estimates based on Gumbel distribution of dynamic pressures and assessment. *Struct. Saf.*, 23, 221-229.
- Smith, R. L. 1989. Extreme value analysis of environmental time series: an application to trend detection in ground level ozone (with discussion). *Statist. Sci.*, 4, 367-393.
- Smith, R. L., 2009: Answers to the five questions. *Evaluation of the statistical methods currently used to determine boundary conditions: Workshop proceedings* (Deltares Report H5098.70, Eds. S. Cairnes and D. Dillingh), 50-54.
- Smits, A., 2001: *Analysis of the Rijkoort-Weibull model*. Technical Report, TR-232, Royal Netherlands Meteorological Institute (KNMI).
- Smits, A., 2003: *Estimation of extreme return levels of wind speed: a modification of the Rijkoort-Weibull model*. KNMI-HYDRA project Phase report 6. KNMI (<http://www.knmi.nl/samenw/hydra/documents/phasereports/ph06.pdf>).
- Smits, A., A. M. G. Klein Tank and G. P. Können, 2005: Trends in storminess over the Netherlands, 1962-2002. *International Journal of Climatology*, 25 (10), pp. 1331-1344/
- Rijkoort, P. J., 1983: *A compound Weibull model for the description of surface wind velocity distributions*. Scientific Report, WR 83-13, Royal Netherlands Meteorological Institute (KNMI).
- Tajvidi, N., 2003: Confidence Intervals and Accuracy Estimation for heavy-tailed Generalized Pareto Distributions. *Extremes*, 6, 111-123.
- Taminiau, C., 2004: *Wind (extremen) in het IJsselmeergebied* (In Dutch). RIZA werkdokument 2004.138x, 60 pp., RWS RIZA
- The KNMI and Deltares wind modelling team, 2008: *Extreme wind statistics for the Netherlands: Plan of Approach*. Deltares Report H5098.40.
- Verkaik, J. W., A. Smits and J. Ettema, 2003: *Wind climate assessment of the Netherlands 2003: Extreme value analysis and spatial interpolation methods for the determination of extreme return levels of wind speed*. KNMI-HYDRA project Phase report 9. KNMI (<http://www.knmi.nl/samenw/hydra/documents/phasereports/ph09.pdf>).
- Van den Brink, H. W. and G. Können, 2008: The statistical distribution of meteorological outliers. *Geophysical Res. letters*, 3, 5L23702, doi:10.1029/2008GL035967.
- Van Twuiver, H.C. and C.P.M. Geerse, 1999: *Achtergronden Hydraulische Belastingen Dijken IJsselmeergebied. Deelrapport 3 Windstatistiek*. RIZA-rapport 99.040 (In Dutch).
- Wever, N and G. Groen, 2009: *Improving potential wind for extreme wind statistics*. KNMI Scientific Report WR2009-02, March 2009.
- Wieringa, J., and P. J. Rijkoort, 1983: *Windklimaat van Nederland* (In Dutch). Staatsdrukkerij, 's Gravenhage (NL).

A Report review

A.1 Review report

Document: memo PR1601 Review extreme wind stat Juli31



memorandum

PR1610.10

Project : SBW – Belastingen - Wind
Date : July 31, 2009
Subject : Review on report "Extreme wind statistics for the inference of the hydraulic boundary conditions for the Dutch primary water defences".
From : Chris Geerse
To : Sofia Caires (Deltares)

1 Introduction

In the project "Extreme wind for the WTI-2011", carried out by KNMI and Deltares, extreme wind statistics for the Netherlands have to be derived [Plan of Approach, 2008]. The project concerns several phases. In phase 1, already completed, newly derived potential wind time series were established, for several wind stations in the Netherlands [Wever and Groen, 2009]. In phase 2 of the project, currently in progress, extreme value statistics have been derived. The analysis and the results are described in the preliminary report [Caires, 2009], written by Sofia Caires from Deltares.

I was asked, in accordance with section 3.6 of the [Plan of Approach, 2008], to review the preliminary report [Caires, 2009]. In a mail by Sofia Caires from Juli 14, 2009, the review instructions are given. The review has to cover the following aspects:

1. Are the background and objectives given in the report clear and unequivocal?
2. Is the chosen approach suitable to fulfil the objectives?
3. Are the objectives met?
4. Does the report provide the desired insight?
5. Are the results reasonably concrete and applicable?

In the following these aspects are treated in several chapters. Items 1, 2 and 4 are treated in chapters 2, 3 and 4, whereas items 3 and 5 are treated together in chapter 5. Chapter 6 gives a brief overall conclusion.

As a side remark, I note that this review can not be looked upon as "completely independent", since I visited some of the team meetings of the Deltares/KNMI wind modelling team, and took part in some of the discussions.

2 Are the background and objectives given in the report clear?

2.1 Background

The backgrounds of the analyses in the report [Caires, 2009] are described in section 1.2 of the report. In short, these backgrounds cover:

1. The need for extreme value distributions as input for the probabilistic Hydra-models, which models are used to derive the Hydraulic Boundary Conditions (HBC) for the Dutch primary water defences.
2. The history of the Hydra-project, running from 1998 to 2005, in which a first attempt was made to derive the extreme value distributions needed.

3. The *curvature problem*, which became apparent in the Hydra-project, i.e. the problem that land stations after extrapolation often lead to higher extreme wind speeds than coastal stations, which is contrary to the expectations. This problem was one of the main obstacles in the Hydra-project to obtain reliable wind statistics.
4. Brief discussion of the curvature problem in relation with the newly derived potential wind series of [Wever and Groen, 2009], in which it is concluded that the curvature problem is still present, though perhaps to a slightly lesser extent. It is also mentioned that the curvature problem partly might have a physical explanation, because of differences in stability properties for land and coastal stations.
5. Comparison of preliminary derived extreme wind speeds by [Wever and Groen, 2009] with the "old" Rijkooort Weibull model (RW-model) currently used in the determination of the Dutch HBC.

My comments on these backgrounds are the following. All in all, it is a brief, but rather complete summary of aspects relevant for the determination of extreme wind speeds, which is the aim of the analyses in the report [Caires, 2009]. Moreover, I would add the following:

- I would include a reference concerning the Hydra-models in point 1. There is a lot of literature about these models, but f.i. referring to [Beckers et al, 2009] would do, since this report contains an extensive list of appropriate references.
- Concerning point 4, I would add that the curvature problem will be discussed in more detail in section 3.3 of the report, since there are more remarks to be made about it than given in section 1.2 (this section seems to imply that stability problems are the only explanation). Also, I would stress more clearly that the curvature problem largely will be ignored in the extreme value analyses in the remainder of the report.
- Concerning point 5, I would stress more clearly that the preliminary results of [Wever and Groen, 2009] are *very much lower* than the old results of the RW-model, hence their results are really *not comparable* to those of the RW-model. (A difference of 10% of extreme wind speeds has already huge implications for the HBC, let alone a difference of 40%.)
Note: the fact that 10% difference in extreme wind speed need not be very large compared to statistical uncertainties, should not be confused with the fact that a difference of 10% is very large for practical applications.

2.2 Objectives

Section 1.3 of the report is titled "Objective". However, the objectives of the study are partly also given in section 1.4, titled "Approach". These objectives seem to be:

1. The determination of extreme wind speed distributions for stations with sufficiently long data series, both omni-directional as per direction (for the 12 directional sectors 15°-45°, 45°-75°, ..., 345°-15°, abbreviated in this review as 30°, 60°, ..., 360°).
2. The determination of Confidence Intervals (CI's) for the extreme value results.

It would be wise to rewrite sections 1.3 and 1.4 a little, in such a way that the objectives are all mentioned in section 1.3. Also, I would add in section 1.4 that the spatial consistency of the results will be judged in a qualitative way.

3 Is the chosen approach suitable?

In chapter 2 of the report the statistical methods used are described. These involve Annual Maxima (AM) and Peaks Over Threshold (POT), for which respectively the Generalised Extreme Value (GEV) and the Generalised Pareto Distribution (GPD) are fitted. This description is brief, but rather clear and to the point. Maybe I would disagree a bit on certain points, or I would stress different aspects, but in my opinion the "best" assumptions and preferred methods are highly subjective. The discussion in chapter 2 certainly makes clear, to my satisfaction, that all kinds of choices are to some extent subjective, and that these assumptions may lead to quite different results. Also I mention that my personal knowledge on the theory of Confidence Intervals is limited. So I take for granted the remarks concerning the theory of these intervals.

After a description of the data in chapter 3, chapter 4 of the report performs the actual analyses. In the following subsections I will treat a number of aspects which I think are relevant.

3.1 Choice of extreme value distributions

The analyses in the report consider AM/GEV and POT/GPD methods. These analyses are standard and basic in Extreme Value Theory, and many people, as I am aware of, favor these methods. My personal view is that a more pragmatic approach should also be possible, in which other kinds of distributions are fitted, which often yield equally convincing, or even better results. A big disadvantage, in my opinion, of the GEV and GPD is that these distributions often yield very non-robust results, unless the shape parameter ξ is put equal to 0, in which case the more robust Gumbel and exponential distribution result. Precisely this choice of ξ is, in combination with some transformations, extensively studied in the report. On the whole, I agree with the approach of the report.

3.2 No information about seasons and missing data

In the data selection for POT analyses, it is (implicitly) assumed that peaks exceeding a chosen threshold occur with the same frequency throughout the year. This is evidently wrong, as is well known from the RW-model and from [Verkaik et al, 2003]. The most extreme storms occur during the winter, especially in the season january-february. A proper analysis should consider also variants in which selections per season are made. I don't think (personal guess) that these analyses would have a serious impact on the results. I would recommend however, to perform a sensitivity study.

Repeat f.i. the most important POT analyses, per direction, for the most important season jan-feb, and check whether these differ very much from the current results. If both results are almost comparable, or the season jan-feb yields slightly lower extreme wind speeds, the (erroneous) assumption that the threshold frequency does not change during the year (homogeneity in time) seems rather harmless. If, however, the results for jan-feb yield much higher results, there would be a problem. It would also be interesting to study to what extent the second most important season november-december contributes to the exceedances. So I suggest to derive the statistics for the seasons nov-dec and jan-feb, to compare the results, and next to compare those results with the statistics based upon the whole year.

Related to this point is the problem of missing data. On p 12 of the report a correction for missing data is mentioned. This correction does not account for the inhomogeneity in time. So if there would be a lot of missing data, this correction will be a poor one. Actually, the report does not

provide much information on the amount of missing data. There is information on the accompanying CD-ROM, but no summary of the amount of missing data is present. I think more information about missing data should be present in the report, and some comments on the correction of p 12 should be given.

3.3 Analysis variants: U, U^k and U²

An important analysis in the report is to fit the AM with the GEV, which is done for U, U to the power $k > 1$, and U to the power 2. The transformations in terms of powers > 1 of U are considered because they are assumed to "speed up convergence of the distribution of the AM" to the Gumbel-distribution (GEV with shape parameter $\xi = 0$), with the AM here built from a parent distribution that is not a GEV. Such a transformation should be especially suitable if the parent distribution is rather concentrated around the mean, such as the normal one. The value of k is obtained by fitting the Weibull distribution to hourly measurements U of the whole dataset (k is the shape parameter of the fitted Weibull).

The assumption in the report is that the best analysis corresponding to U, U^k or U², is the one leading to a GEV distribution with shape parameter $\xi = 0$, i.e. the Gumbel distribution, motivated by the assumption, shared by several experts, that the wind parent distribution should belong to the domain of attraction of the Gumbel distribution. I share this opinion. In the following, based on the information of the report and the accompanying CD-ROM, results will be discussed for the three variants of the analyses (in terms of U, U^k and U²). After conclusions are drawn, at the end of the current section 3.3, some additional comments on the transformation U^k will be given in the next section 3.4.

Omni-directional

The analysis in the report is only given for the omni-directional case, for 21 stations. The corresponding results per direction are given on the (accompanying) CD-ROM. For the omni-directional case the results for U seem to be more satisfying than those for U^k and U². The reasons are:

1. The shape parameters ξ for the 21 stations are closest to 0 for the U-analysis. For the U^k-analysis they are a bit further away from zero, often being positive. For the U²-analysis they are even further away from zero, and even more often positive.
2. The assumption that the true distribution is a Gumbel is rejected in 4 out of the 21 stations for the U²-analysis and only in 1 out of the 21 stations for the U- and U^k-analyses. (The rejection is at the 5%-level, so statistically about 1 rejection out of 20 stations could be expected.)

On the basis of this, the U²-analysis, with 4 rejections, seems inappropriate. It also seems to favor the U-analysis instead of the U^k-analysis, although the evidence against the U^k-analysis seems not really that strong. However, a further investigation of the results (by myself) shows that for the U^k-analysis 5 out of 21 stations have a negative ξ and 16 have a positive ξ , whereas for the U-analysis 10 of the stations have a negative ξ and 11 have a positive ξ . If the proper distribution indeed would be Gumbel, about half of the stations should have negative and half of the stations should have positive ξ 's. So the proper analysis indeed seems to be the U-analysis.

Directional

The CD-ROM contains also results for the 12 directions 30°, 60°, ..., 360°, which are not discussed in the report. These are interesting, though. So I have performed a quick investigation. The results are shown in Table 1 and Figure 1 and Figure 2. The omni-directional case for Table 1 was already discussed (f.i. 10 stations with $\xi < 0$ and 1 station with Gumbel rejected for the U-

analysis). Unfortunately, for the respective directions the situation is much more unclear. The following conclusions can be drawn:

1. The U-analysis seems the proper one, or certainly gives acceptable results, for directions 240°, 270°, 300° and 330°, whereas for the other directions this is not the case.
2. For directions 90°, 120° and 150°, the proper analysis seems to be U^k or U^2 , and not U. For 240° all three types of analyses seem acceptable.

The reason that the preferred analysis for the omni-directional case is in terms of U, is simply that the omni-directional distribution is almost completely determined by the most extreme directions 240°, 270°, 300° (other directions then 240°, 270°, 300° have much lower wind speeds). So the conclusion seems to be that the U-analysis is preferable for the most extreme directions, but not for the other (less extreme) ones.

# stations shape par. < 0 (out of 21 stations)														
	omni	360	30	60	90	120	150	180	210	240	270	300	330	average (excl omni)
U AM	10	18	14	15	18	18	21	20	18	16	11	10	12	15.9
U^2 AM	3	11	9	12	14	8	15	13	17	9	7	7	7	10.8
U^k AM	5	12	10	12	14	9	16	14	17	11	8	8	9	11.7

# stations Gumbel rejected (out of 21 stations)														
	omni	360	30	60	90	120	150	180	210	240	270	300	330	average (excl omni)
U AM	1	2	4	5	3	3	2	5	6	0	1	1	1	2.8
U^2 AM	4	3	3	4	0	0	1	3	3	0	6	4	2	2.4
U^k AM	1	3	3	4	1	0	1	3	3	0	3	3	2	2.2

Table 1 Omni-directional and directional results.

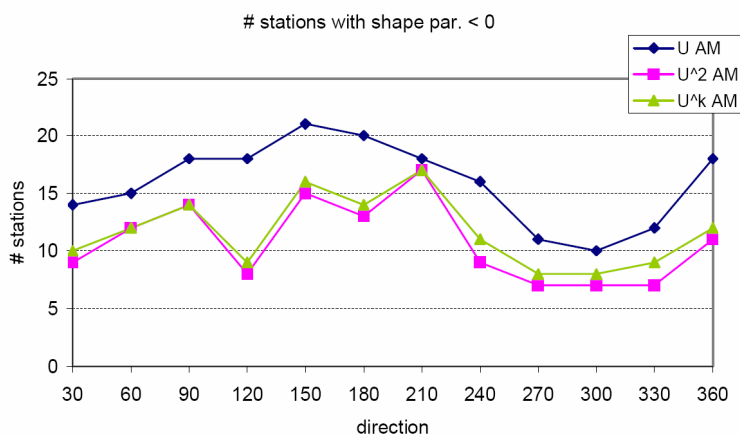


Figure 1 Plot of number of stations with negative ξ for the directional results.

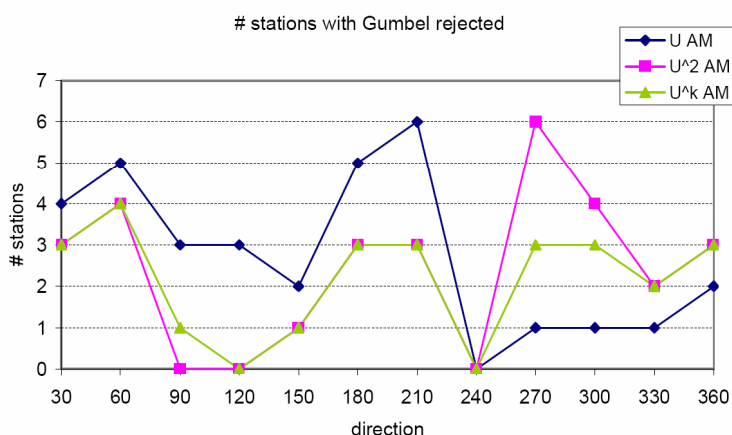


Figure 2 Plot of number of stations for which the Gumbel is rejected, for the directional results.

Consequences of the assumption that ξ should (approximately) equal zero

The final analyses in the report, omni-directional and per direction, are those based on POT analyses in terms of U, with the exponential distribution. Also the GPD is considered, however with a threshold tuned in such a way that effectively the GPD comes very close to the exponential distribution. (The threshold is chosen in such a way that de shape parameter ξ of the GPD becomes close to 0; since the GPD with $\xi = 0$ equals the exponential distribution, this means that effectively the GPD is not considered, but only the exponential one.)

The assumption that $\xi = 0$ (or approximately 0) is based on the conclusion that for the AM analysis the U-analysis in combination with a tail of type 1 had to be preferred (type 1 translates to $\xi = 0$ in the POT analysis). As a comparison, also results are given for the U^k and U^2 analyses, for which exponentials are fitted to the (transformed) data. The latter analyses yield much lower extreme wind speeds.

As shown before (compare Table 1 and Figure 1 and Figure 2) the choice $\xi = 0$ in combination with the U-analysis seems not to be the optimal choice for AM-data for directions 30° until 210° and 360° (directions other then 240°, 270°, 300°, 330°). This suggests that the choice $\xi = 0$ will also be not optimal for the POT-data for directions 30° until 210° and 360°; a different choice should be made for these directions. The results in Table 1 suggest that then a choice $\xi < 0$ would be more appropriate, leading to lower extremes for these directions.

In connection with this, together with the observation that the U^k - and U^2 -analyses yield lower extremes, there is some evidence that the final analyses of the report (U-analysis with exponential fit) overestimate the results for the directions 30° until 210° and 360°. A more suitable approach probably would yield lower extremes for these directions.

In this respect it is interesting to look at the plots on de CD-ROM (figures F.4 and F.5), in which the exponential fits are shown together with the data, both omni-directional and directional (for the U-, U^k - and U^2 -analyses). To interpret the plots properly, it should be kept in mind that people use several kinds of plot positions (an ideal plot position does not exist). In the report the plot

positions are such that the storm peak with rank j , ordered with $j = 1$ as the highest, is assigned a return period $T(j) = (n+1)/(\lambda \cdot j)$, with n the total number of peaks and λ the Poisson parameter, i.e. the average number of storms per year exceeding the threshold. Another plot position is the one by Gringorten, equal to $T(j) = (j-0.44)/[\lambda \cdot (n+0.12)]$. Different plot positions affect the positions of the points in the figures, the higher the observation, the larger it's shift in position. Consider f.i., if λ would be equal to 1, the highest observation in a data set of 39 years. The plot position according to the report then assigns this value return period $T = 40$ years, whereas Gringorten would yield $T = 70$ years. The latter plot position shifts the higher data points towards larger return periods. All other common plot positions in the literature are such that they assign higher return periods to the (higher) data points than the plot position used in the report. This means that when in the report visually the tail of the data seems to be underestimated by the model fit to a certain extent, other plot positions visually would lead to a smaller underestimation (or even an overestimation). So one should not jump to conclusions too quickly when inspecting the plots.

Having said so, my conclusion is that the plots of figures F.4 and F.5 do not really discriminate between the variants of the analyses. My subjective favor, however, is inclined towards (in my view) the most direct analysis: the exponential fit in terms of the U-analysis, which coincides with the final analysis in the report. From the plots I see no compelling reason to disagree with the exponential fit in terms of the U-analysis, taking for granted that the less important directions (30° until 210° and 360°) maybe will be a little overestimated.

General opinion concerning the statistical approaches

Considering the above remarks, and considering all other results in the report, my main conclusions and/or (subjective) preferences are as follows:

1. For directions 240°, 270°, 300°, 330°, of which the first three are the ones with the most extreme wind speeds among all possible directions, the U-analysis with exponential fit (final analysis of the report) seems very appropriate. Thus, for the most important directions 240°, 270°, 300°, the final analysis of the report seems the most appropriate one to obtain extreme wind speeds.
2. For the other directions, i.e. 30° until 210° and 360°, different analyses seem possible, leading probably to lower extremes. On the basis of the plots, the U-analysis with exponential fit, however, seems not a bad choice.
3. The spatial consistency of the results for the final analyses are convincing, both omnidirectional and directional. The choice of fitting exponentials to (untransformed) U-data moreover seems to reduce the influence of the curvature problem: this type of analysis seems rather insensitive to a curvature present in the data. Since there are still questions concerning the curvature problem, from a pragmatic point of view this insensitivity of the analysis seems an advantage.
4. The directional results of the final analyses show a convincing pattern, for each of the stations considered. These patterns seem not very sensitive to statistical fluctuations, meaning that the final analyses are fairly robust regarding directional dependencies.
5. The results of the final analysis are rather close to the ones of the RW-model, which model was derived on the basis of a different and much shorter data period (1962-1976), using a quite different model (see [Rijkoort, 1983], [Geerse, 1999] and [Verkaik et al, 2003] for an extensive description of the model). This is not direct statistical evidence for the correctness

of the final analyses, but it certainly shows that the results are plausible in the opinion of wind experts like Rijkooort and Wieringa.

6. In short: my personal impression is that the final results of the report [Caires, 2009] are satisfying, and sufficiently reliable to use in the determination of the HBC.

3.4 Remarks on the U^k -analysis

The idea to use the transformed wind speed U^k instead of U seems to be introduced in the paper [Cook, 1982]. Here we summarise some aspects of this paper, relevant to the analyses in the report [Caires, 2009]. The basic assumption in the paper is that the parent distribution $F(u)$ of hourly values u of the wind speed is given by a Weibull distribution:

$$F_u(u) = P(U < u) = 1 - \exp\{-(u/a)^k\} \quad (1)$$

where a is the scale parameter and k the shape parameter of the Weibull. Using the transformation $Y = U^k$, the distribution function in terms of Y becomes

$$F_Y(y) = P(Y < y) = 1 - \exp\{-y/a^k\} \quad (2)$$

which is an exponential distribution with scale parameter a^k . If N independent samples are drawn from a parent distribution that is either equal to (1) or (2), and the maximum Z of these samples is considered, it is well known that this maximum, when properly scaled, converges to the Gumbel distribution. The paper motivates and demonstrates that the convergence to the limit is rather slow when considering (1), and very fast when considering (2).

In fact, it is demonstrated that the convergence for case (1), i.e. the U -analysis in the report [Caires, 2009], is so slow that when the *annual* maximum is considered, the distribution of this annual maximum will not have reached the limiting Gumbel form, and that, moreover, fitting a Gumbel distribution to the sequence of annual maxima will *overestimate* the true return levels notably. For instance, fitting a Gumbel to obtain the 1000-year return level, will result in a wind speed that is notably higher than the true value. Clearly, this is unwanted. The paper also demonstrates that when considering case (2), the convergence is so fast that the distribution of the annual maximum based on the transformed values u^k , will be very close to the Gumbel distribution (the reason being that the tail of the Gumbel itself is exponential). In fact, the paper demonstrates that what in [Caires, 2009] is called the U^k -analysis, is the proper analysis when considering annual maxima. Summarizing, the paper demonstrates that the U^k -analysis for the annual maxima is the proper way to obtain extreme return wind speeds, whereas the U -analysis would yield extreme return wind speeds which are too high.

However, this conclusion is based on assumption (1), i.e. that the parent distribution of the hourly wind speed follows a Weibull distribution *over the full range of wind speeds*. If this would be so, I certainly would agree with the conclusion of the paper. But I think it is questionable whether wind speeds do satisfy this property. The most important thing is that I doubt whether the tail of the Weibull distribution (when fitted on hourly values) describes the probabilities with which high wind speeds occur properly. In the following some comments are made.

Do the Weibulls have tails that are decreasing to fast?

The assumption that wind speeds follow a Weibull distribution was a starting point for Rijkooort, when "constructing" the Rijkooort Weibull model (RW-model). At a later stage, however, he

introduced so called "persistencies", compensating for dependencies between adjacent hours, but also for the fact that the tails of the Weibulls *seemed to decrease much too fast*. In fact, it can be verified that the tails of the Weibulls in the RW-model are often "lifted in probability" by a factor 10 or more. Without these adjustments, the 10000 year return levels of the RW-model would decrease by about 4 m/s. See for more information concerning the role of the persistencies [Geerse, 1999] (references [Rijkoort, 1983] and [Verkaik et al, 2003] seem less appropriate concerning this particular issue). If Rijkoort was right in correcting the Weibull tails, the consequence is that assumption (1) does not hold.

Regarding this issue, I mention that in Phase report 6 of [Verkaik et al, 2003], a modified version of the RW-model was considered, in which, among other things, *no tail correction for the hourly Weibull fits was applied*. The results of Appendix D of this phase report show that the modified version of the RW-model (indeed) yields, for a large number of stations, a severe underestimation of the higher observations, indicating again that the Weibull tails decrease too fast. (Since there is only an indirect relation between the outcomes of the RW-model (exceedance frequencies of storms), and the underlying Weibulls for hourly values, the observed underestimation can not be translated directly to the Weibulls.)

Is it correct that the Weibull parameters are determined by the most frequent wind speeds and not by the highest values in the data set?

When fitting, per direction, a Weibull to the whole data set of hourly measurements, it is evident that the parameters a and k will be determined almost completely by the most frequently occurring wind speeds, which are relatively low, and not by the (very) high wind speeds in the data set, which are very rare. So the highest wind speeds in the data set almost bear no relevance to the parameters a and k which are obtained by fitting the Weibull. This seems not a very good starting point when performing an extreme value analysis. Such an analysis should put more, if not all the weight, on the high values in the data set. (In [Cook, 1982], so to speak, the high data values effectively are discarded, and "replaced by the faith" that the Weibull fitted on the whole bunch of data automatically produces the correct tail for hourly data.) In addition, we mention that in the Hydra-project, see in particular Phase report 6 of [Verkaik et al, 2003], it became apparent that the parameters a and k of the Weibulls, fitted per direction, are very sensitive to the treatments of wind speeds as low as 2 m/s, which is certainly something you would not want in an extreme value analysis.

Seasonal dependencies

In [Cook, 1982] it seems to be unnoticed that the occurrence of (high) wind speeds is evidently non-homogeneous throughout the year. As noted before, the most extreme wind speeds occur in the season january-february; in the summer months much lower wind speeds occur. This means that, even if assumption (1) would be satisfied, it can only be satisfied in seasonal periods in which the data are homogeneous in time. (Note that the assumption of a *single* parent distribution (1) implicitly assumes homogeneity in time.) So the U^k -analysis, if it is used, has to be performed for separate seasons, which each can be considered homogeneous in time. Of course, as mentioned in section 3.2, seasonal dependencies are also ignored in the report [Caires, 2009], but I think the U^k -analysis will be more sensitive to seasonal effects than the U -analysis. In the latter analysis only the highest peaks in the data set are considered, whereas in the U^k -analysis all data are used, i.e. for the determination of k , including data from the summer months. The latter months, however, should be irrelevant for the determination of the extreme wind speeds. (As a side remark, note that [Cook, 1982] claims that there occur about 100 independent storms in a year, i.e. roughly one independent weather system every four days; due to the inhomogeneity of

occurrences, however, in a homogeneous seasonal period, lasting only about two months, this number would decrease to about $100/6 = 17$.)

Necessity to check that wind speeds follow a Weibull distribution

The preceding remarks make clear that it is not evident that a Weibull fitted to hourly measurements really fits the highest hourly observations well. When using the obtained fit parameter k in the U^k -analysis, it is therefore necessary to check in advance that the fit to the hourly highest data is sufficiently accurate.

My guess, based on my knowledge of the RW-model, the Hydra-project and the results of [Caires, 2009], is that for most of the stations the Weibulls will underestimate the tail of the data in a notable way, at least for the omnidirectional case and the most important directions 240° , 270° and 300° . If this would be so, the U^k -analysis would be improper to use for these cases. I hope that in the near future, there will be the time and opportunity to check these statements, by using statistical tests and through visual inspection of relevant plots. Note: these checks should be done for all the stations; by considering only a few stations, a systematic underestimation would be "blurred by statistical randomness". Also, the consideration of a proper seasonal, time-homogeneous period, might be an issue for consideration.

3.5 Possible adjustments of final results to obtain consistency between omni-directional and directional results

In some cases the directional extremes exceed the omni-directional ones, which is logically impossible. If this happens, the report advises to put the omni-directional result equal to the highest directional one. This is not a very logical procedure. It is stated that for the WTI-project only directional results are needed. If this would be the case, then no omnidirectional results need to be presented as final results available to others. If however, contrary to what is said, they are needed for practical purposes, they should be consistent with the directional results.

I suggest to derive adjusted omni-directional results from the directional results, in such a way that for every level U , the sum of the exceedance frequencies over the directions equals the omni-directional exceedance frequency of U . My impression is that the adjusted omni-directional levels will be a bit higher than the present levels (in particular this will be the case when three or even more directions are equally extreme).

I want to make another remark. Looking at the results in Figures 5.3 – 5.9 for the 10000 year return values, it is obvious that some directions yield, as a result of statistical randomness, results not plausible compared to adjacent directions. I suggest to adjust the cases in which these deviations are so large that they disturb the pattern. If this is not done, applying the results for the HBC later might raise unnecessary questions. Also, a possible spatial interpolation between stations might become intricate without adjustments.

I recommend (as a "rough guide") to adjust:

- Texelhors: lower sector 360°
- De Kooy: raise 300° , lower 330°
- Schiphol: lower 300°
- Leeuwarden: lower 330°
- L.E. Goeree: raise 300° , lower 330°
- Hoek van Holland: (slightly) adjust 30° , 180° , 210° , 360°
- Eindhoven: lower 300°

This concerns a limited number of adjustments. To perform the adjustments, it would be wise to look at the data again. Actually, in some cases the data seem to indicate that the adjustments are rather plausible (sometimes outliers are responsible for the deviating results). The adjustments should be such that again (now adjusted) exponential fits are used.

3.6 Trends and inhomogeneities

The report discusses briefly trends, and very briefly inhomogeneities in the data. The conclusion is that in 10 out of the 21 stations a significant trend is detected. The only one of the 10 stations with a positive trend is L.E. Goeree, the other 9 have a negative trend. With the results of the CD-ROM (figures F.6) it is seen that 19 out of 21 stations show a negative trend, see Table 2. The positive trend for IJmuiden is very small, hence negligible. The positive trend in L.E. Goeree is very large. Inspection of the plot of annual maxima, however, shows that there is a strong inhomogeneity in the data, almost certainly indicating that the measurements contain serious errors, see Figure 3. It appears that until 1990 all AM's are below 19.5 m/s, whereas they all lie above 19 m/s after 1990. The chance that these measurements will be correct is statistically completely negligible. It seems that the measurements until 1990 suffer from serious systematic errors. It would be wise to reconsider whether the results for L.E. Goeree should not be removed from the final results (the return values, though, seem remarkably plausible).

When L.E. Goeree is removed, the conclusion is that all stations show a negative trend, except for IJmuiden, which has a negligible trend. On average this trend (averaged over 20 remaining stations) equals -6.0 cm/s/yr. In my opinion there is a negative trend for the whole of the Netherlands, which differs, due to all kinds of influences, per station. It seems to me most likely, (slightly contradicting the report, which speaks of multiple origins) that climatological changes will be the main cause in the observed trends. Even if this would be true, however, it is insecure whether such a trend will persist.

I agree with the approach of the report not to adjust the stations for the observed trends. The trouble in doing so would, I think, not substantially improve the result for extreme values.

Station		Annual max (cm/s/yr)
IJmuiden	225	0.69
Texelhors	229	-12.2
De Kooy	235	-11.3
Schiphol	240	-1.5
DeBilt	260	-11.3
Soesterberg	265	-0.75
Leewarden	270	-12.2
Deelen	275	-8.3
Lauwersoog	277	-4.5
Eelde	280	-4.3
Twenthe	290	-2.4
Cadzand	308	-11.7
Viissingen	310	-0.89
L.E. Goeree	320	11.3
Hoek van Holland	330	-1.1
Zestienhoven	344	-7.7
Gilze-Rijen	350	-9.8
Herwijnen	356	-7.4
Eindhoven	370	-7.1
Volkel	375	-4.6
Beek	380	-1.3

Table 2 Trends of stations for the annual maxima.

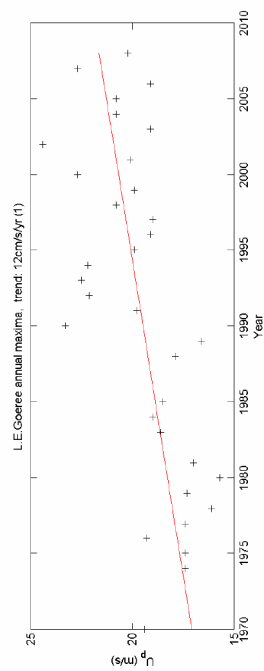


Figure 3 Trend for L.E. Goeree.

4 Does the report provide the desired insight?

4.1 Information on CD-ROM

Accompanying the report is a CD-ROM with a lot of figures and tables. In my opinion a lot of the figures of the CD-ROM should definitely be present in the report itself, preferably in appendices, or in a separate accompanying document. The figures are almost impossible to view clearly from the screen of the PC, whereas in my opinion they are *indispensable to judge the results, and in particular the model fits*. The tables T.2, containing AM/GEV results on which Table 1 is based, and T.3, containing the model parameters for the fits, should also definitely be included in the report.

Concerning the figures I propose to include "on paper":

1. All figures of F.2: return value plots of the omni-directional AM data.
2. Part of the figures of F.3: threshold plots for the omnidirectional cases.
3. Part of the figures of F.4: return value plots of the POT data for the omnidirectional cases.
4. Part of the figures of F.5: comparative return value plots of the POT data for one particular station, f.i. Schiphol, compared with all the other stations (both omnidirectional and directional plots). Remark: the version recently created by Sofia Caires, starting at much lower wind speeds than the thresholds should be used.
5. All figures of F.6: annual maxima time series with linear fits.

With regard to point 4, I note that inspection of these figures is very helpful to judge visually the influence of the curvature problem. (To that purpose, the station common to all the plots should preferably be a land station, yielding a "straighter plot" than a coastal station.) The pictures seem to suggest that the curvature of the plots is mainly present in the relatively low part of the data for the coastal stations, whereas for the higher data the plots for coastal and land stations seem to be much alike (straight lines, fitted rather well with exponentials).

4.2 Layout of tables and pictures in the report

A lot of pictures and tables in the report are so small, that it becomes almost impossible to read them (f.i. Figures 4.1, 4.3, 4.4 and Table 4.4). I would strongly prefer larger figures/tables, even though they might become spread over several pages. A lot of the current pictures and tables are simply not readable. Maybe the report can be checked concerning the size and readability of figures and (to a lesser extent) tables.

4.3 Comparison with the RW-model

In section 5.3 final results are compared with the RW-model. For the RW-model, the "unadjusted results" of [Rijkooort, 1983] are taken, which differ from the ones given in [Rijkooort and Wieringa, 1983]. It is stated that "The latter are to the best of our knowledge, an expert opinion of the values obtained by Rijkooort (1983)". In my opinion, this is not the case. Only results for three stations were manually adjusted by Rijkooort himself, namely Leeuwarden, Deelen and Eelde (see p 16 of Phase report 6 of [Verkaik et al, 2003]), whereas these adjustments, as far as I know, are already present in [Rijkooort, 1983].

I suggest to compare the results with the adjusted version of RW-model, since that is to my knowledge the "official version" of the model. (The adjusted 10000 year values for Leeuwarden, Deelen and Eelde are according to Phase report 6 of [Verkaik et al, 2003] respectively 34.2, 38.0 and 33.8 m/s.)

5 Are the objectives met and the results reasonably concrete and applicale?

The results of the final analyses of extreme value distributions are in my view very concrete, and, compared to the results of the RW-model, relatively easy to apply for the HBC. Where for the RW-model one has to use tables of numbers, or use fits of these numbers, the new analyses yield easy analytic expressions, given in terms of exponential distributions and threshold frequencies.

The necessary parameters are provided in Table T.3 of the CD-ROM (later in the report I hope). A question though, is whether all the parameters have a sufficient number of decimals. It appears f.i. that the scale parameter could use an extra digit.

The unformation concerning confidence intervals (C.I.'s) seems not concrete enough. The report states that the best choices of the C.I.'s are somewhere in between the ones for the exponential fits and the ones for the GPD fits. I agree with this view. For the HBC, however, some definite choices for the C.I.'s have to be made.

As a side remark: at present, C.I.'s are almost never used in the calculations of the HBC; this might change however in the (near) future; also they might be needed in all kinds of studies.

6 General conclusions concerning the final results for the extreme value distributions

Doing extreme value analyses involves, at least in my humble opinion, a lot of subjective choices. Due to this subjectivity, it seems impossible to speak of "the best analysis" to derive extreme wind speeds. Different choices, however, can lead to differences in results which have enormous implications for the HBC.

I personally am rather satisfied with the (subjective) choices in the report [Caires, 2009], amounting to fitting peaks of the (untransformed) wind speed U with exponential distributions. For the most important directions 240° , 270° and 300° (having the most extreme wind speeds) the final approach can relatively well be motivated with statistical arguments. For the other directions, which are less important for the HBC, such a motivation however is lacking. The spatial pattern of the results seems plausible, as does the dependence of the results on the respective directional sectors. I think it will be hard to improve on the results, unless a very extensive additional study is involved. Summarizing, I can agree very well with the final results of the report [Caires, 2009]. See for more comments on the statistical approach section 3.3 of this review.

References

[Beckers et al, 2009]

Uncertainties of the Hydra models. SBW Belastingen. Joost Beckers (editor), Chris Geerse, Nienke Kramer, Robin Nicolai, Karolina Wojciechowska. Deltares report H5098.20 (with contributions by HKV), March 2009.

[Caires, 2009]

Extreme wind statistics for the inference of the hydraulic boundary conditions for the Dutch primary water defences. Preliminary version. Deltares report, Juli 21, 2009.

[Cook, 1982]

Towards better estimation of extreme winds. N.J. Cook. Journal of Wind Engineering and Industrial Aerodynamics, 9 (1982) 295-323.

[Geerse, 1999]

De interpretatie van het Rijkcoort Weibull model. C.P.M. Geerse. RIZA-rapport 99.048. Rijkswaterstaat-RIZA. Lelystad, 20 juli 1999. (In dutch.)

[Plan of Approach, 2008]

Extreme wind statistics for the Netherlands. Plan of approach. By: The KNMI and Deltares wind modelling team. Deltares report H5098.40, August 2008. Prepared for the Waterdienst.

[Rijkcoort, 1983]

A compound Weibull model for the description of surface wind velocity distribution. Rijkcoort P.J. Koninklijk Nederlands Meteorologisch Instituut (KNMI). De Bilt, 1983.

[Verkaik et al, 2003]

KNMI-Hydra project: Phase reports 1 - 16. J.W. Verkaik, A. Smits, J. Ettema. KNMI De Bilt, the Netherlands, may, 2003.

[Wever and Groen, 2009]

Improving potential wind for extreme wind statistics. N. Wever and G. Groen. KNMI Scientific Report WR2009-02, March 2009.

A.2 Acknowledgment of the review

Dr. Chris Geerse's review of a previous version of this report reproduced in the proceeding section, is acknowledged. His advice and suggestions have led to a significant improvement of the exposition and analyses presented in the report. For example, following his suggestion the crude seasonal variability analysis has been added, the influence of the gaps in the data assessed and tables and figures have been added. His review also complements the analyses given in the report and the text refers to it when that is the case.

B Tables

Year\Month	January	February	March	April	May	June	July	August	September	October	November	December
1970	100.00	100.00	100.00	100.00	100.00	100.00	100.00	100.00	100.00	100.00	100.00	100.00
1971	100.00	100.00	100.00	100.00	100.00	100.00	100.00	100.00	100.00	100.00	100.00	100.00
1972	99.87	100.00	99.87	100.00	100.00	100.00	100.00	100.00	100.00	100.00	100.00	100.00
1973	100.00	100.00	100.00	100.00	100.00	100.00	100.00	100.00	100.00	100.00	100.00	100.00
1974	100.00	100.00	100.00	100.00	100.00	100.00	100.00	99.87	100.00	100.00	100.00	100.00
1975	100.00	100.00	99.46	100.00	100.00	98.61	98.92	99.33	99.72	100.00	99.86	99.87
1976	99.87	100.00	100.00	99.58	99.73	99.58	99.73	100.00	99.72	99.87	66.25	99.73
1977	99.60	99.70	99.87	99.58	100.00	99.72	99.46	99.87	98.33	100.00	99.86	100.00
1978	100.00	99.55	100.00	99.03	99.87	99.58	99.87	99.73	100.00	99.73	99.72	100.00
1979	99.60	97.02	99.87	98.75	98.12	99.44	98.79	99.33	98.19	97.04	99.17	99.60
1980	98.39	97.99	97.18	98.06	99.60	98.33	96.64	99.06	97.22	96.91	100.00	99.46
1981	98.52	98.36	99.06	99.31	98.12	99.44	98.92	97.58	97.08	97.98	98.75	97.45
1982	97.58	98.07	96.10	98.89	95.43	95.42	98.39	99.19	97.36	98.79	97.50	98.66
1983	100.00	98.66	99.06	98.06	98.52	98.06	96.64	51.61	0.28	0.00	99.17	55.65
1984	99.87	99.57	98.52	96.94	97.98	99.17	98.66	99.46	98.47	99.33	99.58	100.00
1985	99.87	90.48	0.00	0.00	0.00	0.00	0.00	0.00	0.00	0.00	5.14	5.65
1986	0.00	0.00	0.00	0.00	0.00	94.58	100.00	100.00	99.58	100.00	100.00	100.00
1987	98.66	99.55	100.00	100.00	100.00	100.00	99.87	99.87	99.58	100.00	100.00	100.00
1988	100.00	100.00	100.00	100.00	100.00	100.00	100.00	100.00	100.00	100.00	100.00	100.00
1989	99.87	99.55	100.00	99.86	79.03	99.86	99.73	100.00	99.86	100.00	99.86	100.00
1990	100.00	100.00	99.73	97.50	95.56	94.03	95.30	93.55	96.81	98.79	94.44	97.45
1991	95.43	91.96	95.70	99.03	98.79	98.06	96.51	94.89	95.97	95.97	98.47	94.76
1992	96.24	97.13	99.33	96.94	96.77	98.19	95.83	98.92	96.39	98.52	98.47	96.64
1993	99.33	97.47	98.25	97.36	98.92	97.64	98.25	98.66	96.81	98.52	97.50	97.72
1994	99.06	97.77	98.79	98.06	97.72	96.39	98.12	98.12	98.75	99.33	97.92	99.73
1995	99.46	99.55	99.46	99.17	99.33	100.00	98.79	99.60	99.58	97.85	98.06	98.25
1996	99.87	98.13	99.60	97.78	98.66	97.78	99.19	98.92	98.47	99.33	98.61	97.85
1997	97.04	100.00	98.66	99.58	97.85	99.31	99.19	97.31	99.58	99.06	99.44	99.19
1998	99.06	99.70	99.06	98.47	98.39	99.72	99.19	98.12	99.17	99.60	99.31	99.73
1999	99.33	99.40	98.39	98.89	99.46	99.72	99.19	98.79	99.44	99.73	98.61	99.73
2000	99.46	100.00	99.60	99.44	98.39	99.03	98.66	97.72	99.31	99.87	100.00	99.73
2001	98.79	98.81	100.00	99.72	99.46	98.89	98.25	97.85	99.31	99.60	99.31	99.19
2002	99.06	99.40	99.33	99.17	99.46	99.44	99.46	97.85	99.17	99.19	99.58	99.46
2003	99.73	100.00	99.46	99.72	99.60	99.17	99.87	99.60	99.44	99.73	100.00	99.87
2004	99.87	99.86	99.33	99.58	99.60	99.44	99.60	100.00	100.00	99.73	99.58	99.60
2005	99.73	100.00	99.60	99.03	100.00	100.00	99.73	99.73	99.86	99.87	99.31	100.00
2006	99.60	98.66	99.87	99.72	100.00	99.58	99.33	100.00	99.72	100.00	99.86	99.33
2007	100.00	99.85	100.00	99.86	99.46	99.86	99.73	99.87	100.00	99.46	100.00	100.00
2008	100.00	100.00	99.87	99.72	99.73	99.58	99.73	99.73	99.86	100.00	99.72	99.87
Total	96.74	96.31	94.18	94.02	93.42	96.35	96.40	95.23	93.92	94.20	95.98	95.75

Table T1.225: Percentage of monthly hourly data availability from 1970 until 2008 for station IJmuiden.

Year\Month	January	February	March	April	May	June	July	August	September	October	November	December
1970	96.51	98.66	98.92	96.81	95.56	96.81	97.72	96.77	96.11	98.25	99.17	94.89
1971	99.33	98.96	97.98	96.25	96.77	97.92	96.24	97.85	94.44	97.31	99.58	98.39
1972	99.06	97.70	97.31	99.72	97.18	98.33	95.30	98.25	96.11	97.31	98.06	99.46
1973	98.92	98.96	98.12	98.61	97.31	97.92	97.72	97.31	96.94	97.72	99.86	99.33
1974	100.00	99.55	97.98	98.47	97.72	97.78	99.87	94.76	98.06	96.51	99.44	100.00
1975	99.87	98.07	98.12	98.89	98.52	95.83	95.56	97.04	97.92	98.92	99.72	98.66
1976	99.87	98.99	98.92	96.25	97.72	98.75	98.92	99.33	97.64	98.66	99.17	99.06
1977	99.46	99.55	98.12	98.89	99.46	98.61	97.58	96.24	95.83	99.60	98.89	99.33
1978	100.00	99.70	99.73	99.03	98.92	99.31	98.25	99.06	99.86	96.91	99.31	99.46
1979	98.79	96.58	99.60	98.19	95.83	96.81	94.22	95.30	95.28	95.70	97.92	99.73
1980	98.12	97.56	98.66	97.08	98.25	95.42	96.10	93.41	95.28	95.03	97.92	98.66
1981	97.58	95.98	97.98	95.69	96.24	95.00	96.91	92.61	95.42	98.25	98.75	96.91
1982	97.72	98.51	91.94	96.67	92.07	91.39	94.49	94.49	93.33	97.18	97.92	95.16
1983	99.87	97.62	98.25	96.94	95.70	96.11	94.49	93.41	98.06	97.72	95.83	98.52
1984	99.06	95.98	96.91	95.56	93.82	93.61	94.62	95.83	97.22	98.25	99.58	98.39
1985	97.58	92.41	95.03	98.61	95.97	95.00	97.31	97.98	94.31	92.74	98.47	97.31
1986	98.12	98.96	96.77	95.14	97.85	96.81	92.47	95.83	94.58	95.83	97.64	99.06
1987	96.37	99.26	98.25	96.53	96.64	95.28	93.95	96.10	92.50	95.83	94.58	96.10
1988	98.79	98.99	97.31	96.81	97.58	98.61	98.79	97.58	96.81	96.37	94.58	99.60
1989	98.79	99.55	99.19	96.53	96.37	94.58	96.24	93.68	94.17	98.52	96.25	96.37
1990	99.19	100.00	99.33	98.33	95.83	93.61	94.62	94.62	95.00	98.92	94.86	98.92
1991	95.83	93.45	95.83	98.19	98.25	97.36	95.56	93.15	92.36	94.76	97.64	93.28
1992	95.56	94.97	99.06	96.53	97.04	95.00	94.35	97.31	97.22	97.45	98.33	96.77
1993	98.12	97.32	98.79	96.39	97.85	97.08	97.04	94.89	94.86	96.10	97.92	97.72
1994	99.33	98.36	99.60	96.94	96.77	95.28	94.62	96.64	97.22	95.43	95.00	97.31
1995	98.39	98.51	98.25	97.36	93.01	97.64	93.15	96.51	97.08	93.55	97.08	94.35
1996	99.46	94.97	97.18	96.39	96.24	94.03	95.83	94.22	94.03	96.64	96.39	93.82
1997	93.68	99.55	96.37	95.83	93.95	96.94	96.91	93.95	96.81	94.76	97.78	98.79
1998	96.91	99.26	99.60	96.39	96.77	99.03	98.92	96.64	98.19	99.19	96.67	98.92
1999	97.31	96.88	96.37	97.36	96.51	97.50	97.04	93.41	96.67	97.31	96.53	98.52
2000	98.66	98.56	95.43	95.83	95.30	98.06	97.45	92.61	95.56	98.52	99.72	99.46
2001	95.70	96.13	98.39	96.94	98.66	95.56	96.24	96.91	97.08	99.33	95.42	95.97
2002	97.31	99.11	97.18	97.78	99.06	98.19	98.25	93.41	92.50	96.37	96.81	99.33
2003	99.33	99.70	98.12	99.17	98.66	97.22	98.66	97.04	94.58	98.66	99.72	99.73
2004	99.06	99.14	98.79	97.92	98.12	98.19	96.64	99.19	97.92	99.19	98.47	97.58
2005	99.87	99.55	99.60	99.03	98.79	97.64	97.98	96.64	95.97	98.92	97.50	99.19
2006	98.66	98.51	99.60	99.17	99.73	97.92	98.12	99.33	99.31	98.92	99.72	96.10
2007	99.06	98.66	99.60	99.31	97.31	99.44	99.19	98.52	98.75	97.85	99.17	99.33
2008	100.00	99.57	99.73	98.47	99.60	97.78	98.79	100.00	98.47	99.46	99.44	99.46
Total	98.34	98.05	98.00	97.44	97.00	96.75	96.57	96.10	96.14	97.28	97.87	97.92

Table T1.240: Percentage of monthly hourly data availability from 1970 until 2008 for station Schiphol.

Year\Month	January	February	March	April	May	June	July	August	September	October	November	December
1970	99.46	98.51	99.87	99.03	97.58	97.64	98.92	95.56	98.47	99.19	98.61	96.24
1971	99.33	98.07	98.39	98.33	99.06	96.94	97.85	99.19	97.36	97.45	98.75	99.19
1972	99.73	99.43	99.33	98.75	99.33	99.17	95.70	97.85	96.39	93.41	99.44	99.73
1973	96.77	98.36	99.73	99.72	99.46	100.00	99.33	98.39	98.19	99.19	100.00	99.73
1974	100.00	99.55	98.12	99.72	99.46	99.72	99.73	96.37	99.58	95.70	99.86	100.00
1975	100.00	96.88	99.19	99.44	98.66	96.94	96.64	94.49	98.33	99.46	99.86	99.06
1976	99.73	99.86	98.79	98.61	99.60	96.94	99.60	99.87	99.17	99.73	99.44	99.33
1977	99.87	99.70	99.60	100.00	99.60	99.44	99.60	97.72	97.36	99.87	99.86	99.46
1978	99.87	99.70	99.46	99.17	98.25	98.89	99.06	99.46	100.00	99.87	98.61	99.73
1979	97.85	98.96	100.00	99.03	99.60	99.31	99.19	99.46	97.78	99.46	98.89	99.87
1980	99.46	99.71	99.46	100.00	99.33	99.17	99.87	99.19	99.44	99.33	99.86	99.73
1981	98.92	99.55	100.00	99.03	98.92	99.58	99.87	98.66	99.03	99.19	98.89	96.51
1982	95.70	99.85	98.66	98.06	96.51	98.19	97.85	98.79	98.06	99.06	98.33	97.18
1983	100.00	97.62	98.79	99.03	98.79	99.44	96.24	99.33	99.86	100.00	99.58	100.00
1984	99.73	100.00	99.19	98.19	98.52	98.89	99.06	96.24	98.33	99.46	100.00	99.87
1985	98.12	98.66	95.97	99.03	98.79	98.89	98.12	99.46	97.92	98.12	98.47	99.19
1986	99.19	98.66	99.33	98.61	98.66	99.03	98.25	98.39	95.56	98.92	99.86	99.46
1987	98.92	99.26	97.72	98.19	99.73	98.75	99.73	98.92	99.44	98.52	97.78	99.73
1988	99.60	99.86	99.60	98.75	96.91	99.31	99.73	97.31	99.72	98.39	97.08	99.46
1989	98.79	100.00	98.92	98.33	98.92	94.44	97.72	97.45	97.08	98.52	96.67	98.66
1990	100.00	100.00	96.24	95.97	96.37	96.25	97.72	97.85	98.06	99.73	99.03	97.85
1991	97.98	96.43	97.45	98.61	98.92	96.81	93.55	91.67	96.94	97.04	99.17	96.64
1992	94.35	98.85	99.46	98.89	98.66	97.50	98.66	99.06	99.58	99.46	99.72	100.00
1993	100.00	99.85	99.87	99.17	97.98	97.36	99.19	96.24	97.36	98.52	97.92	98.92
1994	99.87	97.32	99.87	99.58	99.06	99.31	95.97	98.39	98.19	95.97	99.31	98.39
1995	99.33	99.70	100.00	98.89	96.77	99.03	96.37	97.45	98.61	95.56	97.36	95.56
1996	100.00	98.85	99.06	95.00	99.33	97.50	98.39	96.91	96.11	98.79	99.17	97.72
1997	98.39	99.70	98.52	98.47	97.98	99.72	98.79	97.18	92.78	96.64	99.31	99.87
1998	97.58	100.00	99.87	97.64	98.66	99.03	97.85	95.43	98.19	98.66	97.08	99.33
1999	99.33	98.51	97.18	97.78	97.58	95.83	99.19	96.24	98.33	98.52	97.08	99.33
2000	99.73	100.00	97.85	94.44	94.89	95.42	94.09	92.34	97.78	99.87	100.00	98.52
2001	95.30	96.43	97.85	97.78	98.66	96.53	93.01	95.83	96.25	98.92	97.78	96.24
2002	97.85	98.07	98.25	97.78	98.25	97.50	96.64	96.10	95.14	97.31	97.92	97.72
2003	97.72	99.11	97.45	98.61	98.25	97.22	99.60	96.64	98.33	97.98	99.86	98.66
2004	98.39	99.57	98.52	97.92	98.12	97.64	98.25	99.19	99.17	100.00	98.33	99.46
2005	100.00	100.00	99.33	98.47	98.92	98.33	98.66	96.77	99.44	99.46	99.17	99.73
2006	99.33	97.92	98.92	100.00	99.19	97.08	96.51	98.25	98.06	100.00	99.72	98.92
2007	99.46	99.55	99.60	99.44	99.19	99.03	98.79	99.46	99.44	97.45	99.72	98.39
2008	99.46	99.14	99.33	98.75	98.12	98.61	98.79	99.87	98.19	99.60	99.72	99.19
Total	98.85	99.00	98.84	98.52	98.48	98.11	98.00	97.51	98.03	98.52	98.90	98.78

Table T1.270: Percentage of monthly hourly data availability from 1970 until 2008 for station Leeuwarden.

Year/Month	January	February	March	April	May	June	July	August	September	October	November	December
1970	97.85	99.55	99.87	98.75	98.52	97.36	98.25	96.91	98.47	99.60	99.72	99.06
1971	100.00	99.70	99.46	97.08	98.39	95.97	98.79	97.04	97.50	97.85	98.75	99.46
1972	99.46	98.71	98.52	98.06	97.18	95.69	94.89	97.85	96.11	94.62	99.17	99.33
1973	98.25	98.36	97.18	98.33	97.45	98.89	98.79	95.83	97.22	98.25	99.72	99.19
1974	100.00	98.66	98.79	98.75	99.19	99.58	99.87	96.91	98.75	97.72	99.17	99.87
1975	100.00	97.47	98.25	98.33	99.46	97.50	96.37	97.18	98.33	98.92	99.44	99.73
1976	99.73	100.00	98.52	98.89	98.79	93.61	97.98	98.39	96.11	98.66	99.03	98.66
1977	98.12	98.36	98.52	99.72	97.31	98.61	98.92	95.97	95.83	98.52	99.58	98.39
1978	99.06	97.62	99.06	98.61	96.51	96.53	96.91	98.25	98.61	98.79	99.58	97.45
1979	90.59	98.81	99.46	96.39	97.31	97.50	98.66	96.64	96.81	97.58	98.47	99.87
1980	97.31	99.71	99.46	98.61	97.72	98.47	98.39	96.24	96.39	97.85	99.44	99.87
1981	97.98	97.32	99.73	97.92	96.51	97.22	98.66	93.15	95.14	96.51	97.36	97.04
1982	95.83	98.51	96.77	94.31	97.31	96.53	97.58	98.12	95.42	97.85	98.19	97.98
1983	100.00	97.02	99.19	96.53	96.77	97.64	95.30	96.77	99.58	98.39	98.33	97.98
1984	99.60	98.99	99.46	97.08	97.18	96.25	97.18	94.09	97.22	98.66	99.86	96.91
1985	98.52	97.32	96.91	98.75	98.39	94.17	98.52	97.72	95.83	95.30	96.81	98.25
1986	98.39	94.05	95.43	95.69	96.37	95.28	95.83	95.70	91.25	96.37	99.03	98.12
1987	97.72	95.98	92.61	94.17	98.25	93.61	96.77	97.04	92.78	95.16	93.06	96.64
1988	98.92	99.57	98.52	95.56	97.04	96.11	97.98	96.77	94.86	89.11	96.25	98.52
1989	98.79	98.81	98.52	95.42	94.35	88.61	92.07	90.99	90.28	95.56	87.22	89.78
1990	98.12	99.70	97.58	97.36	86.29	84.17	90.99	86.16	92.78	90.32	93.33	95.97
1991	90.32	92.71	90.86	96.39	95.03	91.67	91.13	88.31	84.72	85.08	93.47	92.07
1992	84.68	96.12	97.31	95.14	90.73	89.58	89.52	93.95	87.50	91.40	96.81	85.08
1993	94.22	90.33	93.55	94.44	95.30	90.42	93.82	90.46	88.06	92.88	88.61	98.25
1994	98.79	90.03	98.66	94.58	94.09	94.31	82.66	89.65	92.78	83.60	89.44	91.40
1995	95.16	95.83	98.92	96.25	83.33	93.47	87.37	93.68	90.28	92.07	95.28	93.15
1996	99.06	95.55	98.52	95.42	96.77	91.67	96.91	93.82	91.81	93.68	96.94	94.22
1997	92.88	99.40	97.45	95.56	93.95	95.56	95.16	93.55	89.72	95.03	97.08	98.52
1998	96.91	99.55	98.66	95.28	94.62	97.92	97.04	94.35	93.75	99.73	95.00	98.66
1999	97.31	96.58	95.16	96.81	96.91	93.06	95.16	93.01	95.42	97.98	94.31	97.58
2000	99.06	99.28	97.31	93.61	94.89	95.42	93.68	92.47	94.31	98.52	100.00	97.98
2001	94.76	95.09	97.98	96.67	96.91	96.67	92.74	94.62	94.44	98.25	94.44	94.62
2002	96.10	98.51	98.12	94.17	95.83	96.94	93.68	88.71	91.39	93.01	94.72	98.79
2003	99.19	99.70	98.52	99.31	97.72	96.11	97.85	97.45	93.75	97.04	99.86	99.19
2004	99.19	99.28	99.46	98.19	97.58	97.22	95.97	98.52	98.33	99.46	98.89	98.39
2005	99.73	99.85	98.79	98.33	98.12	97.50	97.98	97.98	95.56	99.46	98.33	99.06
2006	99.06	98.36	98.52	99.44	99.19	96.25	97.04	98.12	99.58	99.60	99.44	99.33
2007	99.73	99.85	99.33	98.47	97.85	96.53	97.72	97.98	99.31	95.03	99.72	98.79
2008	98.92	99.28	99.46	97.36	98.39	97.78	98.52	98.12	96.11	99.73	99.86	99.46
Total	97.42	97.68	97.91	96.92	96.24	95.32	95.71	95.09	94.67	95.98	97.02	97.25

Table T1.280: Percentage of monthly hourly data availability from 1970 until 2008 for station Eelde.

Year\Month	January	February	March	April	May	June	July	August	September	October	November	December
1970	99.06	99.85	99.46	100.00	100.00	100.00	100.00	99.46	99.86	99.60	99.86	99.87
1971	100.00	99.85	100.00	100.00	99.87	100.00	99.73	99.87	100.00	100.00	100.00	99.73
1972	99.19	100.00	99.33	100.00	99.87	99.58	99.73	100.00	100.00	99.60	100.00	99.87
1973	100.00	99.85	99.87	99.86	99.46	99.72	99.60	99.73	99.58	99.73	100.00	99.73
1974	100.00	99.85	99.46	99.72	99.87	100.00	100.00	99.87	99.86	99.46	100.00	100.00
1975	100.00	99.70	99.73	100.00	99.87	99.86	99.87	99.60	99.72	99.73	100.00	99.73
1976	99.87	100.00	99.06	97.78	99.33	99.58	99.46	99.87	99.44	99.60	99.86	99.46
1977	99.73	99.70	99.73	100.00	100.00	99.86	99.87	98.52	99.31	99.73	99.86	99.87
1978	100.00	99.70	99.87	99.86	99.46	99.72	99.87	99.60	99.86	99.19	99.86	99.87
1979	99.73	99.85	100.00	99.86	99.33	98.61	99.87	99.19	99.86	99.87	100.00	99.60
1980	99.87	99.57	99.73	99.86	99.87	100.00	99.87	99.73	99.86	99.73	100.00	100.00
1981	99.46	100.00	99.73	99.58	100.00	100.00	99.87	99.33	100.00	99.19	99.86	99.87
1982	99.87	100.00	99.46	99.72	99.60	98.75	100.00	99.33	99.58	100.00	99.17	99.87
1983	100.00	99.70	100.00	98.61	99.06	99.17	99.33	99.87	99.86	100.00	99.72	99.87
1984	100.00	99.71	99.73	99.44	99.60	99.03	99.19	99.46	100.00	99.73	99.86	99.73
1985	99.60	99.70	99.33	99.58	99.87	99.44	99.06	100.00	99.86	99.46	100.00	100.00
1986	99.87	100.00	99.46	99.44	99.87	99.86	99.19	99.60	99.17	99.87	99.86	100.00
1987	100.00	100.00	99.87	99.72	99.87	99.86	100.00	99.87	99.44	100.00	99.86	100.00
1988	100.00	100.00	100.00	99.86	100.00	100.00	100.00	100.00	99.86	99.87	99.44	100.00
1989	100.00	100.00	100.00	99.72	99.87	100.00	99.87	99.87	99.72	100.00	100.00	100.00
1990	100.00	100.00	100.00	100.00	100.00	99.72	100.00	100.00	100.00	100.00	100.00	99.87
1991	100.00	99.40	99.87	100.00	99.87	99.86	100.00	99.33	100.00	99.60	100.00	99.46
1992	100.00	99.86	99.87	100.00	99.87	99.72	99.73	99.33	100.00	100.00	100.00	99.87
1993	99.87	100.00	99.87	100.00	100.00	99.86	100.00	100.00	99.86	99.73	99.72	100.00
1994	99.87	99.85	100.00	99.58	100.00	99.44	98.66	97.04	99.03	99.19	98.33	99.33
1995	99.19	98.96	99.19	98.19	97.04	98.06	95.03	97.98	97.22	97.85	97.22	99.46
1996	99.46	97.41	96.77	97.08	98.66	95.83	97.85	96.64	98.75	98.92	99.03	99.46
1997	98.25	99.40	96.37	97.64	97.45	97.36	96.51	95.56	98.19	97.85	97.78	99.19
1998	99.60	99.11	99.33	97.08	98.25	98.19	99.06	97.04	98.75	98.92	98.75	99.33
1999	97.31	98.81	98.39	97.92	98.79	97.50	97.31	96.10	99.44	97.31	99.44	99.73
2000	99.46	99.43	97.45	96.25	96.24	97.50	96.91	97.45	99.03	98.66	100.00	99.73
2001	98.12	97.32	99.19	98.89	98.12	98.06	97.72	96.37	97.36	99.60	98.33	98.25
2002	99.06	99.70	97.72	99.31	98.66	98.47	98.66	95.43	95.69	97.98	99.31	100.00
2003	100.00	99.40	99.73	100.00	99.06	99.17	99.87	99.19	98.89	99.87	99.31	99.73
2004	100.00	98.71	99.87	99.44	99.33	99.58	99.46	99.33	100.00	99.73	99.72	99.33
2005	99.73	99.85	99.60	98.89	99.46	99.72	99.19	99.73	99.17	99.46	99.44	100.00
2006	100.00	99.85	99.87	99.86	99.60	99.58	99.46	99.33	99.58	99.60	99.86	99.87
2007	99.60	99.85	99.73	99.72	99.46	98.89	99.33	99.87	99.72	99.33	99.72	100.00
2008	100.00	99.71	99.87	99.03	99.73	98.89	99.46	99.33	99.72	99.87	100.00	100.00
Total	99.63	99.58	99.40	99.27	99.34	99.19	99.19	98.92	99.37	99.43	99.57	99.73

Table T1.310: Percentage of monthly hourly data availability from 1970 until 2008 for station Vlissingen.

Year\Month	January	February	March	April	May	June	July	August	September	October	November	December
1970	92.74	95.24	94.62	95.56	94.09	93.61	97.45	94.76	93.61	96.91	97.64	92.61
1971	97.85	96.13	95.97	95.56	95.30	96.25	91.67	95.30	85.28	94.49	96.94	97.31
1972	98.92	96.41	94.62	97.92	96.10	93.19	96.37	95.43	89.44	95.83	98.61	98.12
1973	96.91	95.54	94.62	96.39	95.16	97.22	94.49	94.62	92.08	93.68	97.36	96.64
1974	99.06	97.62	92.47	97.36	94.22	97.64	98.66	92.20	96.39	91.80	99.72	99.46
1975	99.87	98.07	99.06	97.50	98.66	93.75	94.49	96.37	96.53	97.04	96.11	95.03
1976	98.92	99.14	98.52	94.86	97.85	96.81	96.24	95.97	94.58	97.58	97.36	98.12
1977	96.37	98.07	99.33	96.94	97.85	97.92	97.31	93.28	91.67	98.66	98.47	98.39
1978	99.06	97.32	96.10	96.53	94.76	96.94	96.64	96.51	97.08	92.88	97.78	98.92
1979	97.18	97.17	99.33	97.22	93.01	92.36	93.28	93.95	91.11	94.62	95.97	98.25
1980	98.12	99.14	98.52	98.06	95.56	97.92	97.98	91.53	93.75	95.16	98.33	97.85
1981	95.70	95.24	97.85	96.94	97.31	97.22	97.31	87.90	92.92	97.85	97.08	95.83
1982	98.12	99.11	95.43	97.36	92.20	96.81	95.16	96.64	93.19	96.77	99.86	95.70
1983	100.00	99.26	100.00	98.06	97.98	96.67	91.80	96.24	97.50	93.41	94.17	98.66
1984	98.39	97.56	96.37	92.08	94.62	92.92	96.10	94.76	97.36	98.79	99.58	98.39
1985	96.51	94.64	95.70	98.61	97.72	95.83	97.72	97.98	93.75	93.82	98.06	98.25
1986	97.98	97.92	98.39	97.92	99.06	99.44	96.77	96.51	91.67	98.25	98.06	99.19
1987	96.10	99.11	97.85	96.39	96.37	95.97	92.61	94.89	90.83	95.97	94.72	94.09
1988	98.79	98.99	96.77	96.11	96.77	98.75	98.79	94.89	94.86	93.82	95.28	98.66
1989	97.98	98.21	98.66	95.00	92.34	90.42	92.20	92.34	87.64	95.03	91.39	89.25
1990	98.92	99.55	97.31	95.69	89.52	90.83	91.40	90.86	90.56	97.85	93.75	97.45
1991	94.89	90.33	93.01	96.11	95.16	94.86	90.73	87.63	81.94	88.58	95.42	89.78
1992	92.20	92.82	98.66	96.25	92.34	87.64	88.84	94.09	95.97	92.61	98.47	93.68
1993	97.45	92.41	97.45	94.03	95.30	93.61	93.82	90.05	89.72	93.28	94.17	97.04
1994	98.25	94.79	99.19	96.11	93.28	93.06	88.31	89.52	94.03	90.59	92.78	94.76
1995	97.72	96.58	96.77	93.89	86.96	93.89	88.17	87.37	92.36	87.77	92.64	86.83
1996	96.64	91.95	94.09	93.06	93.95	88.19	91.53	85.75	85.83	92.47	94.44	90.46
1997	87.63	98.66	92.88	91.94	90.19	94.03	92.47	85.48	89.86	87.50	96.11	97.45
1998	97.18	98.96	98.52	96.25	92.07	98.06	95.16	90.32	94.86	99.19	94.31	98.52
1999	95.16	94.64	94.22	95.00	94.62	93.06	94.76	87.23	94.58	93.01	95.42	97.85
2000	97.72	98.13	92.74	92.92	90.05	94.03	90.73	86.02	91.39	96.77	100.00	98.39
2001	96.24	94.20	96.64	96.53	94.76	90.97	90.86	90.73	95.42	98.66	92.50	92.61
2002	95.56	98.66	95.83	93.47	95.70	94.58	94.49	85.48	83.47	96.24	96.81	98.25
2003	98.79	100.00	97.04	99.44	97.45	97.08	98.66	93.68	89.03	97.85	99.03	99.06
2004	99.46	98.28	99.06	97.64	96.91	98.19	96.37	99.60	97.92	97.72	96.53	98.92
2005	99.87	99.40	99.46	98.47	99.19	98.06	97.45	97.31	93.06	97.85	97.50	100.00
2006	99.33	99.55	98.66	99.03	99.33	97.08	98.66	99.33	98.75	99.19	99.86	97.58
2007	98.79	98.21	97.31	97.78	97.04	98.75	98.25	97.45	97.78	95.30	99.17	98.25
2008	99.87	97.27	99.46	96.67	99.46	96.94	97.85	99.33	96.94	97.31	99.44	99.33
Total	97.34	97.03	96.88	96.22	95.13	95.14	94.65	93.06	92.69	95.18	96.69	96.54

Table T1.344: Percentage of monthly hourly data availability from 1970 until 2008 for station Zestienhoven.

Year\Month	January	February	March	April	May	June	July	August	September	October	November	December
1970	94.89	97.47	97.04	96.39	90.46	90.42	95.30	91.67	92.08	95.97	97.08	93.68
1971	98.66	98.36	97.04	97.08	96.77	95.83	90.99	98.12	86.94	95.97	96.81	94.09
1972	97.45	94.40	88.04	99.17	97.45	98.47	97.18	98.52	92.50	95.70	92.50	96.64
1973	88.98	91.96	96.77	99.44	97.85	96.11	98.52	97.98	92.22	92.88	99.17	93.28
1974	99.46	99.55	96.24	99.58	98.52	96.53	99.06	94.49	97.50	94.22	98.47	100.00
1975	99.33	96.88	99.73	94.17	97.04	96.11	94.09	98.79	94.86	97.58	95.69	96.24
1976	98.92	97.13	95.56	90.14	93.82	93.19	95.97	97.45	92.64	96.91	97.64	94.09
1977	96.51	98.51	98.92	98.89	99.06	97.64	98.92	94.22	94.17	98.52	98.89	98.79
1978	99.73	97.62	99.19	97.50	92.07	95.14	95.30	96.24	98.33	94.49	98.33	98.79
1979	97.18	96.73	97.85	97.22	95.83	98.47	98.25	98.25	94.72	98.12	97.78	99.73
1980	99.60	99.71	98.52	97.92	97.58	96.67	99.06	94.49	95.69	95.43	99.17	99.46
1981	97.85	96.28	98.12	98.75	95.30	95.97	97.72	92.47	97.08	98.12	99.17	97.45
1982	97.31	98.07	95.30	98.06	95.56	96.11	97.18	97.31	95.56	99.46	97.78	97.31
1983	99.87	99.55	98.79	96.25	96.77	97.92	96.77	98.66	96.53	97.18	97.22	99.06
1984	99.33	97.41	95.30	95.00	94.76	93.33	95.43	92.74	96.53	97.58	98.19	97.58
1985	95.30	90.33	97.31	96.39	95.43	97.36	95.16	97.31	93.47	91.53	98.19	98.12
1986	98.52	98.36	95.70	96.39	96.10	98.89	94.49	96.10	93.75	98.66	95.97	99.73
1987	96.10	98.96	98.12	95.83	95.70	97.78	98.25	95.97	95.28	98.39	97.64	96.91
1988	99.73	99.43	98.12	97.22	96.91	96.25	97.58	95.03	95.97	96.64	98.33	99.73
1989	98.79	98.07	96.51	95.28	96.37	92.78	92.61	97.72	95.42	98.39	98.75	96.64
1990	100.00	99.55	98.79	98.75	96.77	97.36	97.18	96.24	98.19	99.33	96.94	98.79
1991	99.73	93.60	95.16	96.67	96.91	95.00	93.95	95.03	96.39	95.03	97.64	95.70
1992	95.30	93.97	97.58	96.81	95.43	96.94	95.43	98.52	99.44	99.60	99.86	98.52
1993	99.19	98.51	99.33	97.92	98.52	96.53	99.06	96.37	96.67	98.66	98.89	99.46
1994	99.46	98.21	99.46	96.94	96.77	97.22	95.03	95.16	97.36	95.30	97.08	98.79
1995	99.73	99.55	99.19	97.22	93.68	96.94	94.49	97.85	99.17	97.45	98.06	98.79
1996	99.87	98.85	98.52	96.67	97.85	95.83	97.98	96.77	98.75	97.98	99.72	98.92
1997	97.98	100.00	97.31	96.81	95.56	97.92	96.37	95.83	97.78	98.79	98.61	99.87
1998	99.73	99.85	99.73	96.81	95.70	97.08	96.51	93.55	97.22	95.97	94.03	97.58
1999	97.04	93.90	91.80	95.14	91.53	94.03	94.49	89.78	94.86	96.91	96.81	99.06
2000	95.56	98.28	94.89	94.31	93.68	95.56	95.43	91.67	93.33	98.39	99.58	98.12
2001	92.61	95.68	95.56	97.50	98.52	95.00	94.35	93.01	96.53	97.72	93.19	93.28
2002	97.58	98.66	95.43	95.00	96.24	95.97	96.24	89.92	89.31	95.70	96.67	94.76
2003	98.66	97.47	94.62	97.08	95.56	95.83	95.83	93.68	90.69	98.25	99.72	99.46
2004	99.19	97.84	98.52	98.89	95.83	97.64	92.88	98.39	97.64	98.52	96.81	97.58
2005	99.19	98.96	99.60	97.08	98.12	96.39	96.24	96.64	92.36	98.66	97.64	98.52
2006	99.46	97.62	99.60	98.75	98.52	95.14	96.51	98.79	96.53	99.87	99.72	98.79
2007	99.46	99.85	97.72	97.64	97.85	98.06	97.98	96.24	97.22	95.56	98.61	98.79
2008	100.00	97.13	99.46	96.94	97.98	98.19	95.56	98.79	98.47	98.79	99.44	98.92
Total	98.03	97.49	97.19	96.91	96.16	96.25	96.14	95.79	95.36	97.13	97.74	97.72

Table T1.370: Percentage of monthly hourly data availability from 1970 until 2008 for station Eindhoven.

Station \ Sector	omni-directional	345°N -	15°N -	45°N -	75°N -	105°N -	135°N -	165°N -	195°N -	225°N -	255°N -	285°N -	315°N -
		15°N	45°N	75°N	105°N	135°N	165°N	195°N	225°N	255°N	285°N	315°N	345°N
Ijmuiden	18.3	12.9	10.6	11.9	10.6	8.3	9.5	14.4	16.3	16.2	17.0	15.7	13.9
Texelhors	18.0	15.3	9.7	11.5	10.4	10.4	10.8	14.8	15.1	14.8	15.3	17.1	14.8
De Kooy	16.9	10.7	10.3	9.5	8.9	9.5	10.9	13.8	17.8	17.5	16.8	14.8	11.7
Schiphol	16.6	8.4	9.7	9.2	8.3	6.9	9.4	11.2	12.9	17.2	14.0	14.0	11.3
De Bilt	11.6	8.6	7.4	7.9	6.8	7.5	8.0	9.0	11.5	11.0	9.4	9.5	7.5
Soesterberg	11.5	7.4	7.4	8.5	8.5	8.1	7.5	9.1	9.9	12.2	10.5	9.6	8.3
Leeuwarden	15.0	9.9	9.0	10.3	9.1	9.0	8.2	11.6	13.5	14.6	14.0	14.6	12.1
Deelen	13.4	8.7	8.3	9.1	8.2	9.0	9.0	10.0	11.2	12.5	10.3	9.8	9.9
Lauwersoog	15.9	11.9	11.8	12.0	12.5	10.8	10.4	12.5	14.1	15.9	15.5	14.8	14.9
Eelde	15.3	7.3	8.3	8.4	8.0	7.8	7.5	10.0	12.6	13.2	12.2	10.6	9.7
Twenthe	12.1	6.5	6.3	6.7	6.8	5.6	7.2	10.0	10.9	11.0	9.8	9.4	7.4
Cadzand	16.9	13.4	11.6	11.3	10.3	7.0	7.8	11.6	15.3	17.9	15.5	12.8	12.7
Vlissingen	17.0	9.2	10.3	9.2	7.9	8.8	9.7	13.1	14.3	16.9	15.4	13.5	10.4
L.E. Goeree	16.3	11.7	11.8	8.8	9.9	8.9	10.7	14.4	13.5	15.4	14.5	14.6	12.4
Hoek van Holland	17.3	14.4	12.9	11.0	9.1	9.3	10.0	13.8	16.0	17.0	17.0	15.3	16.7
Zestienhoven	14.5	9.2	8.2	9.4	8.1	7.4	8.4	11.1	13.7	13.5	13.1	13.1	10.2
Gilze-Rijen	12.1	7.6	7.9	9.2	7.3	7.1	7.1	9.9	10.7	12.9	11.1	10.9	7.8
Herwijnen	15.0	8.2	7.3	6.9	8.0	7.3	8.4	9.3	13.6	15.1	14.6	11.4	8.1
Eindhoven	13.3	7.4	7.1	8.1	7.1	8.1	7.0	9.2	11.2	12.2	13.4	11.0	8.6
Volkel	13.0	6.6	6.8	9.0	8.0	8.3	6.4	8.3	11.9	11.1	11.5	8.5	6.7
Beek	14.4	6.9	7.2	8.6	7.5	6.6	6.0	10.0	13.1	15.7	10.0	9.1	7.8

Table T3.1: Threshold used is the U_p POT/exponential model.

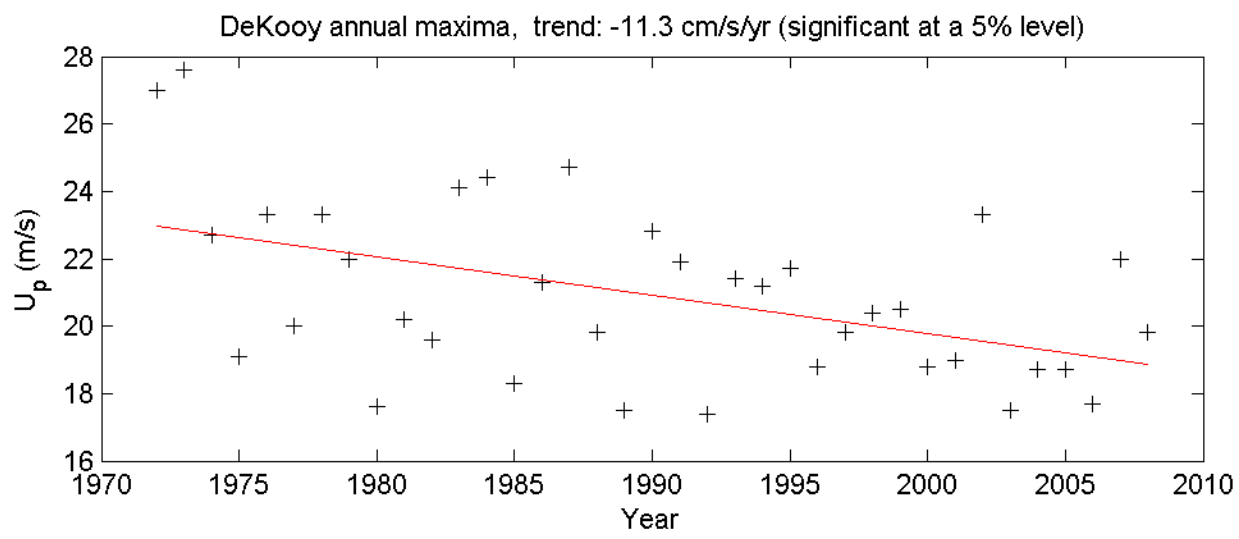
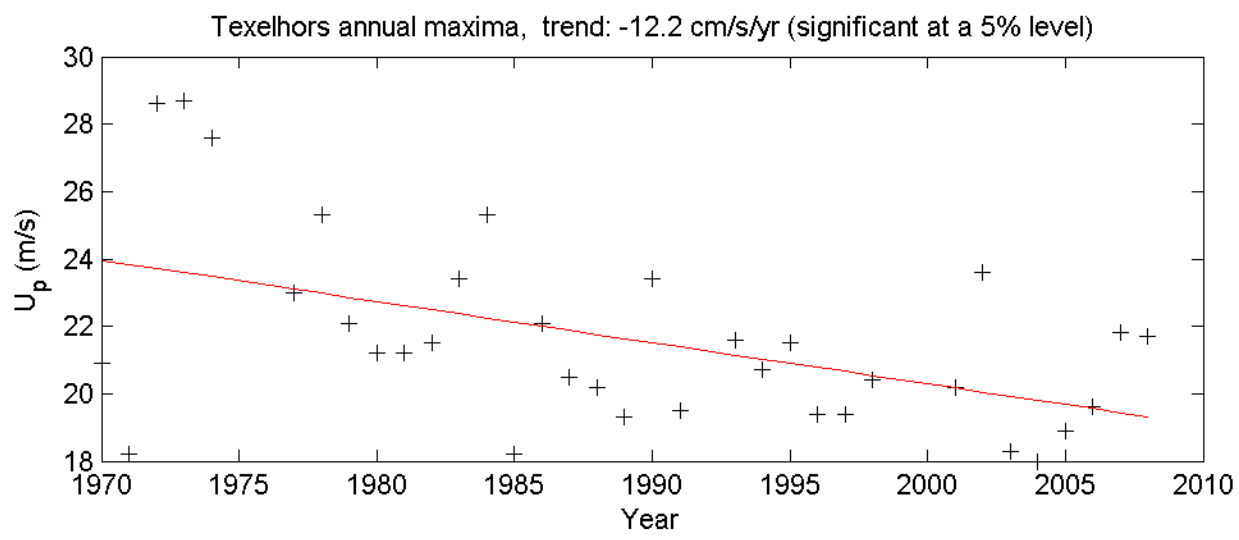
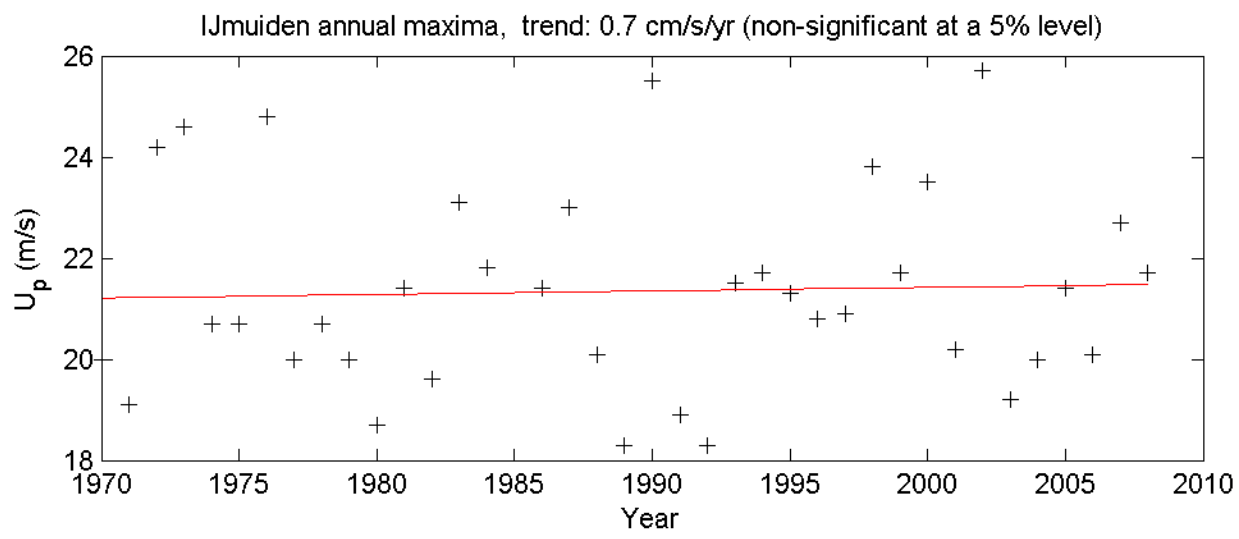
Station \ Sector	omni-directional	345°N -	15°N -	45°N -	75°N -	105°N -	135°N -	165°N -	195°N -	225°N -	255°N -	285°N -	315°N -
		15°N	45°N	75°N	105°N	135°N	165°N	195°N	225°N	255°N	285°N	315°N	345°N
Ijmuiden	3.45	3.05	5.15	2.10	3.61	4.77	5.02	2.56	4.83	3.96	2.51	2.86	3.32
Texelhors	4.31	1.84	6.77	3.10	5.81	5.03	4.31	3.88	6.44	7.04	5.39	2.35	4.06
De Kooy	4.04	2.54	2.48	4.80	5.21	2.59	2.05	1.99	1.39	1.45	1.91	2.73	3.76
Schiphol	2.99	6.24	2.65	4.59	3.20	6.80	3.23	3.17	4.30	1.78	2.94	1.89	2.73
De Bilt	6.04	1.67	4.61	3.13	4.93	3.05	2.62	3.68	3.02	4.93	5.75	2.44	4.45
Soesterberg	6.60	5.74	4.58	2.13	2.26	2.32	5.42	2.48	5.66	2.96	6.06	4.63	5.33
Leeuwarden	4.52	3.82	3.77	2.03	3.22	2.60	5.51	2.75	2.52	2.83	3.09	1.71	3.09
Deelen	4.01	2.64	3.80	2.66	3.98	1.18	2.85	3.71	5.11	4.04	7.00	5.46	2.48
Lauwersoog	7.24	4.76	2.92	2.94	1.67	1.95	1.98	3.54	4.68	2.78	3.77	3.38	2.63
Eelde	2.54	7.50	3.88	3.20	3.57	2.69	4.78	4.97	3.33	4.84	4.60	4.49	4.23
Twenthe	3.99	6.08	5.81	6.27	4.68	7.15	2.72	2.97	3.82	3.41	5.61	4.60	6.74
Cadzand	5.14	2.13	3.85	2.78	2.16	4.97	6.34	4.91	2.72	2.27	3.48	7.33	4.80
Vlissingen	3.43	4.17	1.39	3.38	5.46	3.14	3.38	3.07	3.38	2.71	2.60	2.06	3.38
L.E. Goeree	5.89	5.34	3.40	8.36	3.11	5.54	3.56	2.20	8.87	5.08	5.25	3.76	5.76
Hoek van Holland	4.09	2.08	2.45	3.25	4.14	3.44	4.50	2.60	2.24	2.16	1.90	3.62	1.09
Zestienhoven	5.72	4.34	5.67	1.86	3.59	4.92	4.60	4.79	3.22	6.20	4.12	2.55	4.95
Gilze-Rijen	6.66	5.32	4.50	2.27	5.08	4.14	5.48	4.37	5.85	2.21	4.98	3.11	6.85
Herwijnen	3.40	3.92	5.46	5.58	4.04	4.15	2.64	5.58	2.09	2.41	1.92	3.81	7.50
Eindhoven	4.43	5.30	6.54	3.74	4.74	1.71	4.74	4.66	5.88	4.32	2.16	2.98	4.85
Volkel	3.88	5.52	5.46	2.43	3.33	1.48	6.99	6.83	3.96	6.72	3.25	4.48	6.23
Beek	3.18	5.66	6.18	1.89	4.63	2.03	6.16	4.10	4.47	1.29	5.76	3.76	3.50

Table T3.2: λ_u estimates of the U_p POT/exponential model.

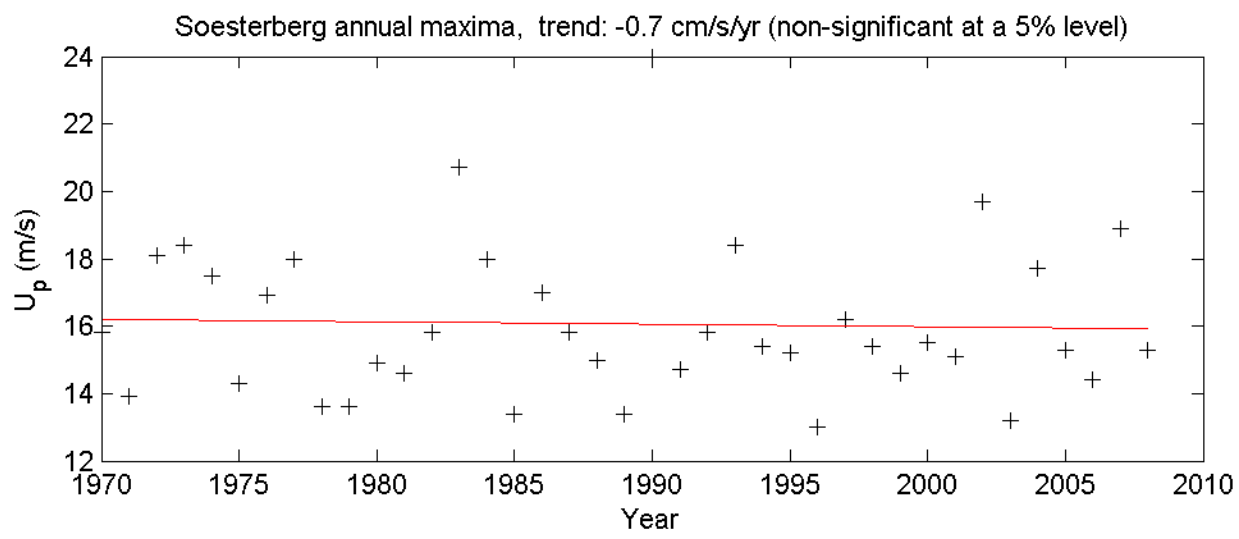
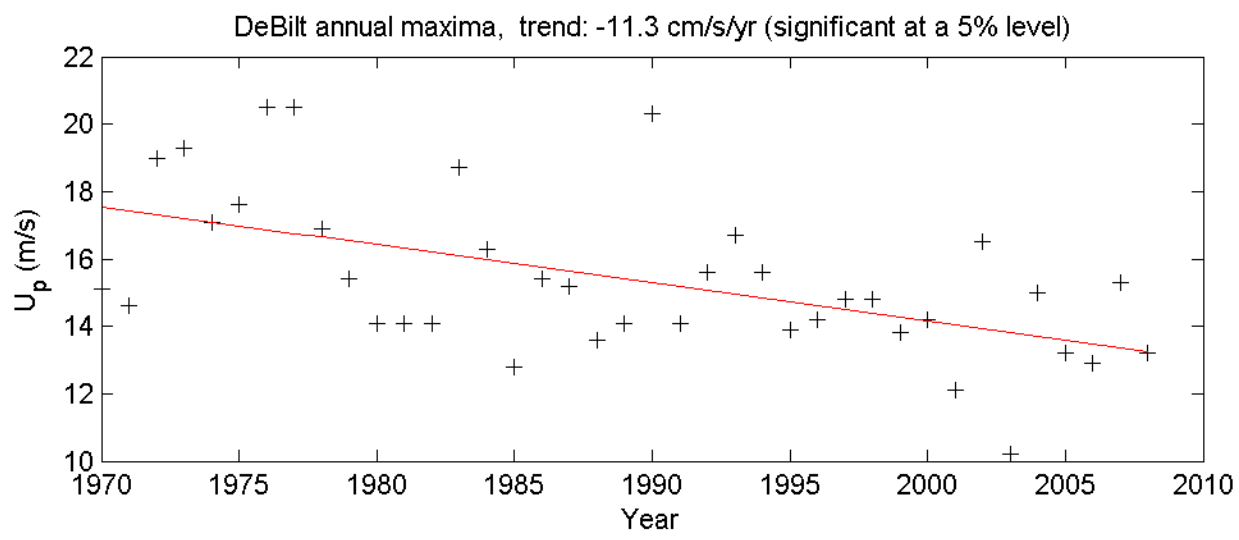
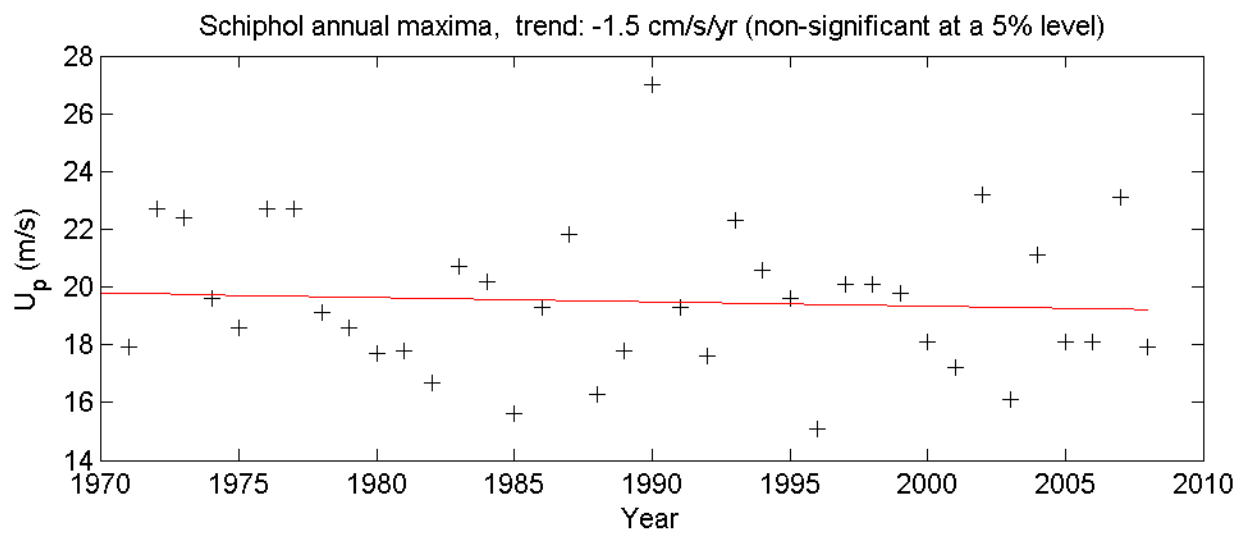
Station \ Sector	omni-directional						
IJmuiden	1.65 (1.40, 1.93)						
Texelhors	1.95 (1.63, 2.30)						
De Kooy	2.03 (1.72, 2.36)						
Schiphol	1.86 (1.53, 2.20)						
De Bilt	1.80 (1.57, 2.04)						
Soesterberg	2.03 (1.78, 2.28)						
Leeuwarden	2.13 (1.81, 2.46)						
Deelen	1.97 (1.68, 2.29)						
Lauwersoog	1.82 (1.61, 2.03)						
Eelde	1.90 (1.54, 2.29)						
Twenthe	2.09 (1.76, 2.43)						
Cadzand	1.90 (1.63, 2.19)						
Vlissingen	1.76 (1.47, 2.05)						
L.E. Goeree	1.76 (1.55, 2.00)						
Hoek van Holland	1.65 (1.43, 1.90)						
Zestienhoven	1.96 (1.71, 2.22)						
Gilze-Rijen	1.88 (1.66, 2.11)						
Herwijnen	2.05 (1.71, 2.44)						
Eindhoven	1.65 (1.41, 1.90)						
Volkel	1.93 (1.61, 2.26)						
Beek	1.77 (1.49, 2.08)						
Station \ Sector	345°N -15°N	15°N -45°N	45°N -75°N	75°N -105°N	105°N -135°N	135°N -165°N	
IJmuiden	1.56 (1.32, 1.87)	1.44 (1.23, 1.66)	1.22 (0.96, 1.50)	1.40 (1.19, 1.62)	1.17 (1.01, 1.35)	1.57 (1.36, 1.80)	
Texelhors	1.59 (1.24, 1.97)	2.01 (1.77, 2.28)	1.53 (1.24, 1.81)	1.78 (1.55, 2.01)	1.58 (1.36, 1.81)	1.95 (1.65, 2.26)	
De Kooy	1.90 (1.53, 2.31)	1.92 (1.57, 2.30)	2.00 (1.71, 2.32)	1.71 (1.48, 1.94)	1.18 (0.95, 1.45)	1.36 (1.07, 1.65)	
Schiphol	1.70 (1.50, 1.91)	1.23 (1.01, 1.48)	1.38 (1.19, 1.57)	1.30 (1.11, 1.52)	1.08 (0.95, 1.20)	1.09 (0.92, 1.29)	
De Bilt	0.97 (0.76, 1.22)	1.19 (1.02, 1.37)	1.28 (1.07, 1.49)	1.26 (1.10, 1.43)	1.04 (0.87, 1.22)	0.94 (0.77, 1.14)	
Soesterberg	1.12 (0.99, 1.27)	1.00 (0.86, 1.15)	0.76 (0.60, 0.92)	0.95 (0.78, 1.14)	0.69 (0.57, 0.83)	0.86 (0.76, 0.97)	
Leeuwarden	1.72 (1.48, 1.99)	1.40 (1.18, 1.60)	1.85 (1.43, 2.34)	1.45 (1.22, 1.70)	0.98 (0.81, 1.16)	1.37 (1.20, 1.55)	
Deelen	1.10 (0.89, 1.29)	1.10 (0.95, 1.27)	1.17 (0.96, 1.39)	1.14 (0.98, 1.33)	0.96 (0.70, 1.24)	1.05 (0.87, 1.24)	
Lauwersoog	1.80 (1.56, 2.02)	1.39 (1.15, 1.65)	1.42 (1.18, 1.67)	1.26 (1.00, 1.54)	0.99 (0.78, 1.22)	1.26 (1.00, 1.55)	
Eelde	1.35 (1.21, 1.49)	1.03 (0.87, 1.19)	1.26 (1.06, 1.48)	1.09 (0.93, 1.27)	0.96 (0.77, 1.15)	1.32 (1.14, 1.51)	
Twenthe	1.08 (0.95, 1.22)	1.13 (0.98, 1.31)	0.99 (0.88, 1.12)	0.91 (0.79, 1.04)	0.93 (0.83, 1.03)	1.13 (0.93, 1.34)	
Cadzand	1.93 (1.53, 2.36)	1.23 (1.03, 1.43)	1.41 (1.15, 1.67)	1.42 (1.13, 1.76)	1.21 (1.04, 1.39)	1.58 (1.38, 1.78)	
Vlissingen	1.30 (1.11, 1.50)	0.95 (0.74, 1.17)	1.23 (1.05, 1.43)	1.32 (1.16, 1.49)	1.35 (1.14, 1.55)	1.40 (1.20, 1.62)	
L.E. Goeree	1.74 (1.50, 1.98)	1.45 (1.18, 1.72)	1.78 (1.58, 1.98)	1.53 (1.19, 1.94)	1.47 (1.28, 1.68)	1.28 (1.07, 1.48)	
Hoek van Holland	1.44 (1.14, 1.74)	1.54 (1.25, 1.87)	1.35 (1.13, 1.59)	1.26 (1.09, 1.44)	1.22 (1.03, 1.42)	1.34 (1.15, 1.53)	
Zestienhoven	1.59 (1.36, 1.80)	1.45 (1.27, 1.64)	0.89 (0.71, 1.08)	1.10 (0.93, 1.29)	1.02 (0.87, 1.19)	1.22 (1.06, 1.40)	
Gilze-Rijen	1.31 (1.15, 1.49)	1.19 (1.01, 1.36)	1.09 (0.89, 1.31)	1.30 (1.14, 1.47)	1.02 (0.87, 1.16)	1.03 (0.90, 1.17)	
Herwijnen	1.28 (1.08, 1.47)	1.35 (1.18, 1.53)	1.46 (1.27, 1.66)	1.31 (1.09, 1.55)	1.21 (1.03, 1.42)	1.11 (0.90, 1.32)	
Eindhoven	1.26 (1.11, 1.43)	1.11 (0.99, 1.24)	1.16 (1.00, 1.33)	1.06 (0.93, 1.20)	0.94 (0.72, 1.16)	1.00 (0.86, 1.13)	
Volkel	0.99 (0.86, 1.12)	1.02 (0.90, 1.15)	1.00 (0.82, 1.22)	1.11 (0.92, 1.29)	0.81 (0.62, 1.03)	1.13 (1.00, 1.26)	
Beek	1.20 (1.06, 1.35)	1.15 (1.02, 1.28)	0.86 (0.68, 1.07)	1.19 (1.03, 1.36)	1.21 (0.95, 1.51)	1.38 (1.22, 1.55)	
Station \ Sector	165°N -195°N	195°N -225°N	225°N -255°N	255°N -285°N	285°N -315°N	315°N -345°N	
IJmuiden	1.52 (1.23, 1.82)	1.74 (1.51, 1.97)	1.99 (1.72, 2.31)	1.83 (1.51, 2.20)	1.74 (1.43, 2.06)	1.83 (1.56, 2.12)	
Texelhors	1.63 (1.36, 1.92)	1.82 (1.60, 2.06)	2.17 (1.91, 2.45)	2.11 (1.80, 2.44)	1.98 (1.55, 2.48)	1.81 (1.49, 2.16)	
De Kooy	1.65 (1.31, 2.01)	1.34 (0.99, 1.74)	1.58 (1.21, 1.97)	2.06 (1.65, 2.55)	1.88 (1.54, 2.27)	2.21 (1.86, 2.58)	
Schiphol	1.39 (1.16, 1.64)	1.89 (1.62, 2.19)	1.78 (1.37, 2.24)	2.08 (1.72, 2.45)	1.95 (1.56, 2.37)	1.89 (1.54, 2.26)	
De Bilt	1.21 (1.02, 1.40)	1.50 (1.27, 1.77)	2.00 (1.71, 2.26)	2.08 (1.83, 2.34)	1.70 (1.36, 2.07)	1.52 (1.30, 1.77)	
Soesterberg	1.09 (0.90, 1.30)	1.46 (1.29, 1.66)	2.03 (1.68, 2.41)	2.02 (1.76, 2.30)	1.75 (1.50, 2.00)	1.43 (1.23, 1.64)	
Leeuwarden	1.45 (1.21, 1.71)	2.04 (1.67, 2.45)	1.98 (1.64, 2.33)	2.12 (1.78, 2.51)	1.84 (1.41, 2.37)	2.01 (1.67, 2.39)	
Deelen	1.21 (1.02, 1.40)	1.41 (1.24, 1.59)	2.02 (1.74, 2.33)	2.10 (1.84, 2.37)	1.89 (1.64, 2.17)	1.30 (1.07, 1.56)	
Lauwersoog	1.58 (1.35, 1.81)	1.94 (1.68, 2.21)	1.89 (1.59, 2.24)	1.89 (1.59, 2.20)	1.90 (1.60, 2.21)	1.66 (1.36, 1.99)	
Eelde	1.35 (1.17, 1.54)	1.70 (1.42, 1.98)	1.93 (1.66, 2.19)	1.92 (1.65, 2.21)	1.85 (1.59, 2.13)	1.44 (1.23, 1.68)	
Twenthe	1.17 (0.96, 1.39)	1.27 (1.08, 1.48)	2.02 (1.66, 2.37)	2.06 (1.79, 2.36)	1.96 (1.68, 2.25)	1.30 (1.14, 1.47)	
Cadzand	1.62 (1.43, 1.84)	1.63 (1.32, 1.94)	1.70 (1.35, 2.09)	2.04 (1.74, 2.39)	2.13 (1.89, 2.37)	1.89 (1.63, 2.16)	
Vlissingen	1.48 (1.23, 1.75)	1.50 (1.27, 1.76)	1.83 (1.49, 2.19)	1.93 (1.58, 2.30)	1.71 (1.37, 2.07)	1.57 (1.31, 1.83)	
L.E. Goeree	1.13 (0.88, 1.38)	1.72 (1.51, 1.92)	1.81 (1.53, 2.10)	1.96 (1.68, 2.24)	1.90 (1.61, 2.20)	2.06 (1.78, 2.34)	
Hoek van Holland	1.39 (1.15, 1.65)	1.24 (1.01, 1.48)	1.69 (1.38, 2.04)	1.80 (1.43, 2.21)	1.84 (1.56, 2.14)	1.42 (1.03, 1.86)	
Zestienhoven	1.30 (1.14, 1.48)	1.39 (1.16, 1.63)	1.96 (1.72, 2.20)	2.14 (1.83, 2.47)	2.15 (1.70, 2.63)	2.00 (1.73, 2.28)	
Gilze-Rijen	1.45 (1.23, 1.69)	1.61 (1.42, 1.80)	2.02 (1.64, 2.46)	2.02 (1.76, 2.29)	1.94 (1.63, 2.27)	1.32 (1.17, 1.49)	
Herwijnen	1.42 (1.25, 1.62)	1.34 (1.04, 1.64)	1.96 (1.56, 2.36)	2.19 (1.71, 2.67)	2.14 (1.77, 2.52)	1.69 (1.51, 1.89)	
Eindhoven	1.17 (1.01, 1.35)	1.52 (1.34, 1.68)	1.74 (1.50, 1.99)	1.68 (1.35, 2.04)	1.79 (1.47, 2.15)	1.40 (1.21, 1.59)	
Volkel	1.36 (1.21, 1.53)	1.49 (1.26, 1.74)	1.96 (1.73, 2.20)	2.08 (1.70, 2.48)	1.93 (1.65, 2.24)	1.24 (1.07, 1.40)	
Beek	1.43 (1.22, 1.64)	1.34 (1.17, 1.52)	1.56 (1.18, 1.94)	2.10 (1.84, 2.38)	1.70 (1.43, 1.98)	1.28 (1.09, 1.50)	

Table T3.3: $\tilde{\sigma}$ estimates of the U_p POT/exponential model.

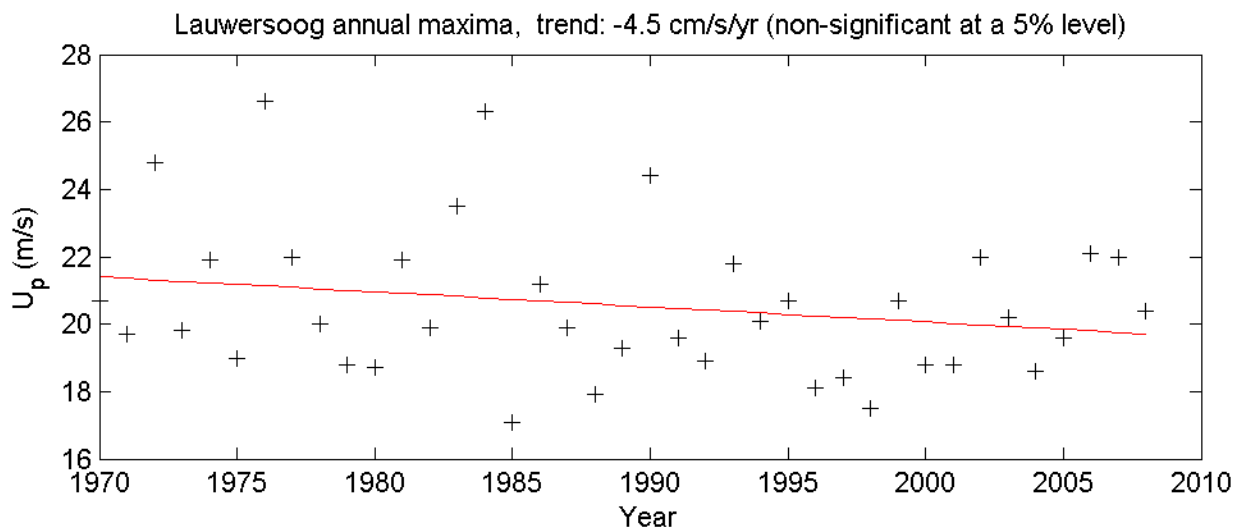
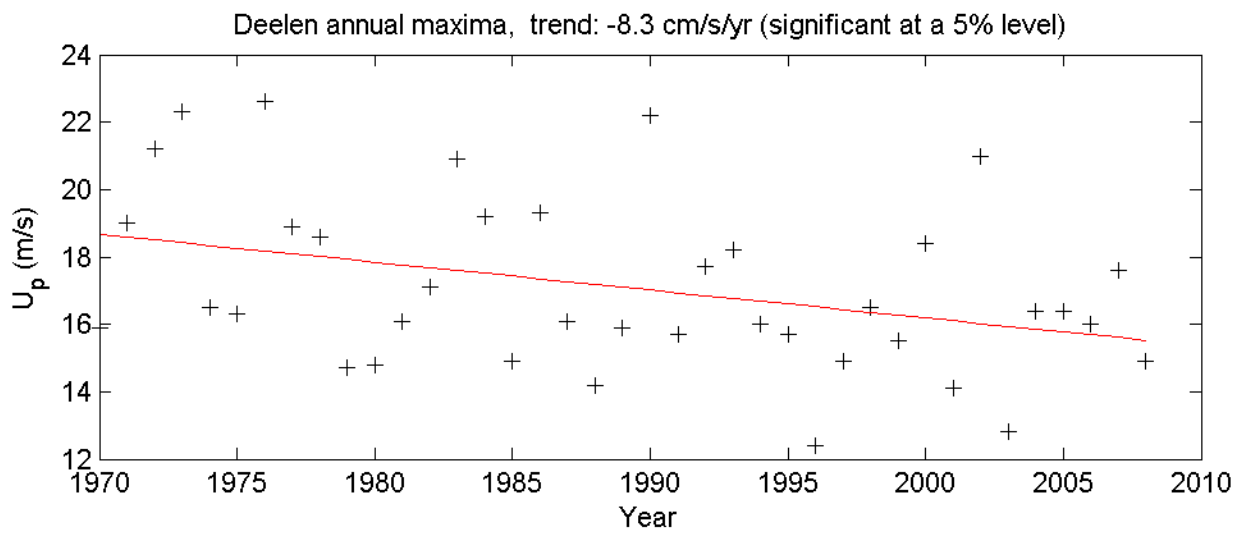
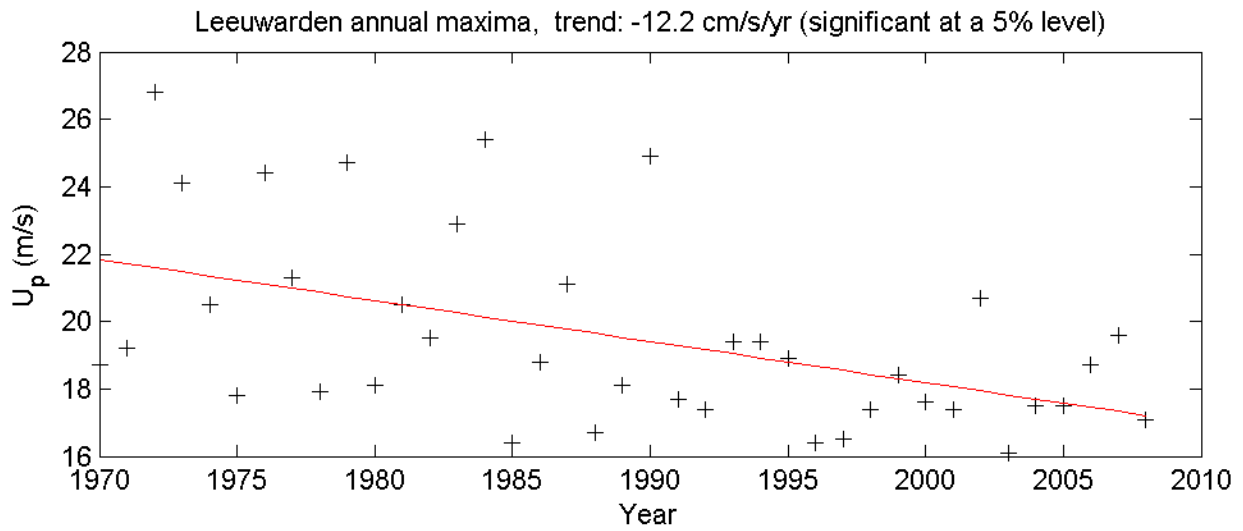
C Figures



Annual maxima timeseries and linear fits		
	1970-2008	
Deltares	1200264-005	Fig. F.1.1

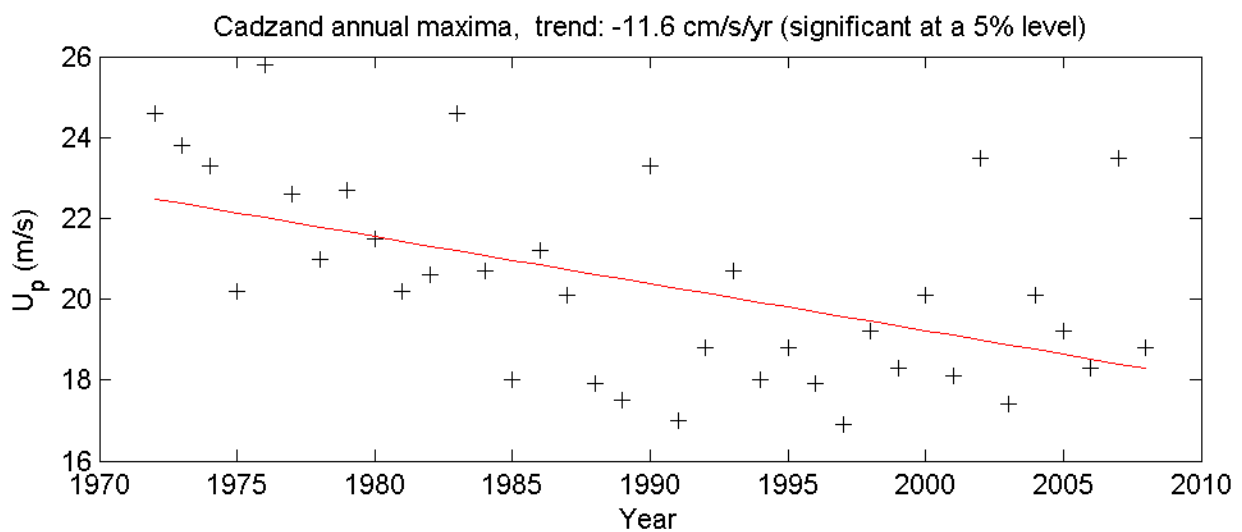
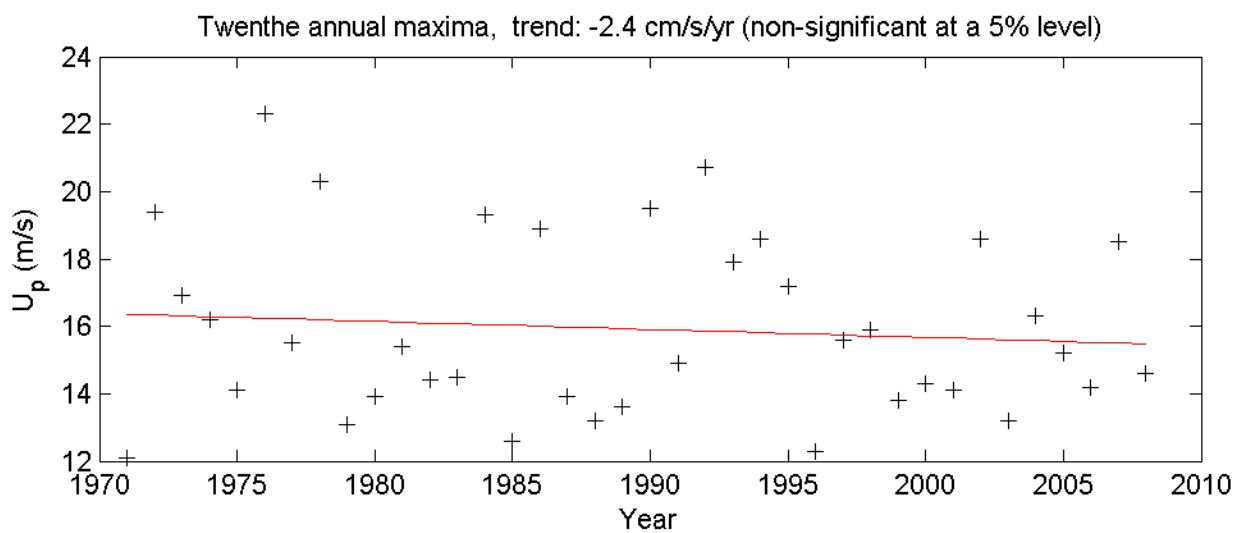
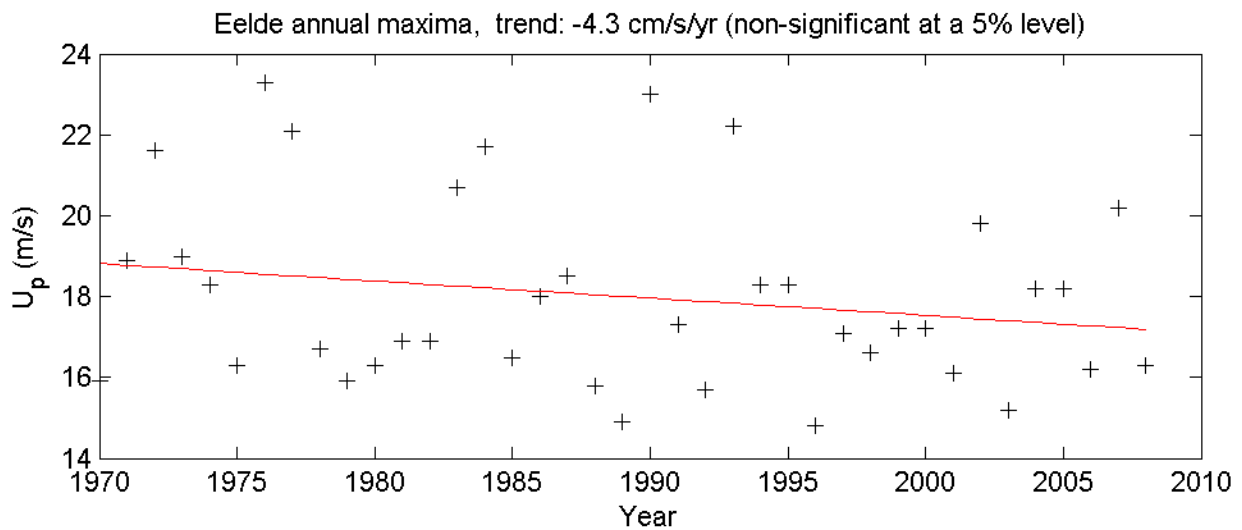


Annual maxima timeseries and linear fits		
	1970-2008	
Deltares	1200264-005	Fig. F.1.2



Annual maxima timeseries and linear fits

1970-2008



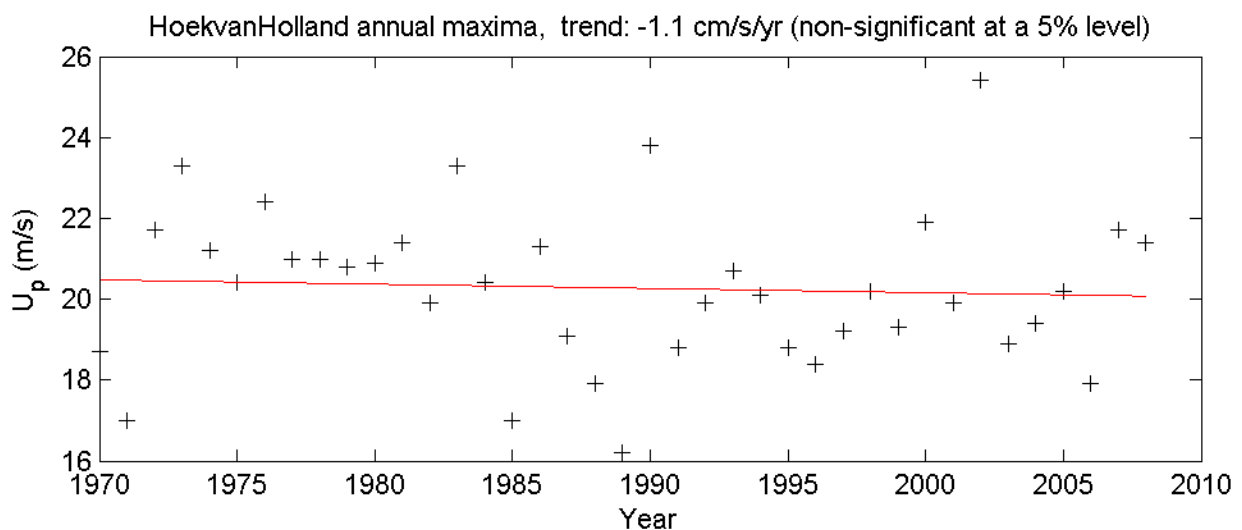
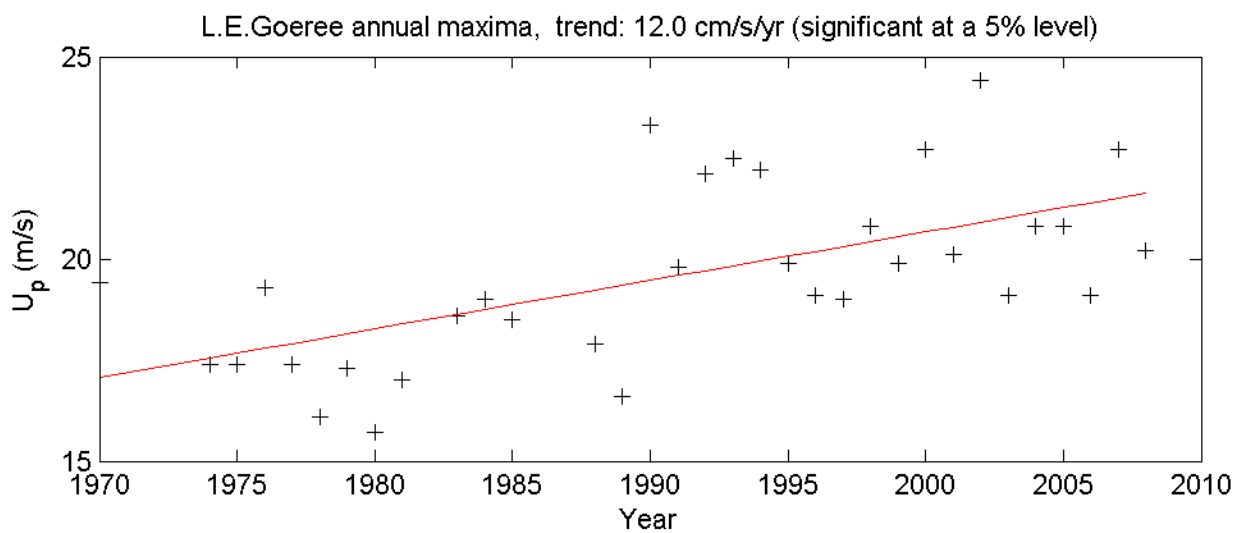
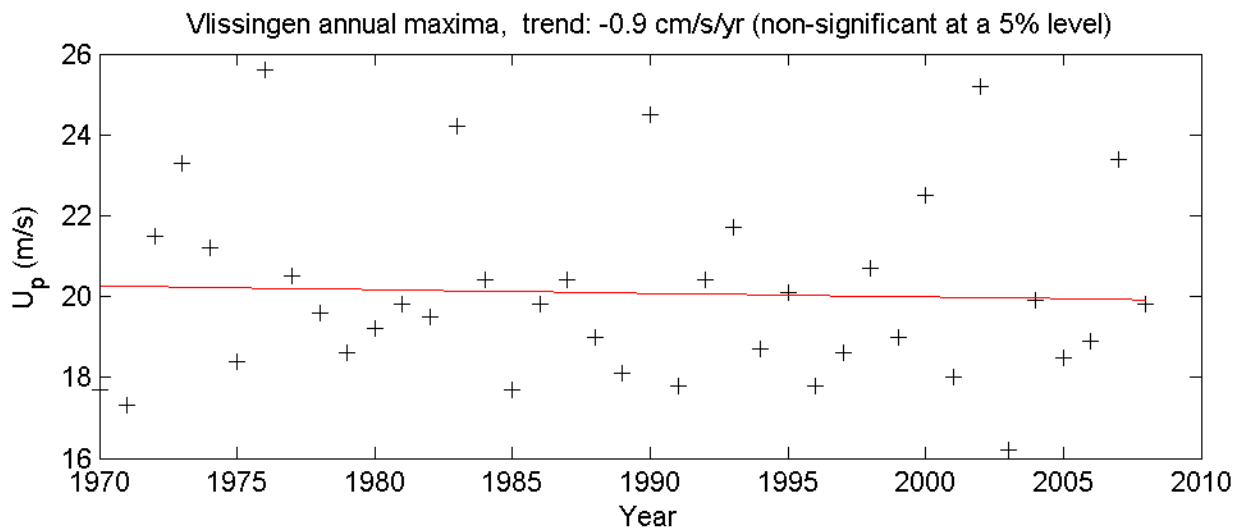
Annual maxima timeseries and linear fits

1970-2008

Deltares

1200264-005

Fig. F.1.4



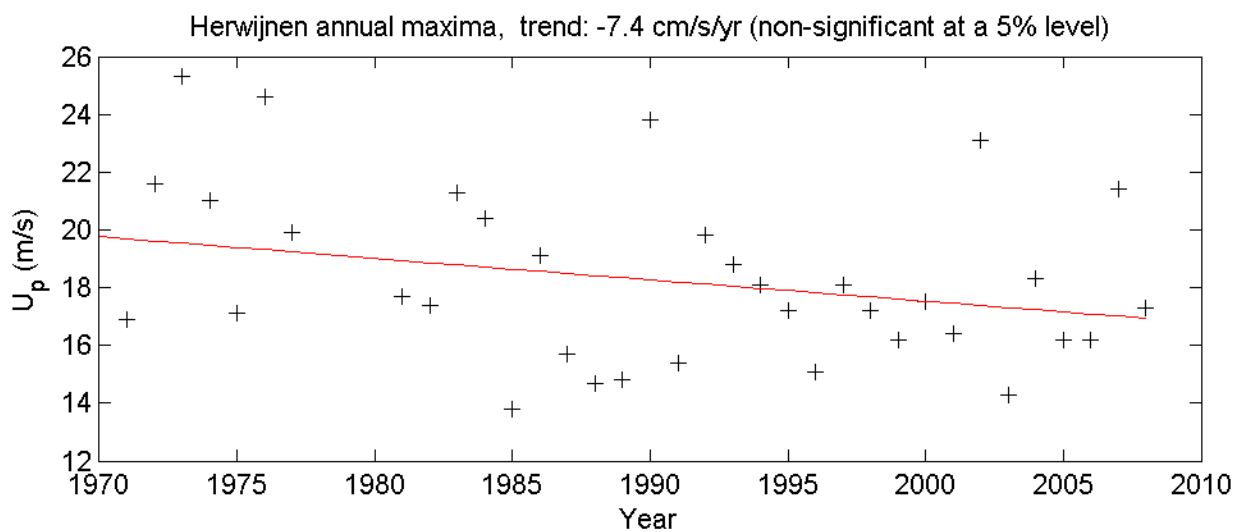
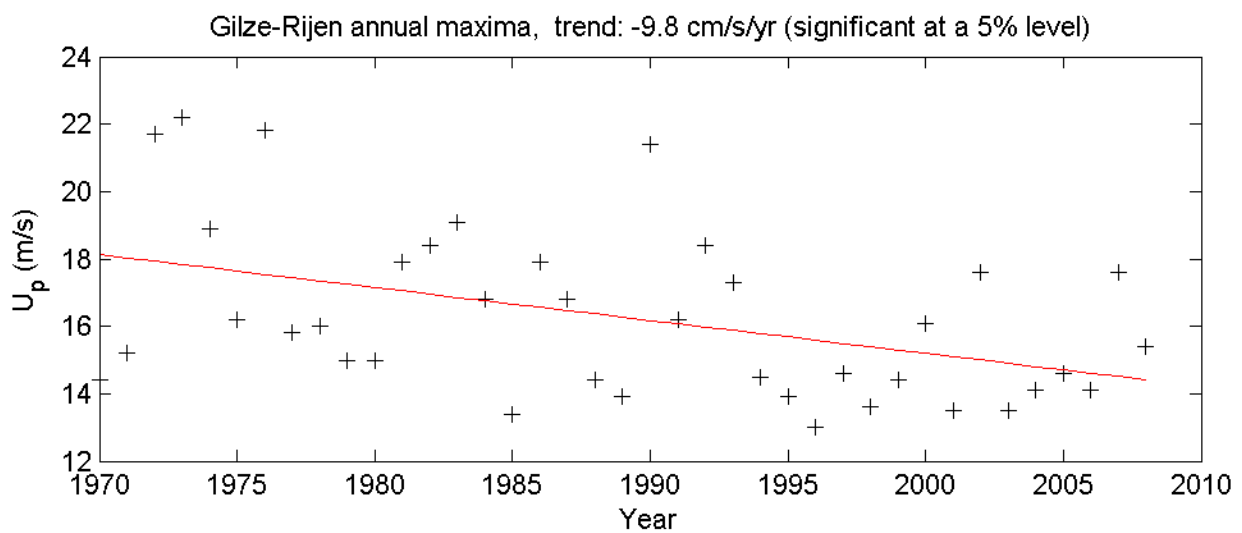
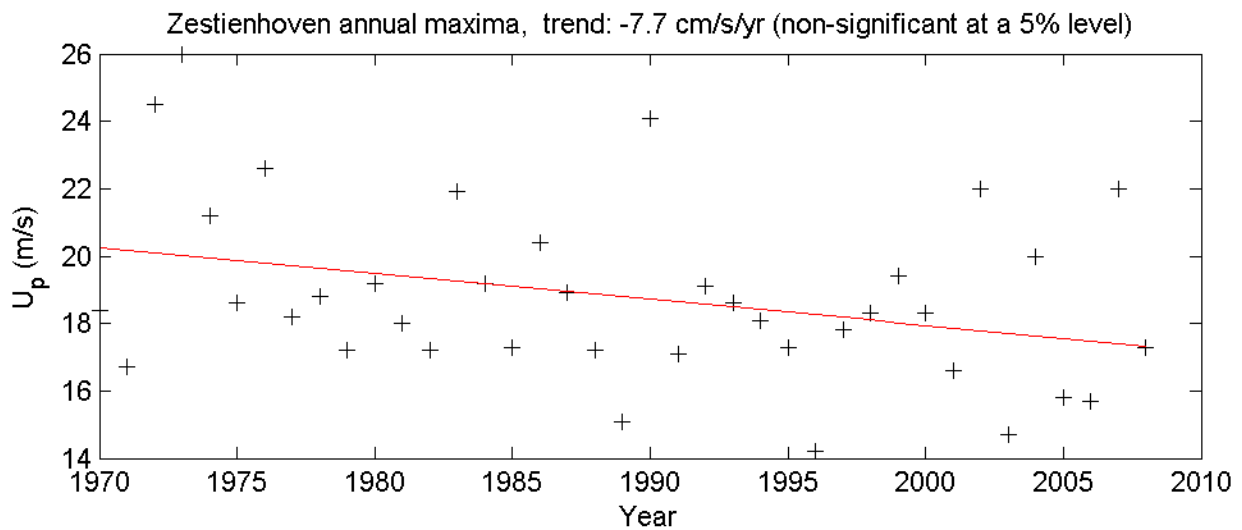
Annual maxima timeseries and linear fits

1970-2008

Deltares

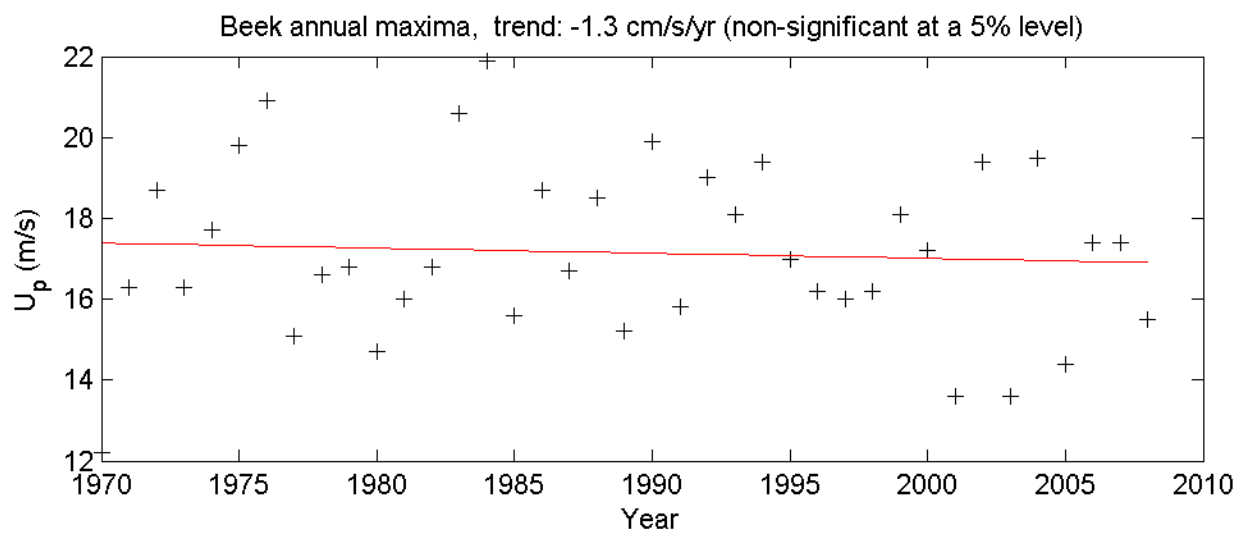
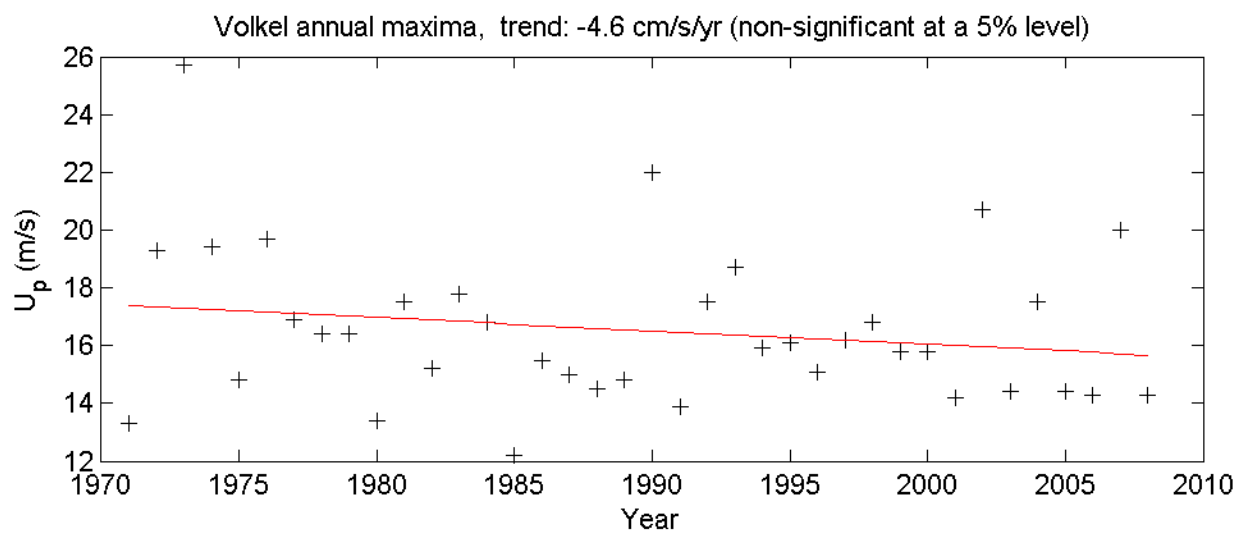
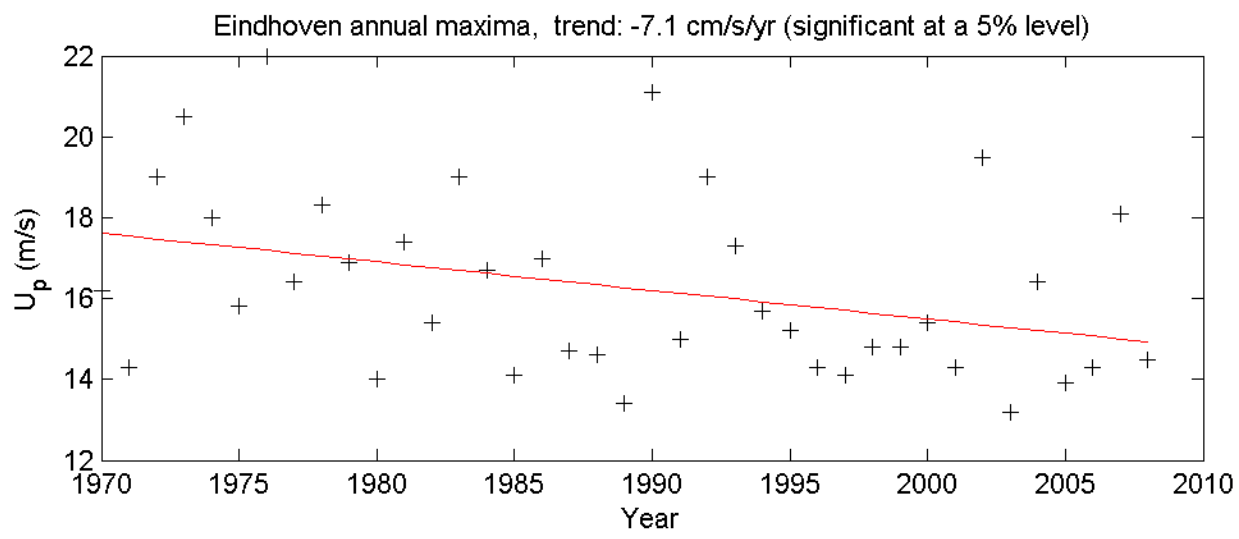
1200264-005

Fig. F.1.5

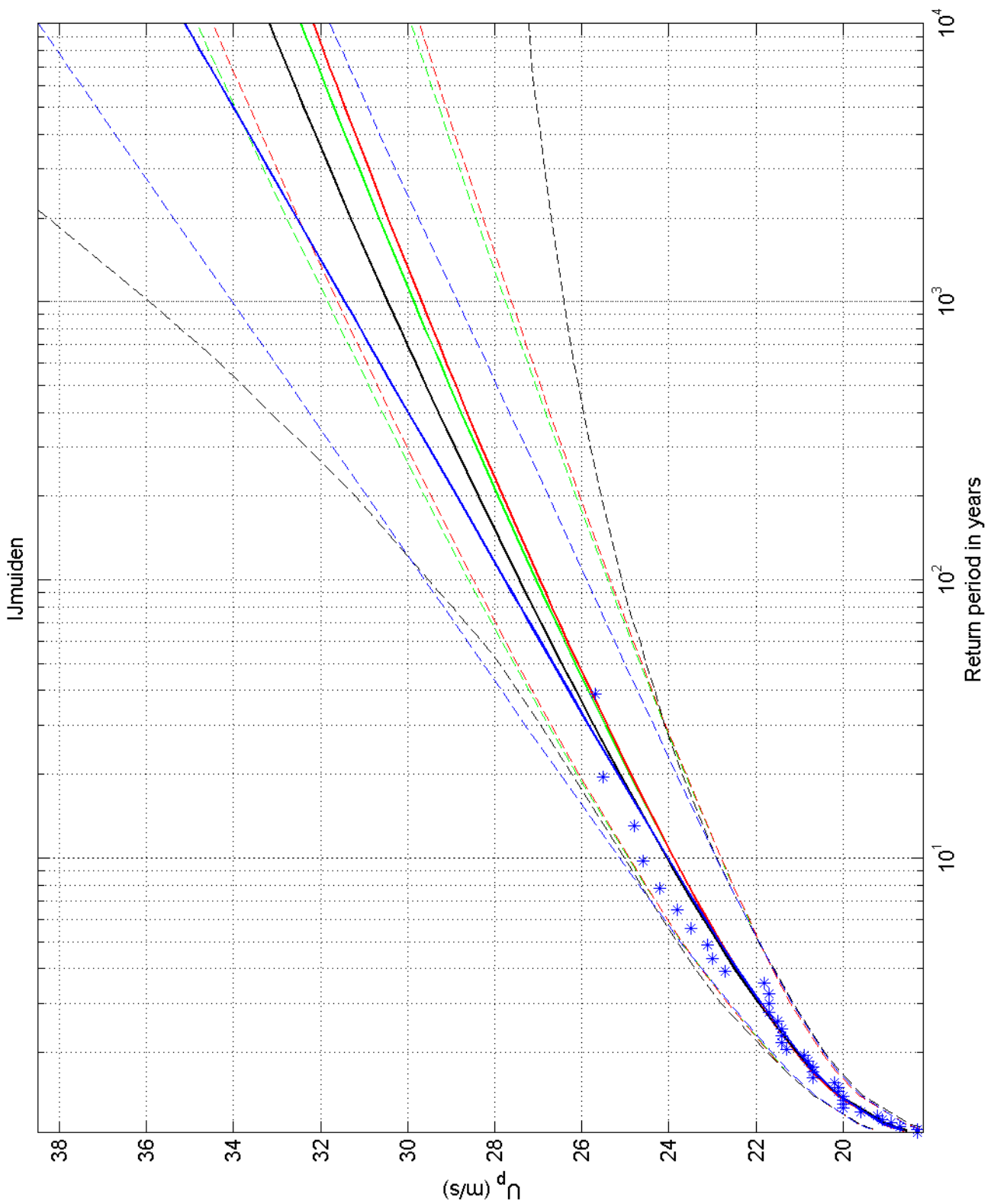


Annual maxima timeseries and linear fits

1970-2008



Annual maxima timeseries and linear fits		
	1970-2008	
Deltares	1200264-005	Fig. F.1.7



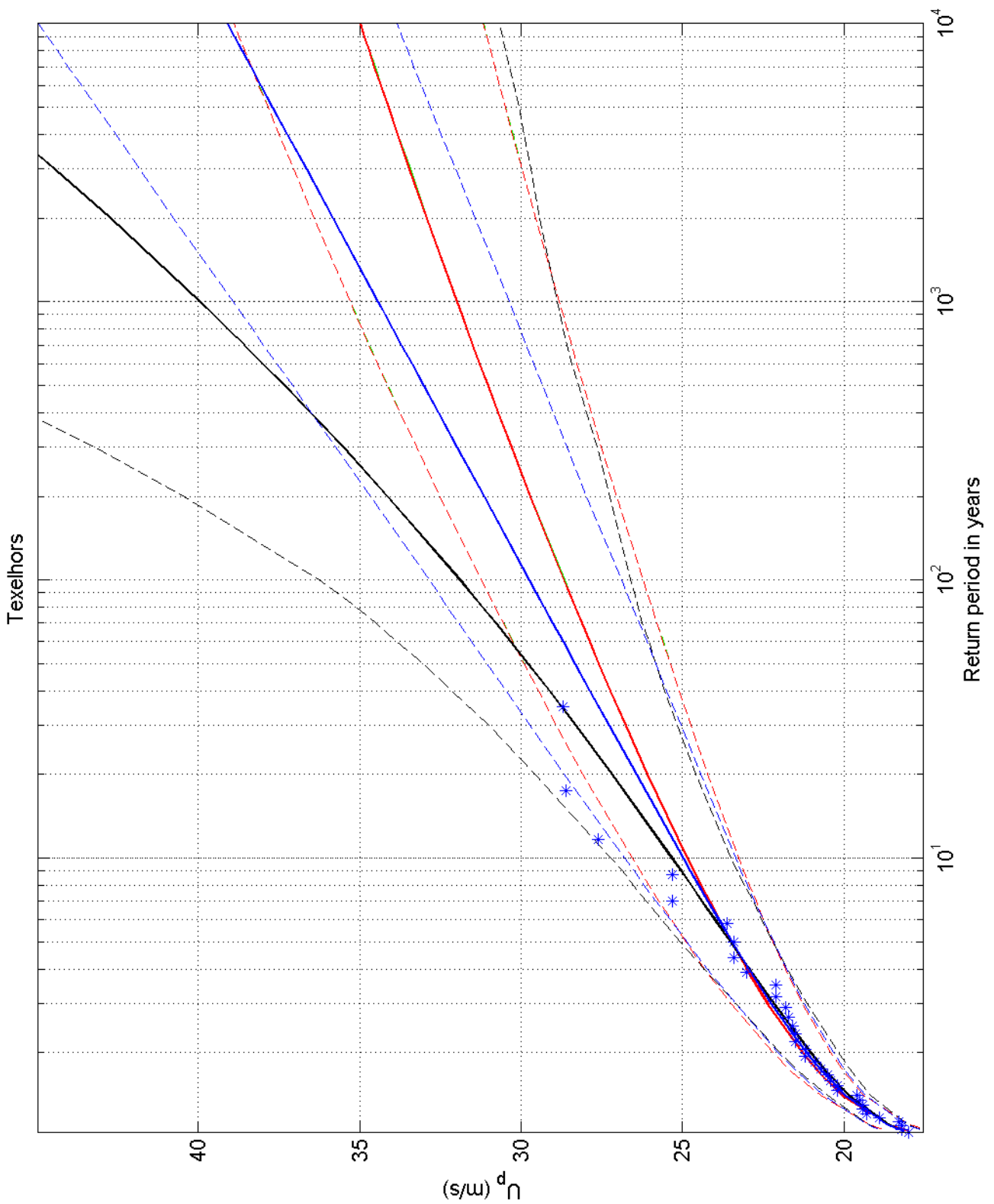
Return value plot with Gumbel (blue) and GEV (black) fit to U ,
 Gumbel (red) fit to U_p^2 and Gumbel (green) fit to U_p
 Plotting positions: x_i vs $(n+1)/(n+1-i)$

IJmuiden

Deltares

1200264-005

Fig. F.2.225



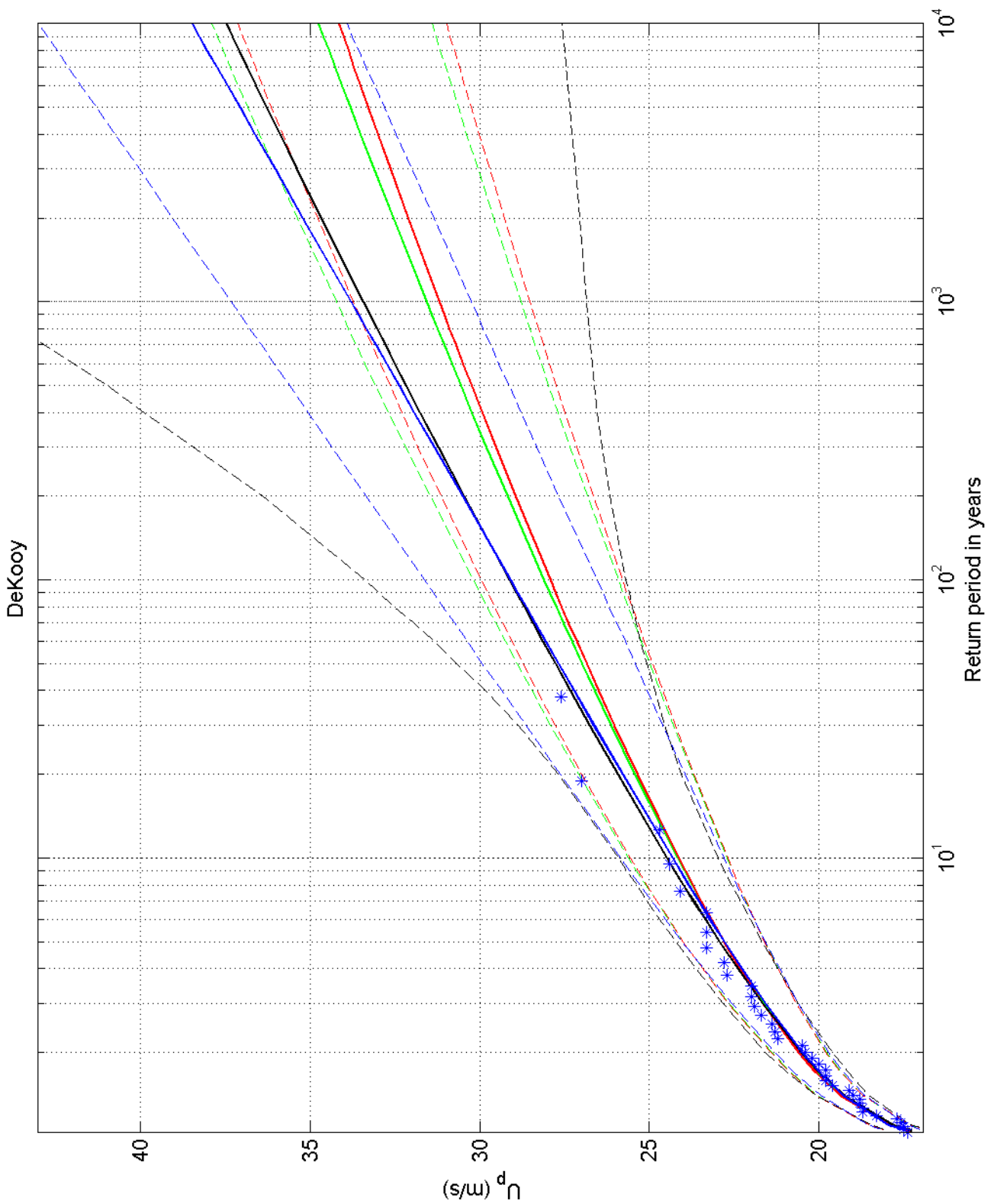
Return value plot with Gumbel (blue) and GEV (black) fit to U ,
 Gumbel (red) fit to U_p^2 and Gumbel (green) fit to U_p
 Plotting positions: x_i vs $(n+1)/(n+1-i)$

Texelhors

Deltares

1200264-005

Fig. F.2.229



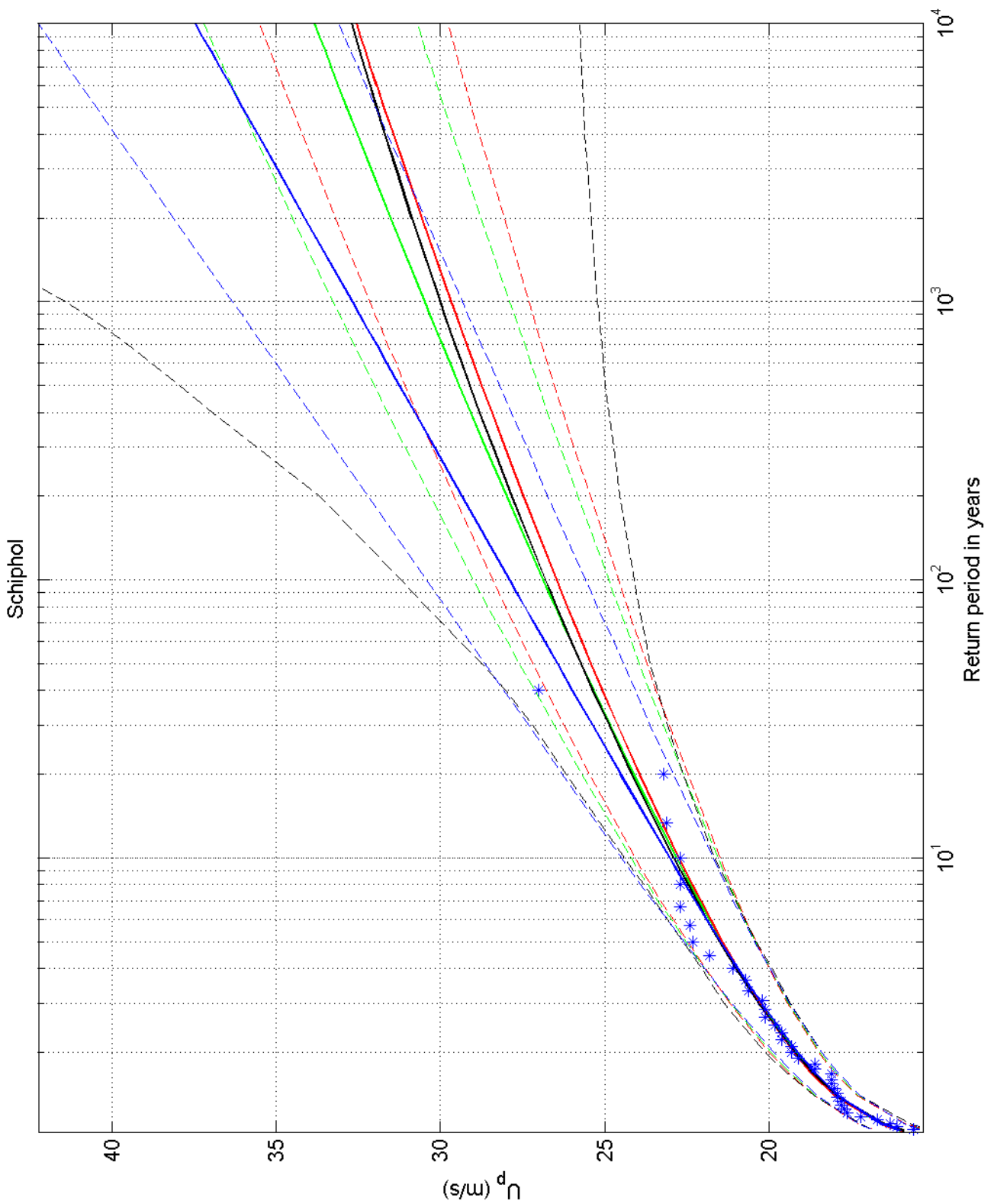
Return value plot with Gumbel (blue) and GEV (black) fit to U ,
 Gumbel (red) fit to U_p^2 and Gumbel (green) fit to U_p
 Plotting positions: x_i vs $(n+1)/(n+1-i)$

DeKooy

Deltares

1200264-005

Fig. F.2.235



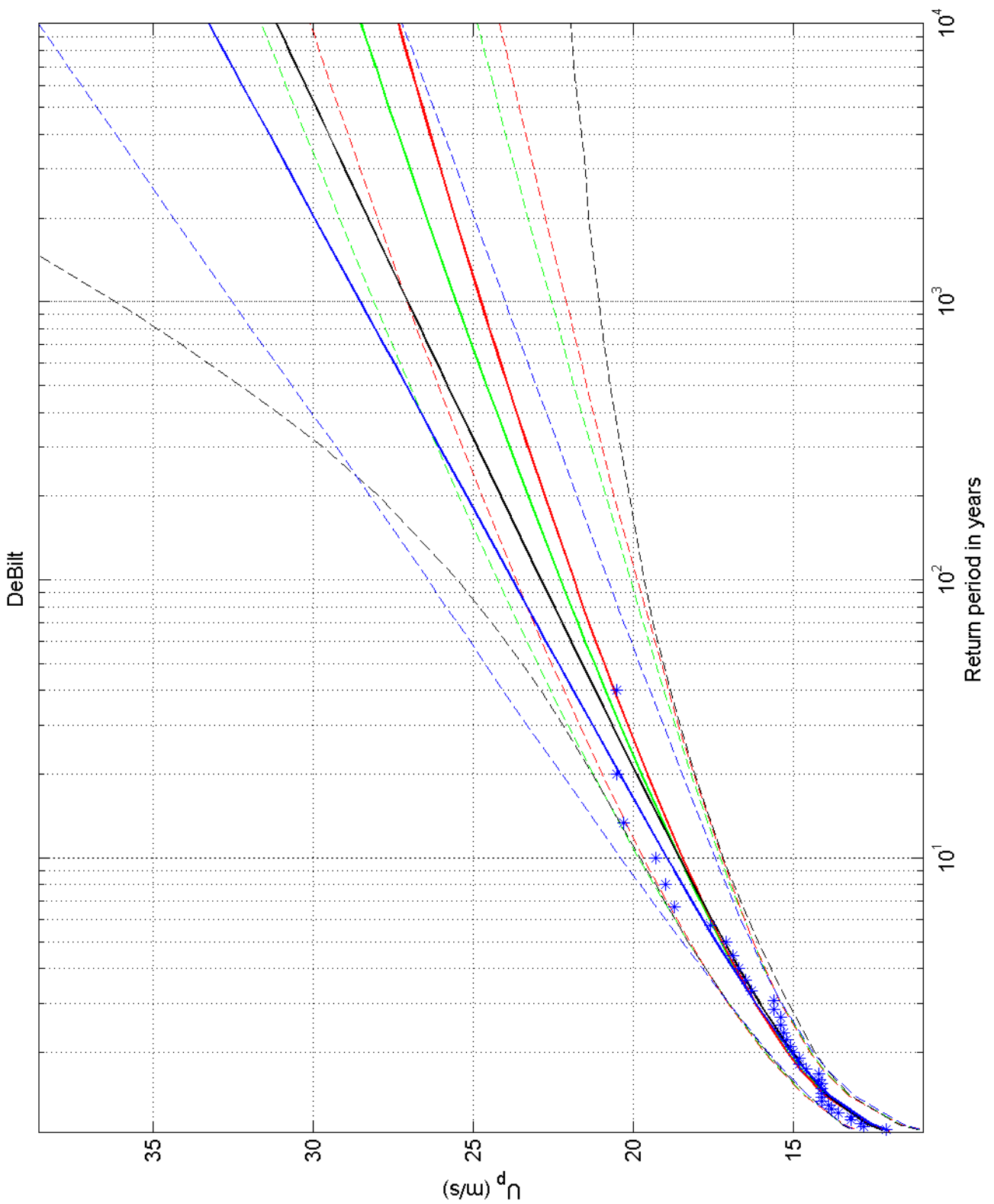
Return value plot with Gumbel (blue) and GEV (black) fit to U,
 Gumbel (red) fit to U_p^2 and Gumbel (green) fit to U_p^k
 Plotting positions: x_i vs $(n+1)/(n+1-i)$

Schiphol

Deltares

1200264-005

Fig. F.2.240



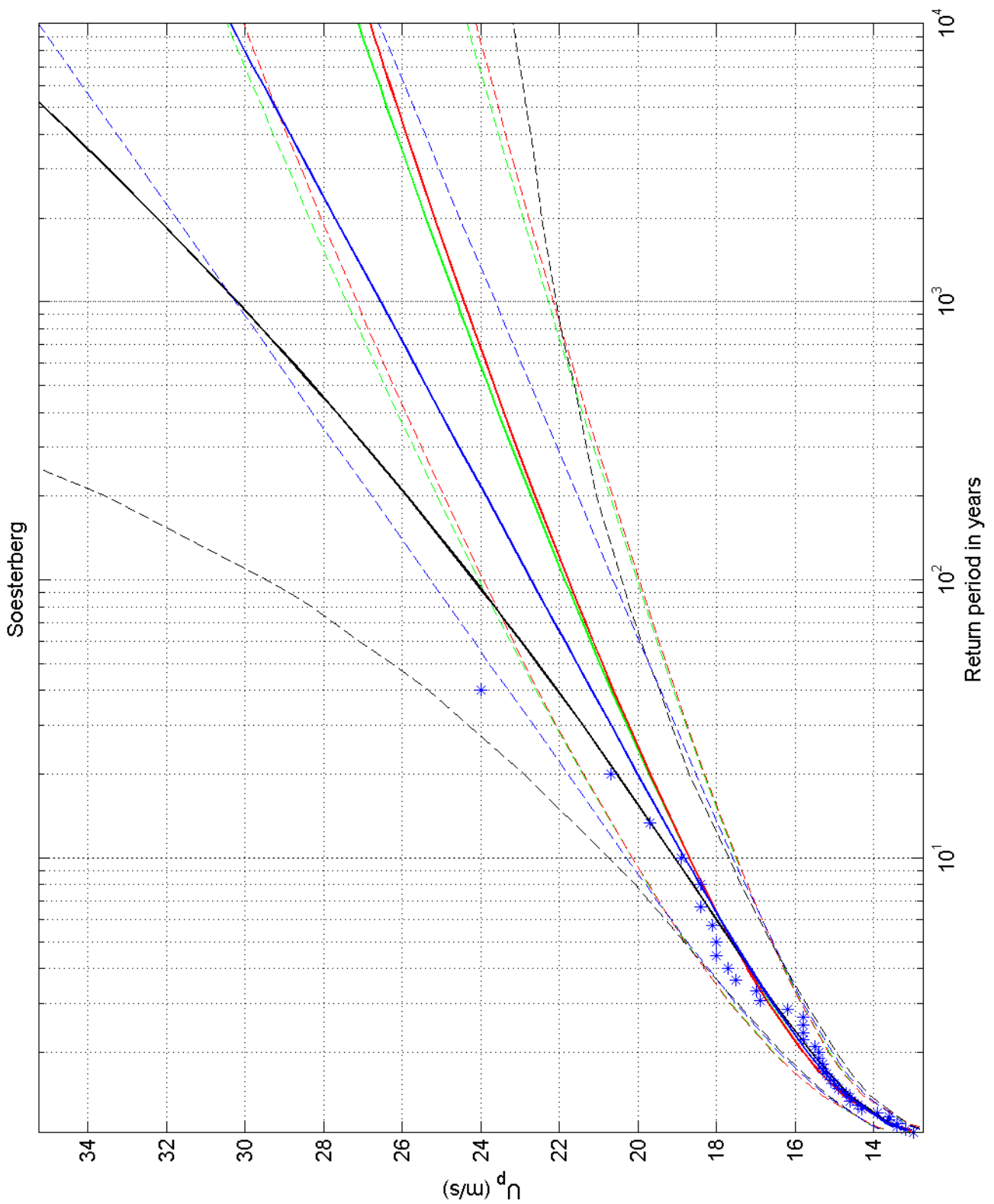
Return value plot with Gumbel (blue) and GEV (black) fit to U ,
 Gumbel (red) fit to U_p^2 and Gumbel (green) fit to U_p^k
 Plotting positions: x_i vs $(n+1)/(n+1-i)$

DeBilt

Deltares

1200264-005

Fig. F.2.260



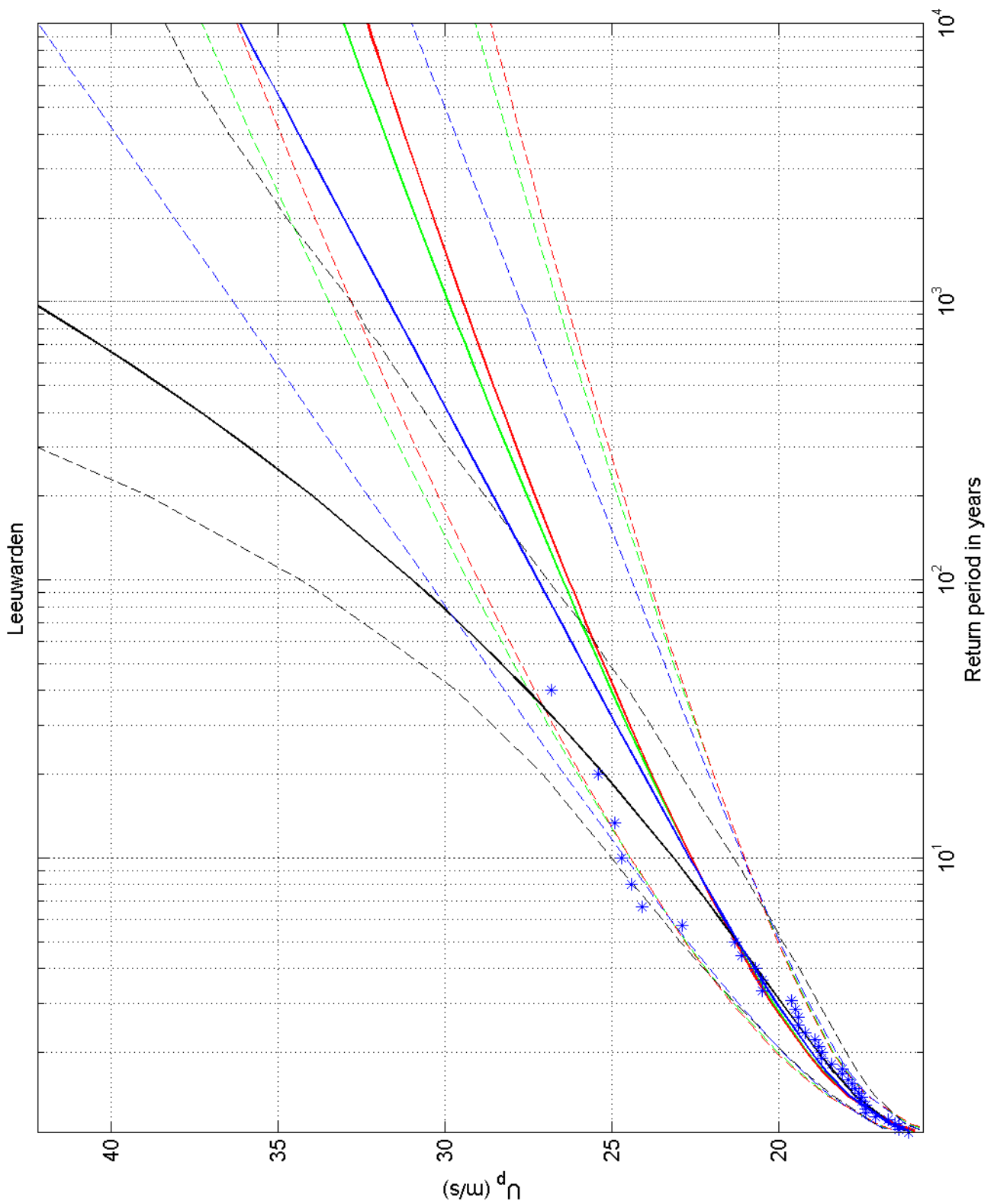
Return value plot with Gumbel (blue) and GEV (black) fit to U ,
 Gumbel (red) fit to U_p^2 and Gumbel (green) fit to U_p
 Plotting positions: x_i vs $(n+1)/(n+1-i)$

Soesterberg

Deltares

1200264-005

Fig. F.2.265



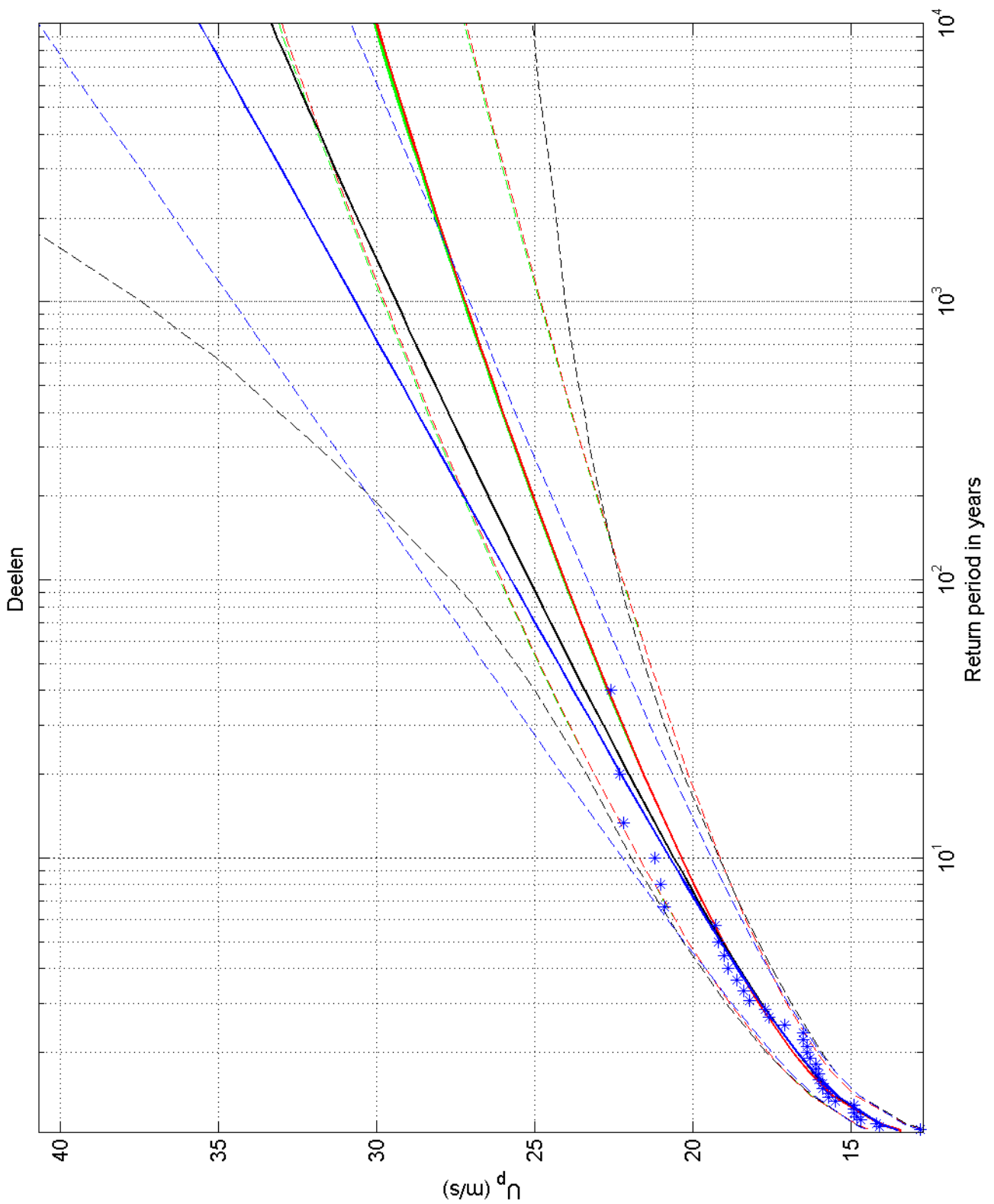
Return value plot with Gumbel (blue) and GEV (black) fit to U ,
 Gumbel (red) fit to U_p^2 and Gumbel (green) fit to U_p
 Plotting positions: x_i vs $(n+1)/(n+1-i)$

Leeuwarden

Deltares

1200264-005

Fig. F.2.270



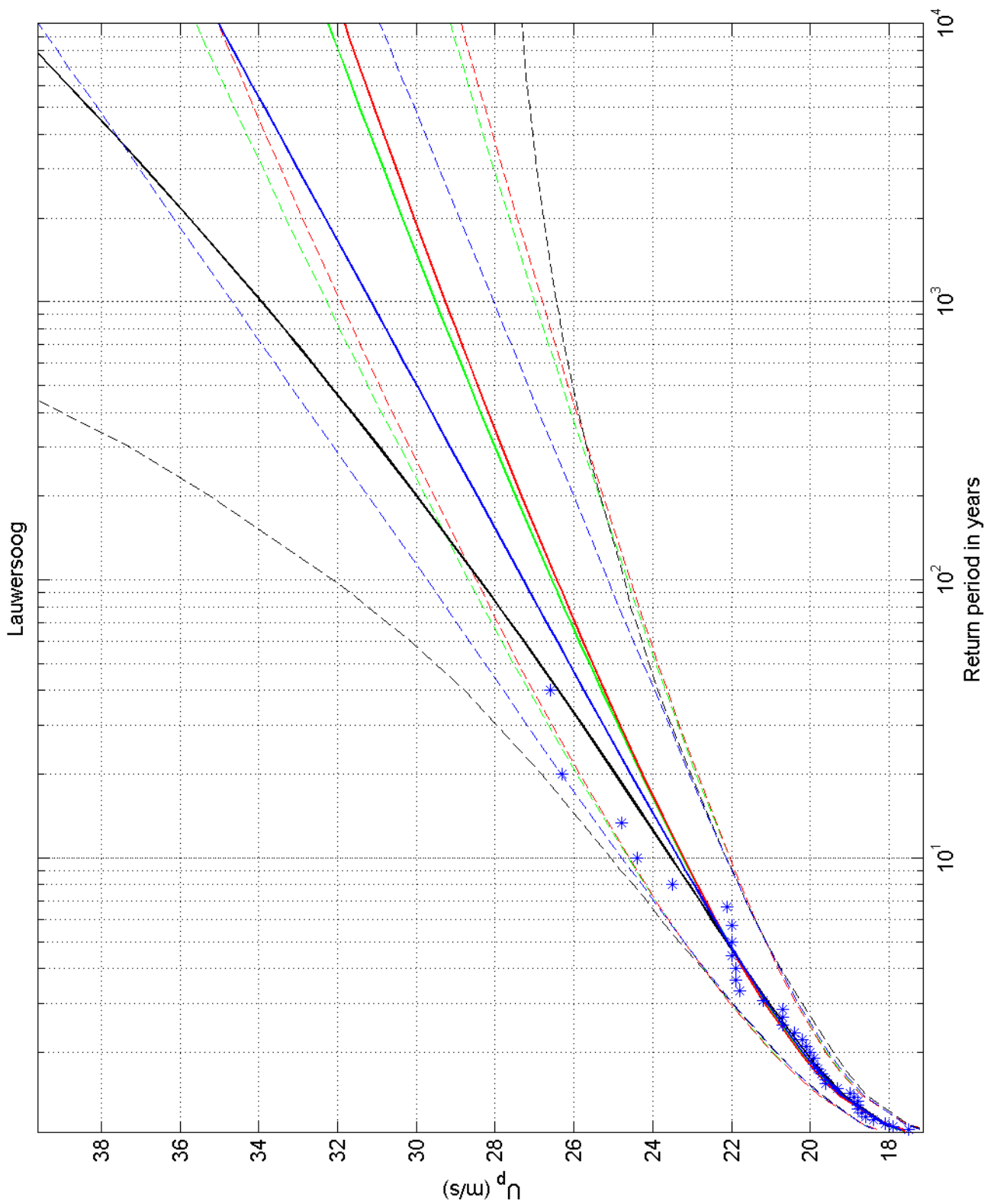
Return value plot with Gumbel (blue) and GEV (black) fit to U,
 Gumbel (red) fit to U_p^2 and Gumbel (green) fit to U_p^k
 Plotting positions: x_i vs $(n+1)/(n+1-i)$

Deelen

Deltares

1200264-005

Fig. F.2.275



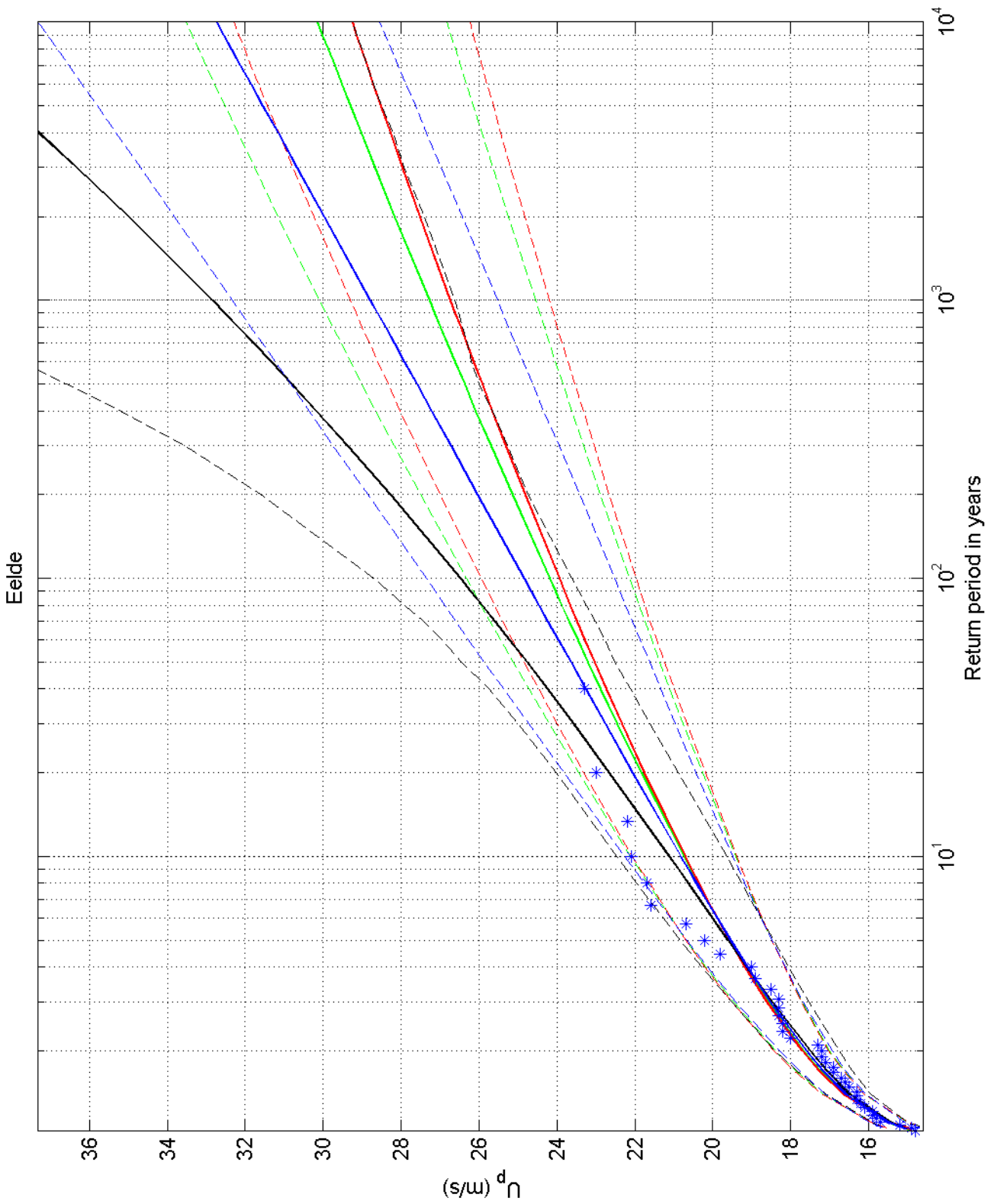
Return value plot with Gumbel (blue) and GEV (black) fit to U ,
 Gumbel (red) fit to U_p^2 and Gumbel (green) fit to U_p
 Plotting positions: x_i vs $(n+1)/(n+1-i)$

Lauwersoog

Deltares

1200264-005

Fig. F.2.277



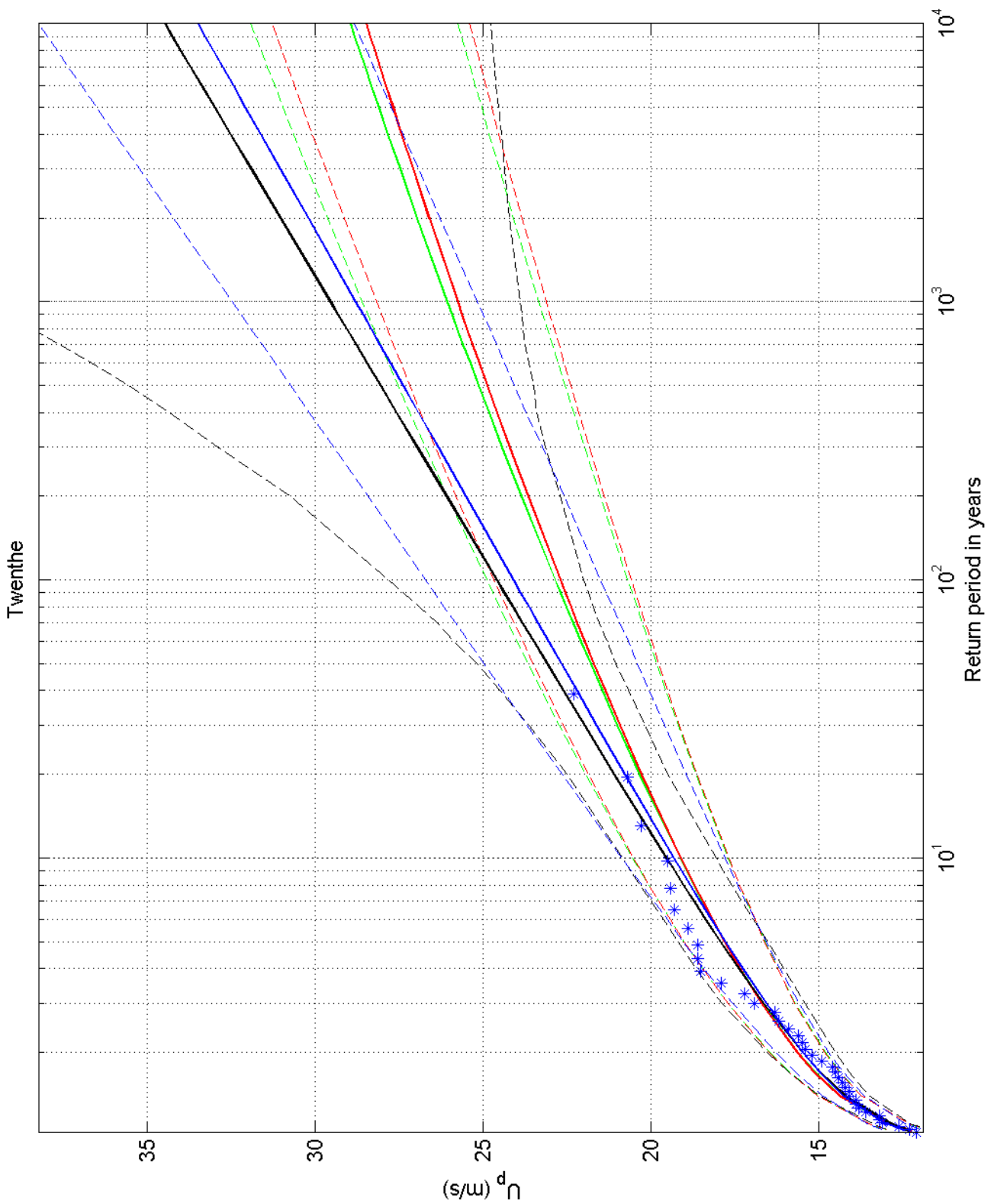
Return value plot with Gumbel (blue) and GEV (black) fit to U ,
 Gumbel (red) fit to U_p^2 and Gumbel (green) fit to U_p
 Plotting positions: x_i vs $(n+1)/(n+1-i)$

Eelde

Deltares

1200264-005

Fig. F.2.280



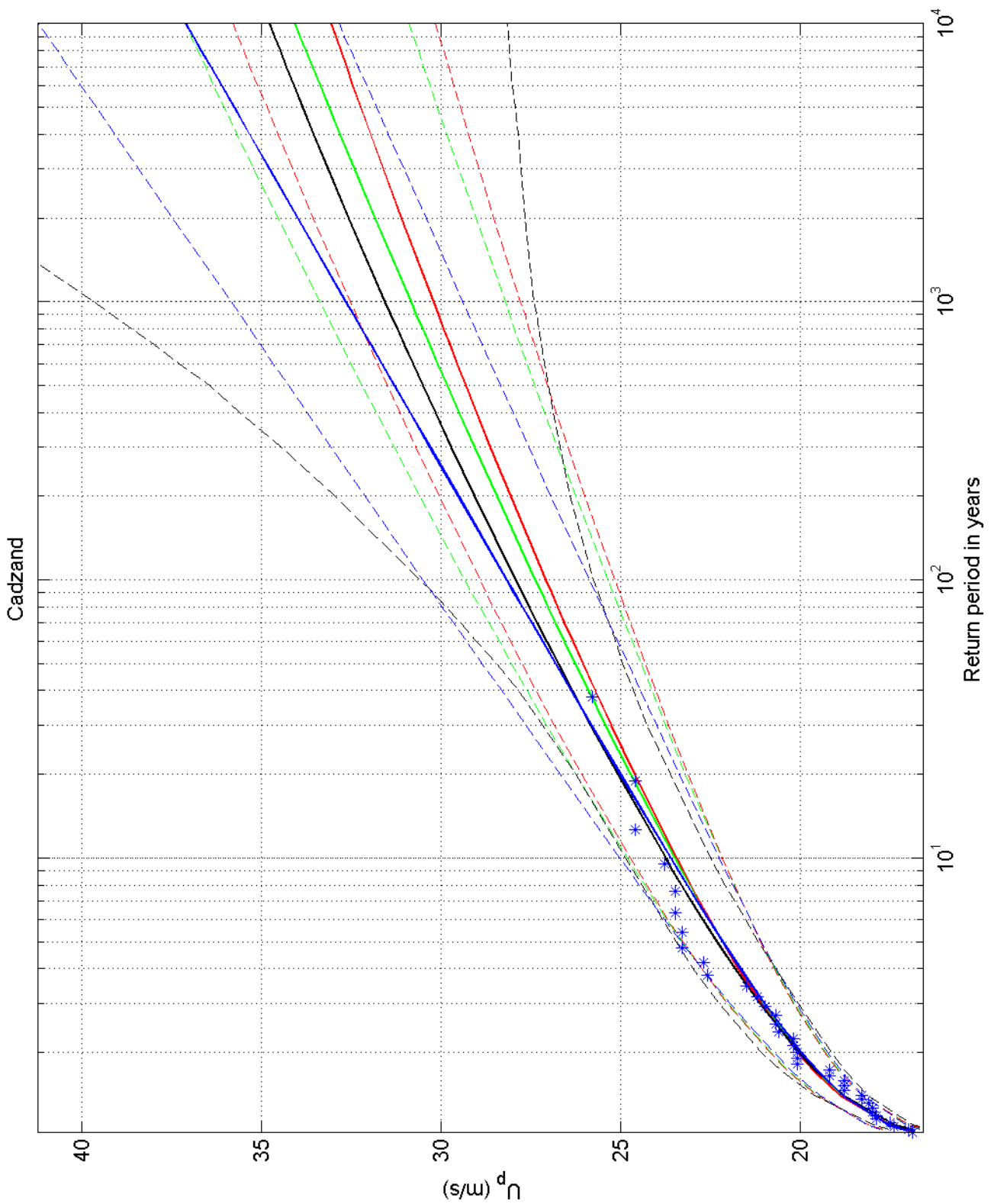
Return value plot with Gumbel (blue) and GEV (black) fit to U ,
 Gumbel (red) fit to U_p^2 and Gumbel (green) fit to U_p
 Plotting positions: x_i vs $(n+1)/(n+1-i)$

Twenthe

Deltares

1200264-005

Fig. F.2.290



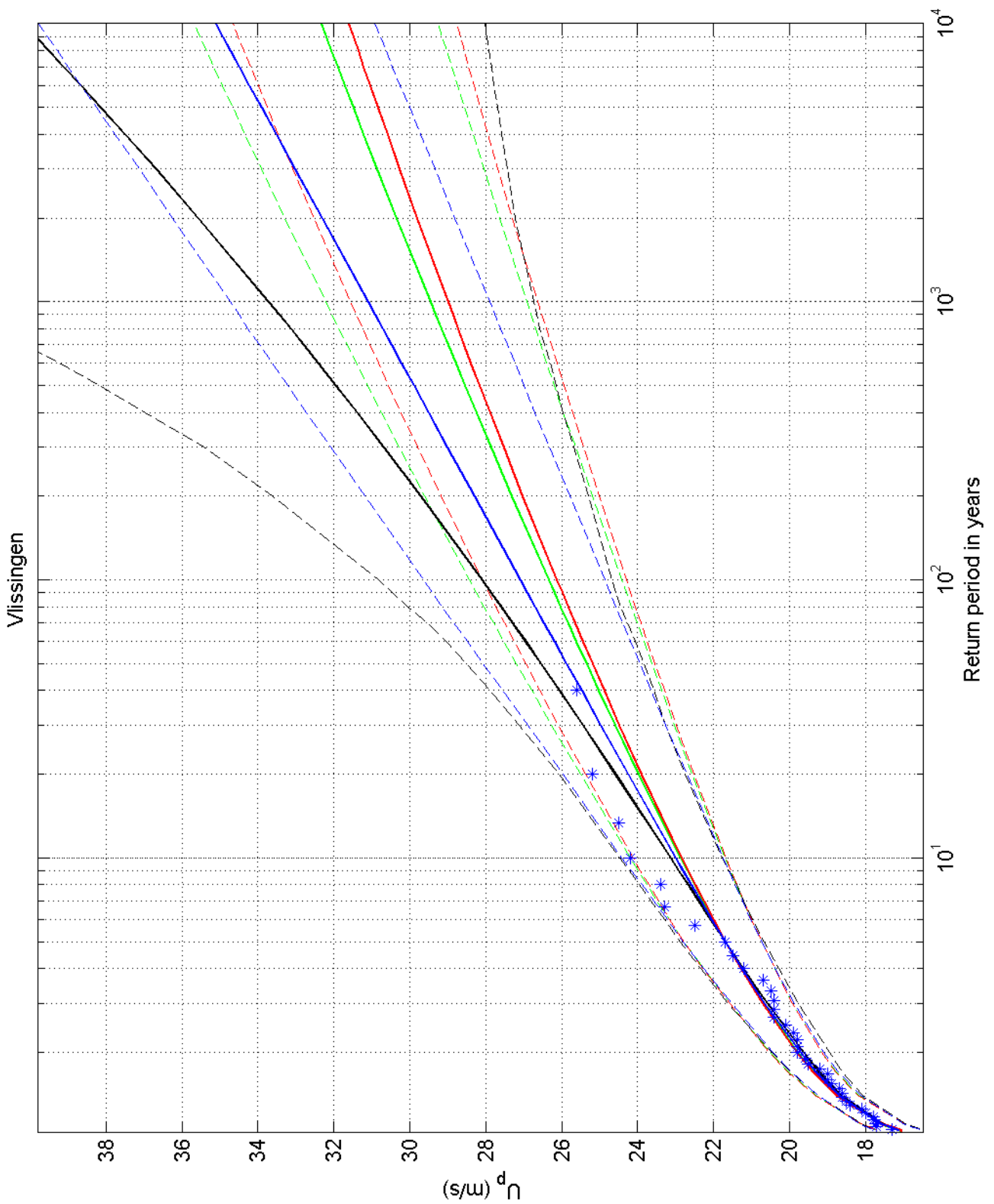
Return value plot with Gumbel (blue) and GEV (black) fit to U ,
 Gumbel (red) fit to U_p^2 and Gumbel (green) fit to U_p^k
 Plotting positions: x_i vs $(n+1)/(n+1-i)$

Cadzand

Deltares

1200264-005

Fig. F.2.308



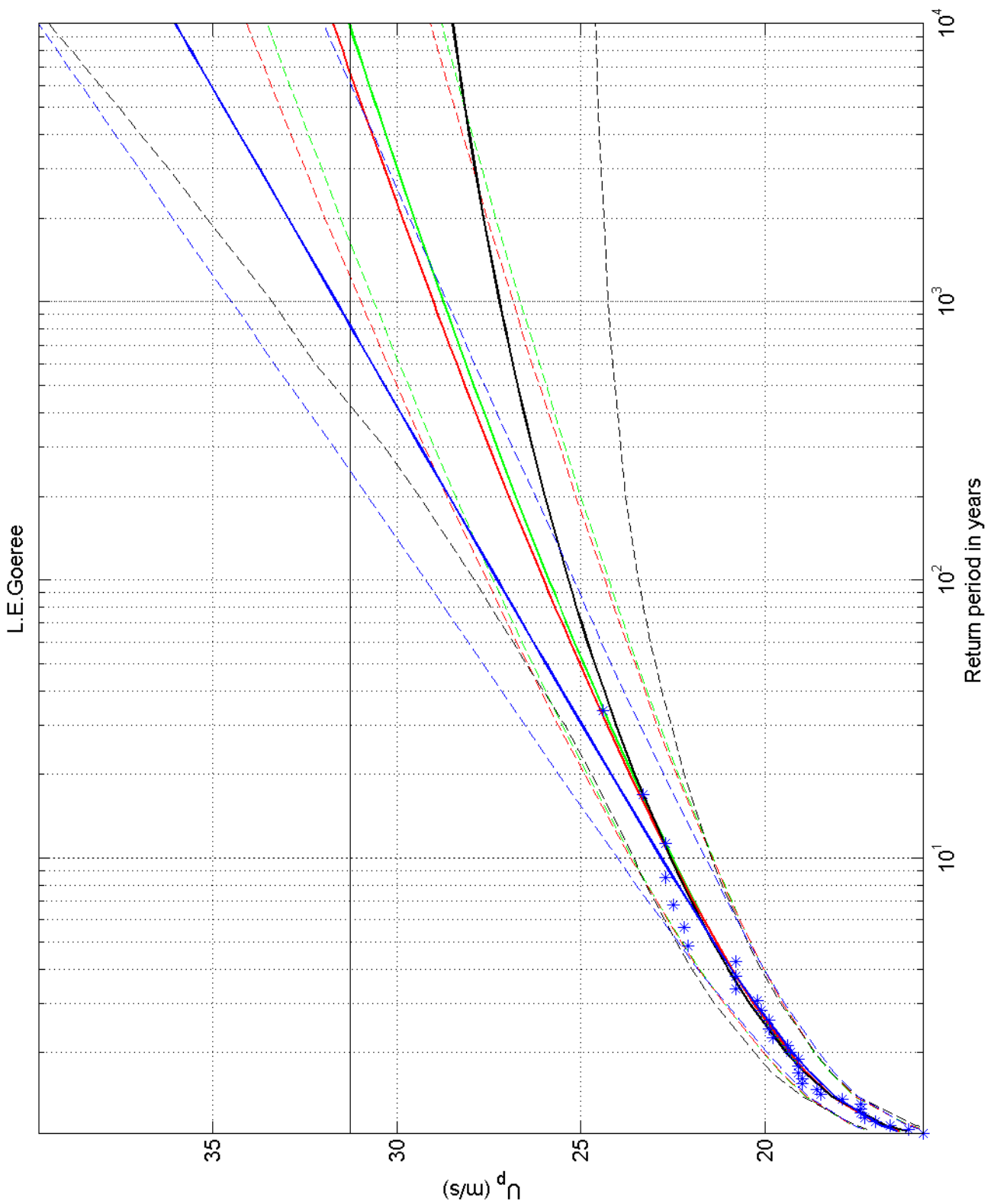
Return value plot with Gumbel (blue) and GEV (black) fit to U ,
 Gumbel (red) fit to U_p^2 and Gumbel (green) fit to U_p^k
 Plotting positions: x_i vs $(n+1)/(n+1-i)$

Vlissingen

Deltares

1200264-005

Fig. F.2.310



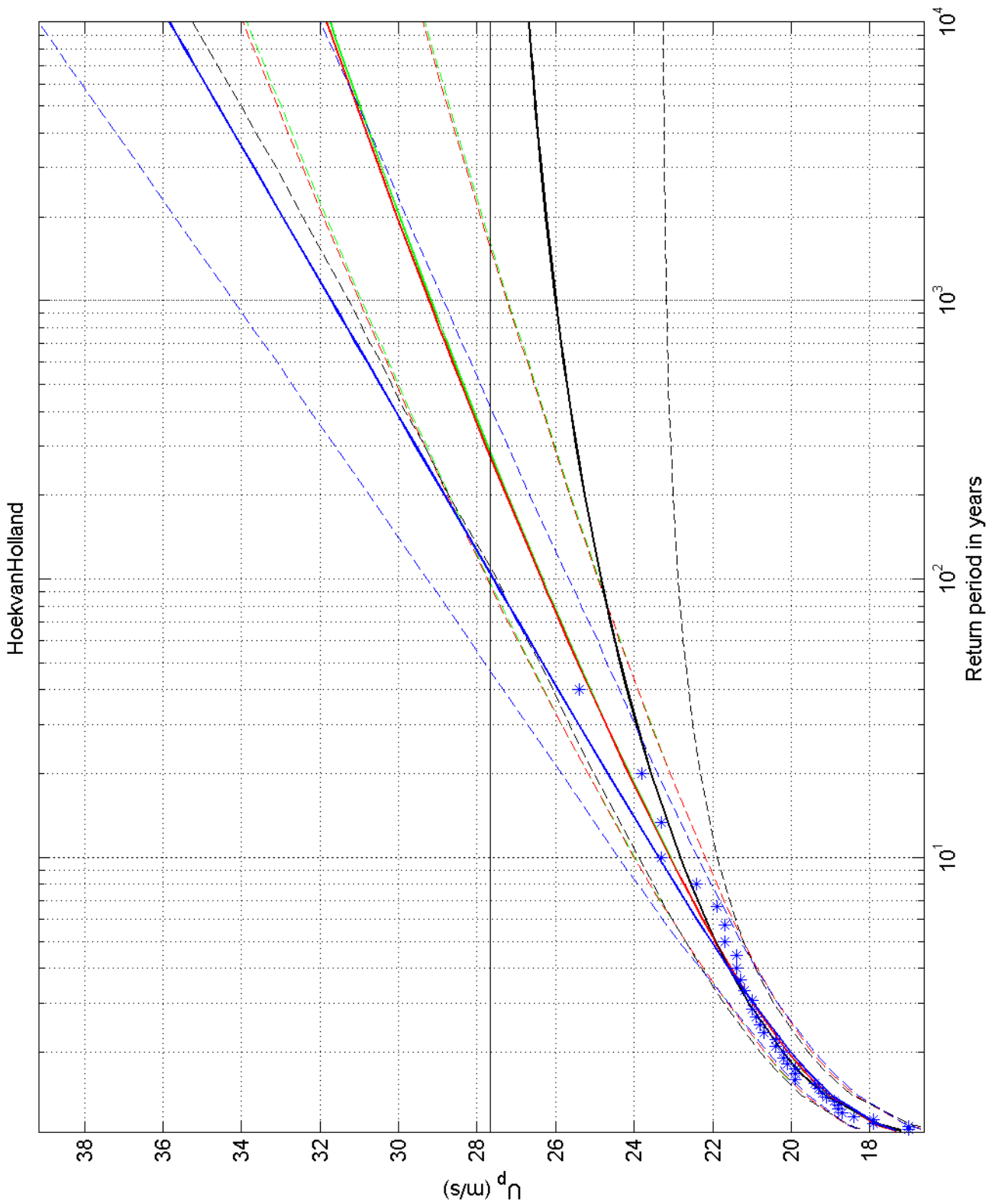
Return value plot with Gumbel (blue) and GEV (black) fit to U ,
 Gumbel (red) fit to U_p^2 and Gumbel (green) fit to U_p
 Plotting positions: x_i vs $(n+1)/(n+1-i)$

L.E. Goeree

Deltares

1200264-005

Fig. F.2.320



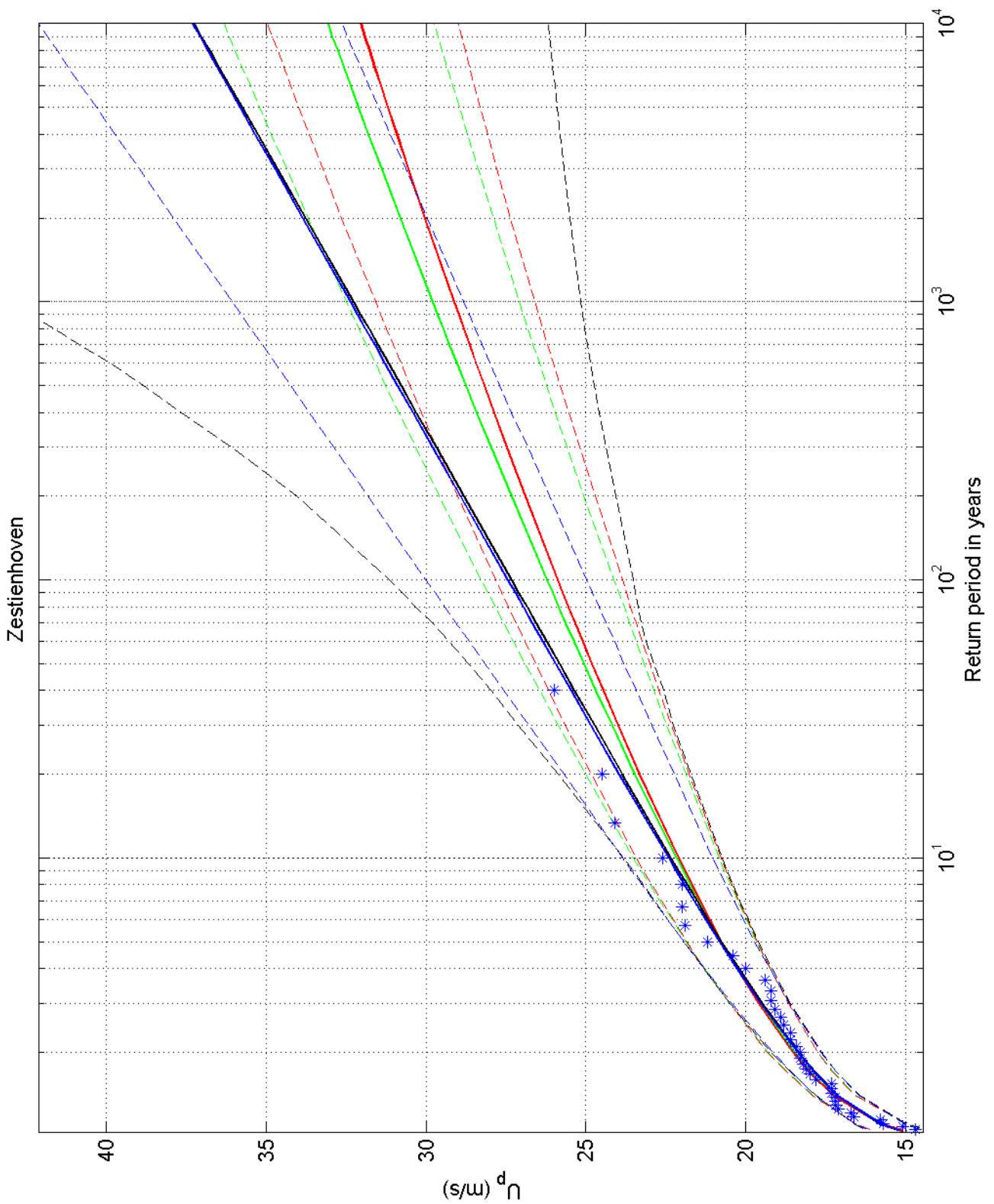
Return value plot with Gumbel (blue) and GEV (black) fit to U,
 Gumbel (red) fit to U_p^2 and Gumbel (green) fit to U_p
 Plotting positions: x_i vs $(n+1)/(n+1-i)$

HoekvanHolland

Deltares

1200264-005

Fig. F.2.330



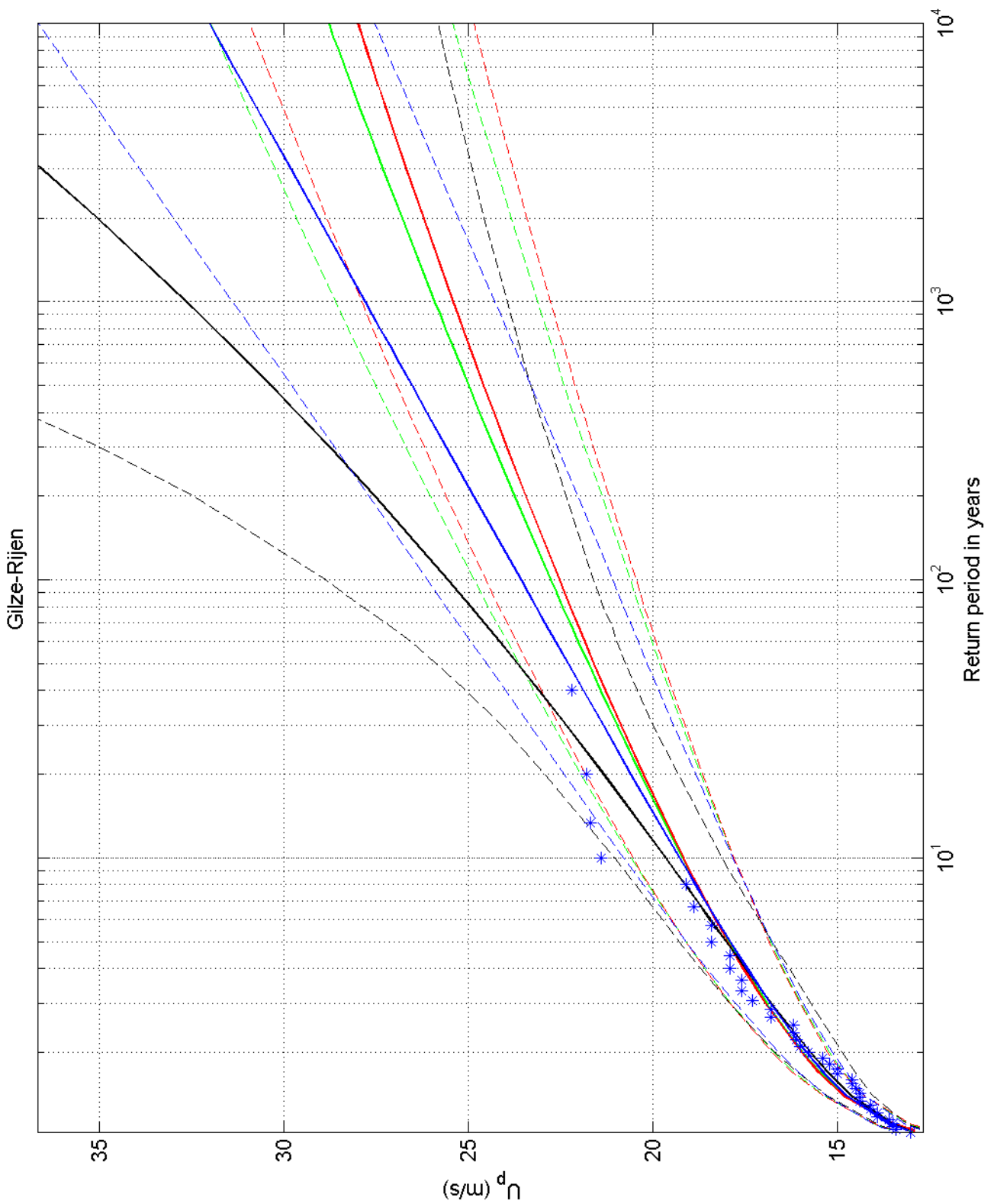
Return value plot with Gumbel (blue) and GEV (black) fit to U ,
 Gumbel (red) fit to U_p^2 and Gumbel (green) fit to U_p
 Plotting positions: x_i vs $(n+1)/(n+1-i)$

Zestienhoven

Deltares

1200264-005

Fig. F.2.344



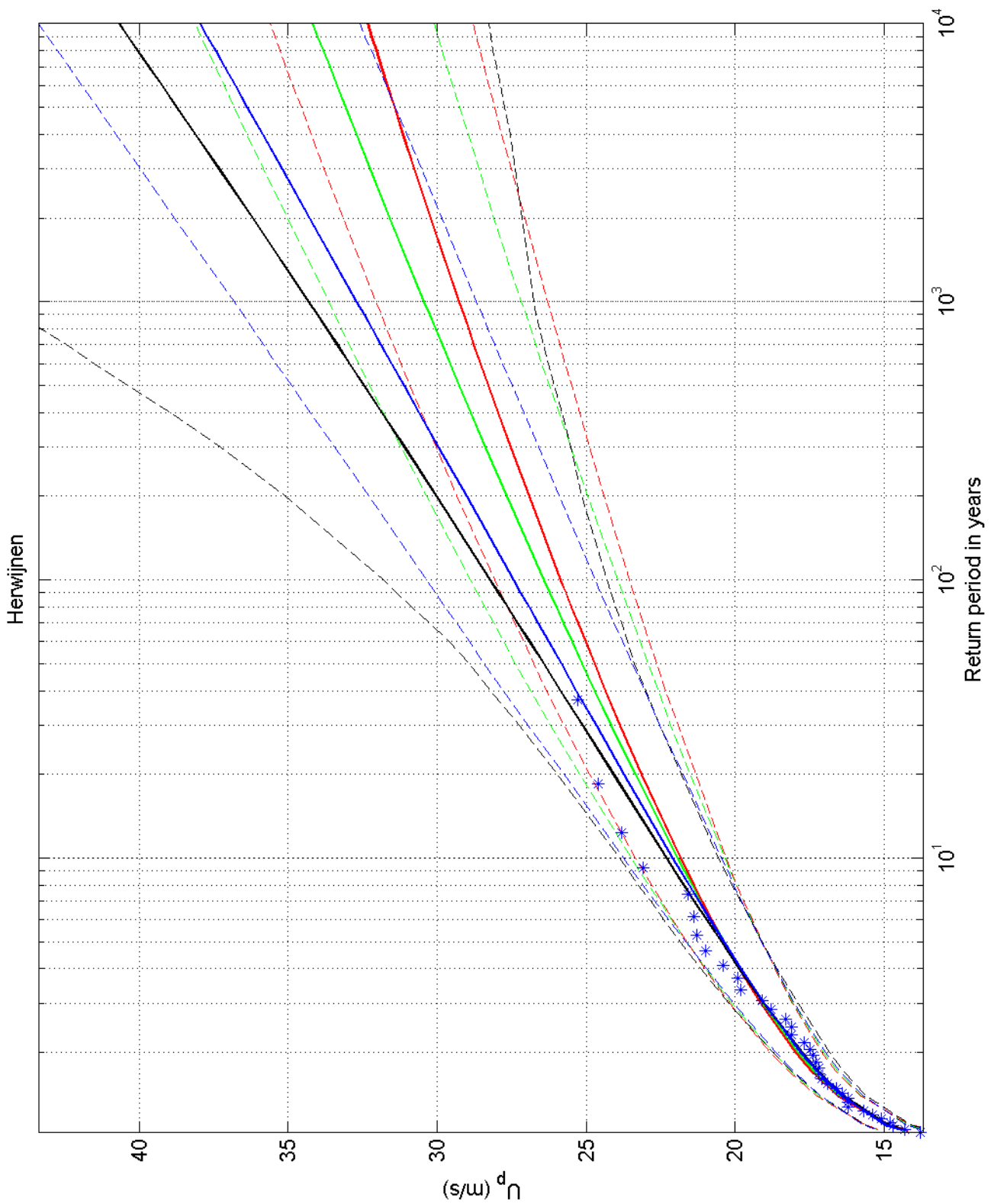
Return value plot with Gumbel (blue) and GEV (black) fit to U ,
 Gumbel (red) fit to U_p^2 and Gumbel (green) fit to U_p
 Plotting positions: x_i vs $(n+1)/(n+1-i)$

Gilze-Rijen

Deltares

1200264-005

Fig. F.2.350



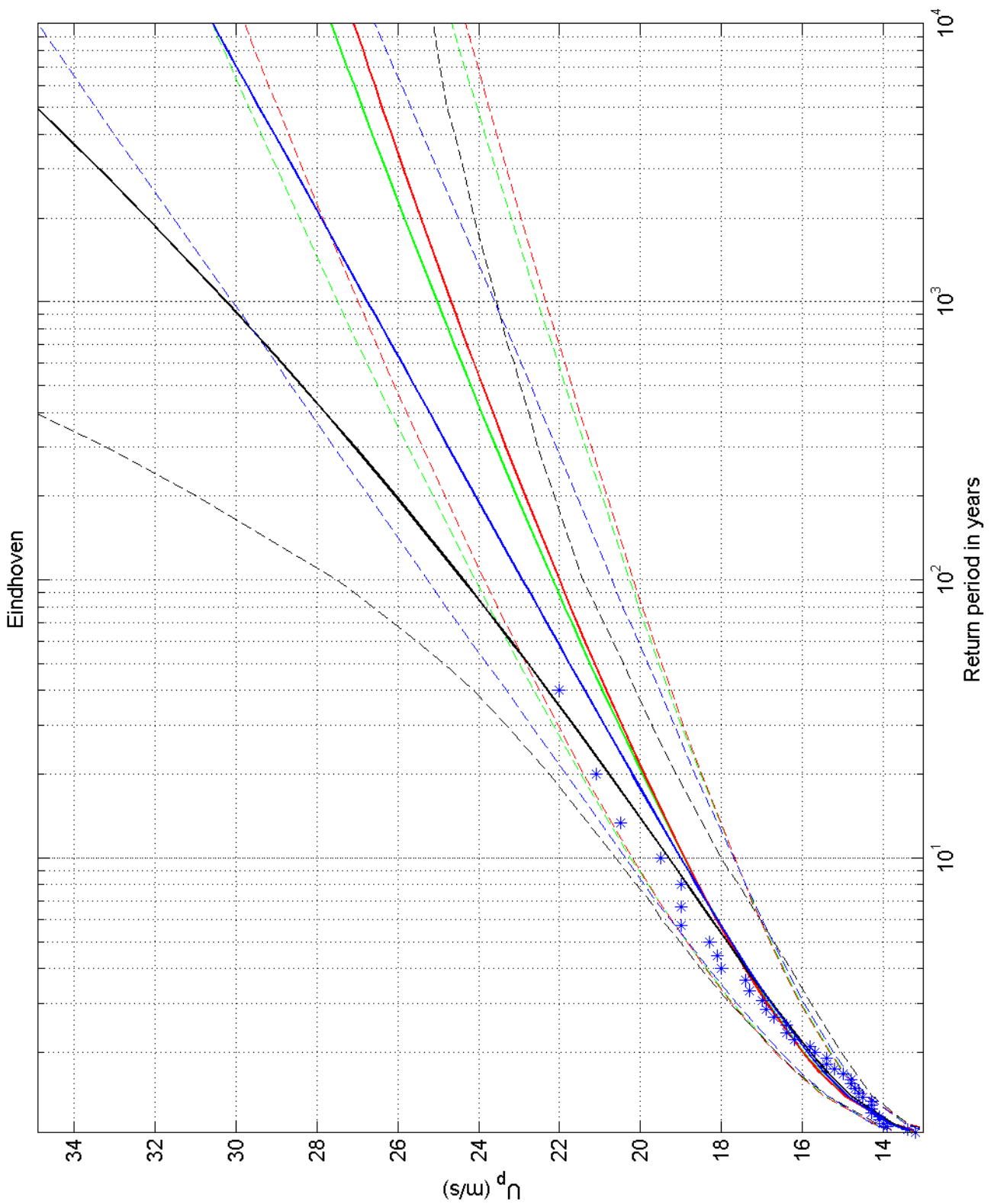
Return value plot with Gumbel (blue) and GEV (black) fit to U ,
 Gumbel (red) fit to U_p^2 and Gumbel (green) fit to U_p
 Plotting positions: x_i vs $(n+1)/(n+1-i)$

Herwijnen

Deltares

1200264-005

Fig. F.2.356



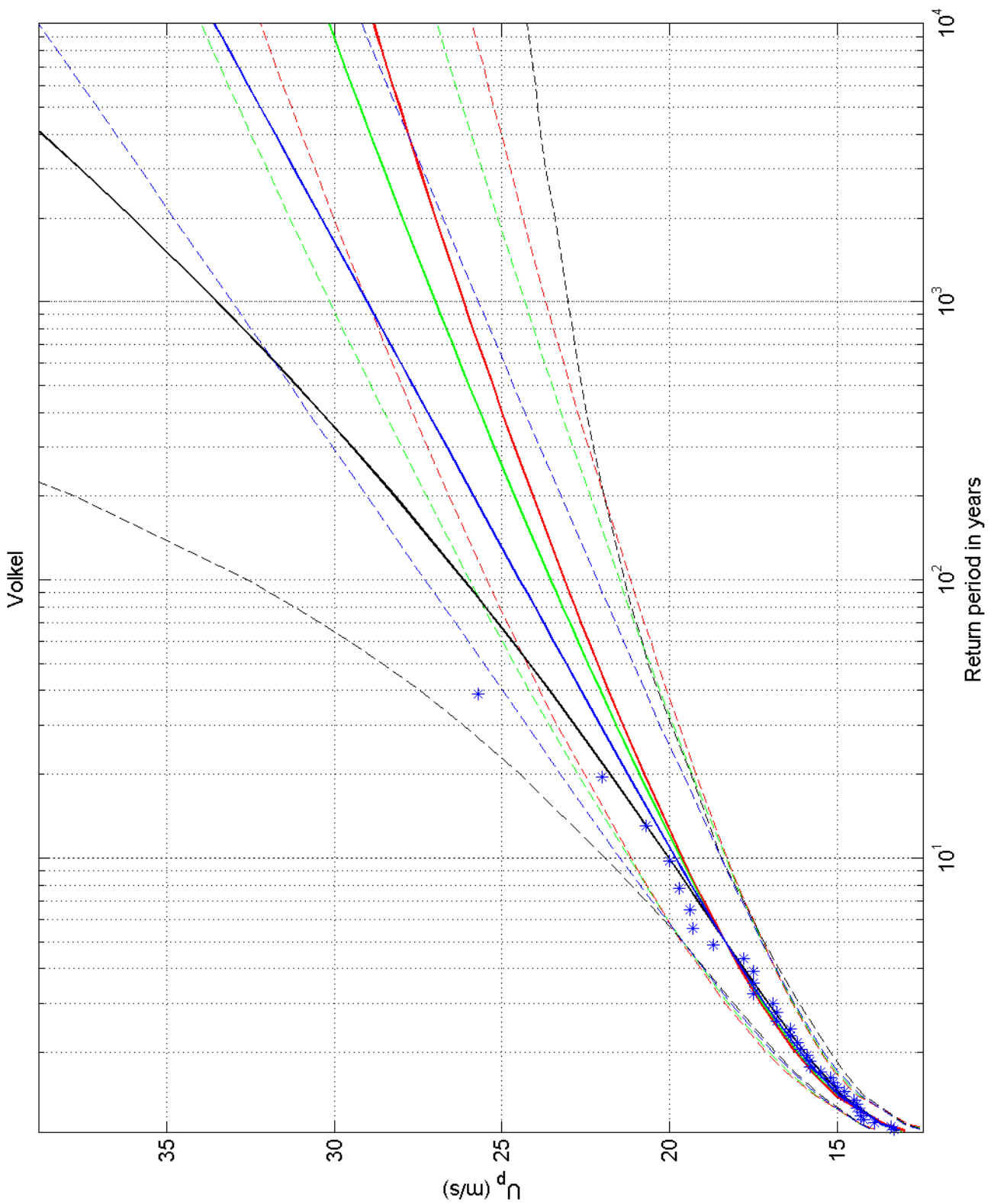
Return value plot with Gumbel (blue) and GEV (black) fit to U ,
 Gumbel (red) fit to U_p^2 and Gumbel (green) fit to U_p
 Plotting positions: x_i vs $(n+1)/(n+1-i)$

Eindhoven

Deltares

1200264-005

Fig. F.2.370



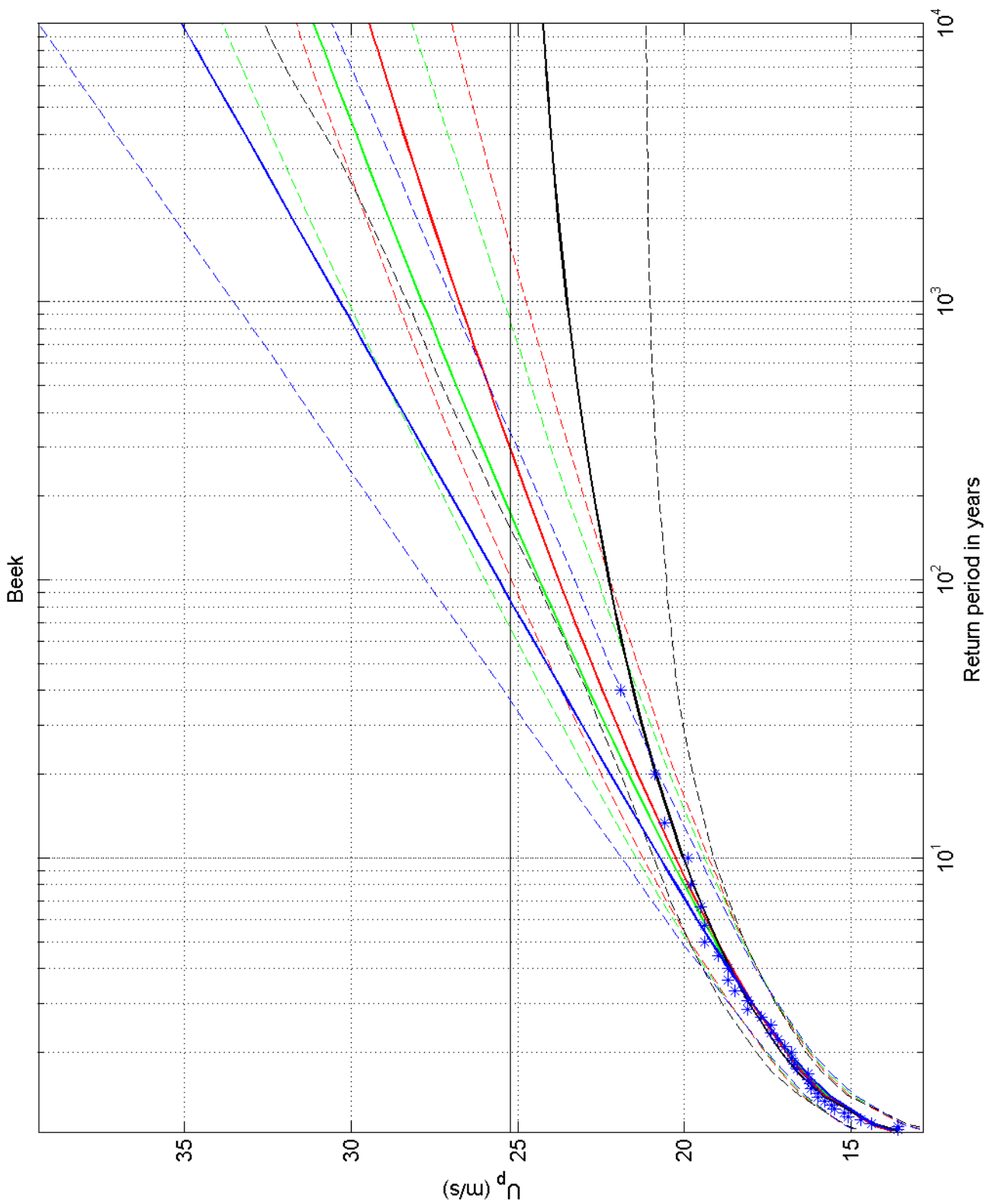
Return value plot with Gumbel (blue) and GEV (black) fit to U ,
 Gumbel (red) fit to U_p^2 and Gumbel (green) fit to U_p^k
 Plotting positions: x_i vs $(n+1)/(n+1-i)$

Volkrel

Deltares

1200264-005

Fig. F.2.375



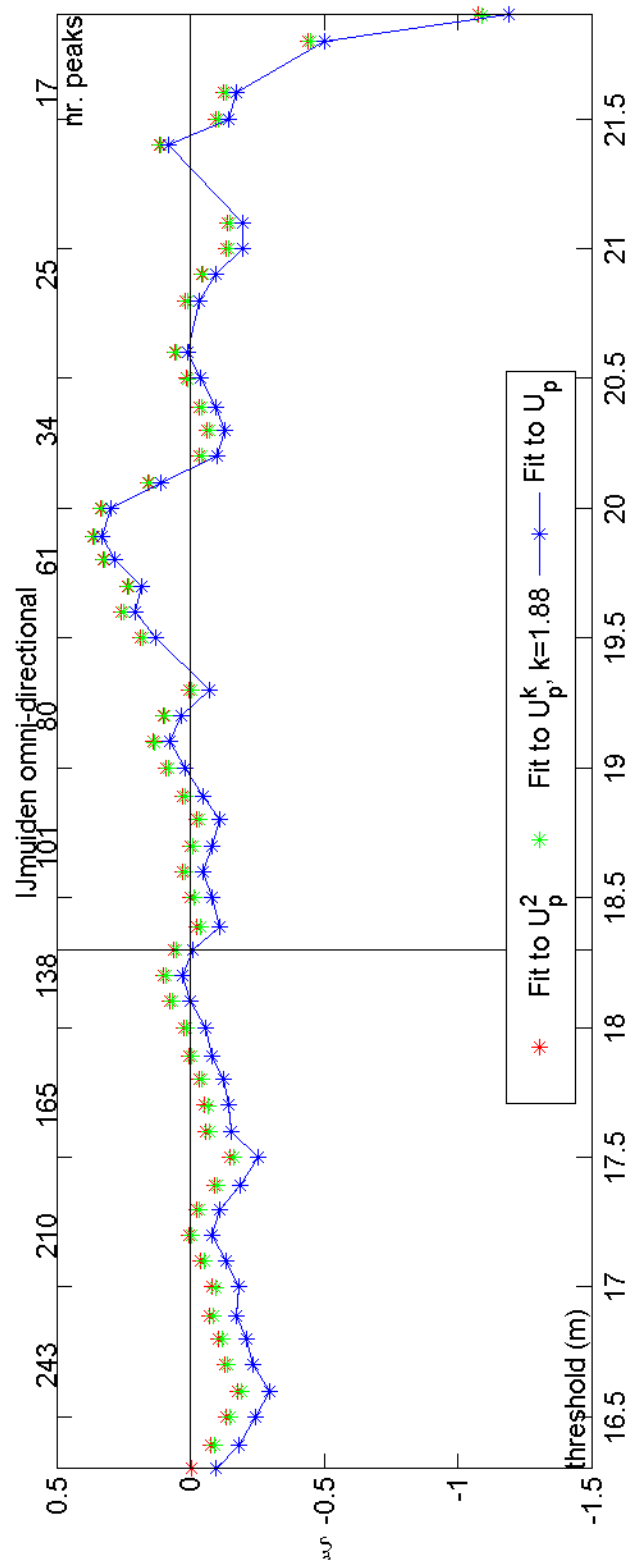
Return value plot with Gumbel (blue) and GEV (black) fit to U ,
 Gumbel (red) fit to U_p^2 and Gumbel (green) fit to U_p^k
 Plotting positions: x_i vs $(n+1)/(n+1-i)$

Beek

Deltares

1200264-005

Fig. F.2.380



Threshold plot
omni-directional

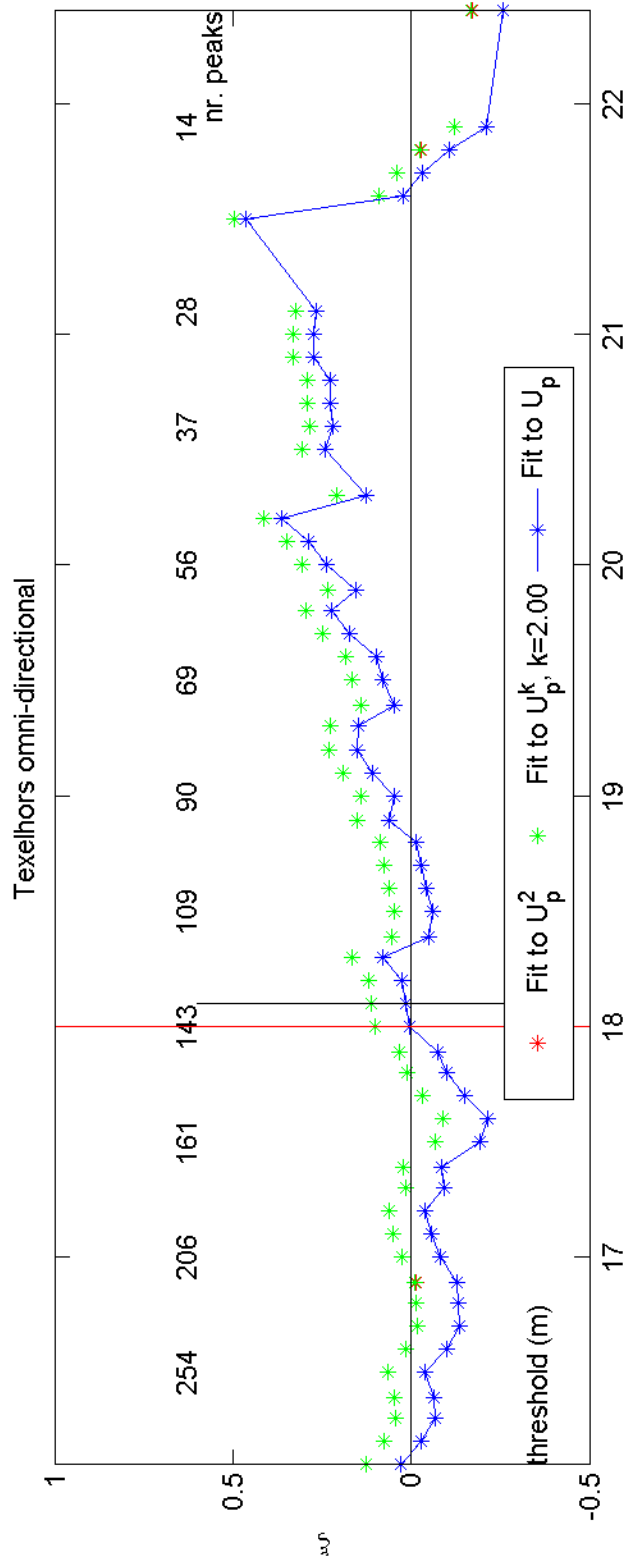
1970-2008

Ijmuiden

Deltares

1200264-005

Fig. F.3.225



Threshold plot
omni-directional

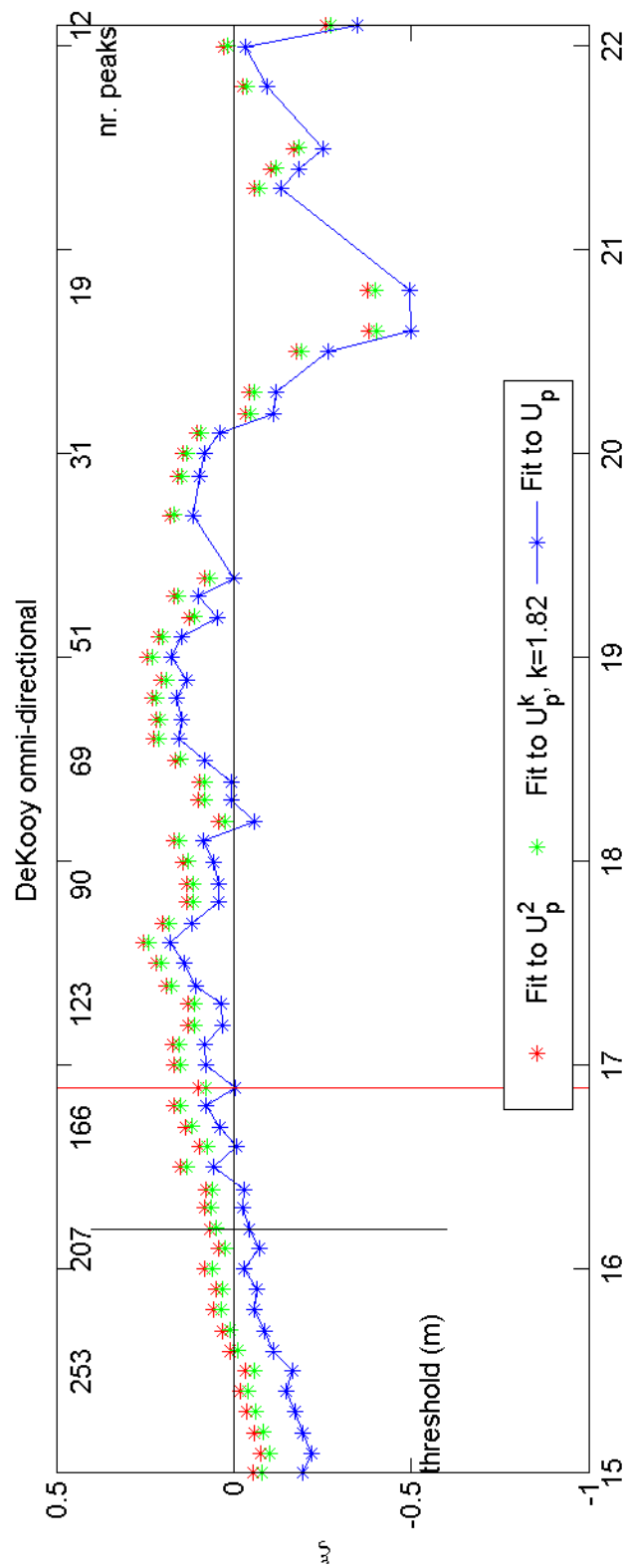
1970-2008

Texelhors

Deltares

1200264-005

Fig. F.3.229



Threshold plot
omni-directional

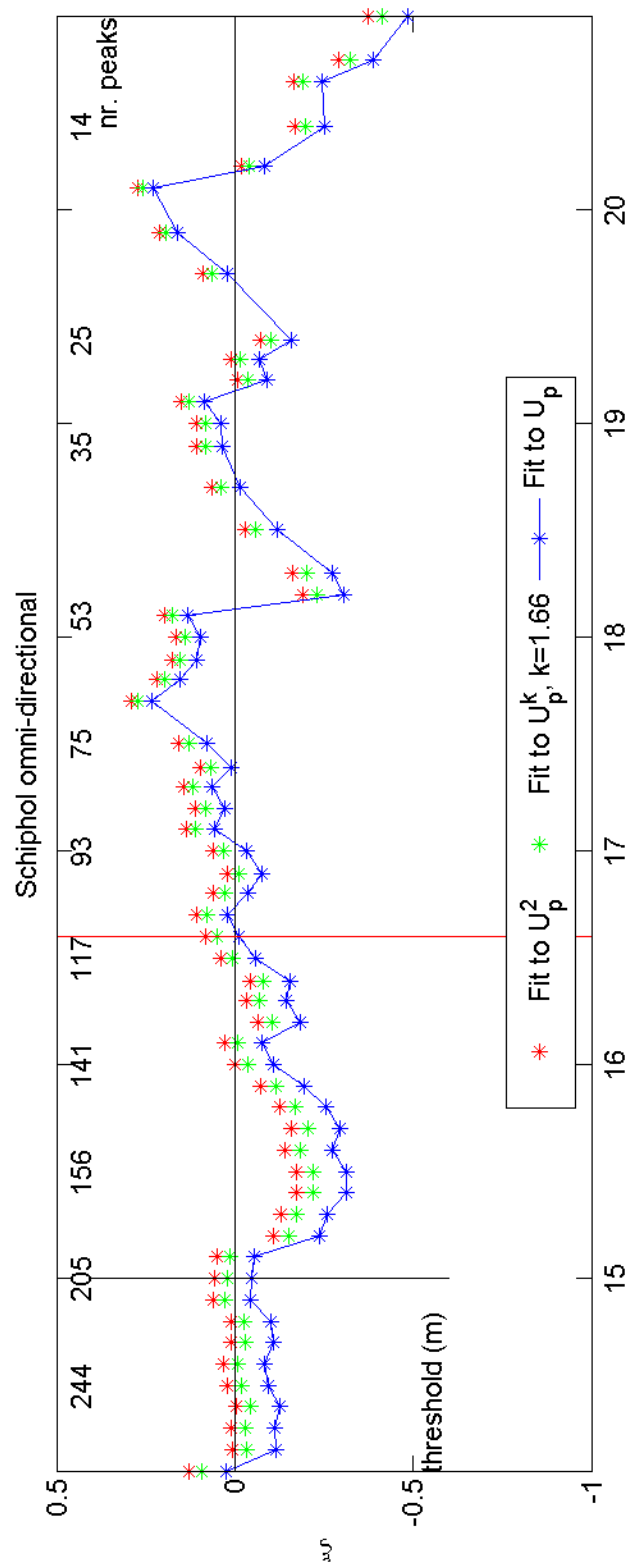
1970-2008

DeKooy

Deltares

1200264-005

Fig. F.3.235



Threshold plot
omni-directional

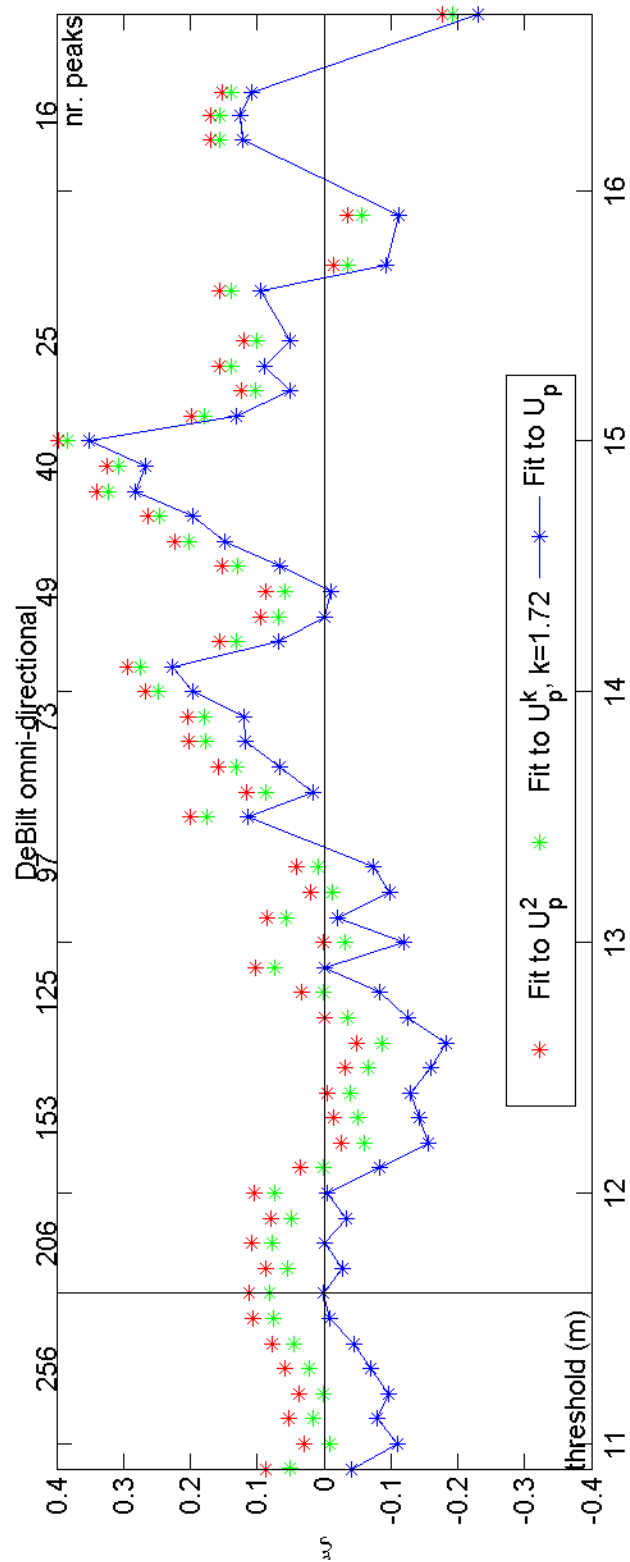
1970-2008

Schiphol

Deltares

1200264-005

Fig. F.3.240



Threshold plot
omni-directional

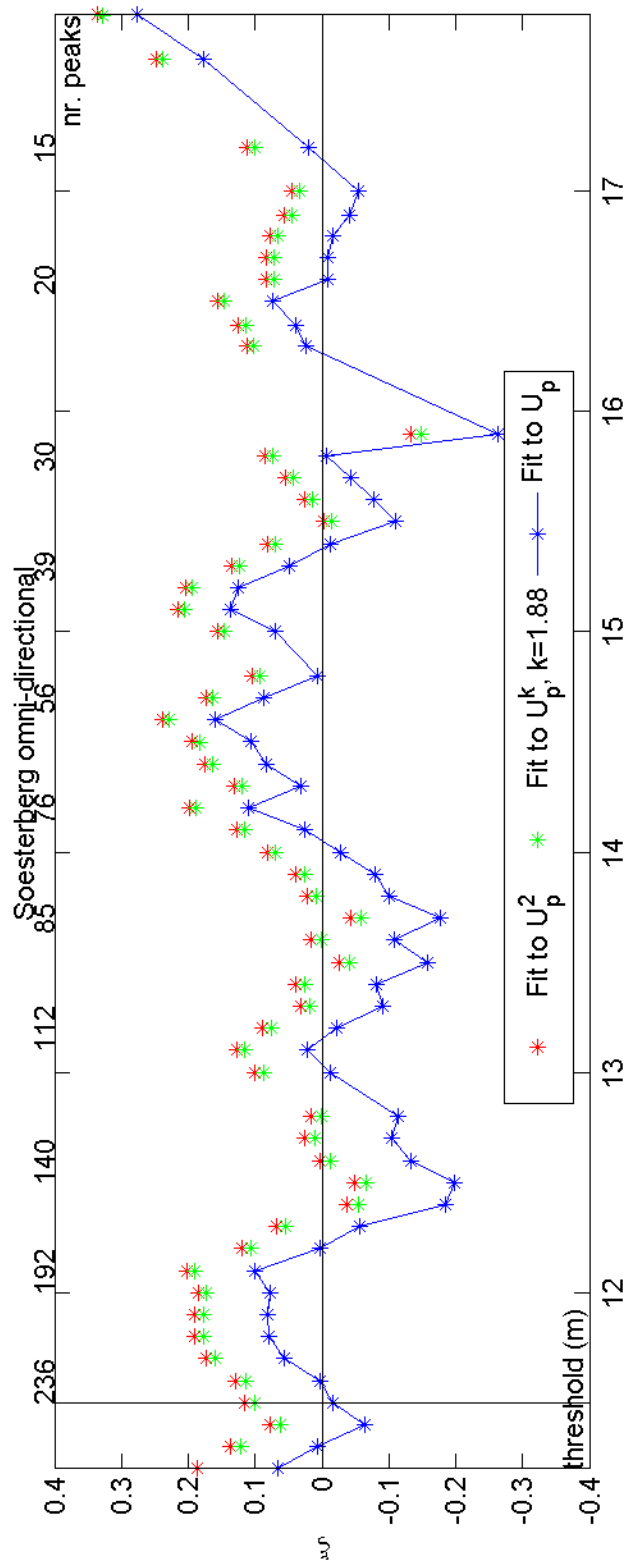
1970-2008

DeBilt

Deltares

1200264-005

Fig. F.3.260



Threshold plot
omni-directional

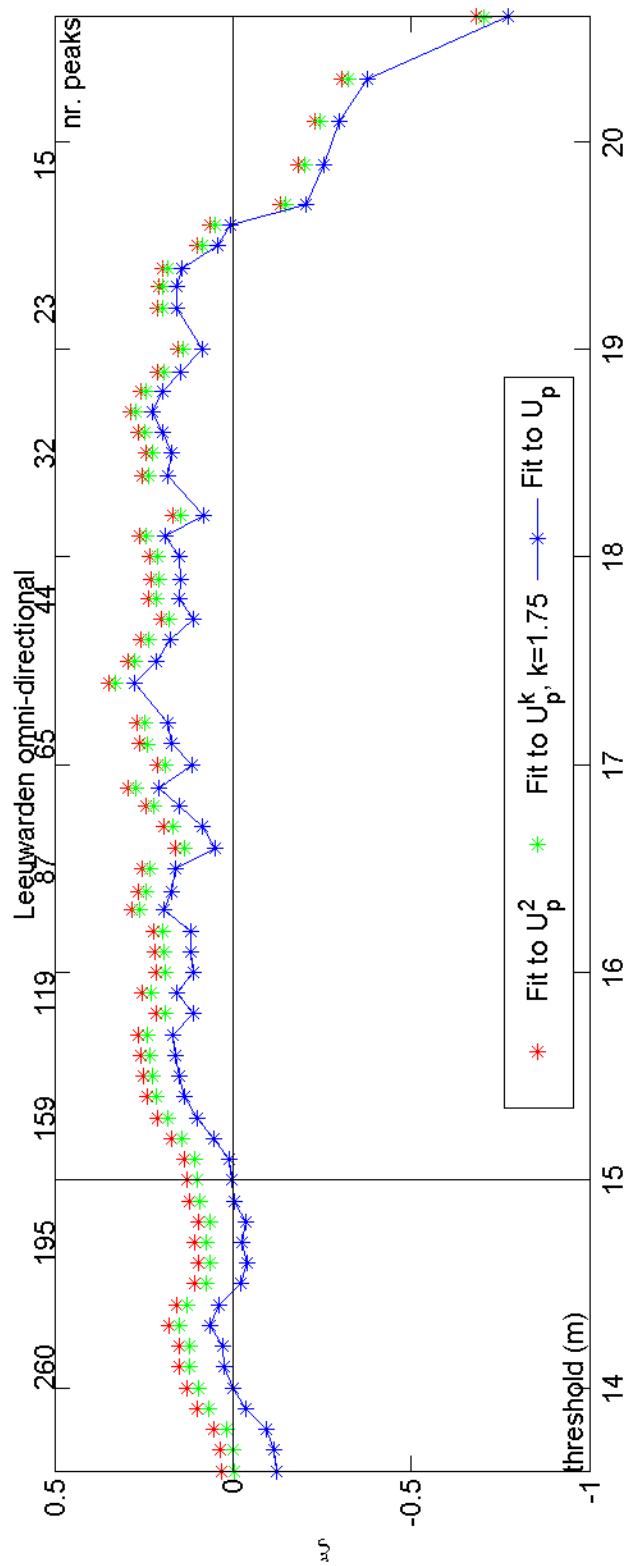
1970-2008

Soesterberg

Deltares

1200264-005

Fig. F.3.265



Threshold plot
omni-directional

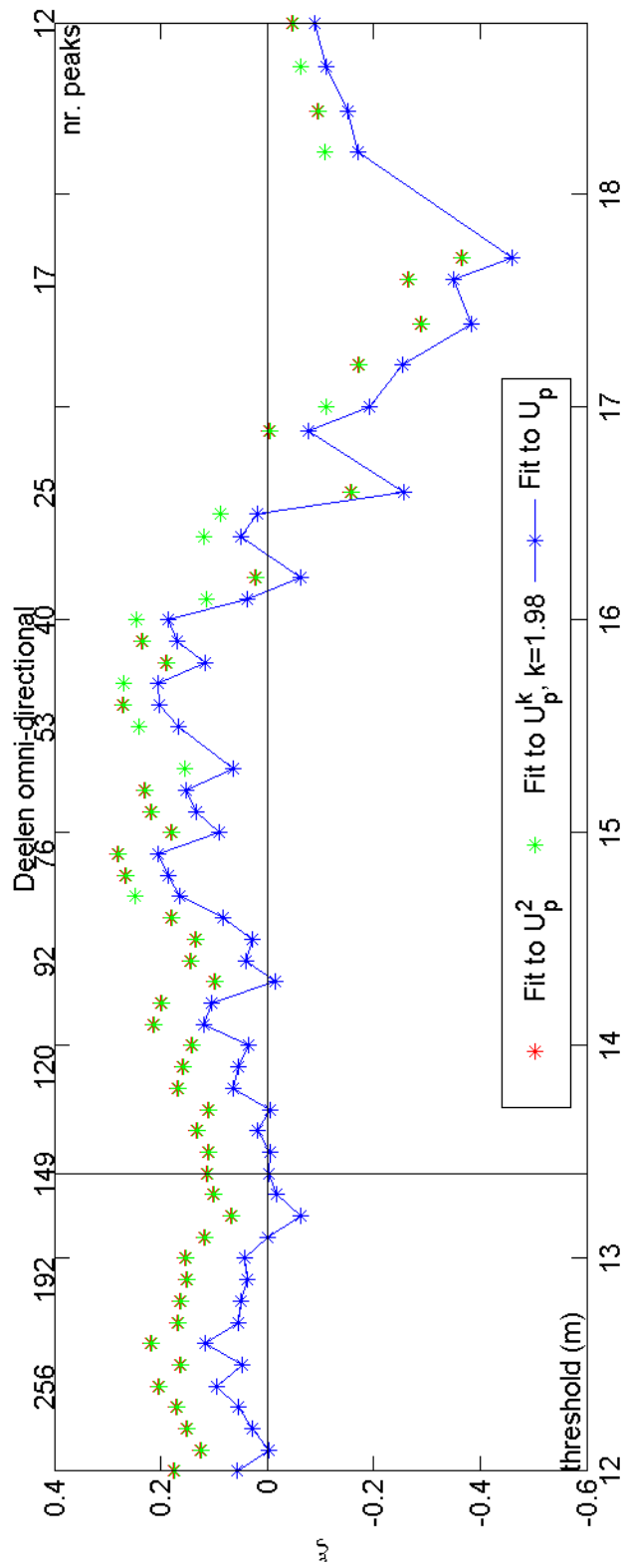
1970-2008

Leeuwarden

Deltares

1200264-005

Fig. F.3.270



Threshold plot
omni-directional

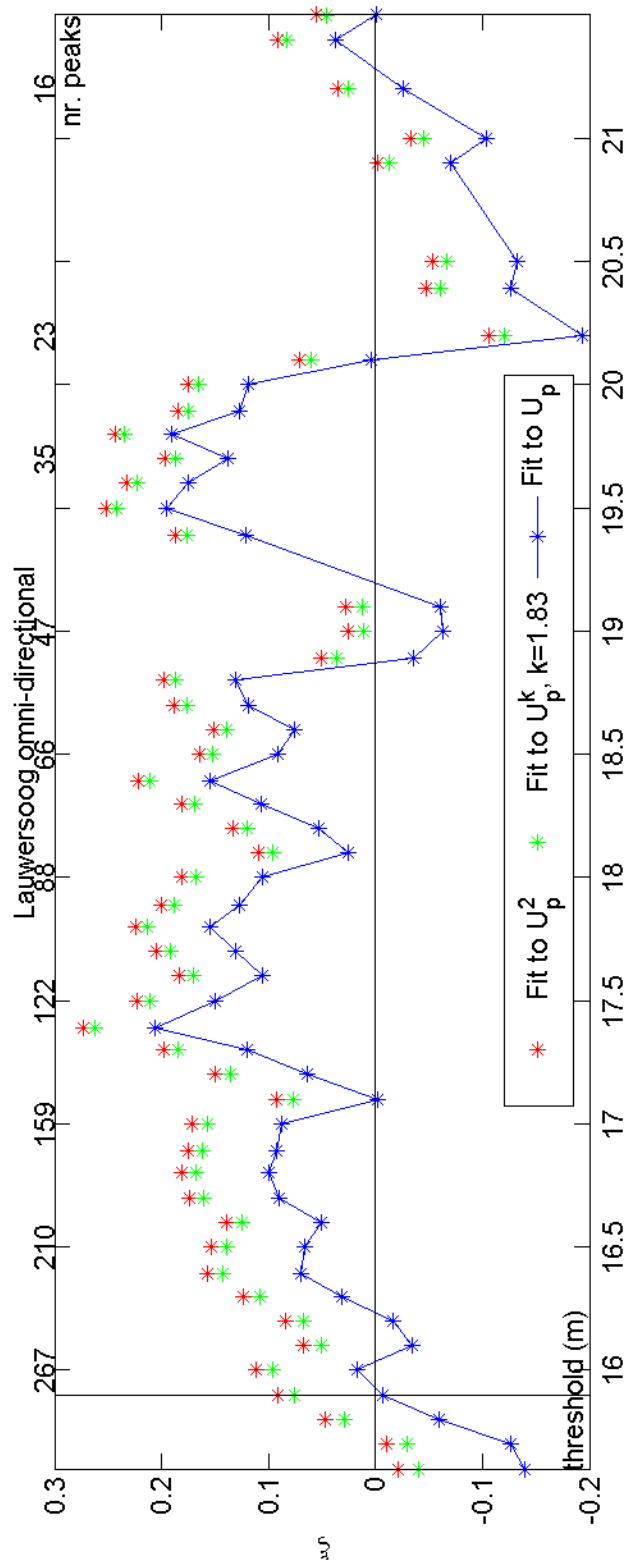
1970-2008

Deelen

Deltares

1200264-005

Fig. F.3.275



Threshold plot
omni-directional

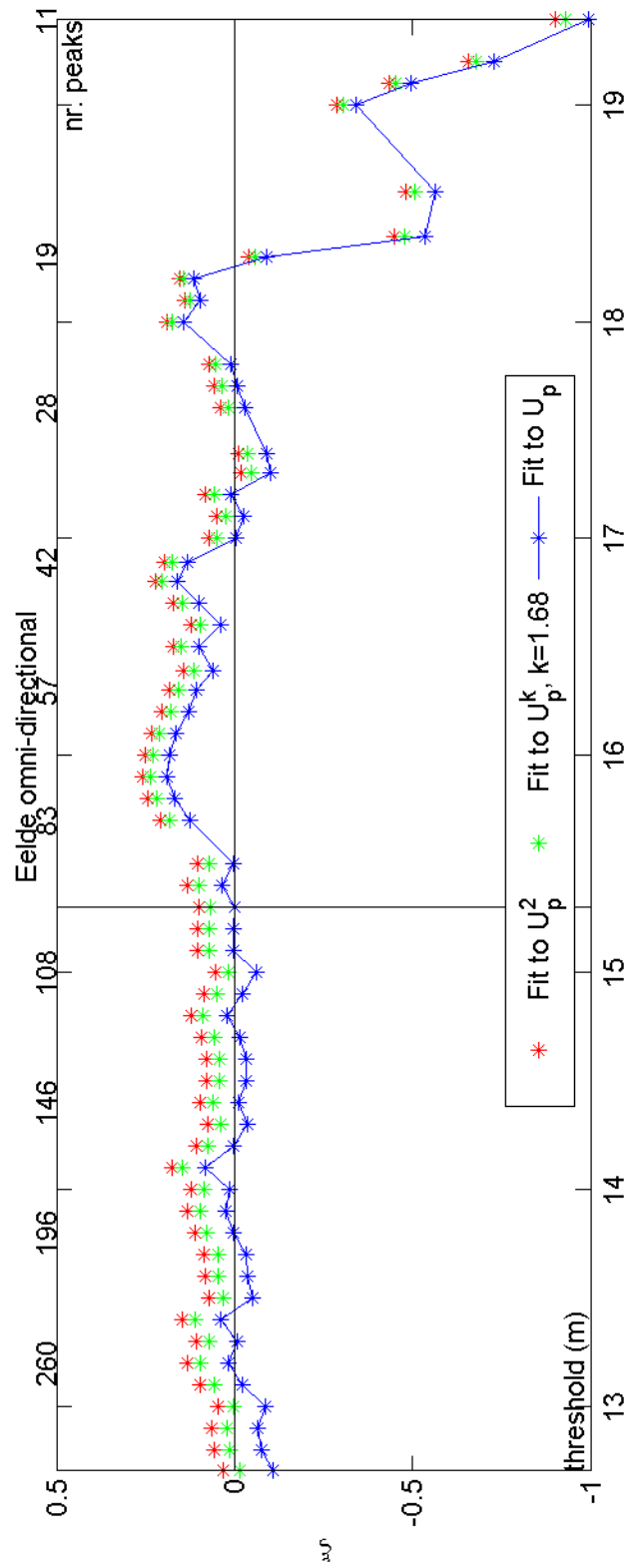
1970-2008

Lauwersoog

Deltares

1200264-005

Fig. F.3.277



Threshold plot
omni-directional

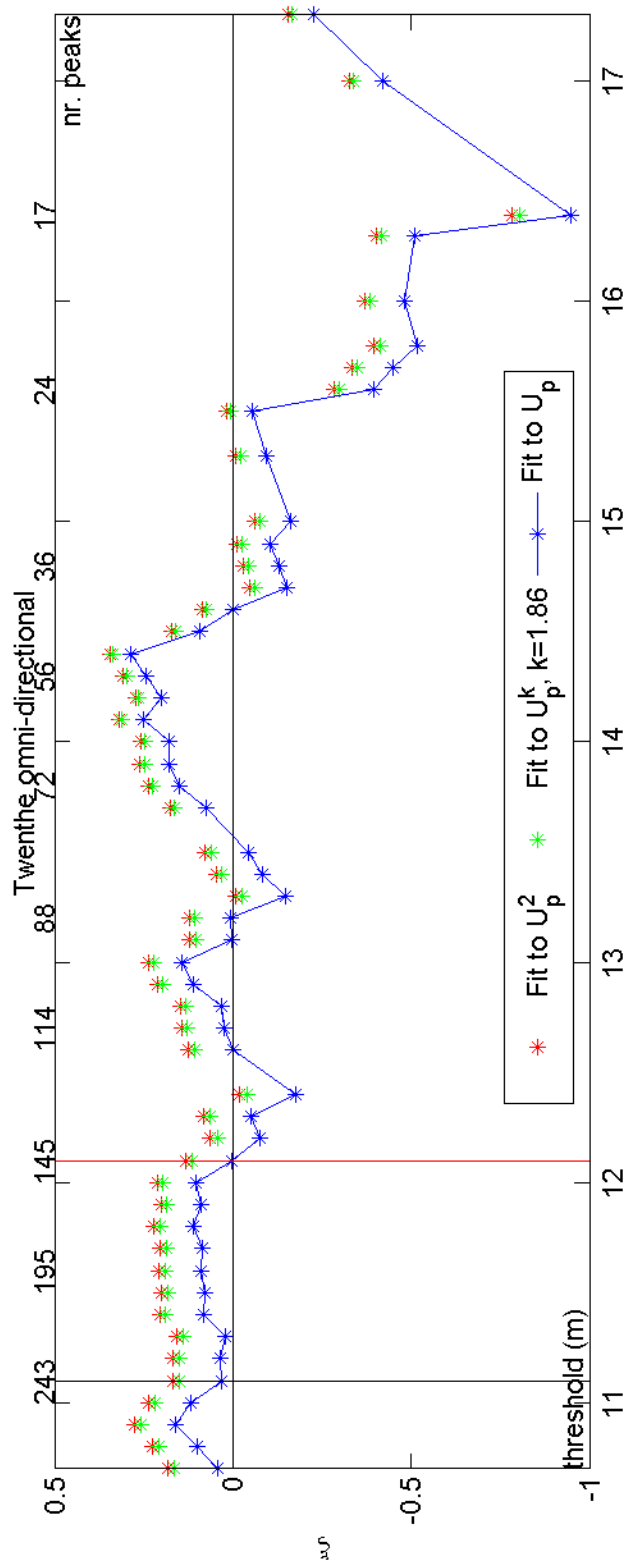
1970-2008

Eelde

Deltares

1200264-005

Fig. F.3.280



Threshold plot
omni-directional

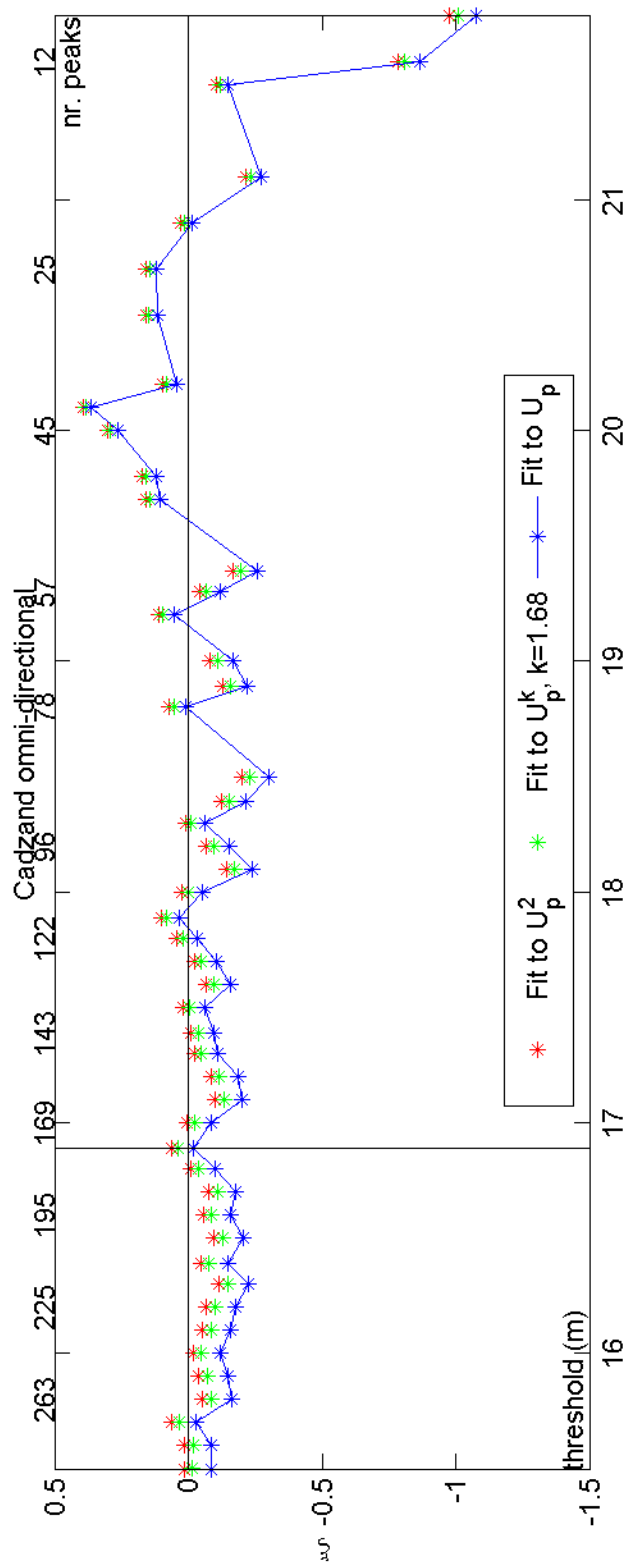
1970-2008

Twenthe

Deltares

1200264-005

Fig. F.3.290



Threshold plot
omni-directional

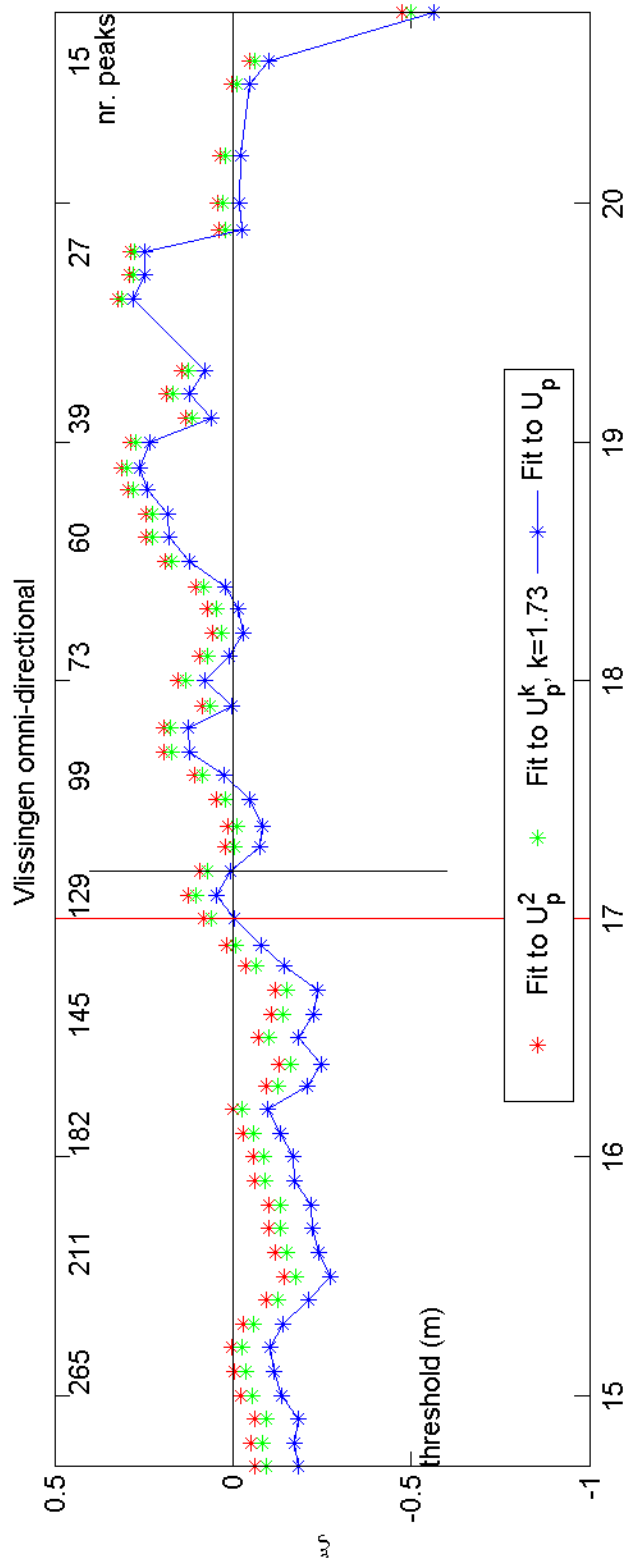
1970-2008

Cadzand

Deltares

1200264-005

Fig. F.3.308



Threshold plot
omni-directional

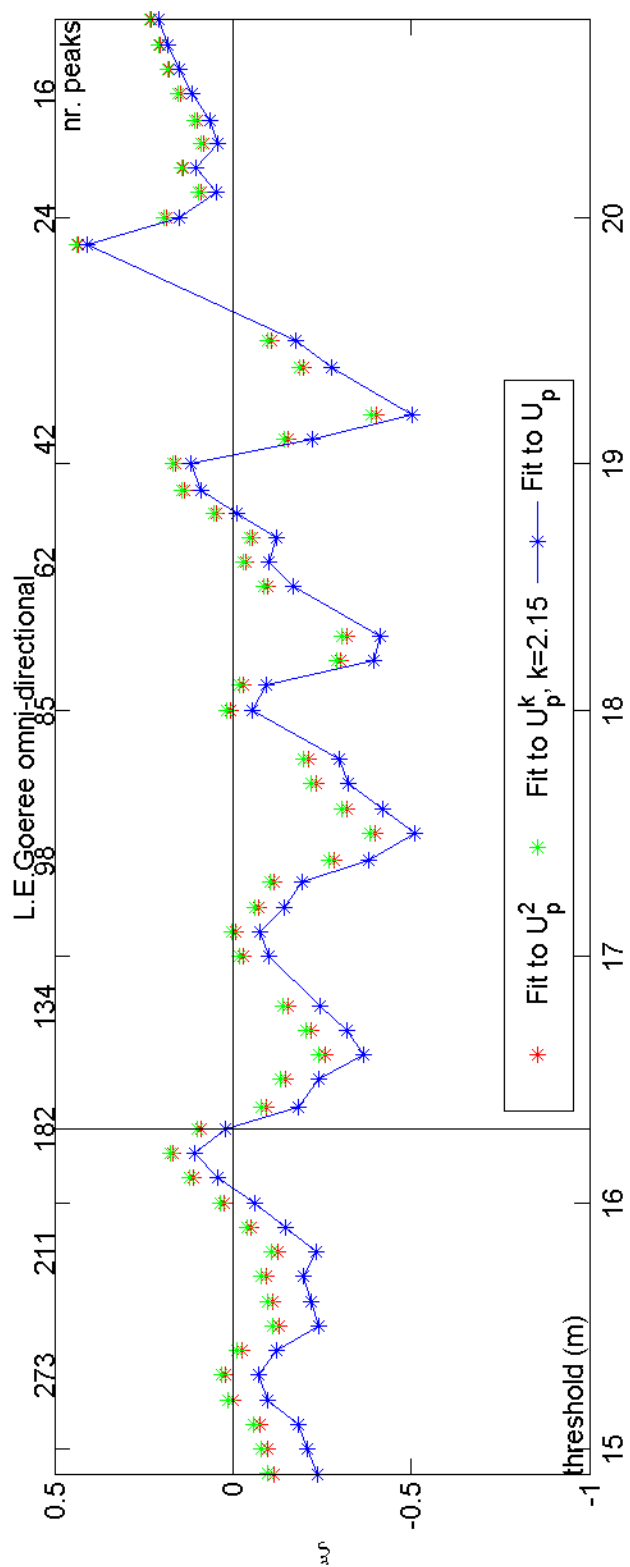
1970-2008

Vissingen

Deltares

1200264-005

Fig. F.3.310



Threshold plot
omni-directional

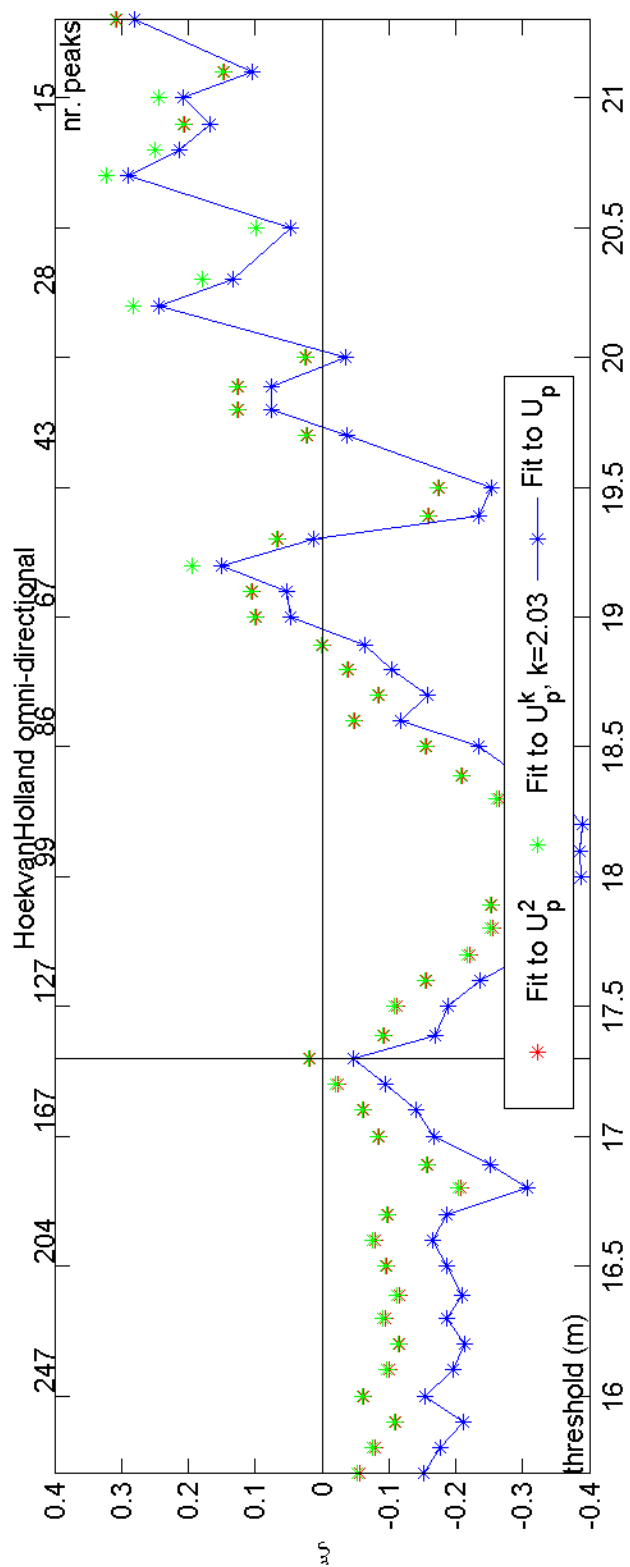
1970-2008

L.E. Goeree

Deltares

1200264-005

Fig. F.3.320



Threshold plot
omni-directional

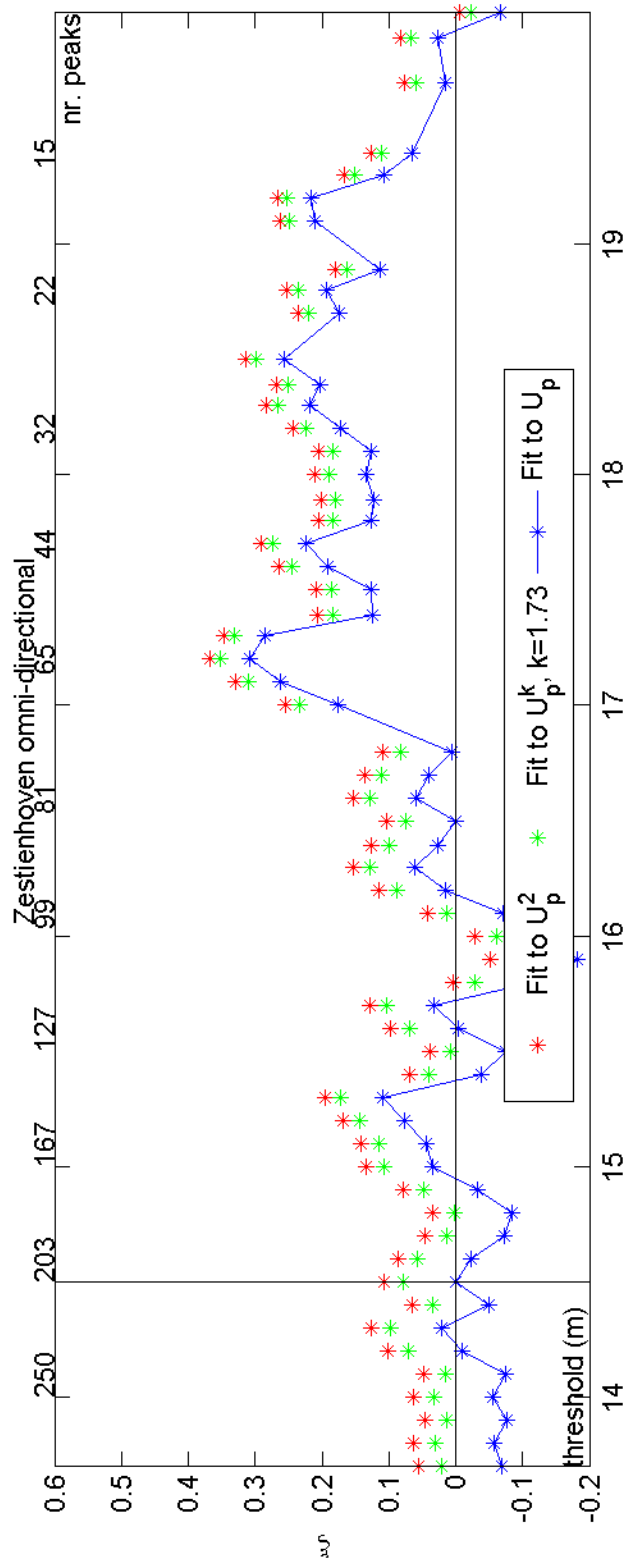
1970-2008

HoekvanHolland

Deltares

1200264-005

Fig. F.3.330



Threshold plot
omni-directional

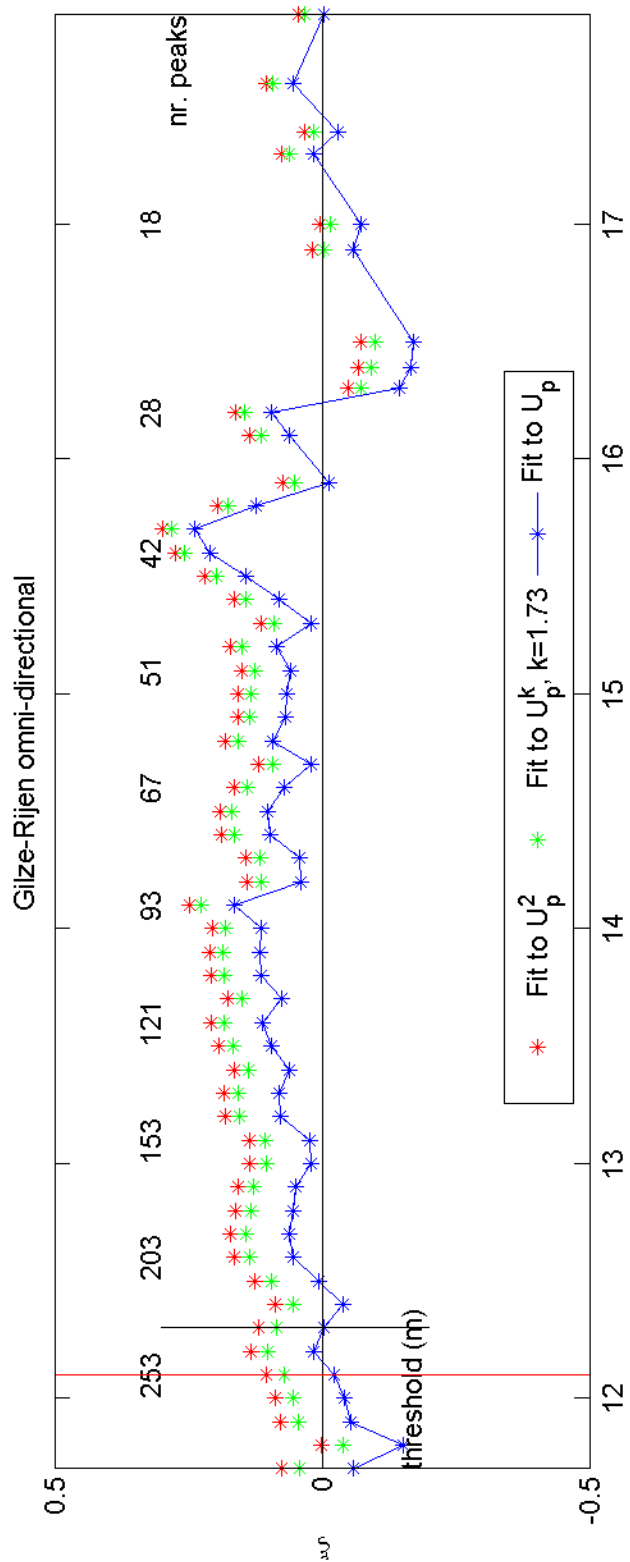
1970-2008

Zestienhoven

Deltares

1200264-005

Fig. F.3.344



Threshold plot
omni-directional

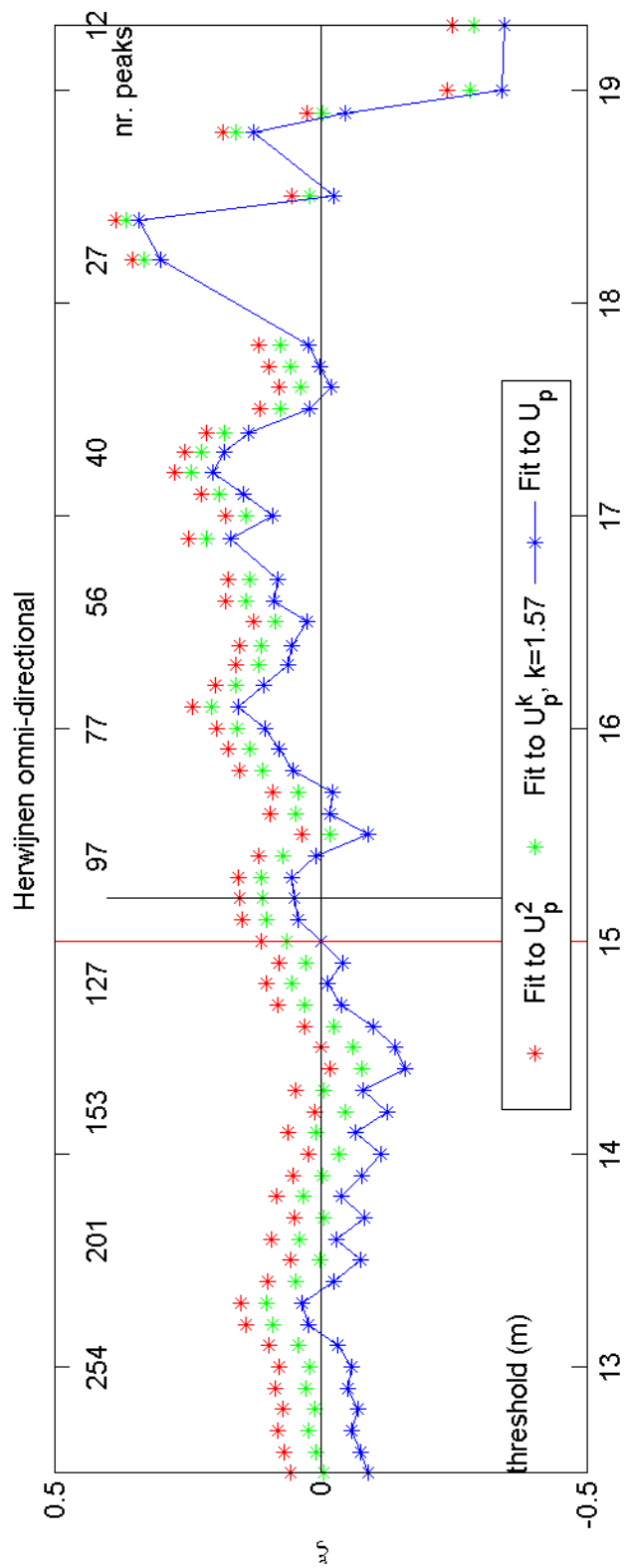
1970-2008

Gilze-Rijen

Deltares

1200264-005

Fig. F.3.350



Threshold plot
omni-directional

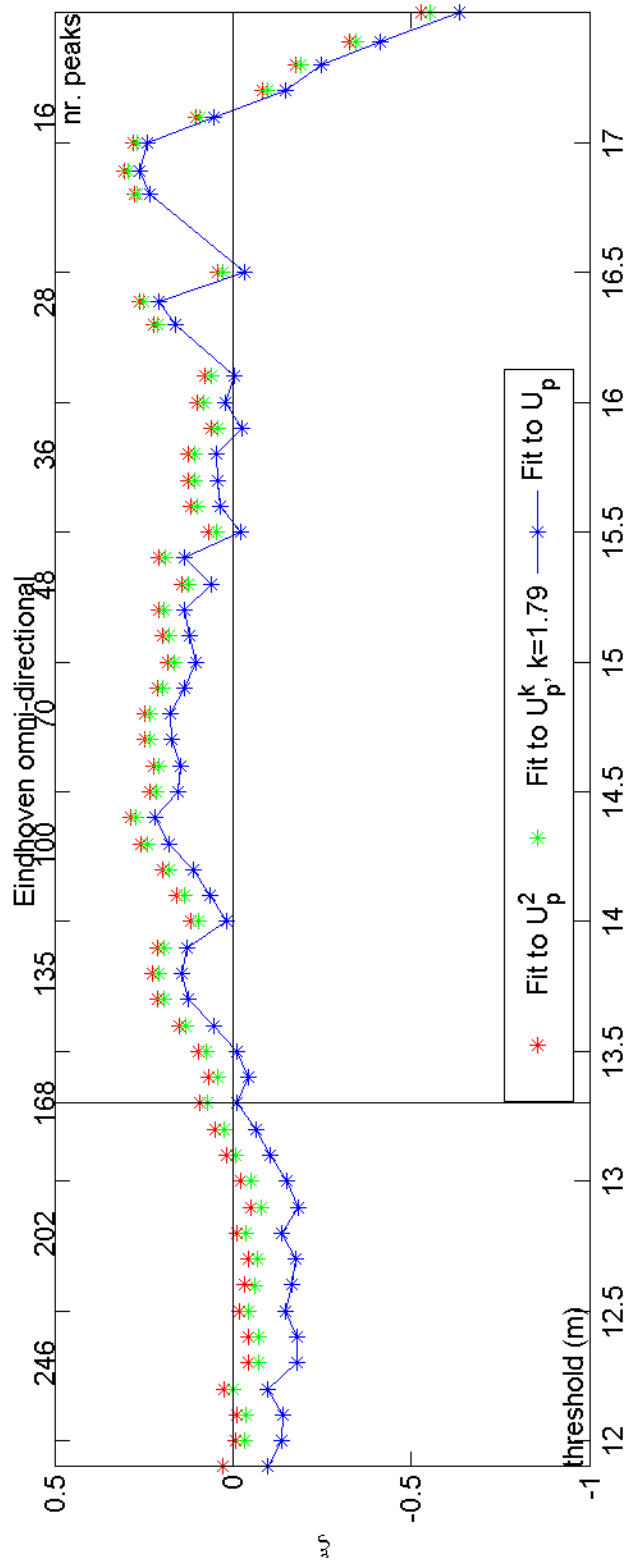
1970-2008

Herwijnen

Deltares

1200264-005

Fig. F.3.356



Threshold plot
omni-directional

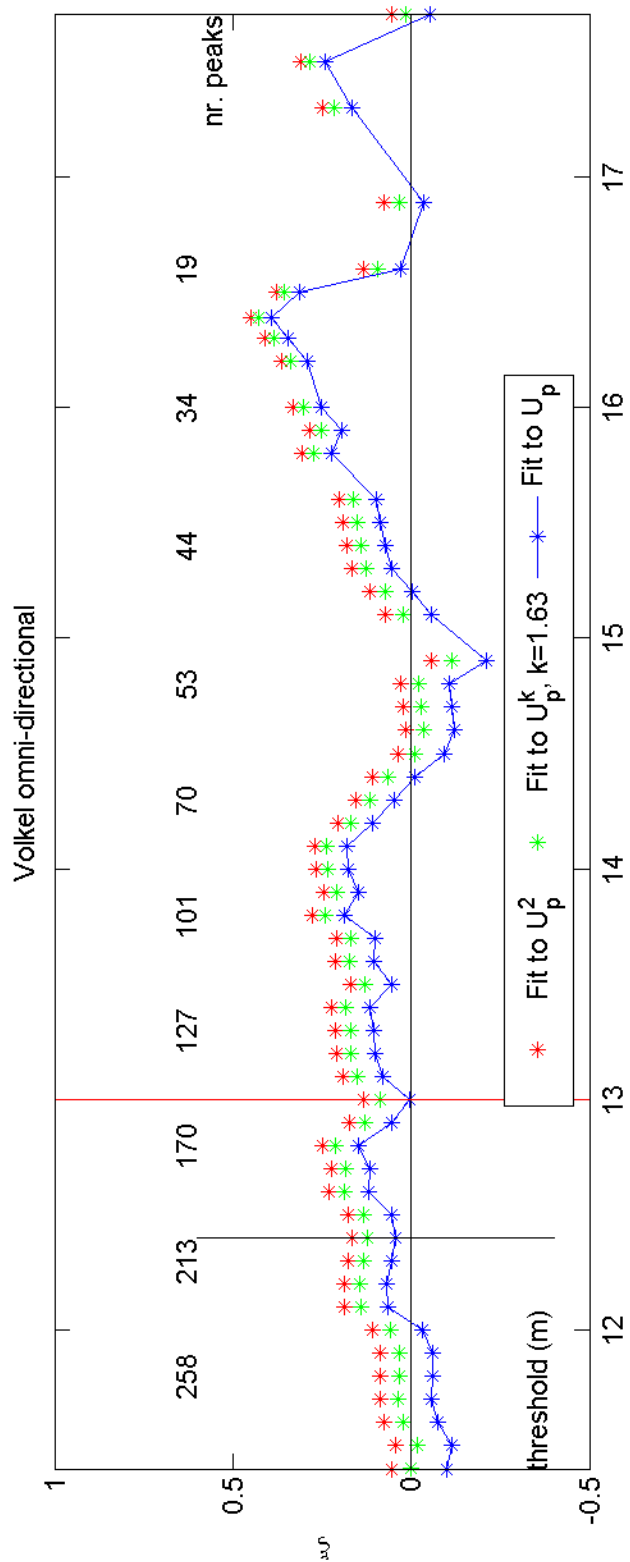
1970-2008

Eindhoven

Deltares

1200264-005

Fig. F.3.370



Threshold plot
omni-directional

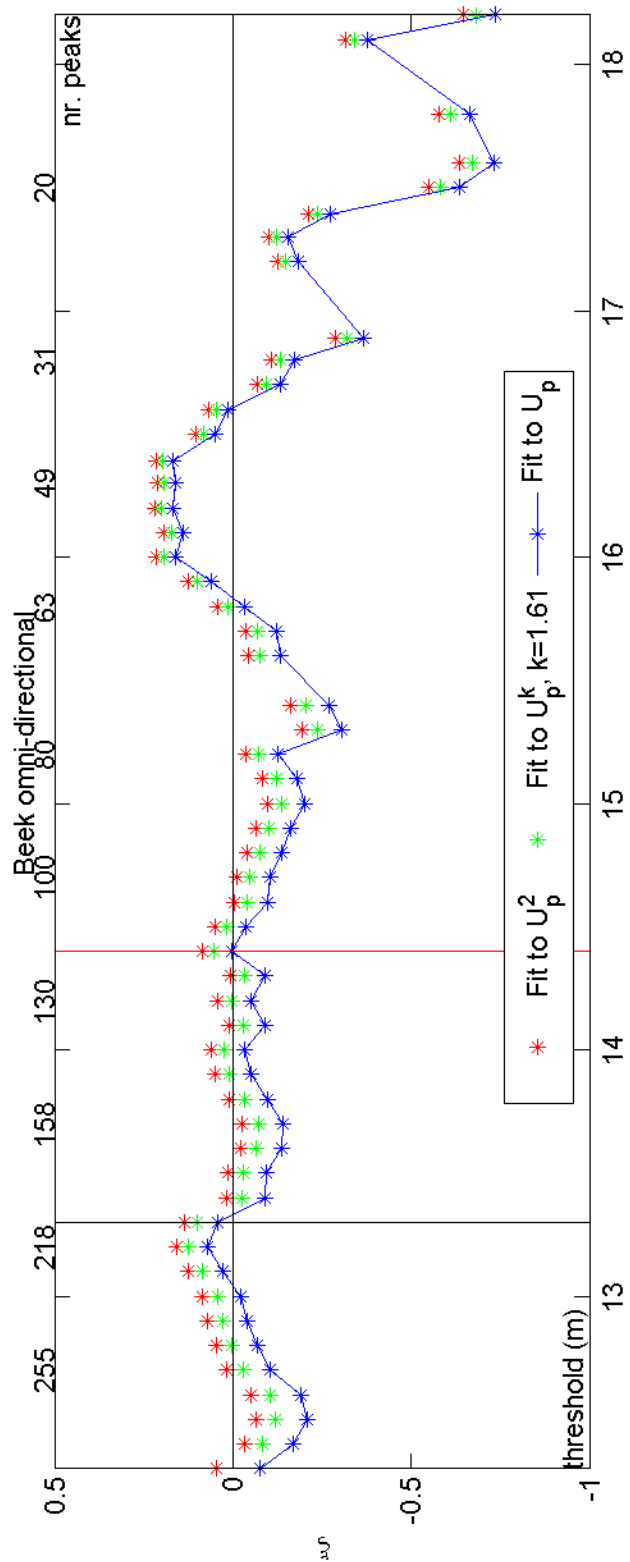
1970-2008

Volkel

Deltares

1200264-005

Fig. F.3.375



Threshold plot
omni-directional

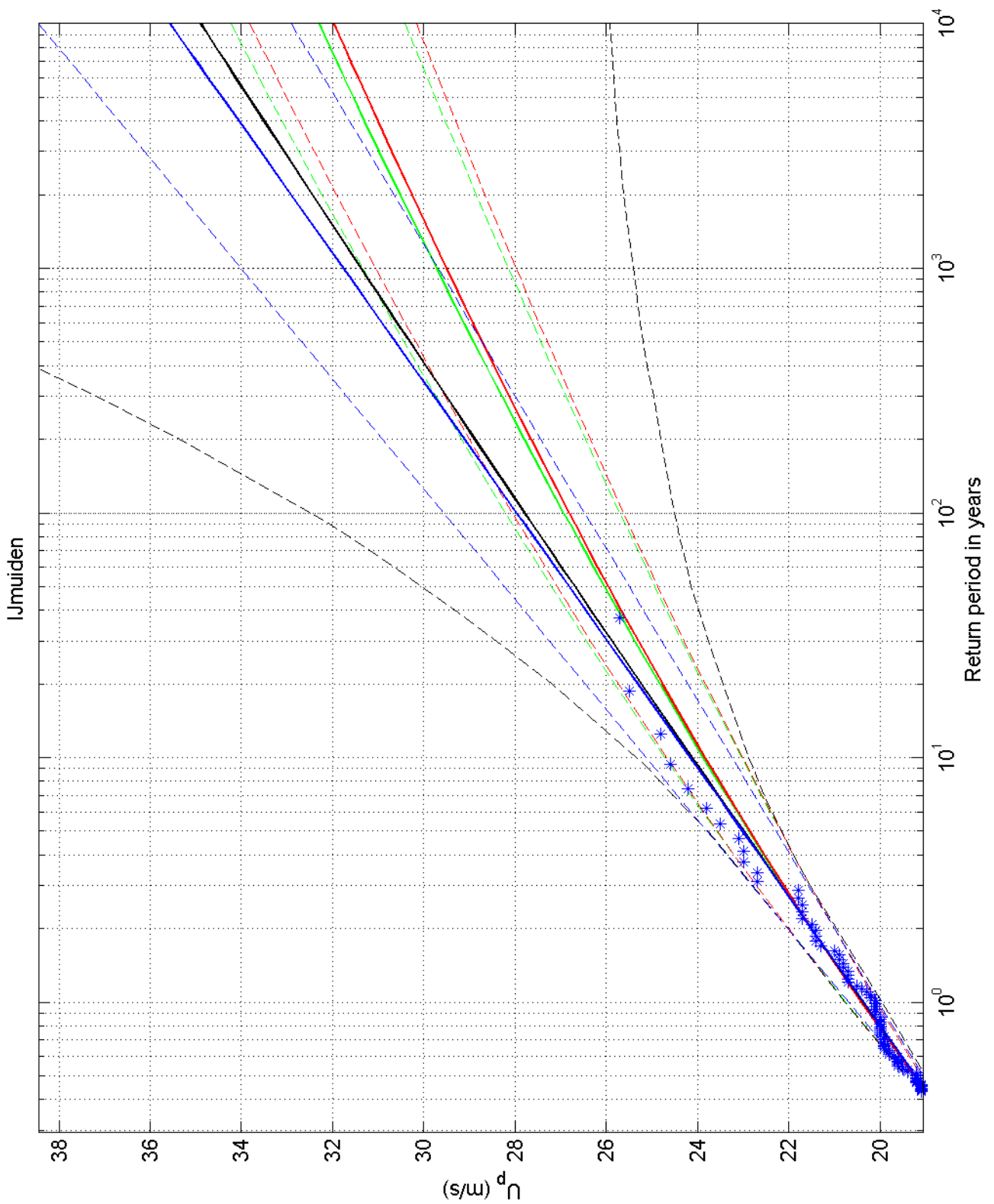
1970-2008

Beek

Deltares

1200264-005

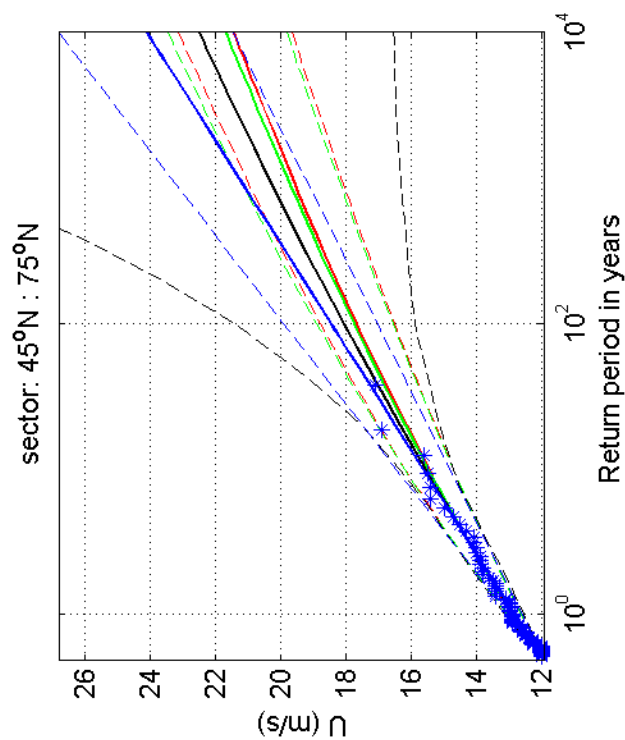
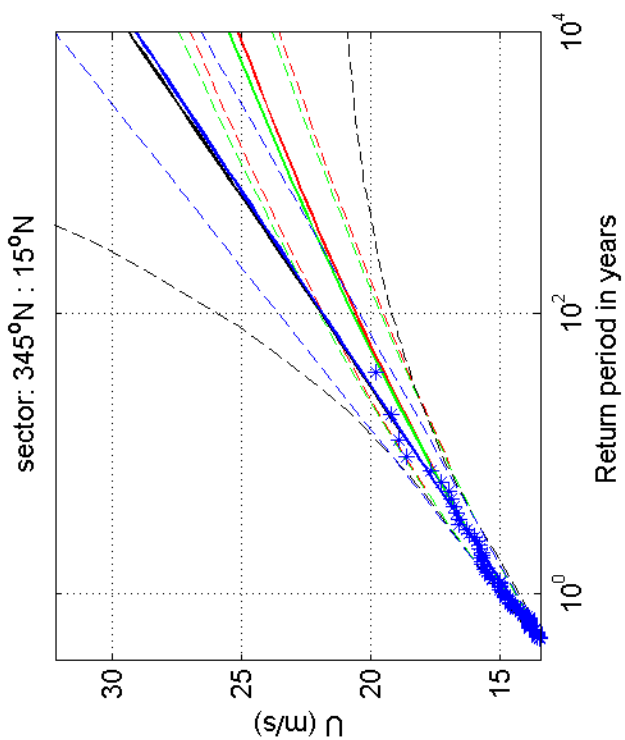
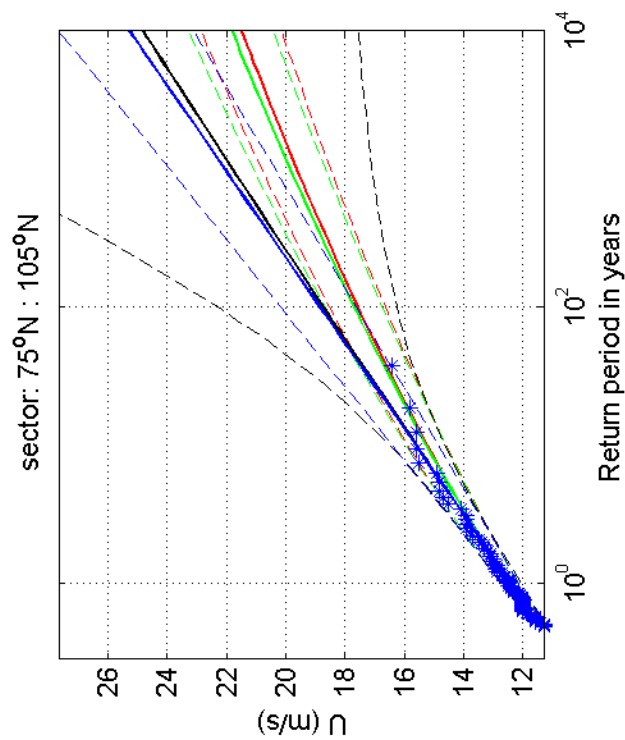
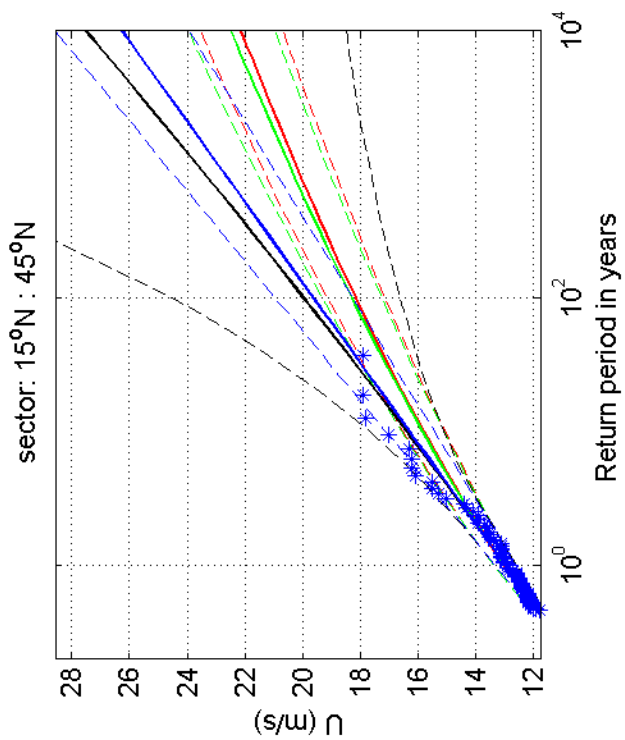
Fig. F.3.380



Return value plot with exponential (blue) and GPD (black) fit to U_p ,
 exponential (red) fit to U_p^2 and exponential (green) fit to U_p^k
 Plotting positions: x_i vs $(n+1)/(\lambda(n+1-i))$

omni-directional	1970-2008
IJmuiden	
1200264-005	Fig. F.4.225

Deltares



Return value plot with exponential (blue) and GPD (black) fit to U ,
 exponential (red) fit to U_p^2 and exponential (green) fit to U_p^k
 Plotting positions: x_i vs $(n+1)/(\lambda(n+1-i))$

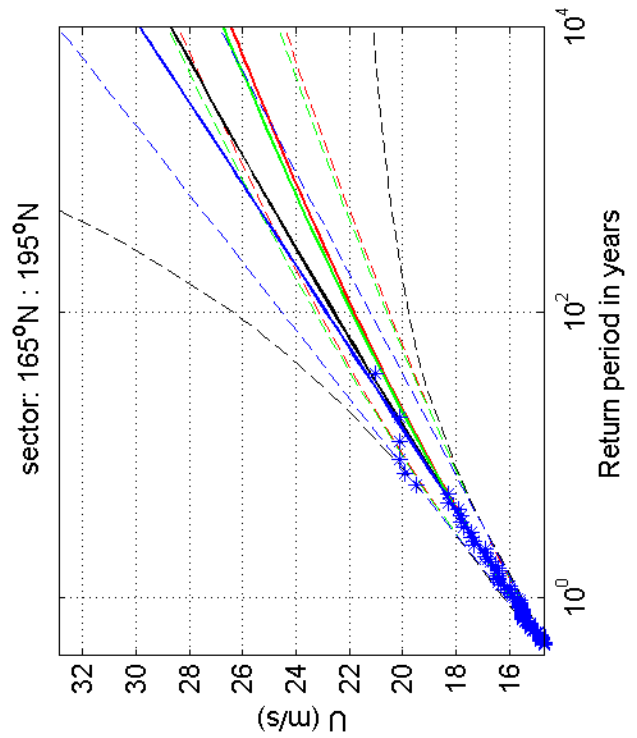
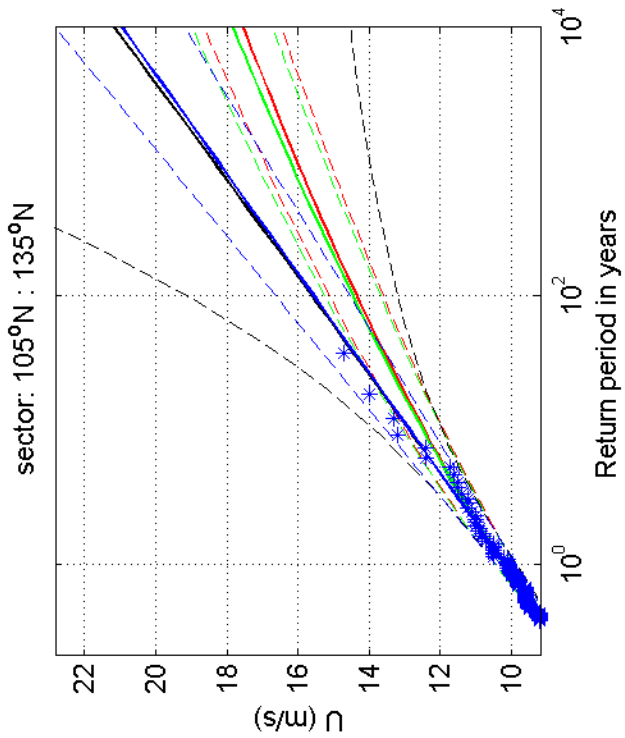
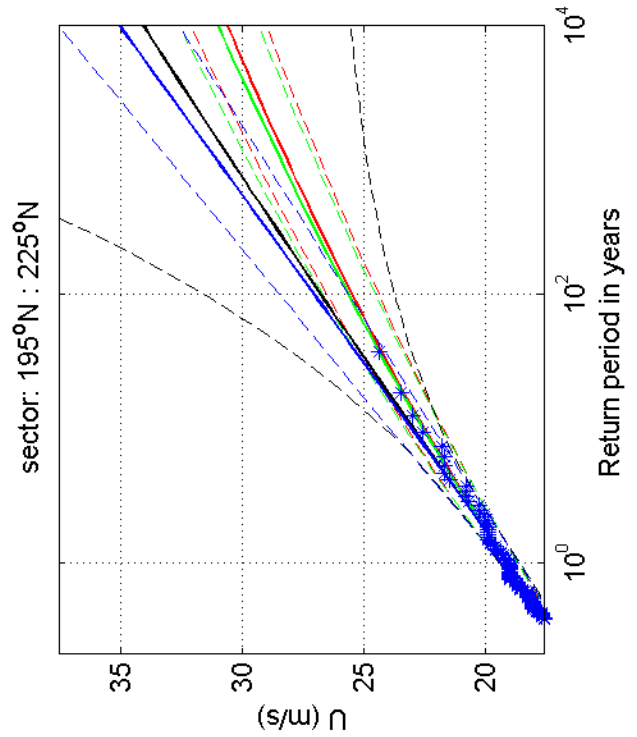
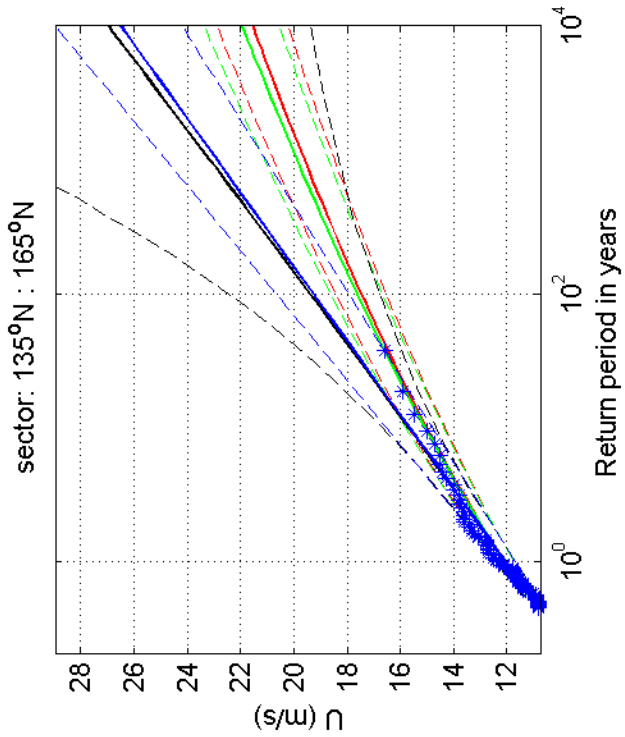
1970-2008

IJmuiden

Deltares

1200264-005

Fig. F.4.225.1



Return value plot with exponential (blue) and GPD (black) fit to U , exponential (red) fit to U_p^2 and exponential (green) fit to U_p^k
 Plotting positions: x_i vs $(n+1)/(\lambda(n+1-i))$

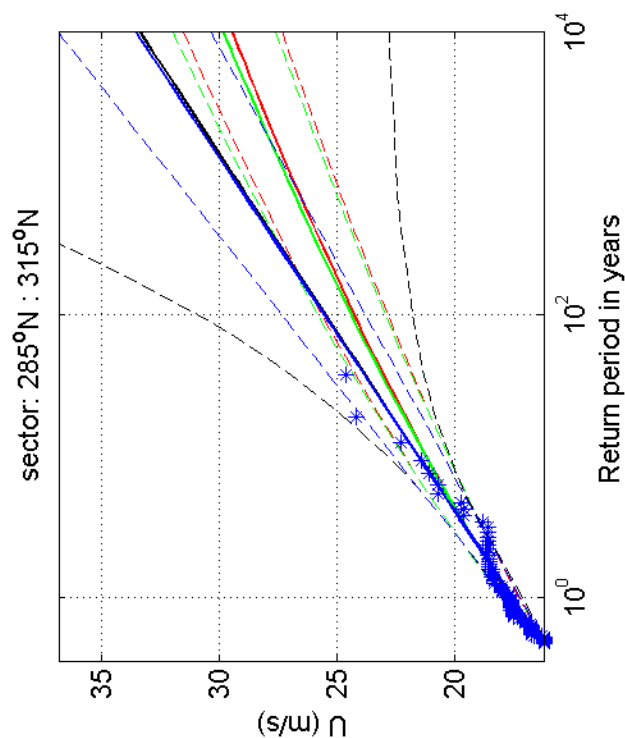
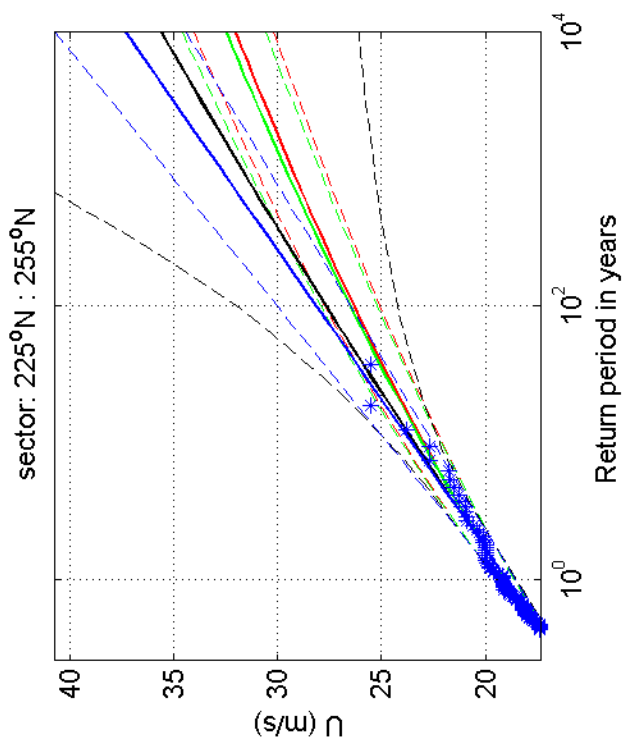
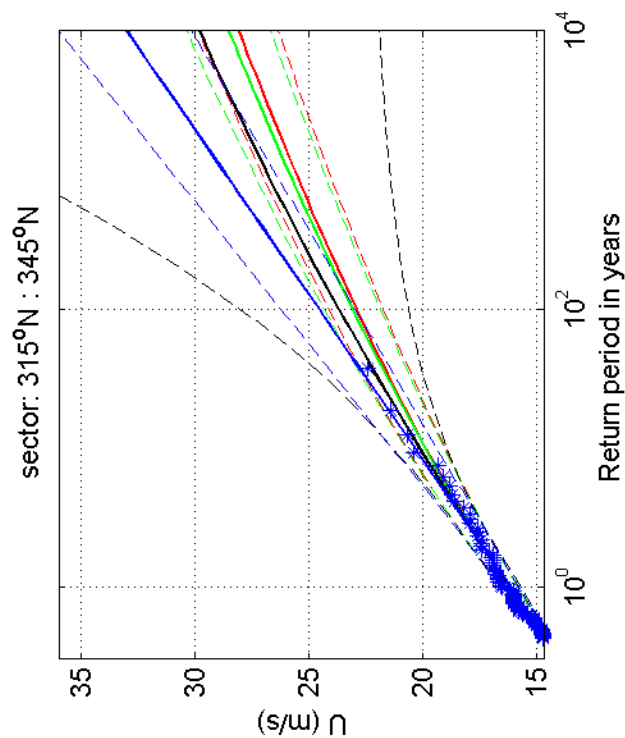
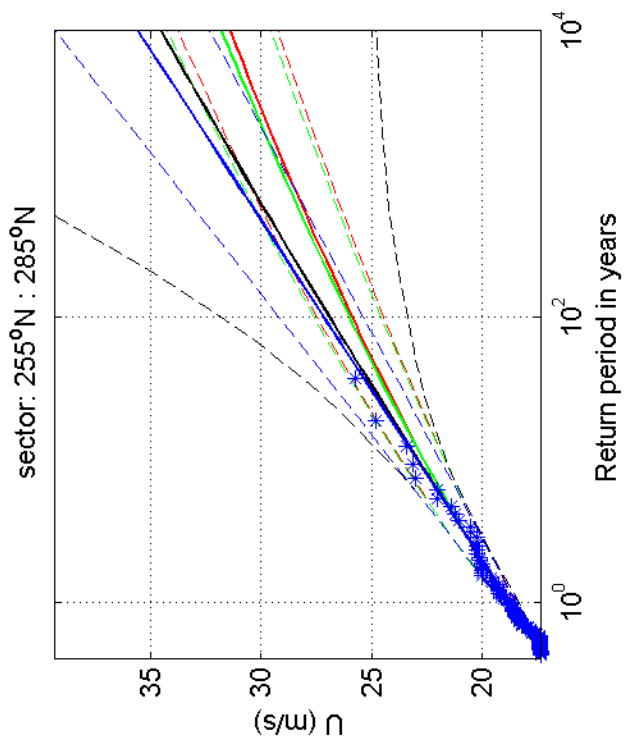
1970-2008

IJmuiden

Deltares

1200264-005

Fig. F.4.225.5



Return value plot with exponential (blue) and GPD (black) fit to U ,
 exponential (red) fit to U_p^2 and exponential (green) fit to U_p^k
 Plotting positions: x_i vs $(n+1)/(\lambda(n+1-i))$

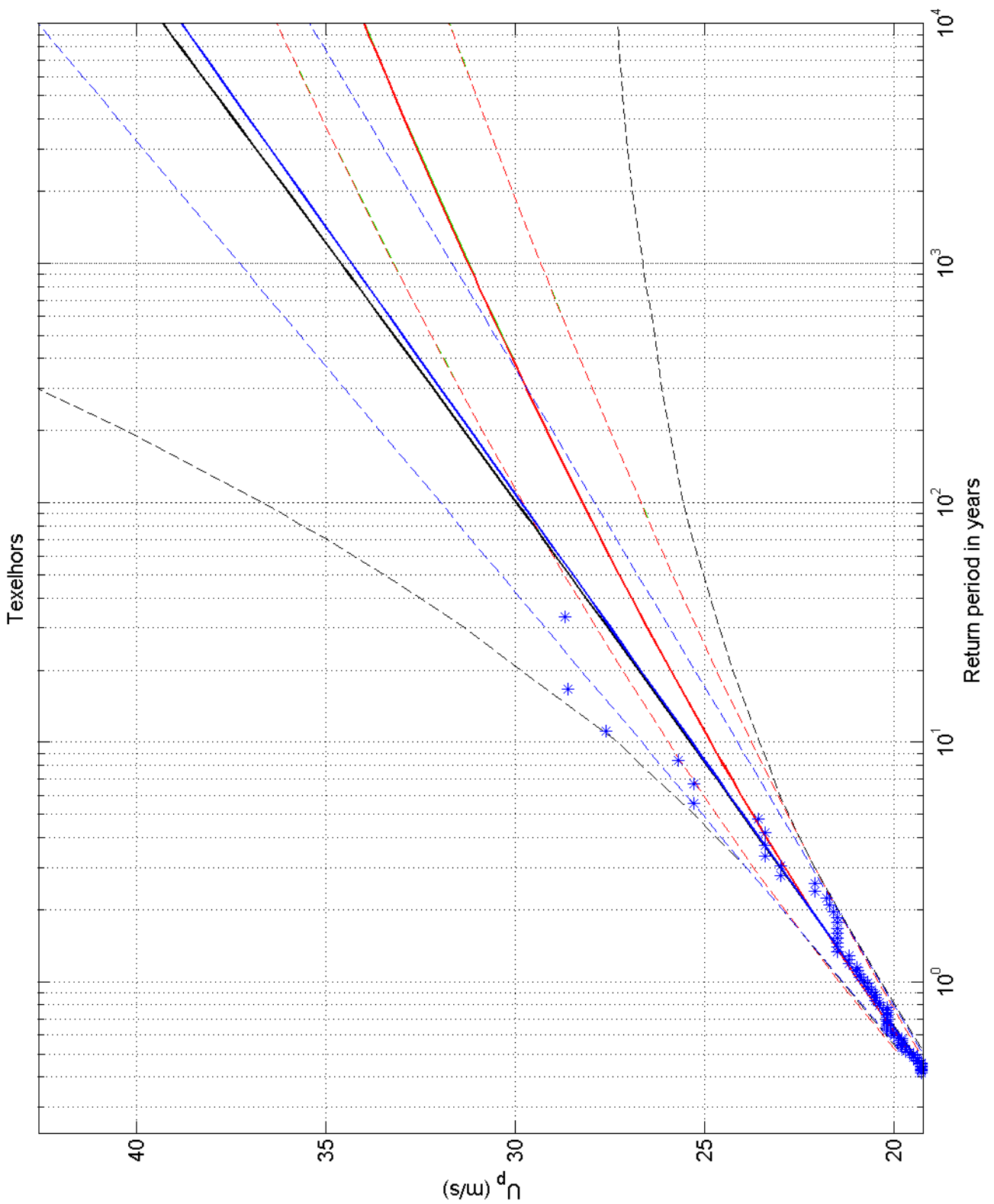
1970-2008

IJmuiden

Deltares

1200264-005

Fig. F.4.225.9



Return value plot with exponential (blue) and GPD (black) fit to U_p ,
 exponential (red) fit to U_p^2 and exponential (green) fit to U_p^k
 Plotting positions: x_i vs $(n+1)/(\lambda(n+1-i))$

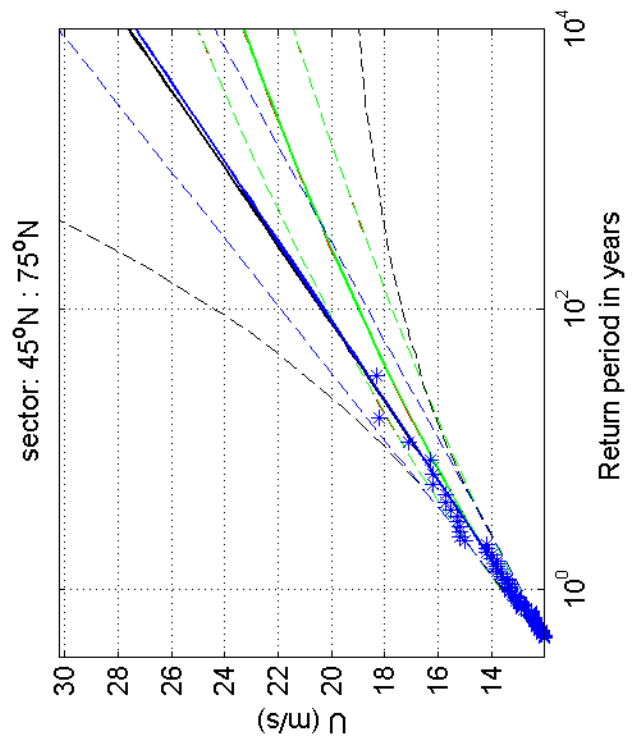
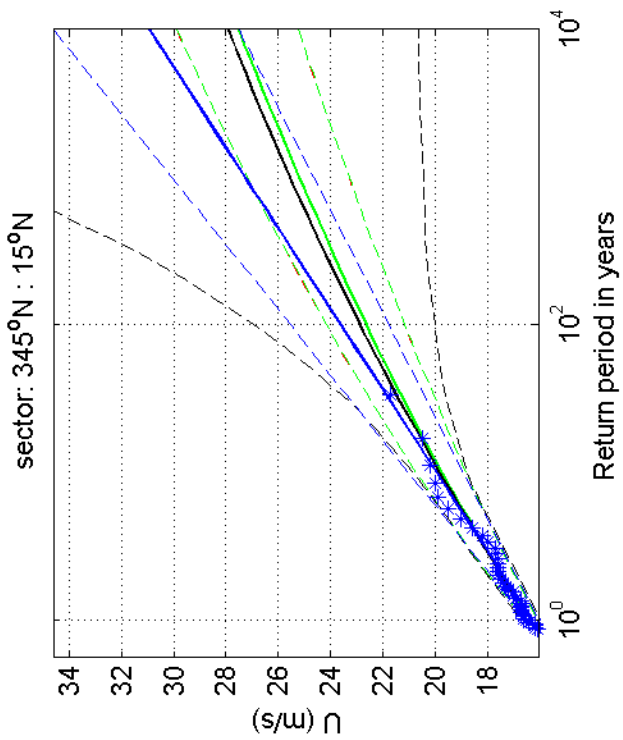
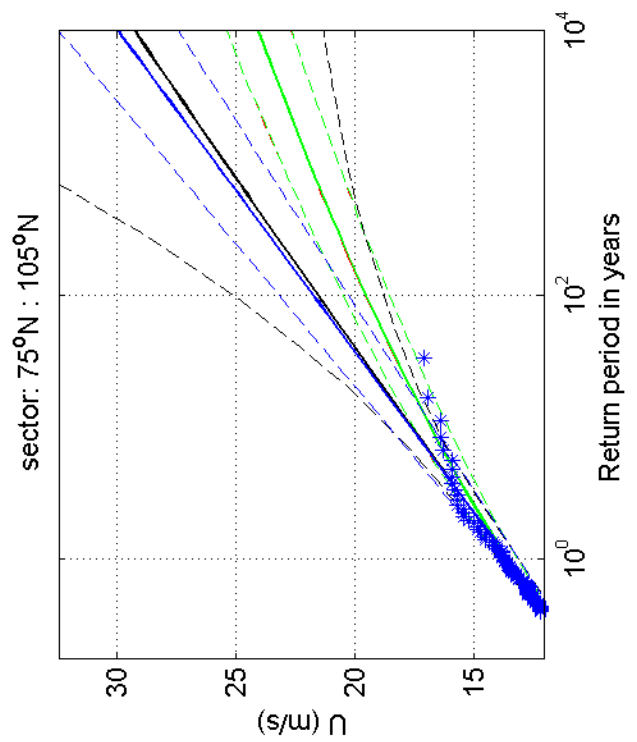
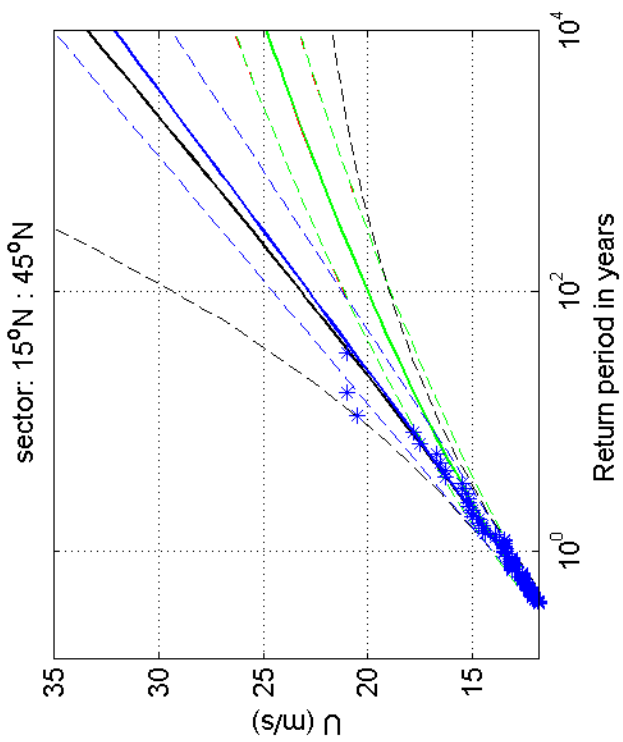
omni-directional 1970-2008

Texelhors

Deltares

1200264-005

Fig. F.4.229



Return value plot with exponential (blue) and GPD (black) fit to U ,
 exponential (red) fit to U_p^2 and exponential (green) fit to U_p^k
 Plotting positions: x_i vs $(n+1)/(\lambda(n+1-i))$

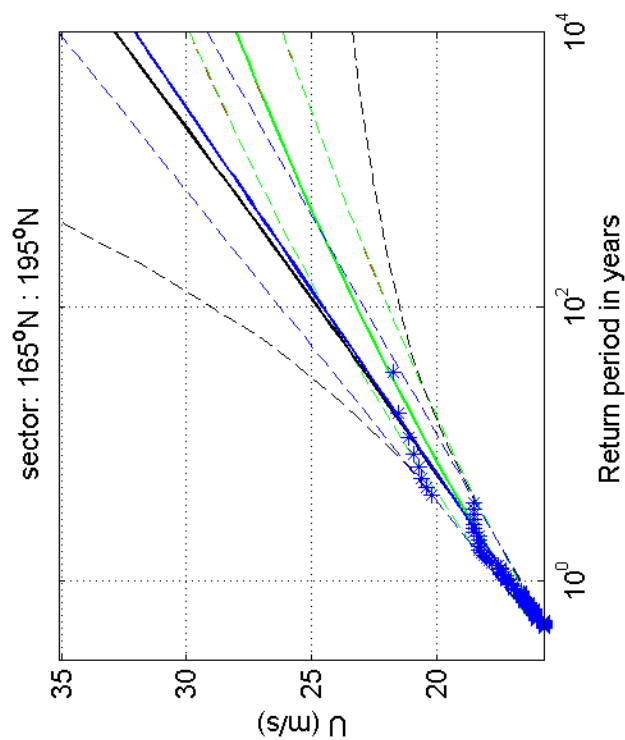
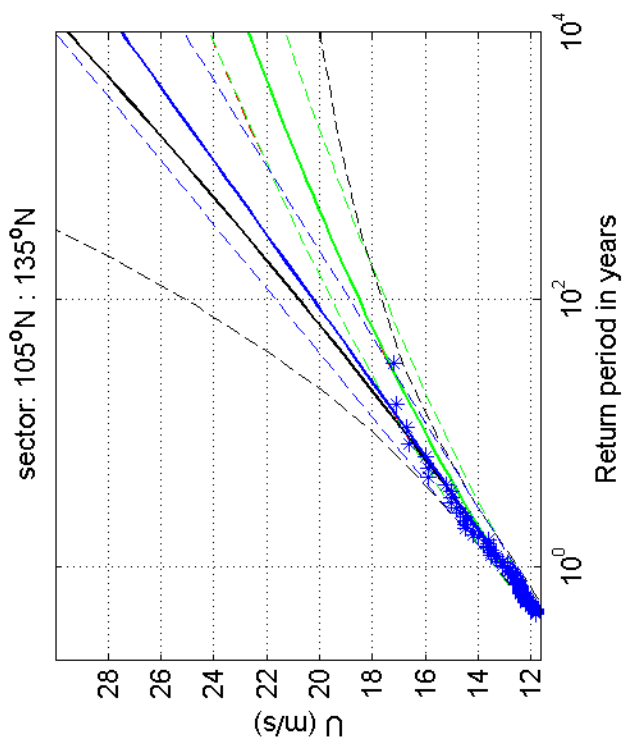
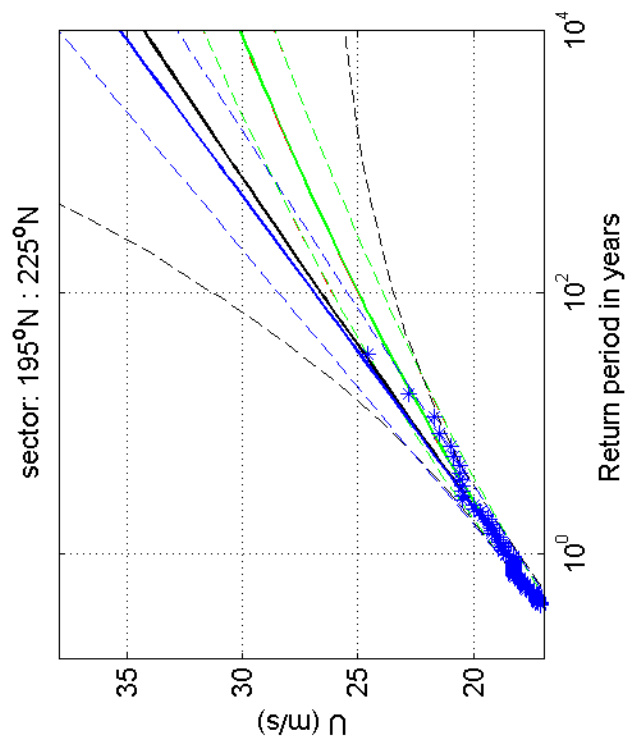
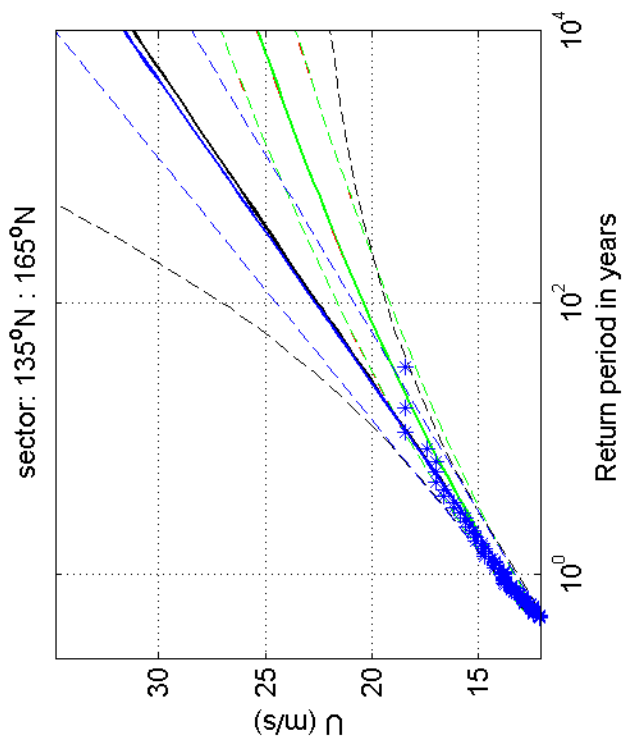
1970-2008

Texelhors

Deltares

1200264-005

Fig. F.4.229.1



Return value plot with exponential (blue) and GPD (black) fit to U ,
 exponential (red) fit to U_p^k and exponential (green) fit to U_p^k
 Plotting positions: x_i vs $(n+1)/(\lambda(n+1-i))$

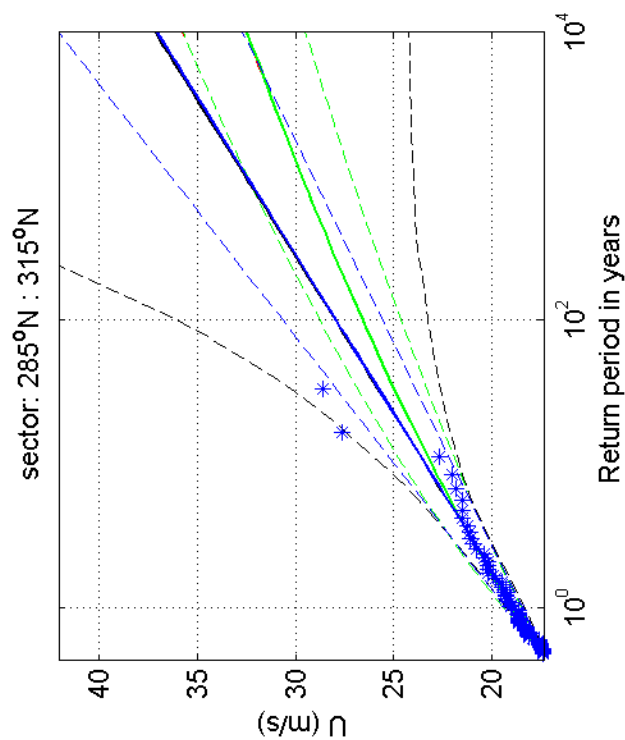
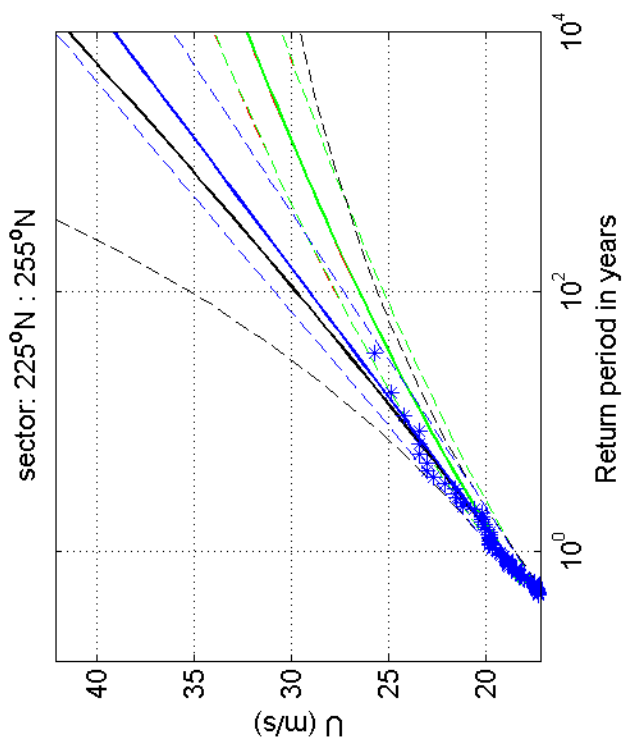
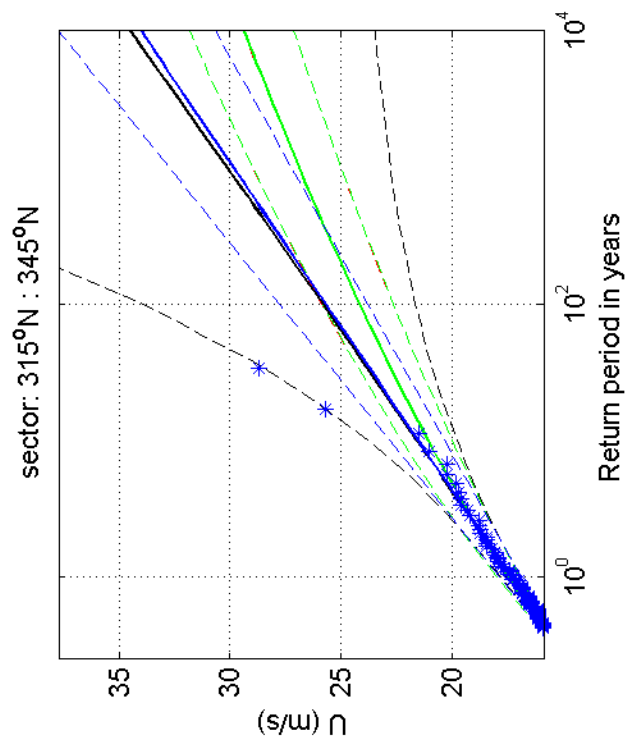
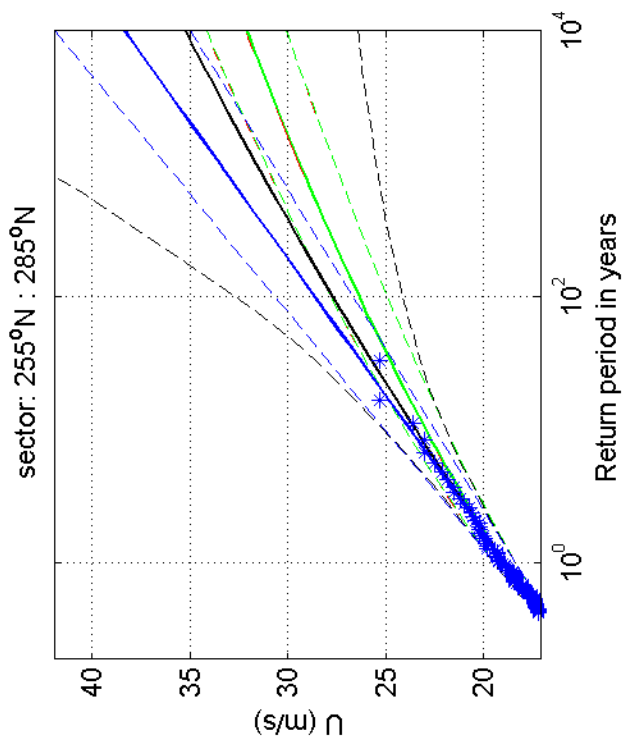
1970-2008

Texelhors

Deltares

1200264-005

Fig. F.4.229.5



Return value plot with exponential (blue) and GPD (black) fit to U ,
 exponential (red) fit to U_p^2 and exponential (green) fit to U_p^k
 Plotting positions: x_i vs $(n+1)/(\lambda(n+1-i))$

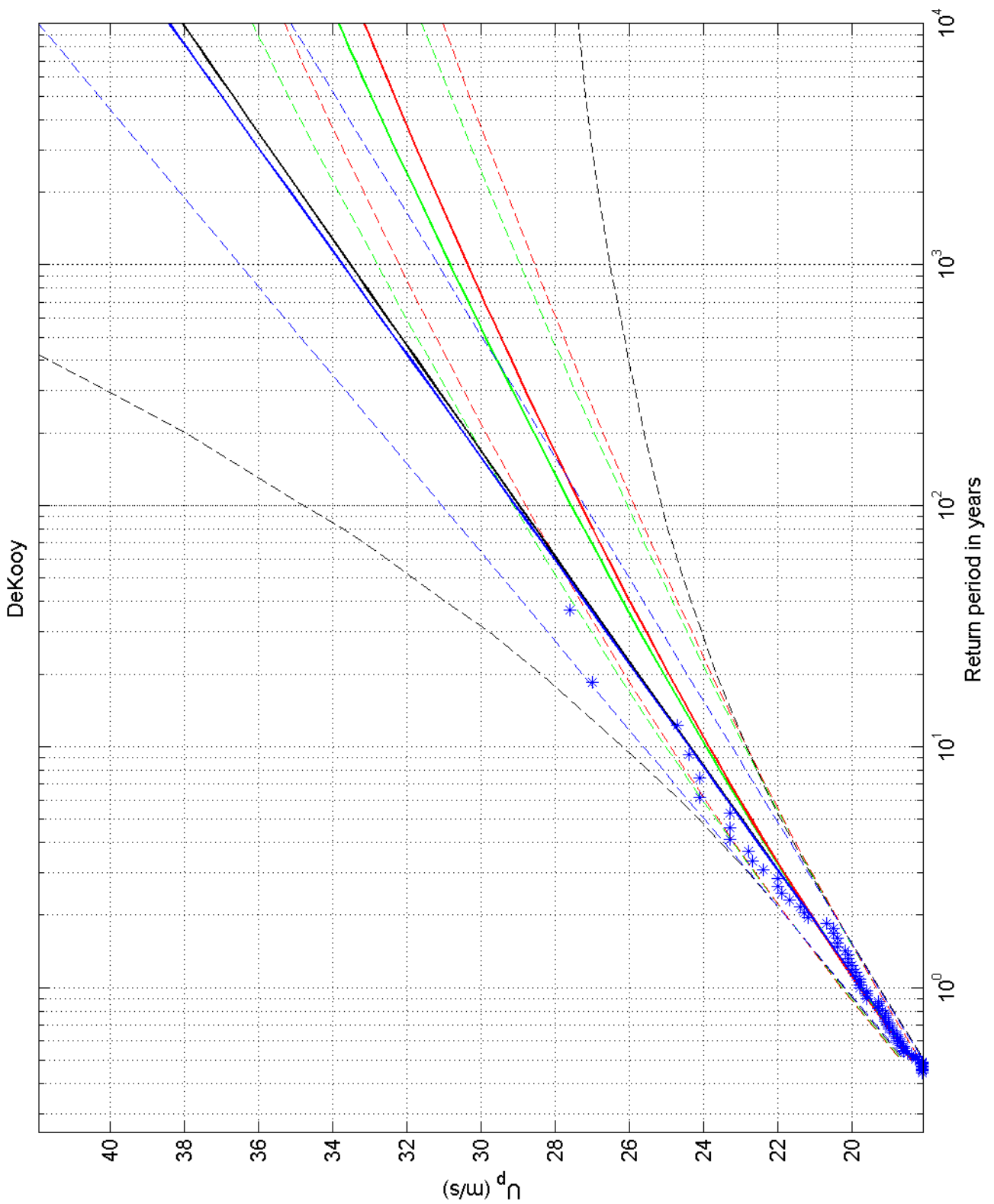
1970-2008

Texelhors

Deltares

1200264-005

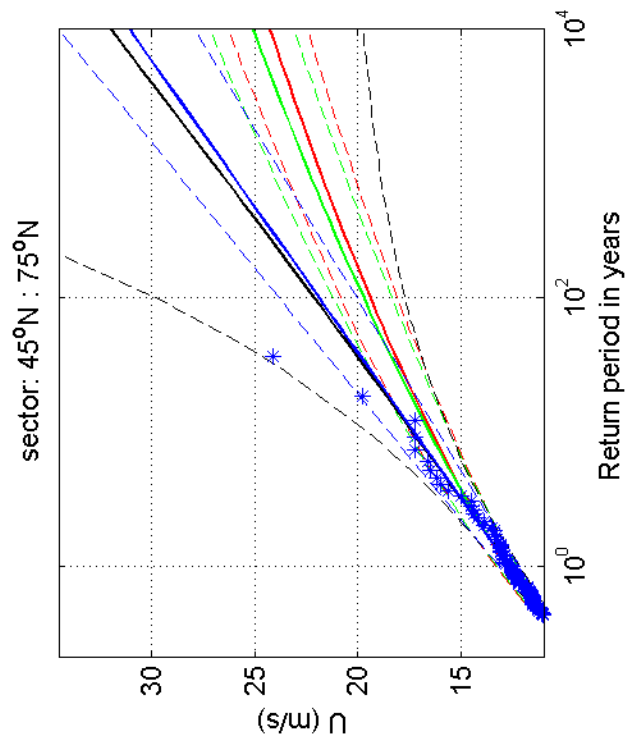
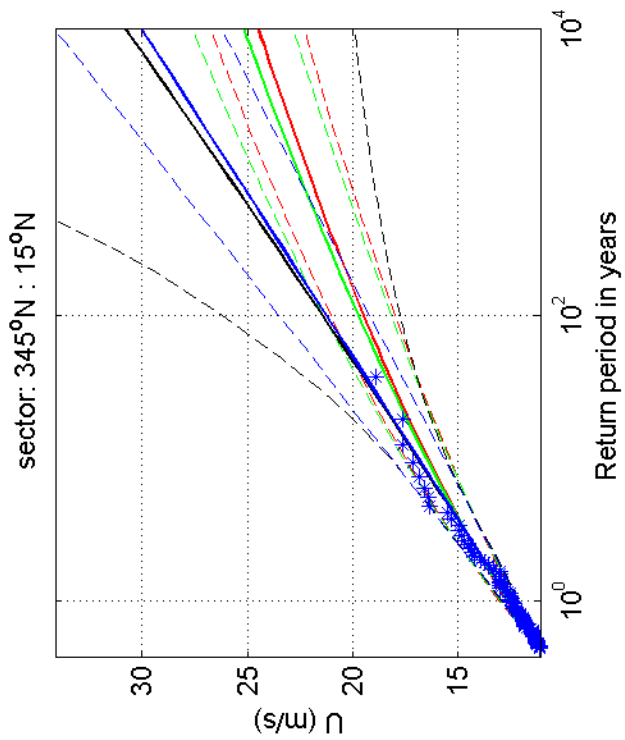
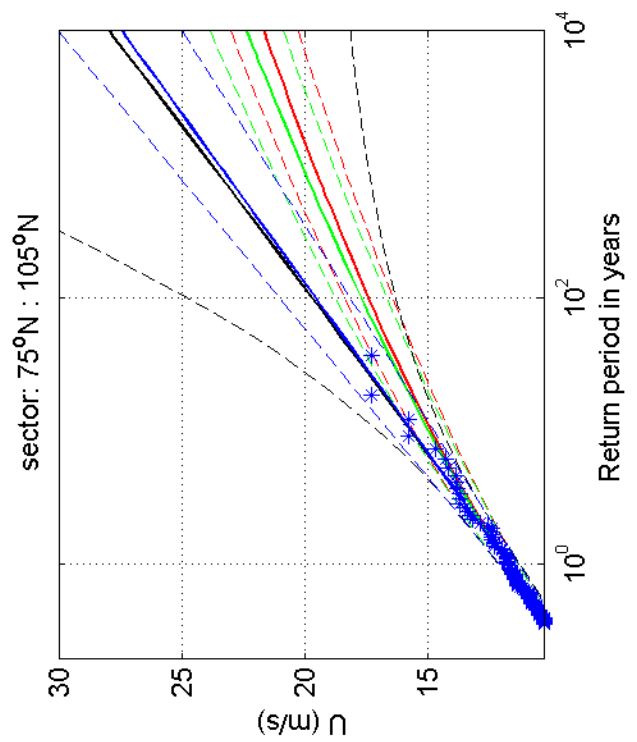
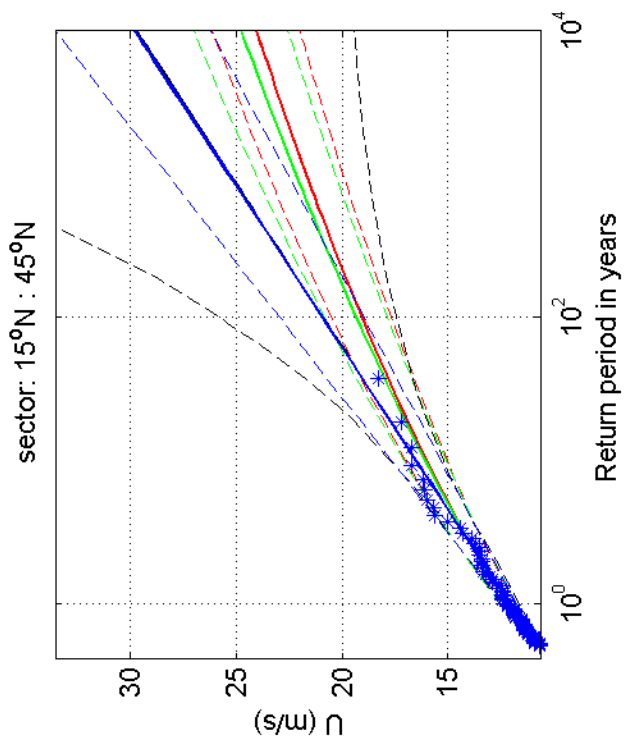
Fig. F.4.229.9



Return value plot with exponential (blue) and GPD (black) fit to U_p ,
 exponential (red) fit to U_p^2 and exponential (green) fit to U_p^k
 Plotting positions: x_i vs $(n+1)/(\lambda(n+1-i))$

omni-directional	1970-2008
DeKooy	
1200264-005	Fig. F.4.235

Deltares



Return value plot with exponential (blue) and GPD (black) fit to U ,
 exponential (red) fit to U_p^k and exponential (green) fit to U_p^k
 Plotting positions: x_i vs $(n+1)/(\lambda(n+1-i))$

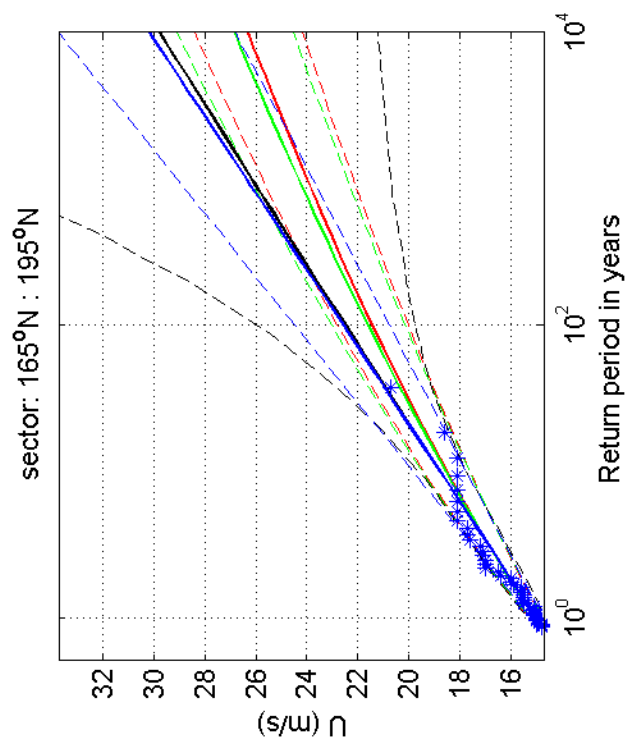
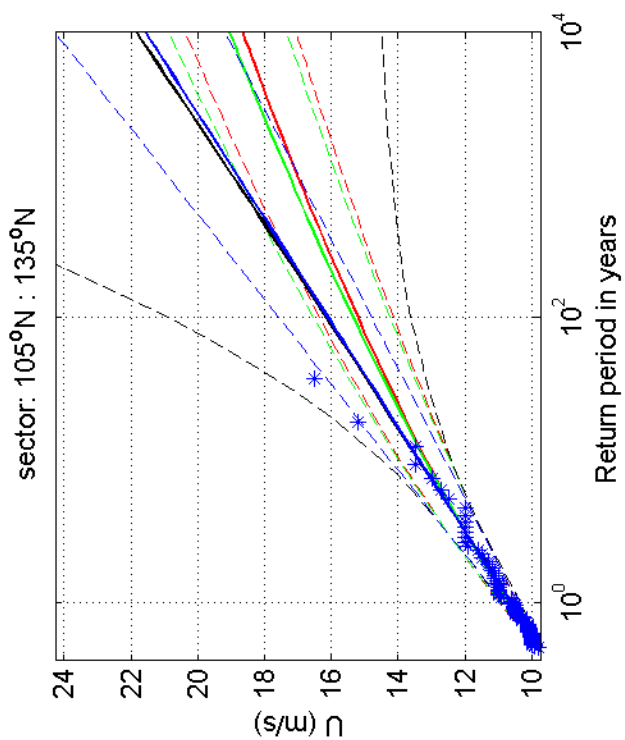
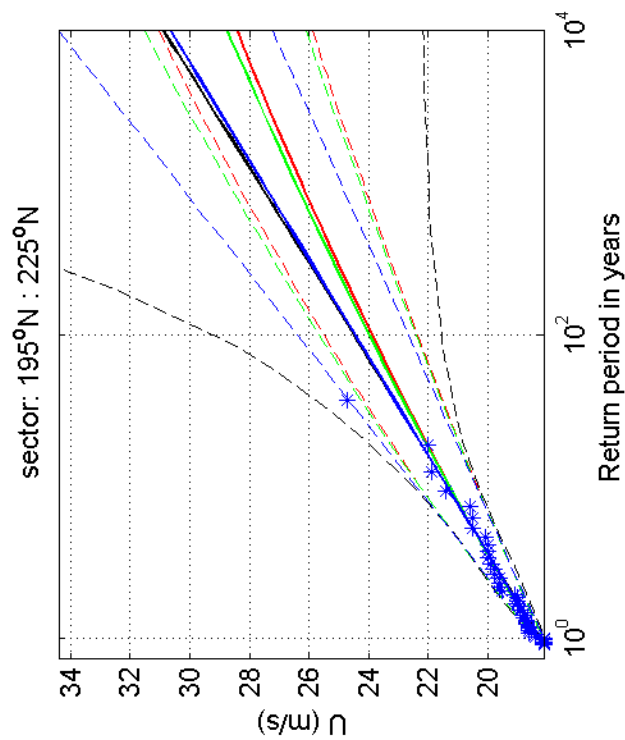
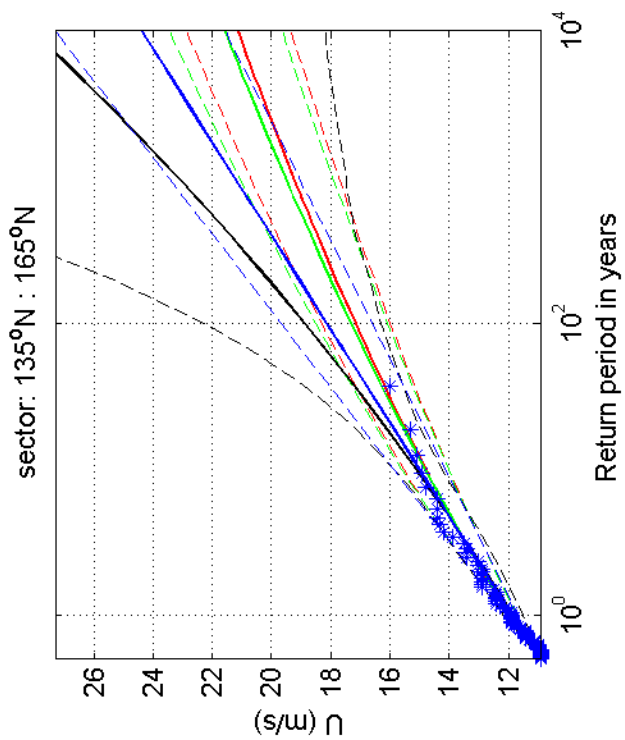
1970-2008

DeKooy

Deltares

1200264-005

Fig. F.4.235.1



Return value plot with exponential (blue) and GPD (black) fit to U ,
 exponential (red) fit to U_p^2 and exponential (green) fit to U_p^k
 Plotting positions: x_i vs $(n+1)/(\lambda(n+1-i))$

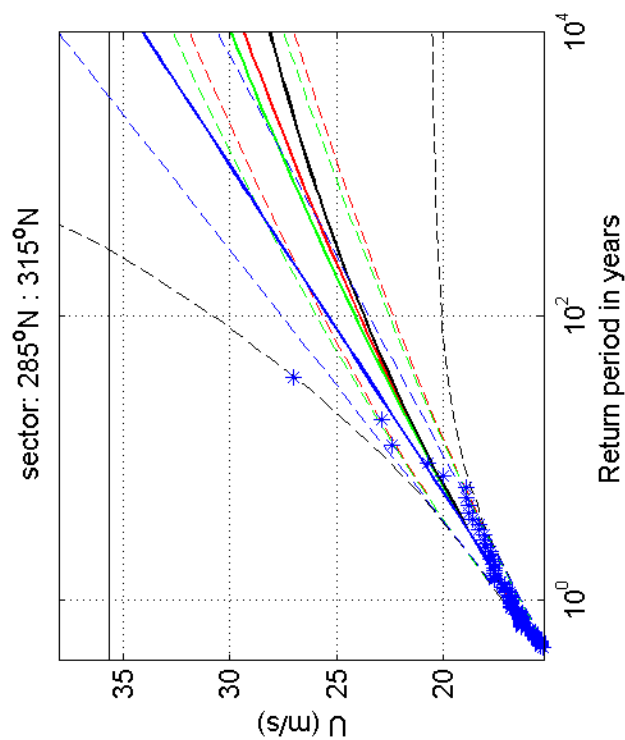
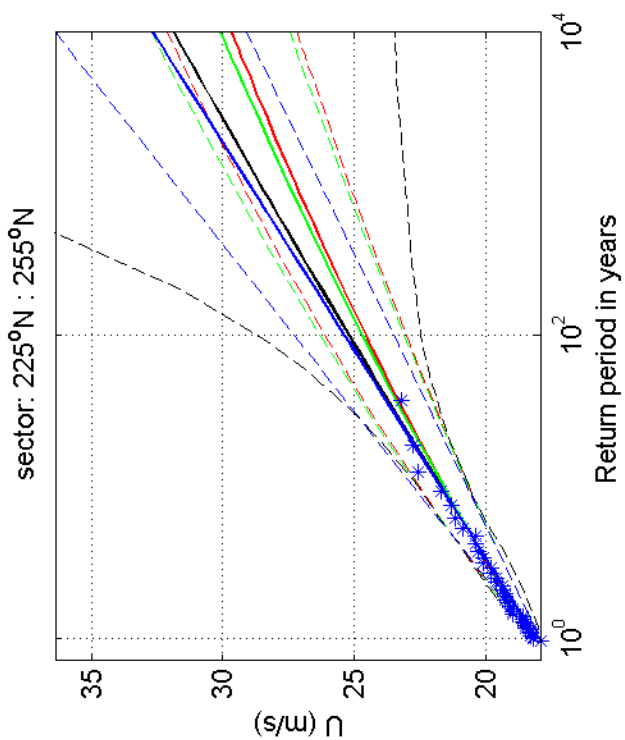
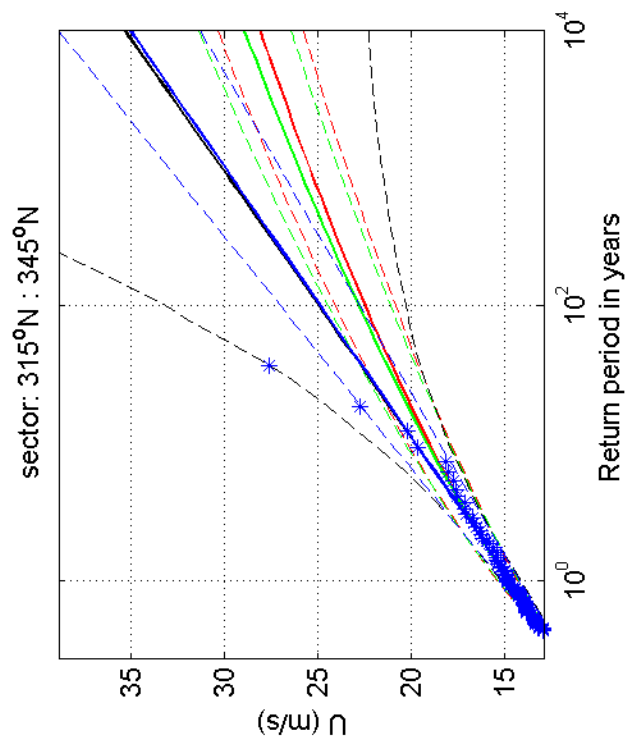
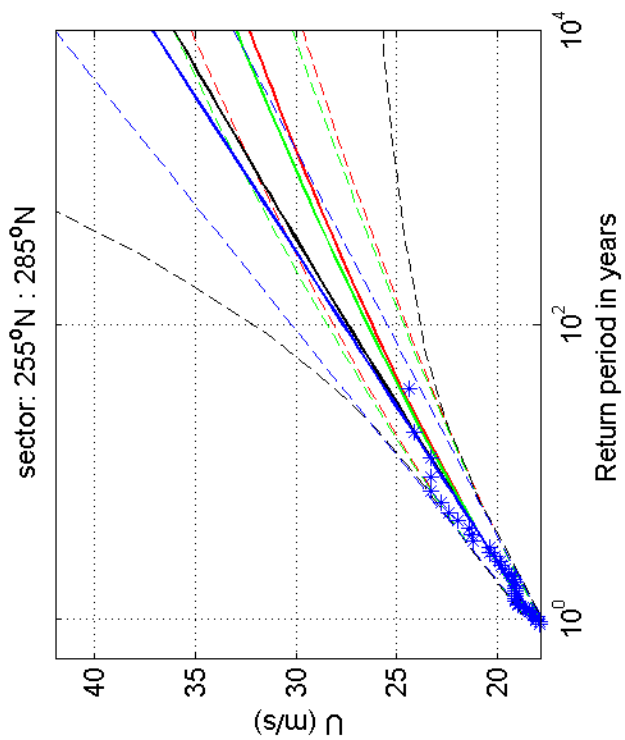
1970-2008

DeKooy

Deltares

1200264-005

Fig. F.4.235.5



Return value plot with exponential (blue) and GPD (black) fit to U ,
 exponential (red) fit to U_p^2 and exponential (green) fit to U_p^k
 Plotting positions: x_i vs $(n+1)/(\lambda(n+1-i))$

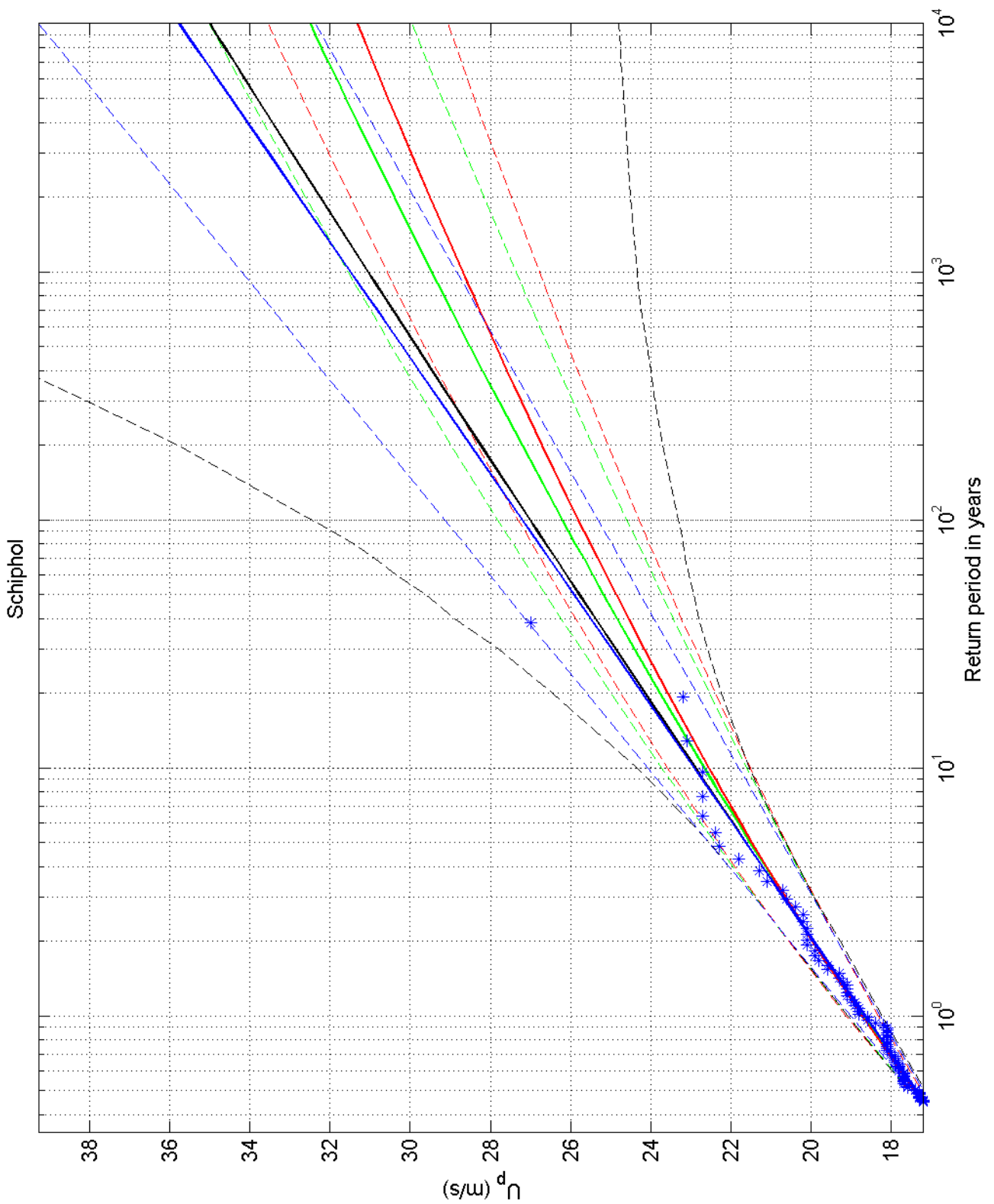
1970-2008

DeKooy

Deltares

1200264-005

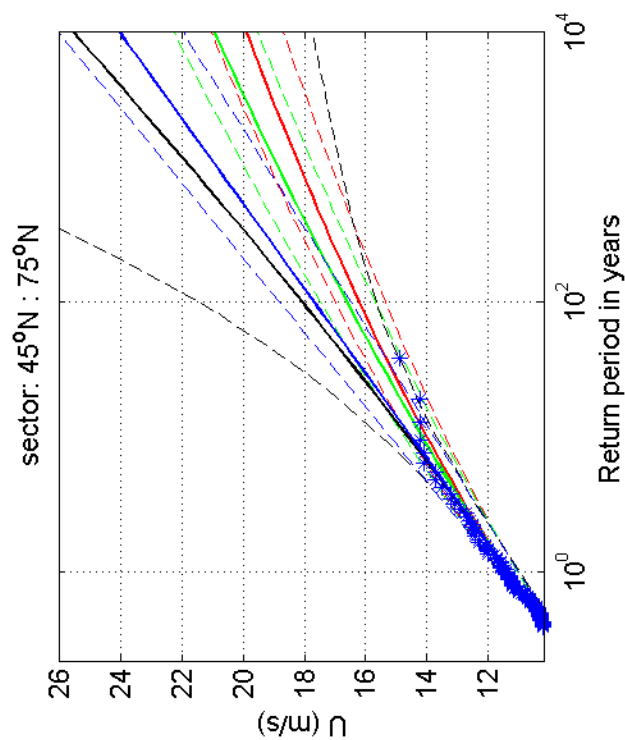
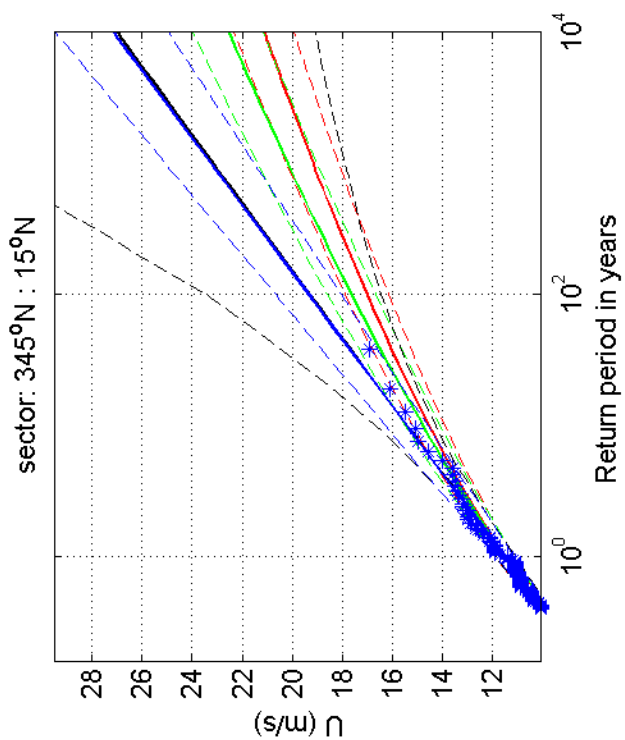
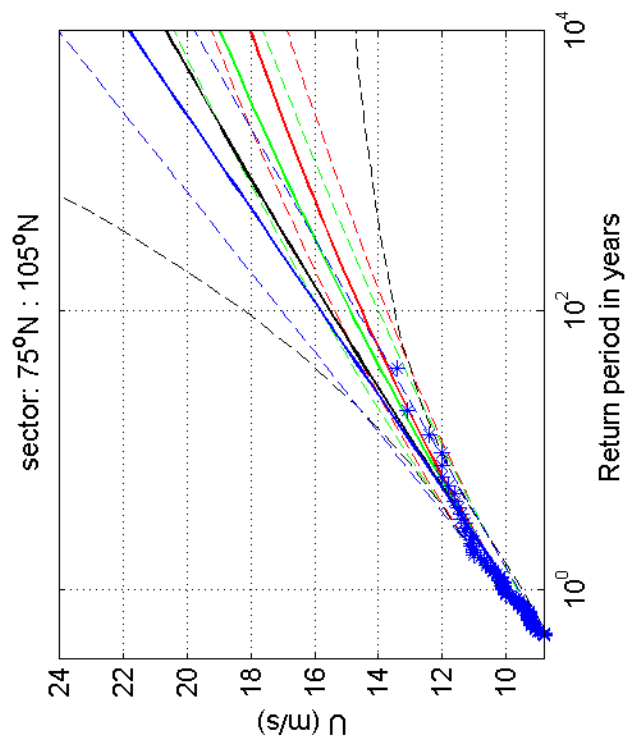
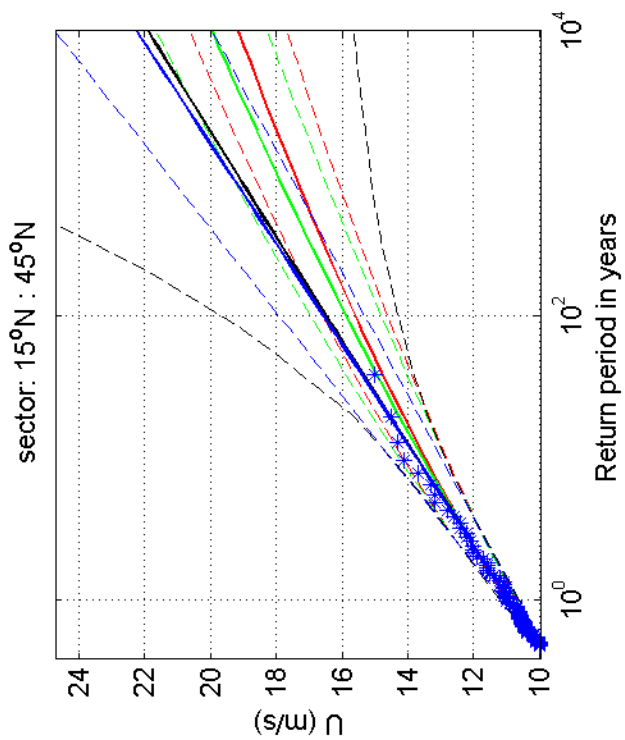
Fig. F.4.235.9



Return value plot with exponential (blue) and GPD (black) fit to U_p ,
 exponential (red) fit to U_p^2 and exponential (green) fit to U_p^k
 Plotting positions: x_i vs $(n+1)/(\lambda(n+1-i))$

omni-directional	1970-2008
Schiphol	
1200264-005	Fig. F.4.240

Deltares



Return value plot with exponential (blue) and GPD (black) fit to U ,
 exponential (red) fit to U_p^2 and exponential (green) fit to U_p^k
 Plotting positions: x_i vs $(n+1)/(\lambda(n+1-i))$

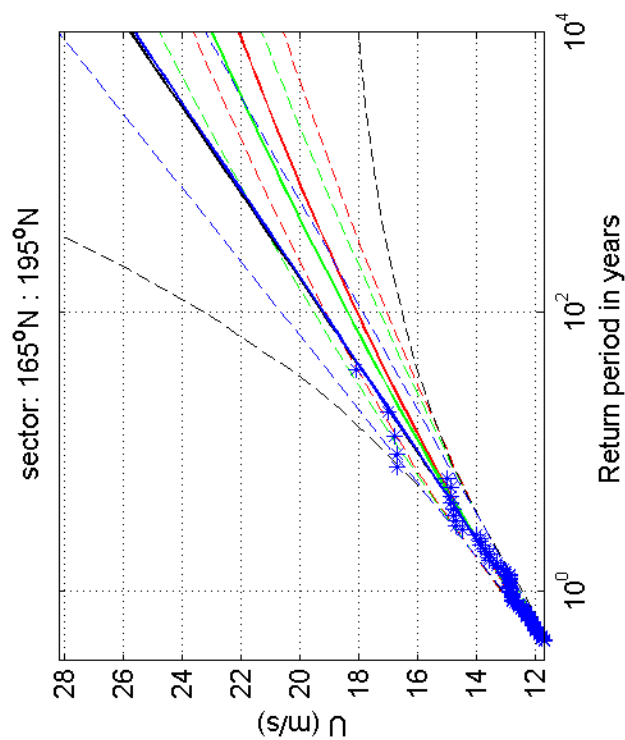
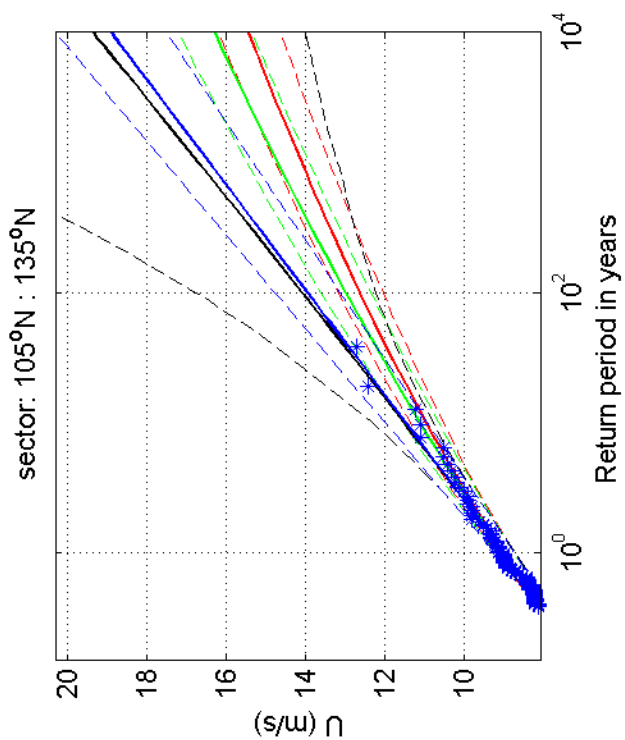
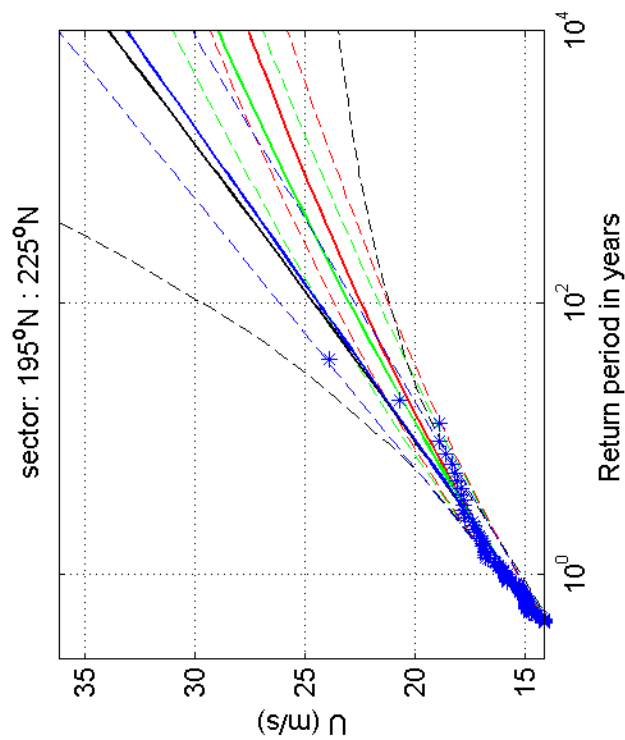
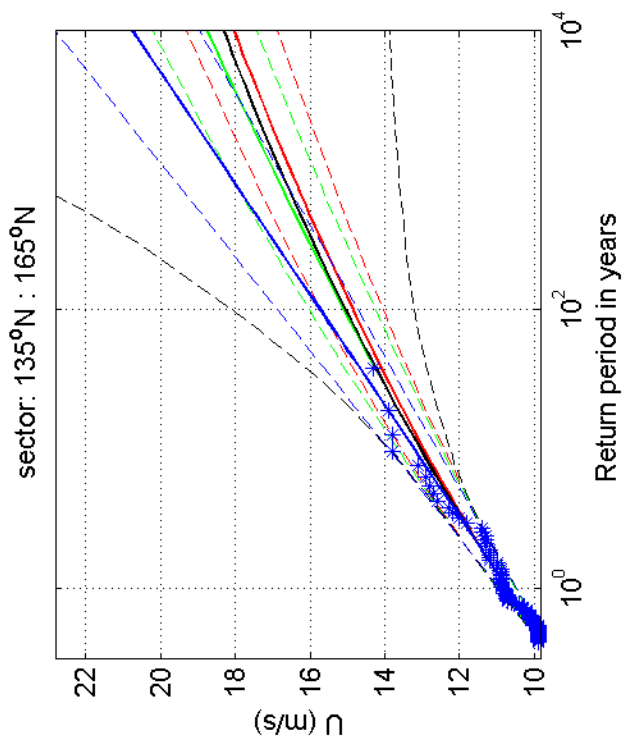
1970-2008

Schiphol

Deltares

1200264-005

Fig. F.4.240.1



Return value plot with exponential (blue) and GPD (black) fit to U ,
 exponential (red) fit to U_p^2 and exponential (green) fit to U_p^k
 Plotting positions: x_i vs $(n+1)/(\lambda(n+1-i))$

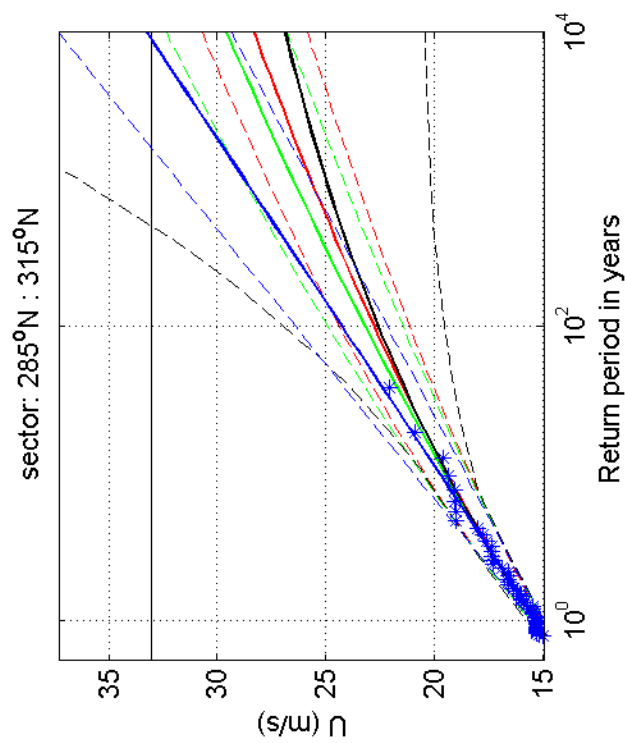
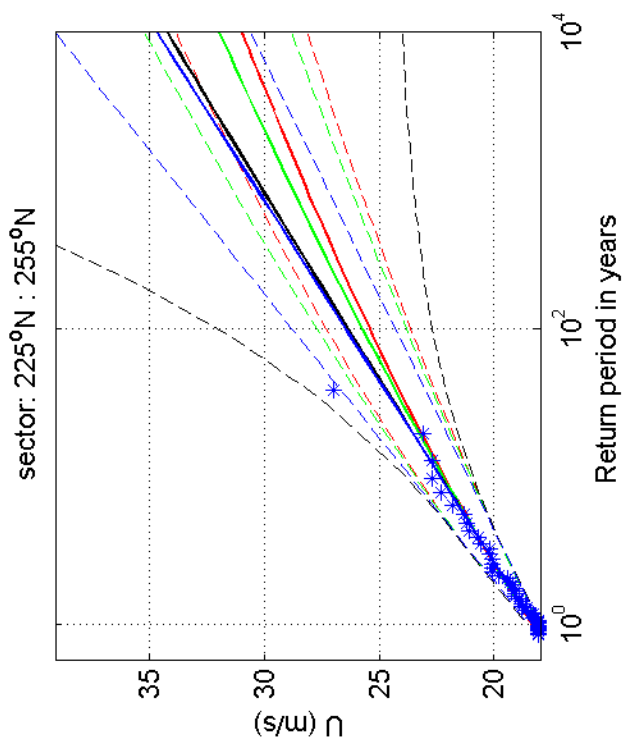
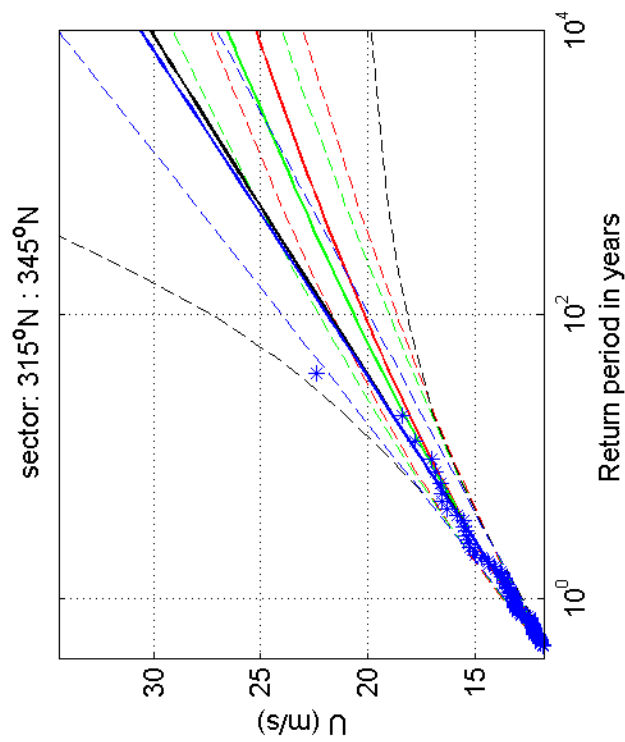
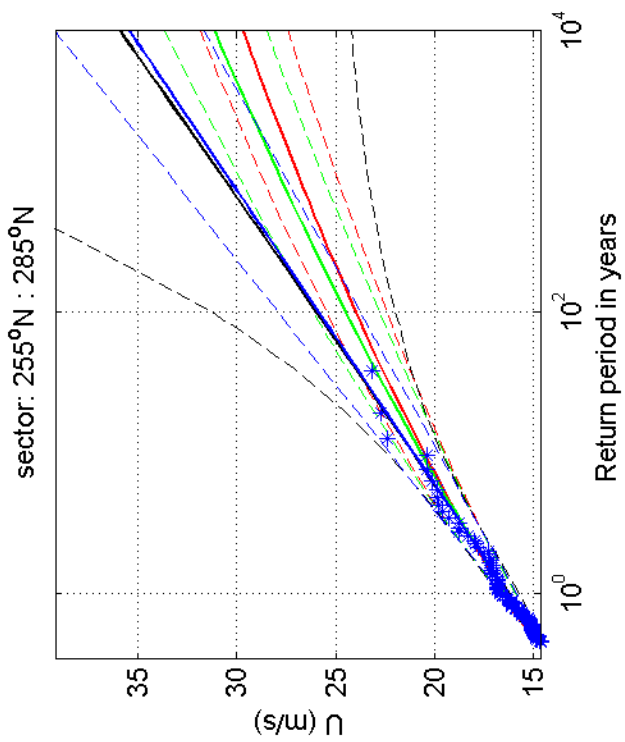
1970-2008

Schiphol

Deltares

1200264-005

Fig. F.4.240.5



Return value plot with exponential (blue) and GPD (black) fit to U ,
 exponential (red) fit to U_p^2 and exponential (green) fit to U_p^k
 Plotting positions: x_i vs $(n+1)/(\lambda(n+1-i))$

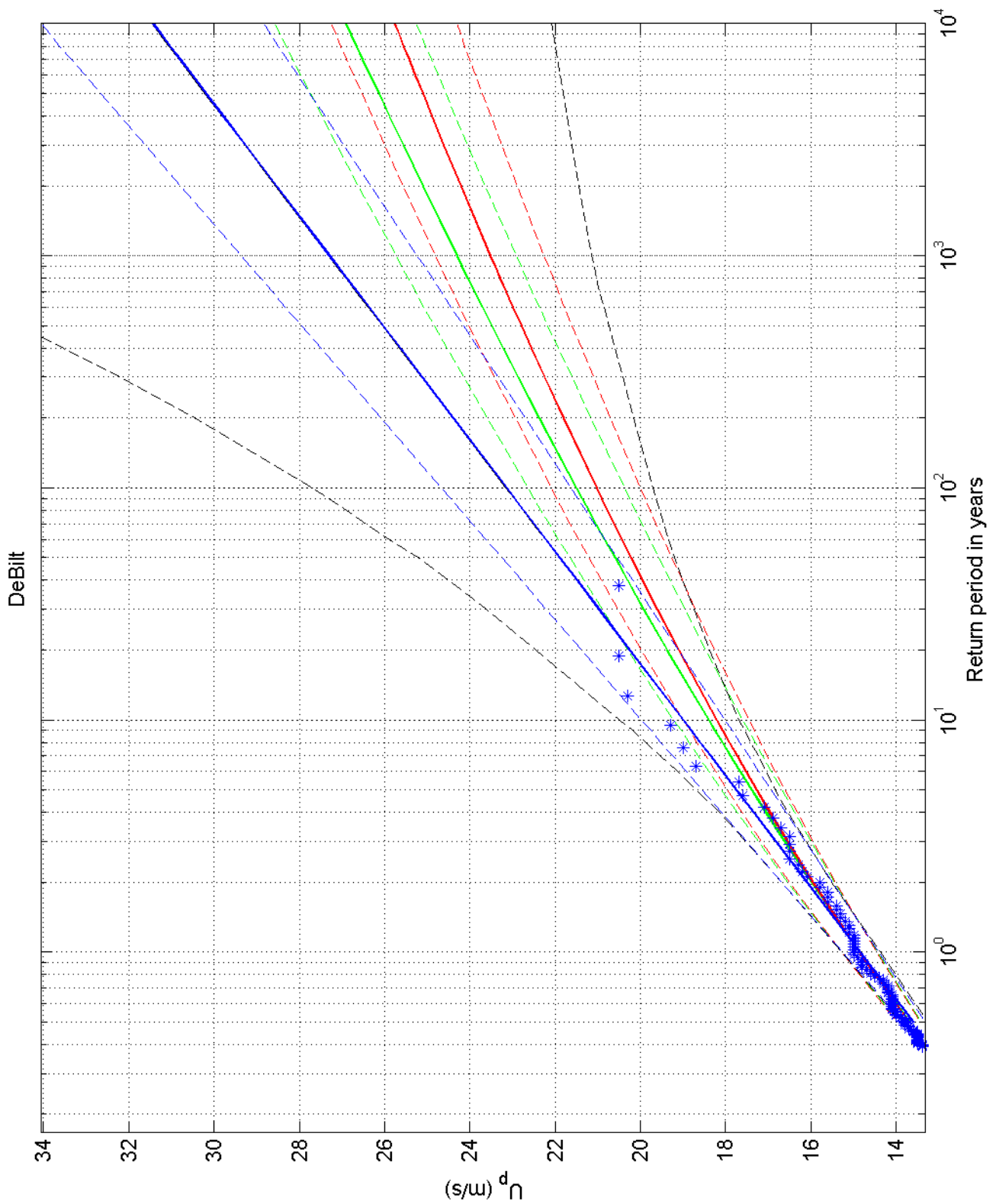
1970-2008

Schiphol

Deltares

1200264-005

Fig. F.4.240.9



Return value plot with exponential (blue) and GPD (black) fit to U_p ,
 exponential (red) fit to U_p^2 and exponential (green) fit to U_p^k
 Plotting positions: x_i vs $(n+1)/(\lambda(n+1-i))$

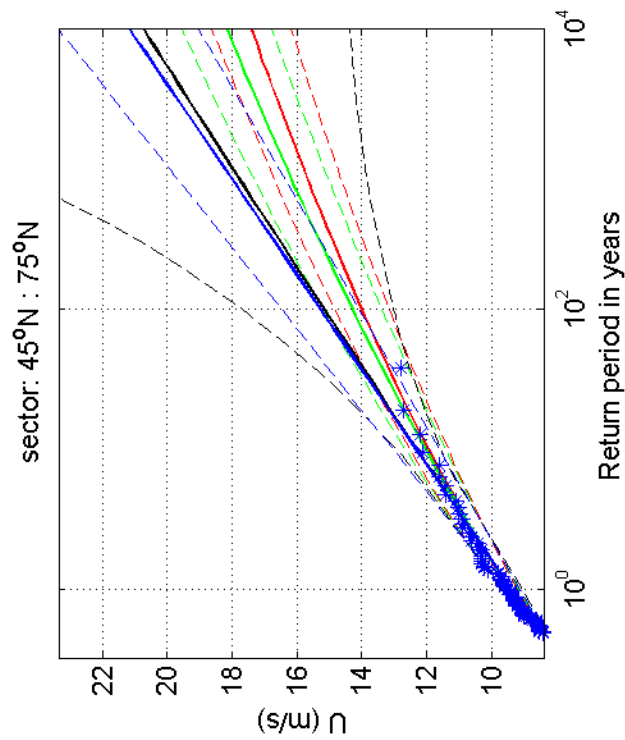
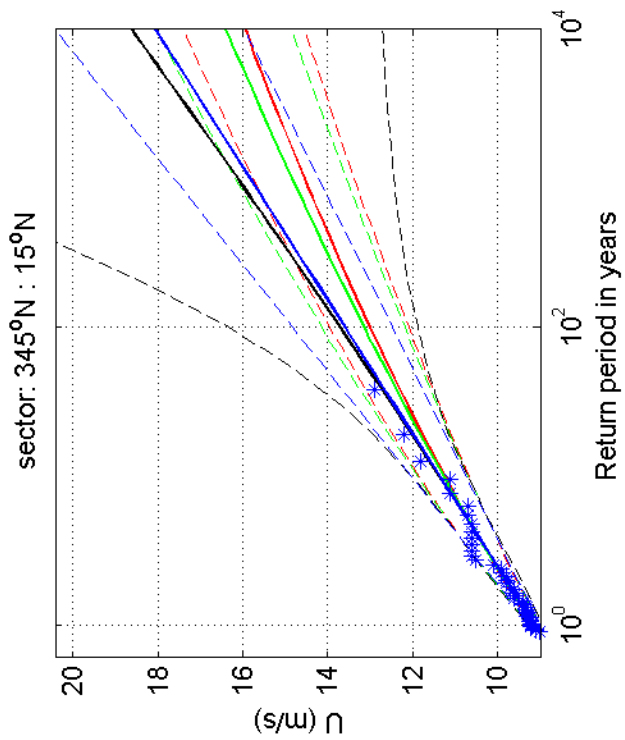
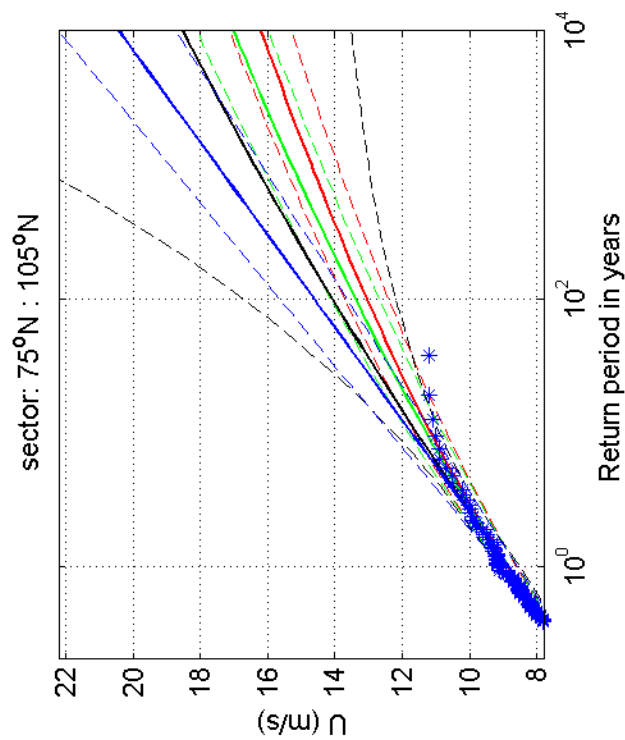
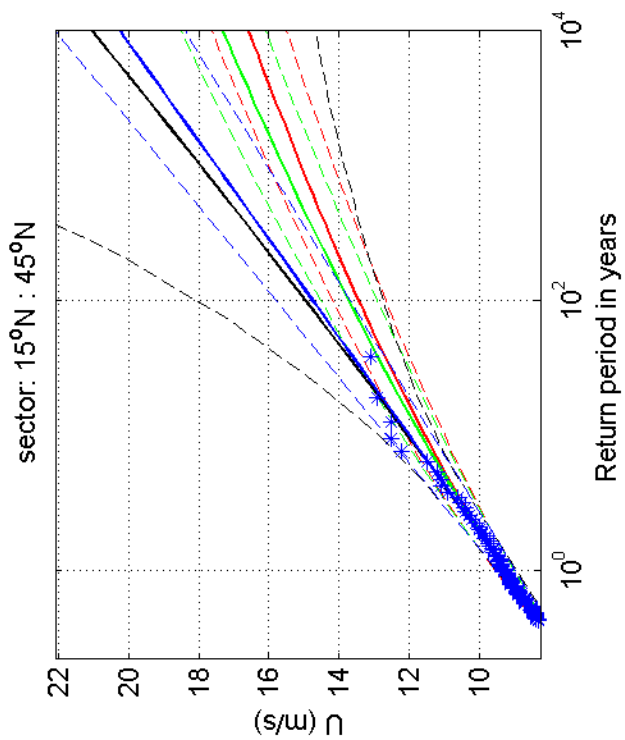
omni-directional 1970-2008

DeBilt

Deltares

1200264-005

Fig. F.4.260



Return value plot with exponential (blue) and GPD (black) fit to U ,
 exponential (red) fit to U_p^2 and exponential (green) fit to U_p^k
 Plotting positions: x_i vs $(n+1)/(\lambda(n+1-i))$

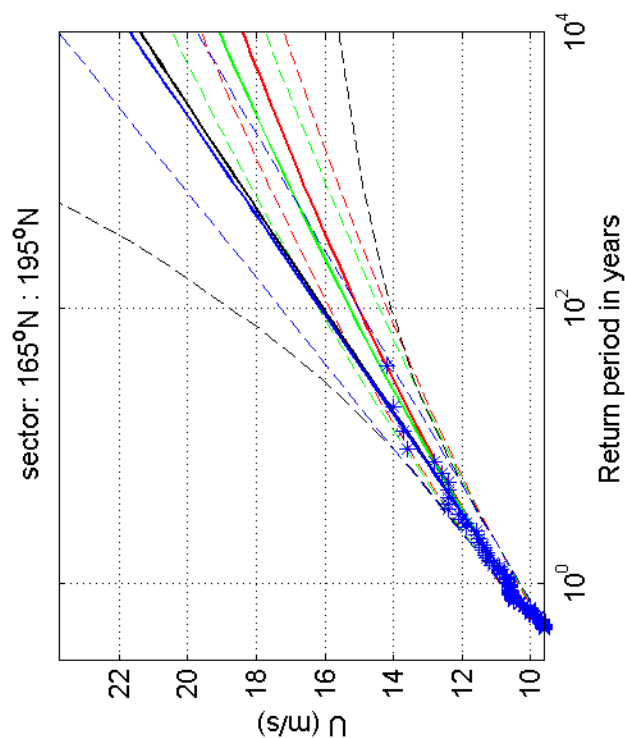
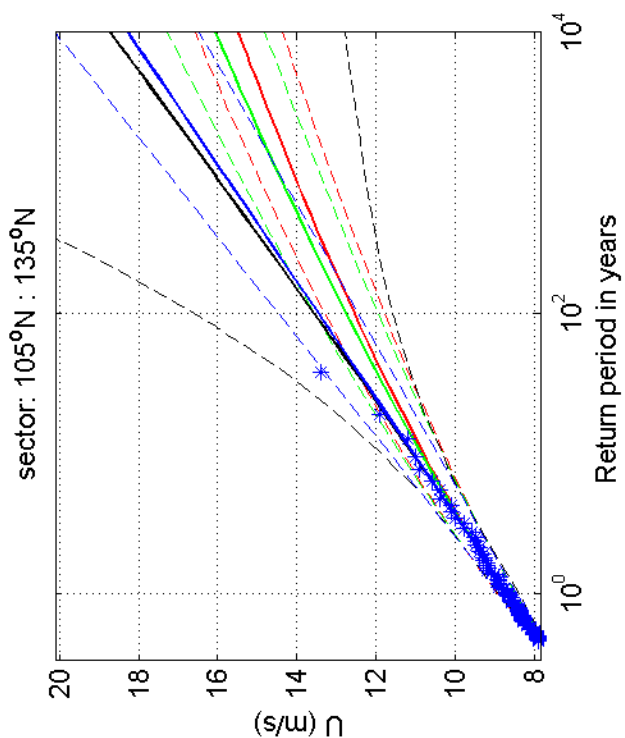
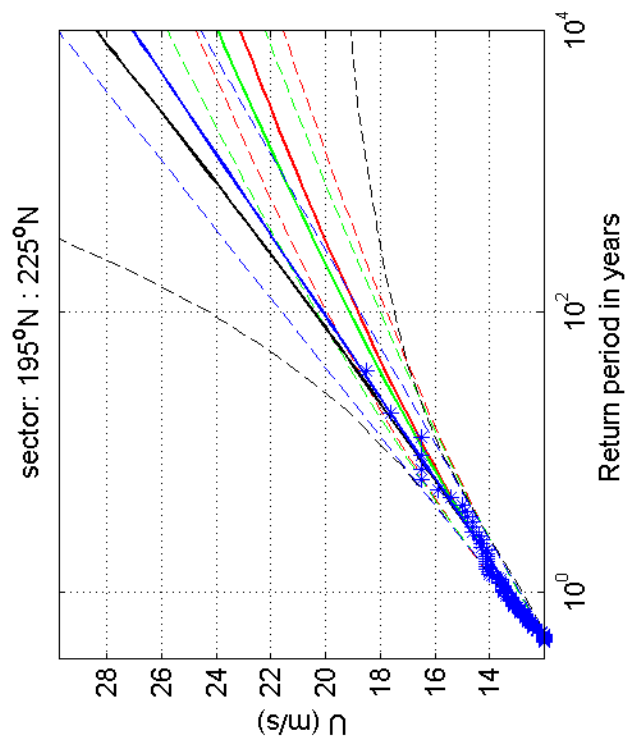
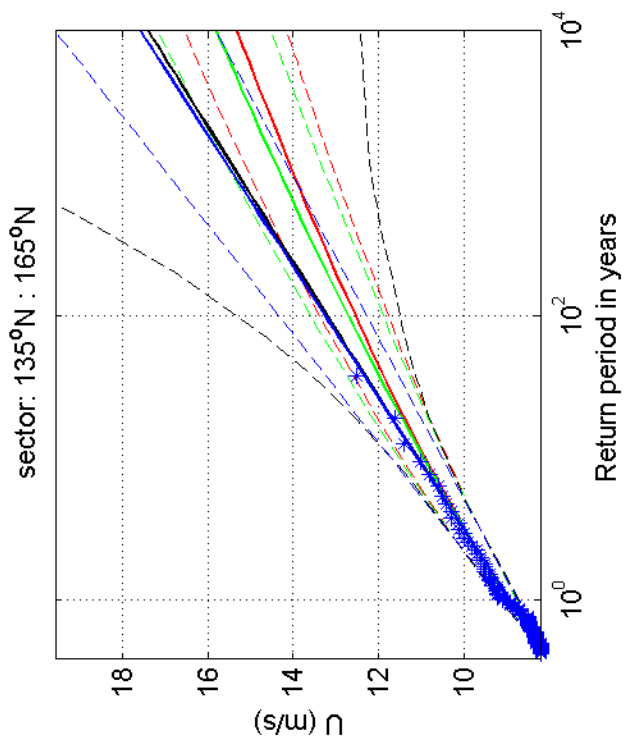
1970-2008

DeBilt

Deltares

1200264-005

Fig. F.4.260.1



Return value plot with exponential (blue) and GPD (black) fit to U ,
 exponential (red) fit to U_p^2 and exponential (green) fit to U_p^k
 Plotting positions: x_i vs $(n+1)/(\lambda(n+1-i))$

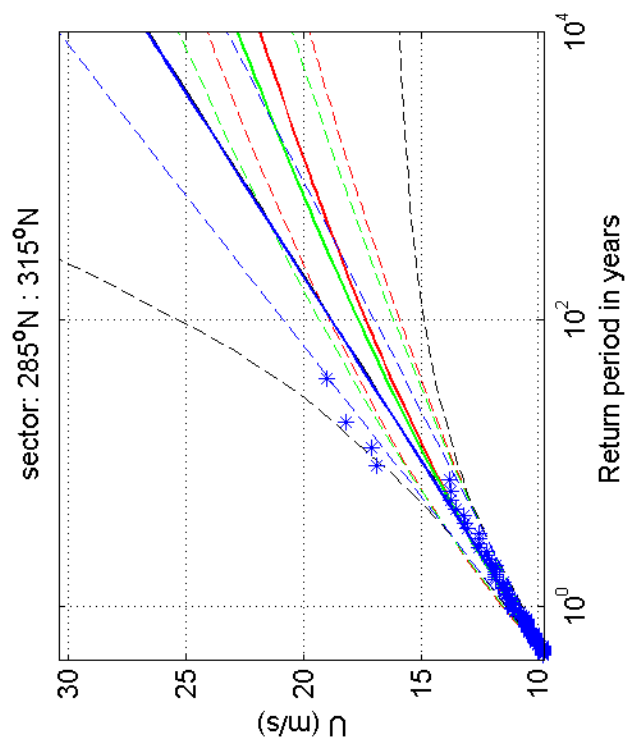
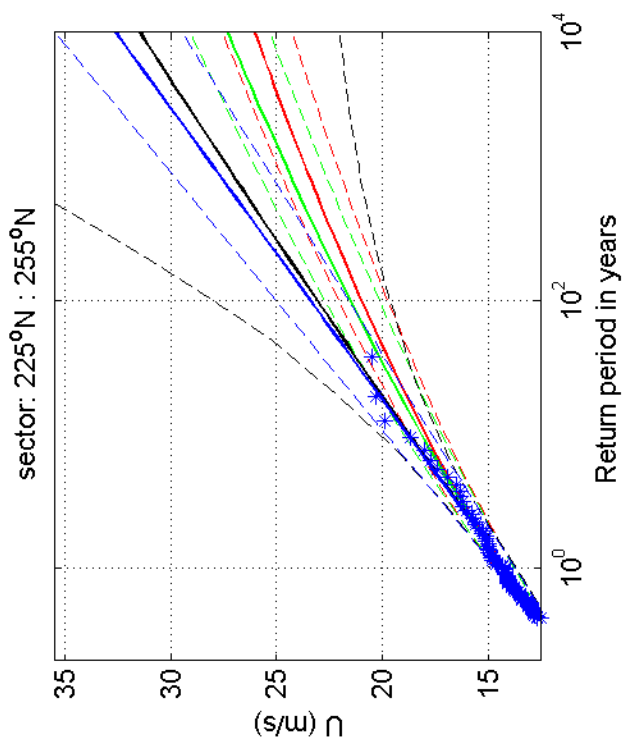
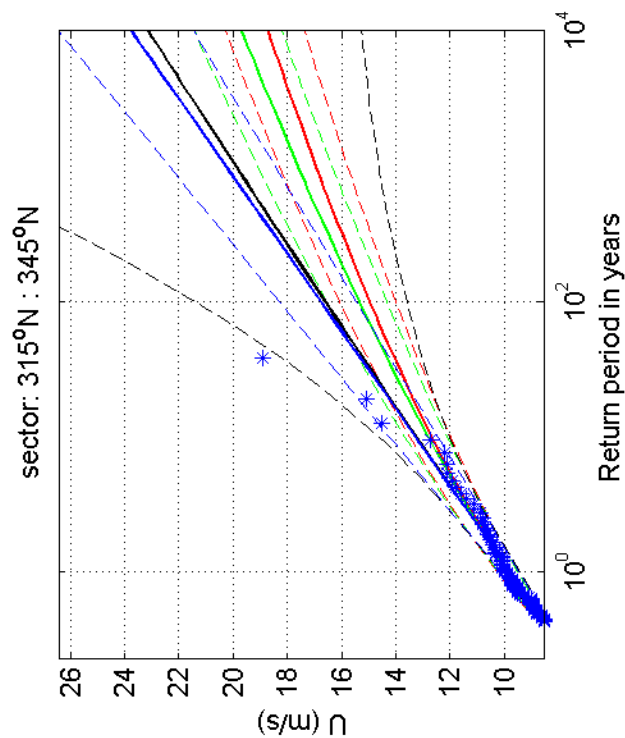
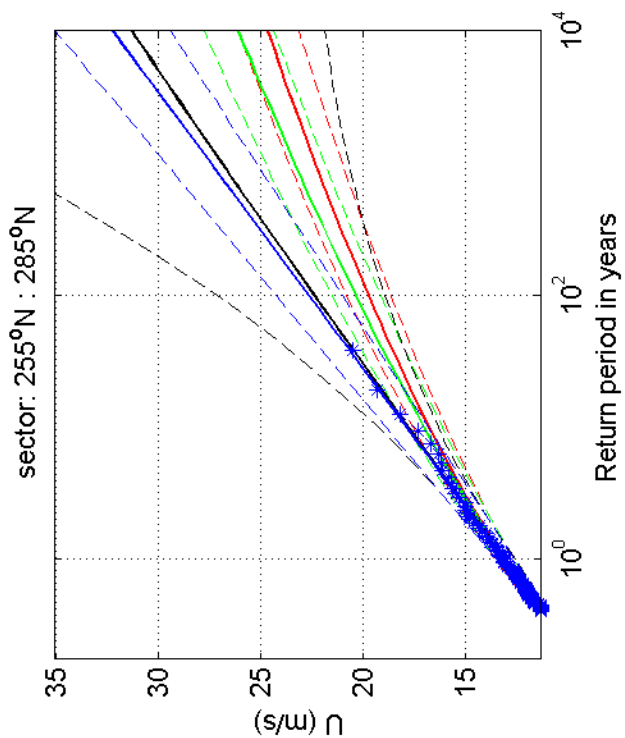
1970-2008

DeBilt

Deltares

1200264-005

Fig. F.4.260.5



Return value plot with exponential (blue) and GPD (black) fit to U ,
 exponential (red) fit to U_p^2 and exponential (green) fit to U_p^k
 Plotting positions: x_i vs $(n+1)/(\lambda(n+1-i))$

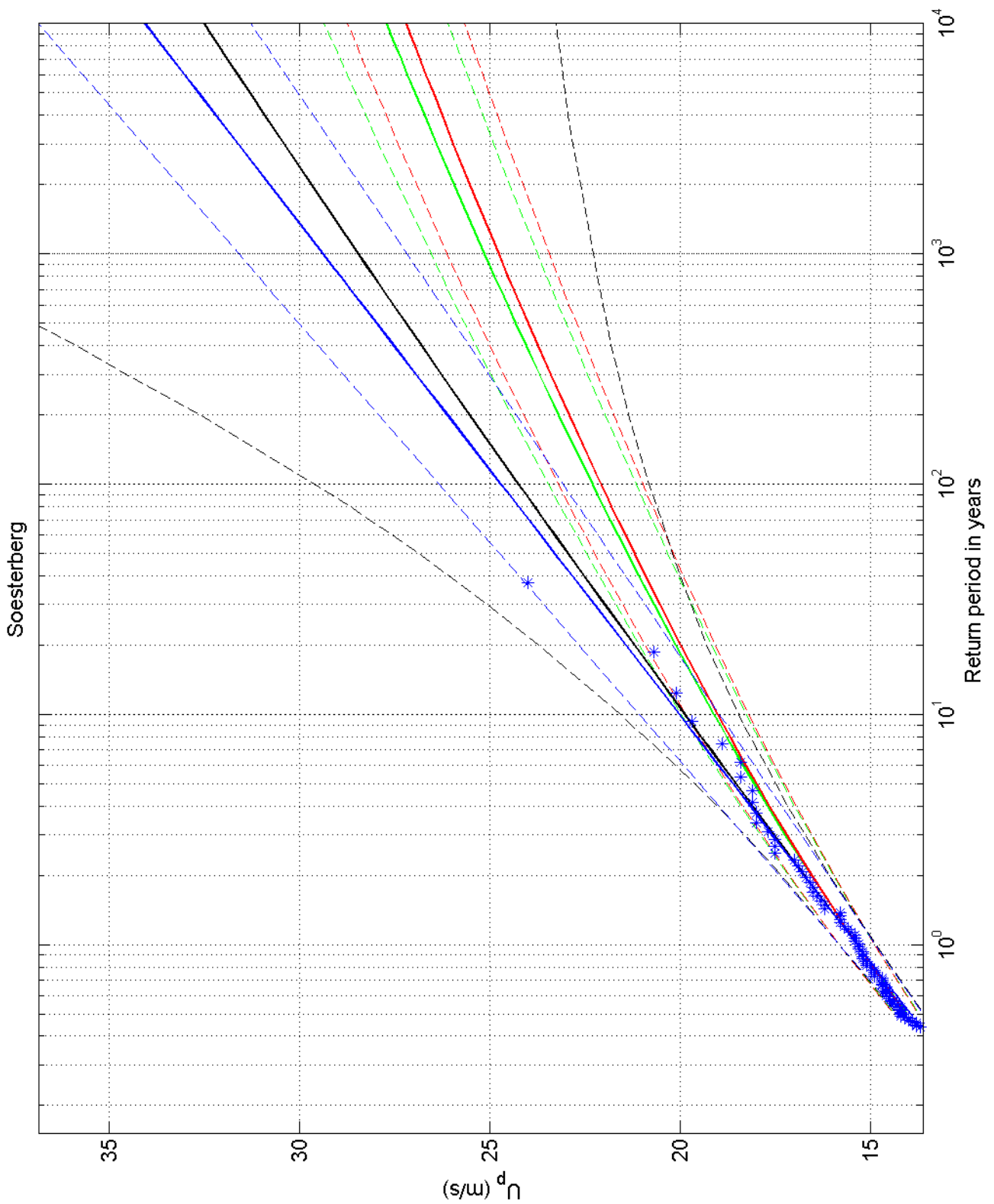
1970-2008

DeBilt

Deltares

1200264-005

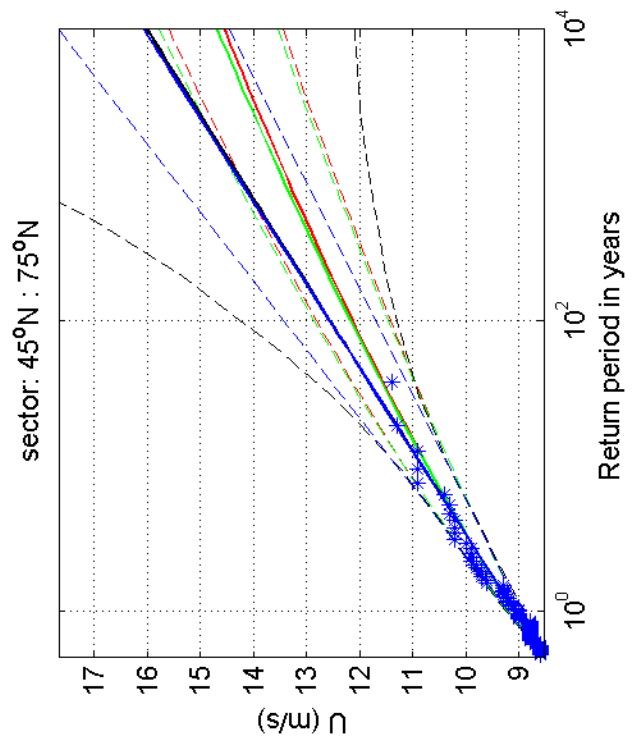
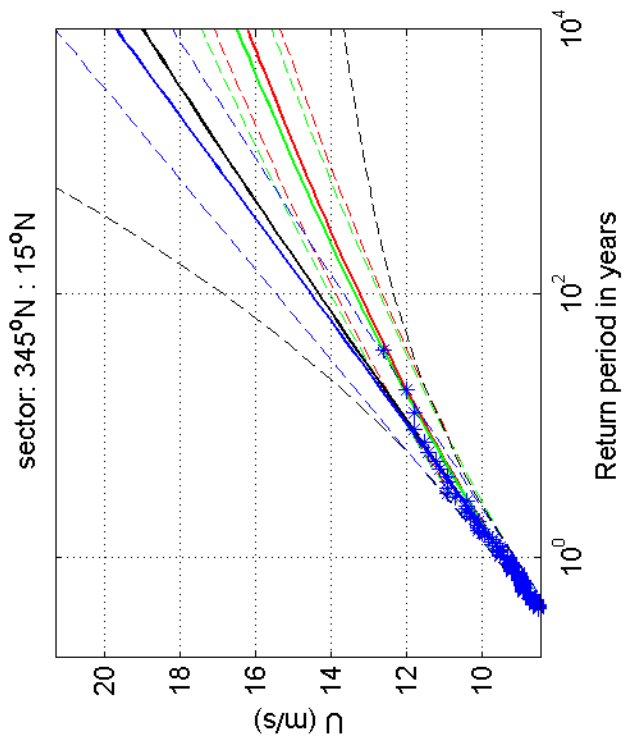
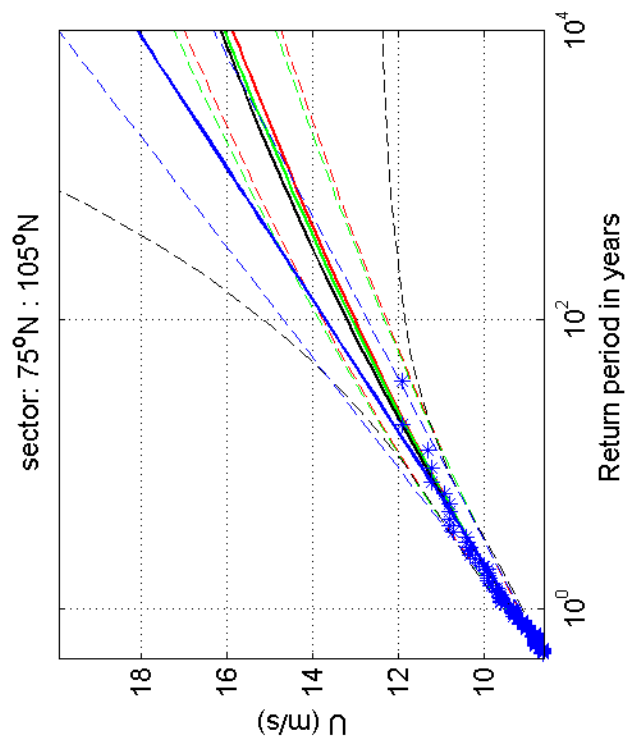
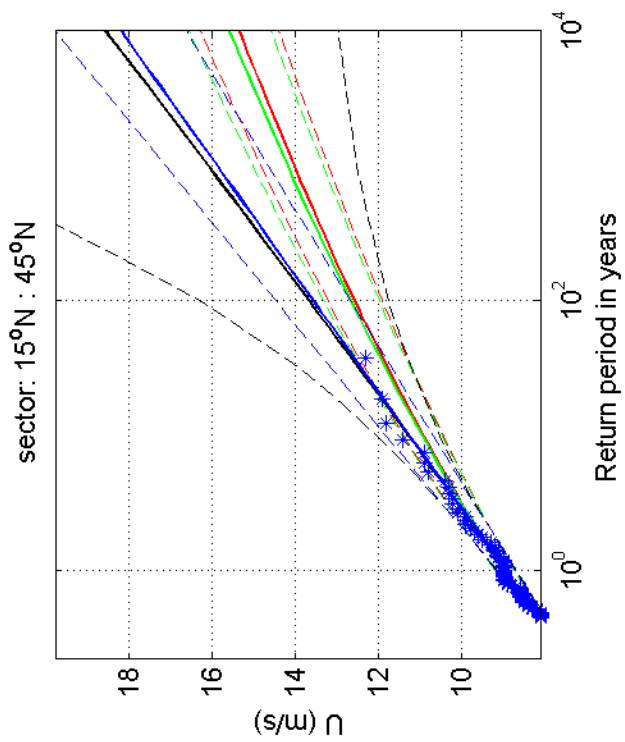
Fig. F.4.260.9



Return value plot with exponential (blue) and GPD (black) fit to U_p ,
 exponential (red) fit to U_p^2 and exponential (green) fit to U_p^k
 Plotting positions: x_i vs $(n+1)/(\lambda(n+1-i))$

omni-directional	1970-2008
Soesterberg	
1200264-005	Fig. F.4.265

Deltares



Return value plot with exponential (blue) and GPD (black) fit to U ,
 exponential (red) fit to U_p^2 and exponential (green) fit to U_p^k
 Plotting positions: x_i vs $(n+1)/(\lambda(n+1-i))$

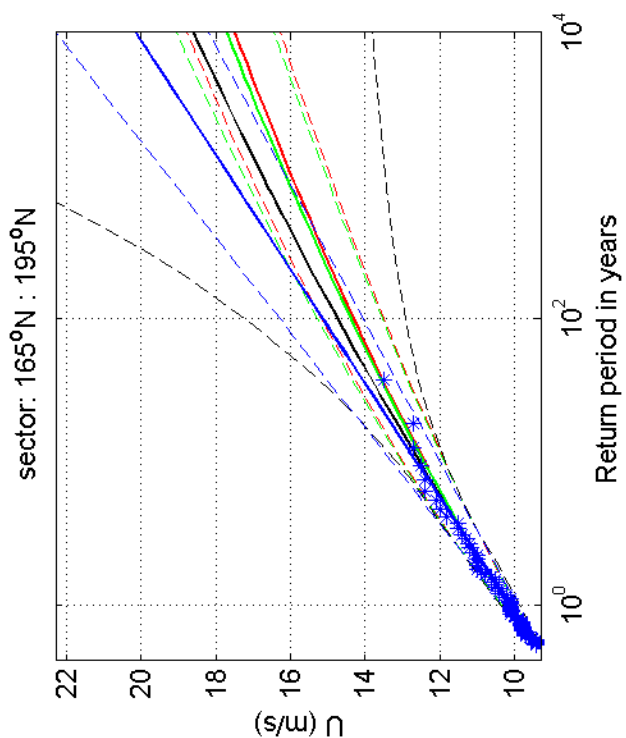
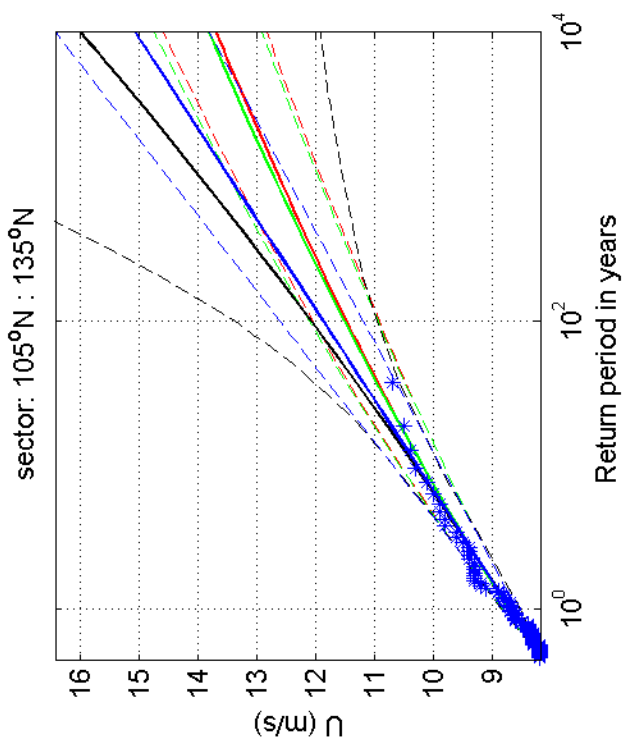
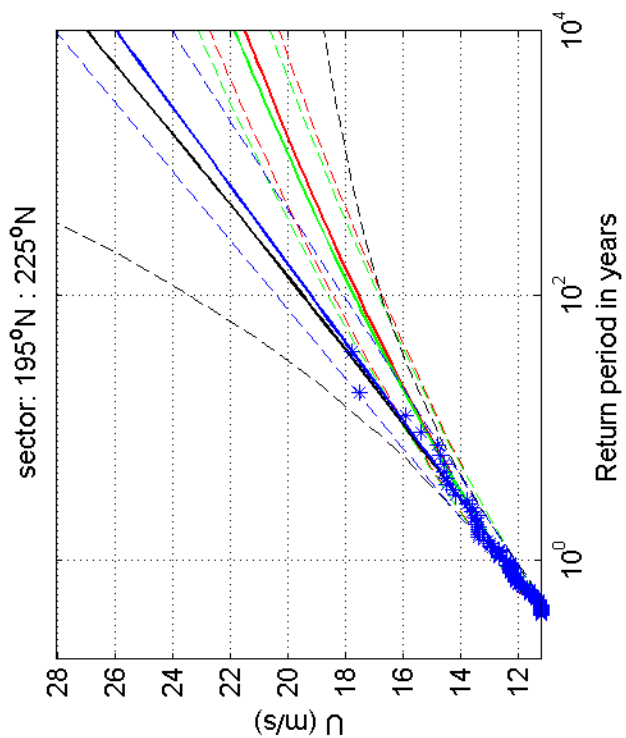
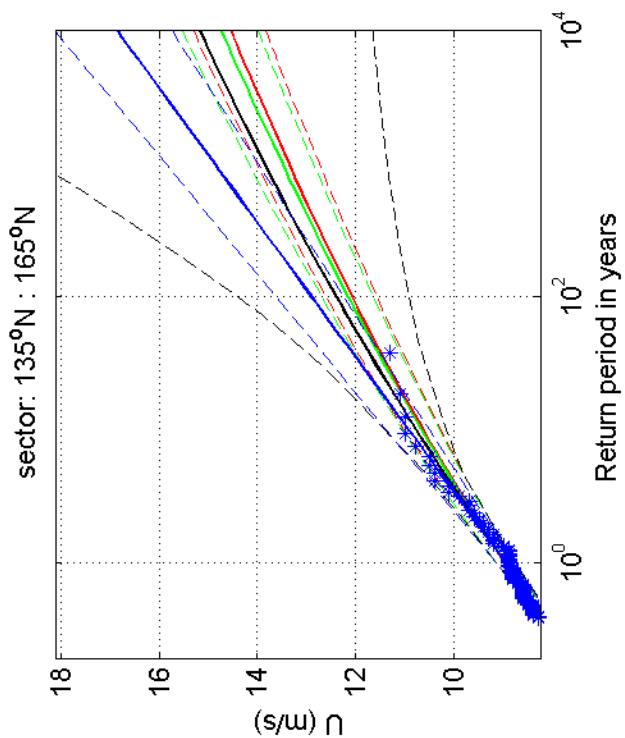
1970-2008

Soesterberg

Deltares

1200264-005

Fig. F.4.265.1



Return value plot with exponential (blue) and GPD (black) fit to U ,
 exponential (red) fit to U_p^k and exponential (green) fit to U_p^k
 Plotting positions: x_i vs $(n+1)/(\lambda(n+1-i))$

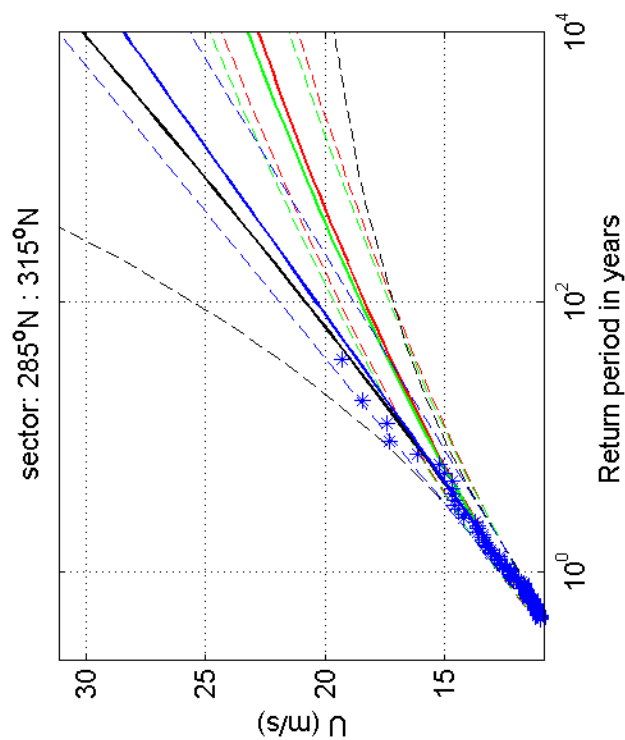
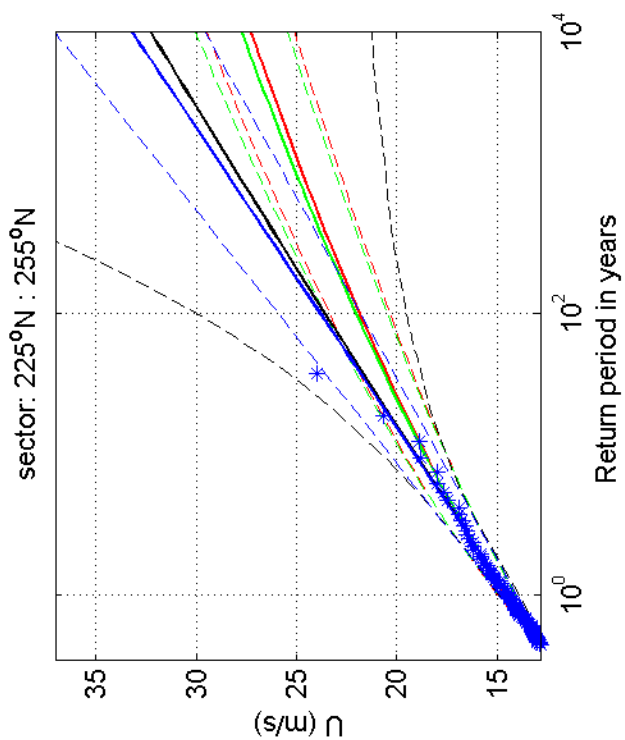
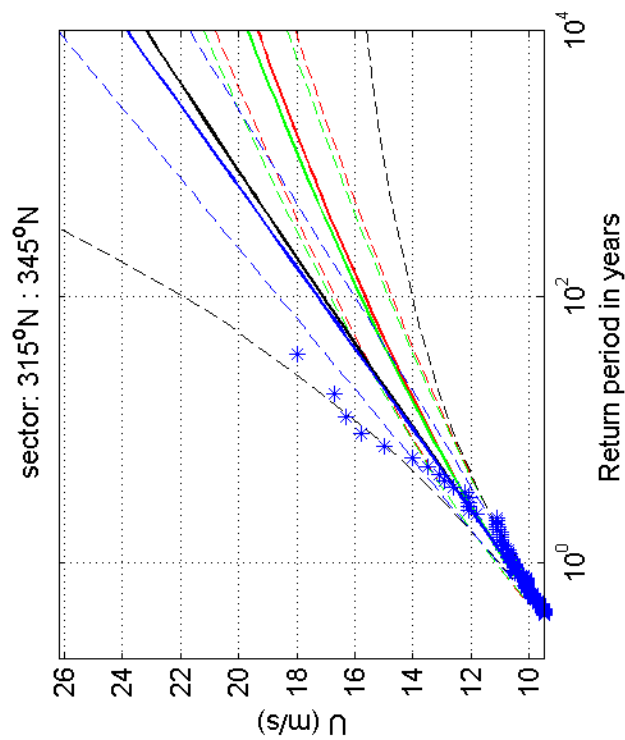
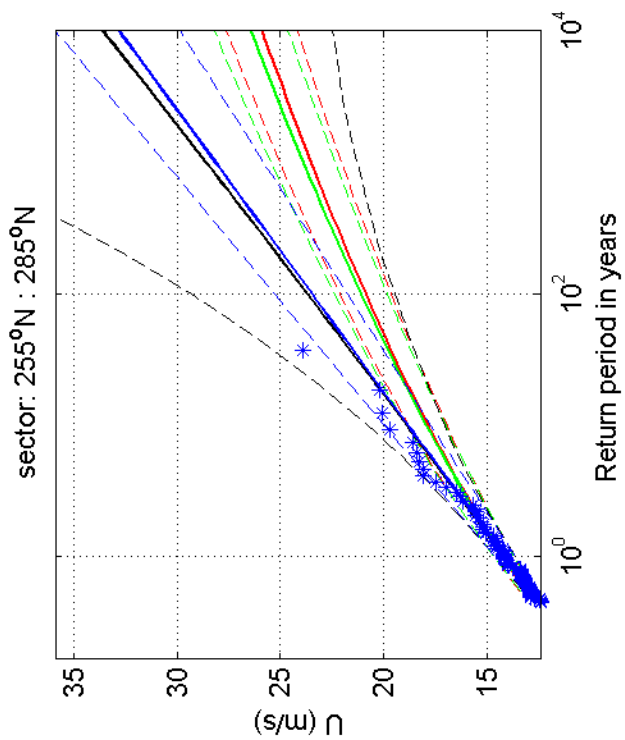
1970-2008

Soesterberg

Deltares

1200264-005

Fig. F.4.265.5



Return value plot with exponential (blue) and GPD (black) fit to U ,
 exponential (red) fit to U_p^2 and exponential (green) fit to U_p^k
 Plotting positions: x_i vs $(n+1)/(\lambda(n+1-i))$

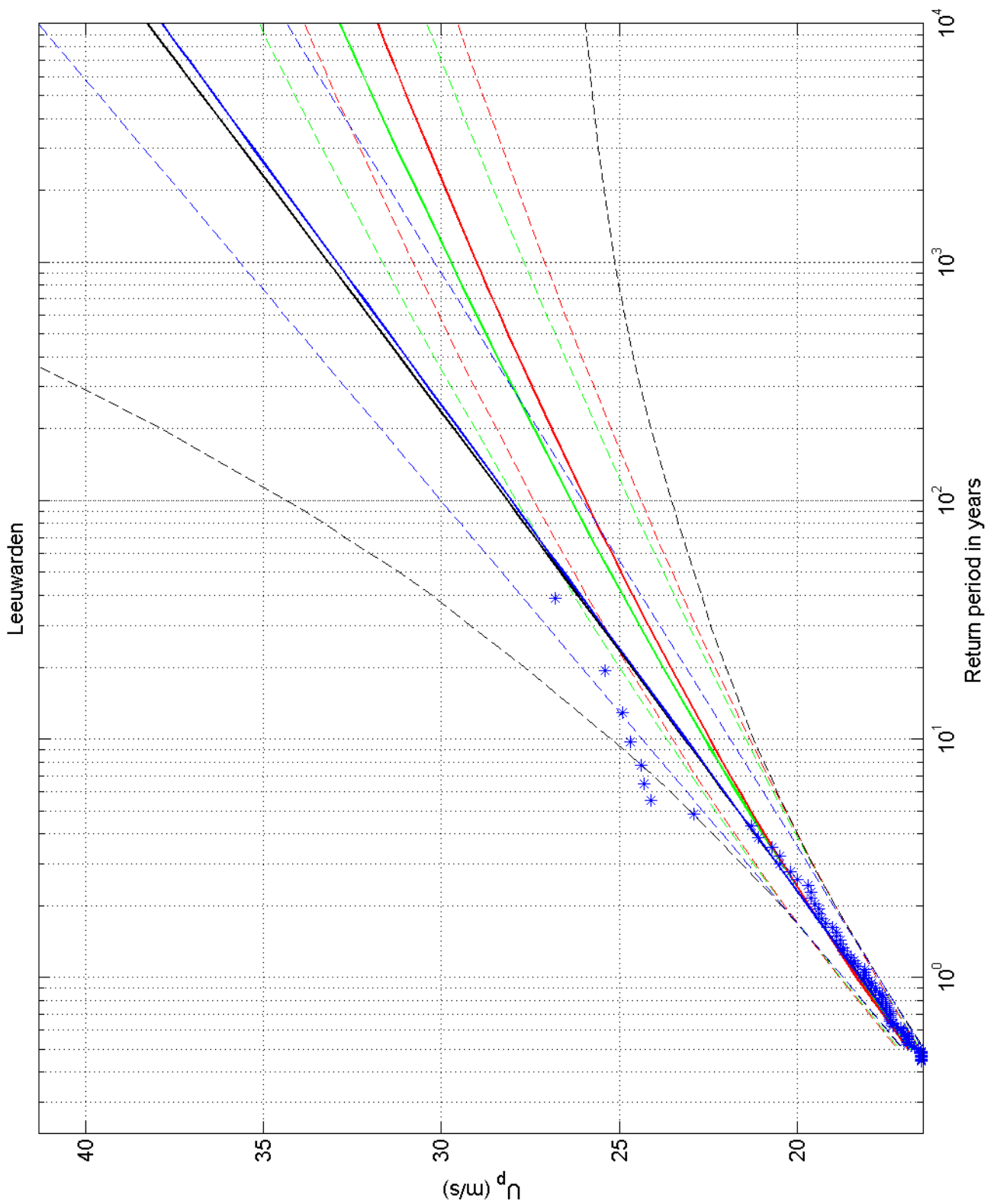
1970-2008

Soesterberg

Deltares

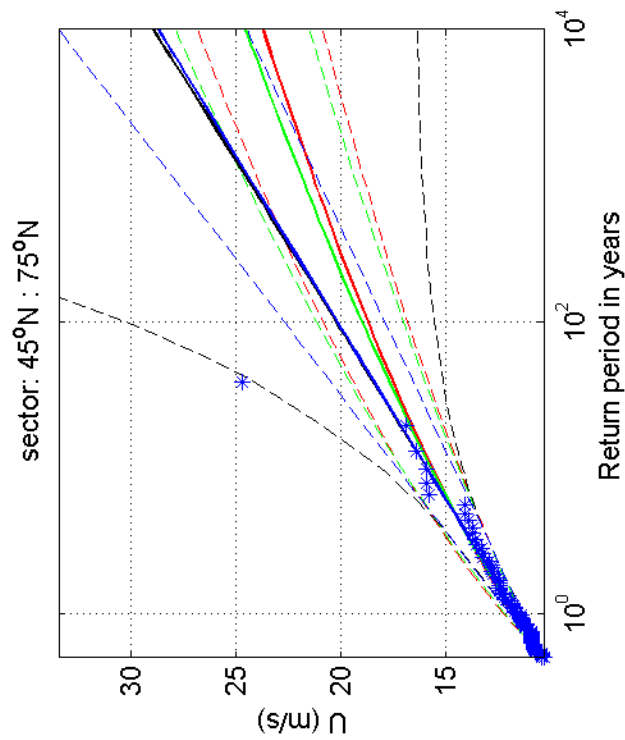
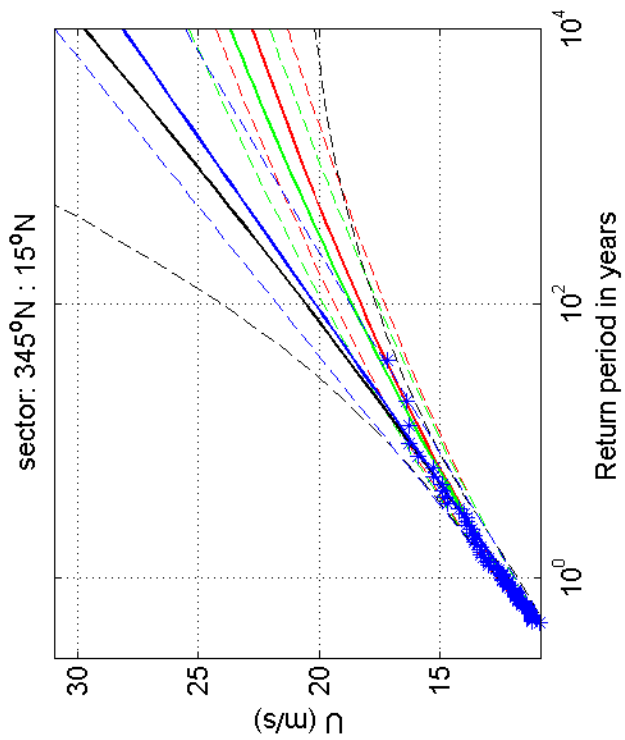
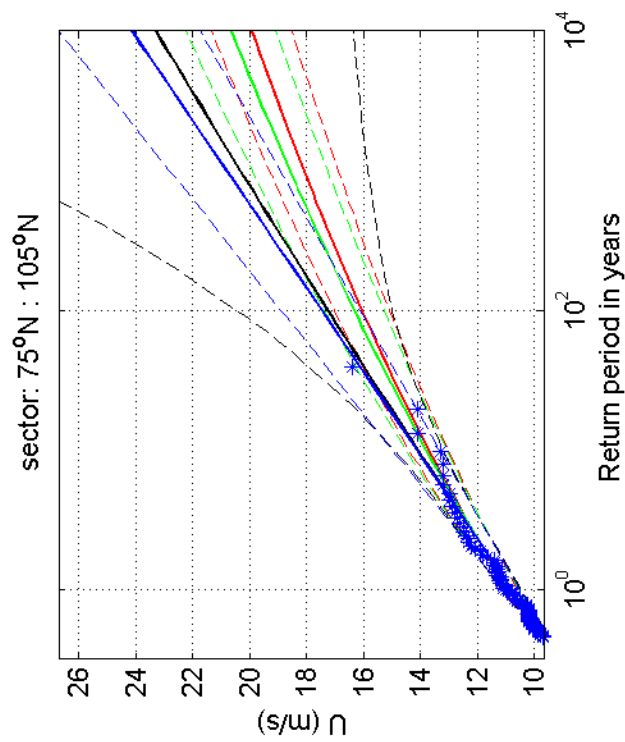
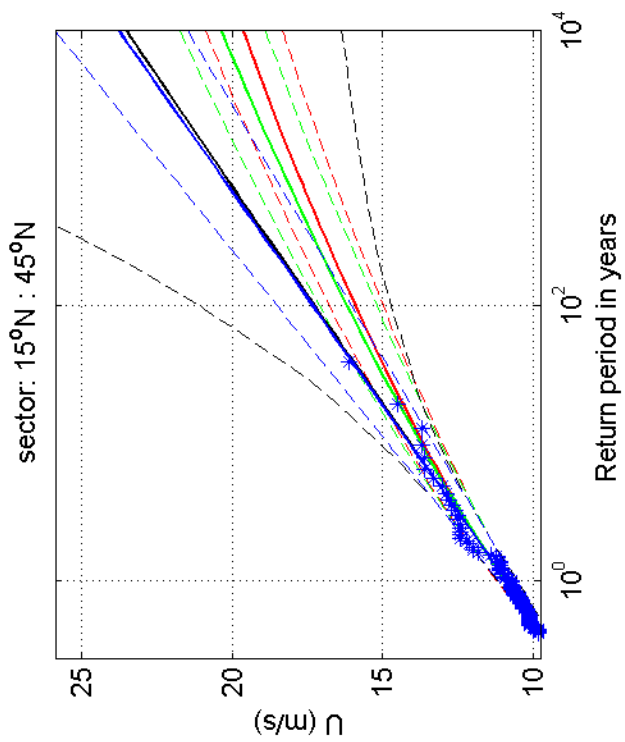
1200264-005

Fig. F.4.265.9



Return value plot with exponential (blue) and GPD (black) fit to U_p ,
 exponential (red) fit to U_p^2 and exponential (green) fit to U_p^k
 Plotting positions: x_i vs $(n+1)/(\lambda(n+1-i))$

omni-directional	1970-2008
Leeuwarden	
1200264-005	Fig. F.4.270



Return value plot with exponential (blue) and GPD (black) fit to U ,
 exponential (red) fit to U_p^2 and exponential (green) fit to U_p^k
 Plotting positions: x_i vs $(n+1)/(\lambda(n+1-i))$

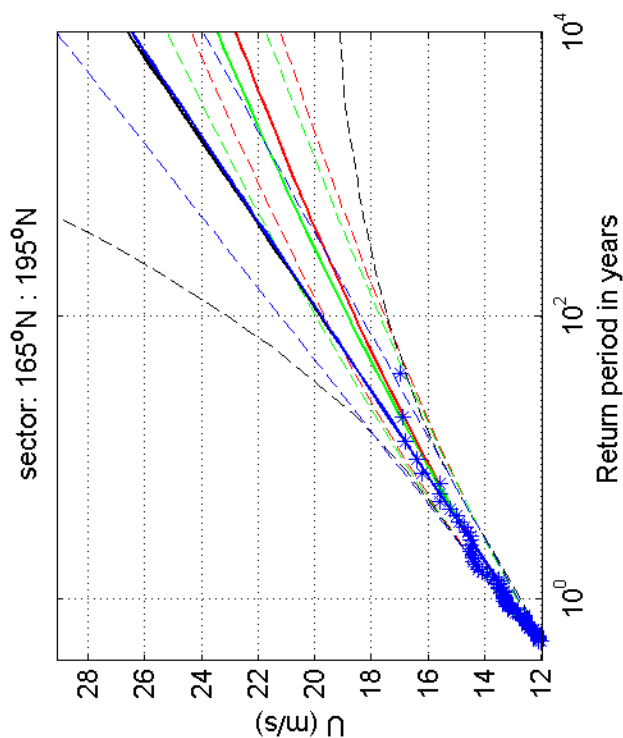
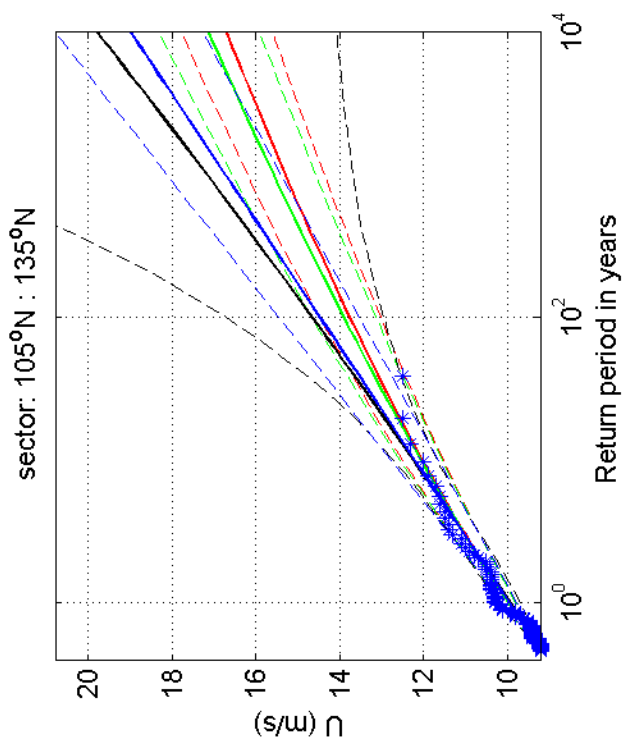
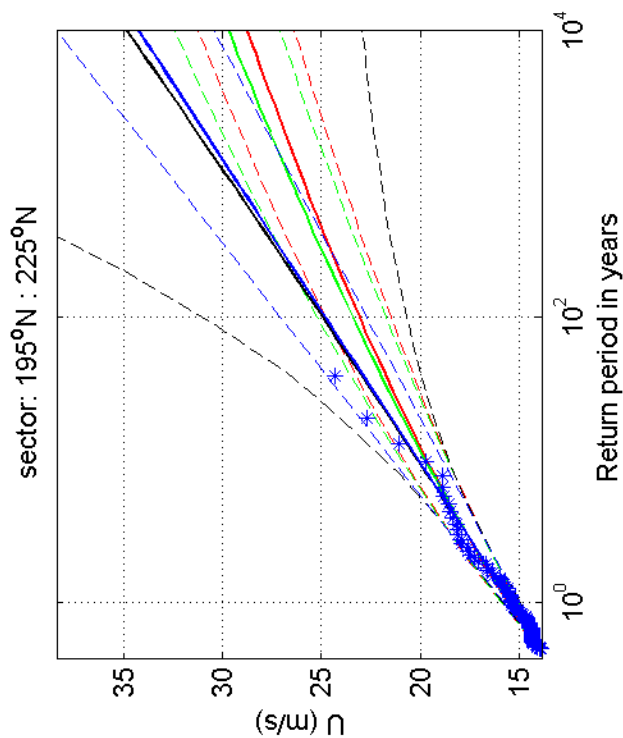
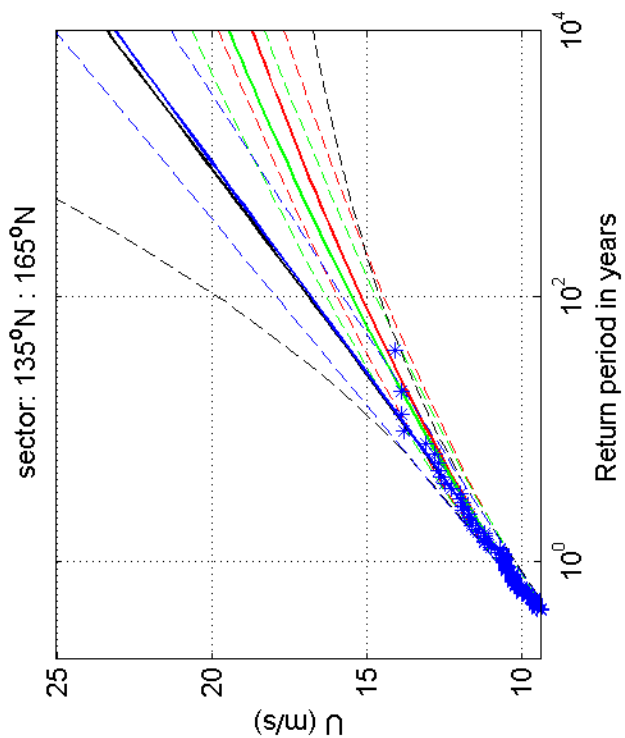
1970-2008

Leeuwarden

Deltares

1200264-005

Fig. F.4.270.1



Return value plot with exponential (blue) and GPD (black) fit to U ,
 exponential (red) fit to U_p^k and exponential (green) fit to U_p^k
 Plotting positions: x_i vs $(n+1)/(\lambda(n+1-i))$

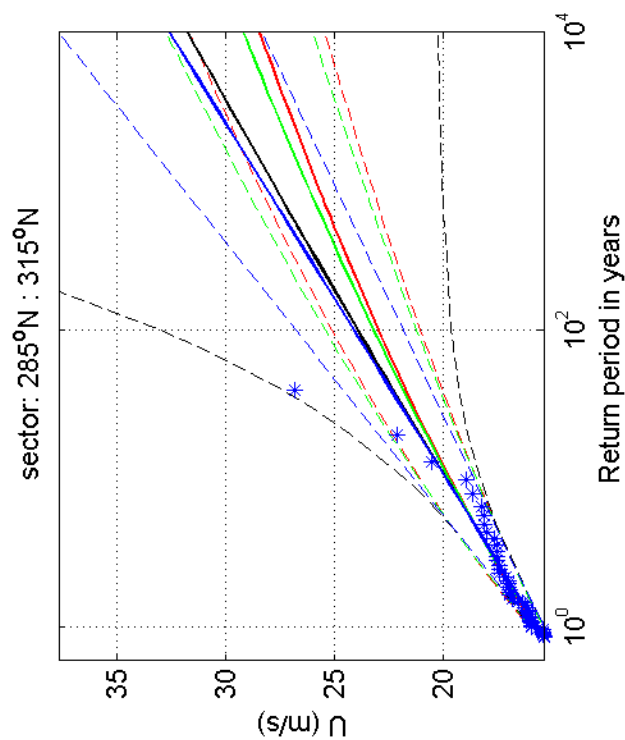
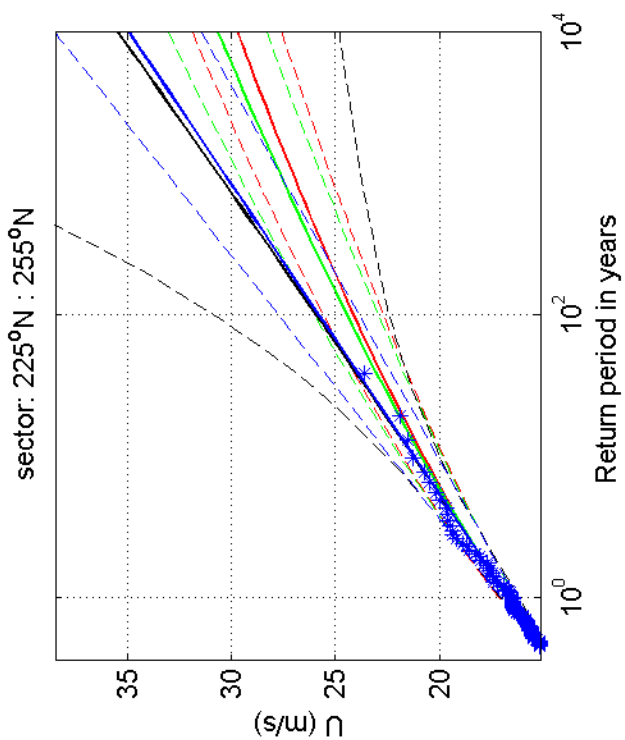
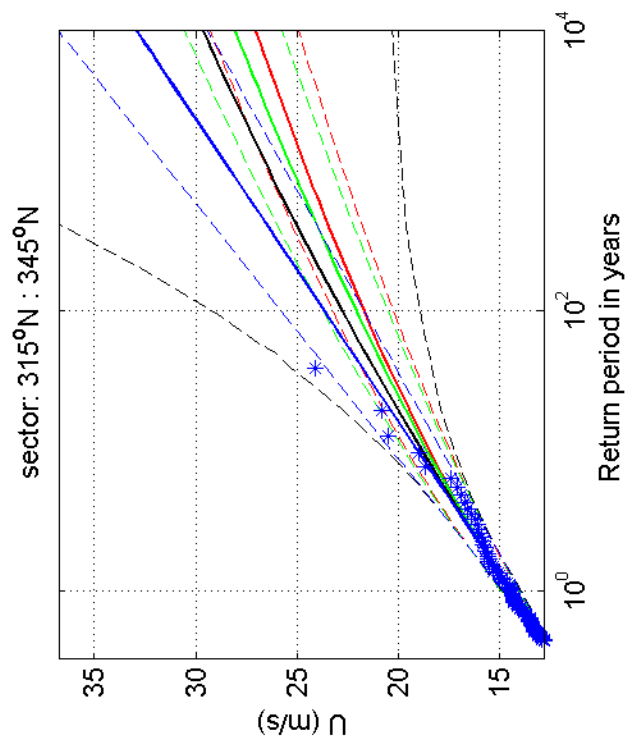
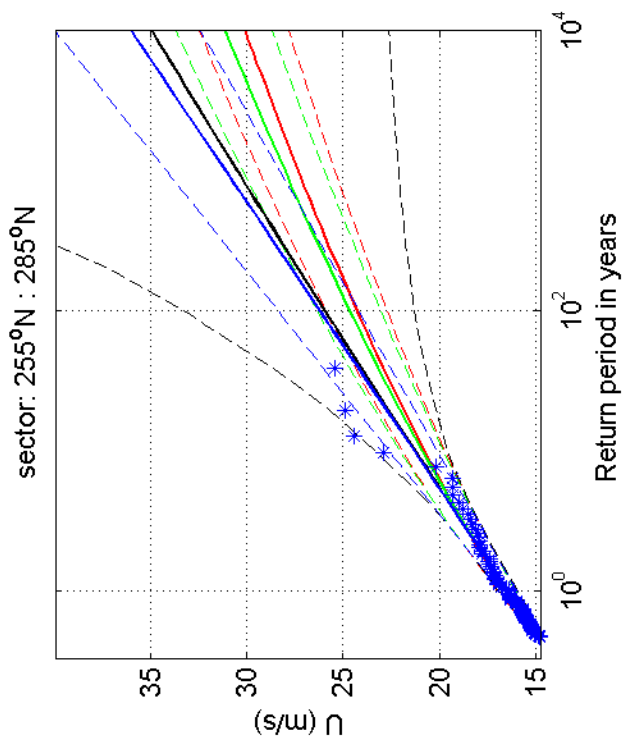
1970-2008

Leeuwarden

Deltares

1200264-005

Fig. F.4.270.5



Return value plot with exponential (blue) and GPD (black) fit to U ,
 exponential (red) fit to U_p^2 and exponential (green) fit to U_p^k
 Plotting positions: x_i vs $(n+1)/(\lambda(n+1-i))$

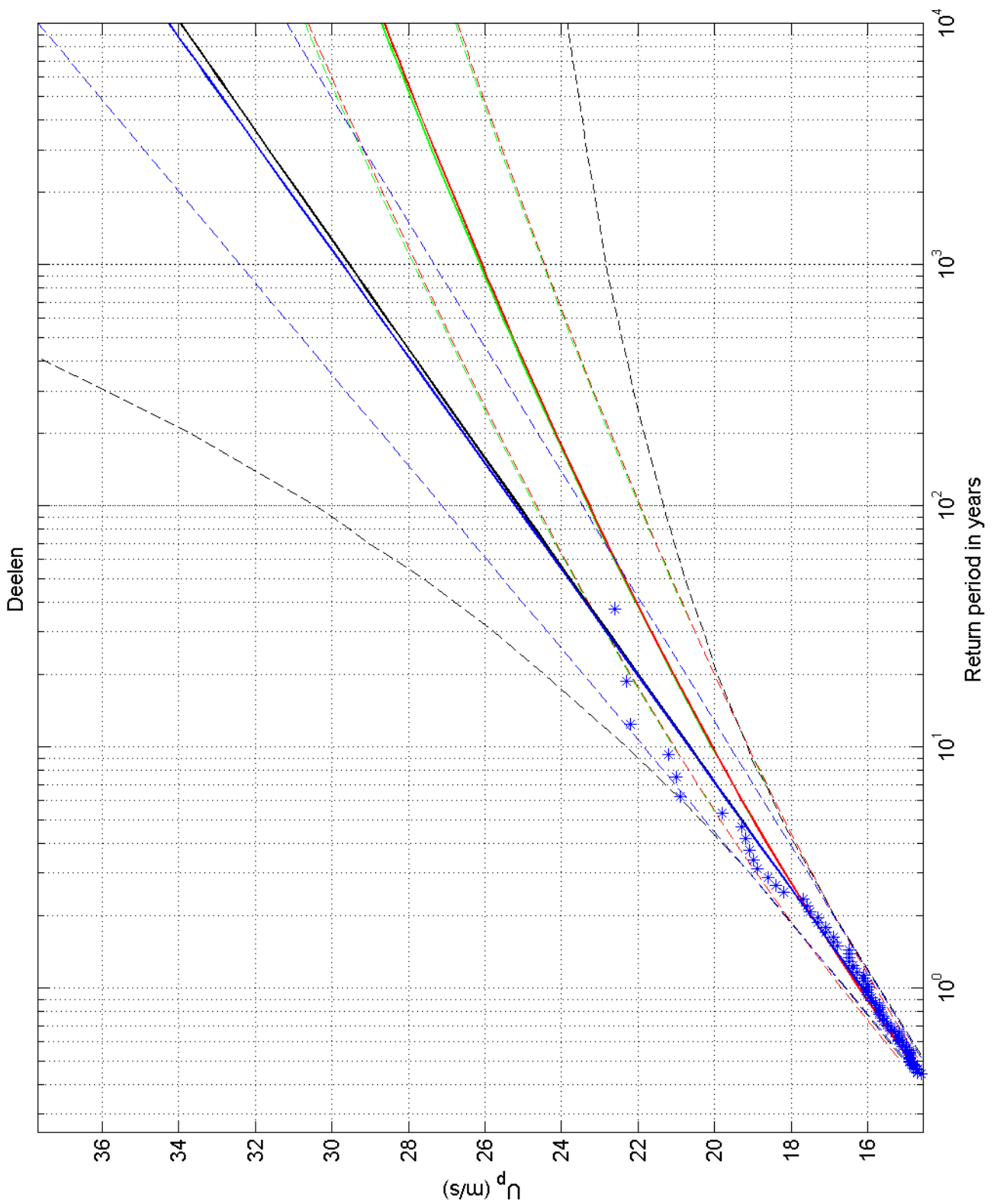
1970-2008

Leeuwarden

Deltares

1200264-005

Fig. F.4.270.9



Return value plot with exponential (blue) and GPD (black) fit to U_p ,
 exponential (red) fit to U_p^2 and exponential (green) fit to U_p^k
 Plotting positions: x_i vs $(n+1)/(\lambda(n+1-i))$

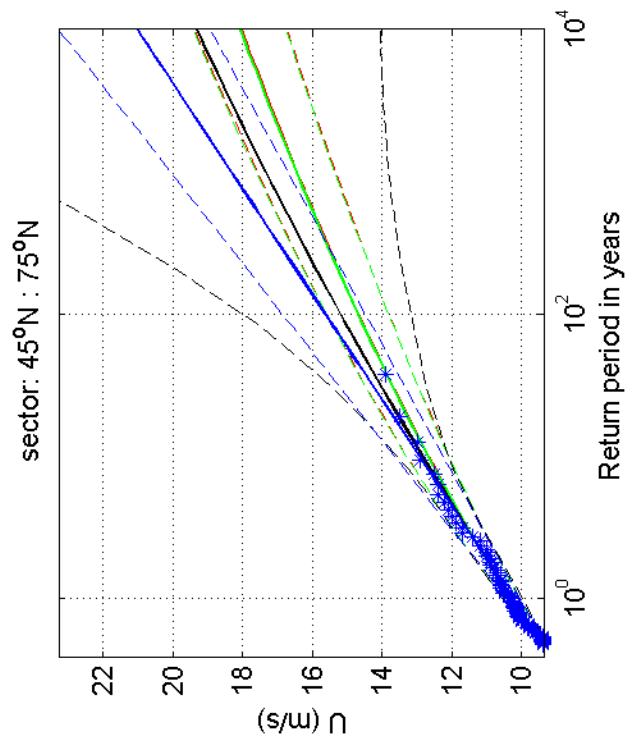
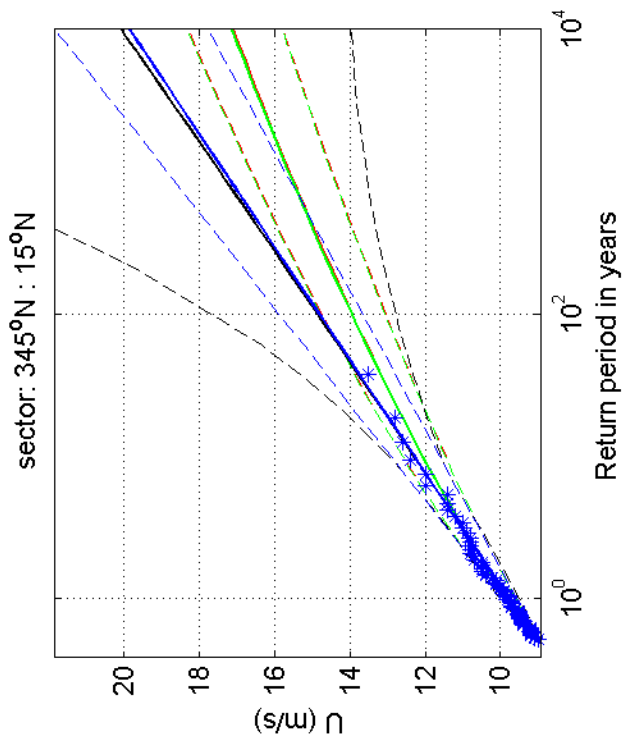
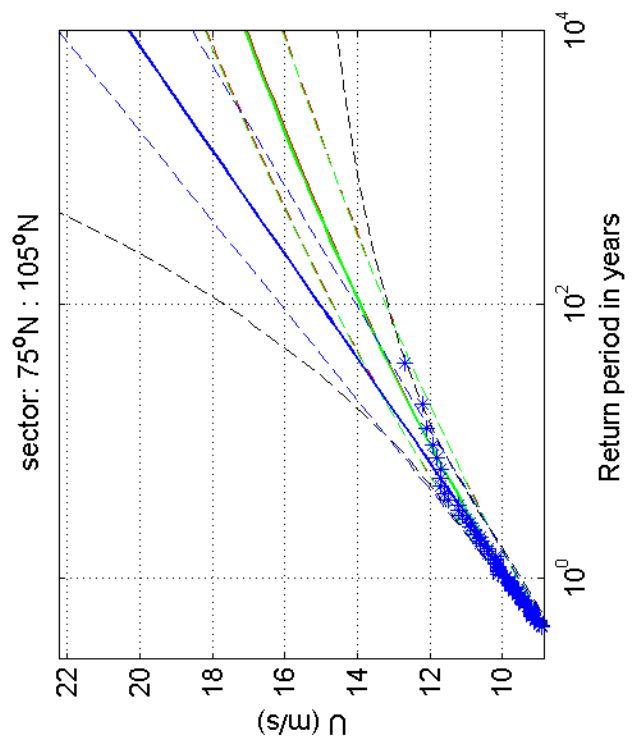
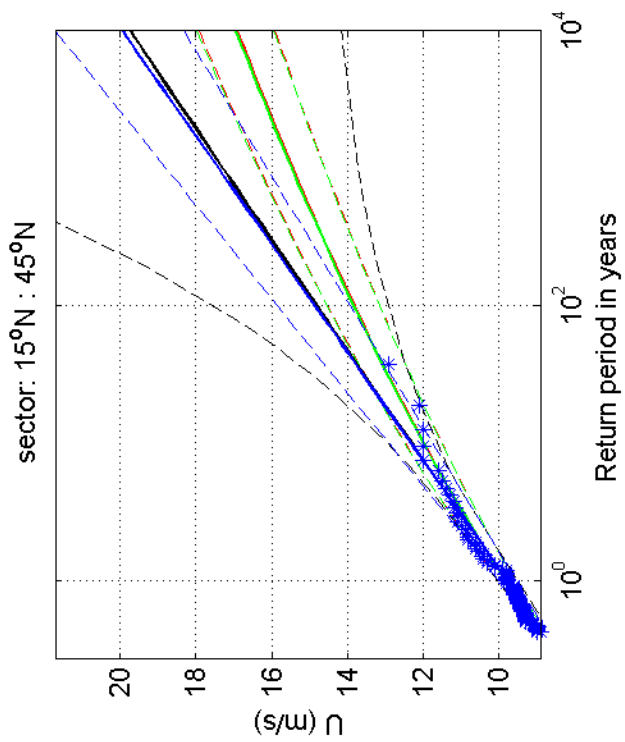
omni-directional 1970-2008

Deelen

Deltares

1200264-005

Fig. F.4.275



Return value plot with exponential (blue) and GPD (black) fit to U ,
 exponential (red) fit to U_p^2 and exponential (green) fit to U_p^k
 Plotting positions: x_i vs $(n+1)/(\lambda(n+1-i))$

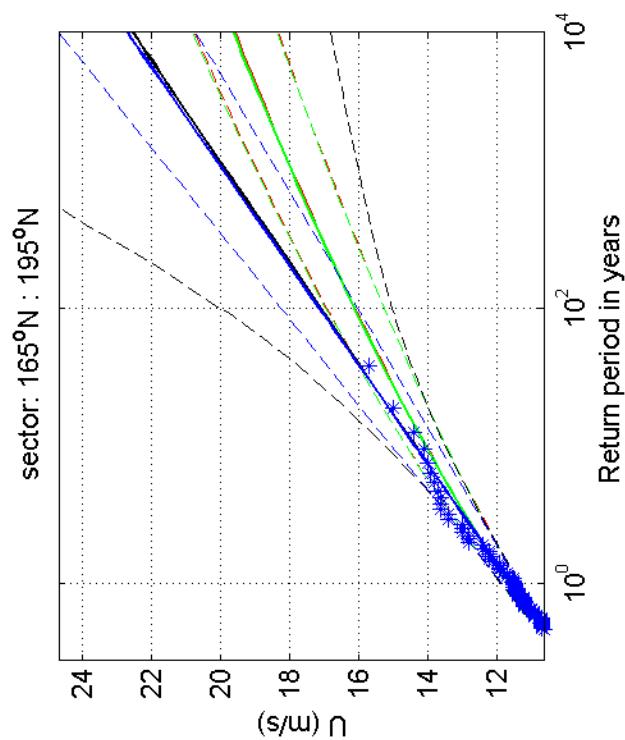
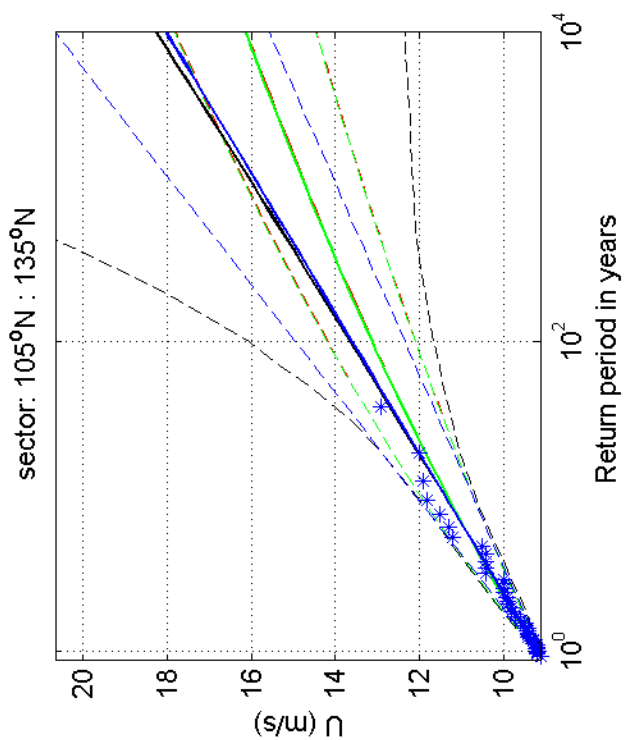
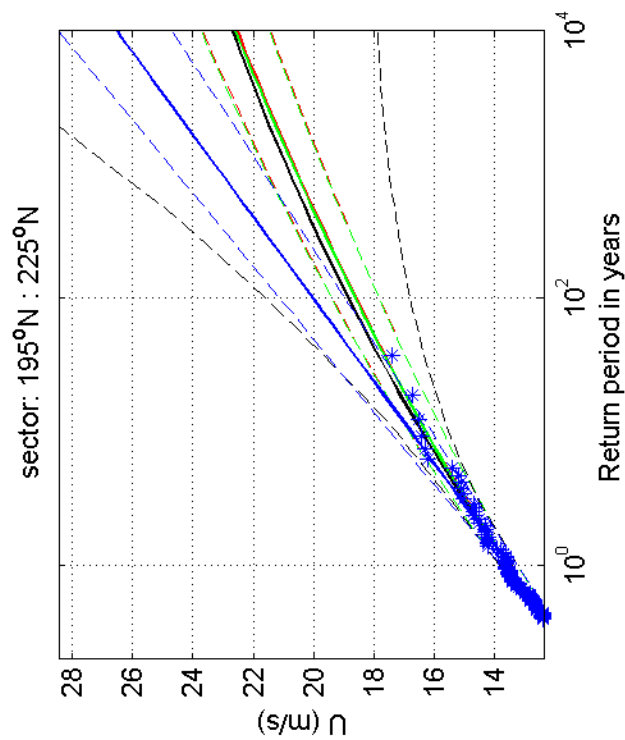
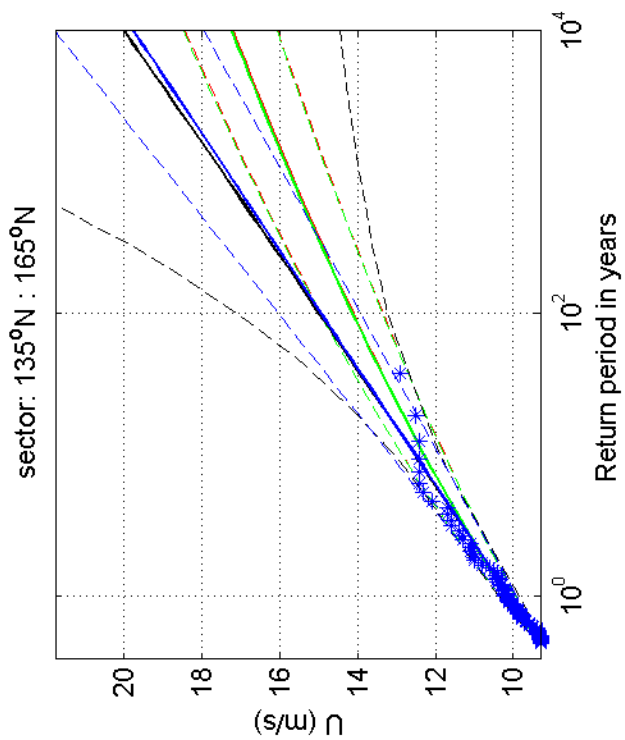
1970-2008

Deelen

Deltares

1200264-005

Fig. F.4.275.1



Return value plot with exponential (blue) and GPD (black) fit to U ,
 exponential (red) fit to U_p^2 and exponential (green) fit to U_p^k
 Plotting positions: x_i vs $(n+1)/(\lambda(n+1-i))$

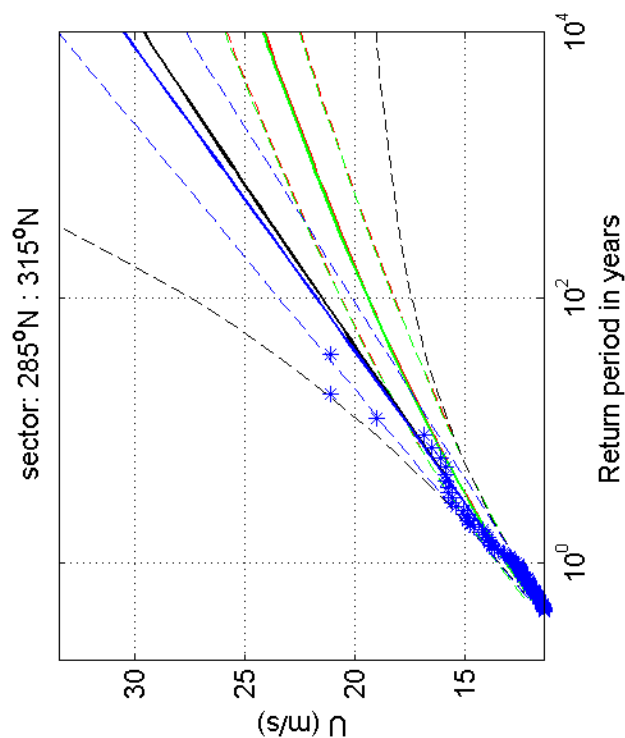
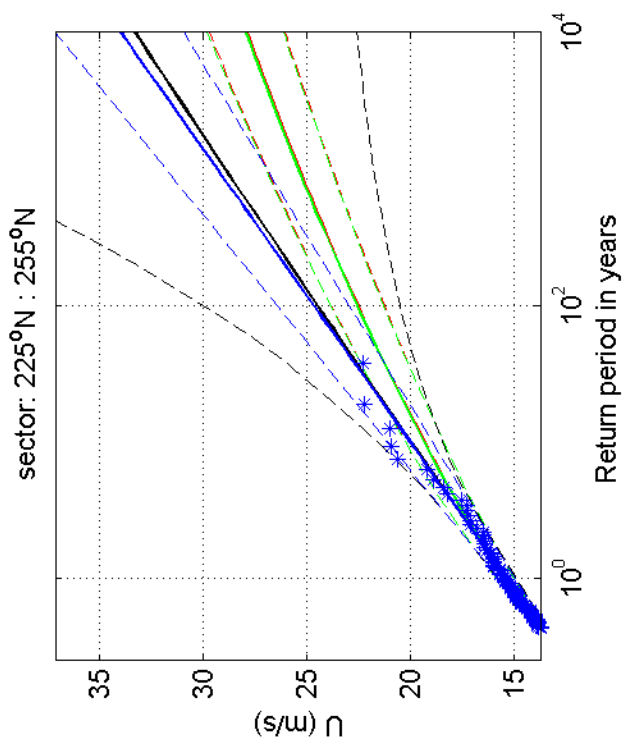
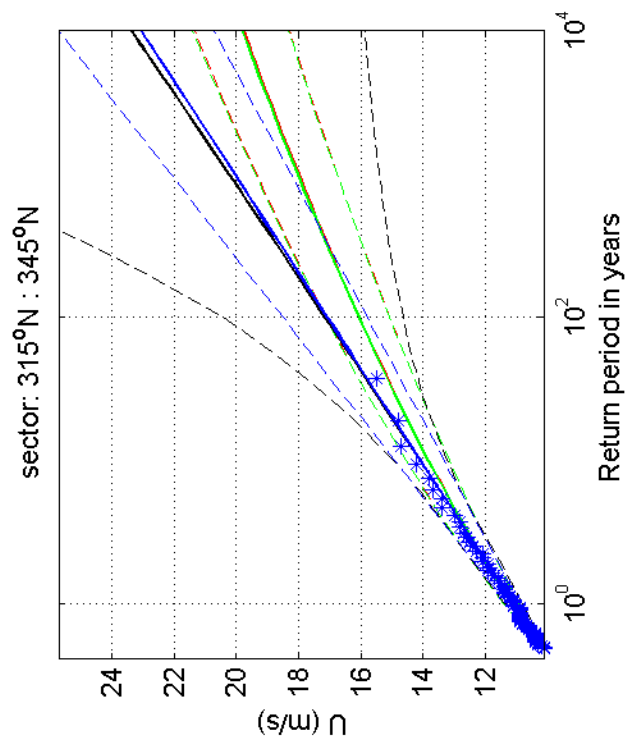
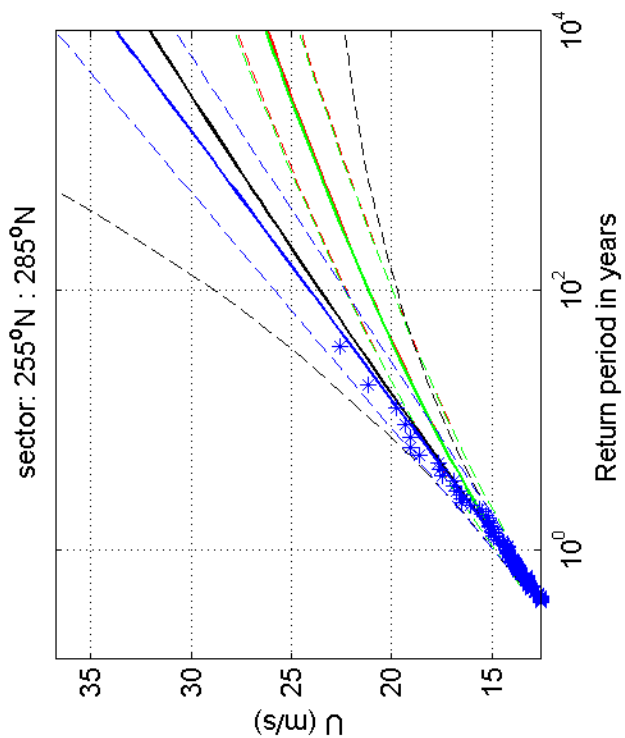
1970-2008

Deelen

Deltares

1200264-005

Fig. F.4.275.5



Return value plot with exponential (blue) and GPD (black) fit to U ,
 exponential (red) fit to U_p^2 and exponential (green) fit to U_p^k
 Plotting positions: x_i vs $(n+1)/(\lambda(n+1-i))$

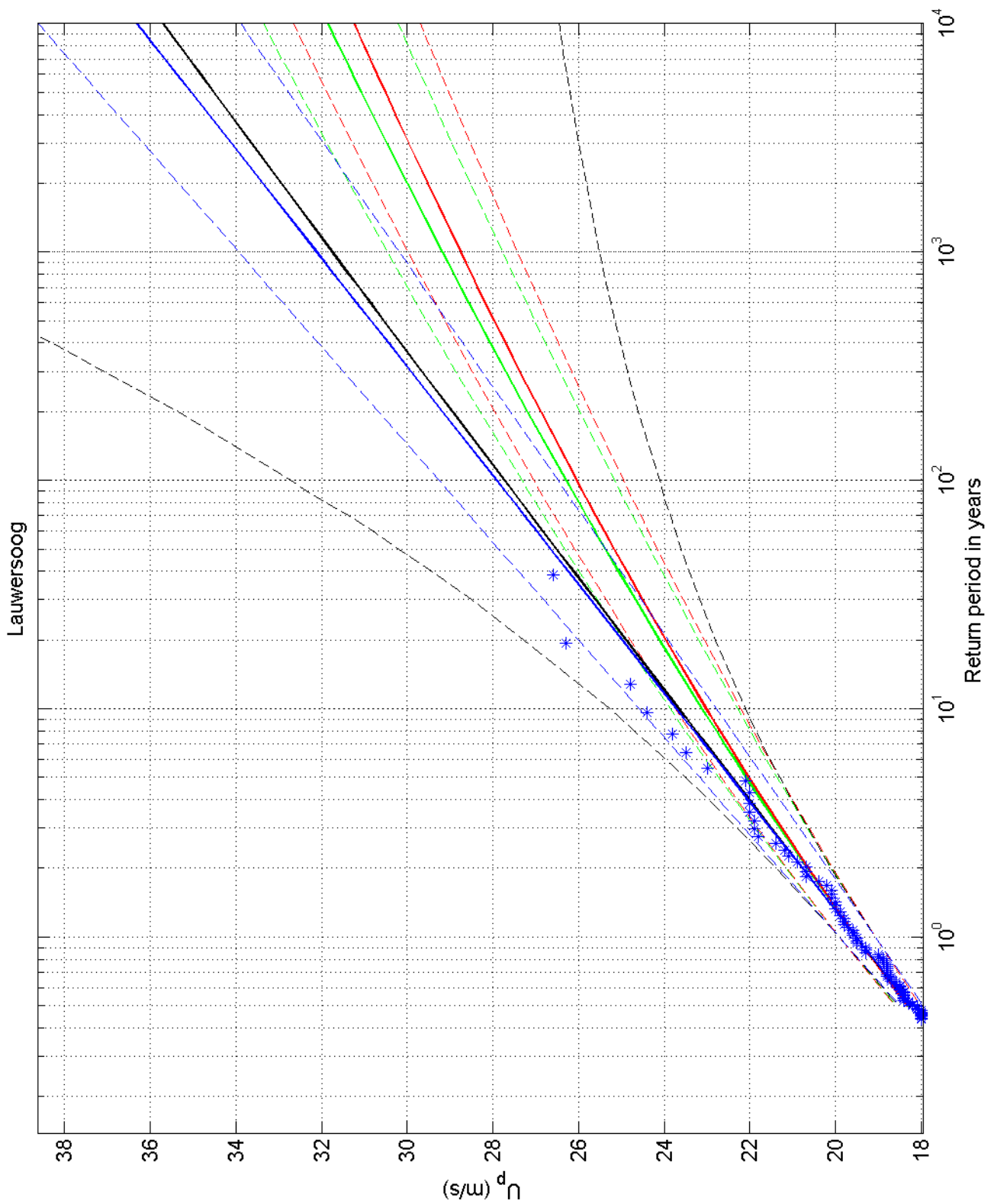
1970-2008

Deelen

Deltares

1200264-005

Fig. F.4.275.9



Return value plot with exponential (blue) and GPD (black) fit to U_p ,
 exponential (red) fit to U_p^2 and exponential (green) fit to U_p^k
 Plotting positions: x_i vs $(n+1)/(\lambda(n+1-i))$

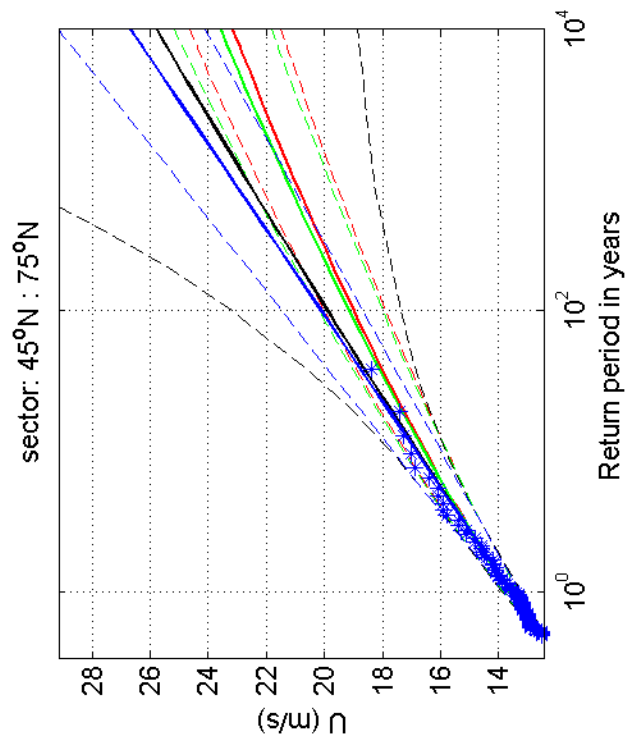
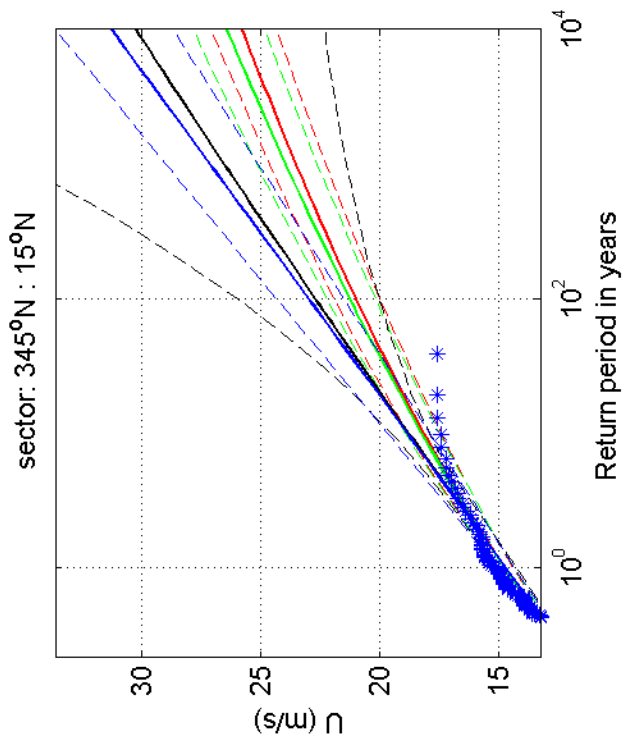
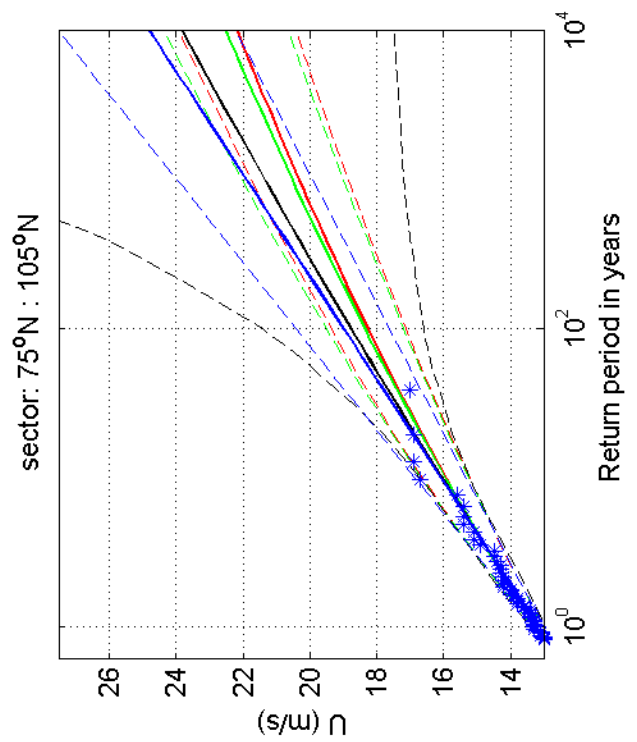
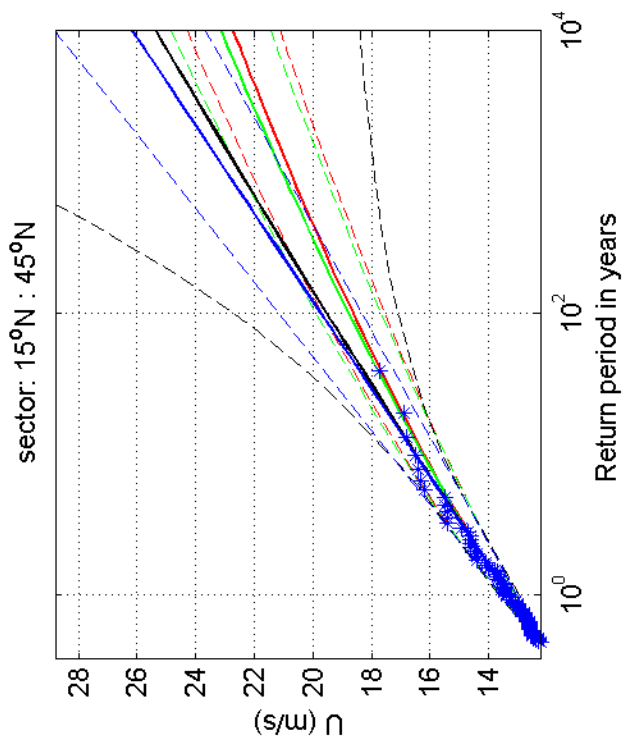
omni-directional 1970-2008

Lauwersoog

Deltares

1200264-005

Fig. F.4.277



Return value plot with exponential (blue) and GPD (black) fit to U ,
 exponential (red) fit to U_p^2 and exponential (green) fit to U_p^k
 Plotting positions: x_i vs $(n+1)/(\lambda(n+1-i))$

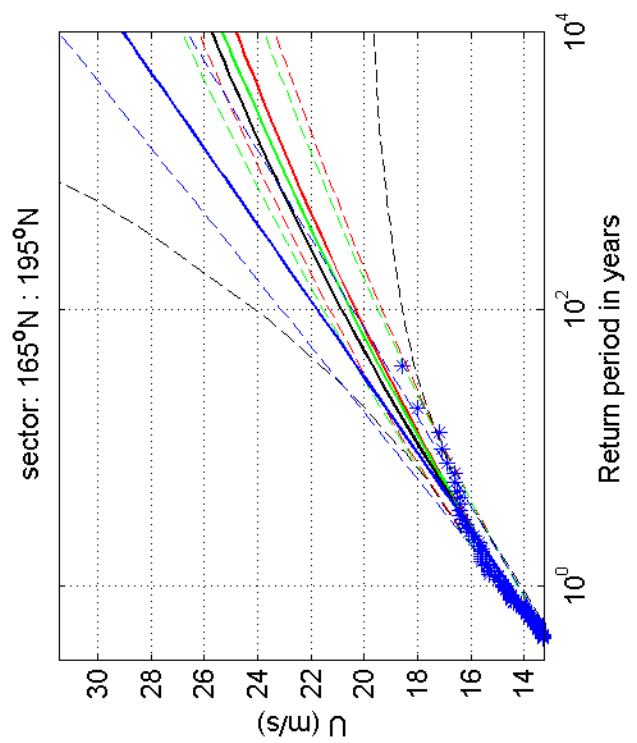
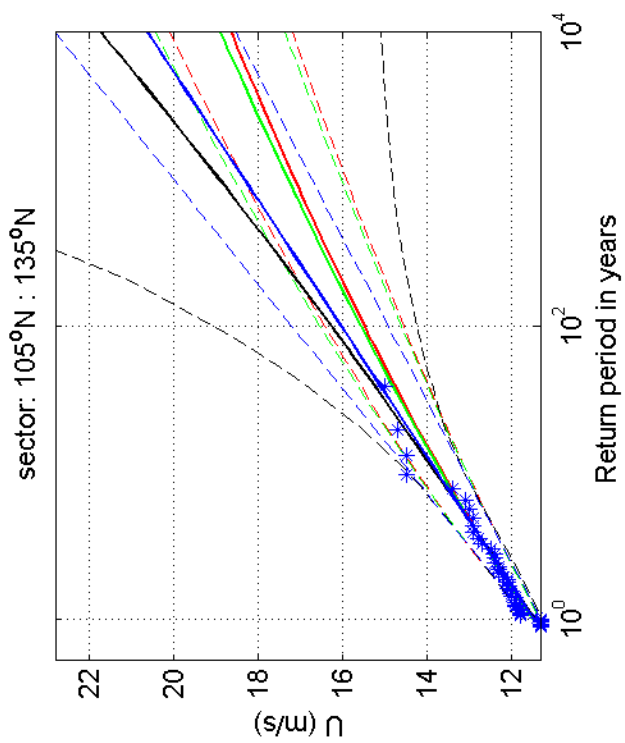
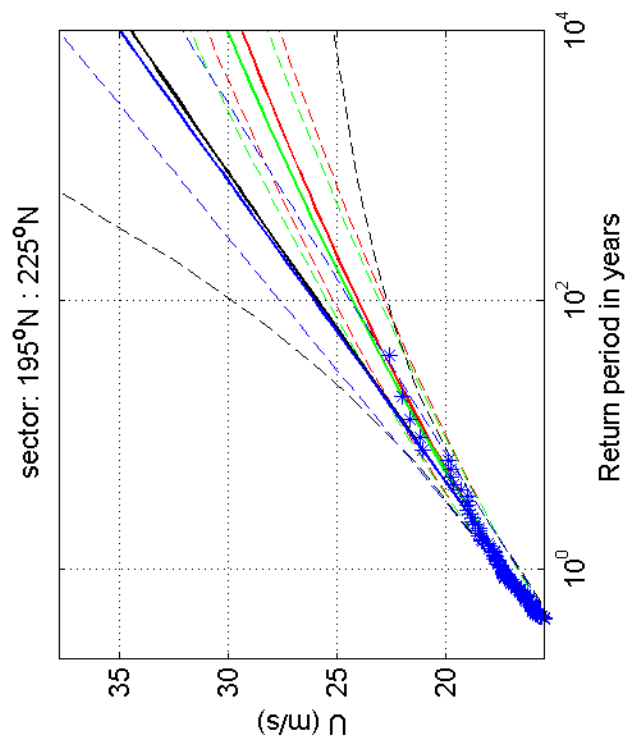
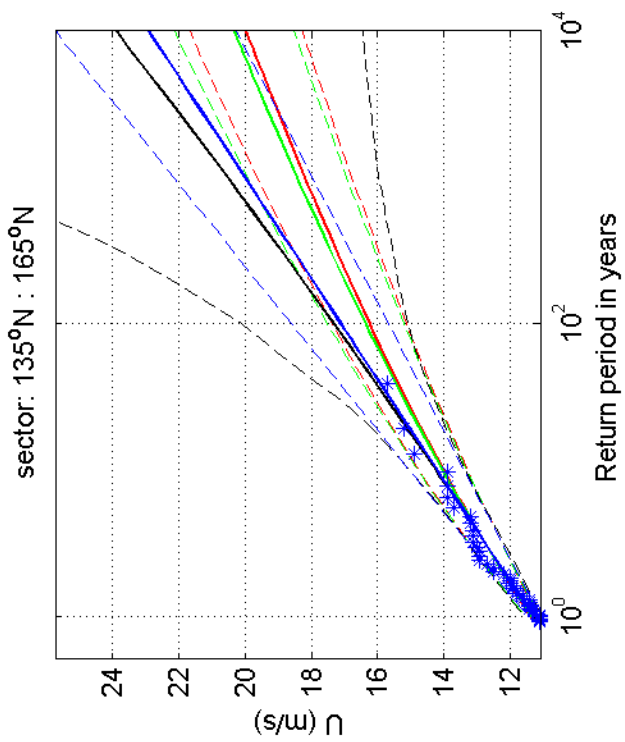
1970-2008

Lauwersoog

Deltares

1200264-005

Fig. F.4.277.1



Return value plot with exponential (blue) and GPD (black) fit to U , exponential (red) fit to U_p^2 and exponential (green) fit to U_p^k
 Plotting positions: x_i vs $(n+1)/(\lambda(n+1-i))$

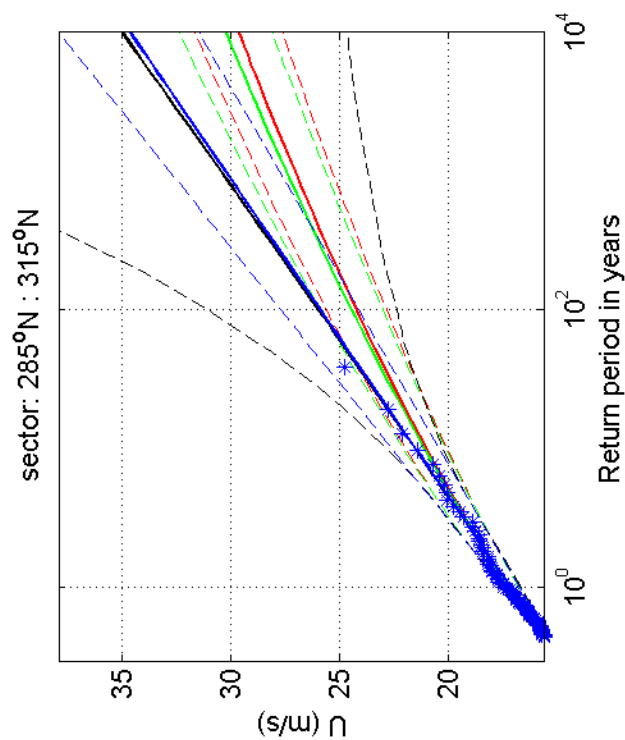
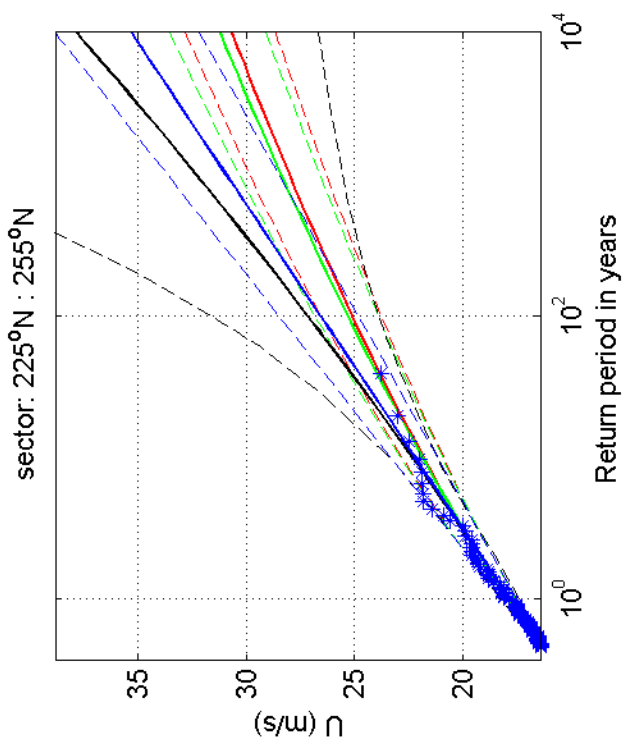
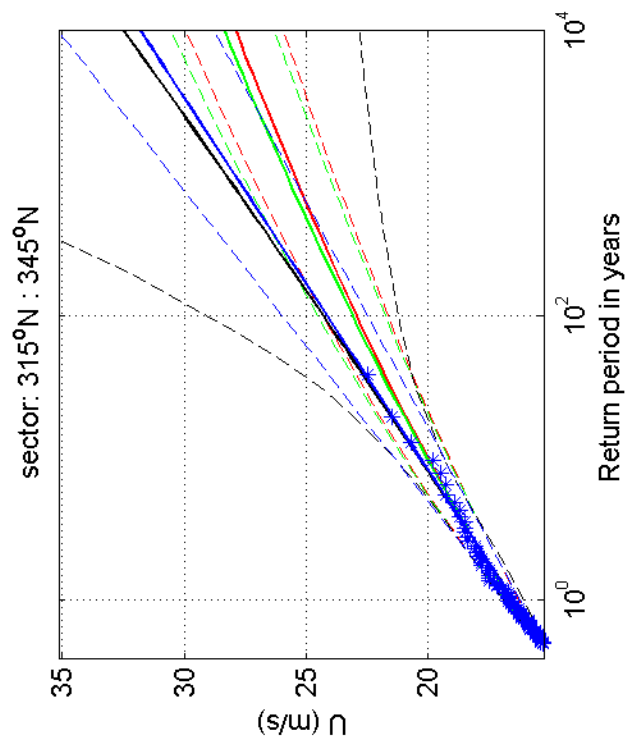
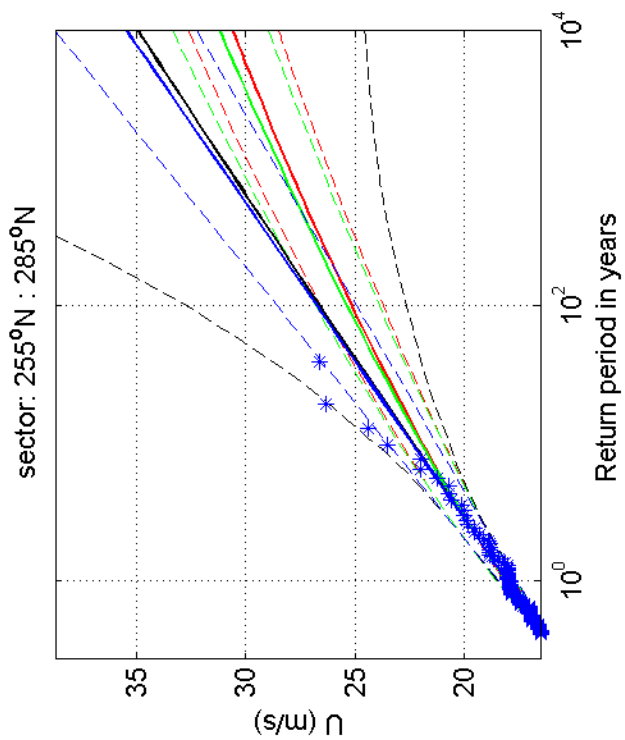
1970-2008

Lauwersoog

Deltares

1200264-005

Fig. F.4.277.5



Return value plot with exponential (blue) and GPD (black) fit to U ,
 exponential (red) fit to U_p^k and exponential (green) fit to U_p^k
 Plotting positions: x_i vs $(n+1)/(\lambda(n+1-i))$

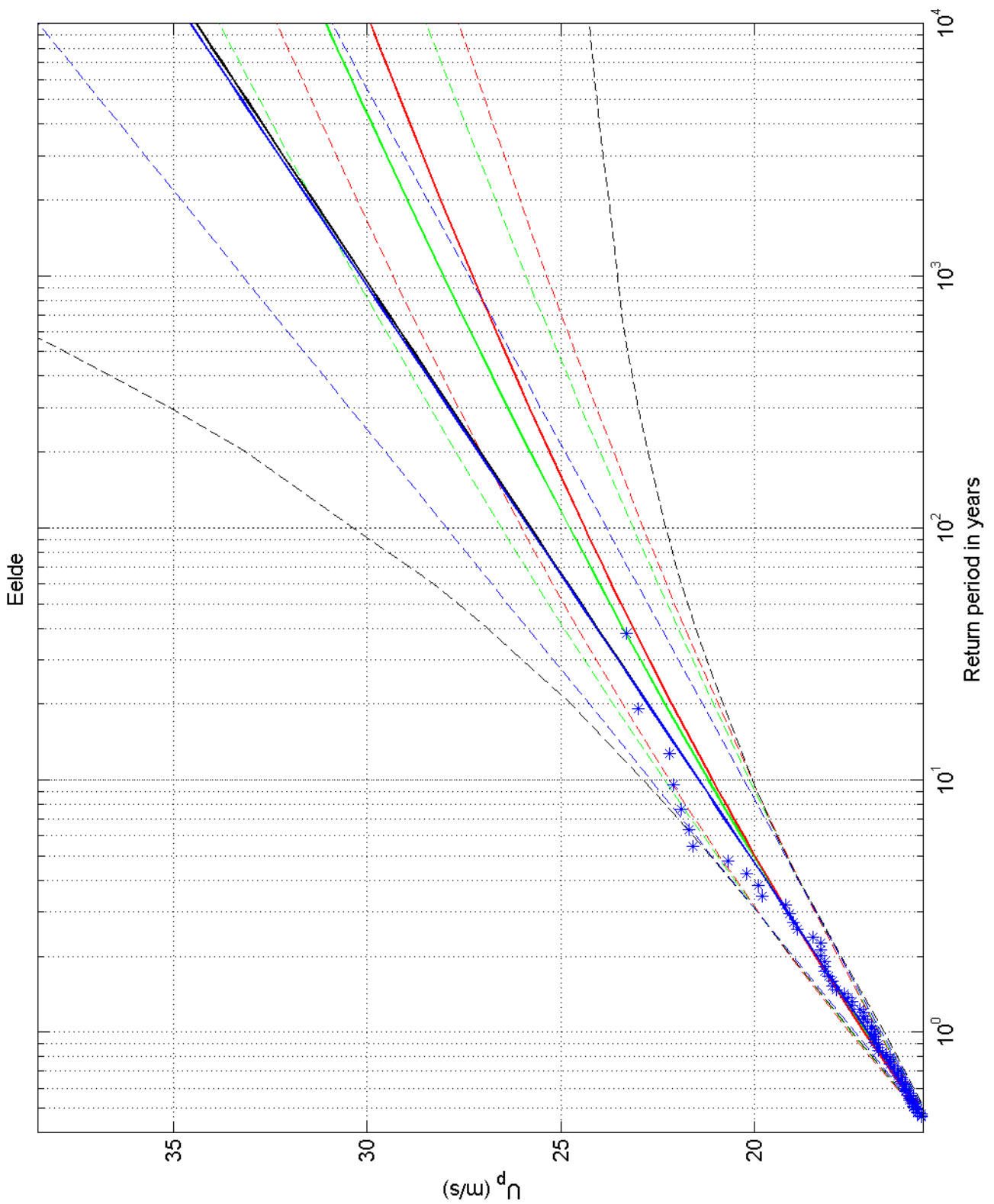
1970-2008

Lauwersoog

Deltares

1200264-005

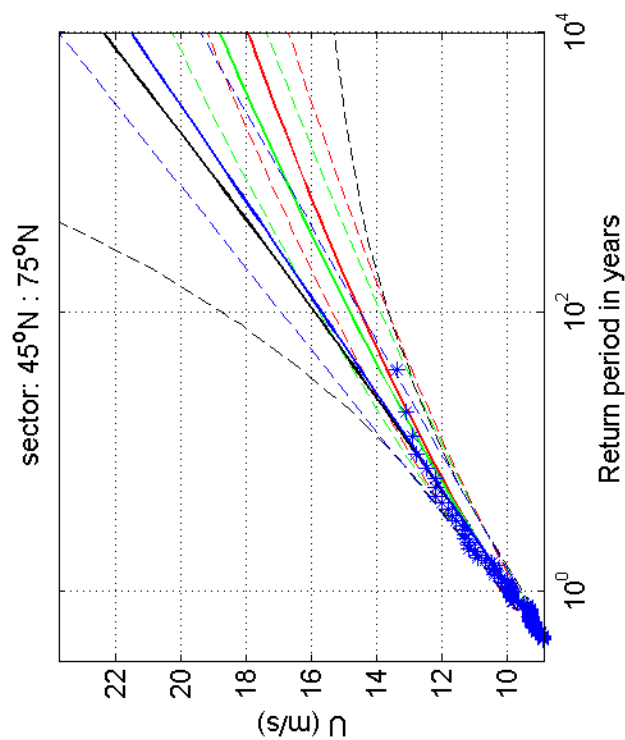
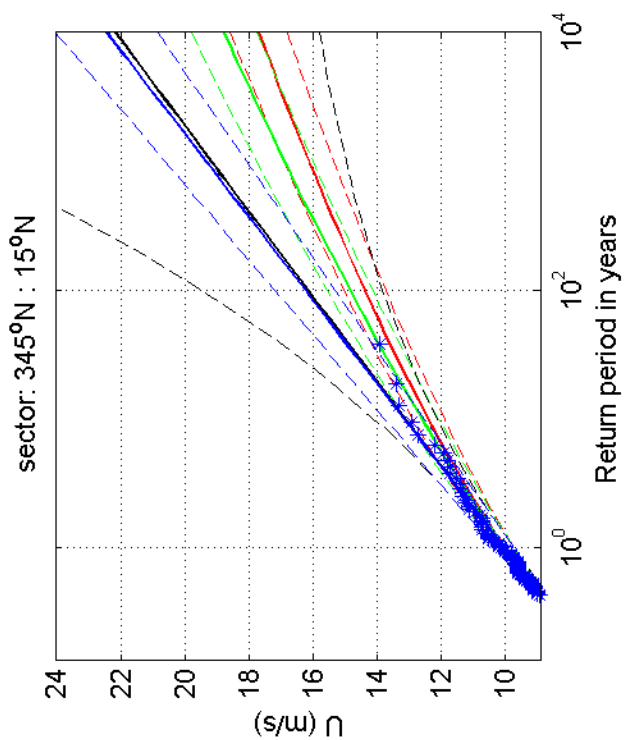
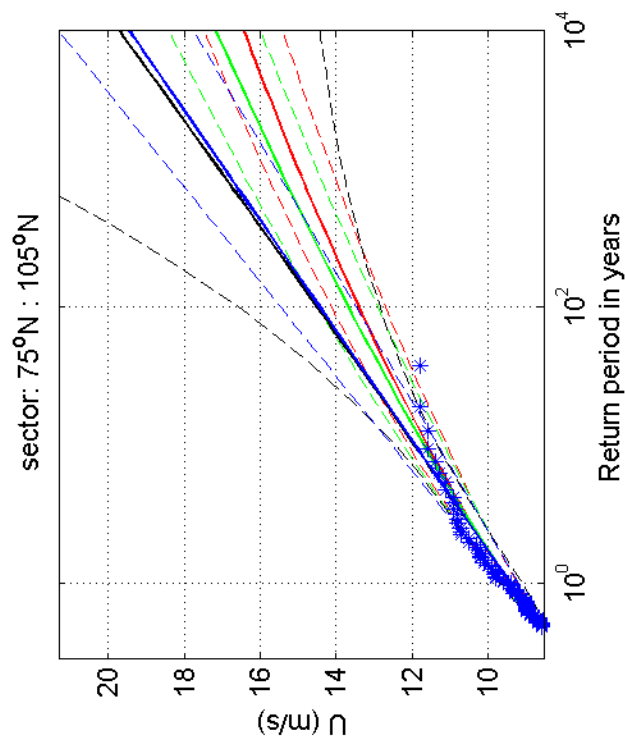
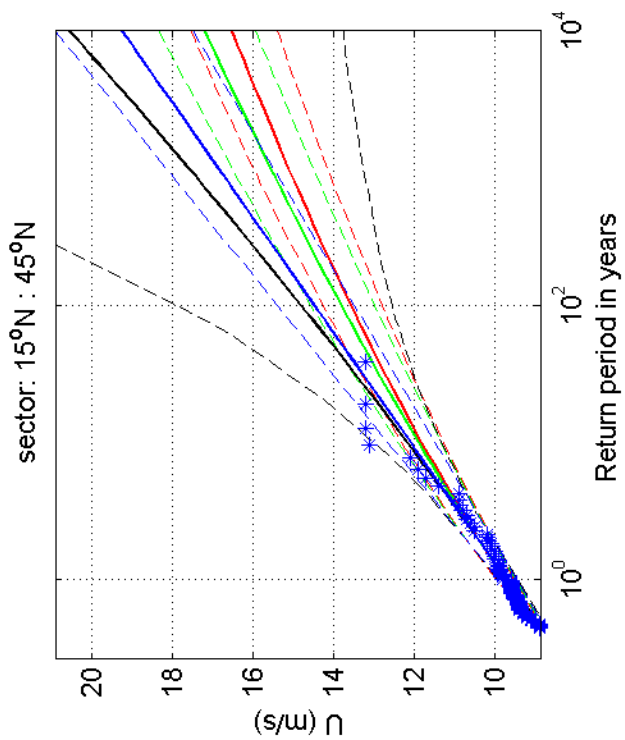
Fig. F.4.277.9



Return value plot with exponential (blue) and GPD (black) fit to U_p ,
 exponential (red) fit to U_p^2 and exponential (green) fit to U_p^k
 Plotting positions: x_i vs $(n+1)/(\lambda(n+1-i))$

omni-directional	1970-2008
Eelde	
1200264-005	Fig. F.4.280

Deltares



Return value plot with exponential (blue) and GPD (black) fit to U ,
 exponential (red) fit to U_p^2 and exponential (green) fit to U_p^k
 Plotting positions: x_i vs $(n+1)/(\lambda(n+1-i))$

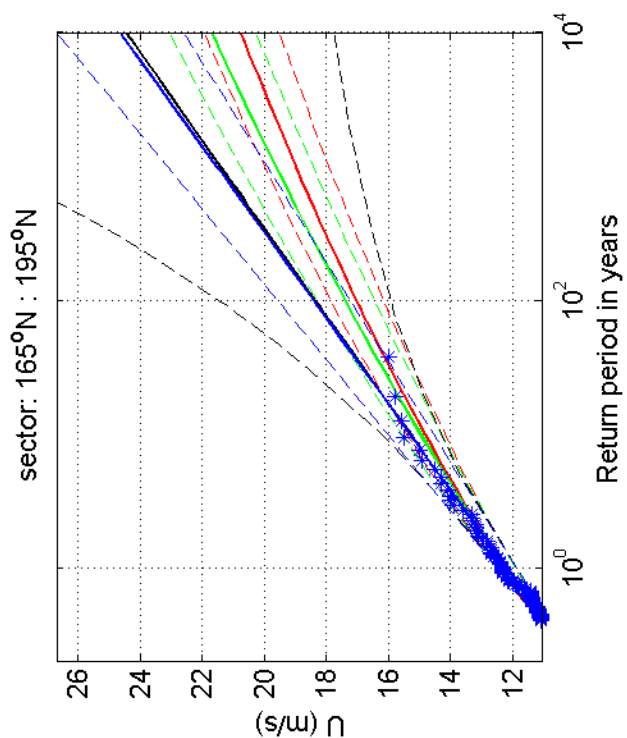
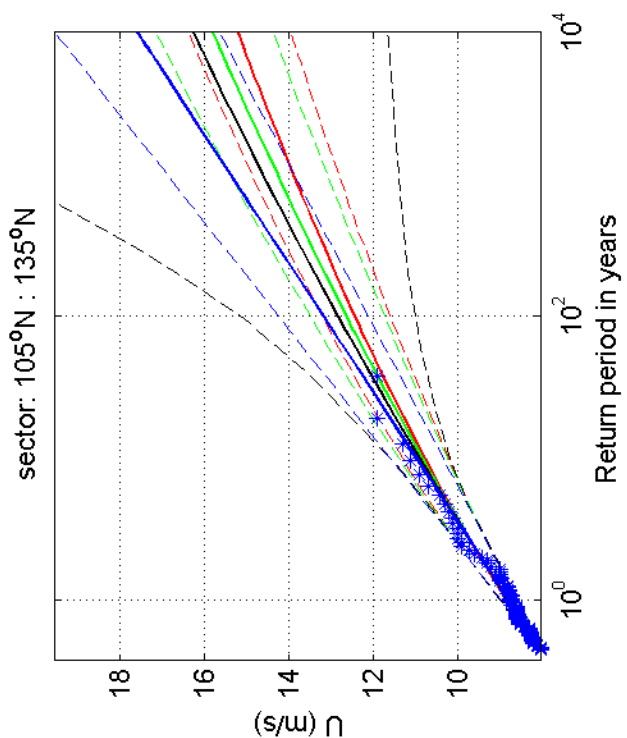
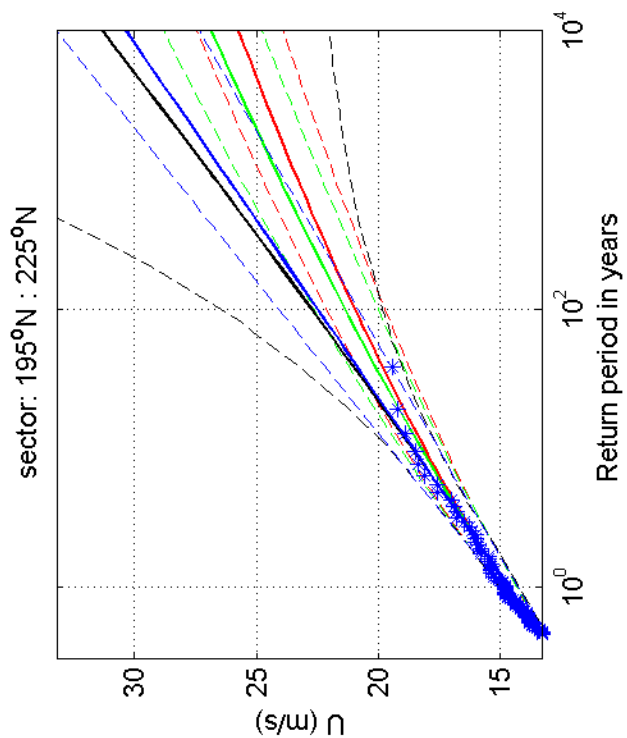
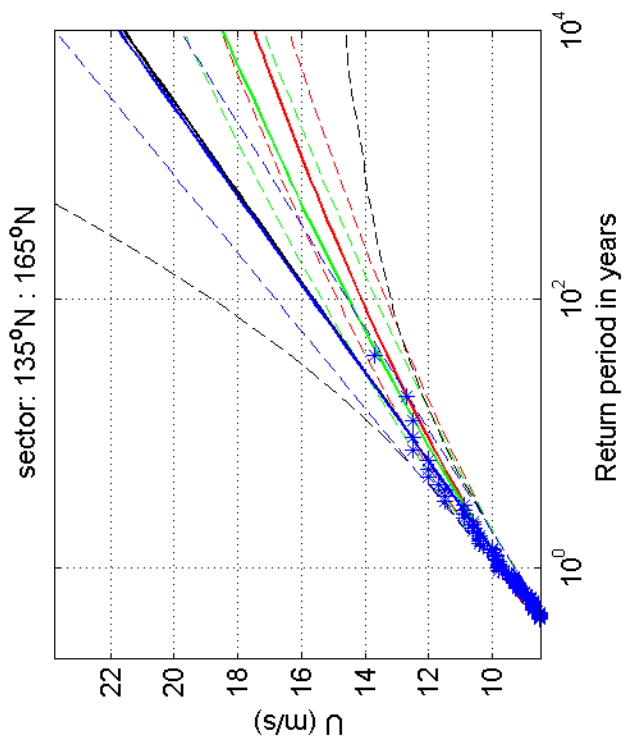
1970-2008

Eelde

Deltares

1200264-005

Fig. F.4.280.1



Return value plot with exponential (blue) and GPD (black) fit to U ,
 exponential (red) fit to U_p^2 and exponential (green) fit to U_p^k
 Plotting positions: x_i vs $(n+1)/(\lambda(n+1-i))$

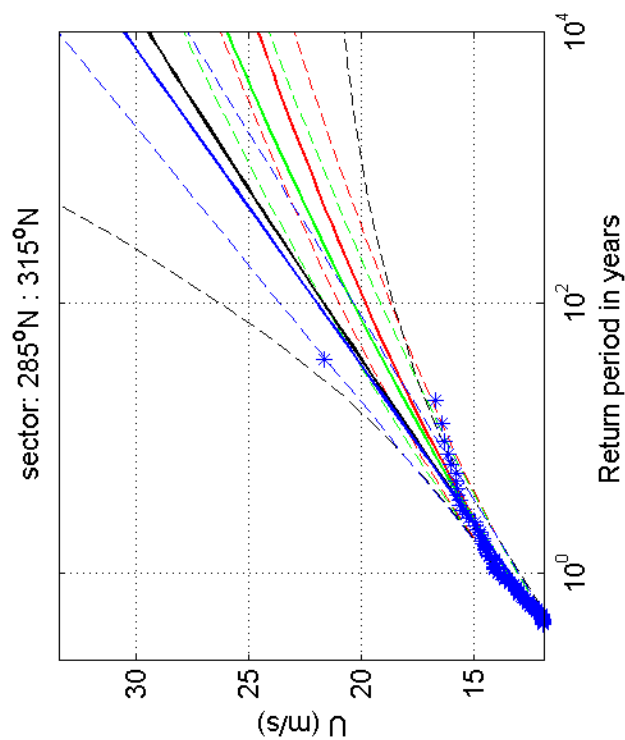
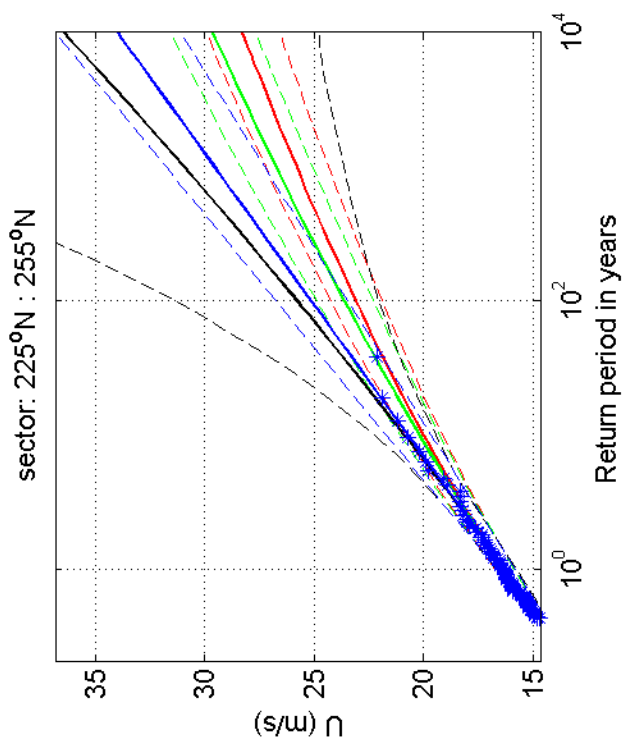
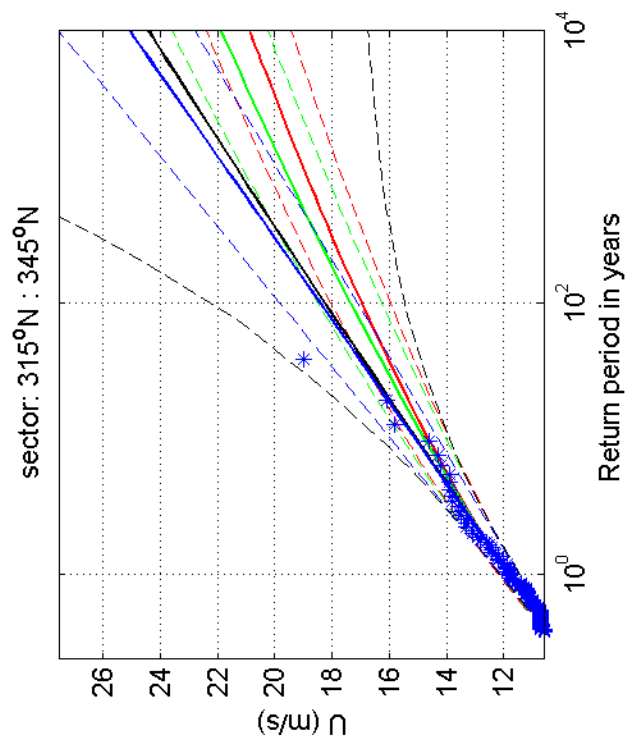
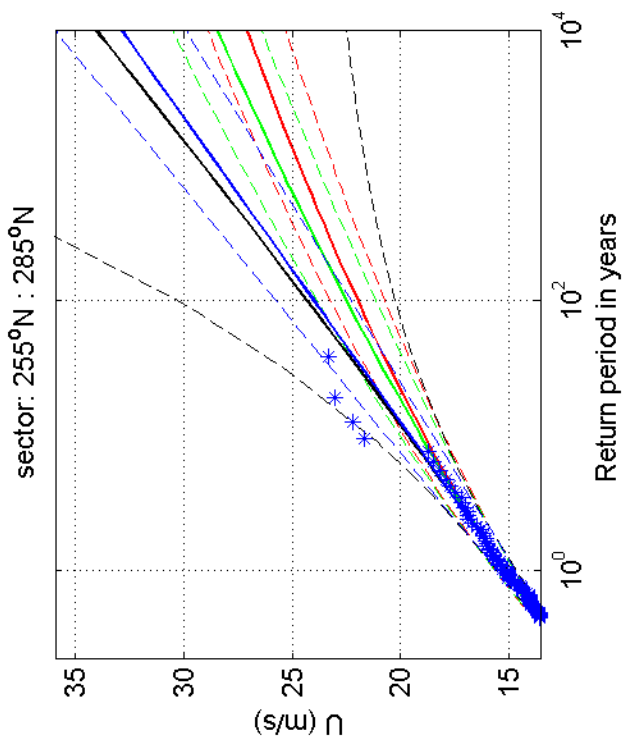
1970-2008

Eelde

Deltares

1200264-005

Fig. F.4.280.5



Return value plot with exponential (blue) and GPD (black) fit to U ,
 exponential (red) fit to U_p^2 and exponential (green) fit to U_p^k
 Plotting positions: x_i vs $(n+1)/(\lambda(n+1-i))$

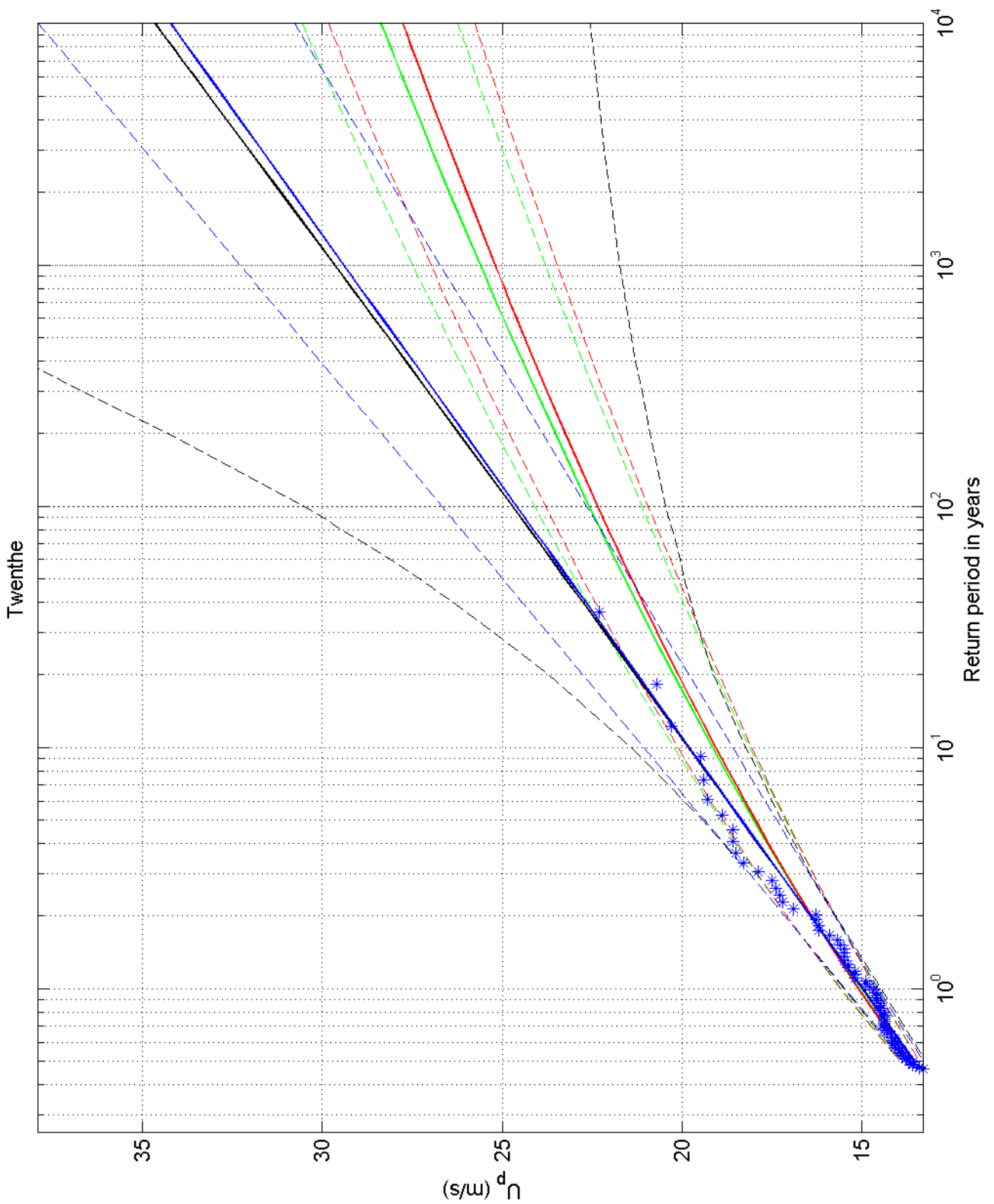
1970-2008

Eelde

Deltares

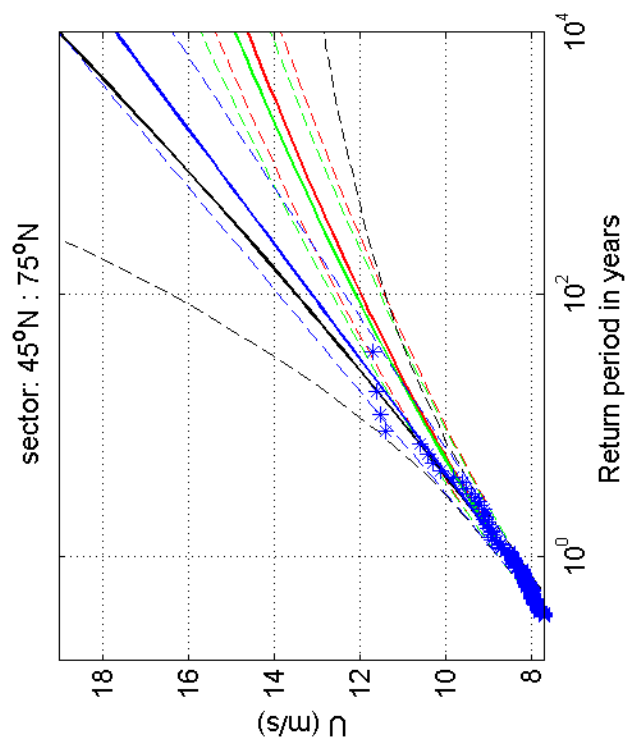
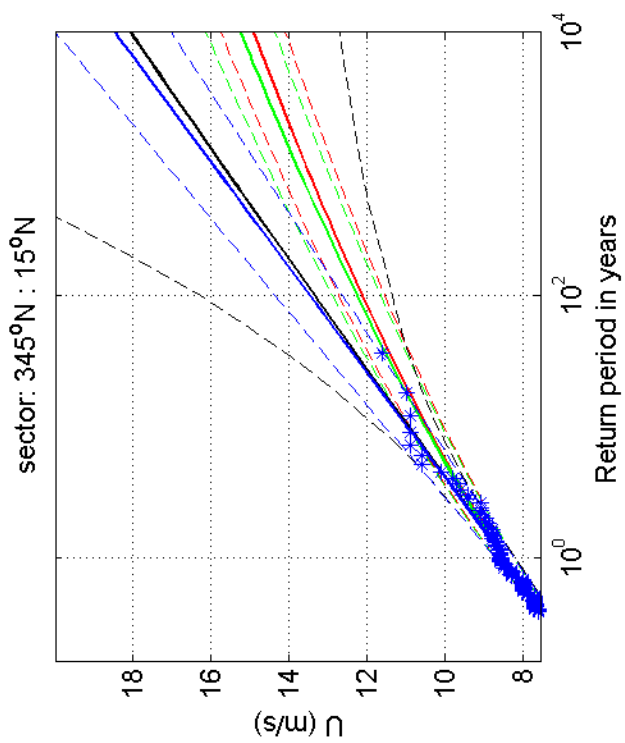
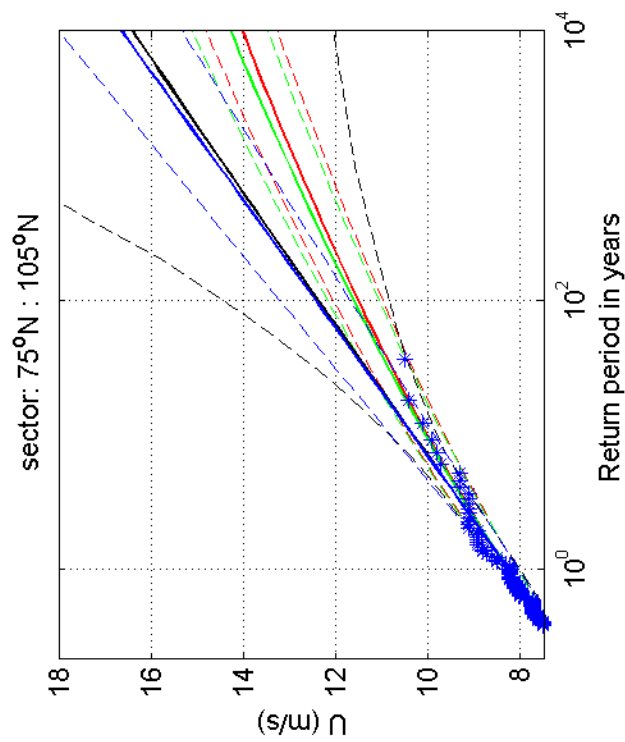
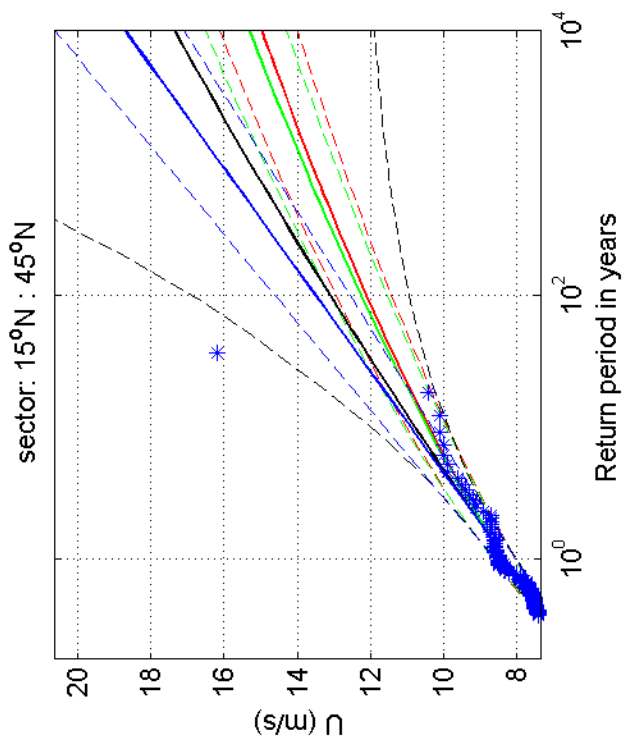
1200264-005

Fig. F.4.280.9



Return value plot with exponential (blue) and GPD (black) fit to U_p ,
 exponential (red) fit to U_p^2 and exponential (green) fit to U_p^k
 Plotting positions: x_i vs $(n+1)/(\lambda(n+1-i))$

omni-directional	1970-2008
Twenthe	
1200264-005	Fig. F.4.290



Return value plot with exponential (blue) and GPD (black) fit to U ,
 exponential (red) fit to U_p^2 and exponential (green) fit to U_p^k
 Plotting positions: x_i vs $(n+1)/(\lambda(n+1-i))$

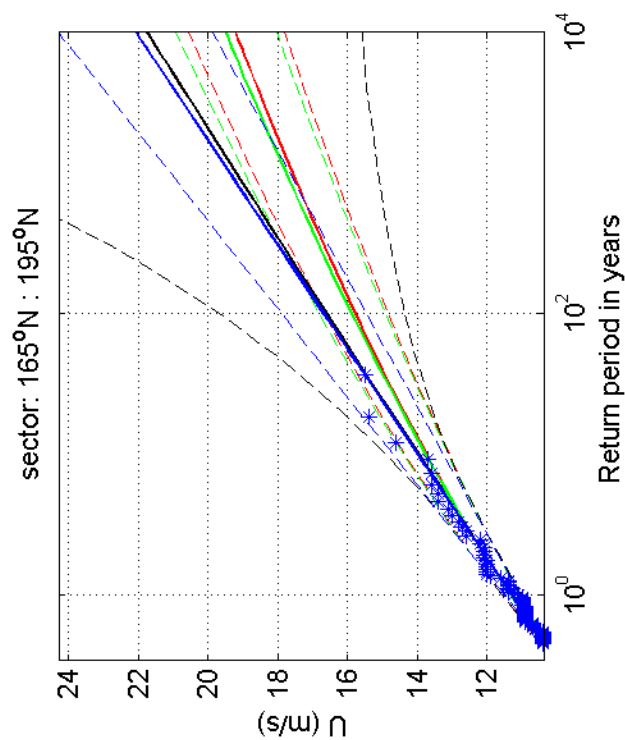
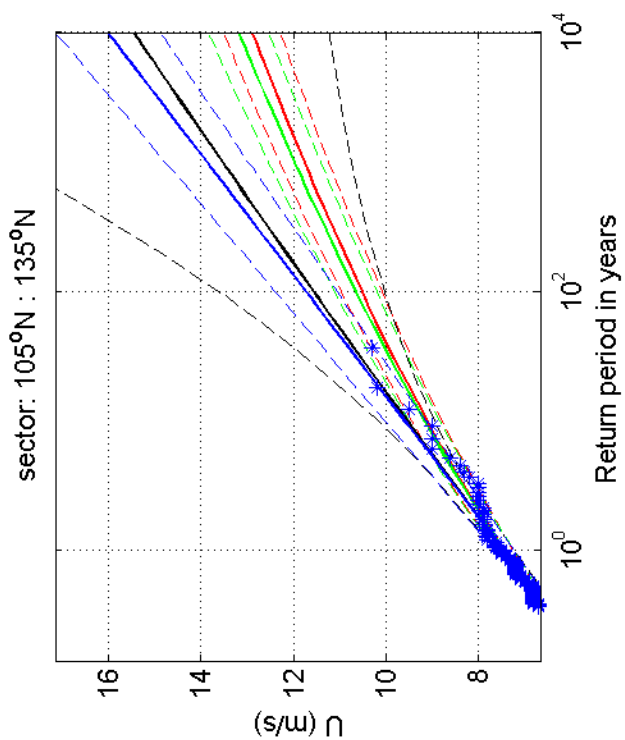
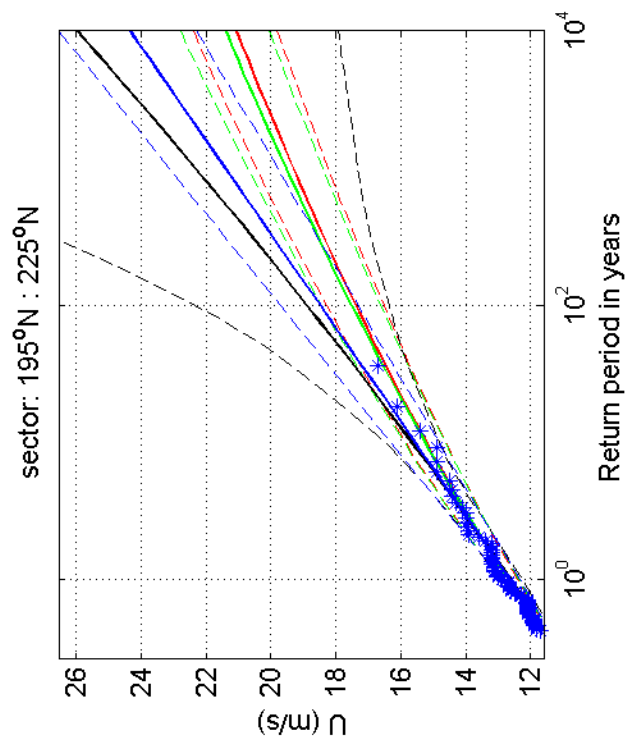
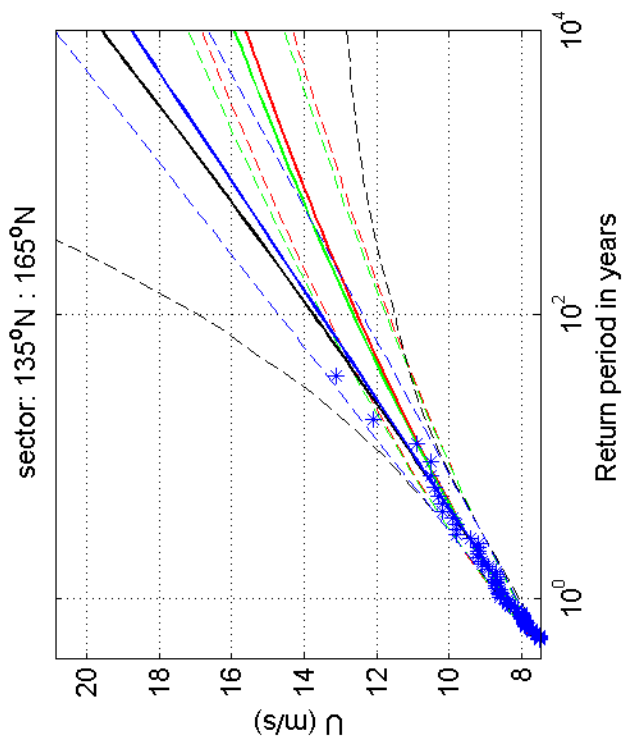
1970-2008

Twenthe

Deltares

1200264-005

Fig. F.4.290.1



Return value plot with exponential (blue) and GPD (black) fit to U ,
 exponential (red) fit to U_p^2 and exponential (green) fit to U_p^k
 Plotting positions: x_i vs $(n+1)/(\lambda(n+1-i))$

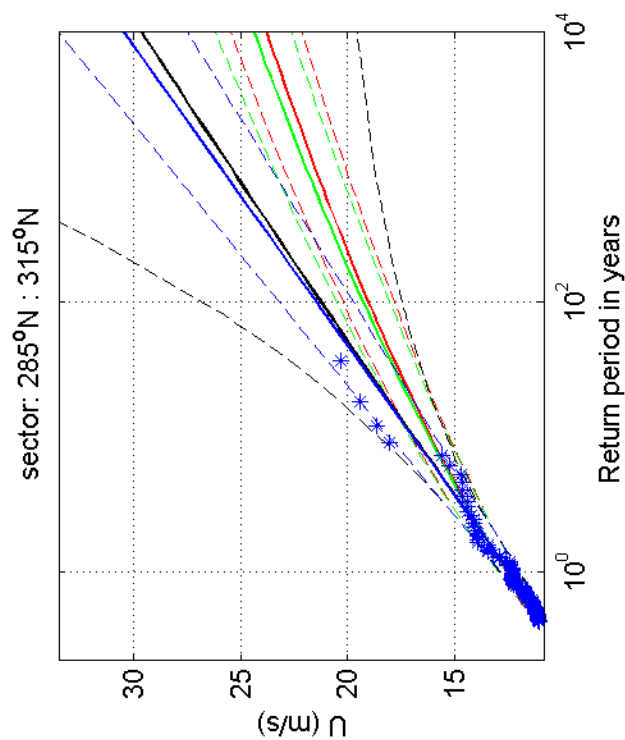
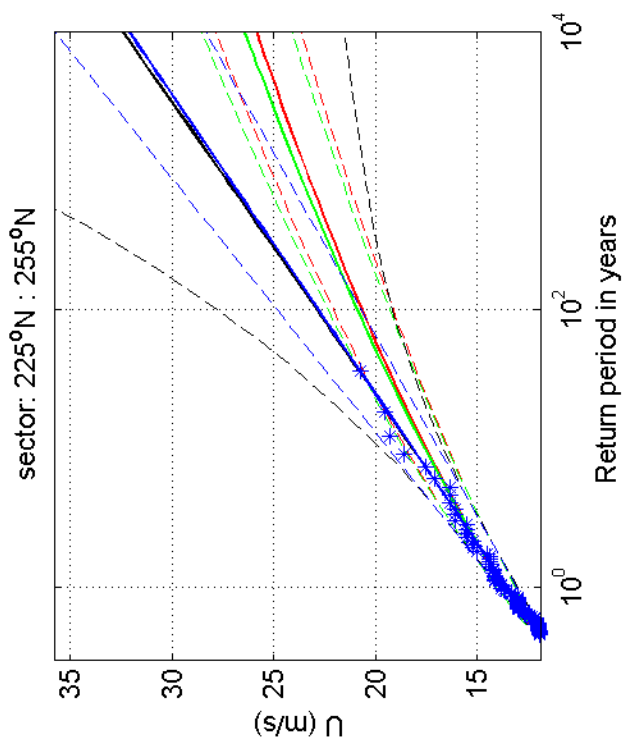
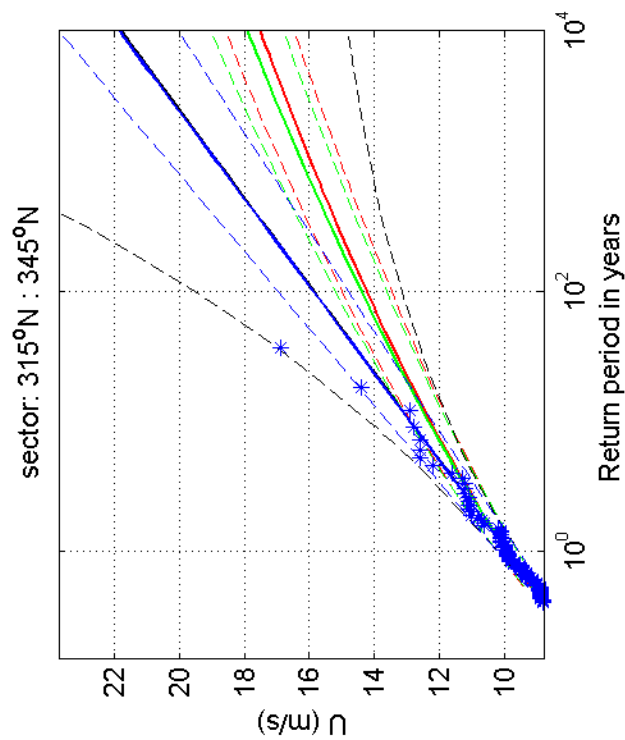
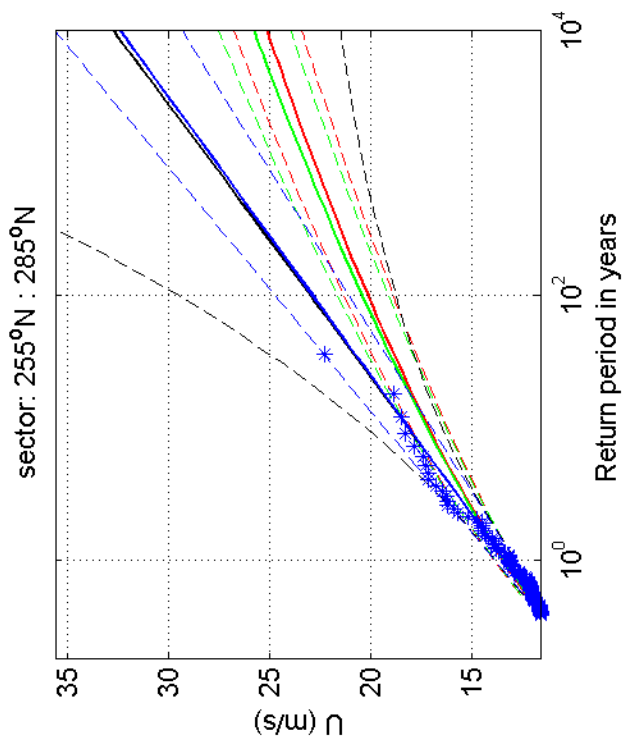
1970-2008

Twenthe

Deltares

1200264-005

Fig. F.4.290.5



Return value plot with exponential (blue) and GPD (black) fit to U ,
 exponential (red) fit to U_p^k and exponential (green) fit to U_p^k
 Plotting positions: x_i vs $(n+1)/(\lambda(n+1-i))$

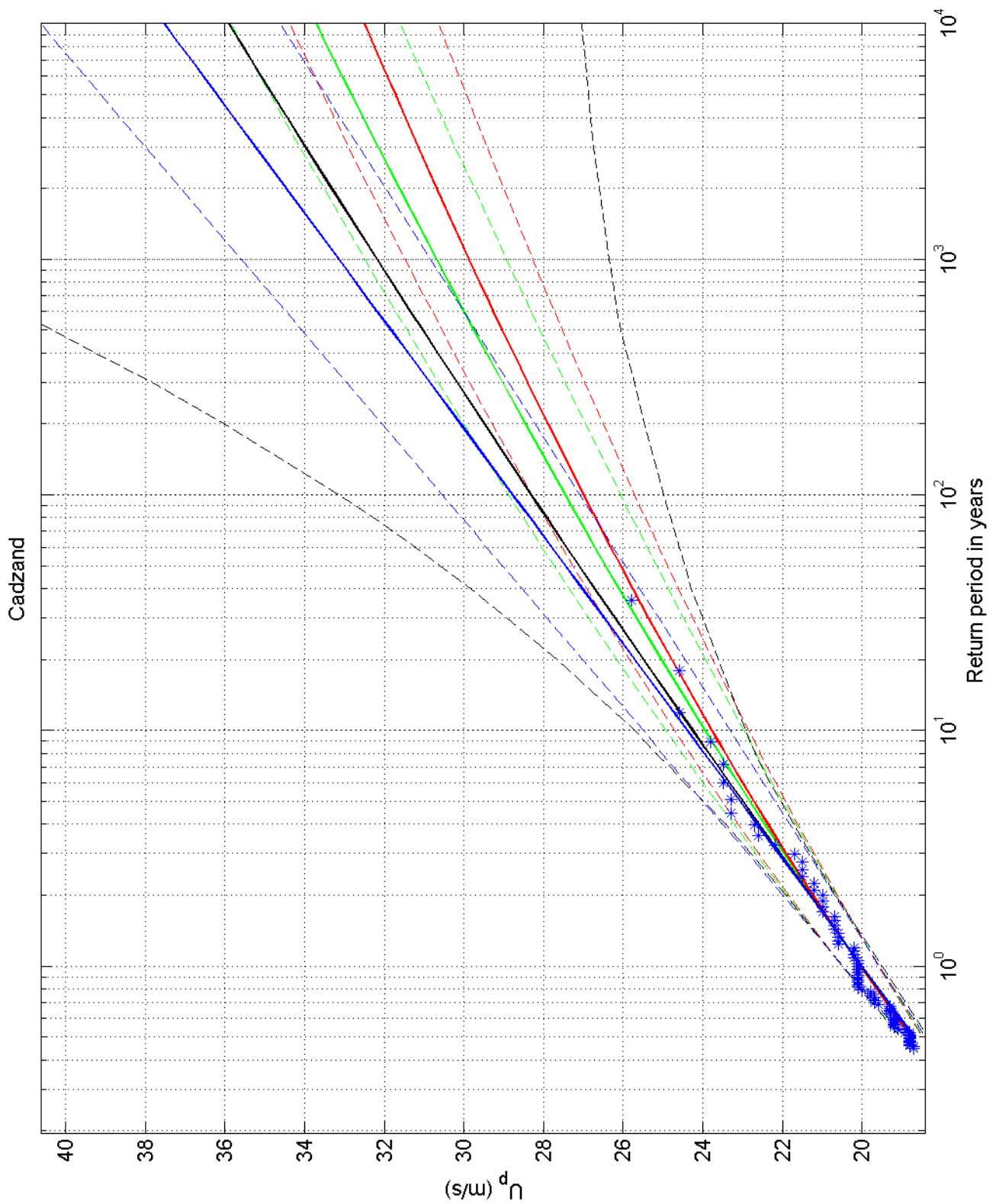
1970-2008

Twenthe

Deltares

1200264-005

Fig. F.4.290.9



Return value plot with exponential (blue) and GPD (black) fit to U_p ,
 exponential (red) fit to U_p^2 and exponential (green) fit to U_p^k
 Plotting positions: x_i vs $(n+1)/(\lambda(n+1-i))$

omni-directional

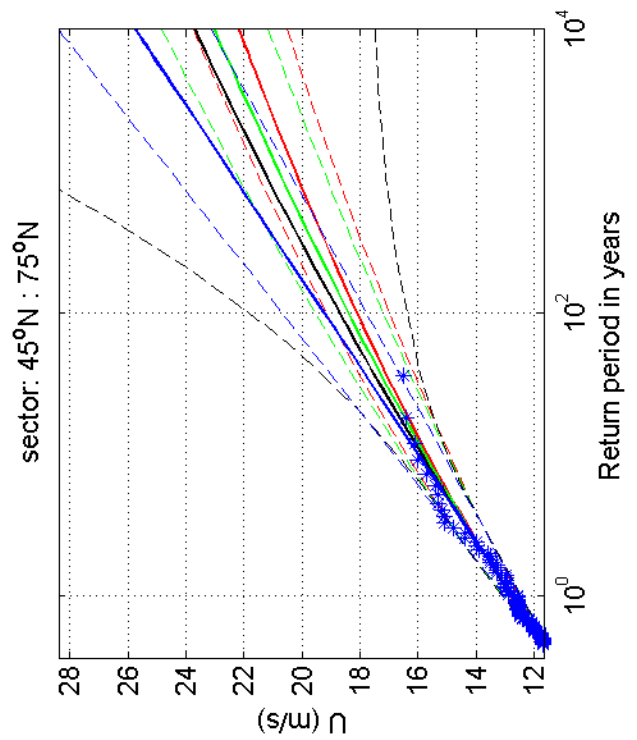
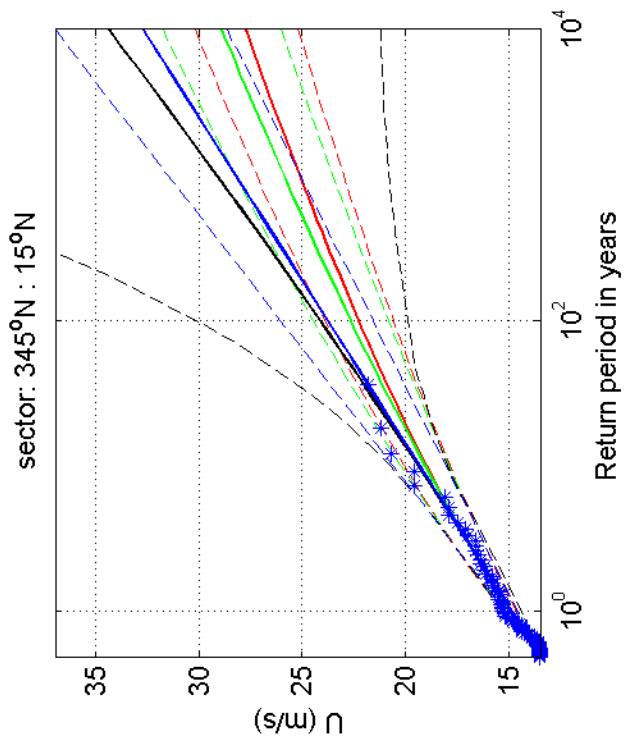
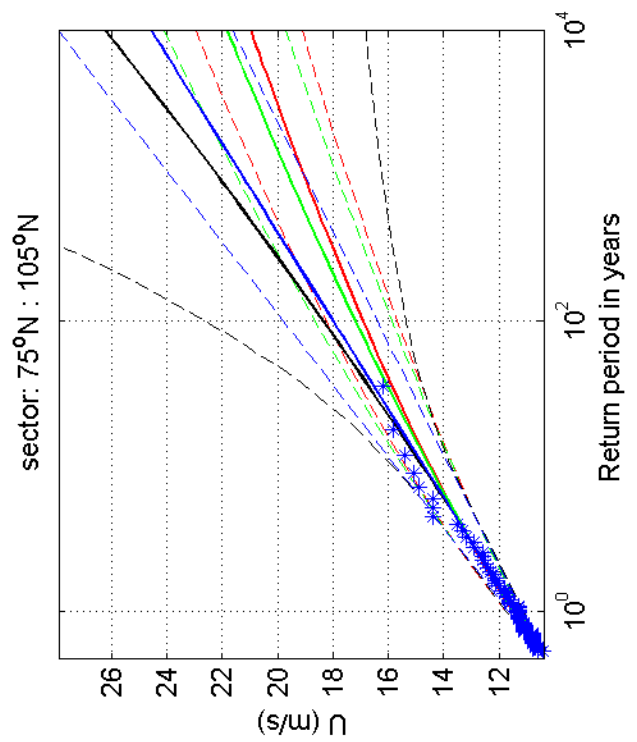
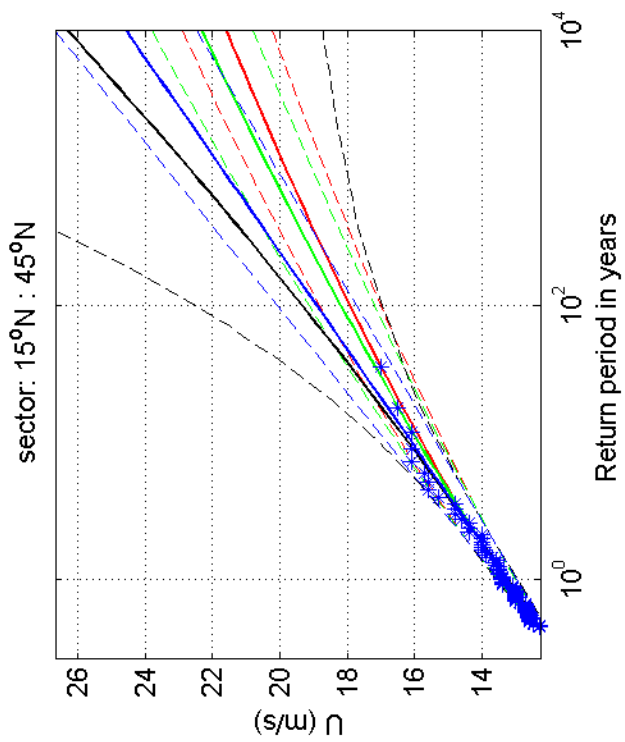
1970-2008

Cadzand

Deltares

1200264-005

Fig. F.4.308



Return value plot with exponential (blue) and GPD (black) fit to U ,
 exponential (red) fit to U_p^2 and exponential (green) fit to U_p^k
 Plotting positions: x_i vs $(n+1)/(\lambda(n+1-i))$

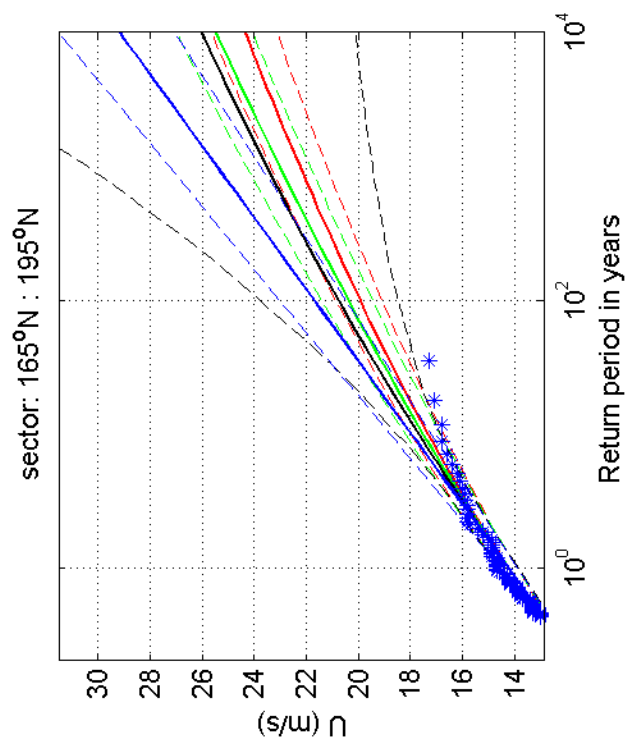
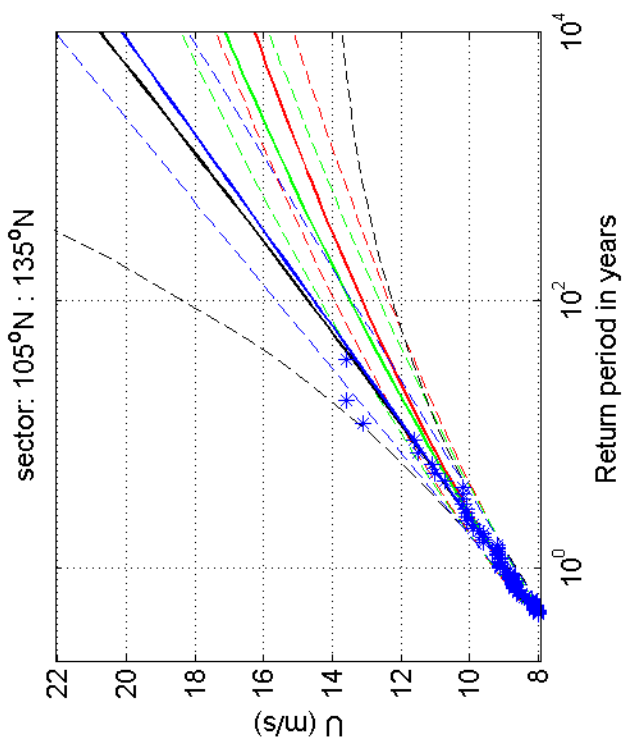
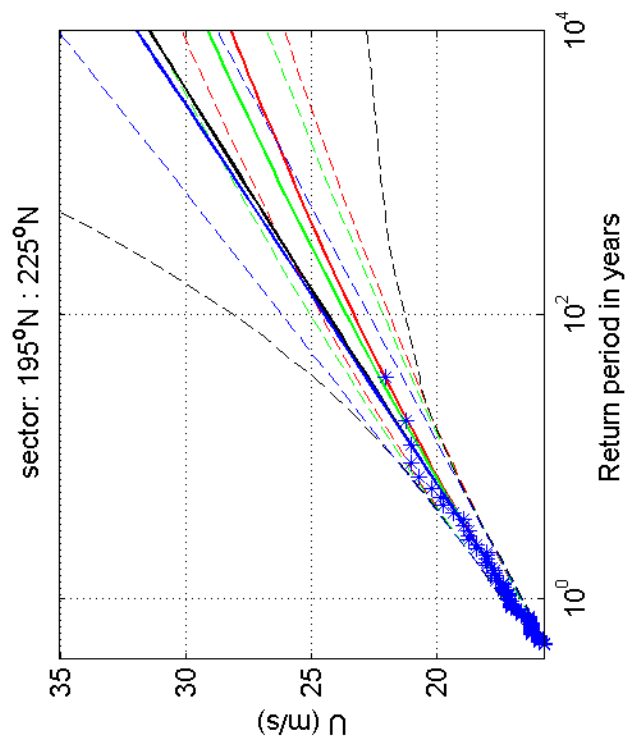
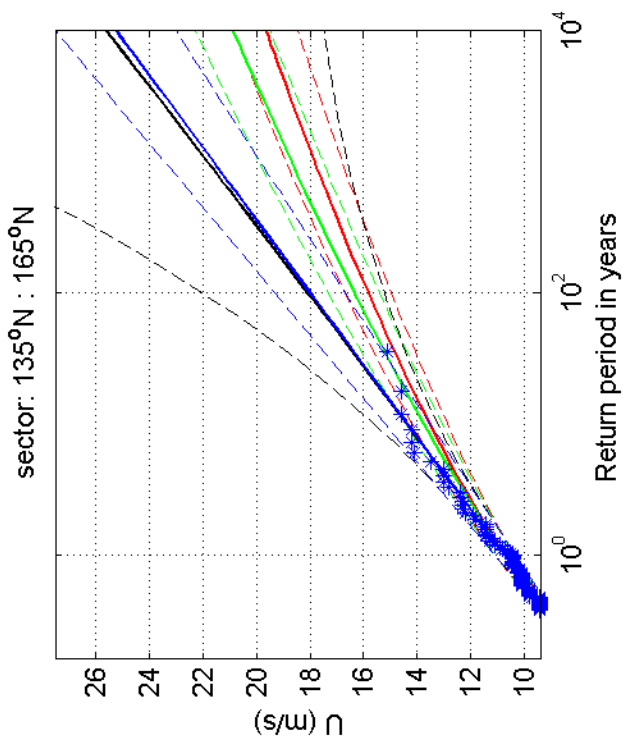
1970-2008

Cadzand

Deltares

1200264-005

Fig. F.4.308.1



Return value plot with exponential (blue) and GPD (black) fit to U ,
 exponential (red) fit to U_p^2 and exponential (green) fit to U_p^k
 Plotting positions: x_i vs $(n+1)/(\lambda(n+1-i))$

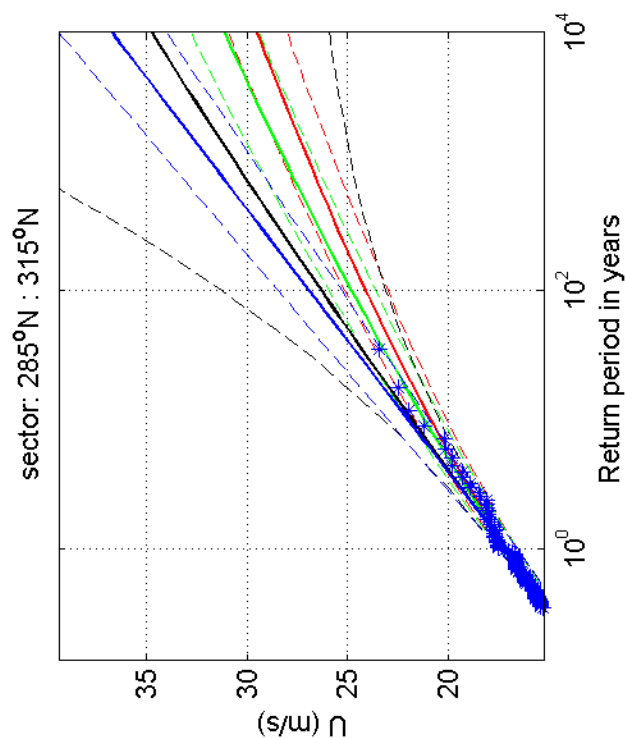
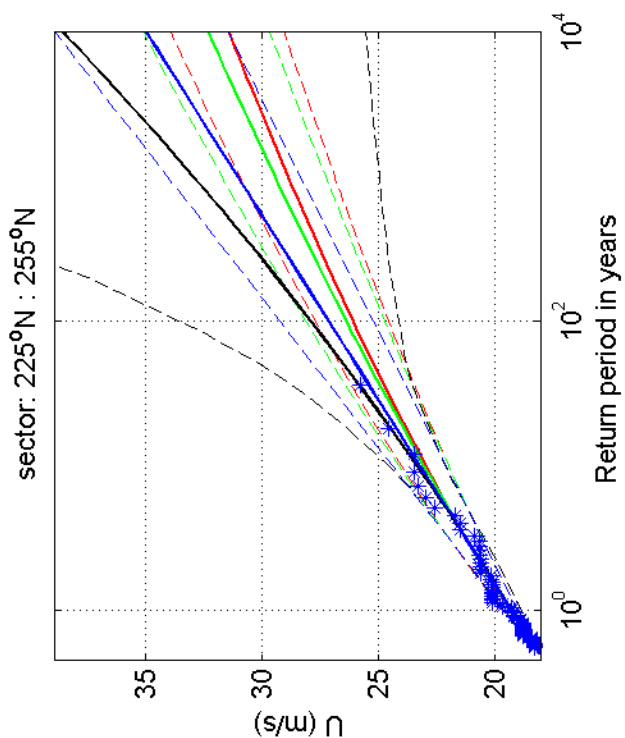
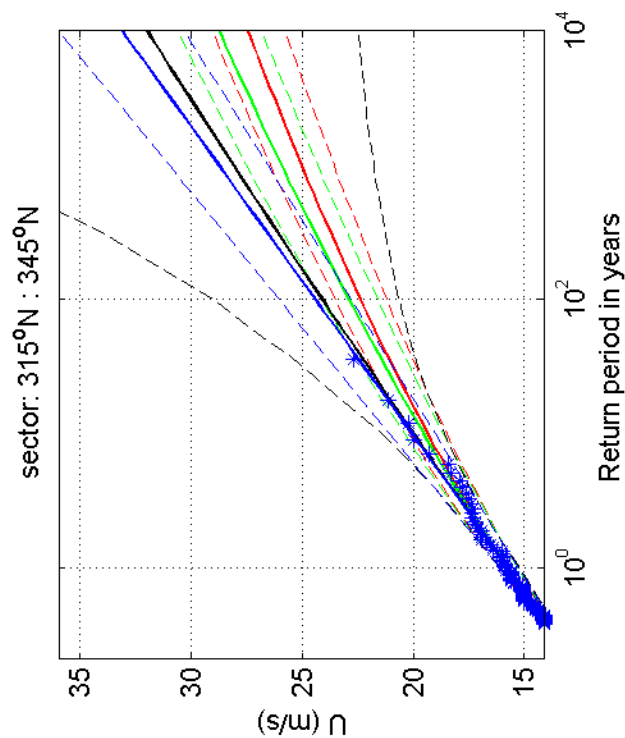
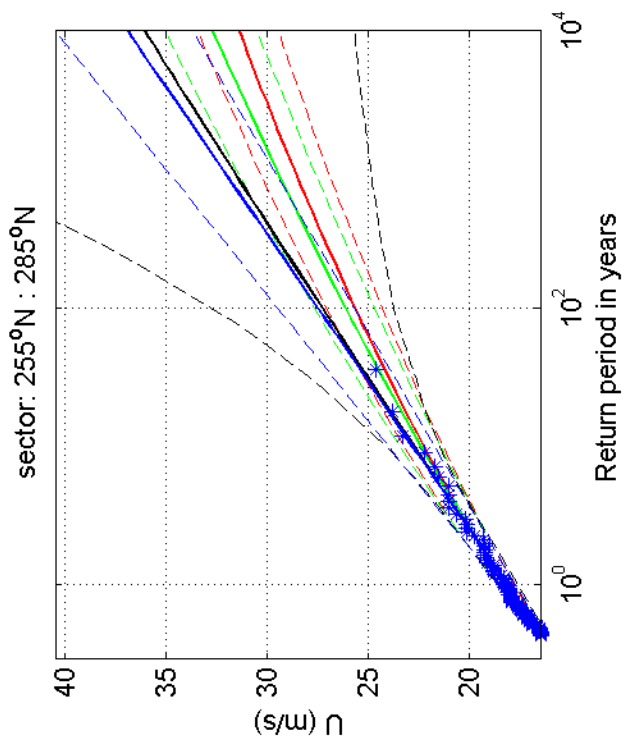
1970-2008

Cadzand

Deltares

1200264-005

Fig. F.4.308.5



Return value plot with exponential (blue) and GPD (black) fit to U ,
 exponential (red) fit to U_p^2 and exponential (green) fit to U_p^k
 Plotting positions: x_i vs $(n+1)/(\lambda(n+1-i))$

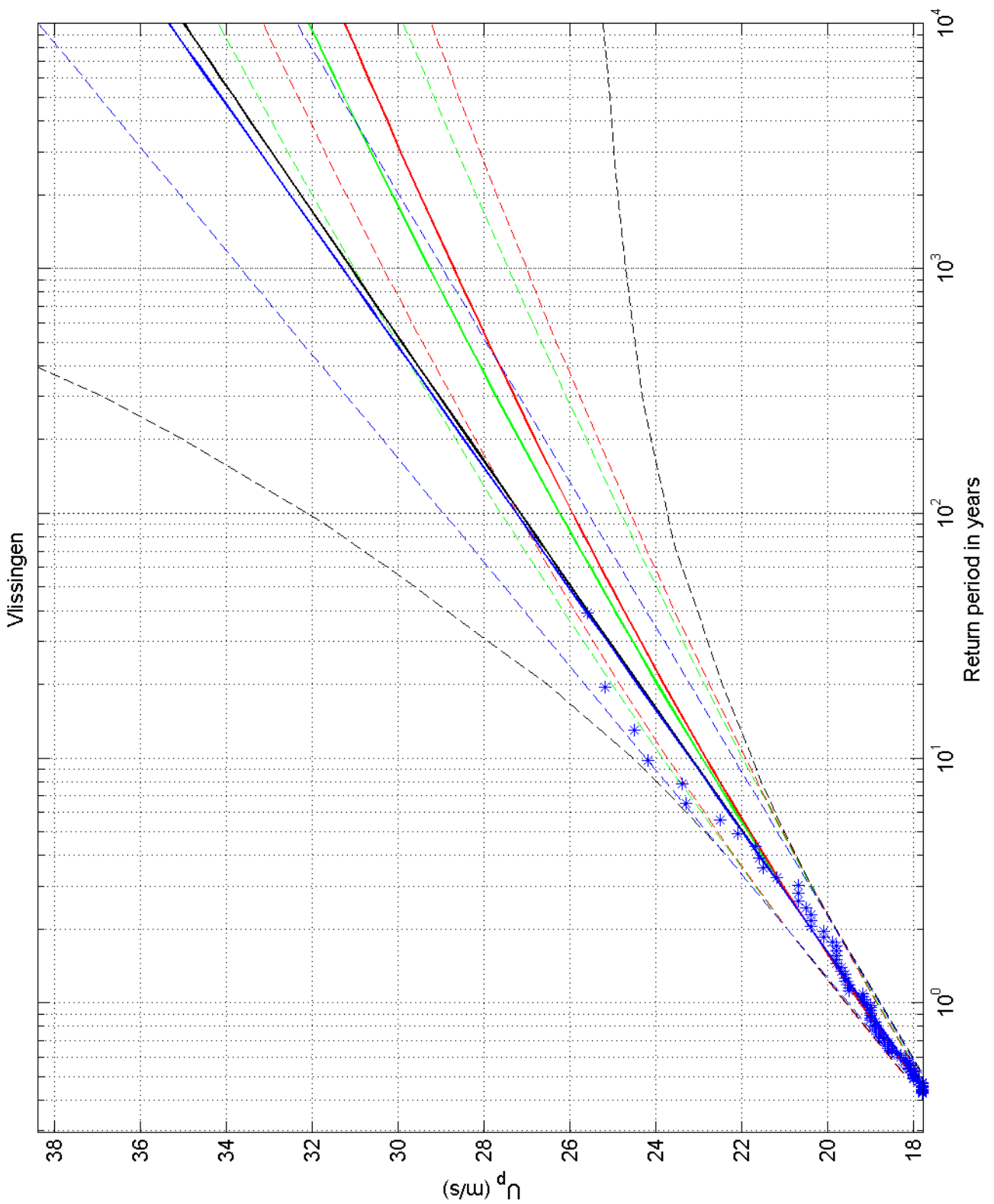
1970-2008

Cadzand

Deltares

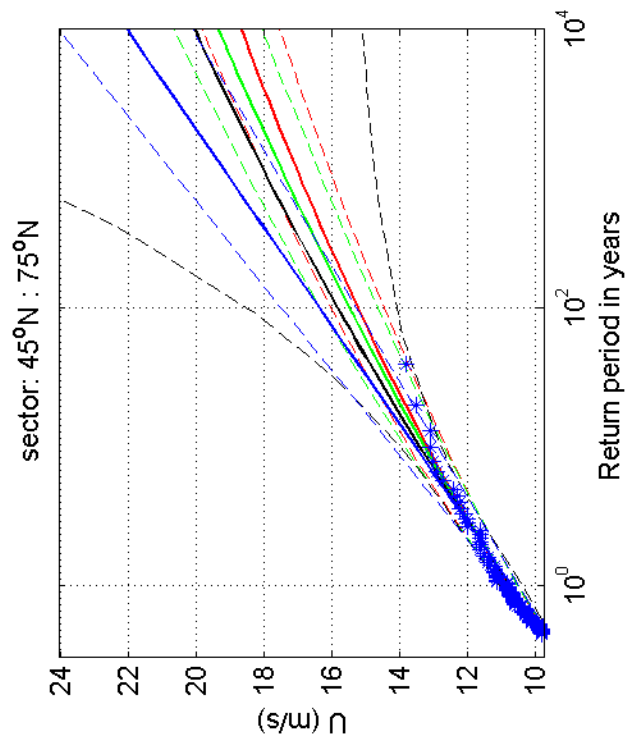
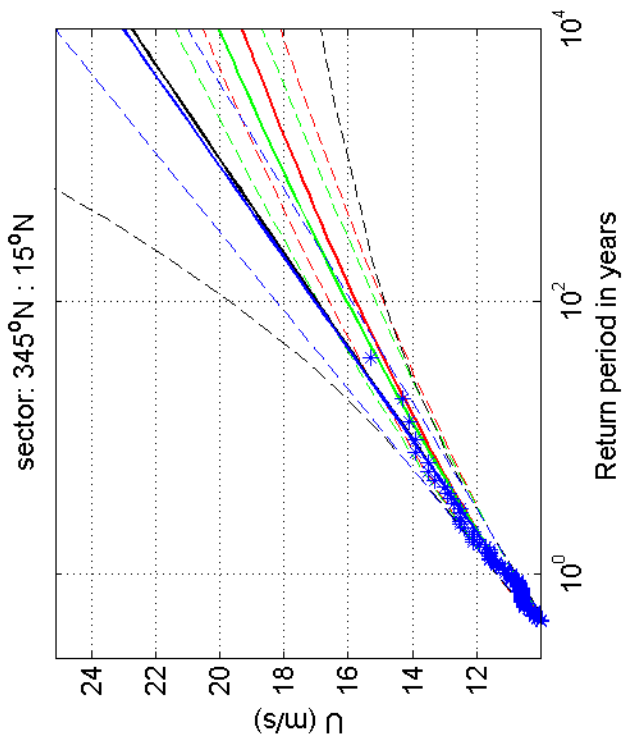
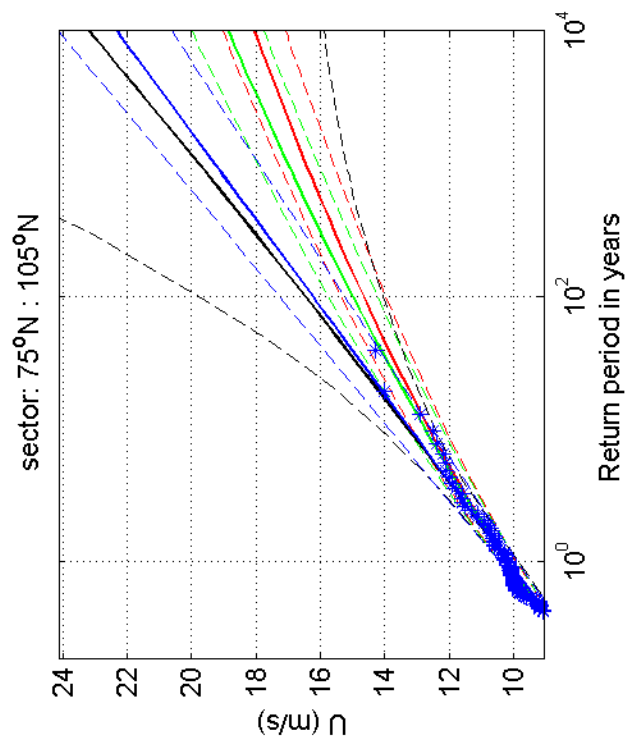
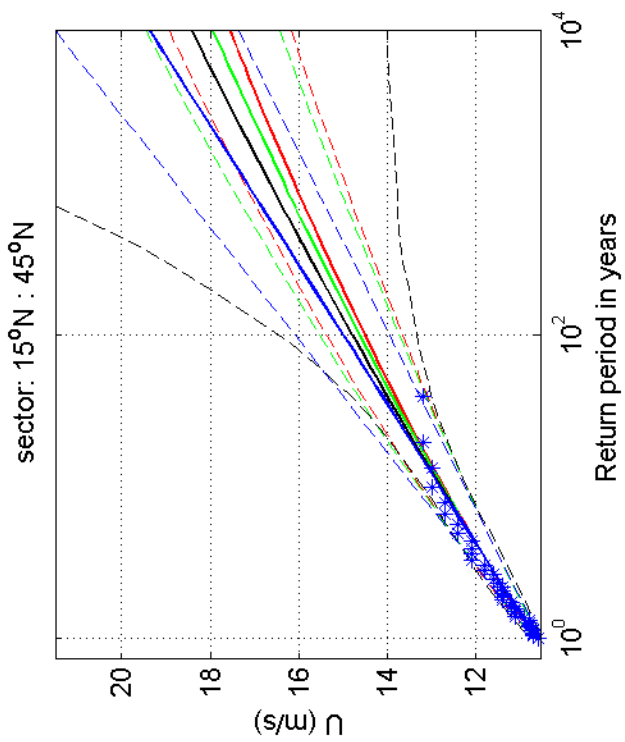
1200264-005

Fig. F.4.308.9



Return value plot with exponential (blue) and GPD (black) fit to U_p ,
 exponential (red) fit to U_p^2 and exponential (green) fit to U_p^k
 Plotting positions: x_i vs $(n+1)/(\lambda(n+1-i))$

omni-directional	1970-2008
Vlissingen	
1200264-005	Fig. F.4.310



Return value plot with exponential (blue) and GPD (black) fit to U ,
 exponential (red) fit to U_p^2 and exponential (green) fit to U_p^k
 Plotting positions: x_1 vs $(n+1)/(\lambda(n+1-i))$

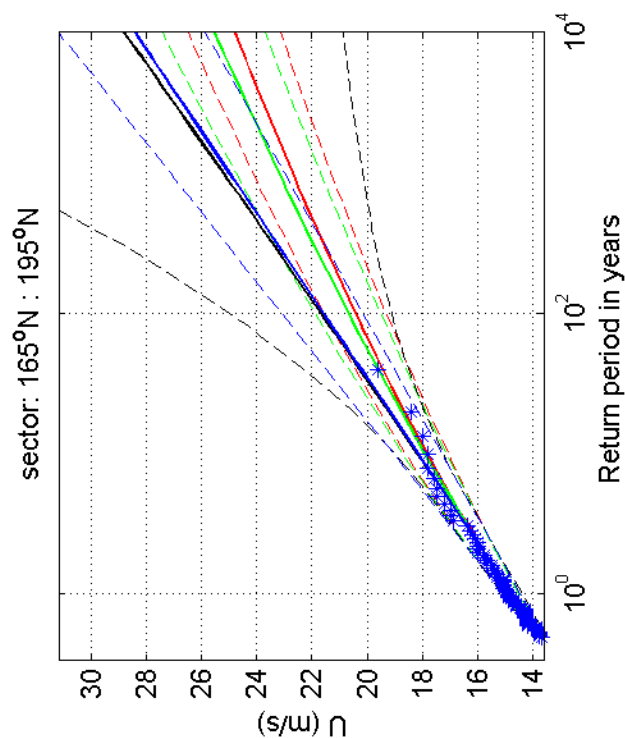
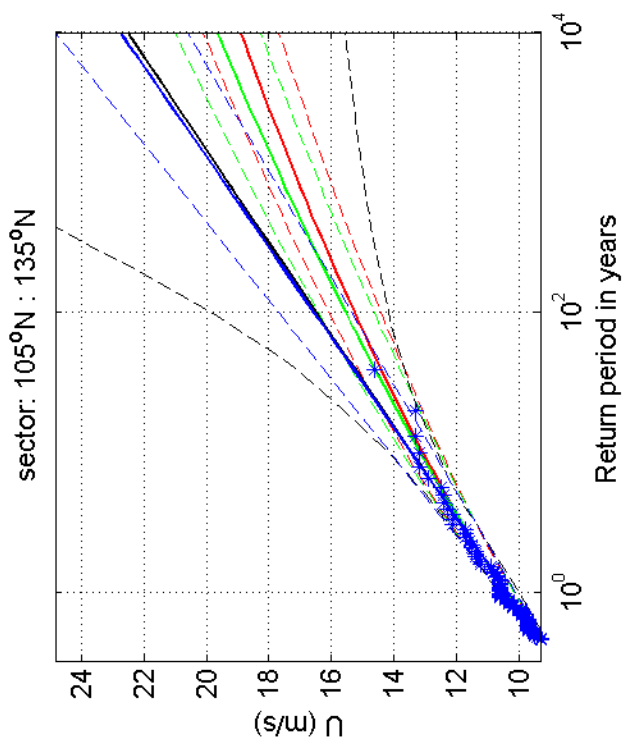
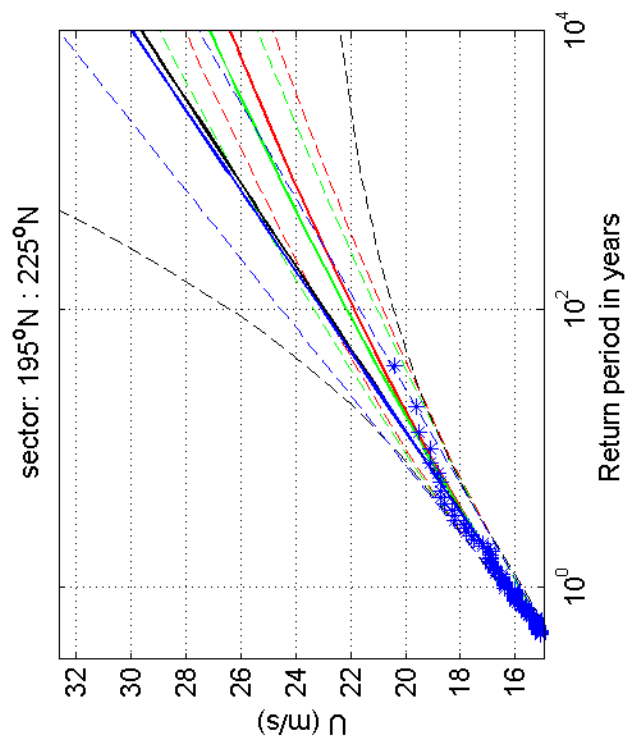
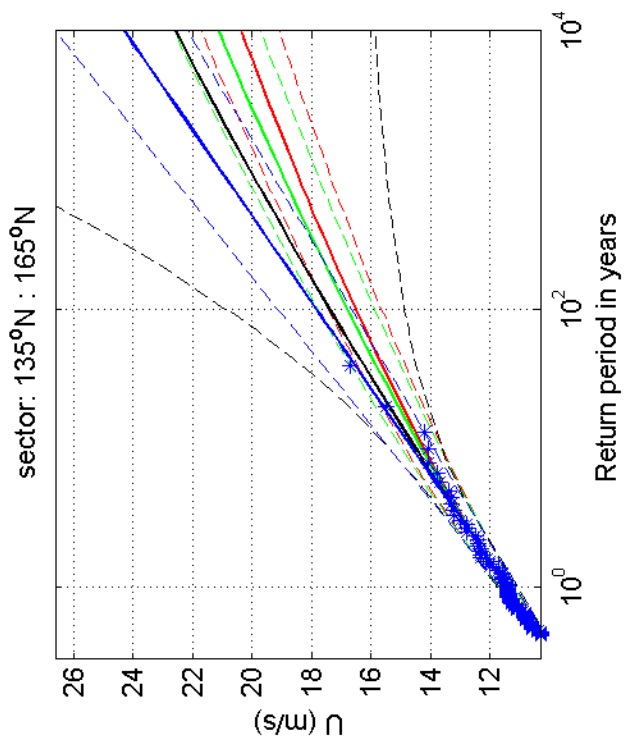
1970-2008

Vlissingen

Deltares

1200264-005

Fig. F.4.310.1



Return value plot with exponential (blue) and GPD (black) fit to U ,
 exponential (red) fit to U_p^2 and exponential (green) fit to U_p^k
 Plotting positions: x_i vs $(n+1)/(\lambda(n+1-i))$

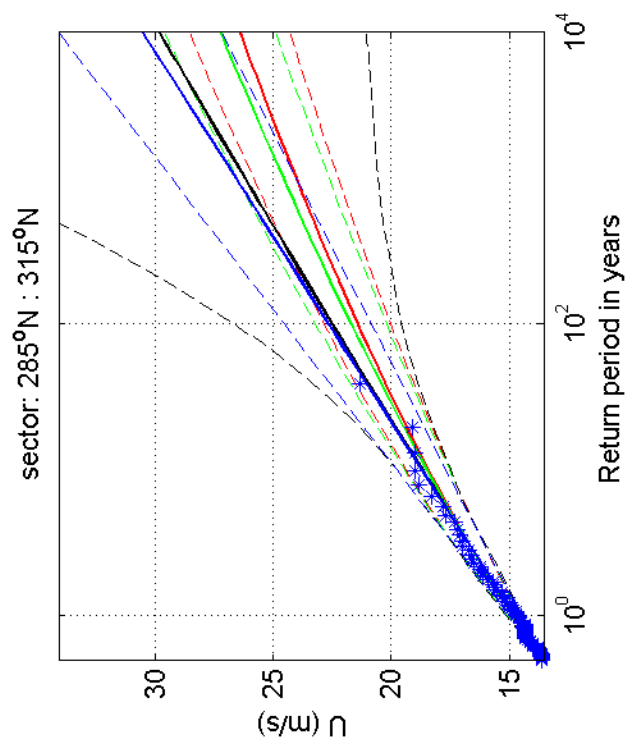
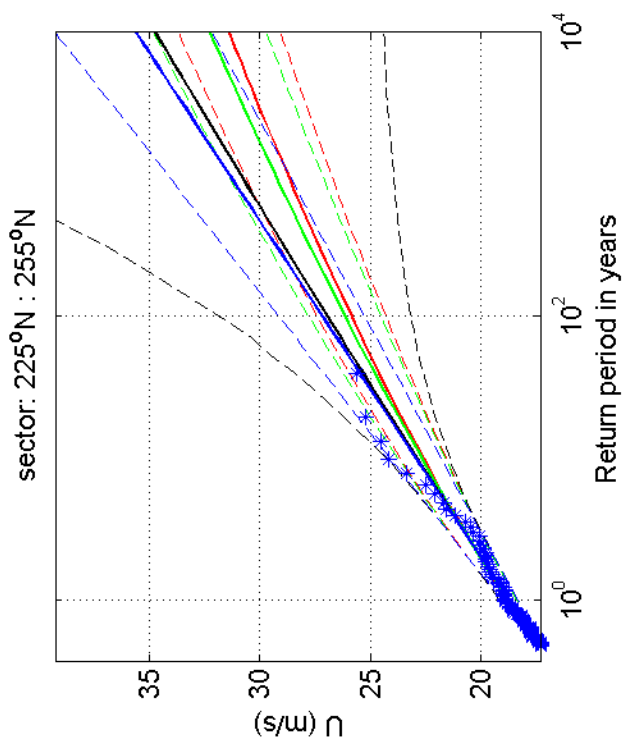
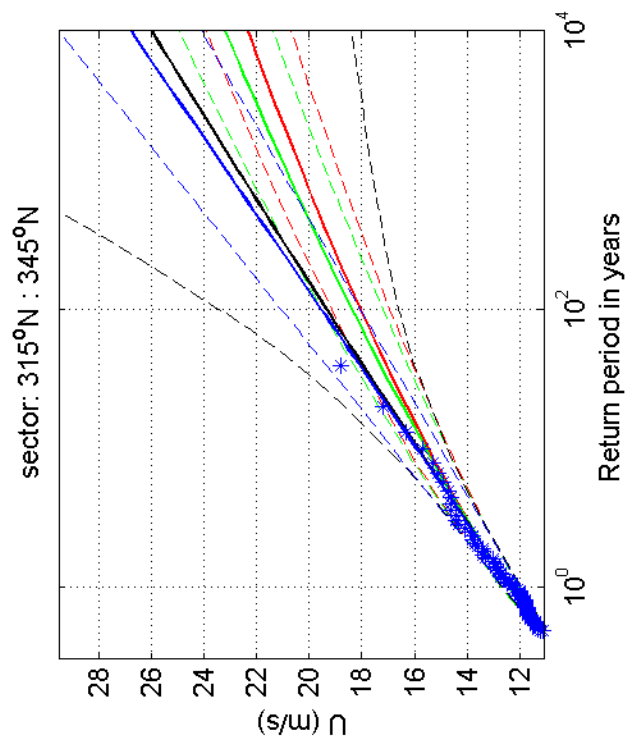
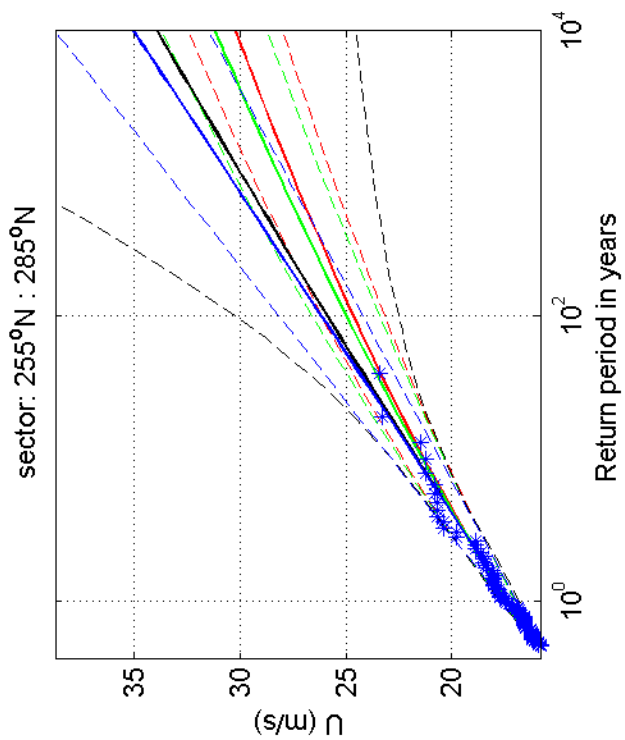
1970-2008

Vlissingen

Deltares

1200264-005

Fig. F.4.310.5



Return value plot with exponential (blue) and GPD (black) fit to U ,
 exponential (red) fit to U_p^2 and exponential (green) fit to U_p^k
 Plotting positions: x_i vs $(n+1)/(\lambda(n+1-i))$

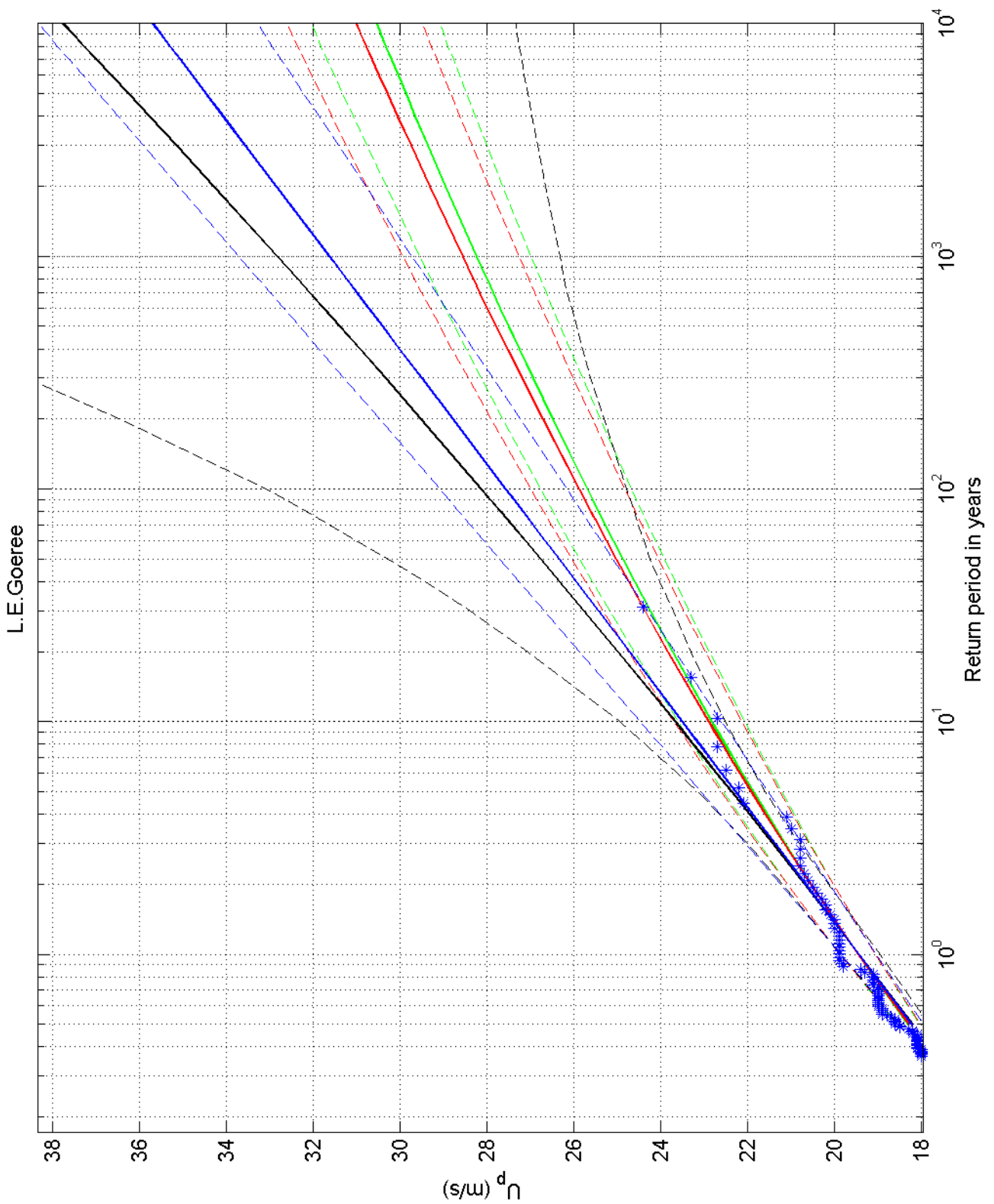
1970-2008

Vlissingen

Deltares

1200264-005

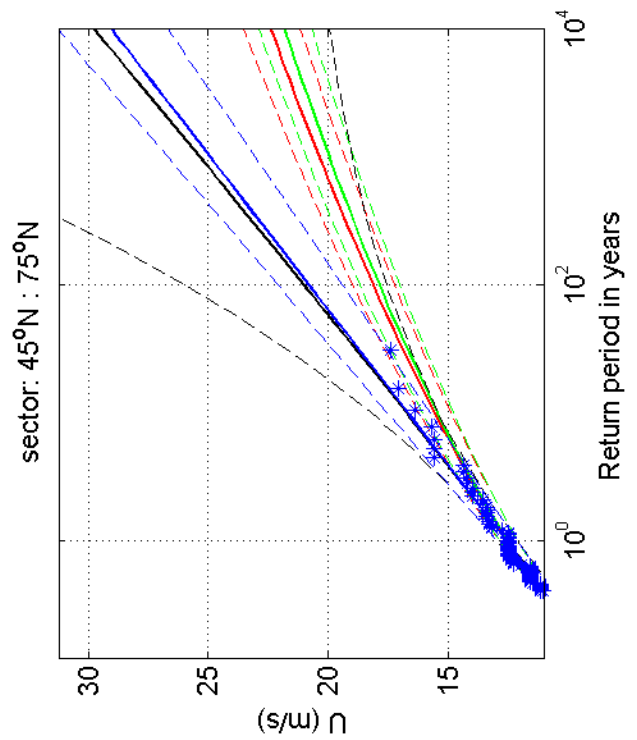
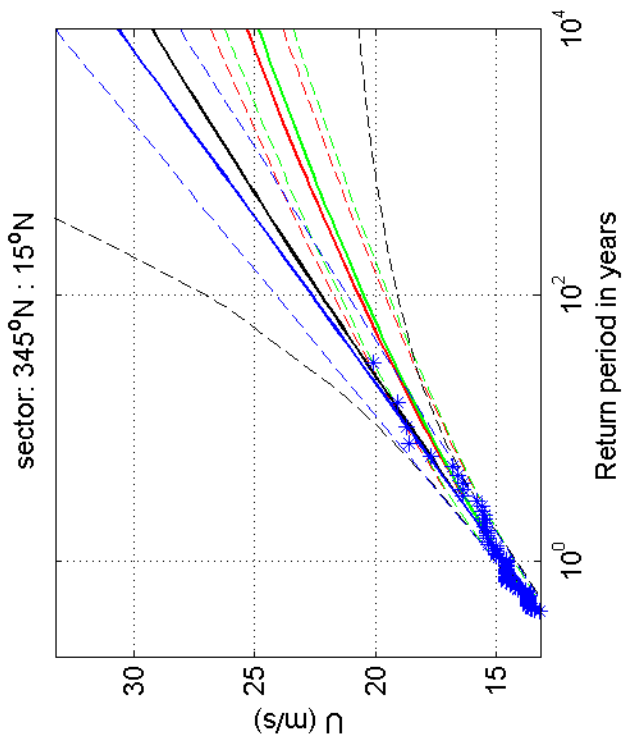
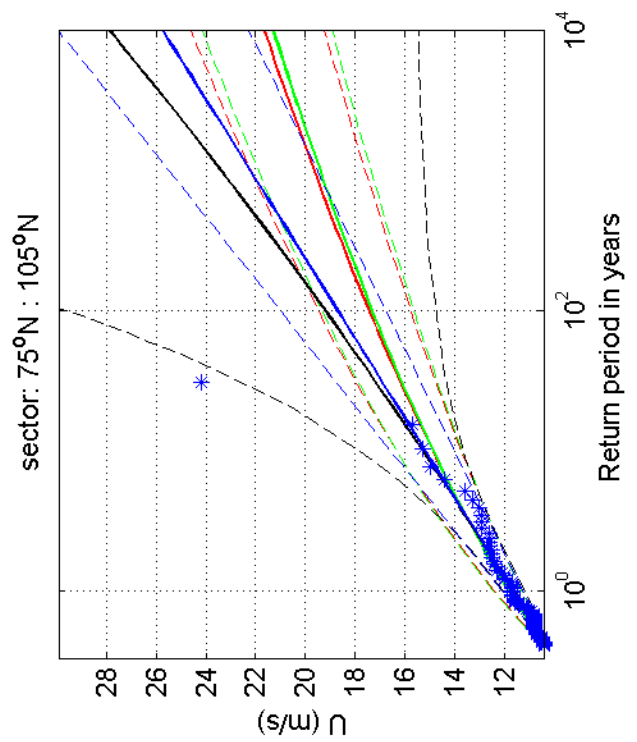
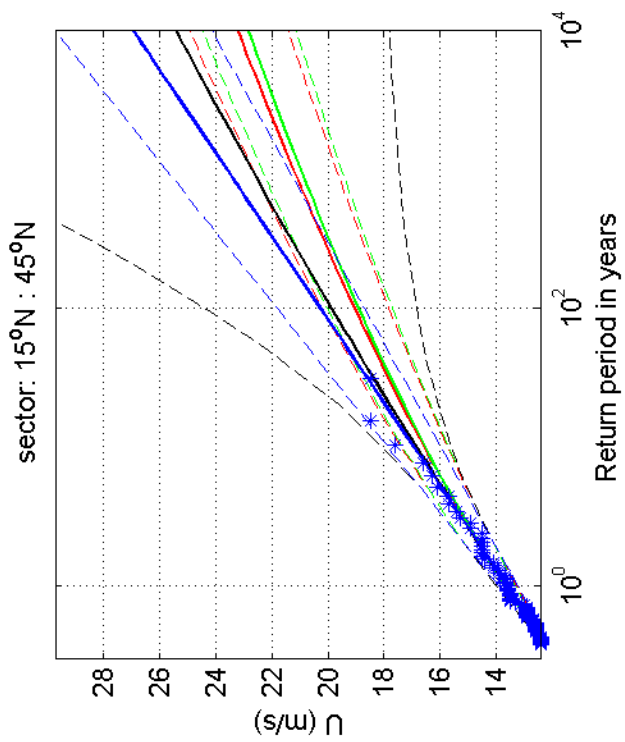
Fig. F.4.310.9



Return value plot with exponential (blue) and GPD (black) fit to U_p ,
 exponential (red) fit to U_p^2 and exponential (green) fit to U_p^k
 Plotting positions: x_i vs $(n+1)/(\lambda(n+1-i))$

omni-directional	1970-2008
L.E. Goeree	
1200264-005	Fig. F.4.320

Deltares



Return value plot with exponential (blue) and GPD (black) fit to U ,
 exponential (red) fit to U_p^2 and exponential (green) fit to U_p^k
 Plotting positions: x_i vs $(n+1)/(\lambda(n+1-i))$

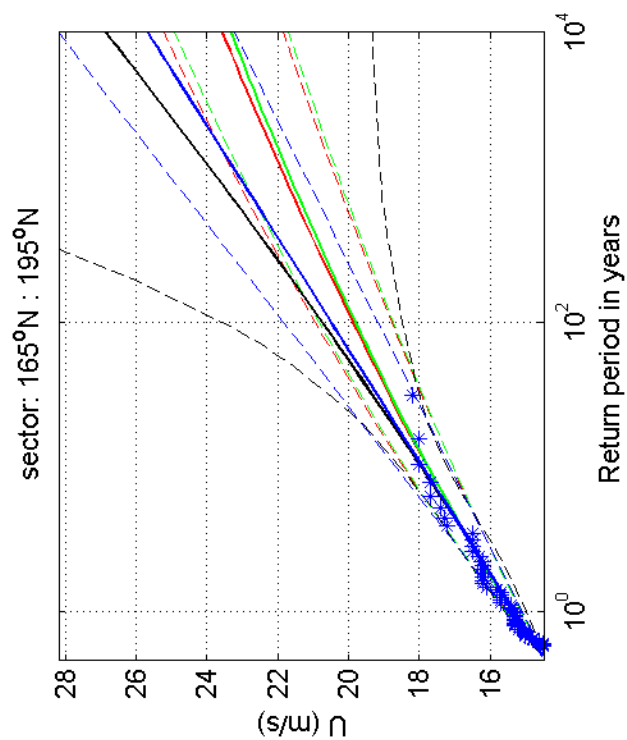
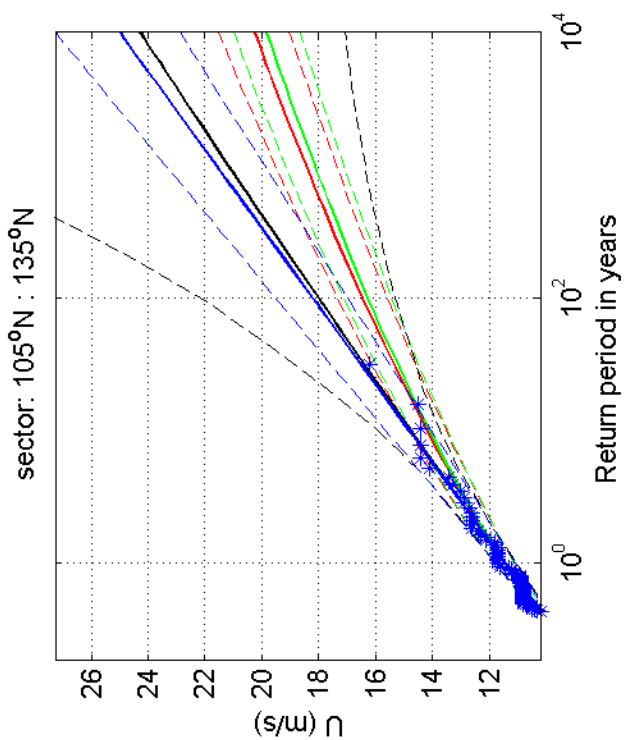
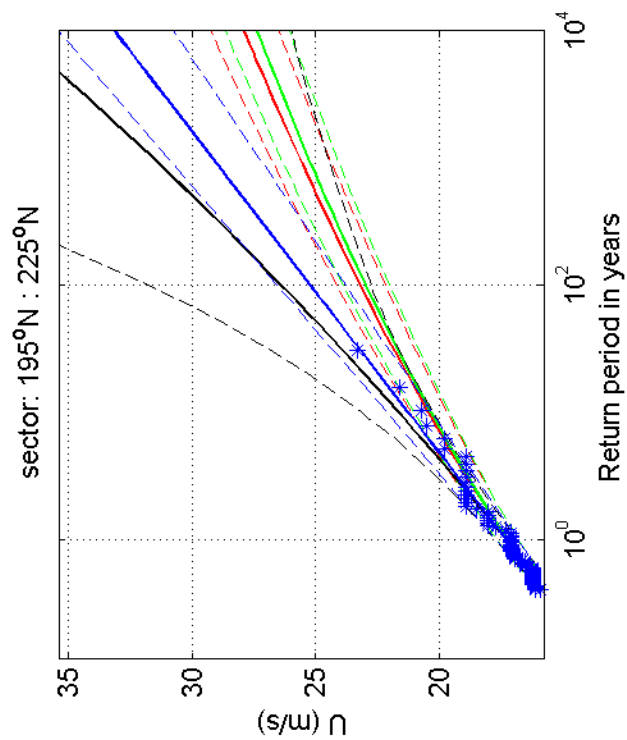
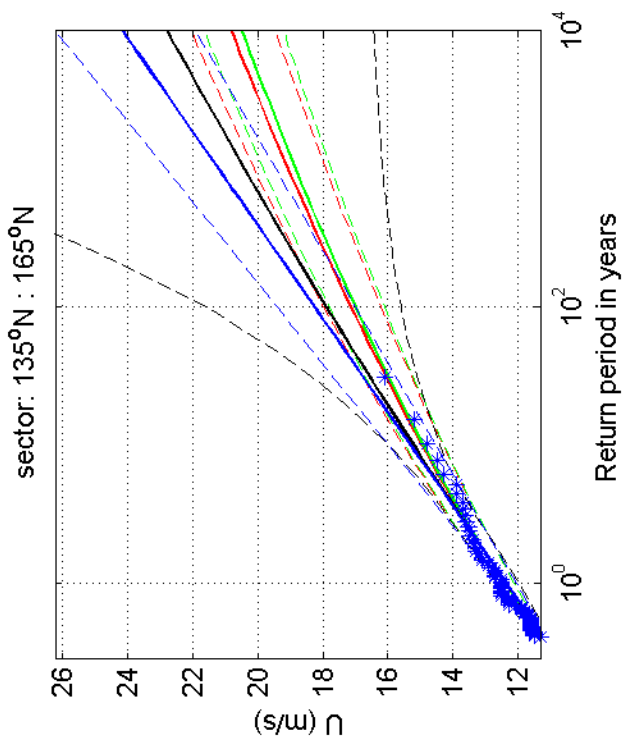
1970-2008

L.E.Goeree

Deltares

1200264-005

Fig. F.4.320.1



Return value plot with exponential (blue) and GPD (black) fit to U ,
 exponential (red) fit to U_p^2 and exponential (green) fit to U_p^k
 Plotting positions: x_i vs $(n+1)/(\lambda(n+1-i))$

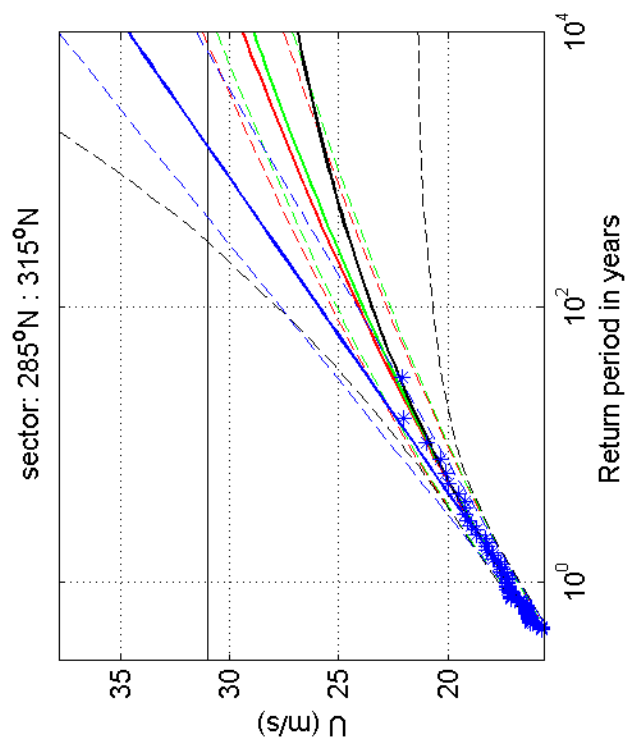
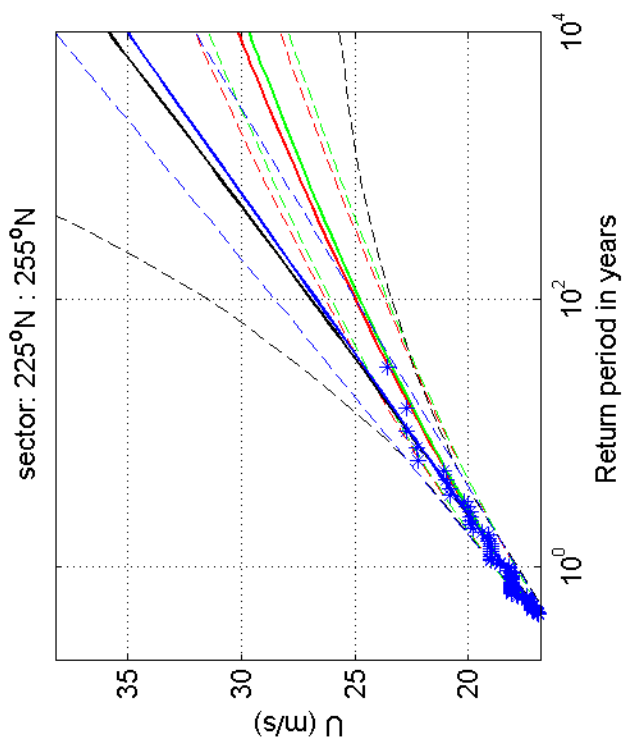
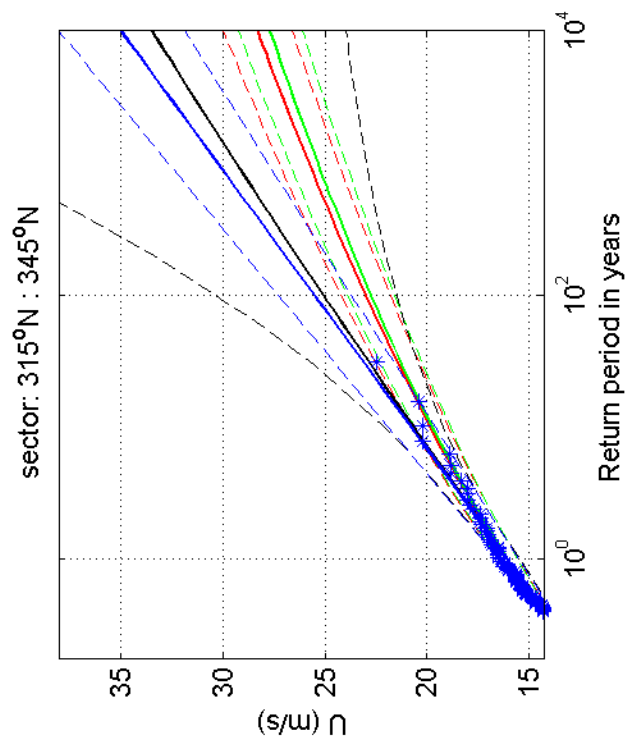
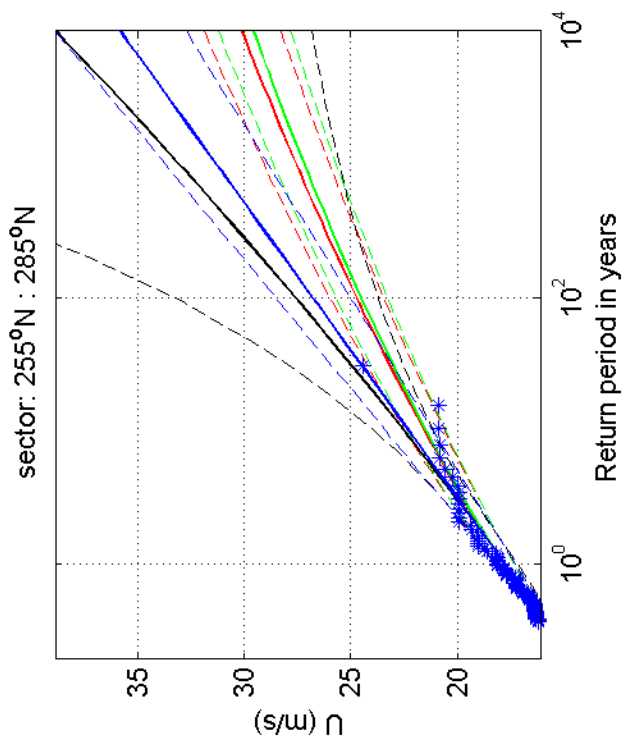
1970-2008

L.E.Goeree

Deltares

1200264-005

Fig. F.4.320.5



Return value plot with exponential (blue) and GPD (black) fit to U ,
 exponential (red) fit to U_p^2 and exponential (green) fit to U_p^k
 Plotting positions: x_i vs $(n+1)/(\lambda(n+1-i))$

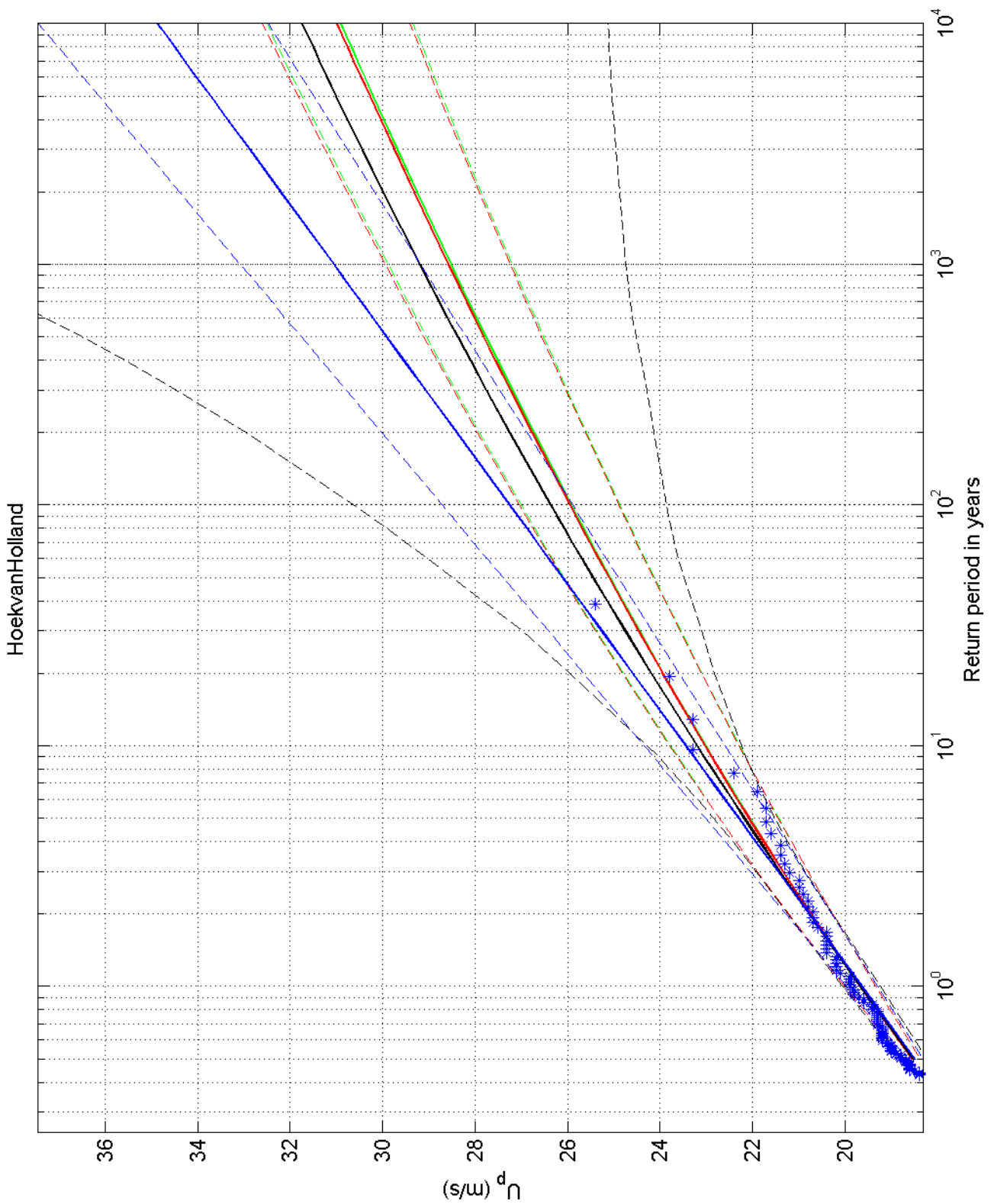
1970-2008

L.E.Goeree

Deltares

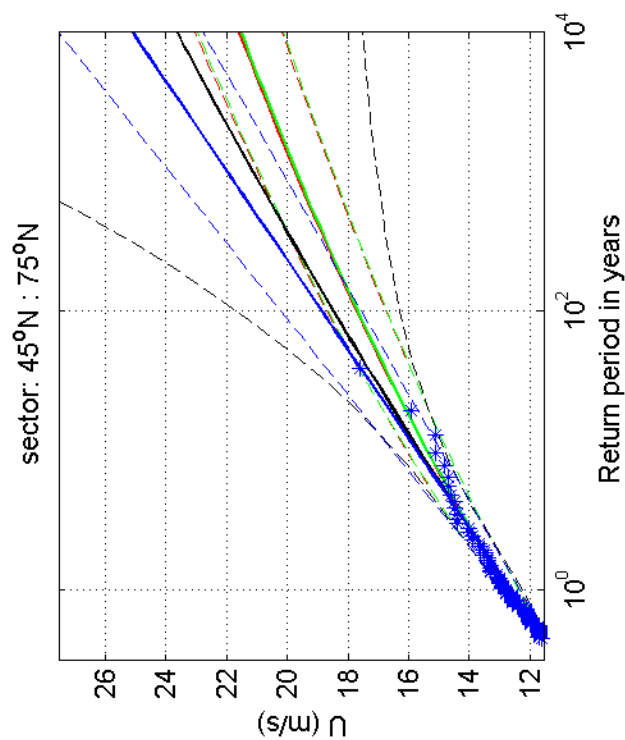
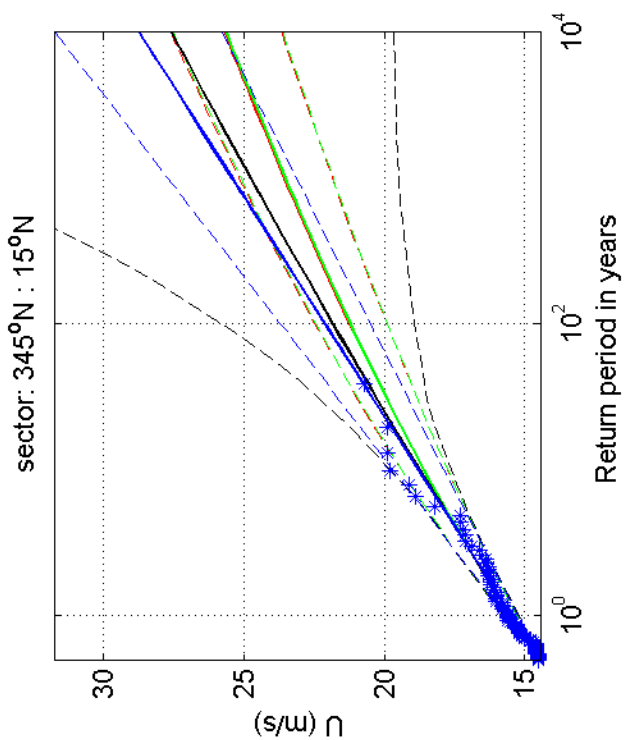
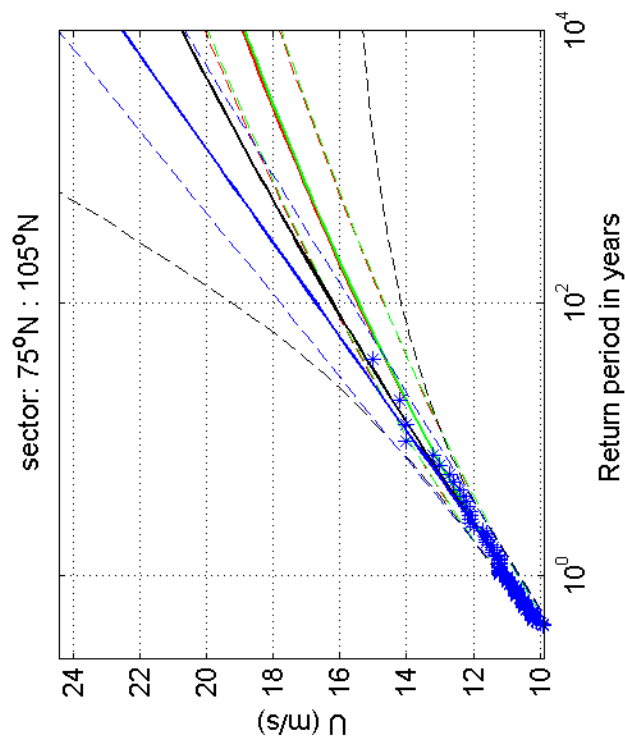
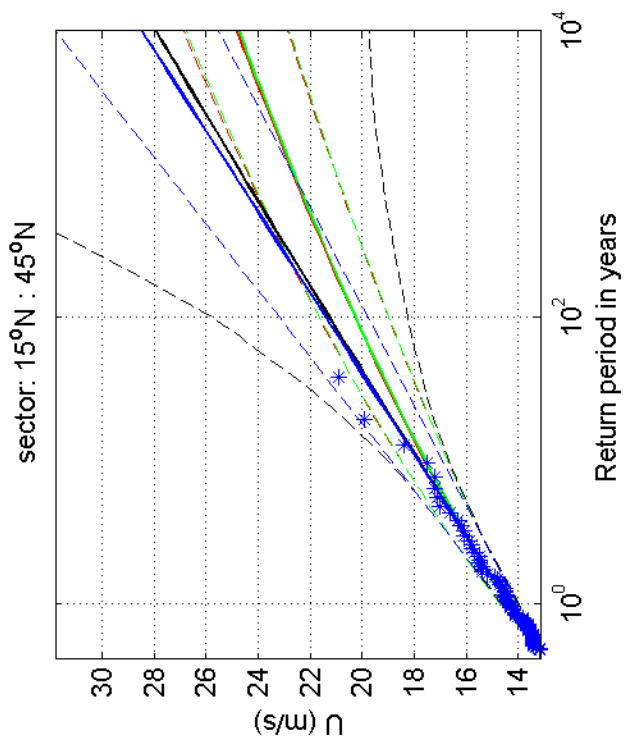
1200264-005

Fig. F.4.320.9



Return value plot with exponential (blue) and GPD (black) fit to U_p ,
 exponential (red) fit to U_p^2 and exponential (green) fit to U_p^k
 Plotting positions: x_i vs $(n+1)/(\lambda(n+1-i))$

omni-directional	1970-2008
HoekvanHolland	
1200264-005	Fig. F.4.330



Return value plot with exponential (blue) and GPD (black) fit to U ,
 exponential (red) fit to U_p^2 and exponential (green) fit to U_p^k
 Plotting positions: x_i vs $(n+1)/(\lambda(n+1-i))$

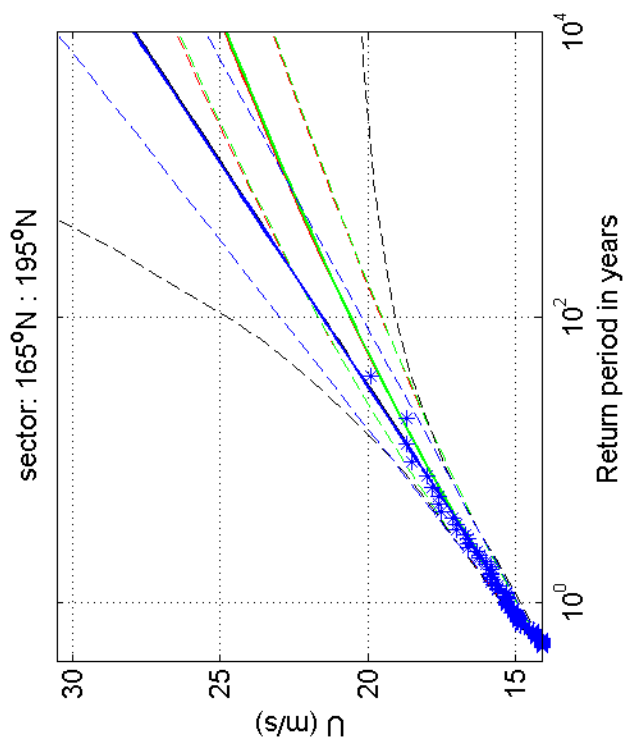
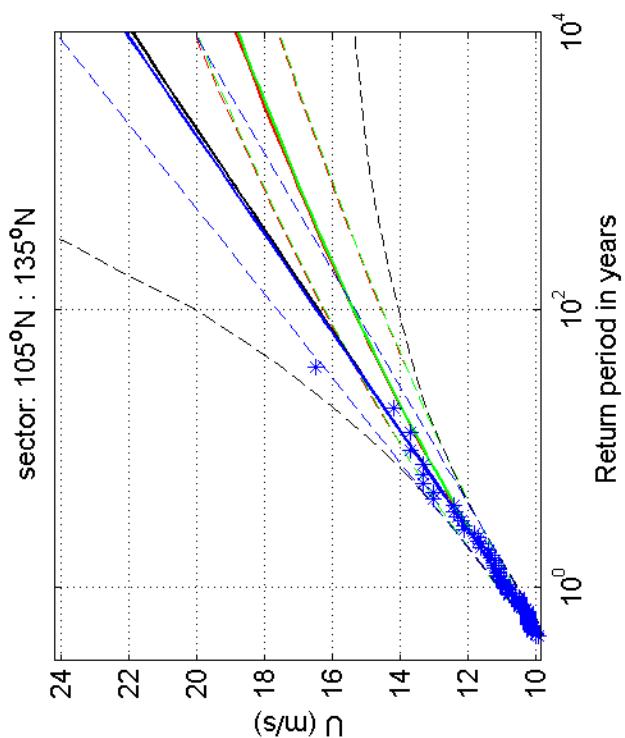
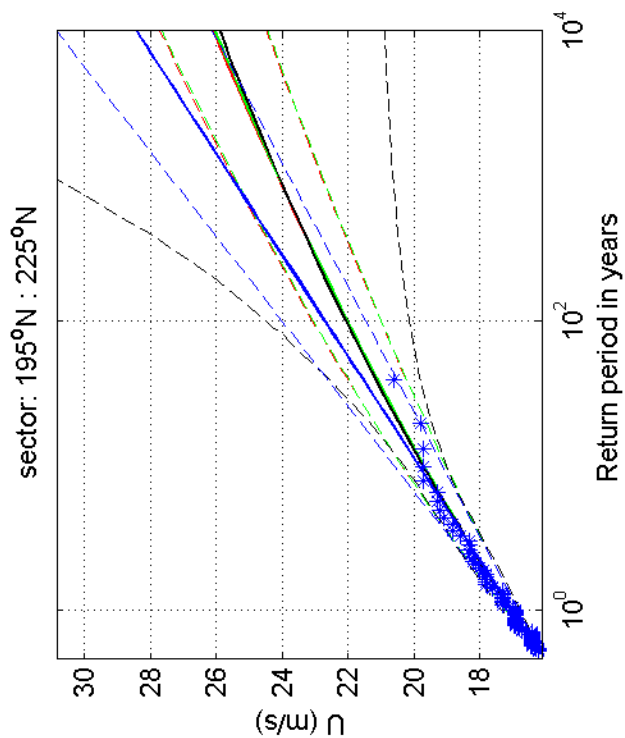
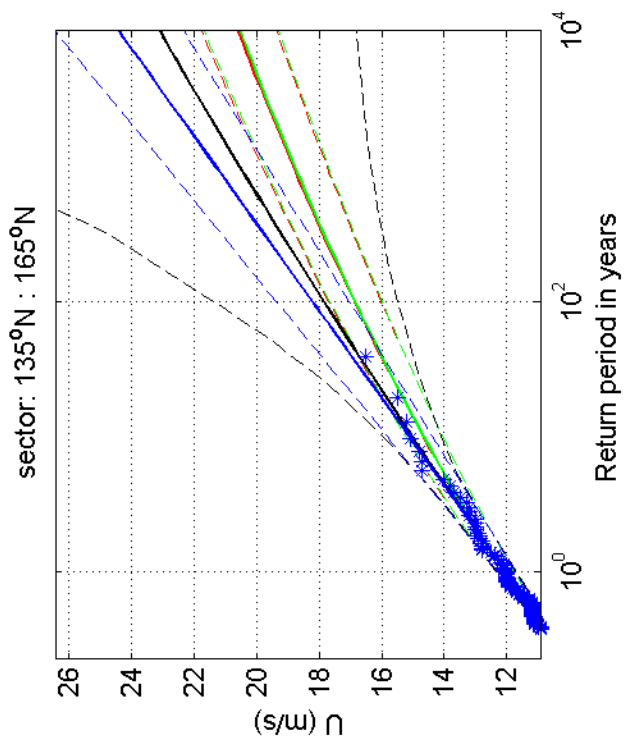
1970-2008

HoekvanHolland

Deltares

1200264-005

Fig. F.4.330.1



Return value plot with exponential (blue) and GPD (black) fit to U ,
 exponential (red) fit to U_p^2 and exponential (green) fit to U_p^k
 Plotting positions: x_i vs $(n+1)/(\lambda(n+1-i))$

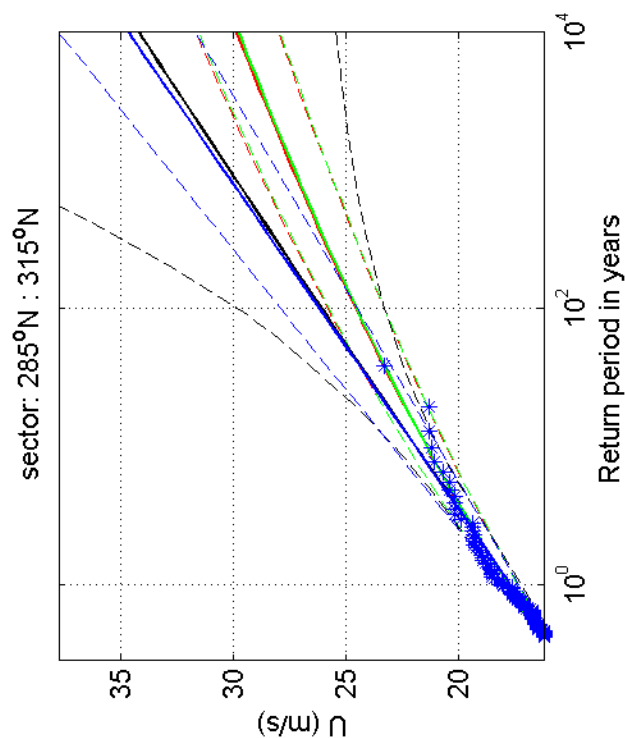
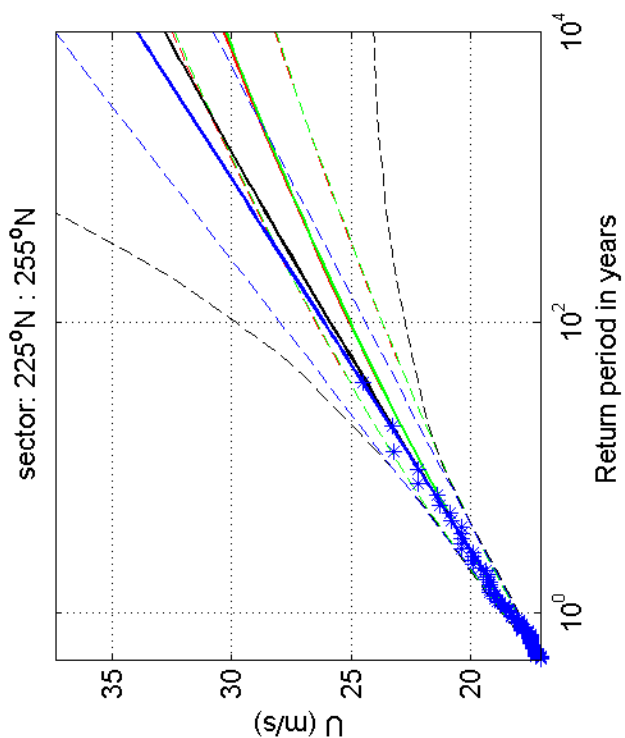
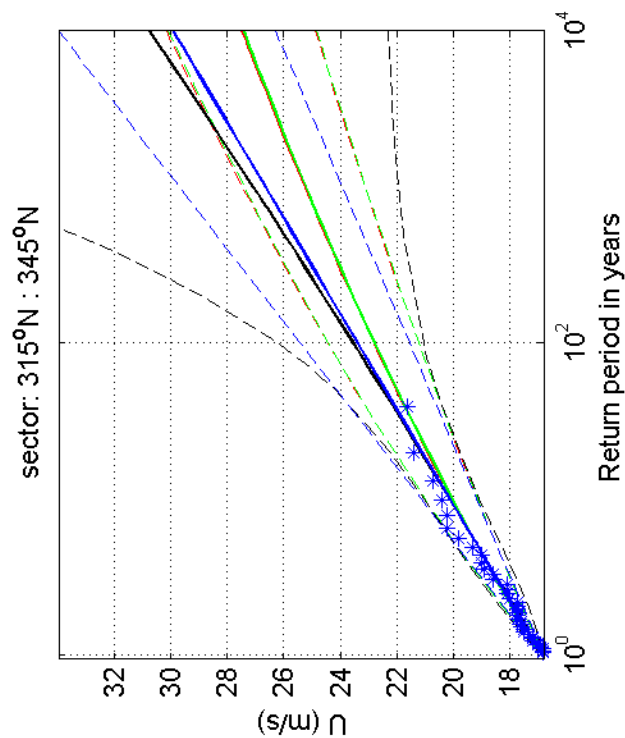
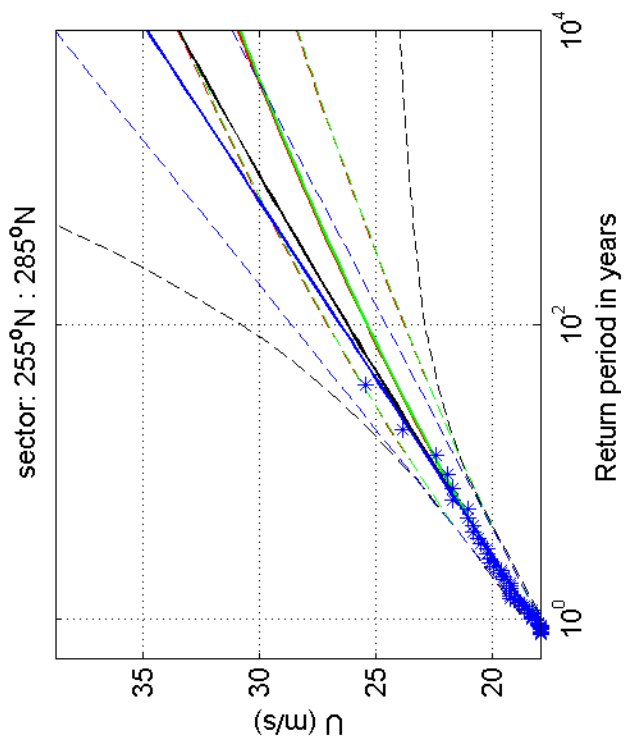
1970-2008

HoekvanHolland

Deltares

1200264-005

Fig. F.4.330.5



Return value plot with exponential (blue) and GPD (black) fit to U ,
 exponential (red) fit to U_p^2 and exponential (green) fit to U_p^k
 Plotting positions: x_i vs $(n+1)/(\lambda(n+1-i))$

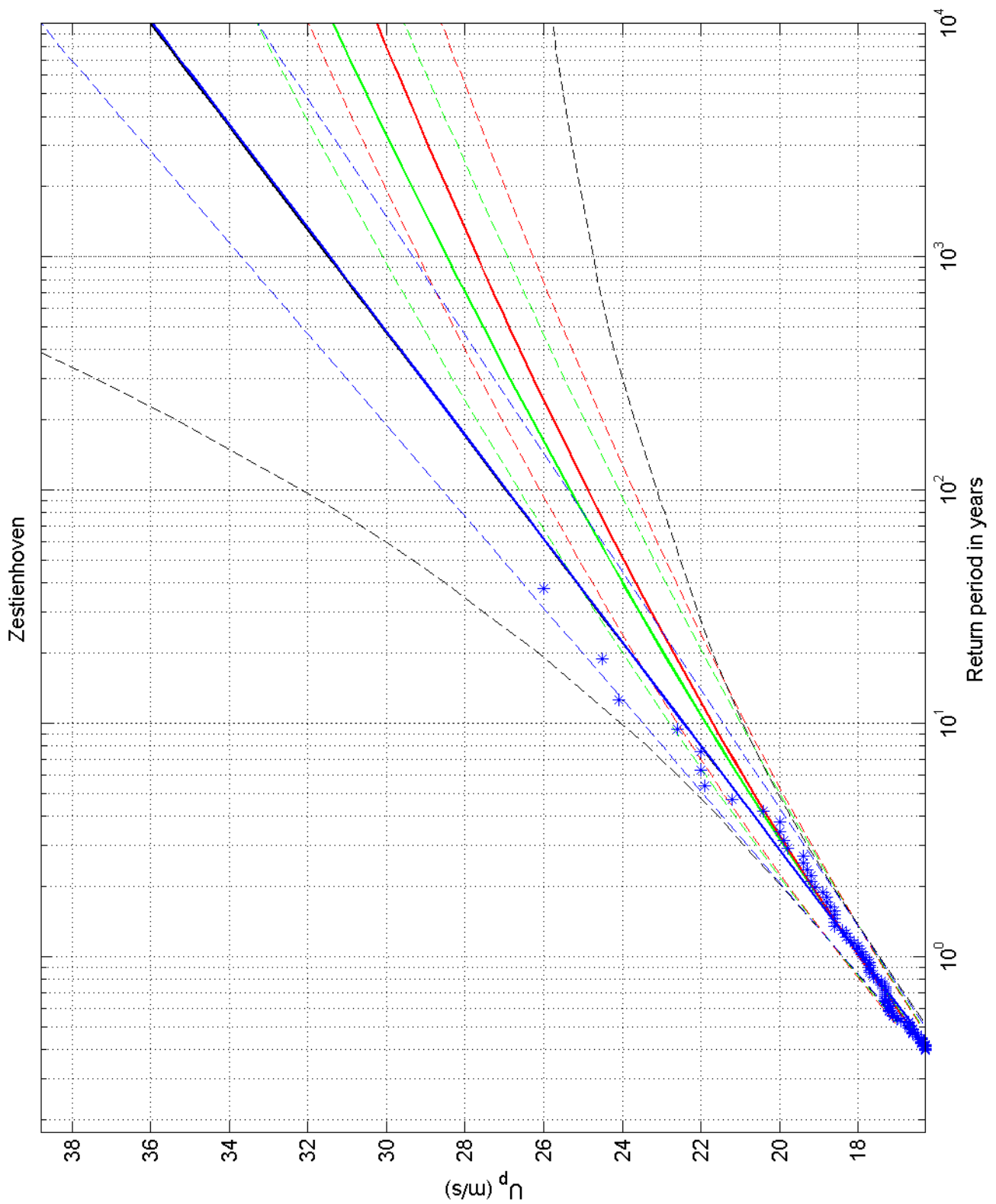
1970-2008

HoekvanHolland

Deltares

1200264-005

Fig. F.4.330.9



Return value plot with exponential (blue) and GPD (black) fit to U_p ,
 exponential (red) fit to U_p^2 and exponential (green) fit to U_p^k
 Plotting positions: x_i vs $(n+1)/(\lambda(n+1-i))$

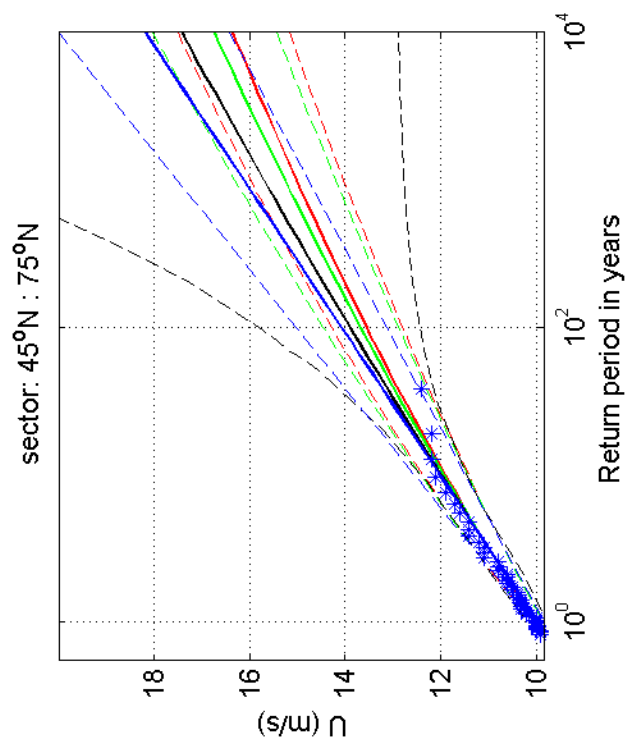
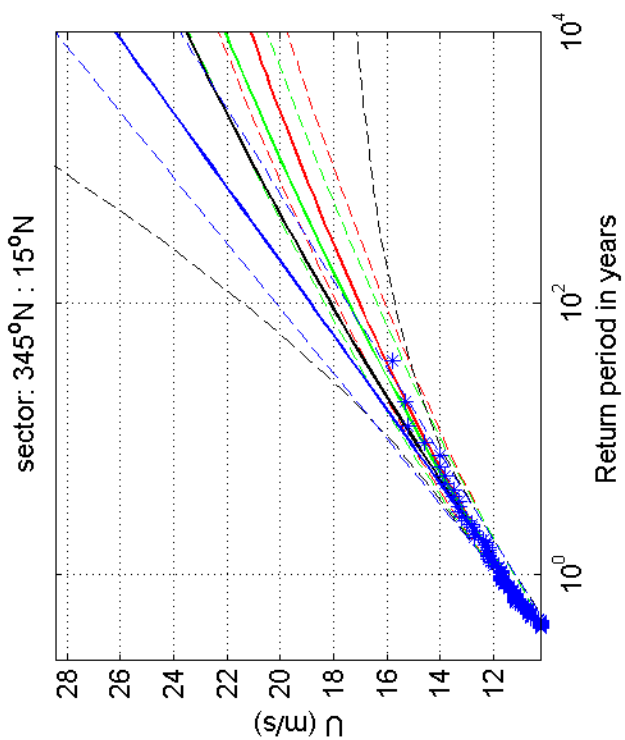
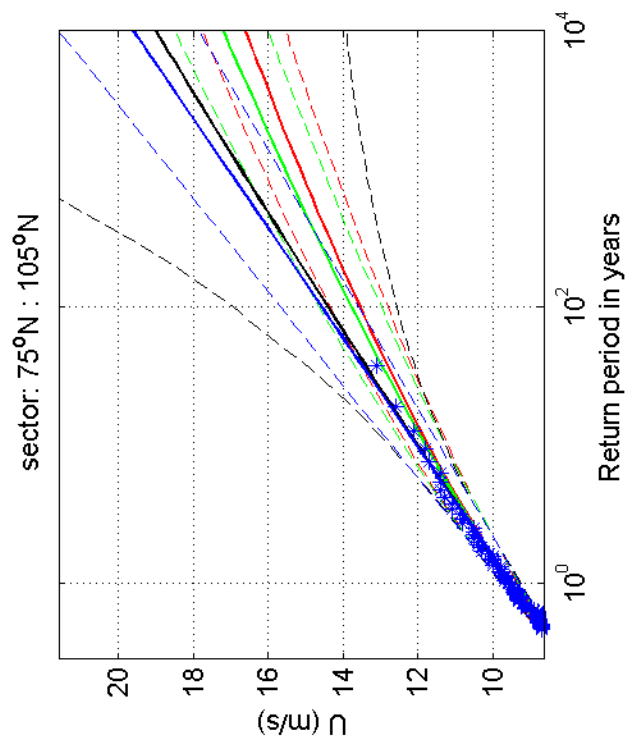
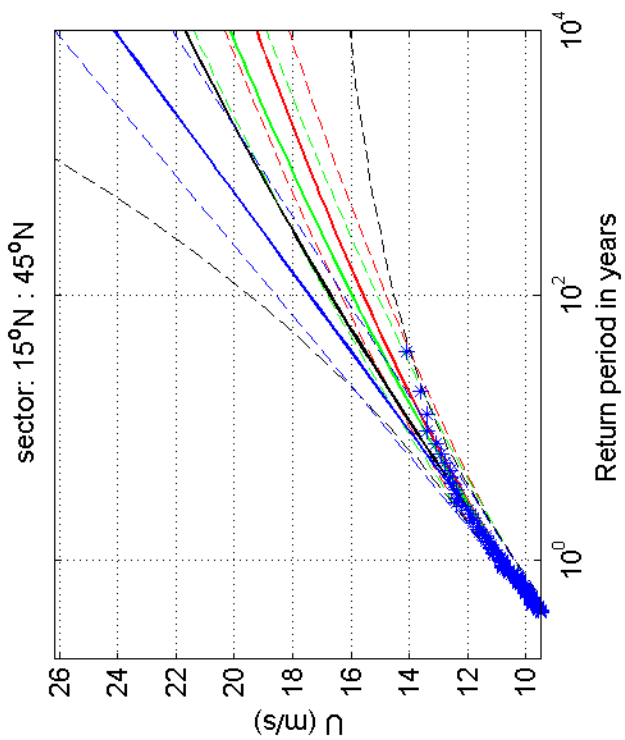
omni-directional 1970-2008

Zestienhoven

Deltares

1200264-005

Fig. F.4.344



Return value plot with exponential (blue) and GPD (black) fit to U ,
 exponential (red) fit to U_p^2 and exponential (green) fit to U_p^k
 Plotting positions: x_i vs $(n+1)/(\lambda(n+1-i))$

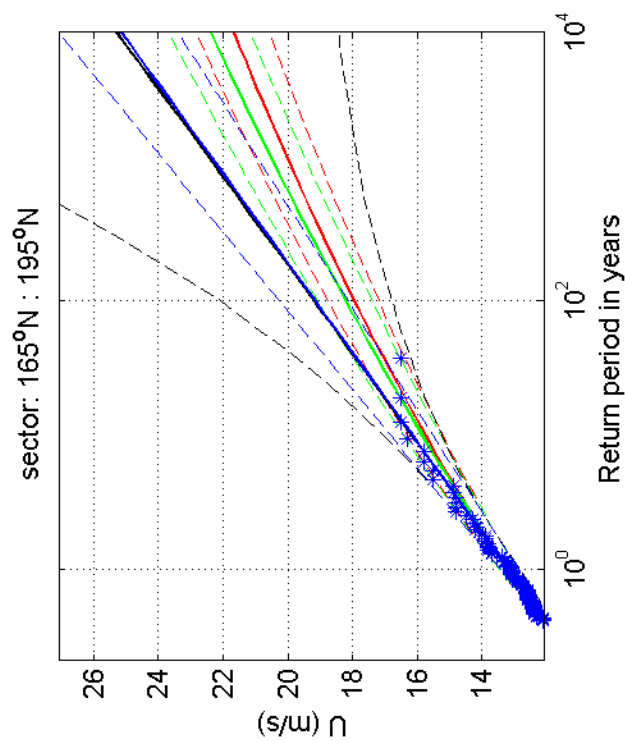
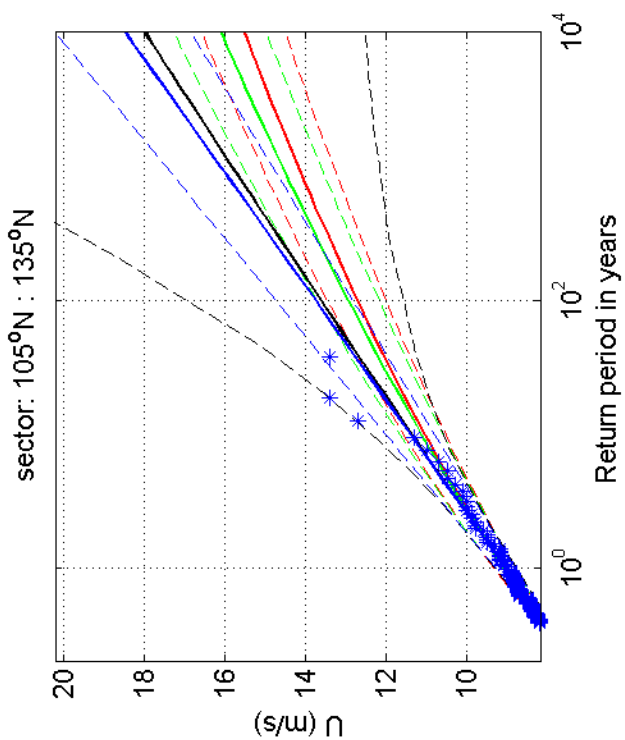
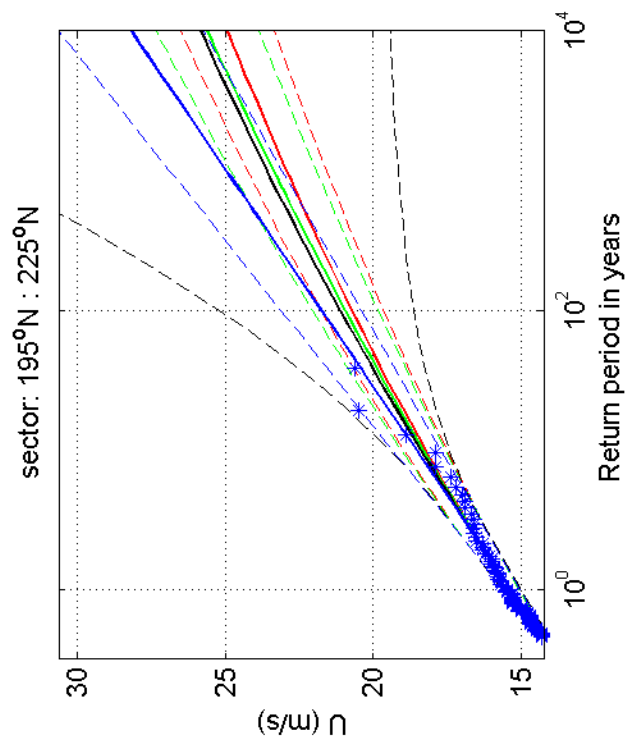
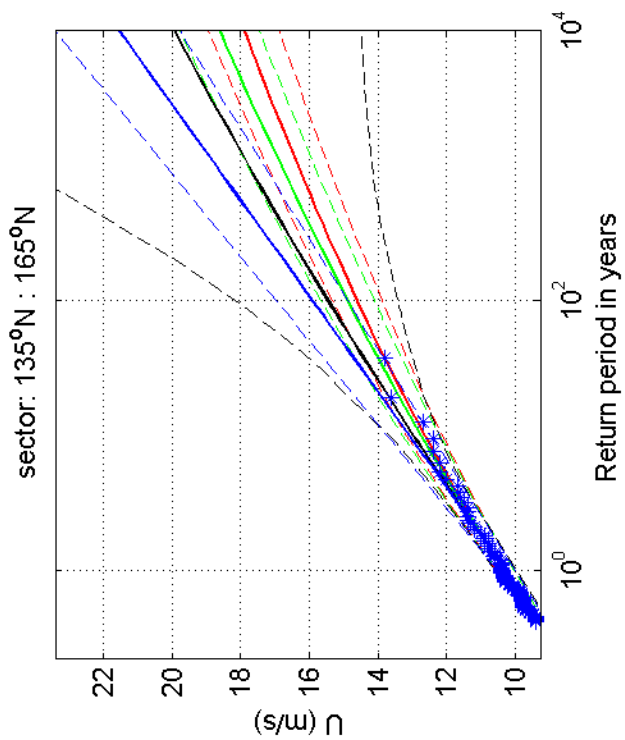
1970-2008

Zestienhoven

Deltares

1200264-005

Fig. F.4.344.1



Return value plot with exponential (blue) and GPD (black) fit to U ,
 exponential (red) fit to U_p^2 and exponential (green) fit to U_p^k
 Plotting positions: x_i vs $(n+1)/(\lambda(n+1-i))$

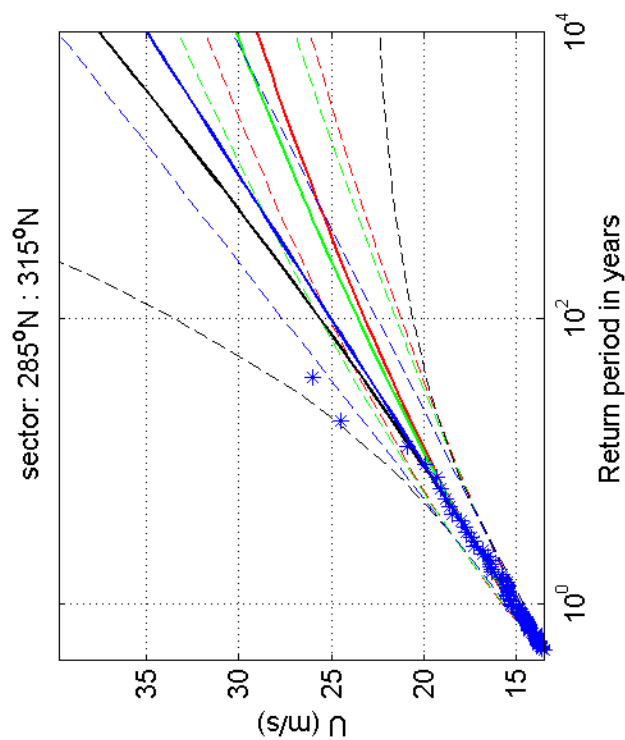
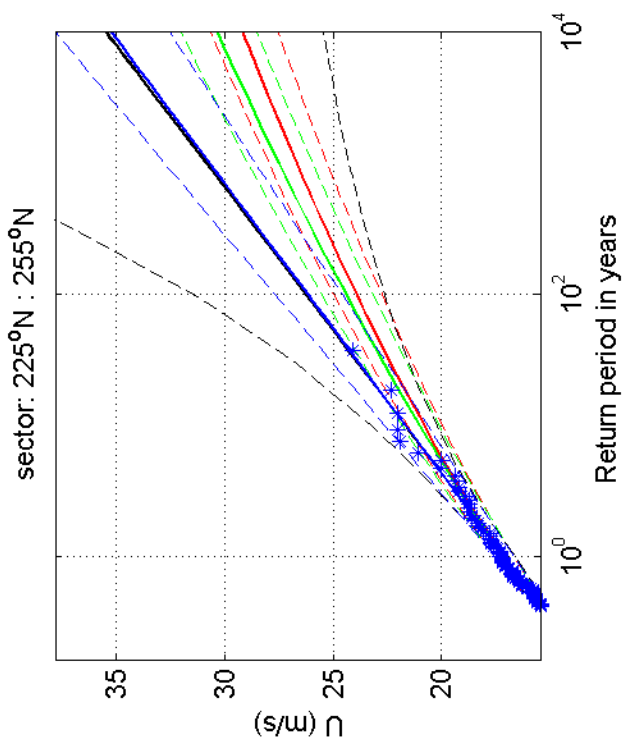
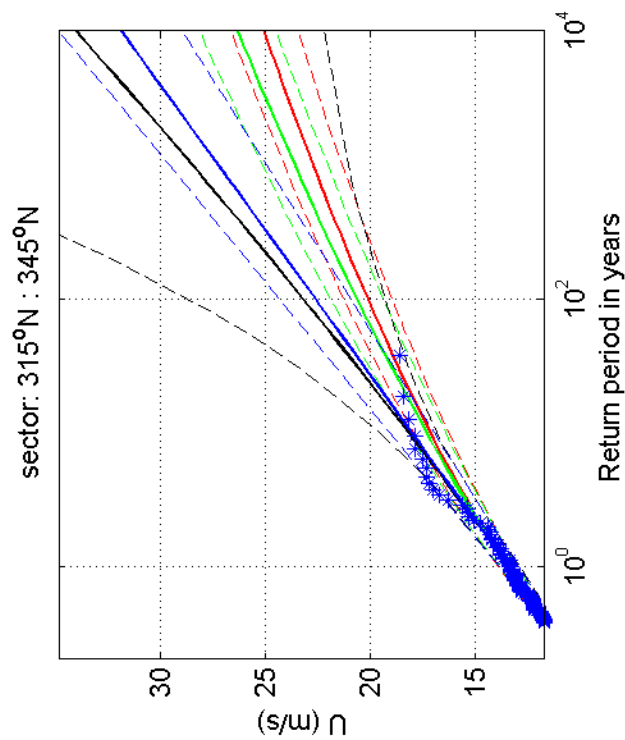
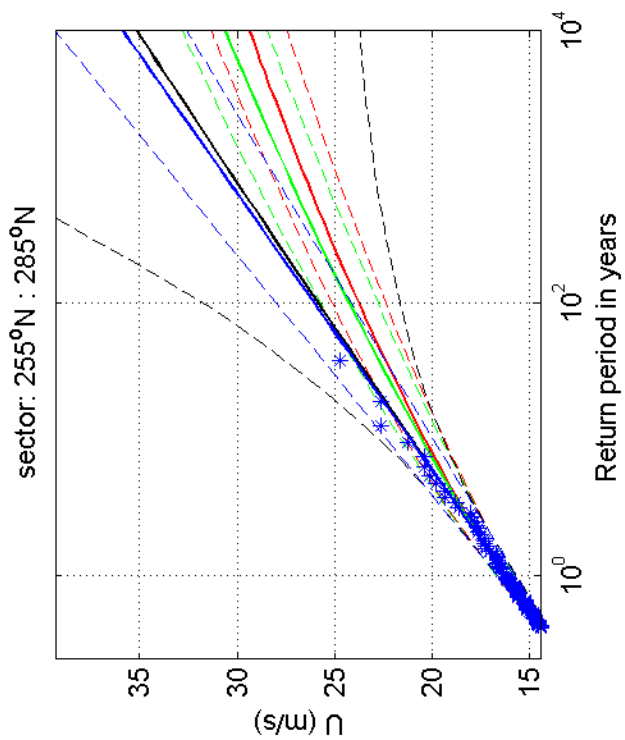
1970-2008

Zestienhoven

Deltares

1200264-005

Fig. F.4.344.5



Return value plot with exponential (blue) and GPD (black) fit to U ,
 exponential (red) fit to U_p^k and exponential (green) fit to U_p^k
 Plotting positions: x_i vs $(n+1)/(\lambda(n+1-i))$

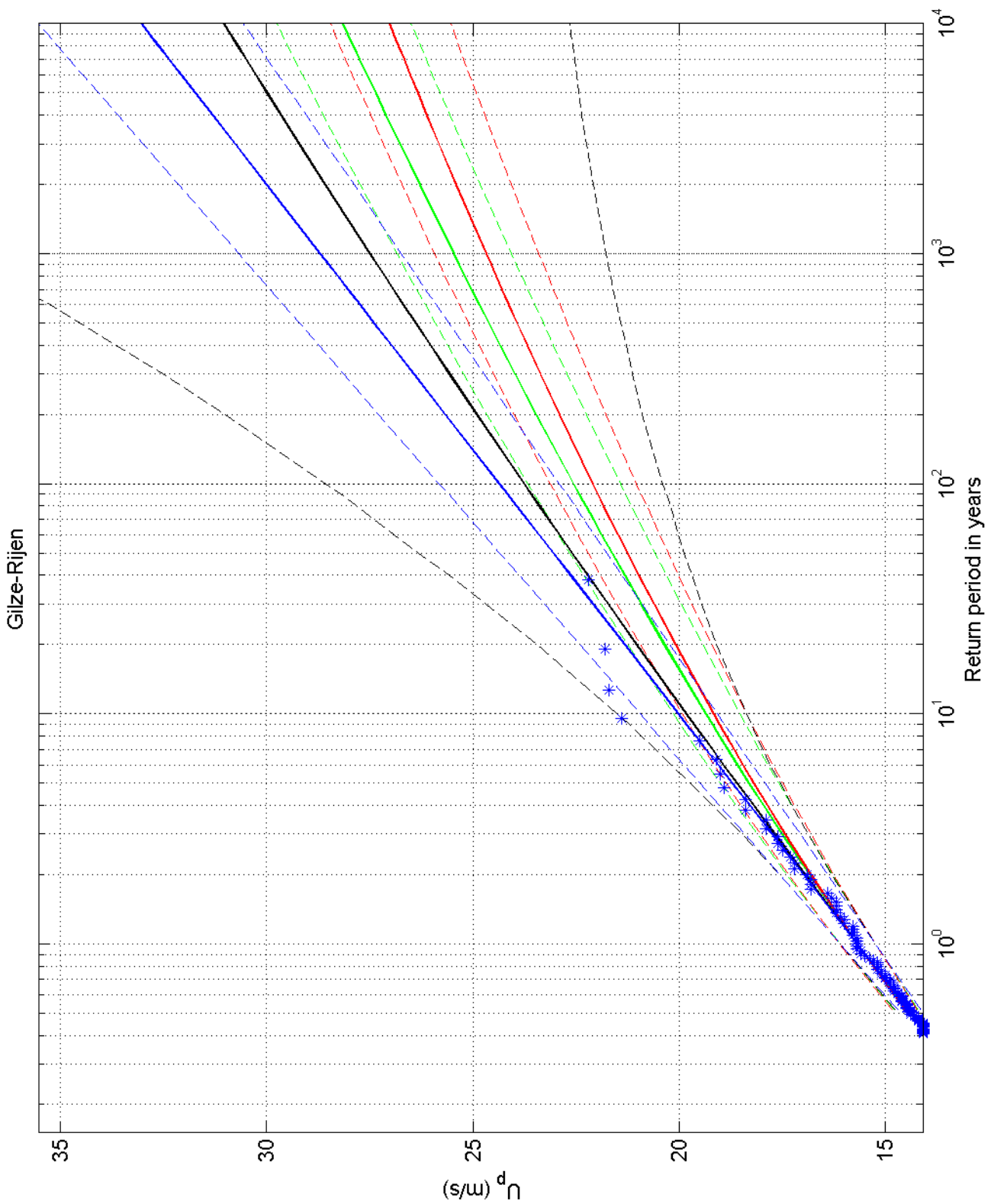
1970-2008

Zestienhoven

Deltares

1200264-005

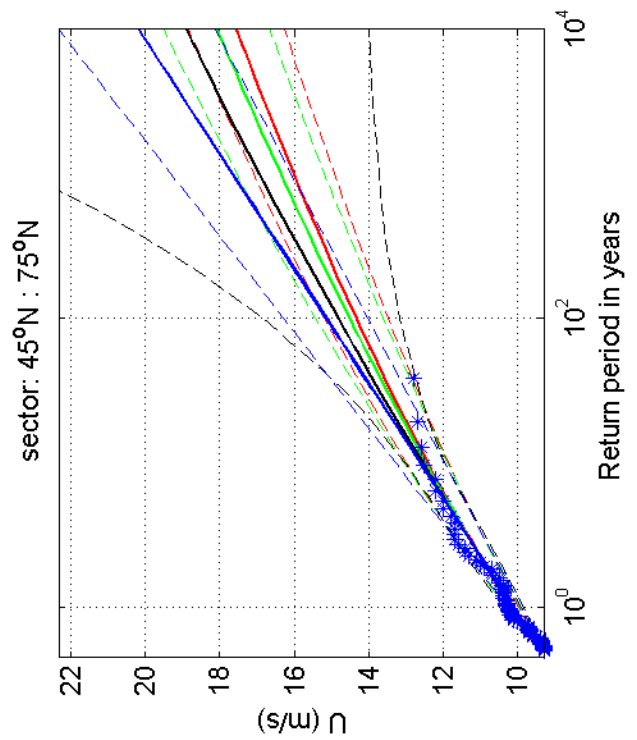
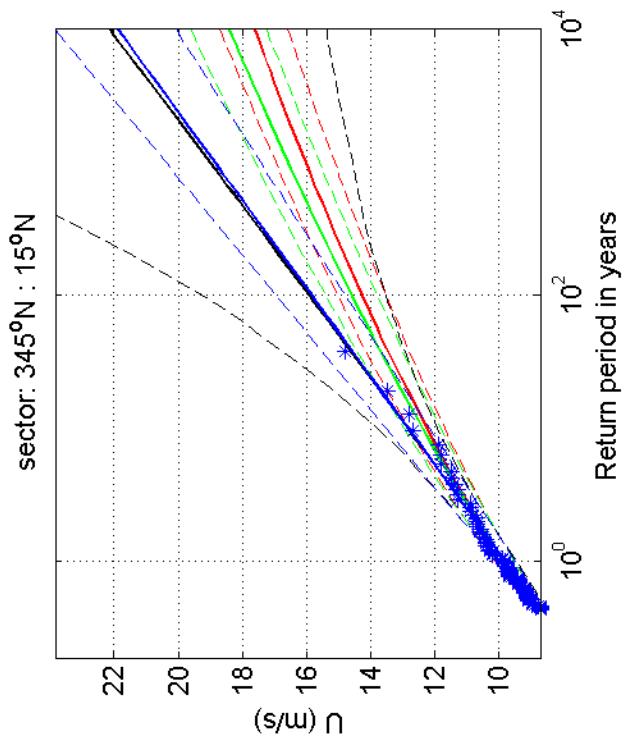
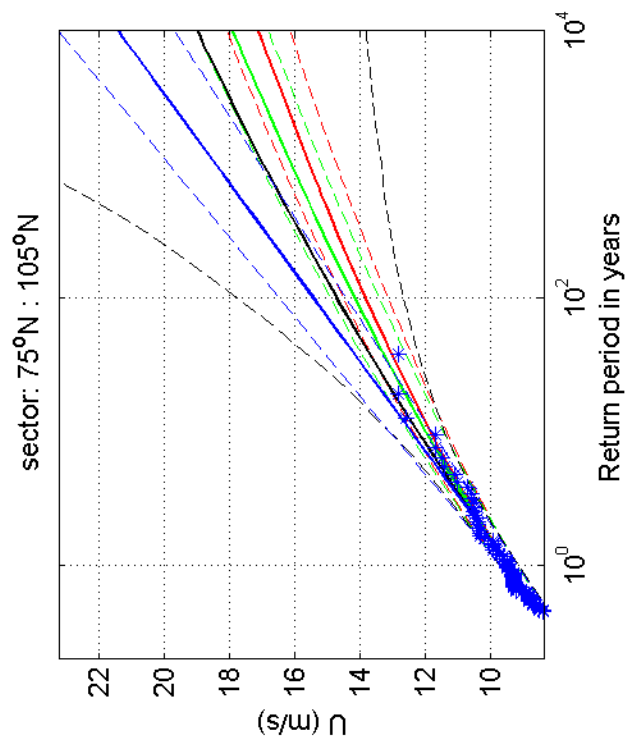
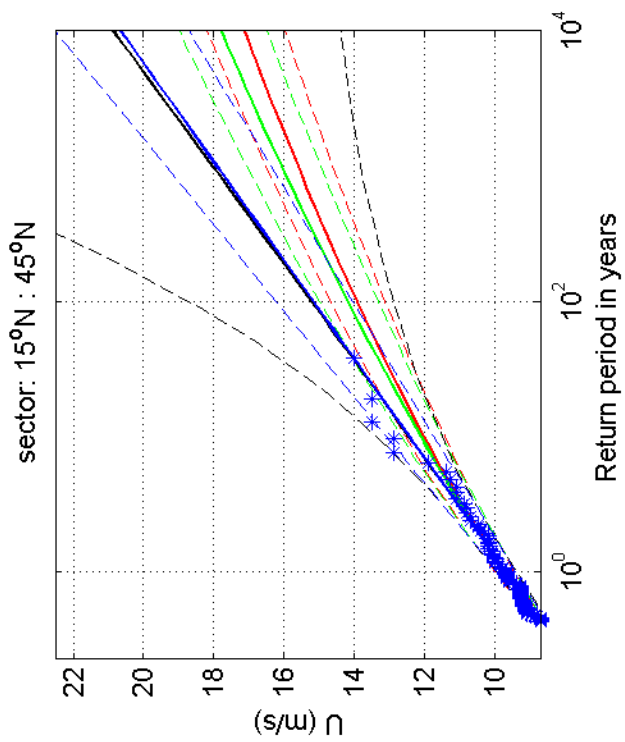
Fig. F.4.344.9



Return value plot with exponential (blue) and GPD (black) fit to U_p ,
 exponential (red) fit to U_p^2 and exponential (green) fit to U_p^k
 Plotting positions: x_i vs $(n+1)/(\lambda(n+1-i))$

omni-directional	1970-2008
Gilze-Rijen	
1200264-005	Fig. F.4.350

Deltares



Return value plot with exponential (blue) and GPD (black) fit to U ,
 exponential (red) fit to U_p^2 and exponential (green) fit to U_p^k
 Plotting positions: x_i vs $(n+1)/(\lambda(n+1-i))$

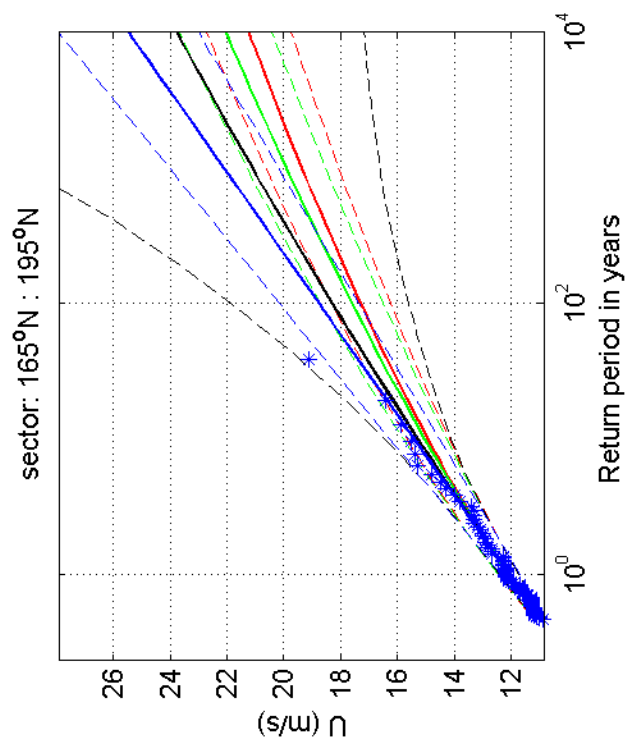
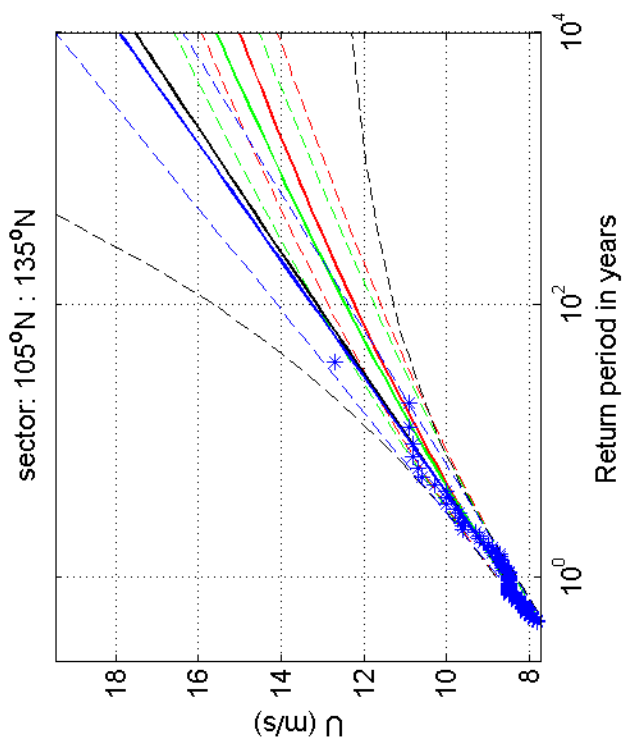
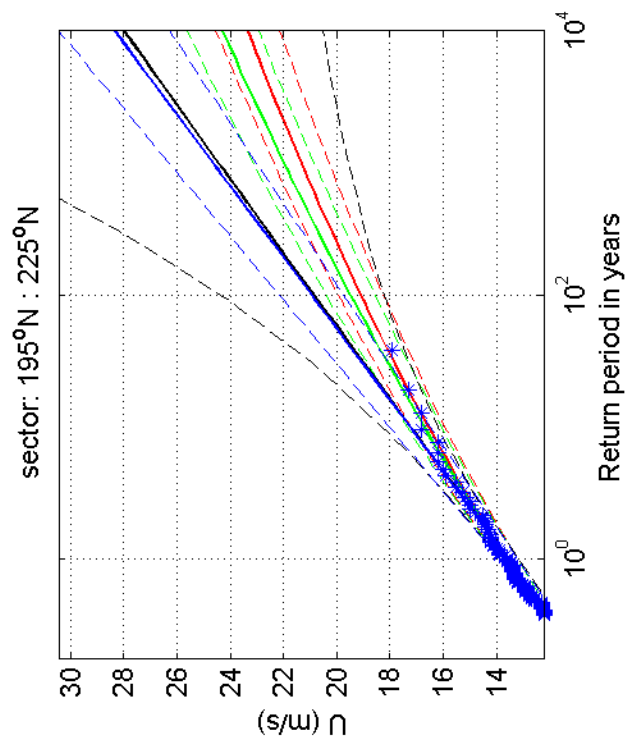
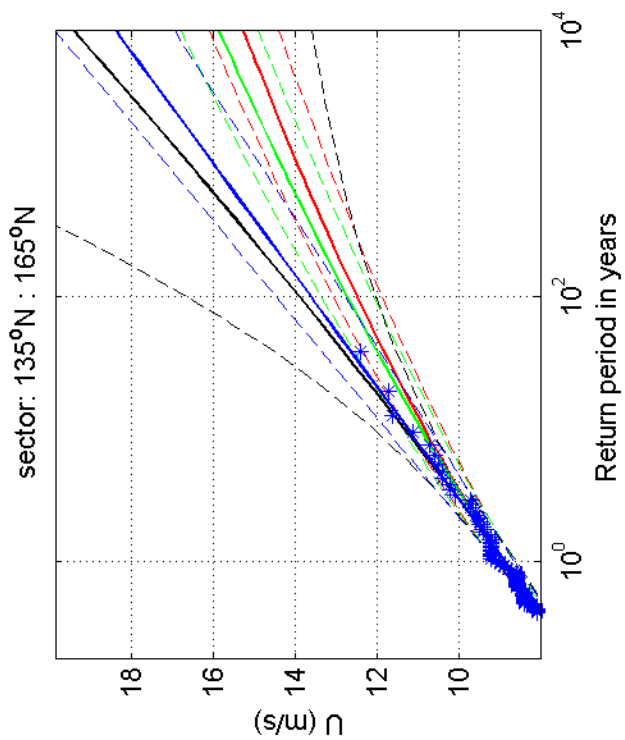
1970-2008

Gilze-Rijen

Deltares

1200264-005

Fig. F.4.350.1



Return value plot with exponential (blue) and GPD (black) fit to U ,
 exponential (red) fit to U_p^2 and exponential (green) fit to U_p^k
 Plotting positions: x_i vs $(n+1)/(\lambda(n+1-i))$

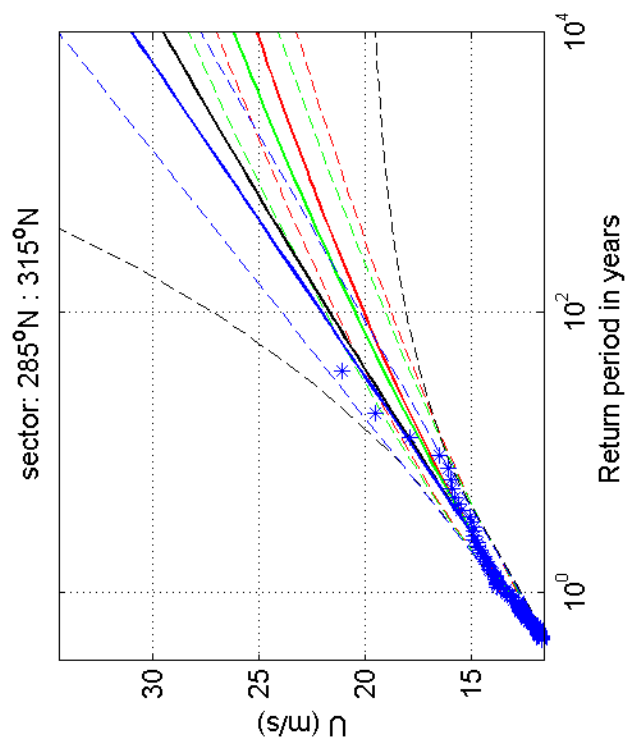
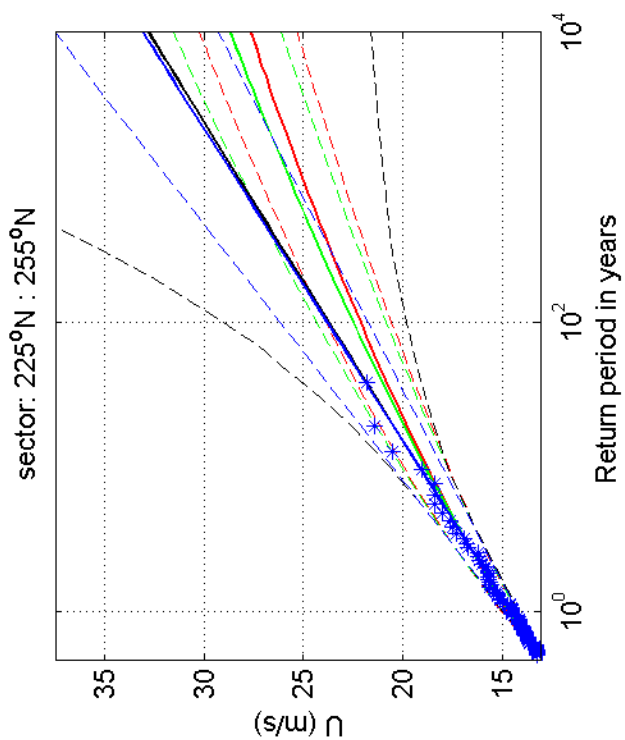
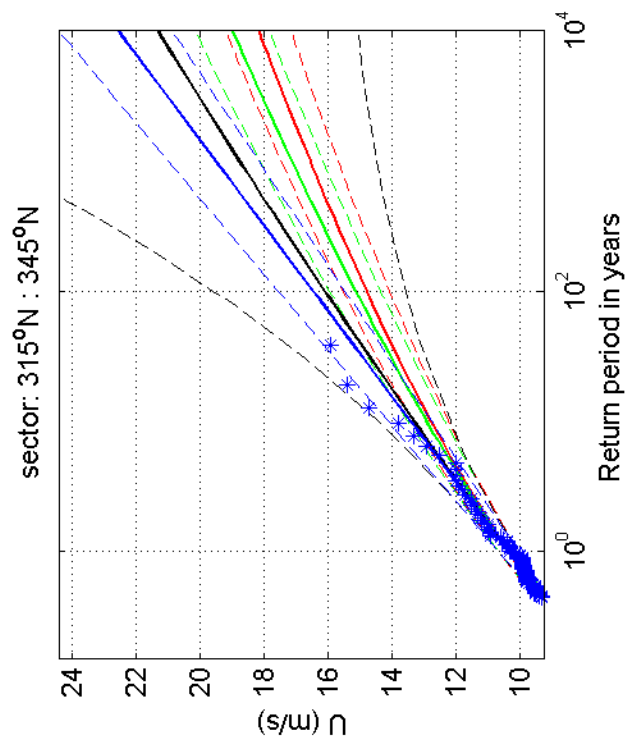
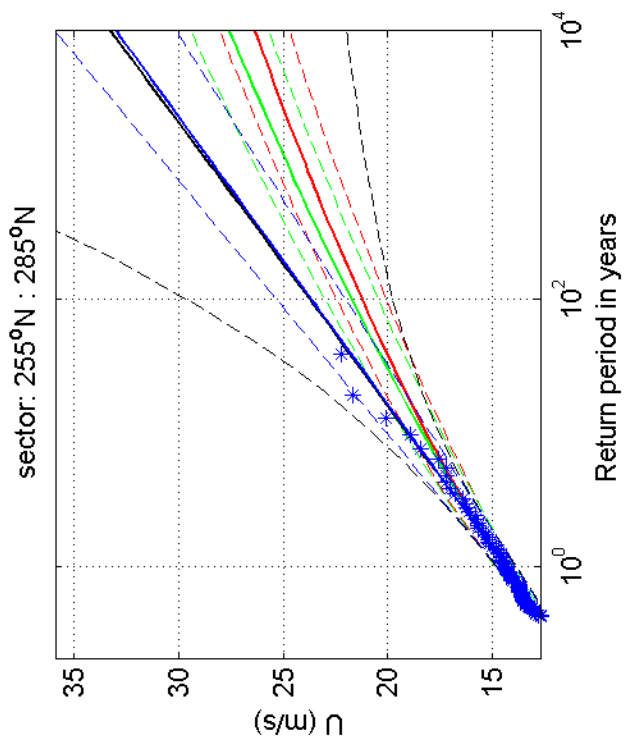
1970-2008

Gilze-Rijen

Deltares

1200264-005

Fig. F.4.350.5



Return value plot with exponential (blue) and GPD (black) fit to U ,
 exponential (red) fit to U_p^2 and exponential (green) fit to U_p^k
 Plotting positions: x_i vs $(n+1)/(\lambda(n+1-i))$

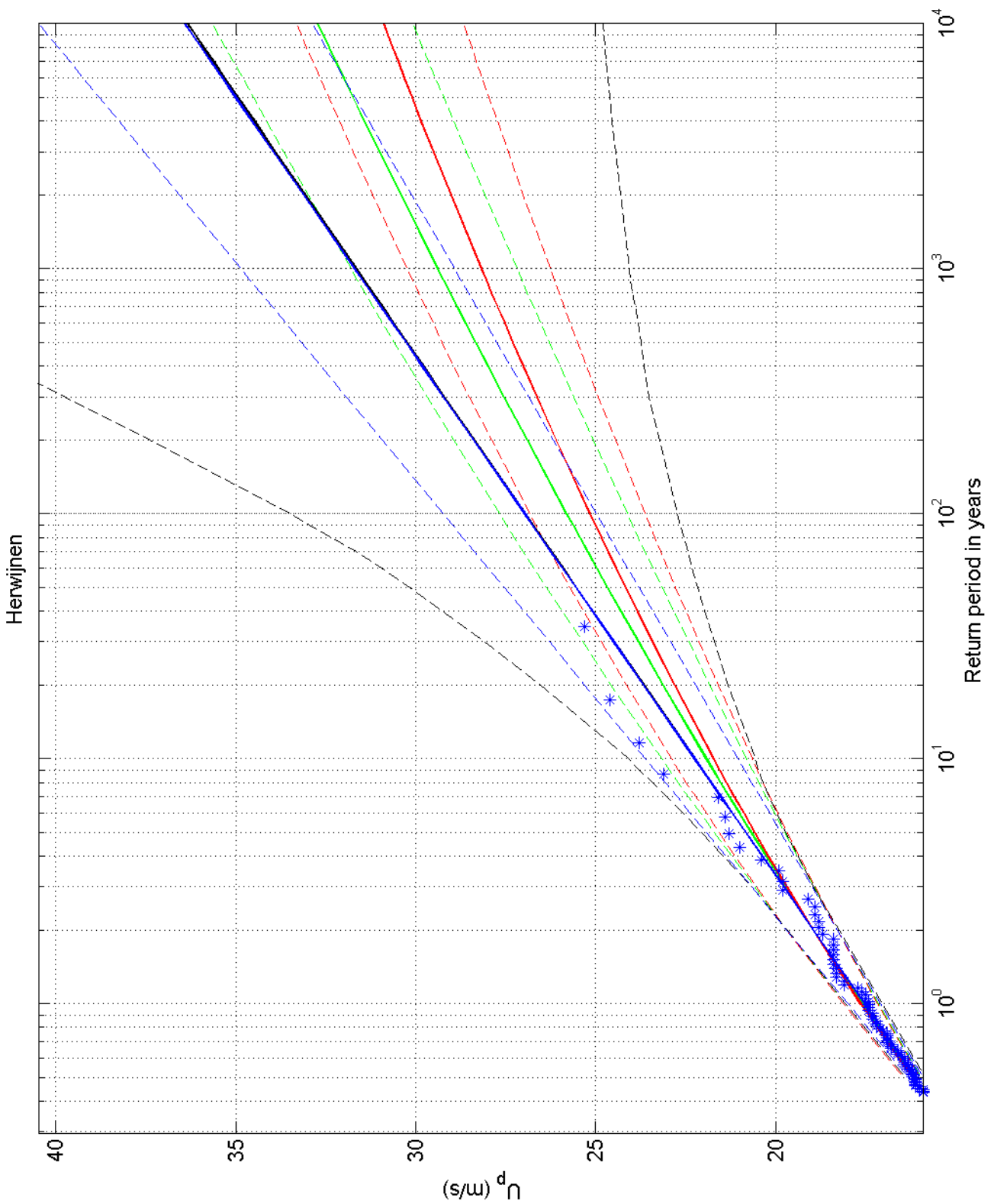
1970-2008

Gilze-Rijen

Deltares

1200264-005

Fig. F.4.350.9



Return value plot with exponential (blue) and GPD (black) fit to U_p ,
 exponential (red) fit to U_p^2 and exponential (green) fit to U_p^k
 Plotting positions: x_i vs $(n+1)/(\lambda(n+1-i))$

omni-directional

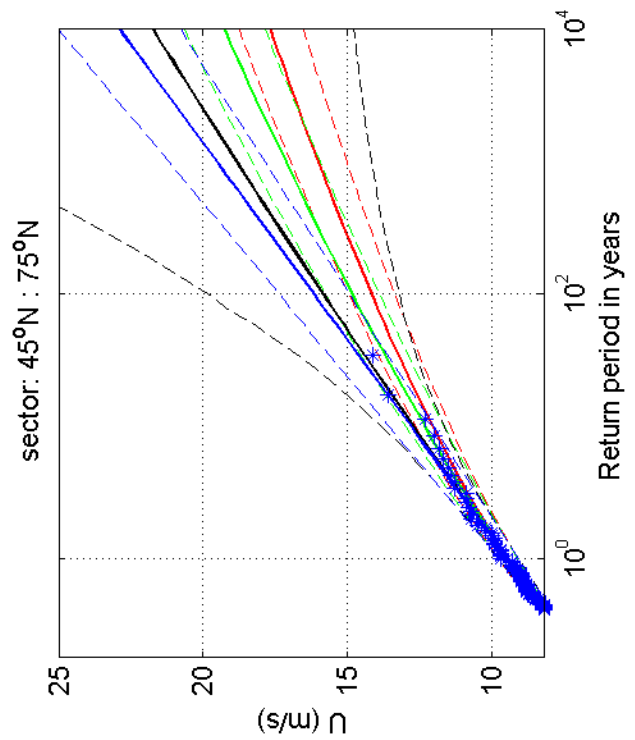
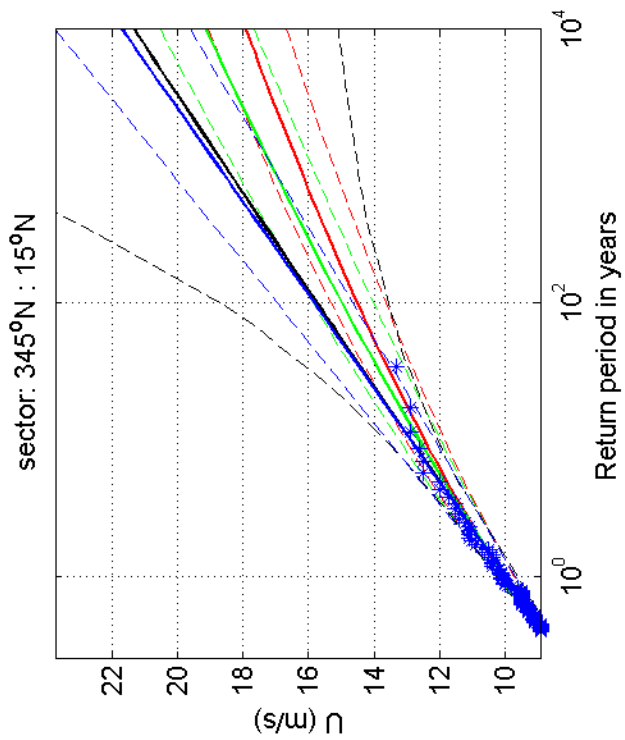
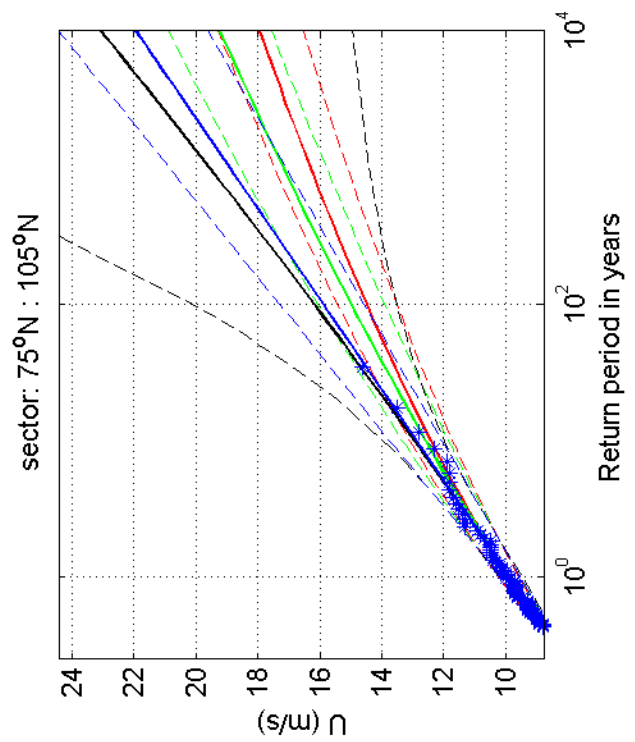
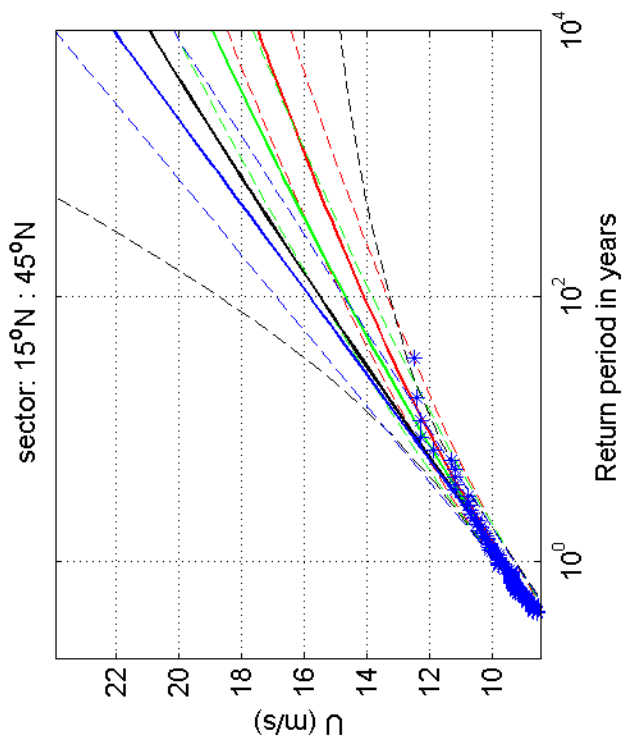
1970-2008

Herwijnen

Deltares

1200264-005

Fig. F.4.356



Return value plot with exponential (blue) and GPD (black) fit to U ,
 exponential (red) fit to U_p^2 and exponential (green) fit to U_p^k
 Plotting positions: x_i vs $(n+1)/(\lambda(n+1-i))$

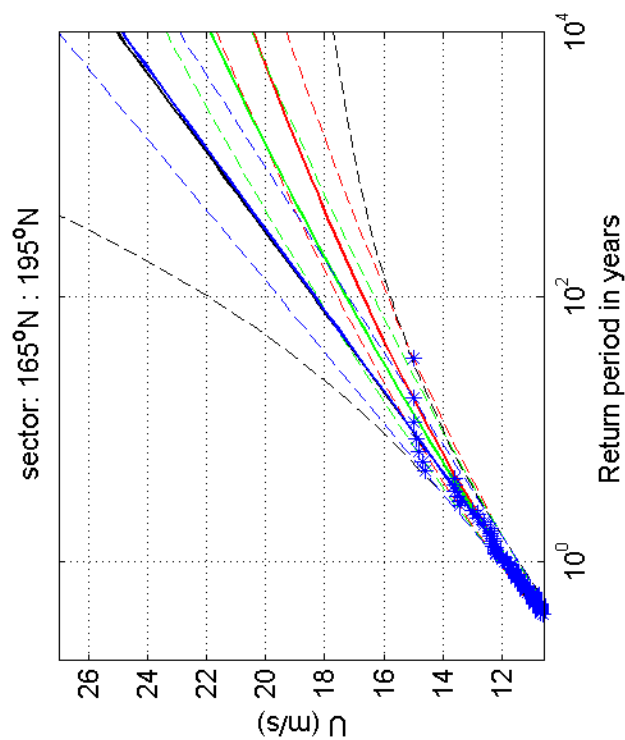
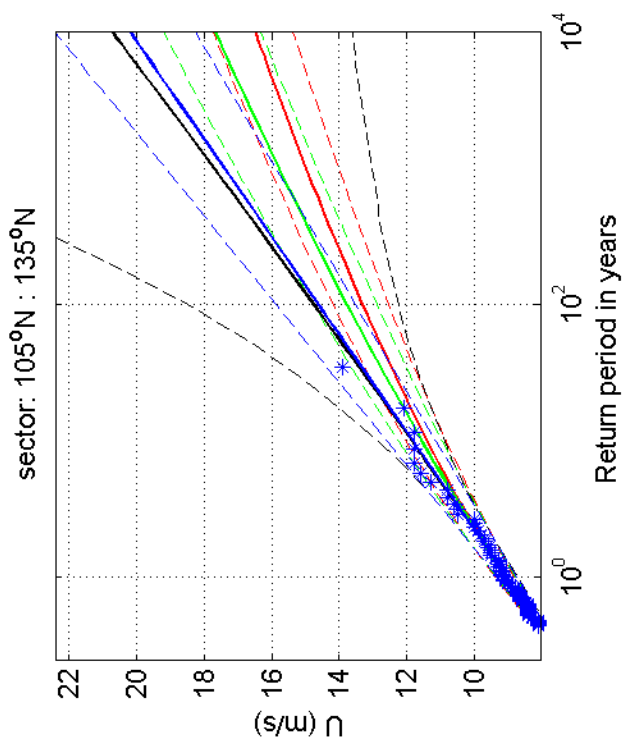
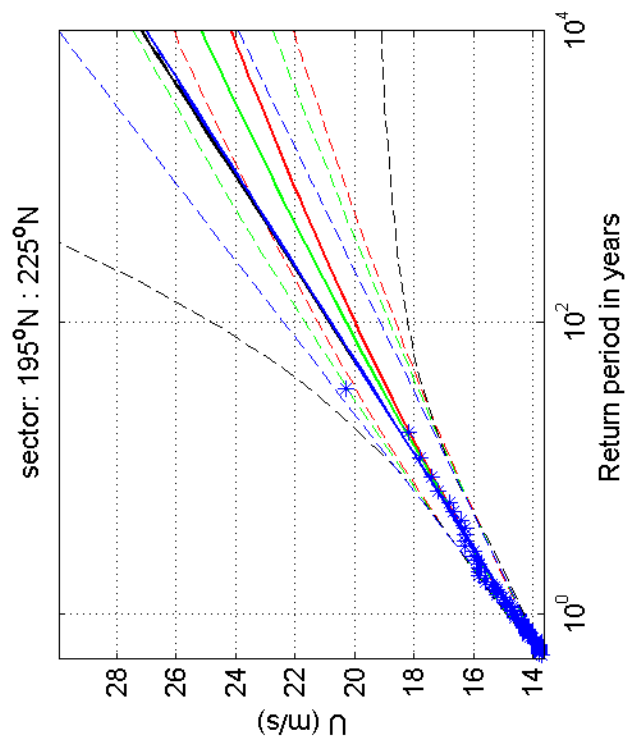
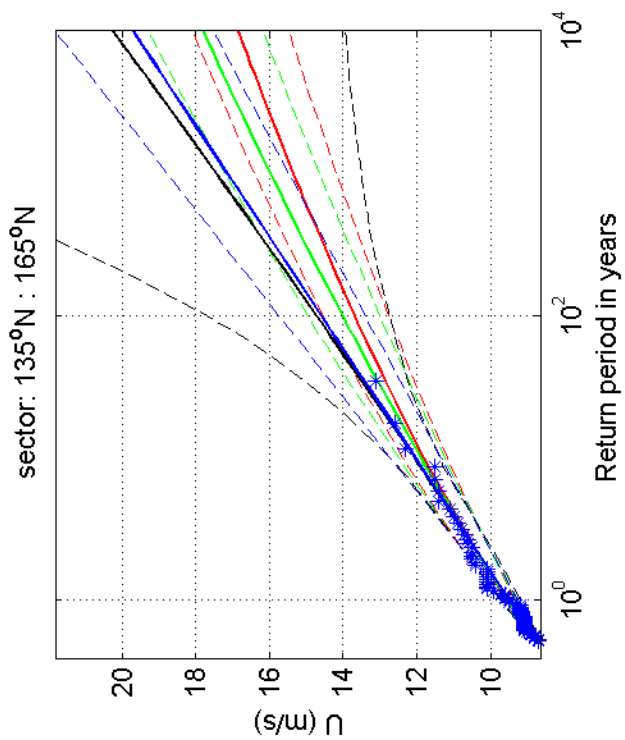
1970-2008

Herwijnen

Deltares

1200264-005

Fig. F.4.356.1



Return value plot with exponential (blue) and GPD (black) fit to U ,
 exponential (red) fit to U_p^2 and exponential (green) fit to U_p^k
 Plotting positions: x_i vs $(n+1)/(\lambda(n+1-i))$

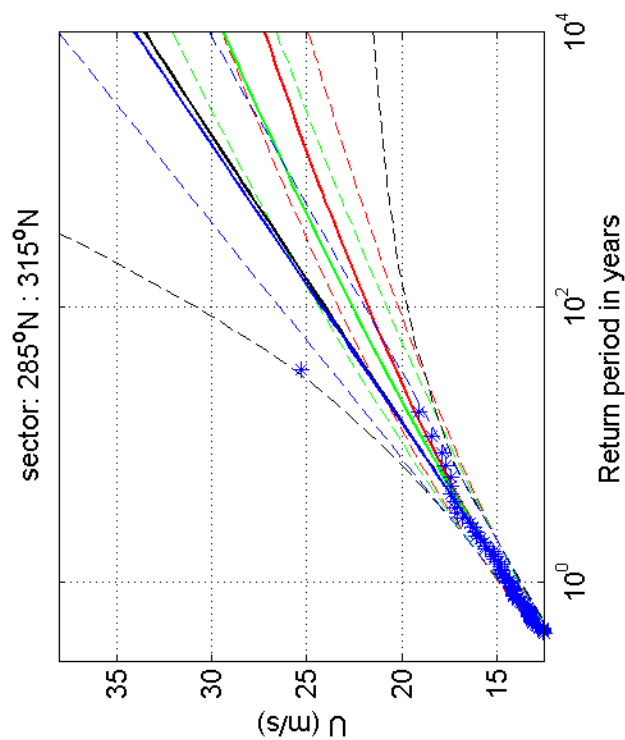
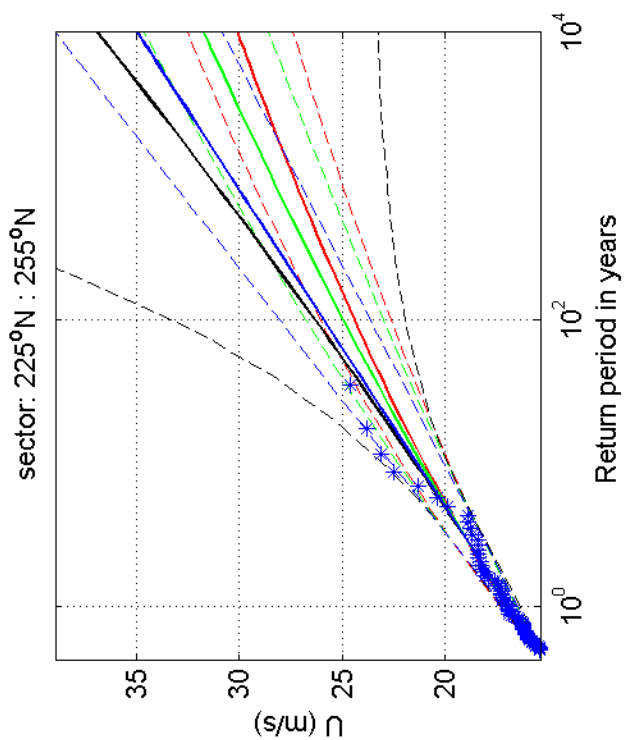
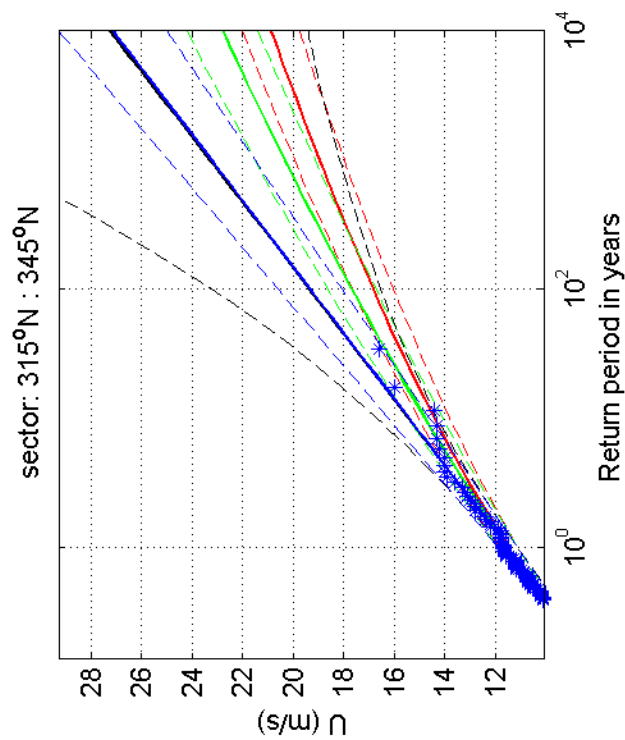
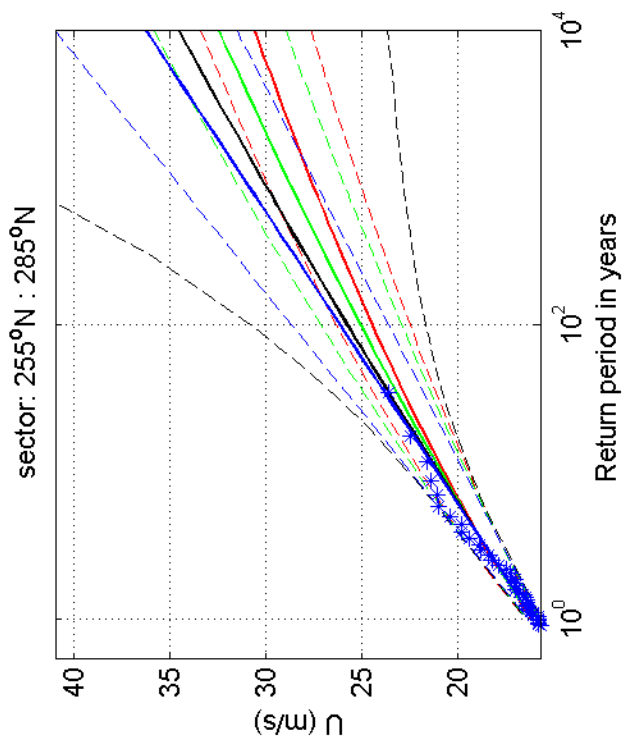
1970-2008

Herwijnen

Deltares

1200264-005

Fig. F.4.356.5



Return value plot with exponential (blue) and GPD (black) fit to U ,
 exponential (red) fit to U_p^2 and exponential (green) fit to U_p^k
 Plotting positions: x_i vs $(n+1)/(\lambda(n+1-i))$

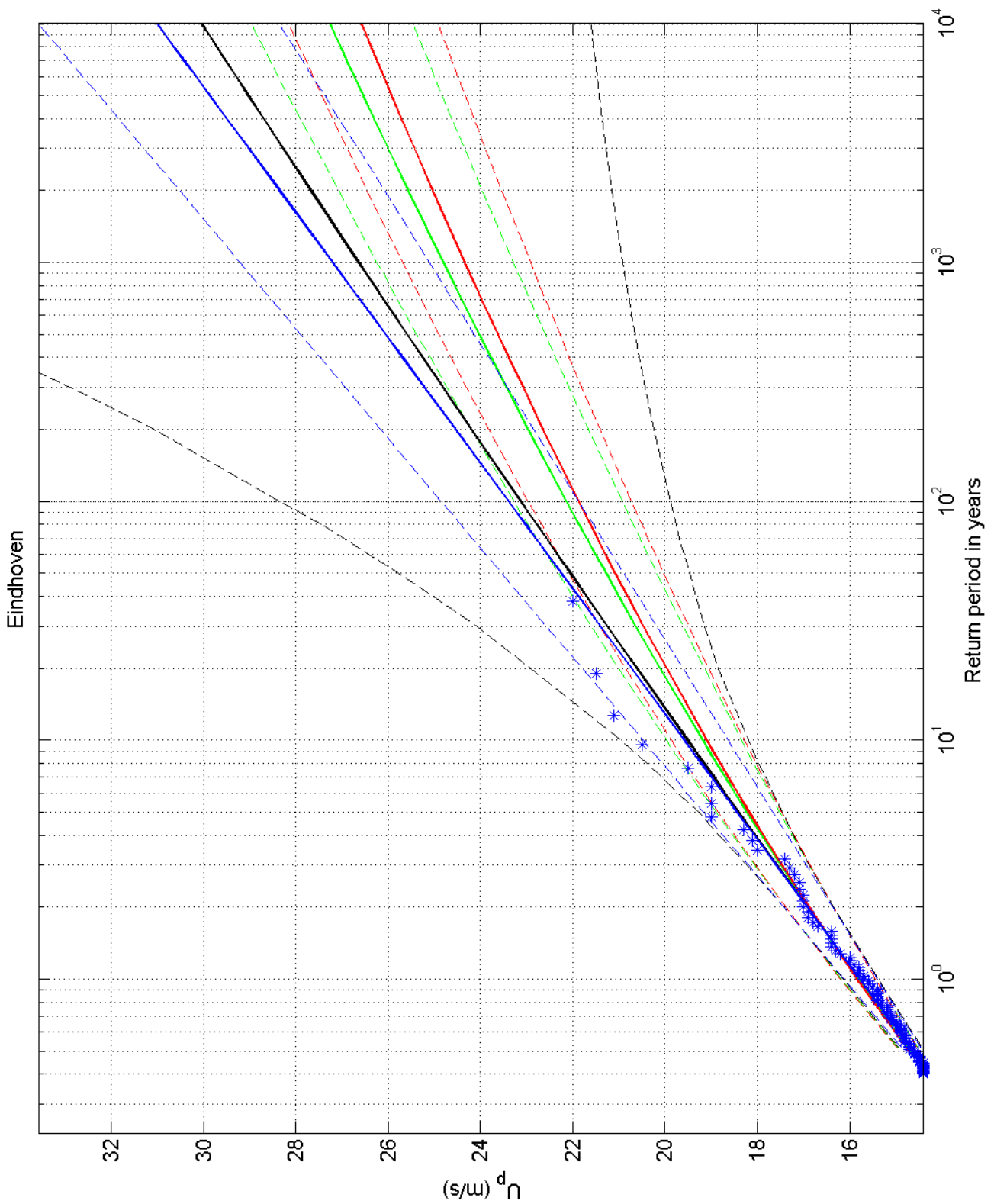
1970-2008

Herwijnen

Deltares

1200264-005

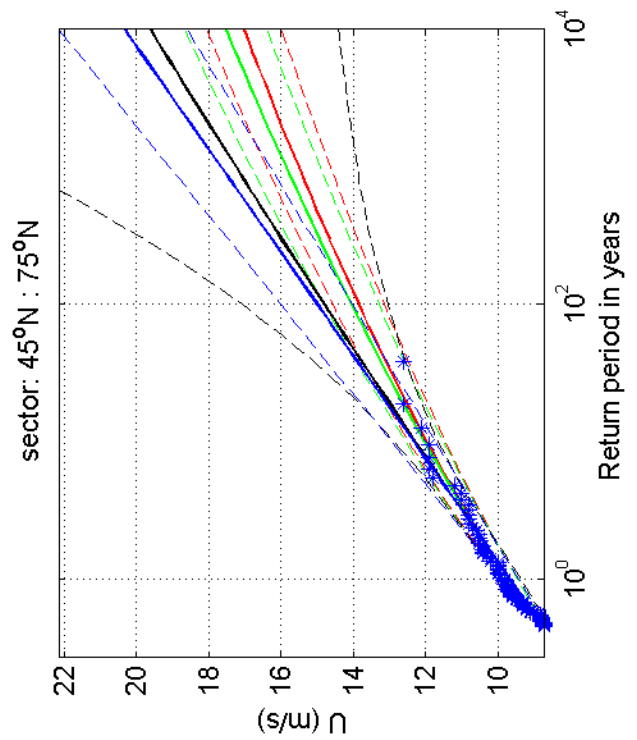
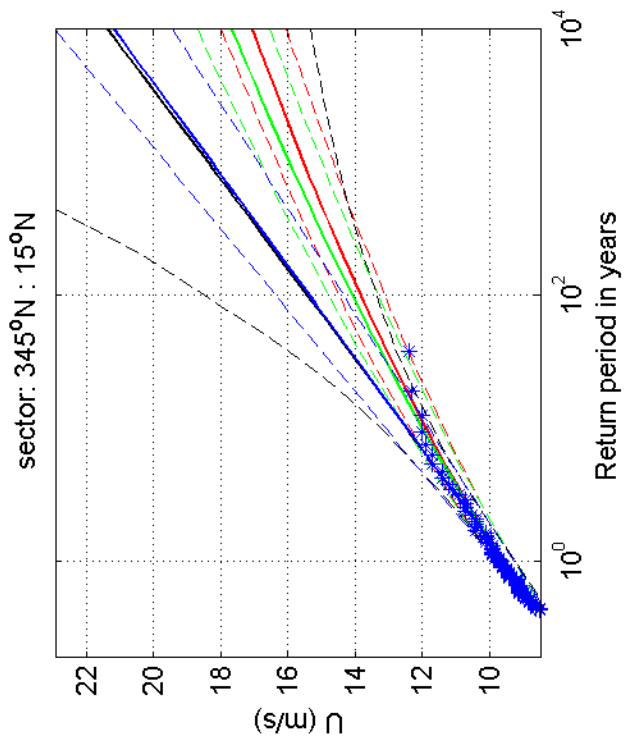
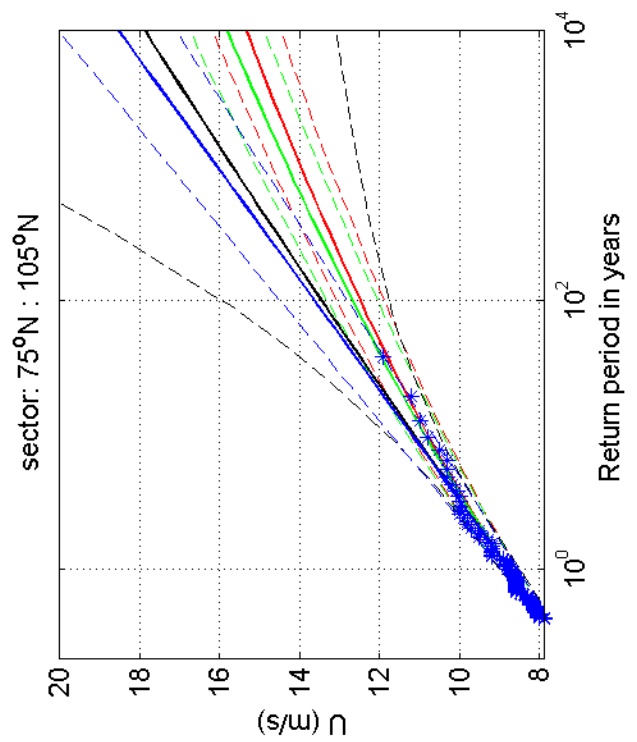
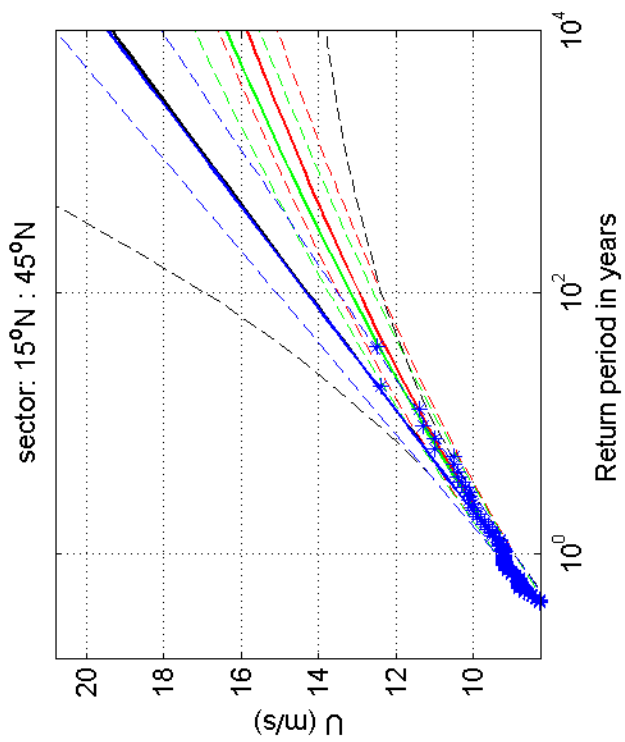
Fig. F.4.356.9



Return value plot with exponential (blue) and GPD (black) fit to U_p ,
 exponential (red) fit to U_p^2 and exponential (green) fit to U_p^k
 Plotting positions: x_i vs $(n+1)/(\lambda(n+1-i))$

omni-directional	1970-2008
Eindhoven	
1200264-005	Fig. F.4.370

Deltares



Return value plot with exponential (blue) and GPD (black) fit to U ,
 exponential (red) fit to U_p^k and exponential (green) fit to U_p^k
 Plotting positions: x_i vs $(n+1)/(\lambda(n+1-i))$

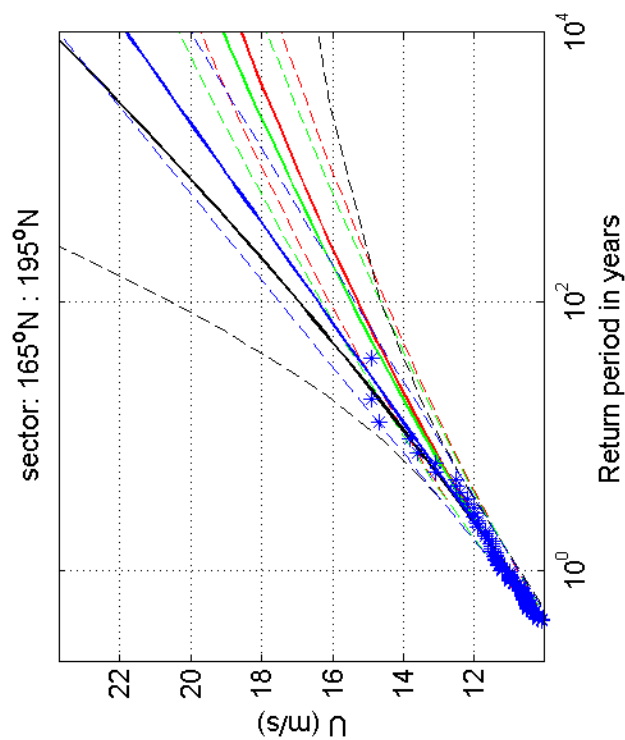
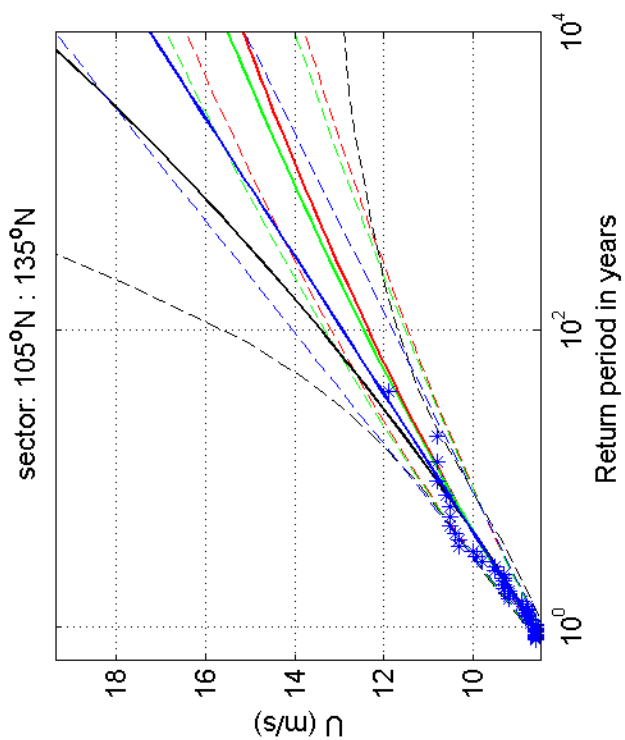
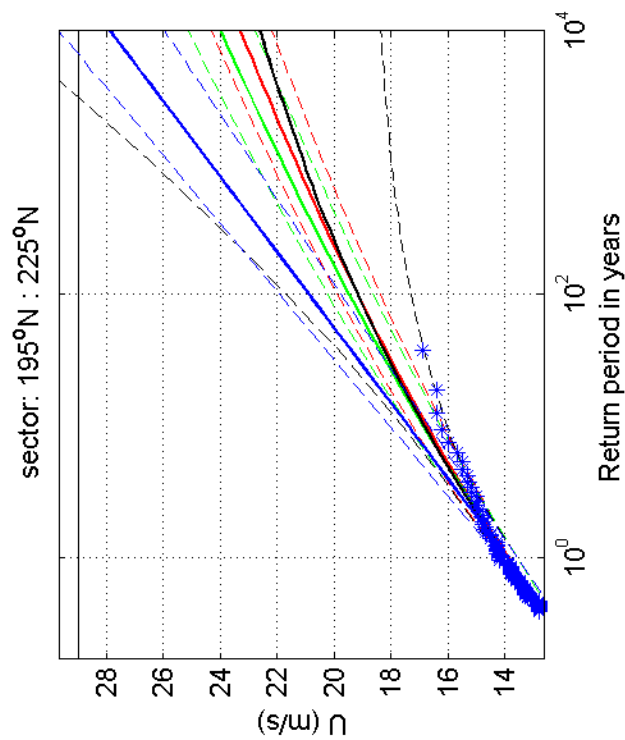
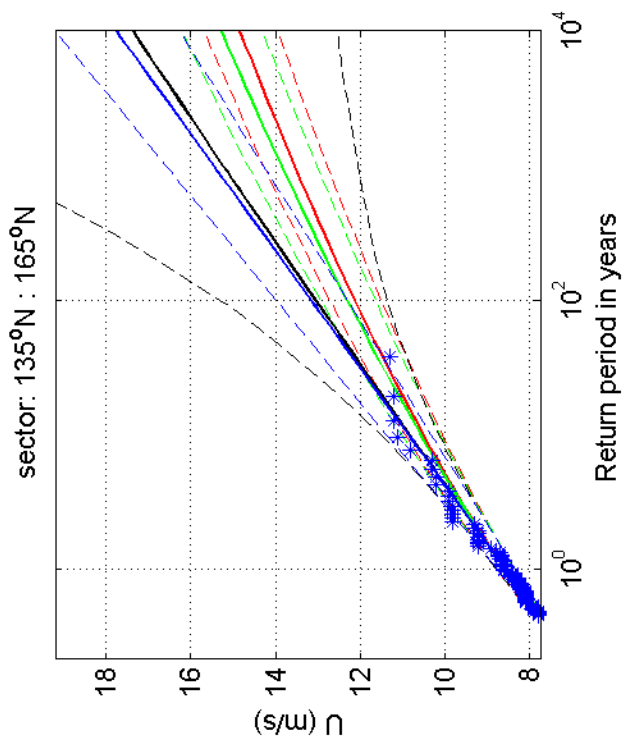
1970-2008

Eindhoven

Deltares

1200264-005

Fig. F.4.370.1



Return value plot with exponential (blue) and GPD (black) fit to U ,
 exponential (red) fit to U_p^2 and exponential (green) fit to U_p^k
 Plotting positions: x_i vs $(n+1)/(\lambda(n+1-i))$

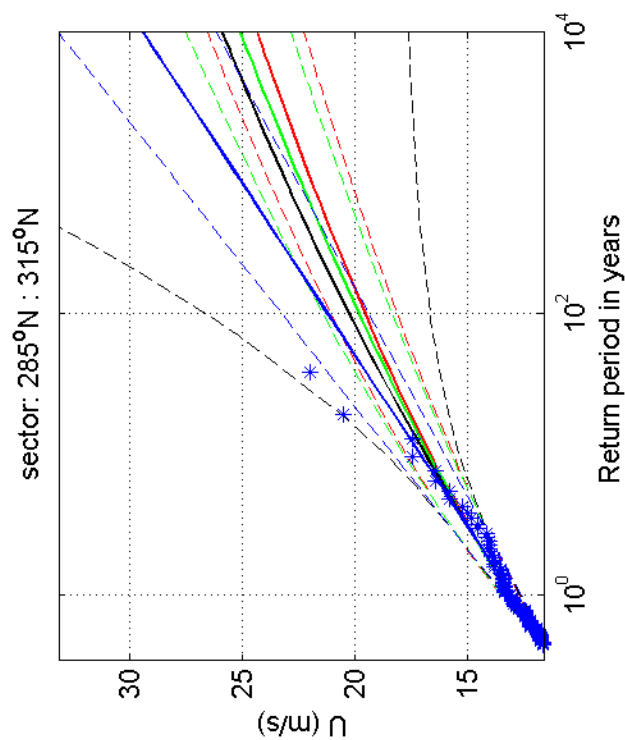
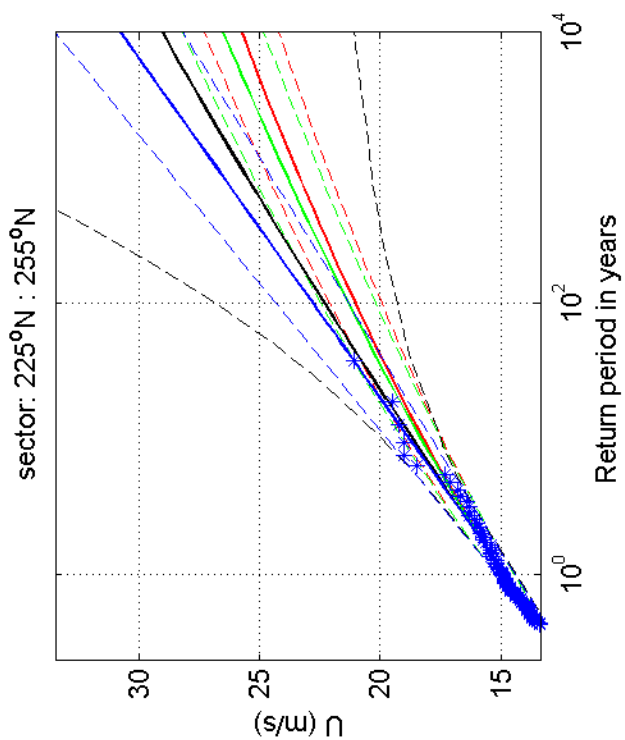
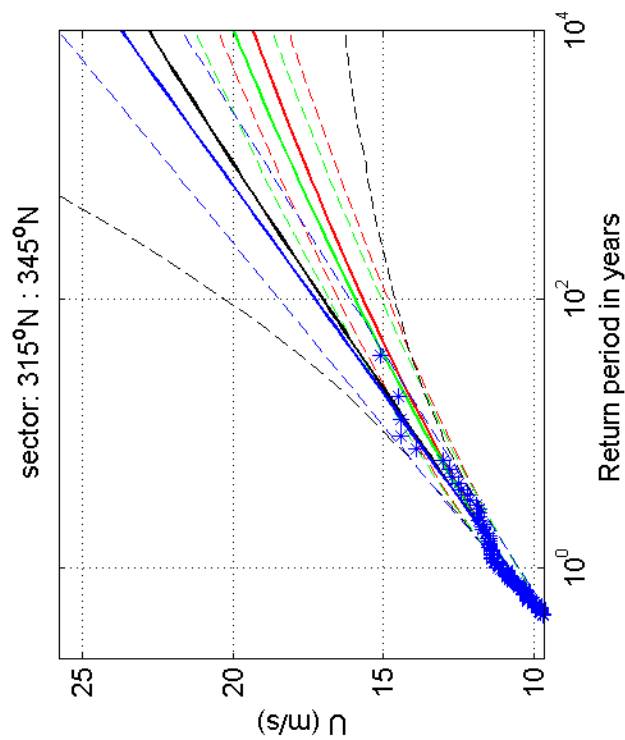
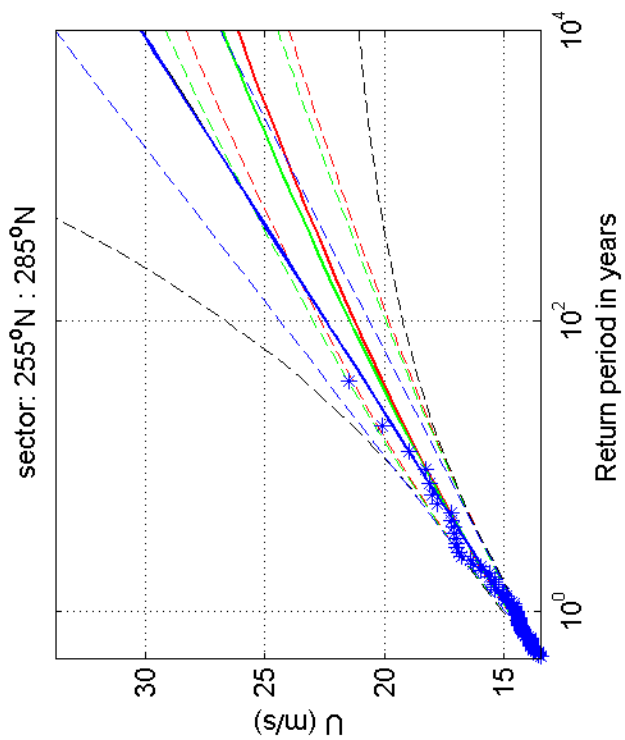
1970-2008

Eindhoven

Deltares

1200264-005

Fig. F.4.370.5



Return value plot with exponential (blue) and GPD (black) fit to U ,
 exponential (red) fit to U_p^2 and exponential (green) fit to U_p^k
 Plotting positions: x_i vs $(n+1)/(\lambda(n+1-i))$

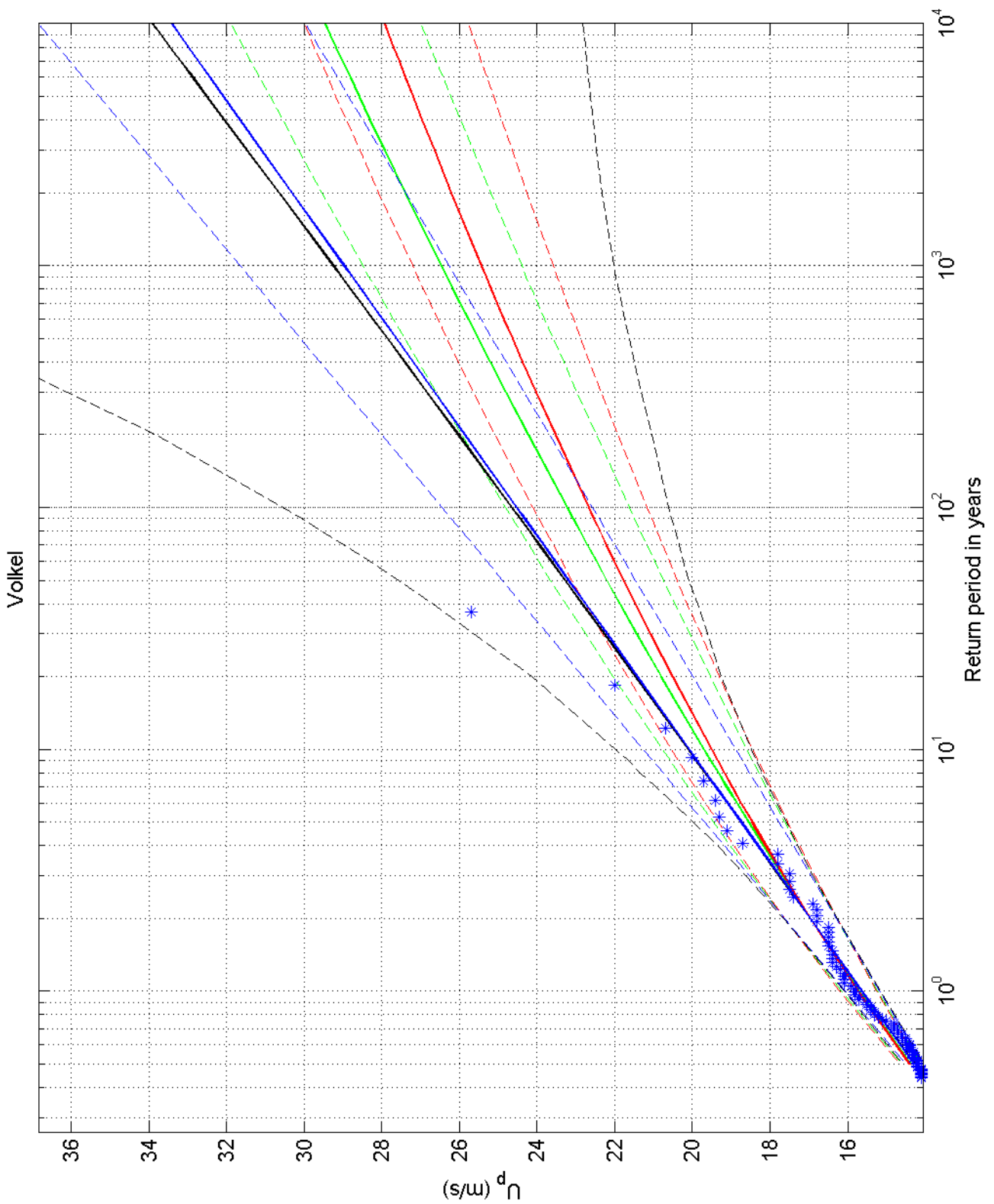
1970-2008

Eindhoven

Deltares

1200264-005

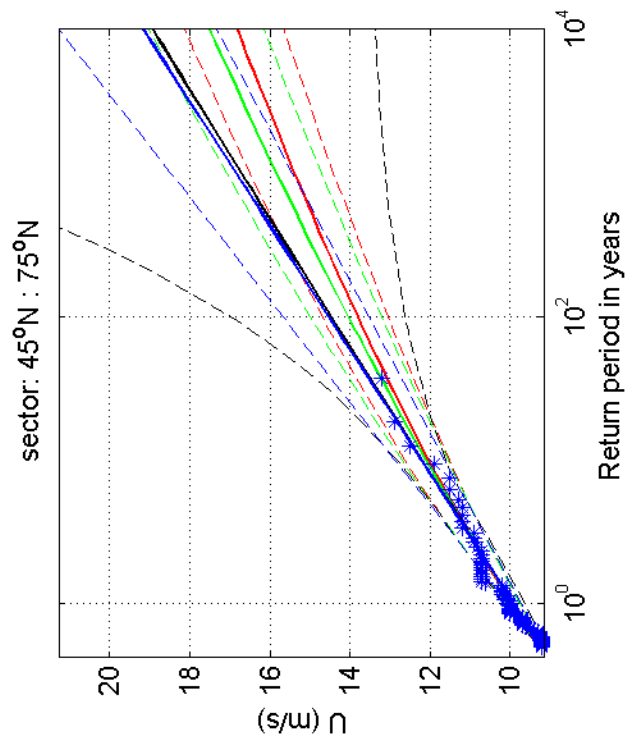
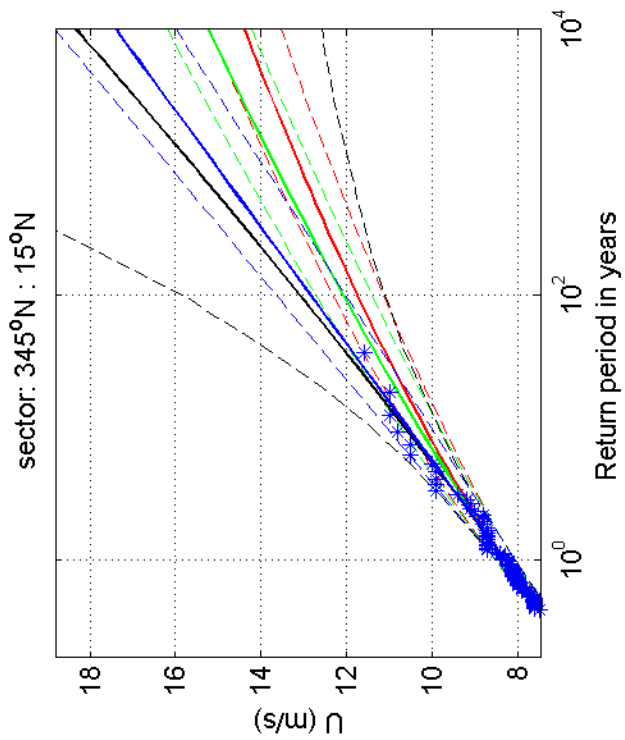
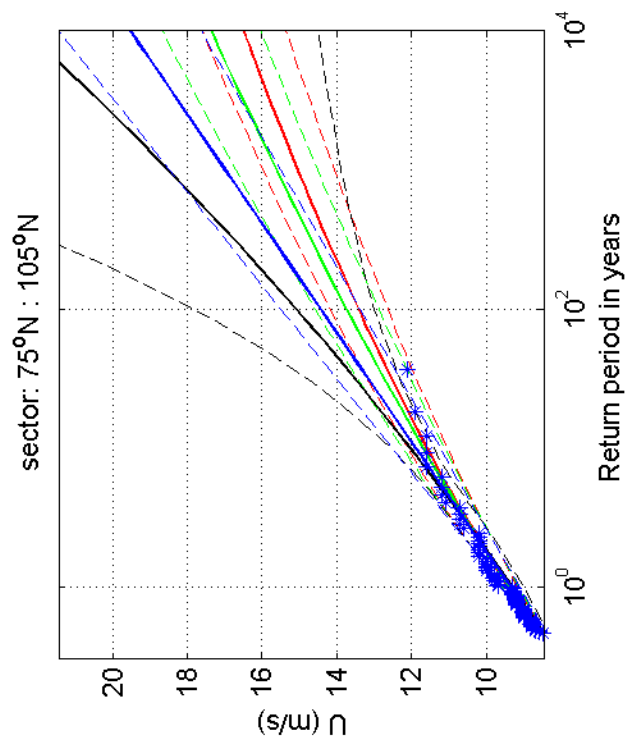
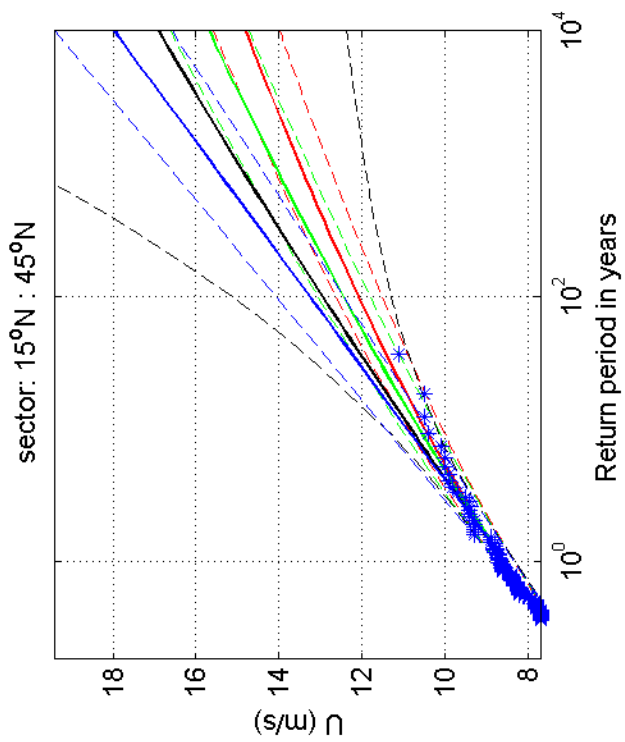
Fig. F.4.370.9



Return value plot with exponential (blue) and GPD (black) fit to U_p ,
 exponential (red) fit to U_p^2 and exponential (green) fit to U_p^k
 Plotting positions: x_i vs $(n+1)/(\lambda(n+1-i))$

omni-directional	1970-2008
Volkel	
1200264-005	Fig. F.4.375

Deltares



Return value plot with exponential (blue) and GPD (black) fit to U ,
 exponential (red) fit to U_p^2 and exponential (green) fit to U_p^k
 Plotting positions: x_i vs $(n+1)/(\lambda(n+1-i))$

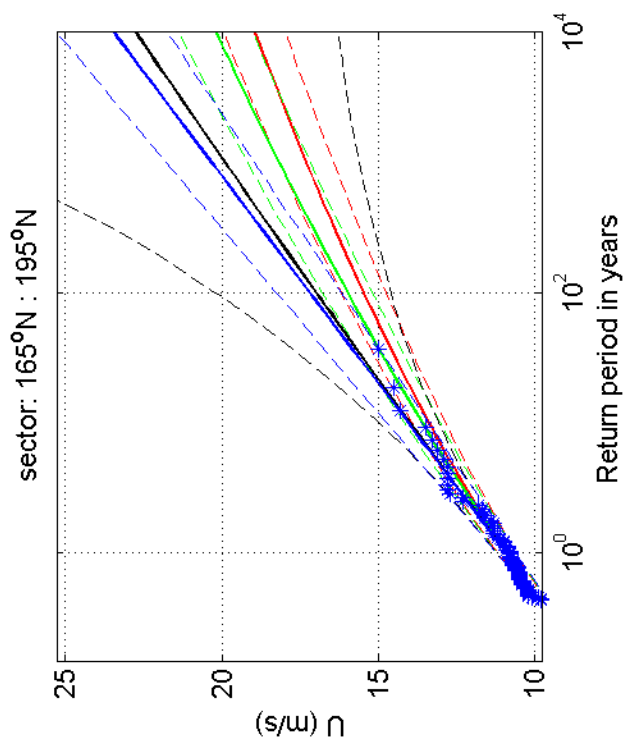
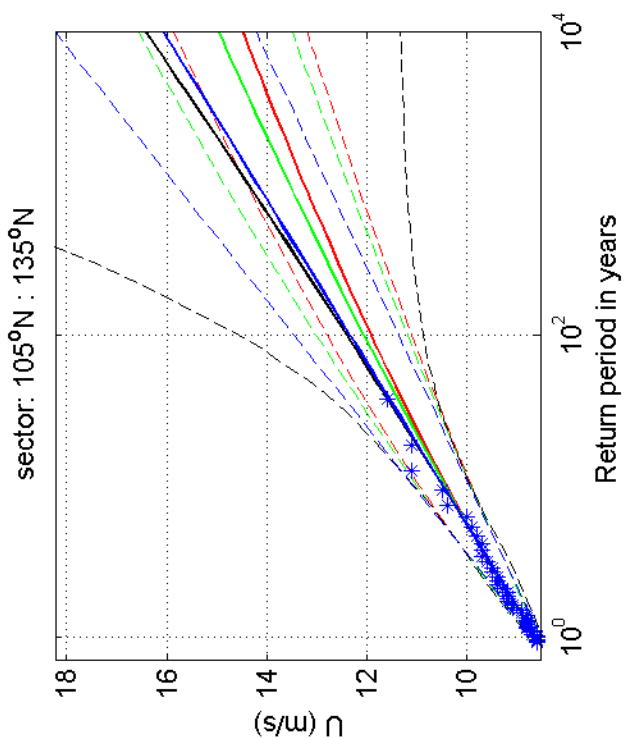
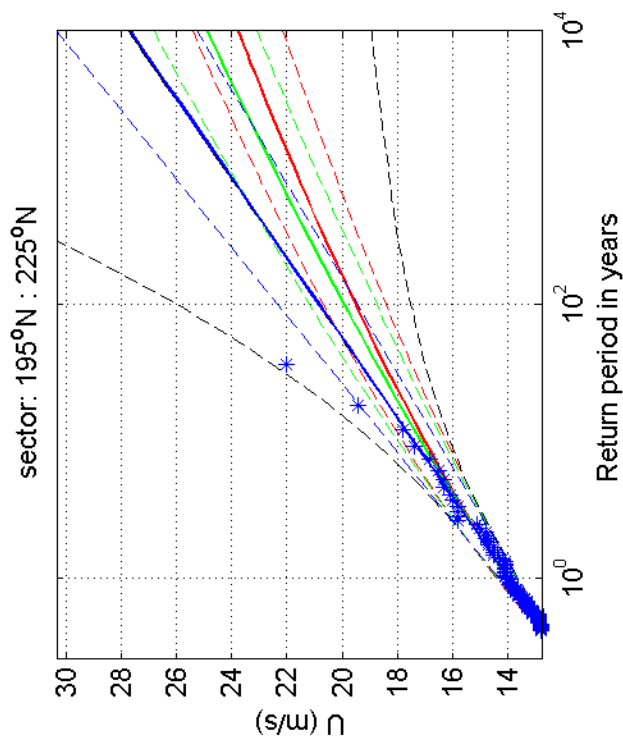
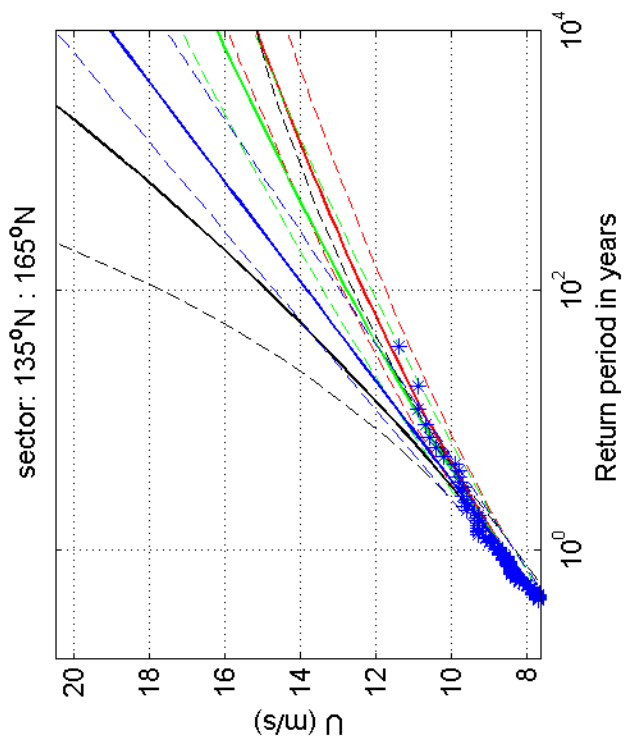
1970-2008

Volkel

Deltares

1200264-005

Fig. F.4.375.1



Return value plot with exponential (blue) and GPD (black) fit to U ,
 exponential (red) fit to U_p^2 and exponential (green) fit to U_p^k
 Plotting positions: x_i vs $(n+1)/(\lambda(n+1-i))$

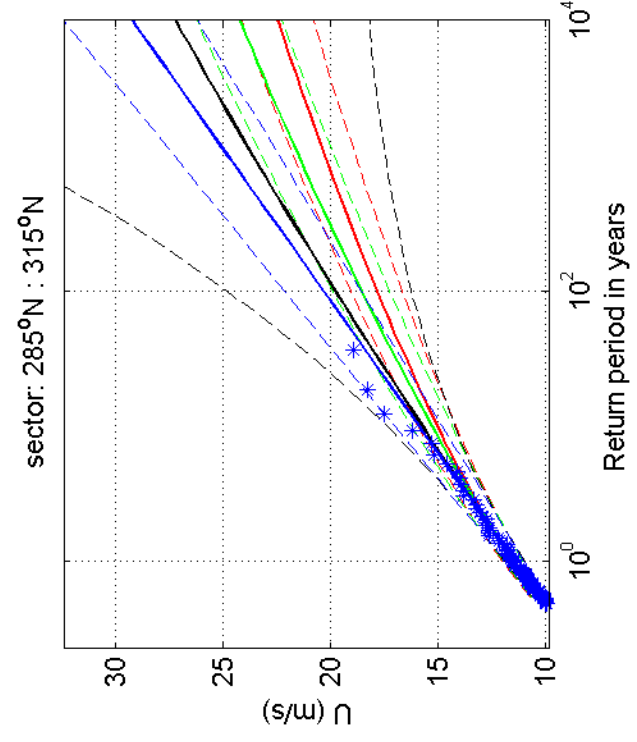
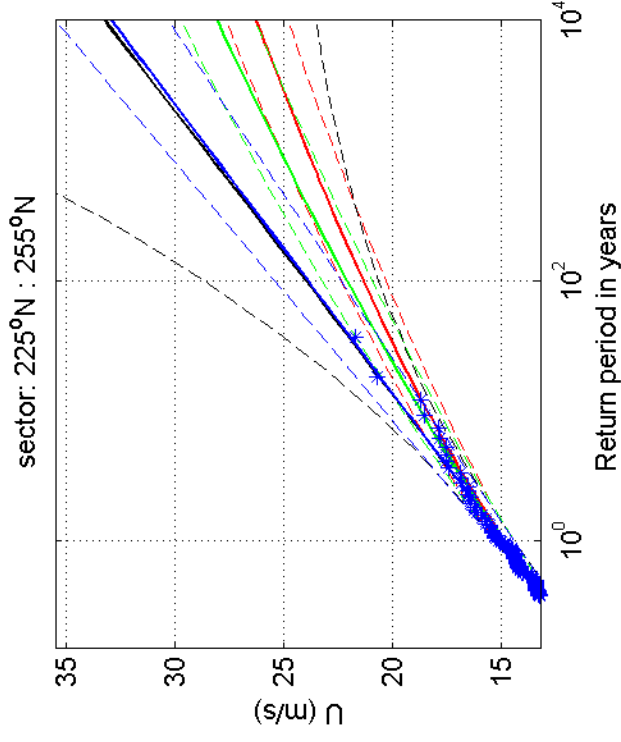
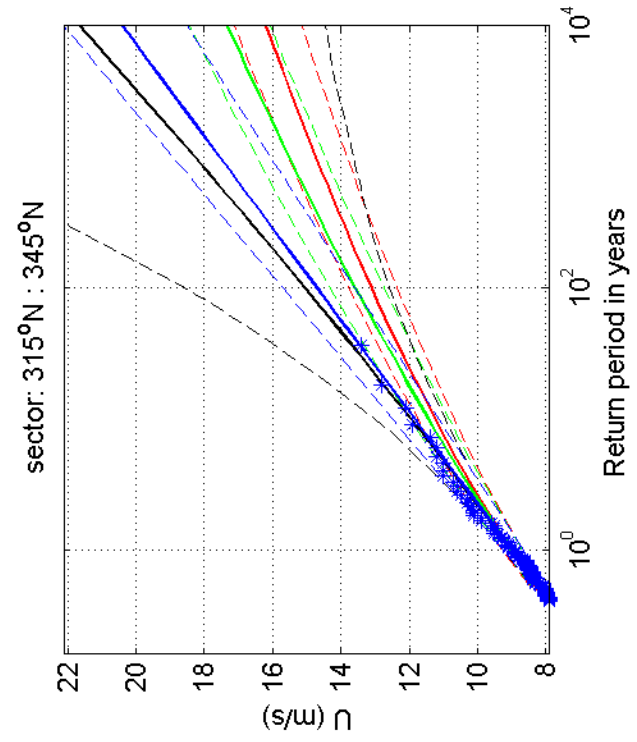
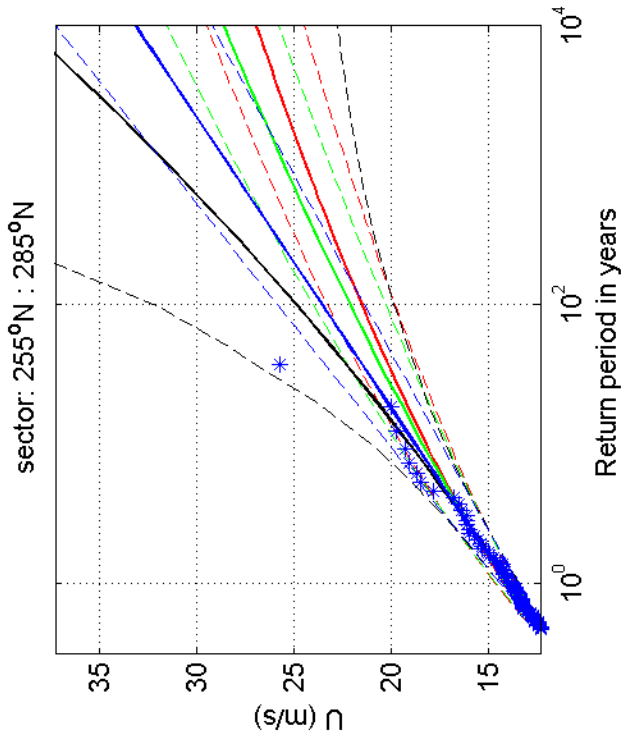
1970-2008

Volkel

Deltares

1200264-005

Fig. F.4.375.5



Return value plot with exponential (blue) and GPD (black) fit to U , exponential (red) fit to U_p^2 and exponential (green) fit to U_p^k
 Plotting positions: x_i vs $(n+1)/(\lambda(n+1-i))$

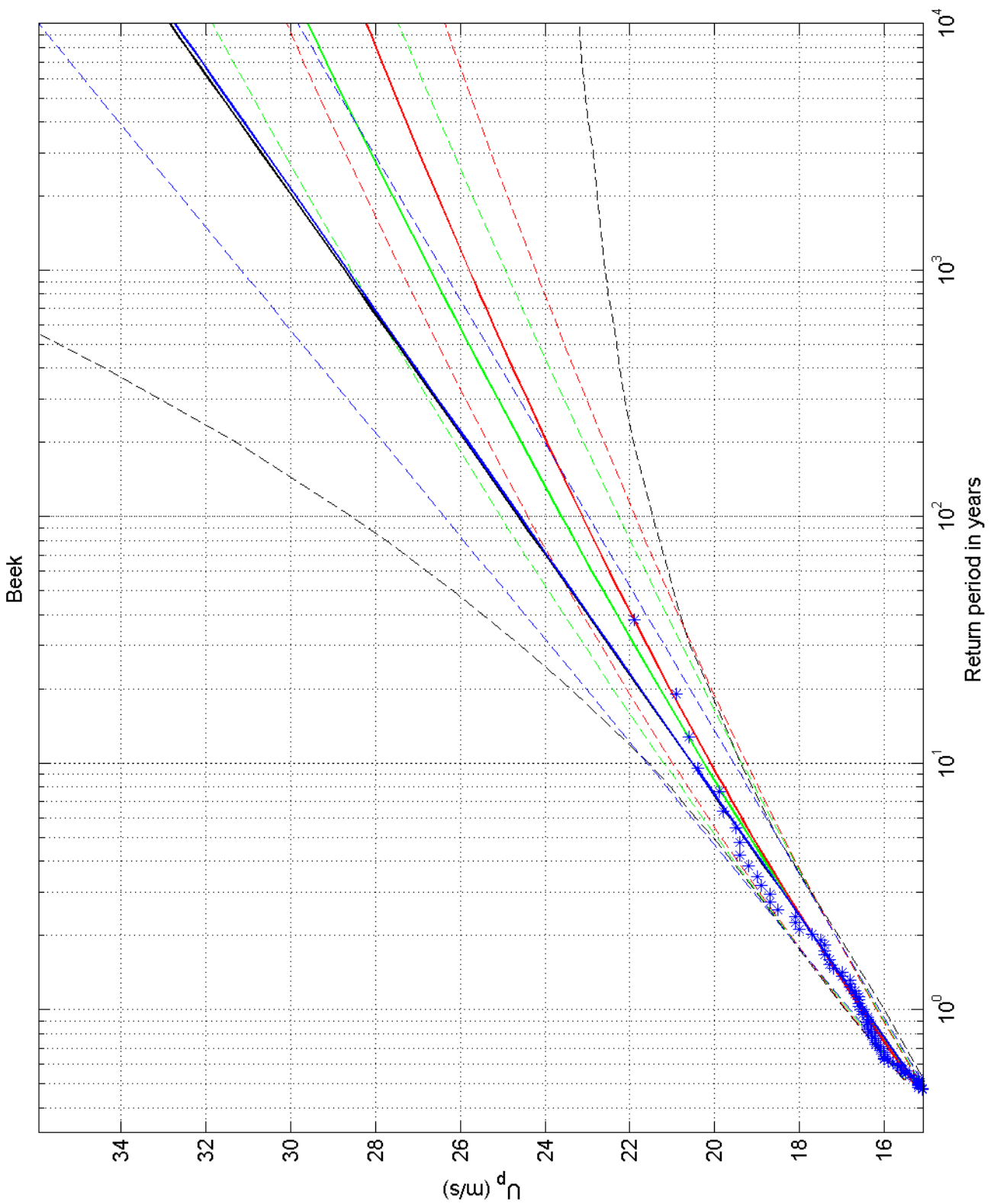
1970-2008

Volkel

Deltares

1200264-005

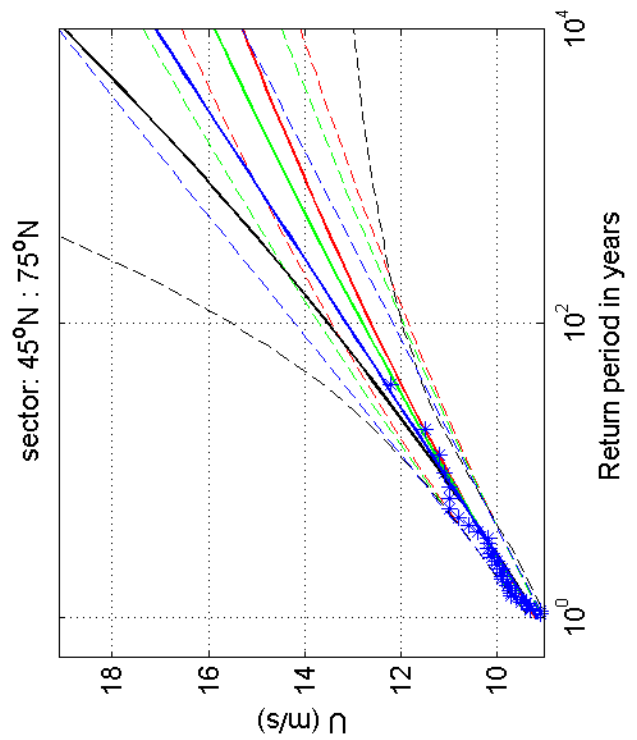
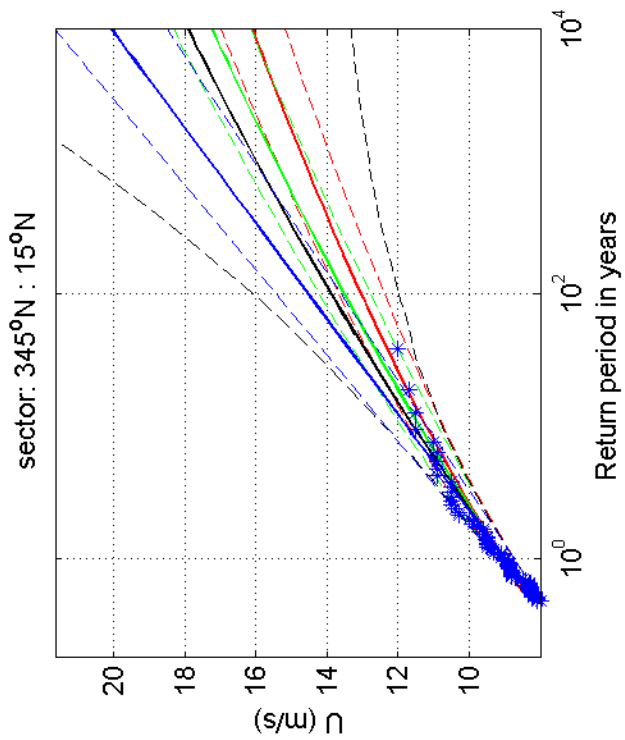
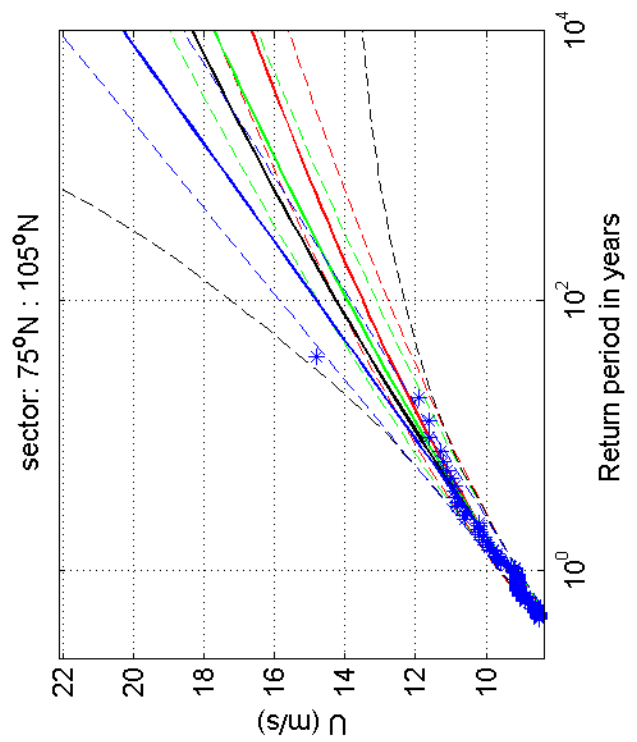
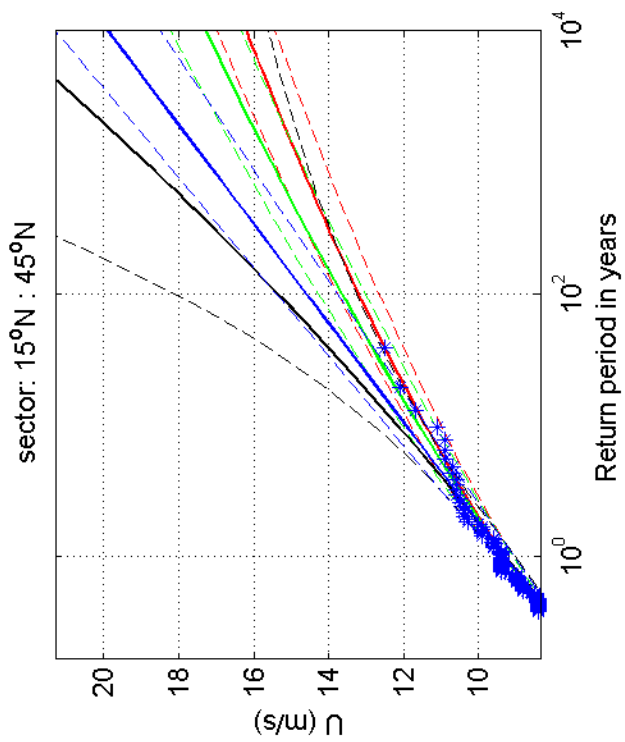
Fig. F.4.375.9



Return value plot with exponential (blue) and GPD (black) fit to U_p ,
 exponential (red) fit to U_p^2 and exponential (green) fit to U_p^k
 Plotting positions: x_i vs $(n+1)/(\lambda(n+1-i))$

omni-directional	1970-2008
Beek	
1200264-005	Fig. F.4.380

Deltares



Return value plot with exponential (blue) and GPD (black) fit to U ,
 exponential (red) fit to U_p^2 and exponential (green) fit to U_p^k
 Plotting positions: x_i vs $(n+1)/(\lambda(n+1-i))$

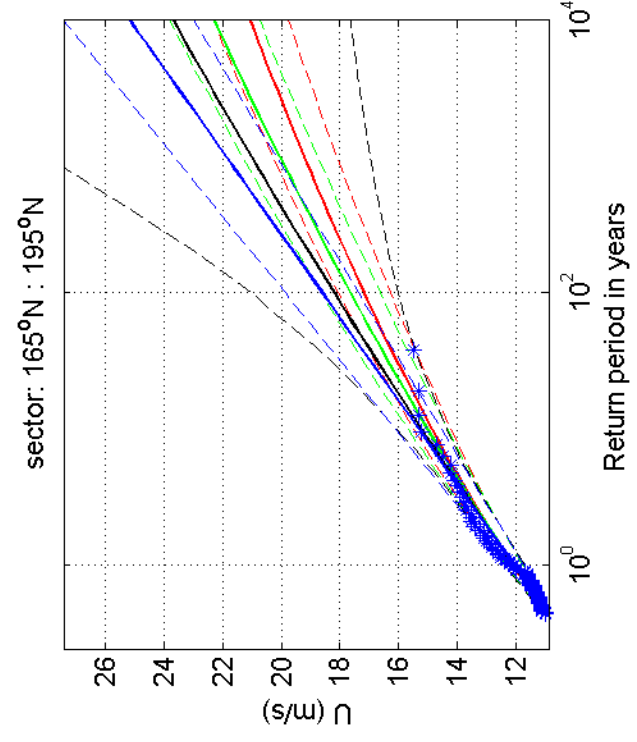
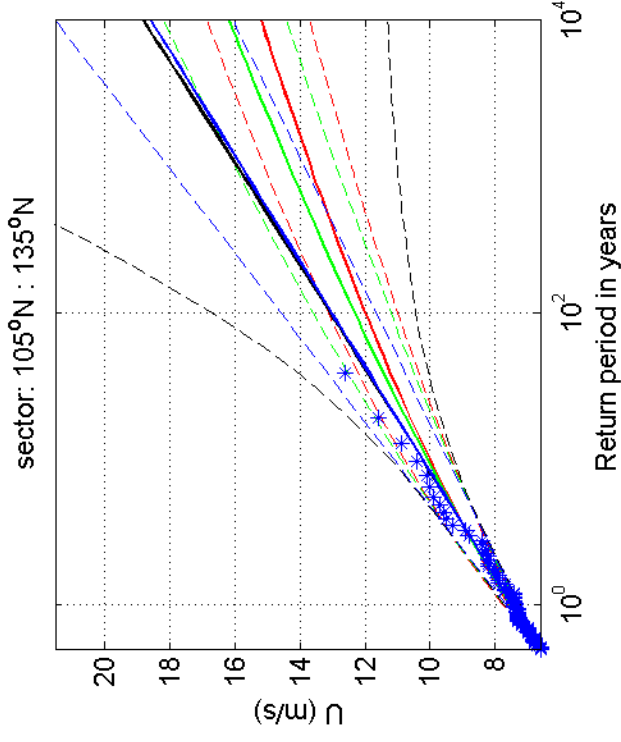
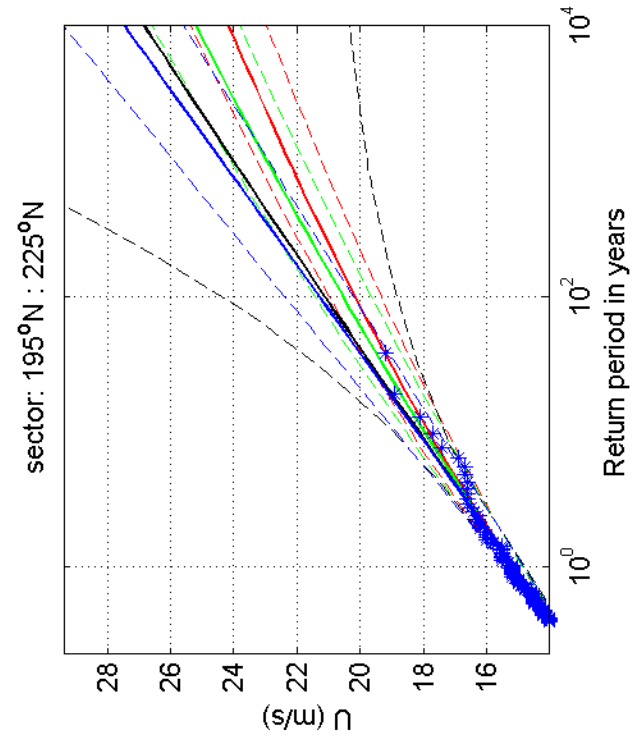
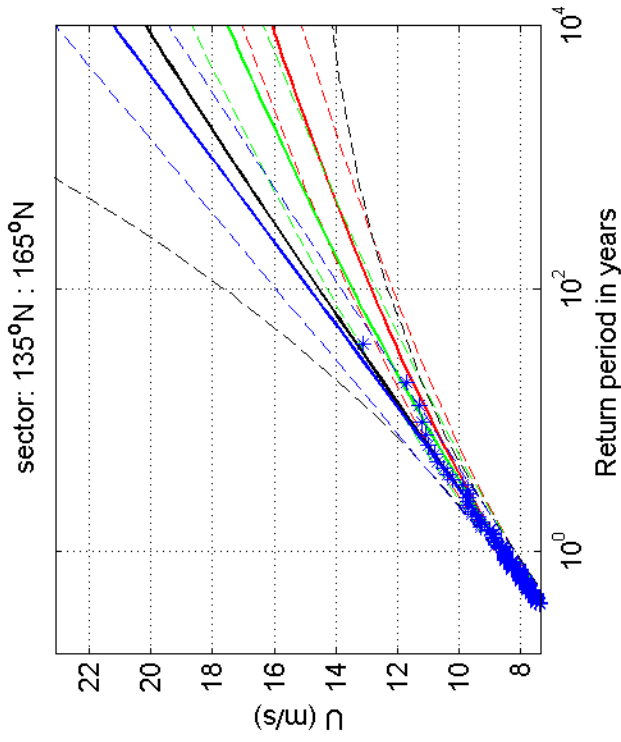
1970-2008

Beek

Deltares

1200264-005

Fig. F.4.380.1



Return value plot with exponential (blue) and GPD (black) fit to U , exponential (red) fit to U_p^2 and exponential (green) fit to U_p^k
 Plotting positions: x_i vs $(n+1)/(\lambda(n+1-i))$

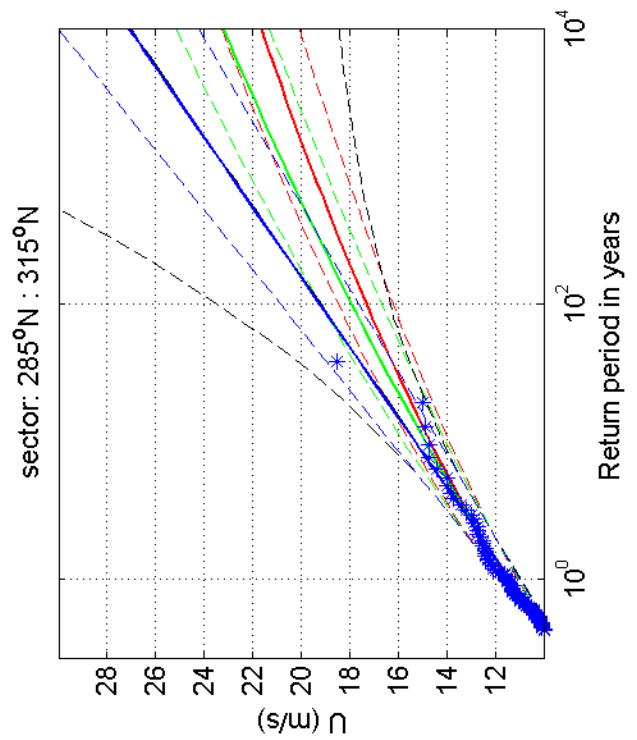
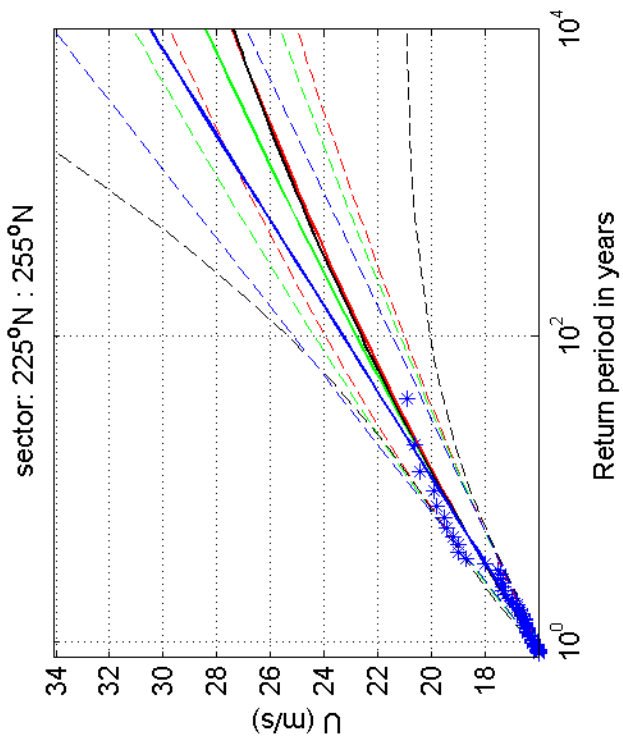
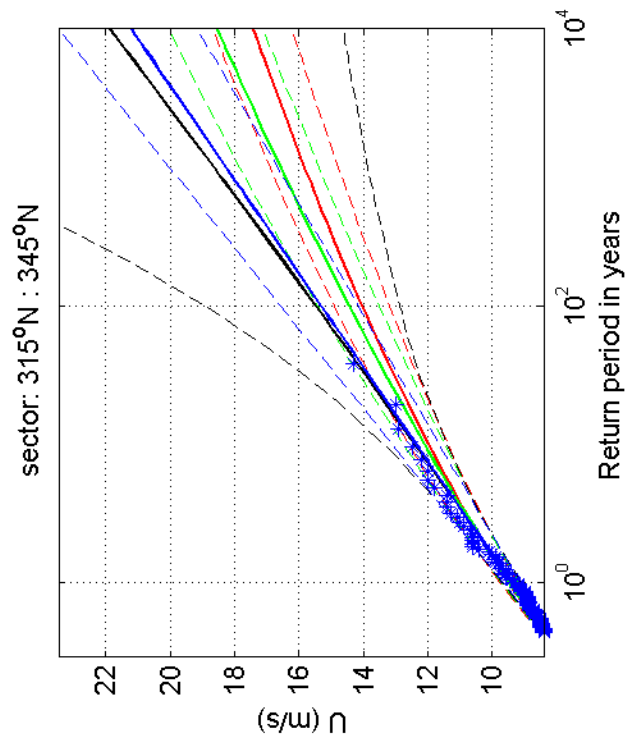
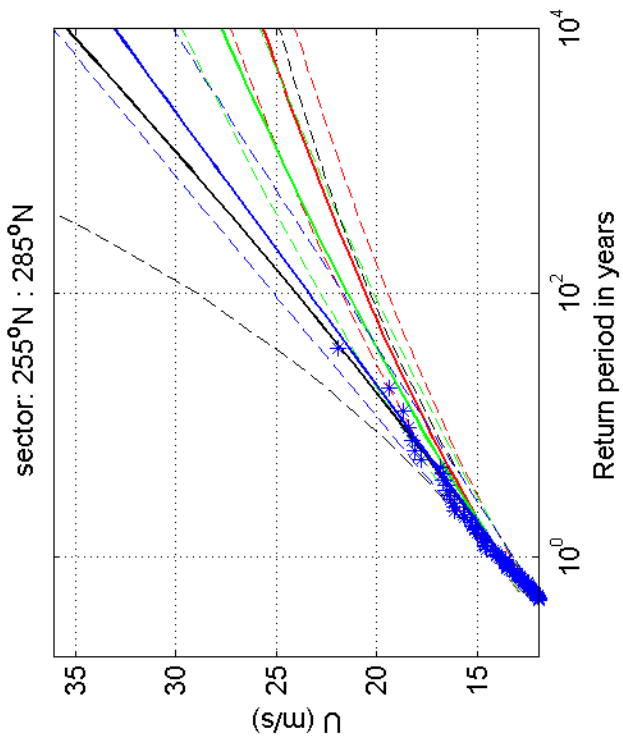
1970-2008

Beek

Deltares

1200264-005

Fig. F.4.380.5



Return value plot with exponential (blue) and GPD (black) fit to U ,
 exponential (red) fit to U_p^2 and exponential (green) fit to U_p^k
 Plotting positions: x_i vs $(n+1)/(\lambda(n+1-i))$

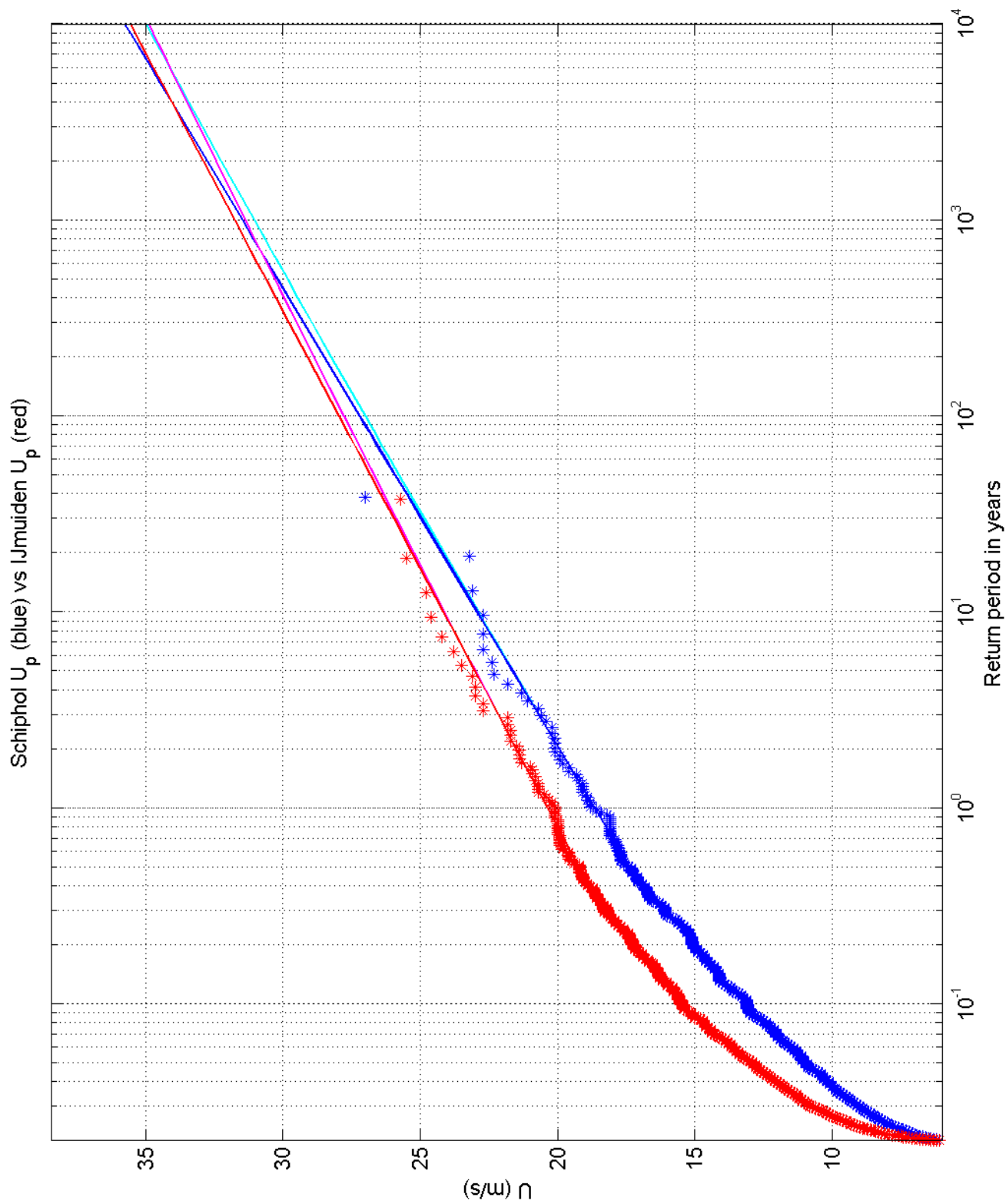
1970-2008

Beek

Deltares

1200264-005

Fig. F.4.380.9



Return value plot of Schiphol (blue) vs IJmuiden (red)
 Exponential (blue, red) and GPD (cyan, magenta) fits to U_p
 Plotting positions: x_i vs $(n+1)/(\lambda(n+1-i))$

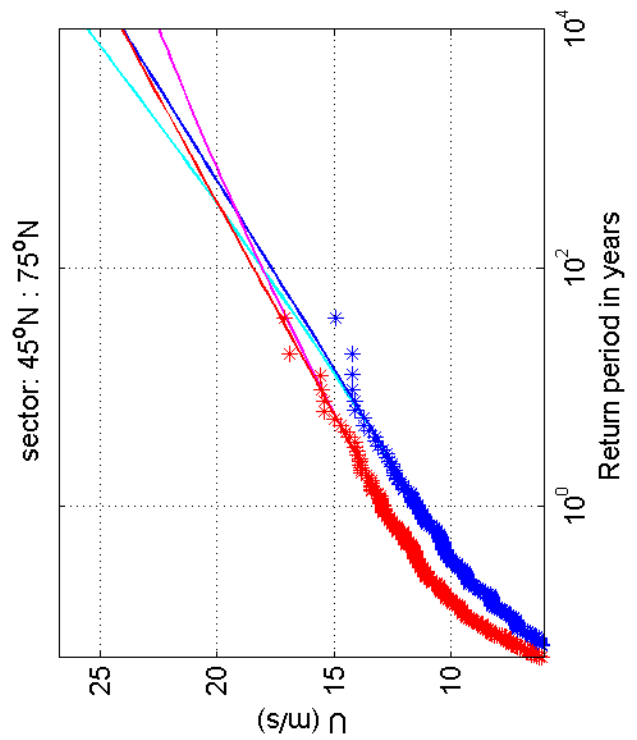
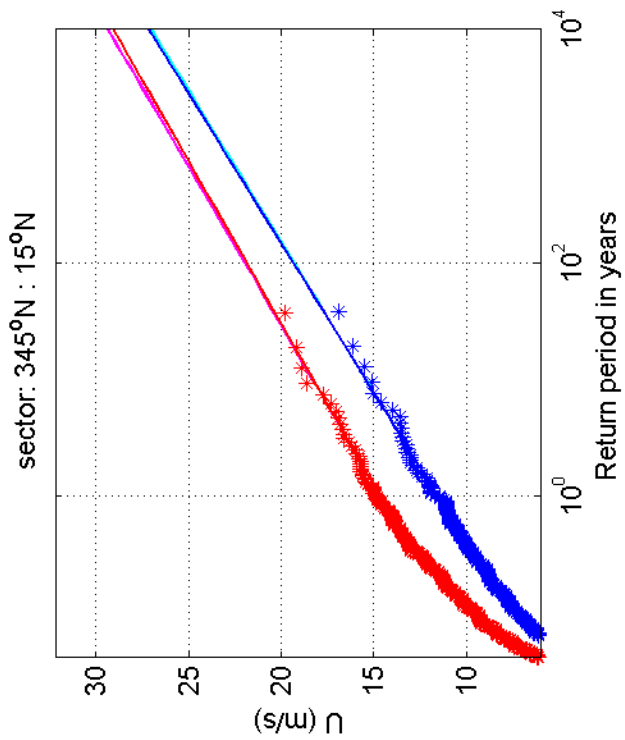
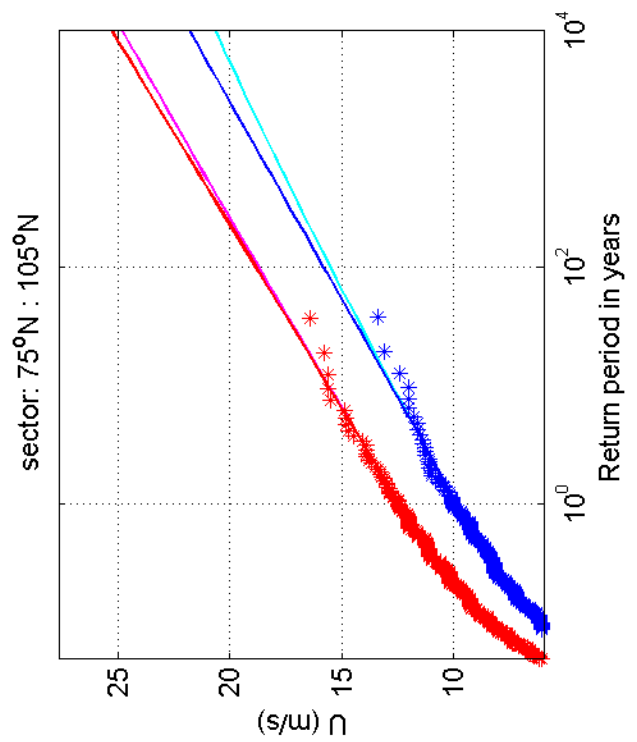
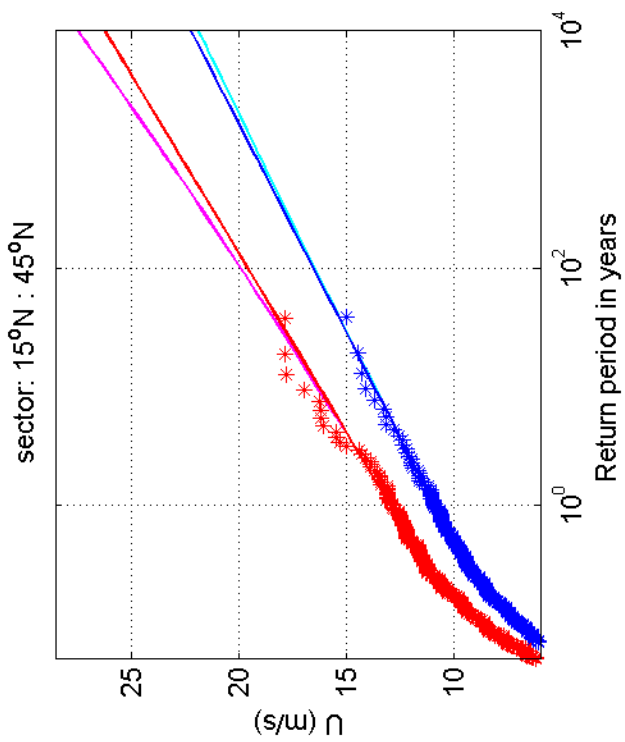
1970-2008

Schiphol vs IJmuiden

Deltares

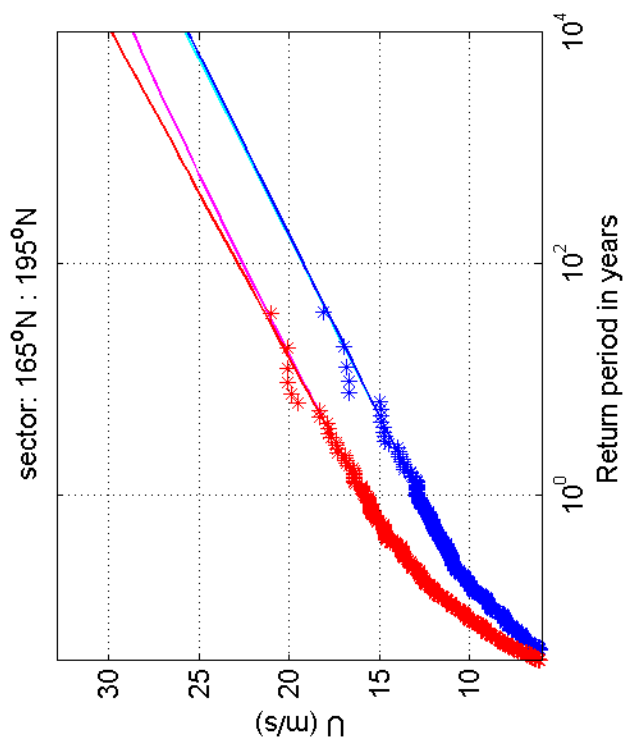
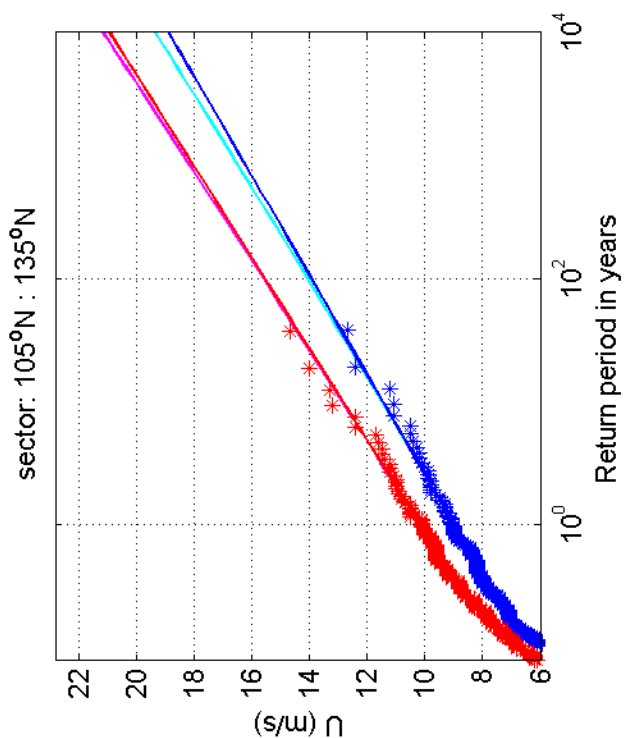
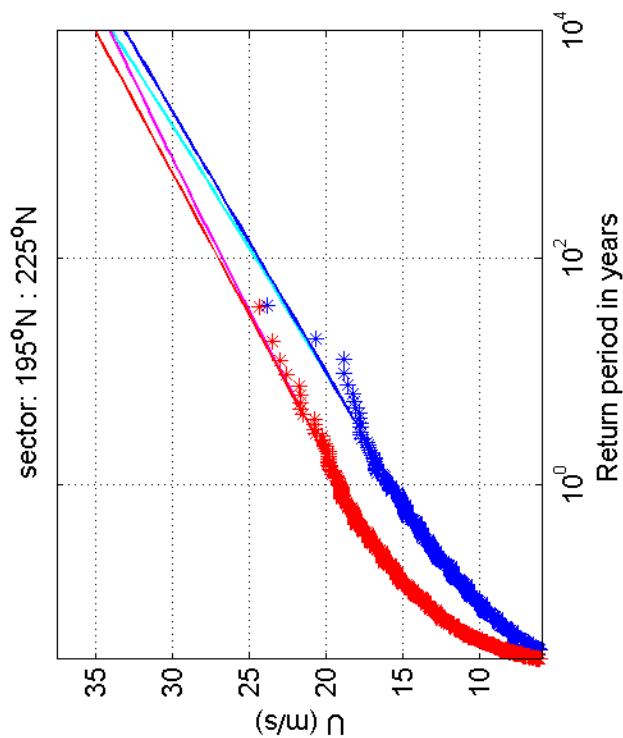
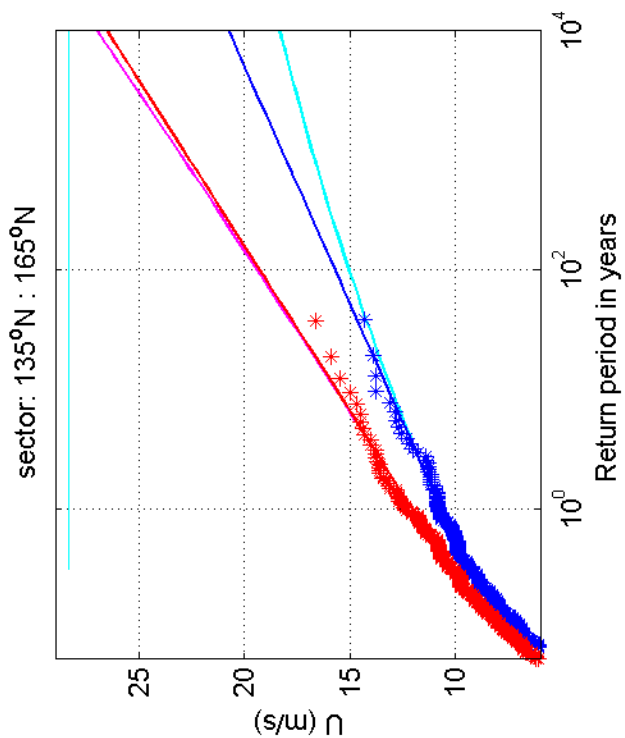
1200264-005

Fig. F.5a.1



Return value plot per sector of Schiphol (blue) vs IJmuiden (red)
 Exponential (blue, red) and GPD (cyan, magenta) fits to U_p
 Plotting positions: x_i vs $(n+1)/(\lambda(n+1-i))$

1970-2008



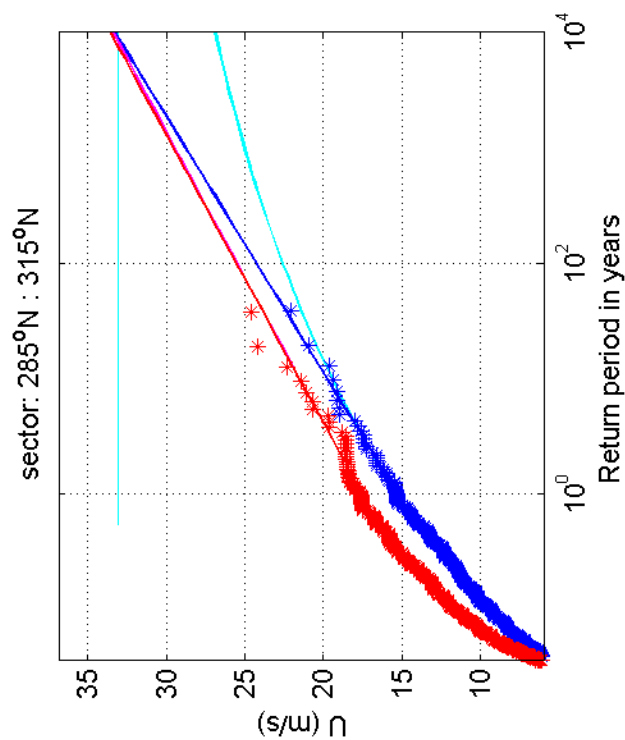
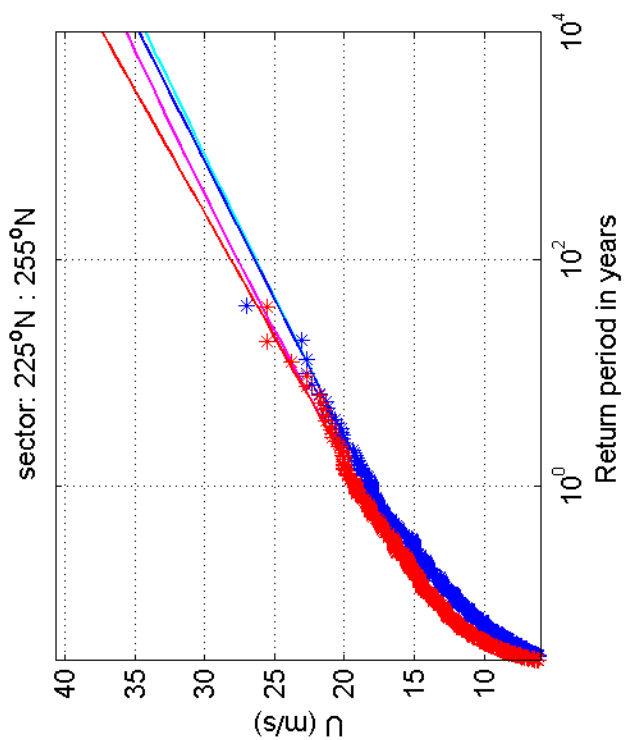
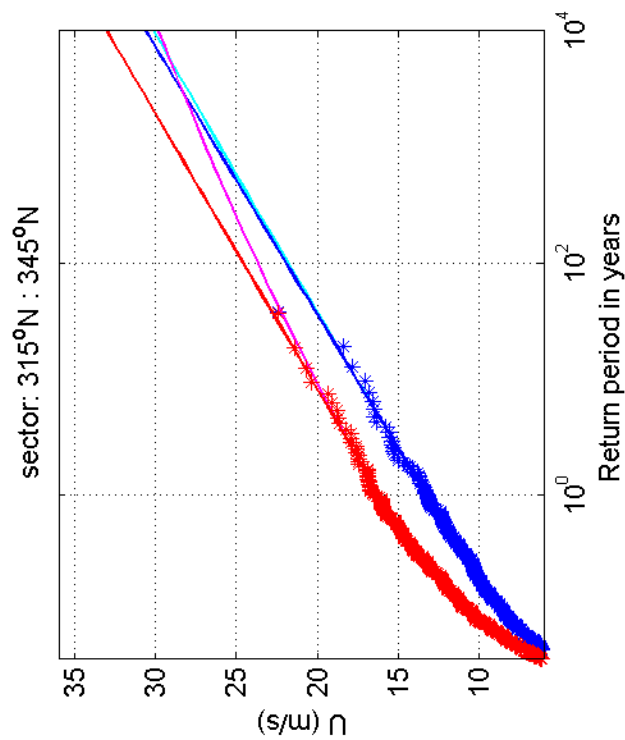
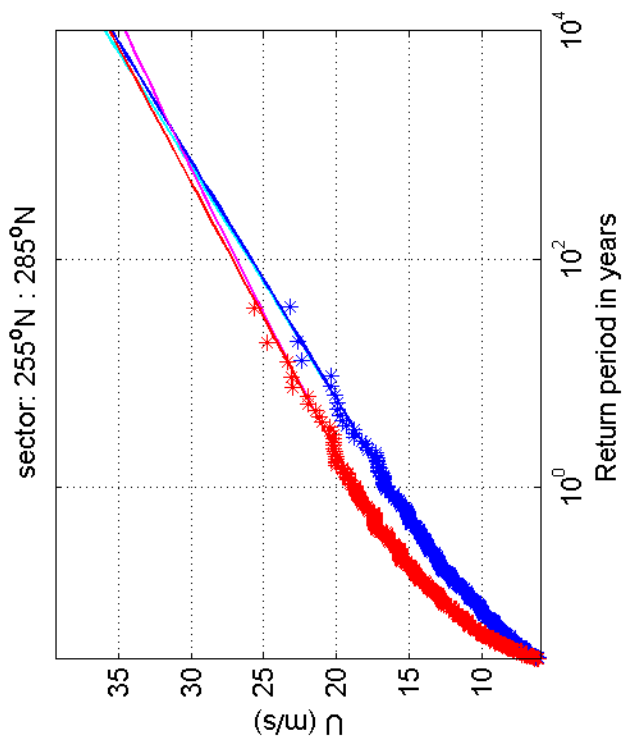
Return value plot per sector of Schiphol (blue) vs IJmuiden (red)
 Exponential (blue, red) and GPD (cyan, magenta) fits to U_p
 Plotting positions: x_i vs $(n+1)/(\lambda(n+1-i))$

1970-2008

Deltares

1200264-005

Fig. F.5c.1



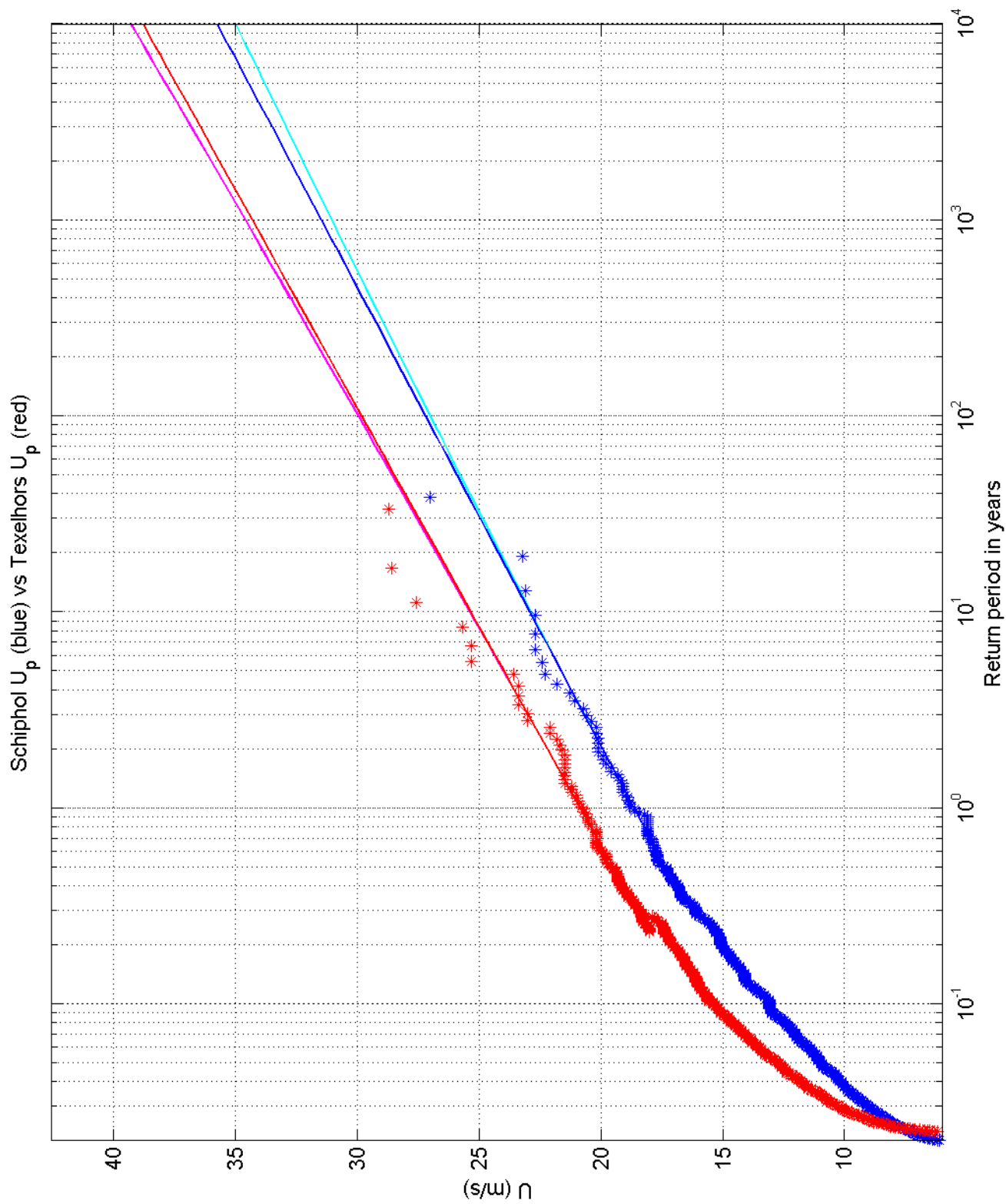
Return value plot per sector of Schiphol (blue) vs IJmuiden (red)
 Exponential (blue, red) and GPD (cyan, magenta) fits to U_p
 Plotting positions: x_i vs $(n+1)/(\lambda(n+1-i))$

1970-2008

Deltares

1200264-005

Fig. F.5d.1



Return value plot of Schiphol (blue) vs Texelhors (red)
 Exponential (blue, red) and GPD (cyan, magenta) fits to U_p
 Plotting positions: x_i vs $(n+1)/(\lambda(n+1-i))$

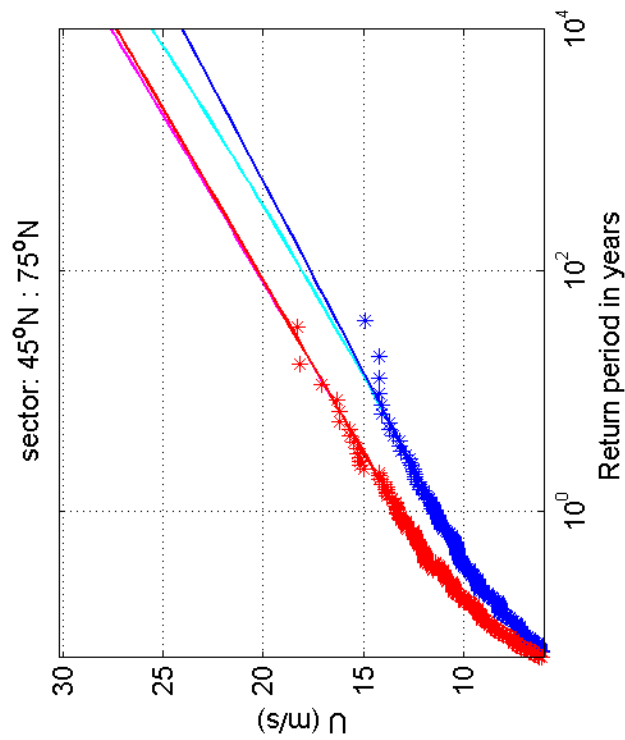
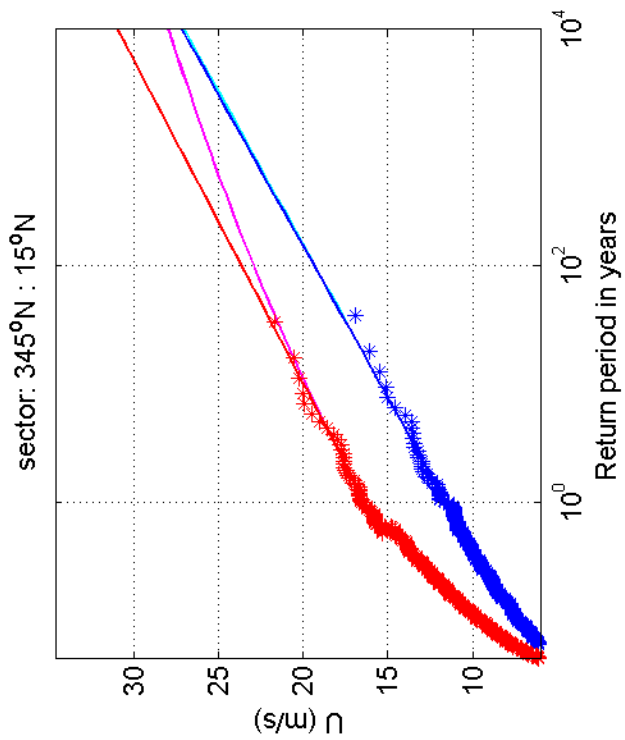
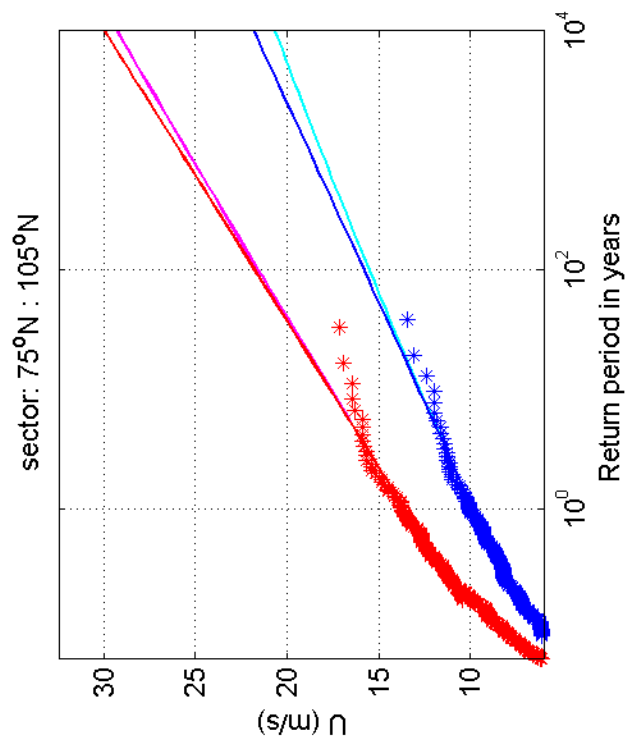
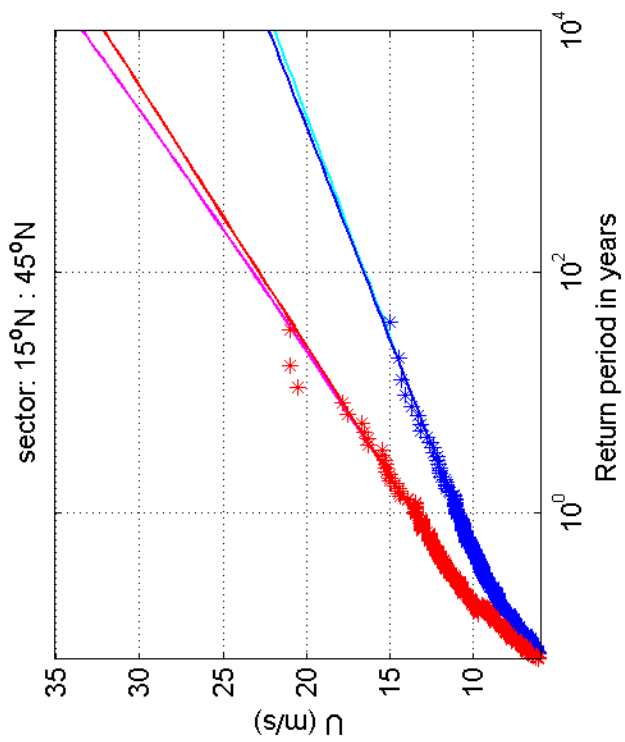
1970-2008

Schiphol vs Texelhors

Deltares

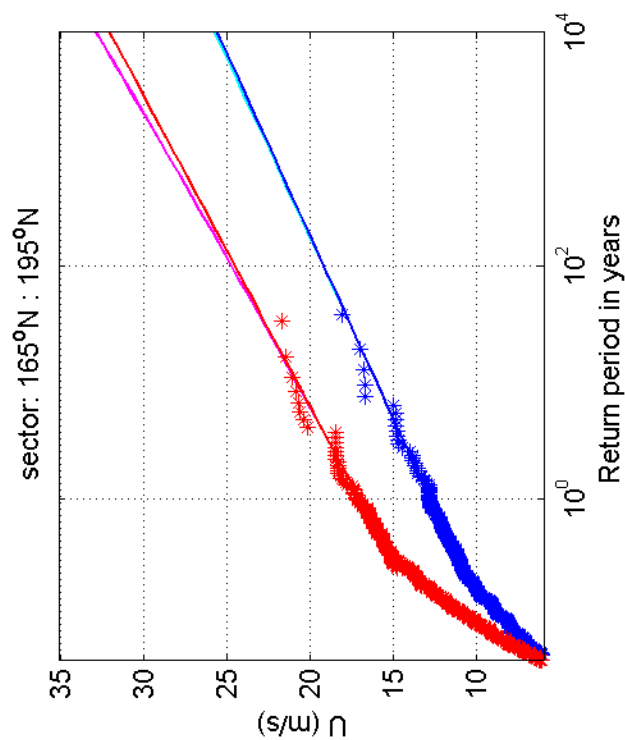
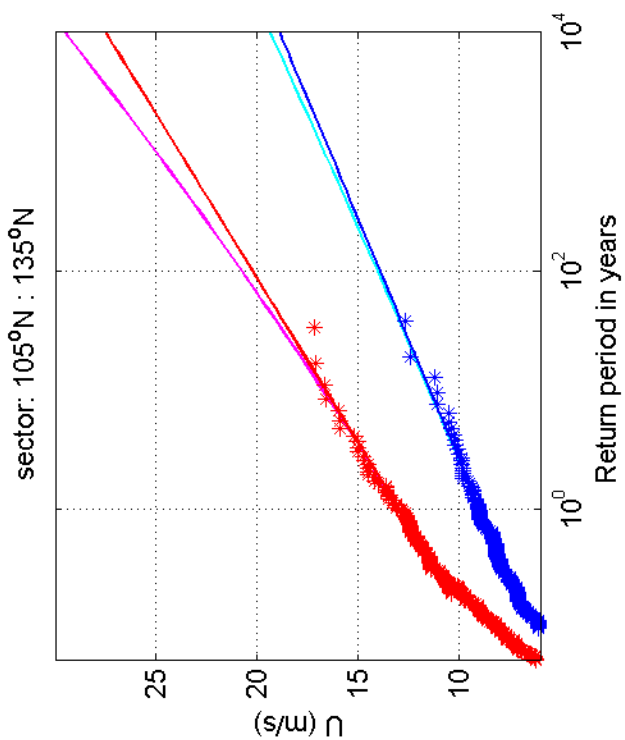
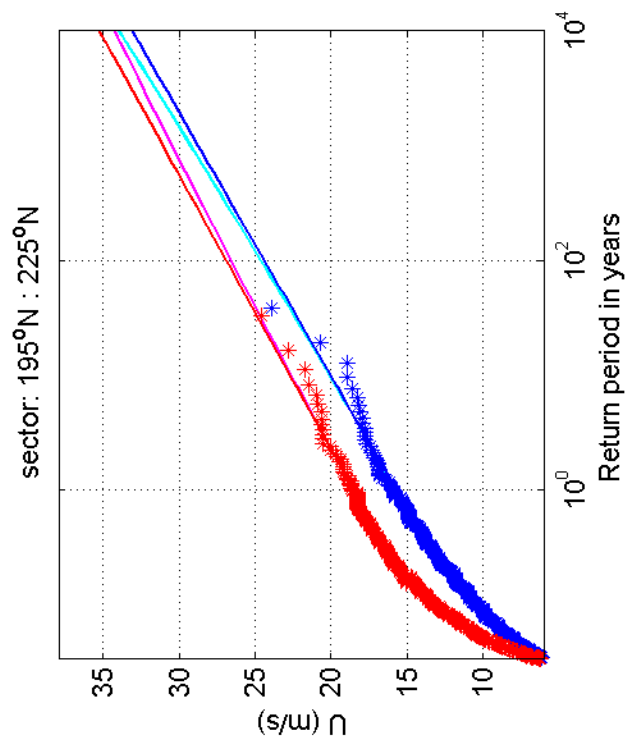
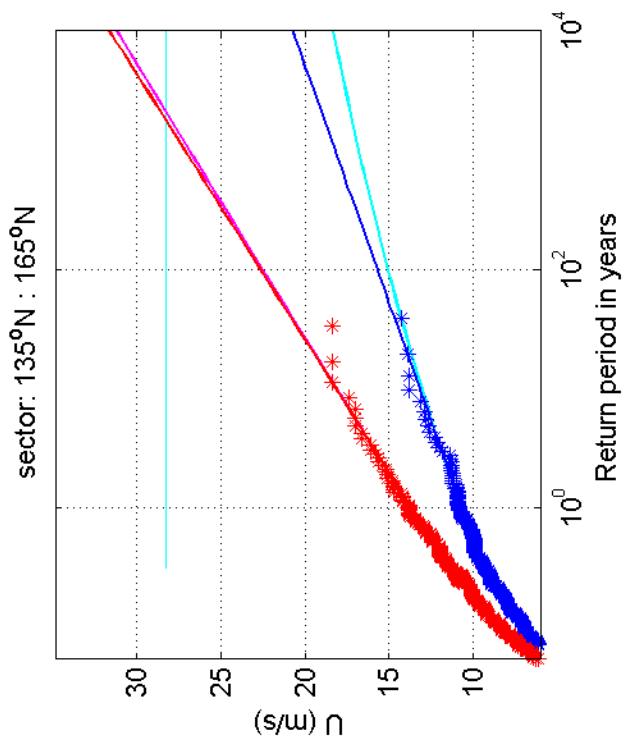
1200264-005

Fig. F.5a.2



Return value plot per sector of Schiphol (blue) vs Texelhors (red)
 Exponential (blue, red) and GPD (cyan, magenta) fits to U_p
 Plotting positions: x_i vs $(n+1)/(\lambda(n+1-i))$

1970-2008



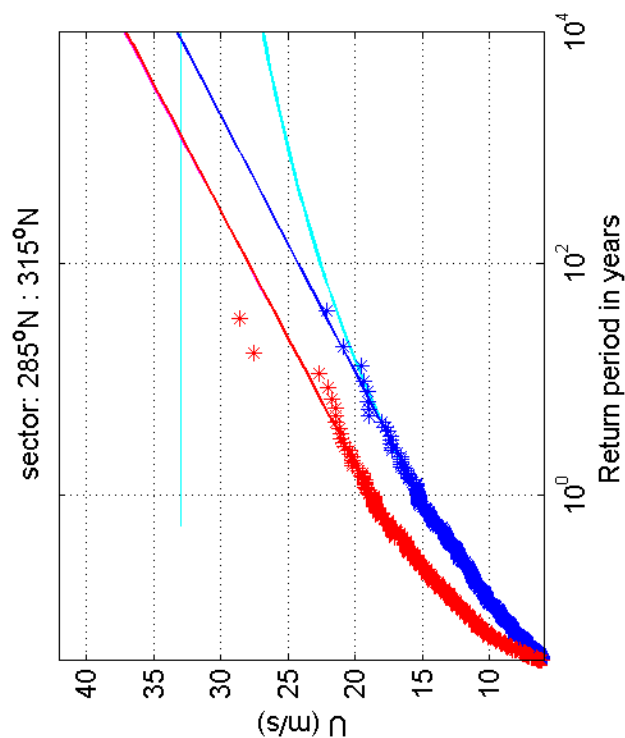
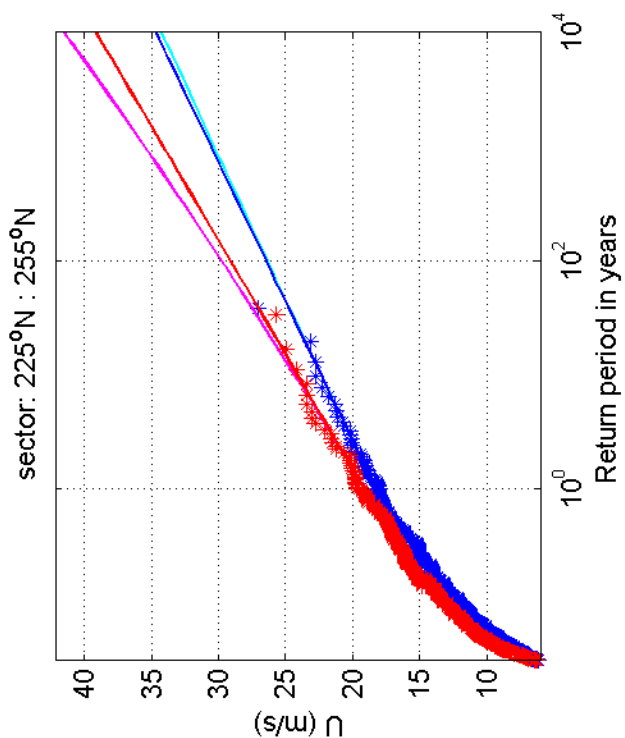
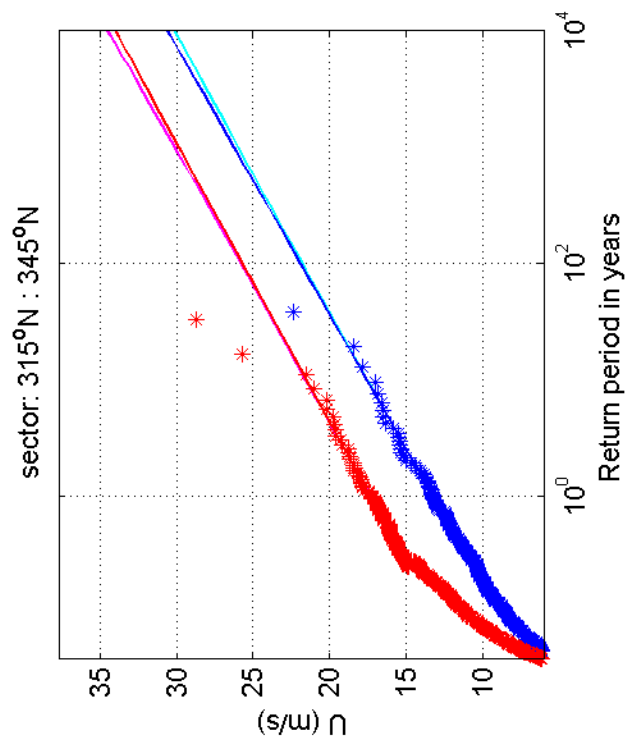
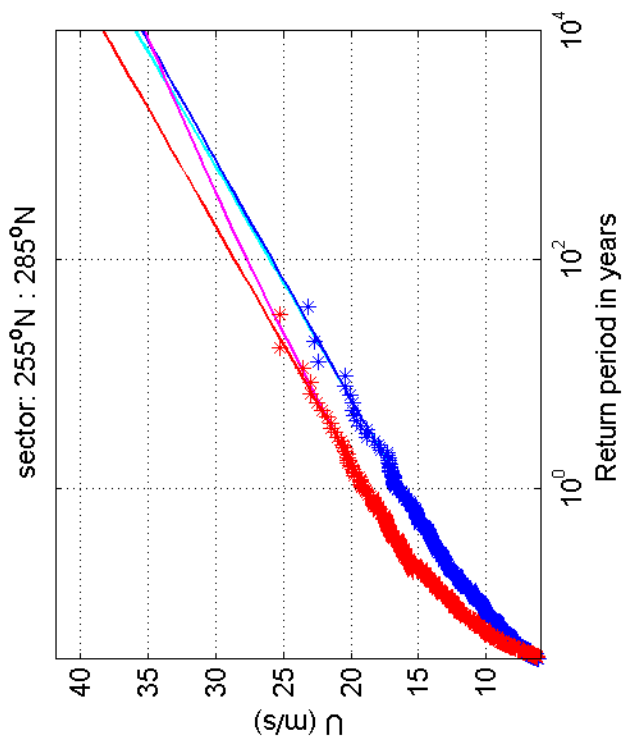
Return value plot per sector of Schiphol (blue) vs Texelhors (red)
 Exponential (blue, red) and GPD (cyan, magenta) fits to U_p
 Plotting positions: x_i vs $(n+1)/(\lambda(n+1-i))$

1970-2008

Deltares

1200264-005

Fig. F.5c.2



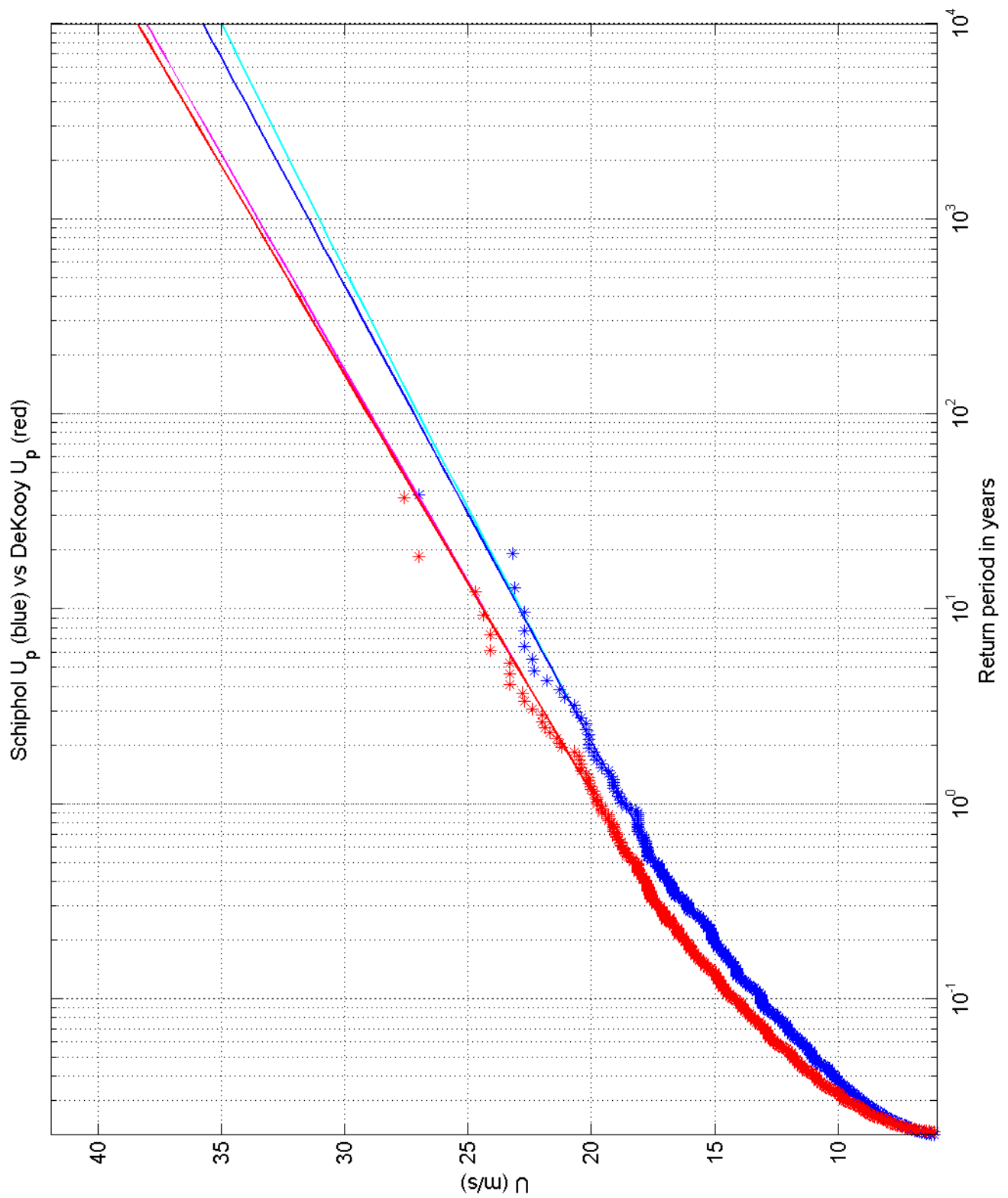
Return value plot per sector of Schiphol (blue) vs Texelhors (red)
 Exponential (blue, red) and GPD (cyan, magenta) fits to U_p
 Plotting positions: x_i vs $(n+1)/(\lambda(n+1-i))$

1970-2008

Deltares

1200264-005

Fig. F.5d.2



Return value plot of Schiphol (blue) vs DeKooy (red)
 Exponential (blue, red) and GPD (cyan, magenta) fits to U_p
 Plotting positions: x_i vs $(n+1)/(\lambda(n+1-i))$

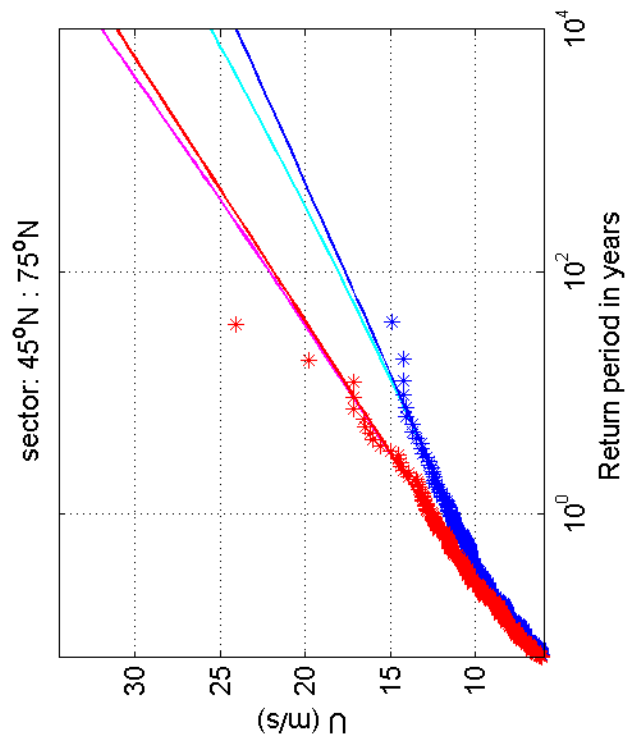
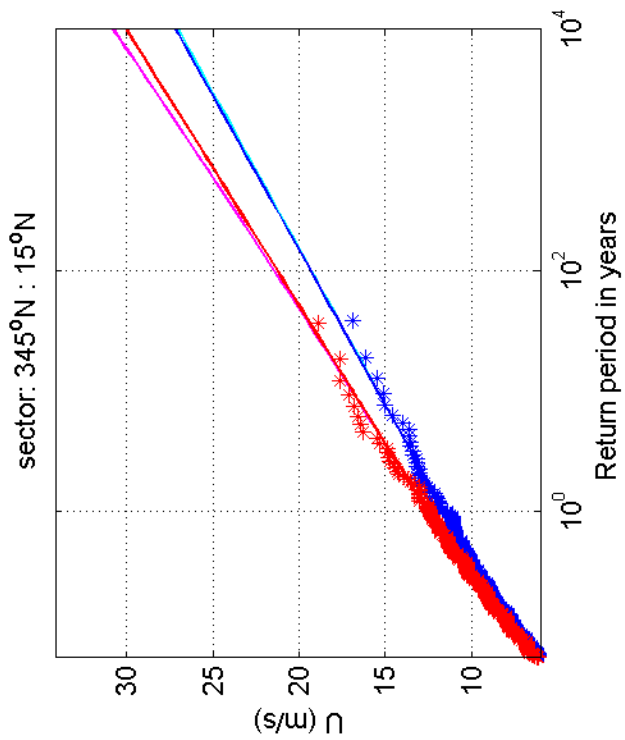
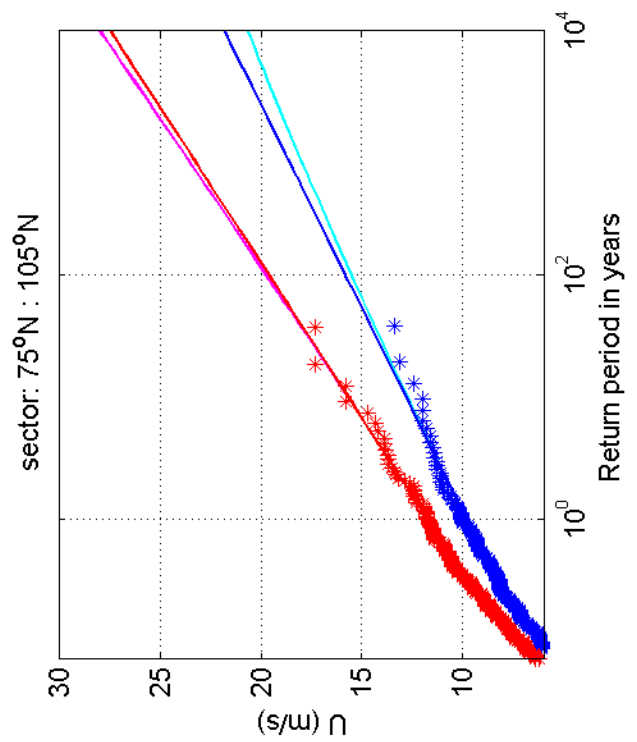
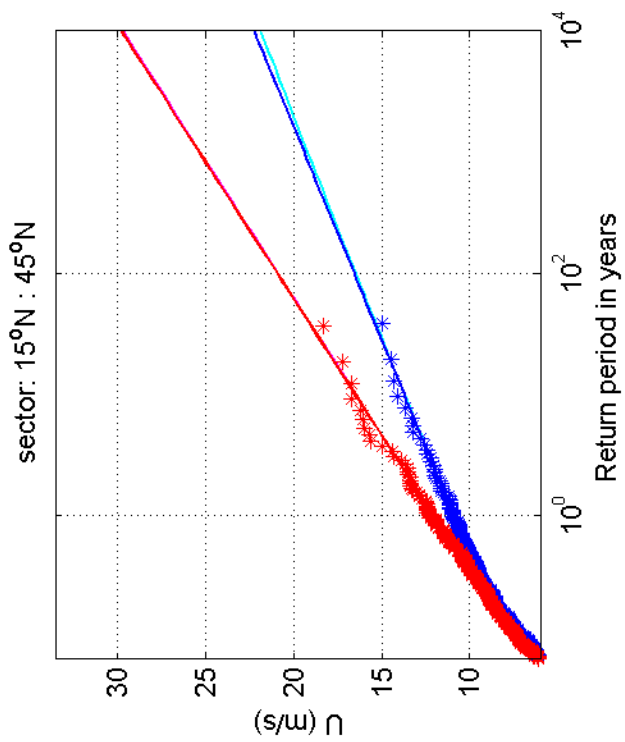
1970-2008

Schiphol vs DeKooy

Deltares

1200264-005

Fig. F.5a.3



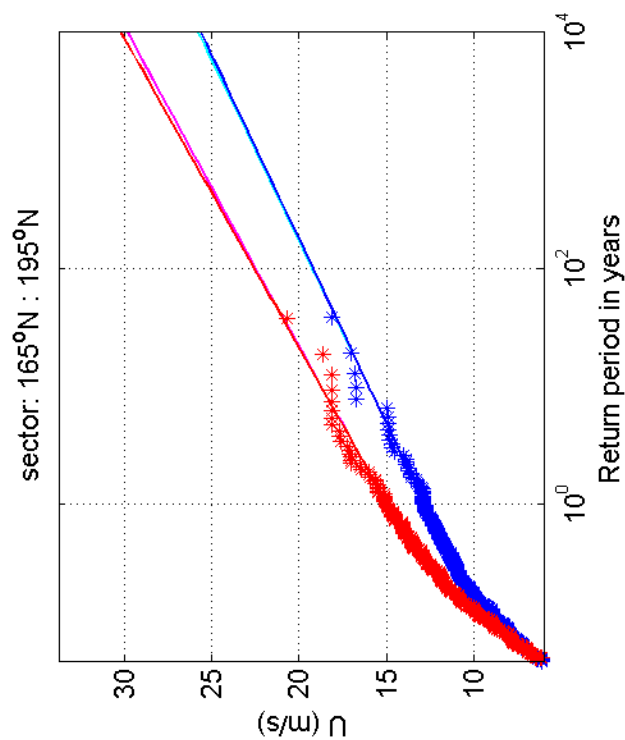
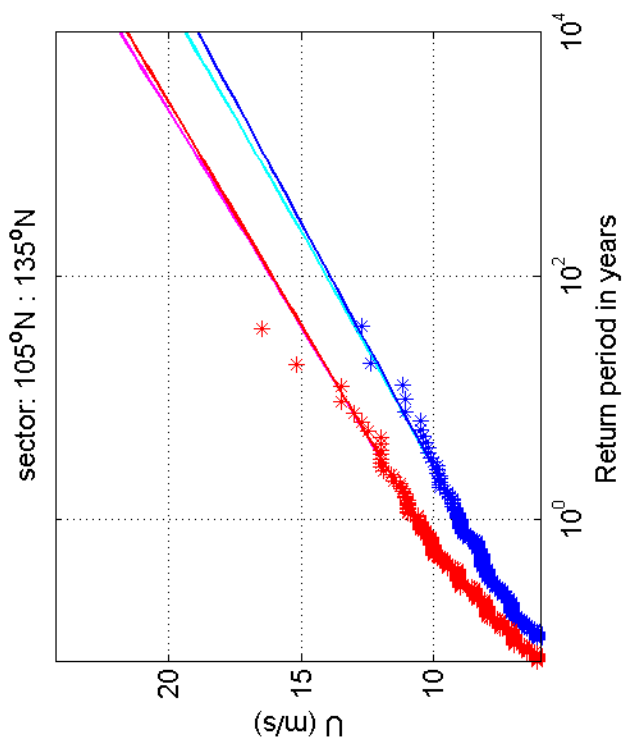
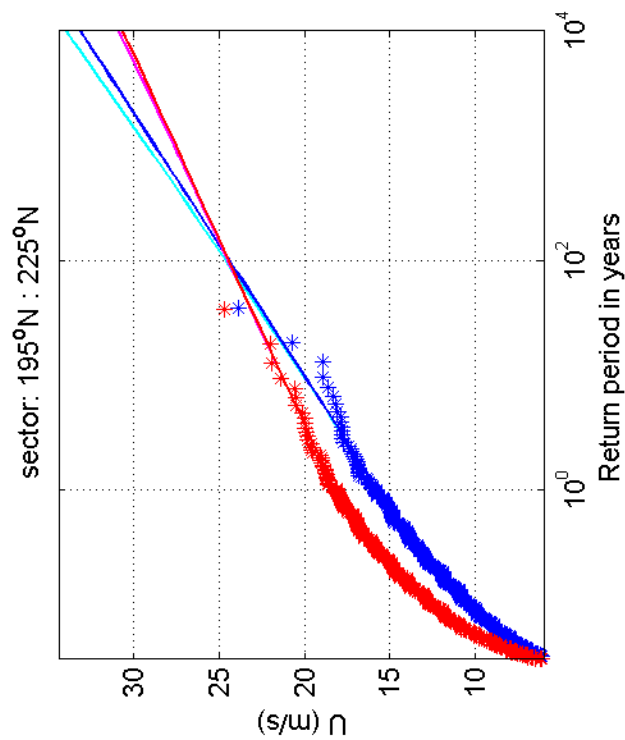
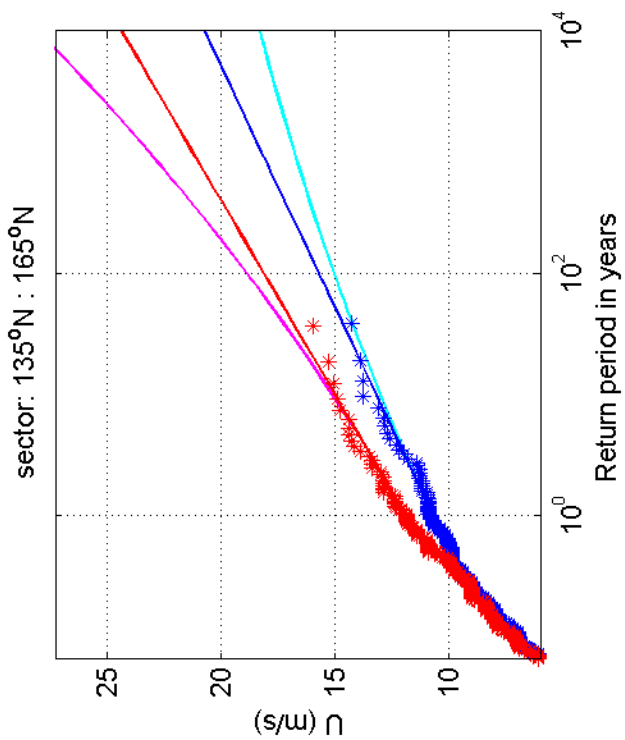
Return value plot per sector of Schiphol (blue) vs DeKooy (red)
 Exponential (blue, red) and GPD (cyan, magenta) fits to U_p
 Plotting positions: x_i vs $(n+1)/(\lambda(n+1-i))$

1970-2008

Deltares

1200264-005

Fig. F.5b.3



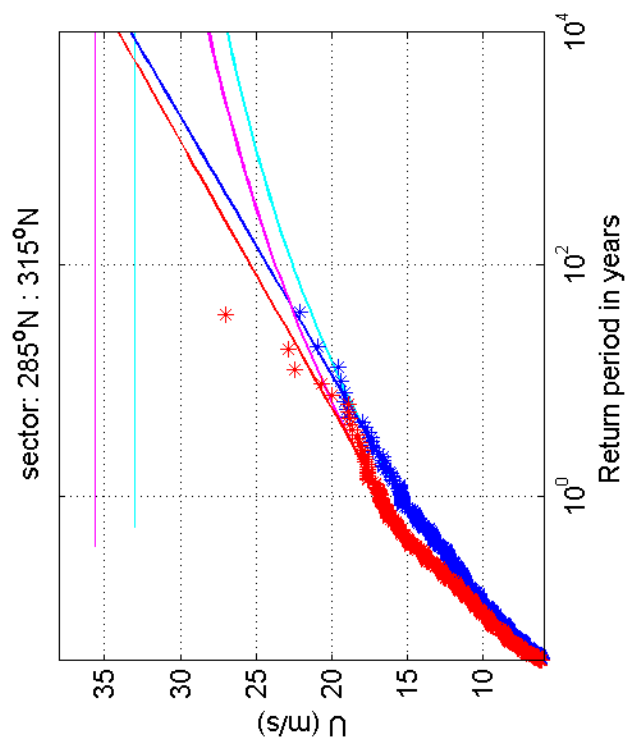
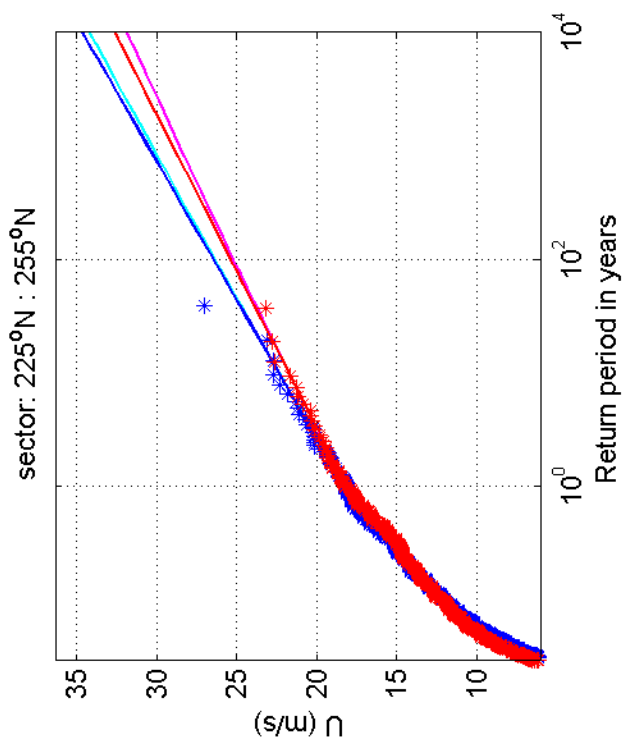
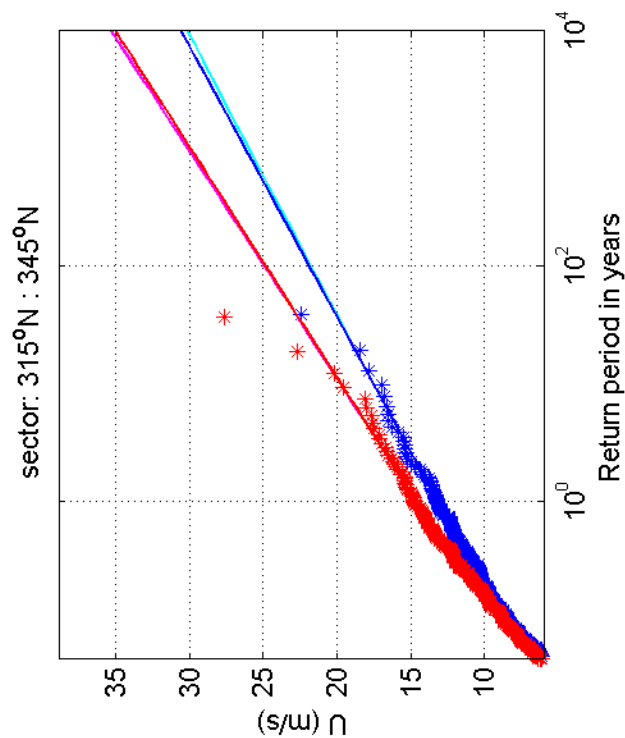
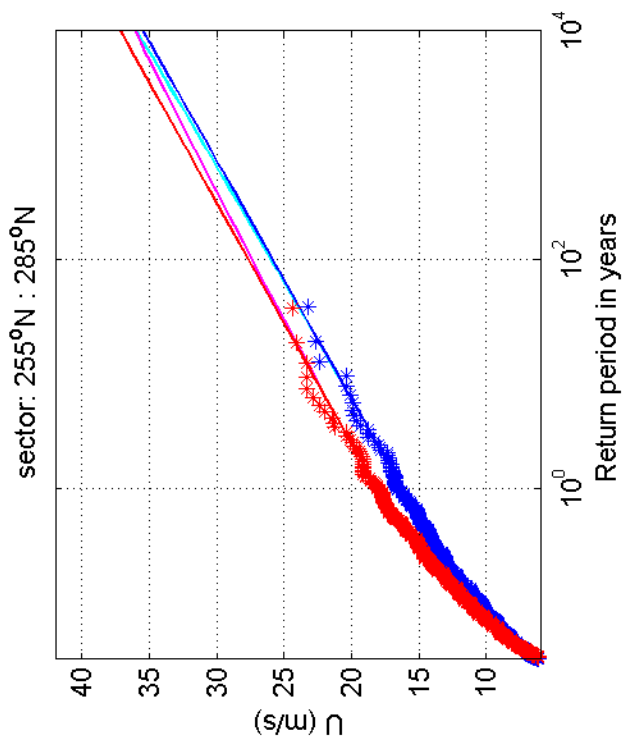
Return value plot per sector of Schiphol (blue) vs DeKooy (red)
 Exponential (blue, red) and GPD (cyan, magenta) fits to U_p
 Plotting positions: x_i vs $(n+1)/(\lambda(n+1-i))$

1970-2008

Deltares

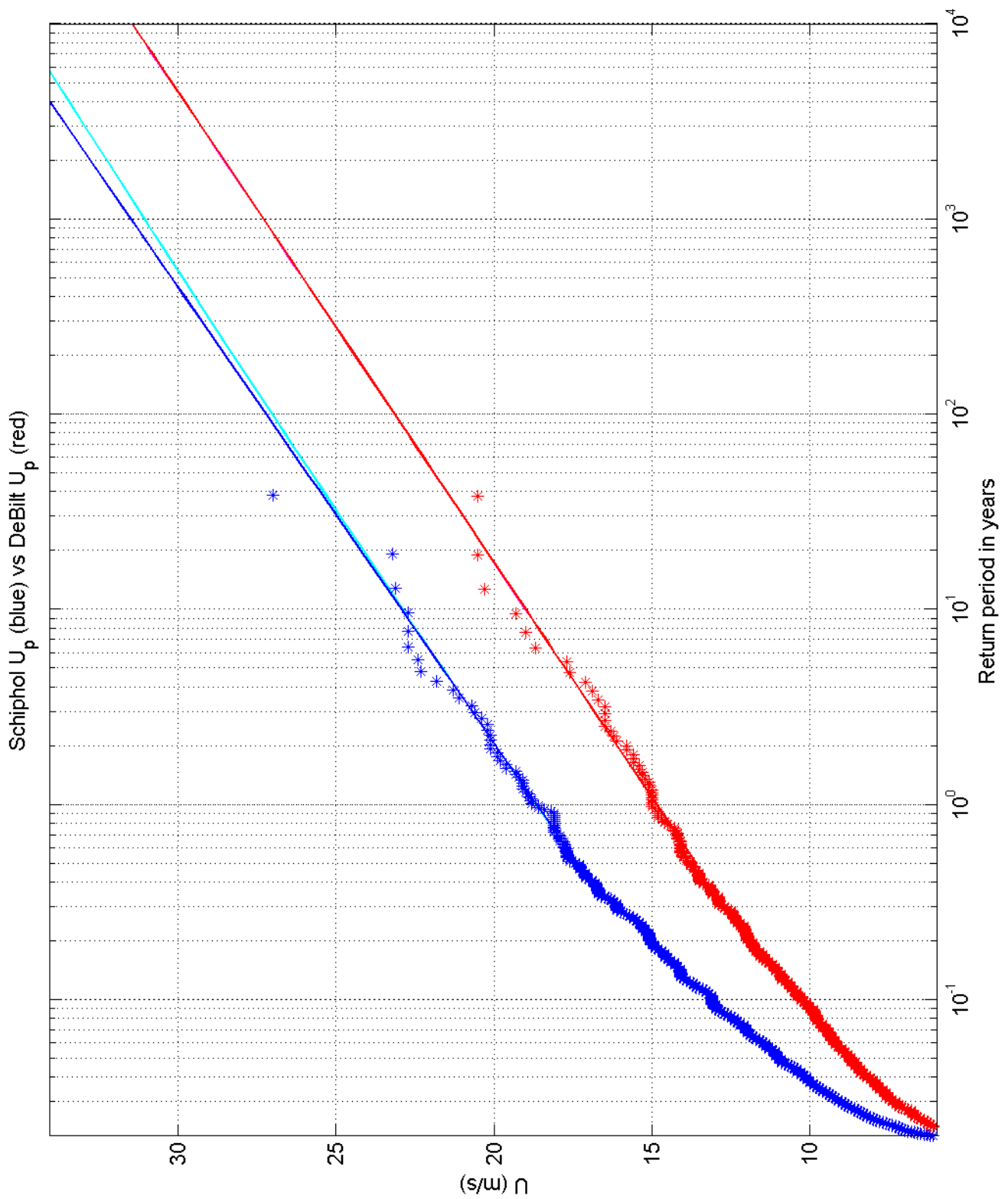
1200264-005

Fig. F.5c.3



Return value plot per sector of Schiphol (blue) vs DeKooy (red)
 Exponential (blue, red) and GPD (cyan, magenta) fits to U_p
 Plotting positions: x_i vs $(n+1)/(\lambda(n+1-i))$

1970-2008



Return value plot of Schiphol (blue) vs DeBilt (red)
 Exponential (blue, red) and GPD (cyan, magenta) fits to U_p
 Plotting positions: x_i vs $(n+1)/(\lambda(n+1-i))$

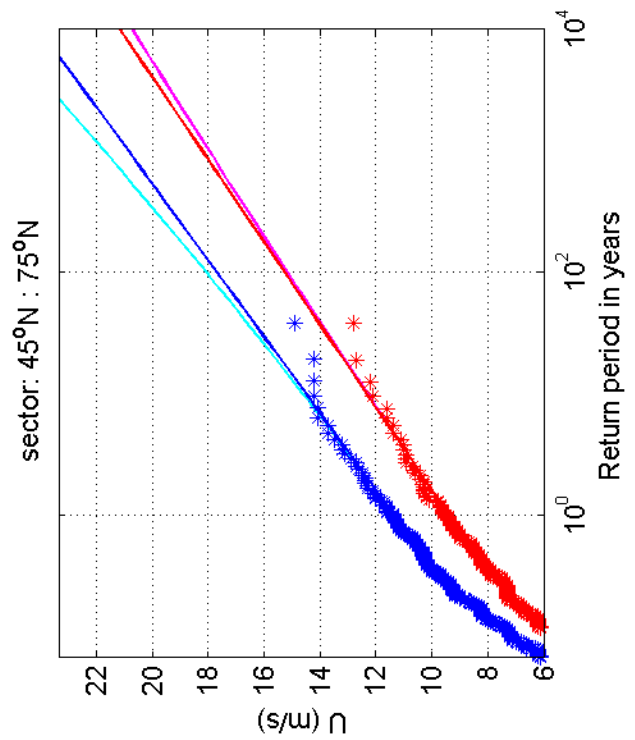
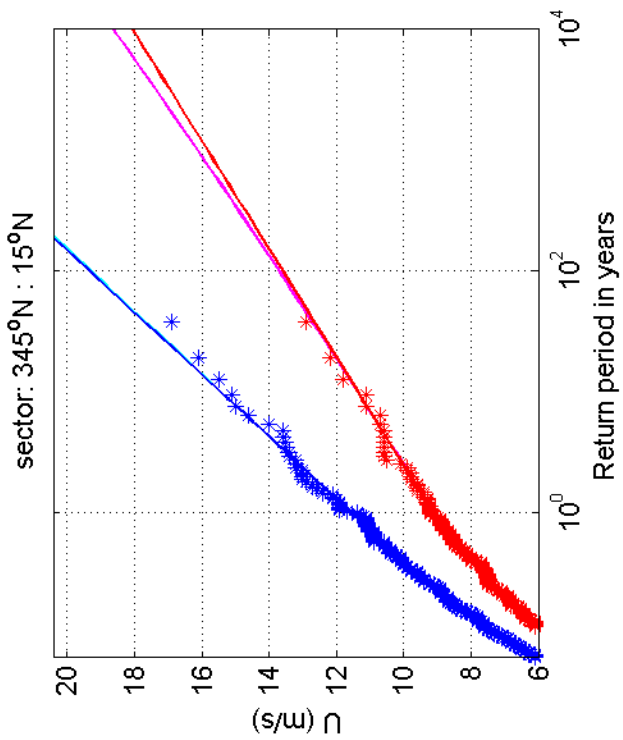
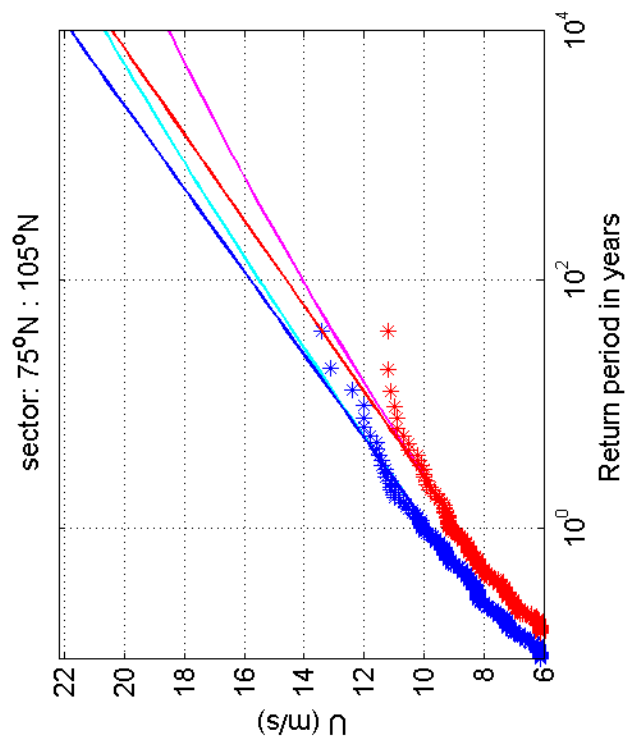
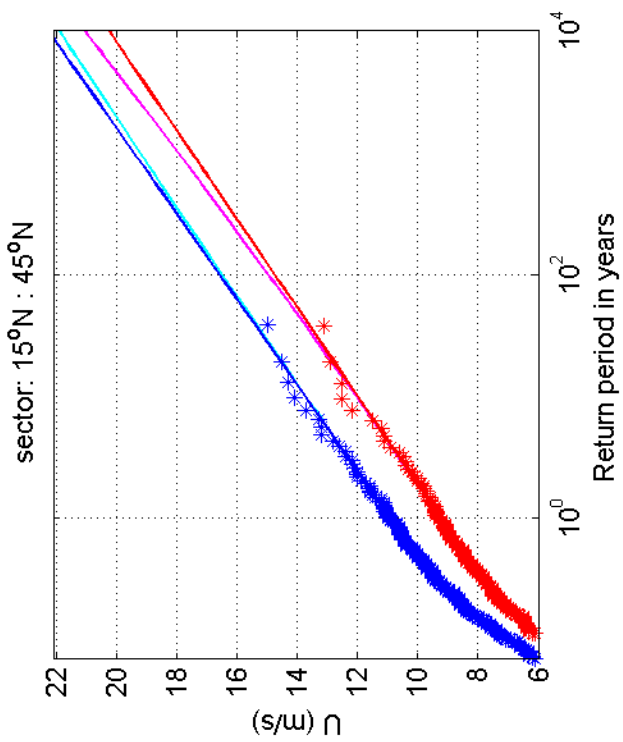
1970-2008

Schiphol vs DeBilt

Deltares

1200264-005

Fig. F.5a.4



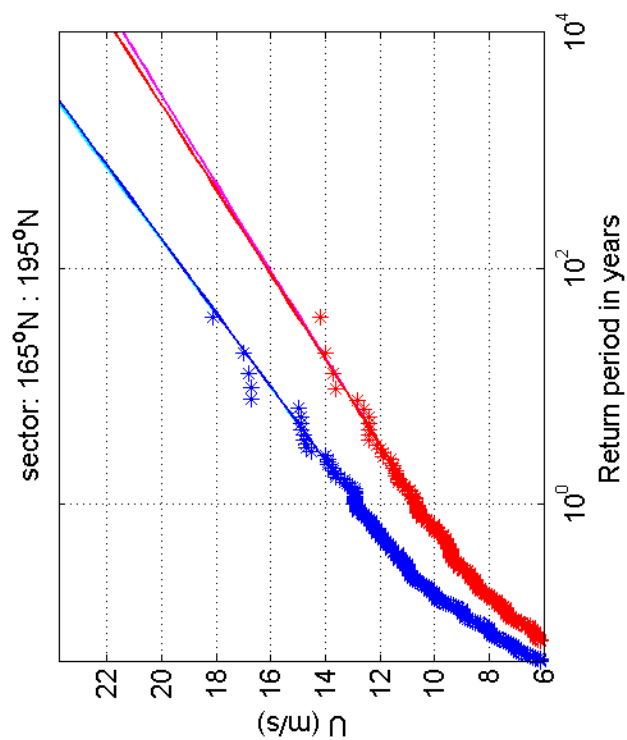
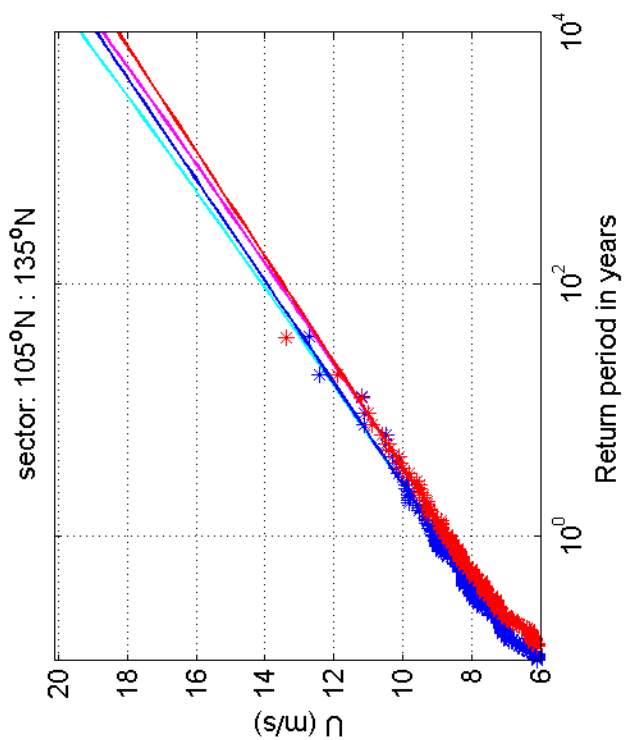
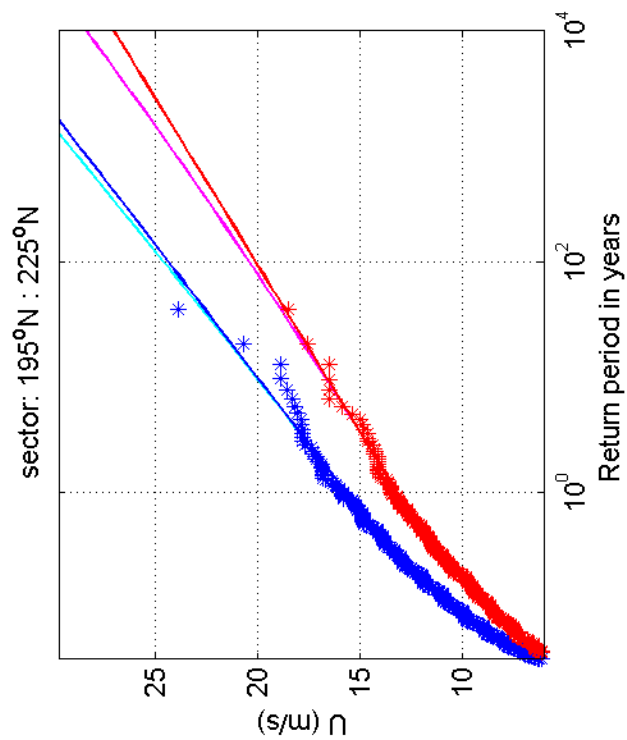
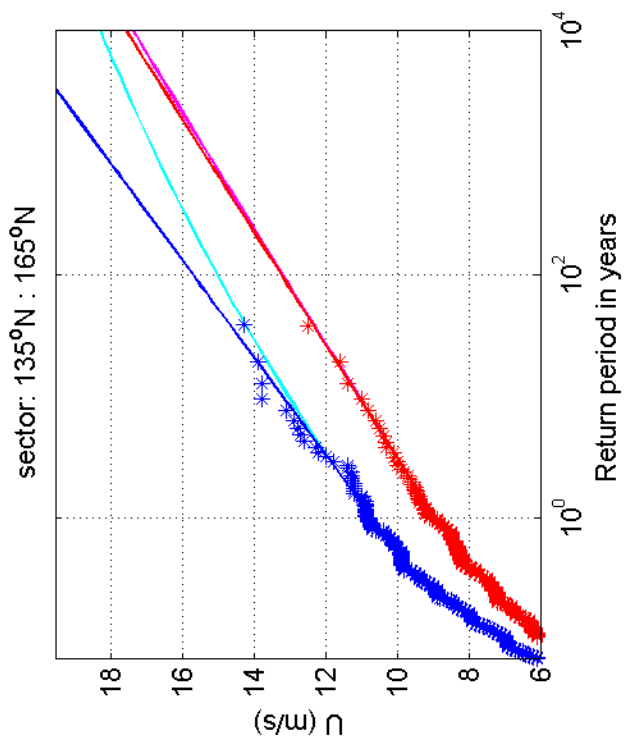
Return value plot per sector of Schiphol (blue) vs DeBilt (red)
 Exponential (blue, red) and GPD (cyan, magenta) fits to U_p
 Plotting positions: x_i vs $(n+1)/(\lambda(n+1-i))$

1970-2008

Deltares

1200264-005

Fig. F.5b.4



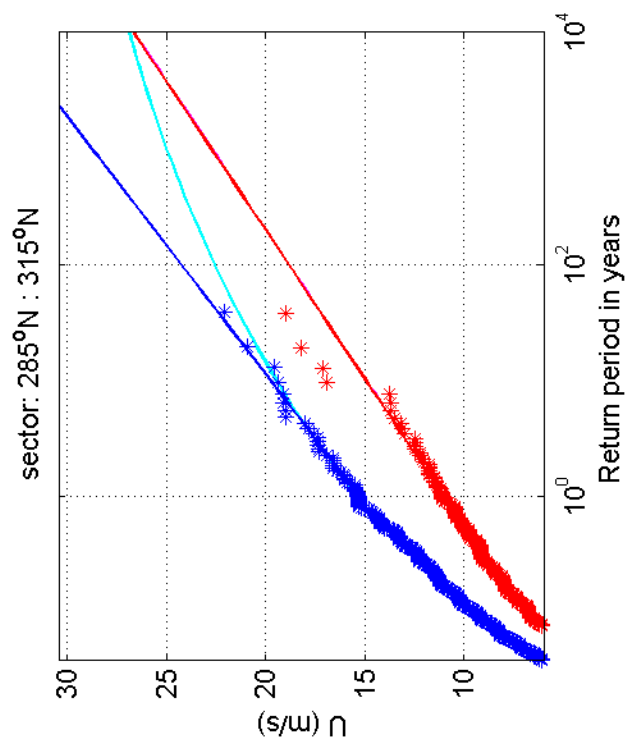
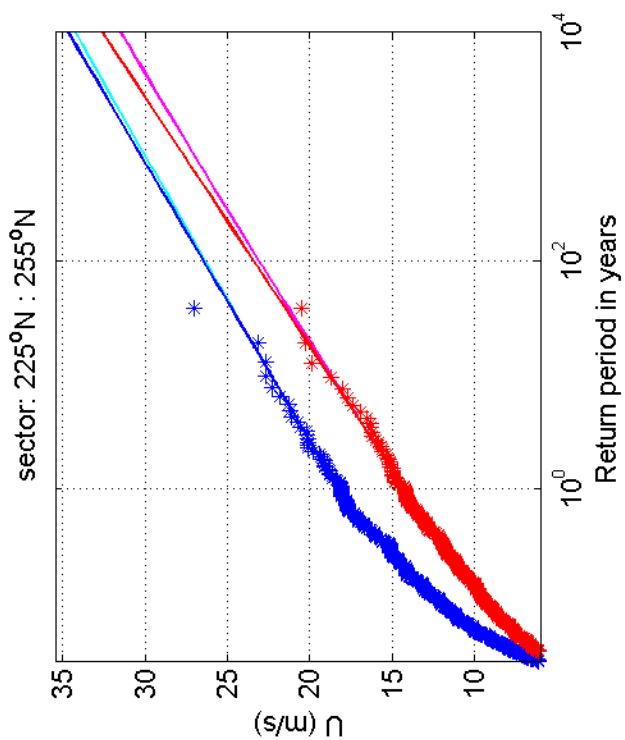
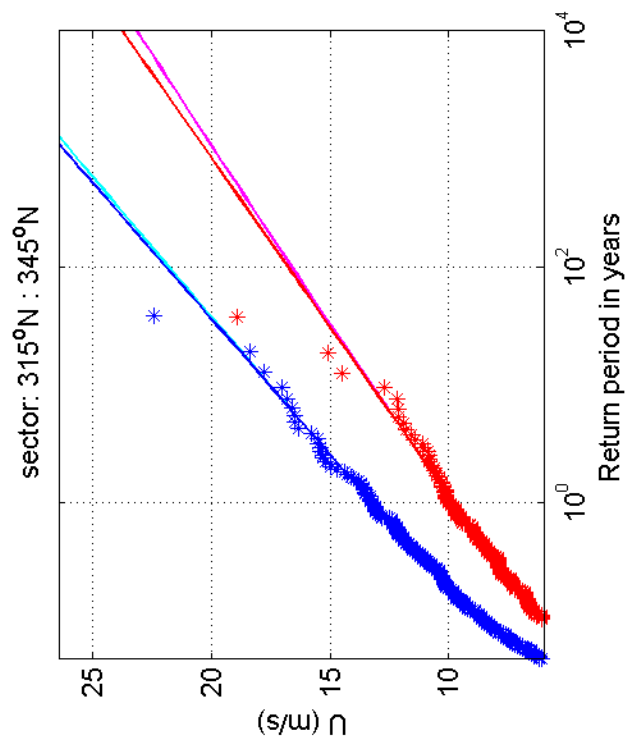
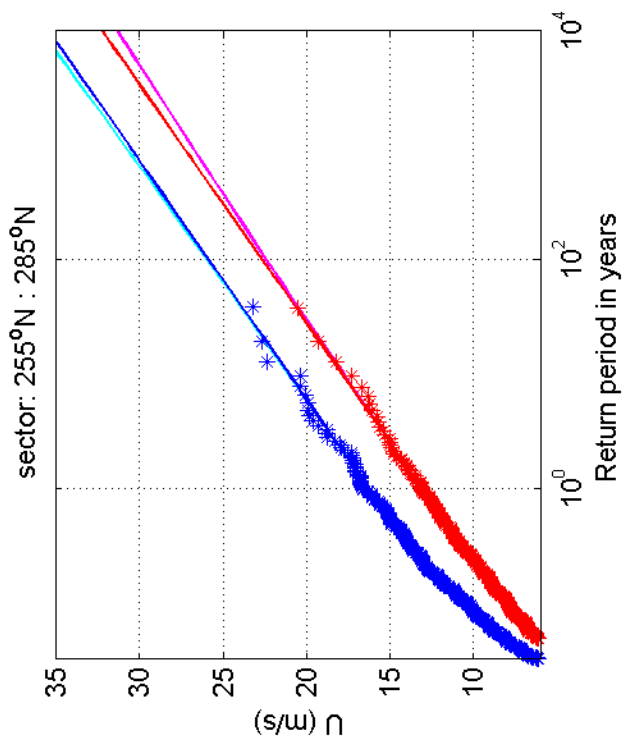
Return value plot per sector of Schiphol (blue) vs DeBilt (red)
 Exponential (blue, red) and GPD (cyan, magenta) fits to U_p
 Plotting positions: x_i vs $(n+1)/(\lambda(n+1-i))$

1970-2008

Deltares

1200264-005

Fig. F.5c.4



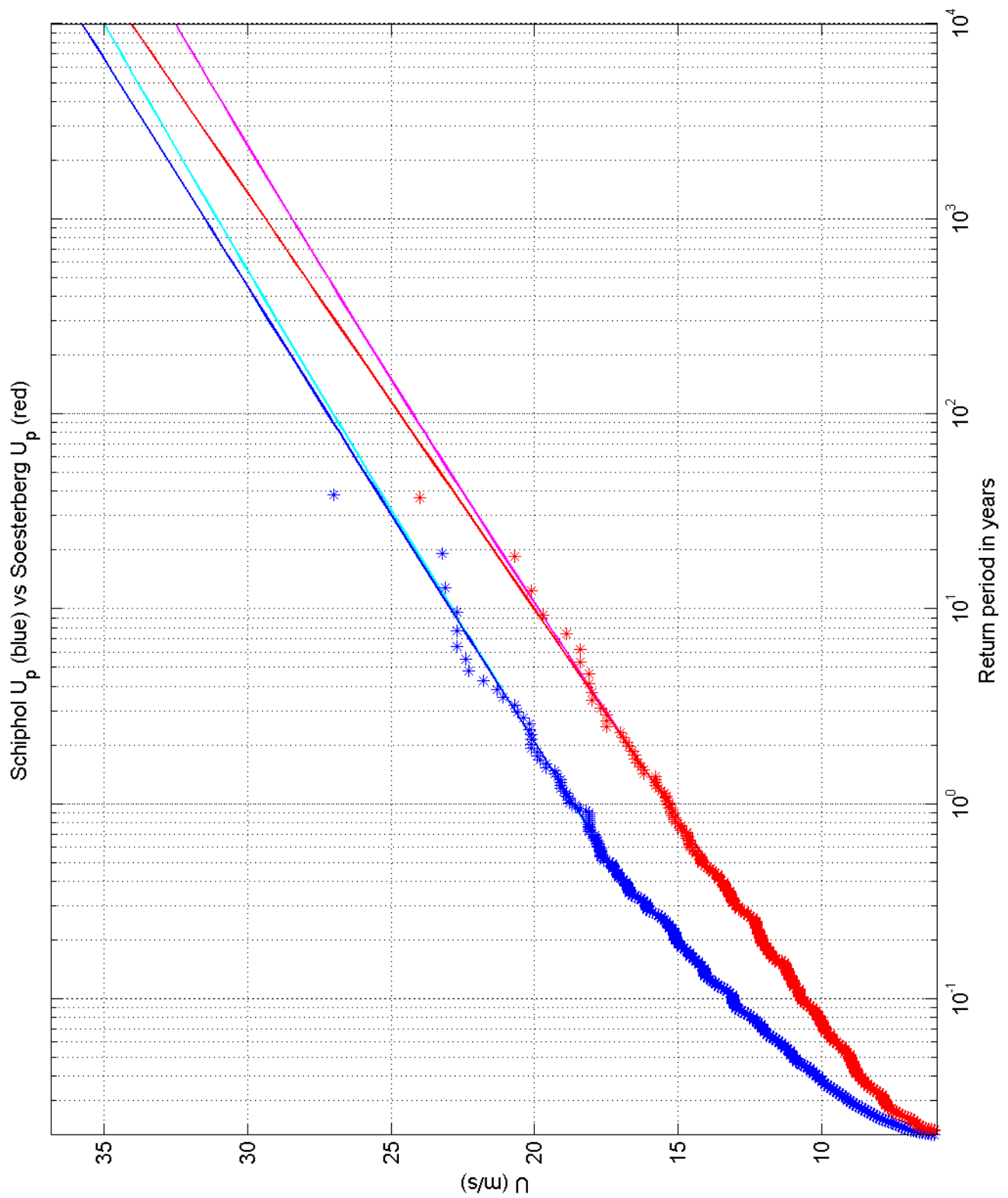
Return value plot per sector of Schiphol (blue) vs DeBilt (red)
 Exponential (blue, red) and GPD (cyan, magenta) fits to U_p
 Plotting positions: x_i vs $(n+1)/(\lambda(n+1-i))$

1970-2008

Deltares

1200264-005

Fig. F.5d.4



Return value plot of Schiphol (blue) vs Soesterberg (red)
 Exponential (blue, red) and GPD (cyan, magenta) fits to U_p
 Plotting positions: x_i vs $(n+1)/(\lambda(n+1-i))$

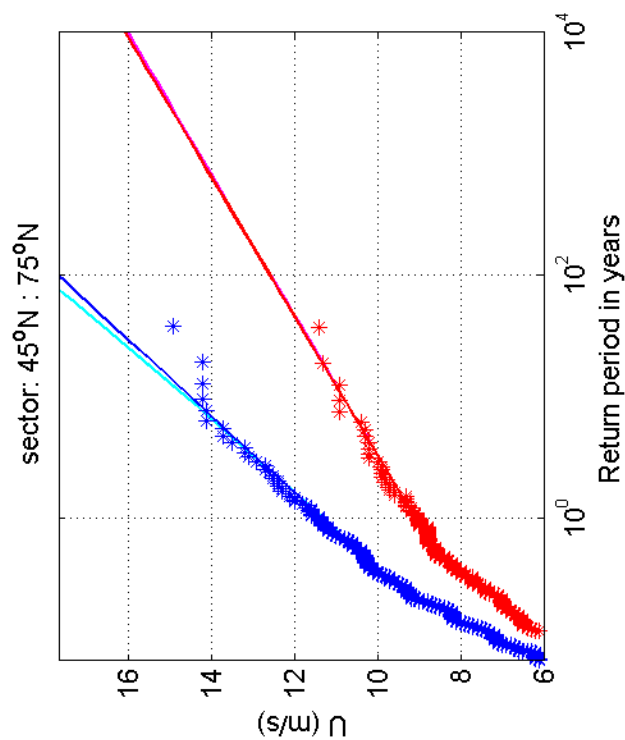
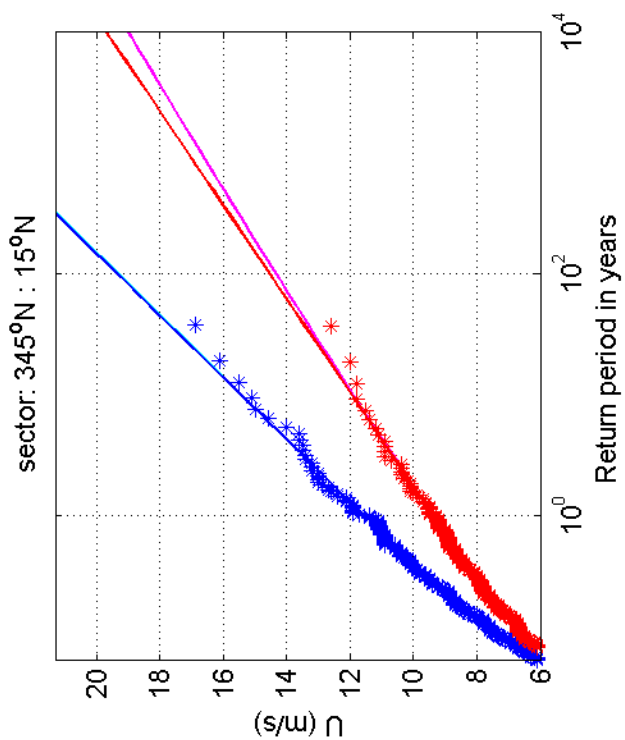
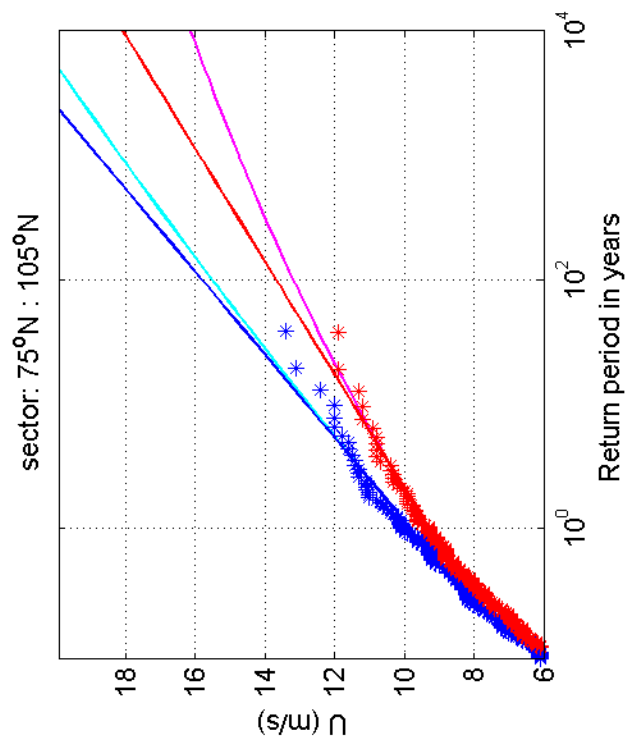
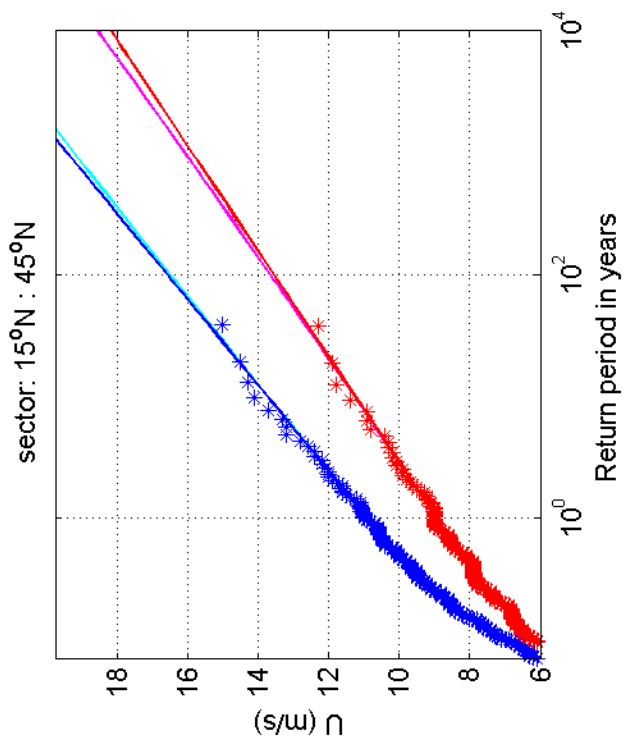
1970-2008

Schiphol vs Soesterberg

Deltares

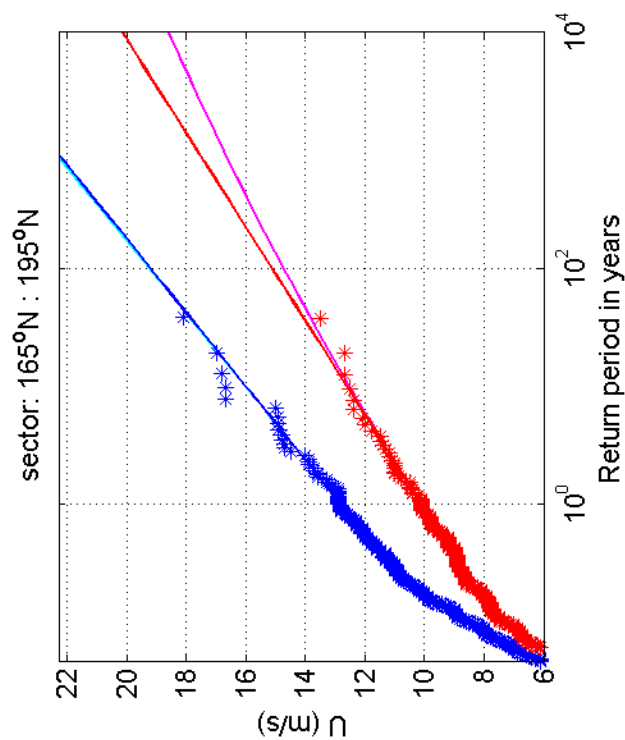
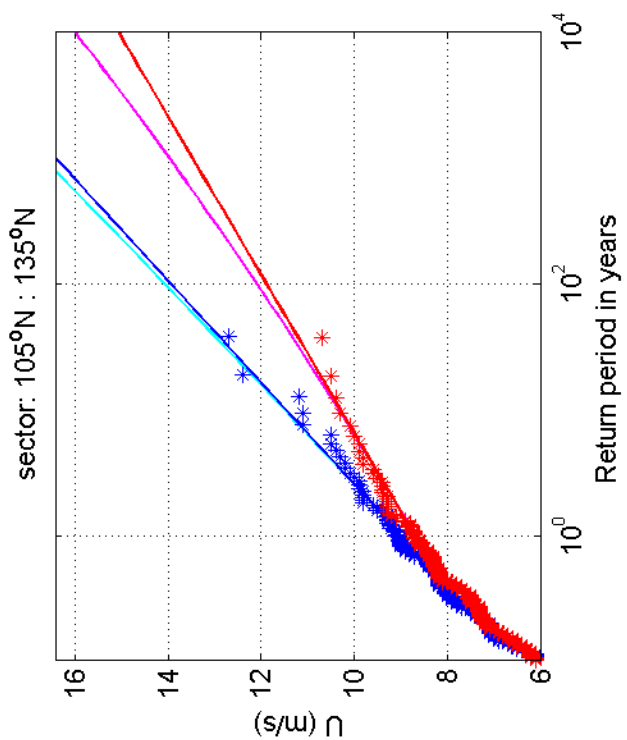
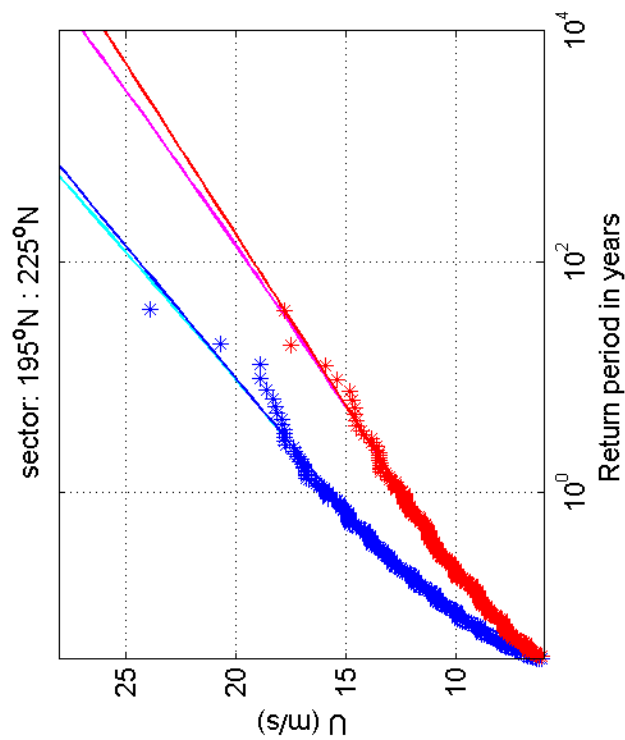
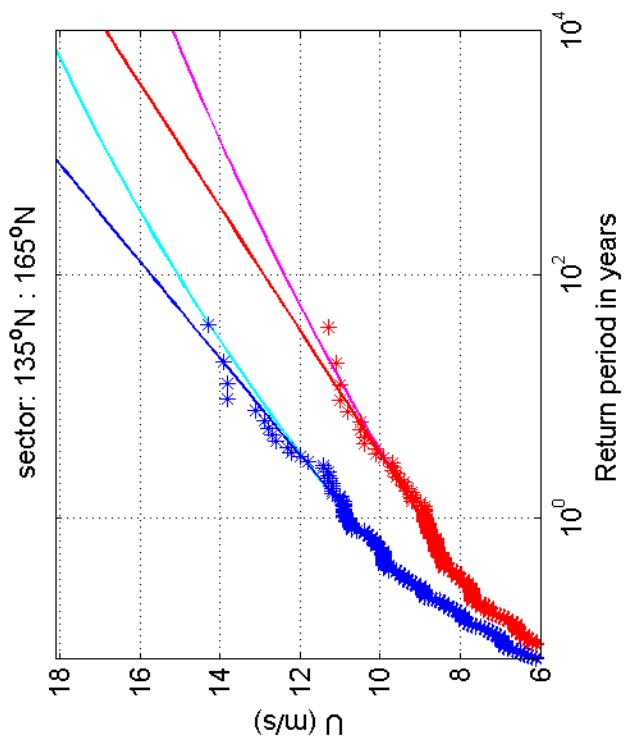
1200264-005

Fig. F.5a.5



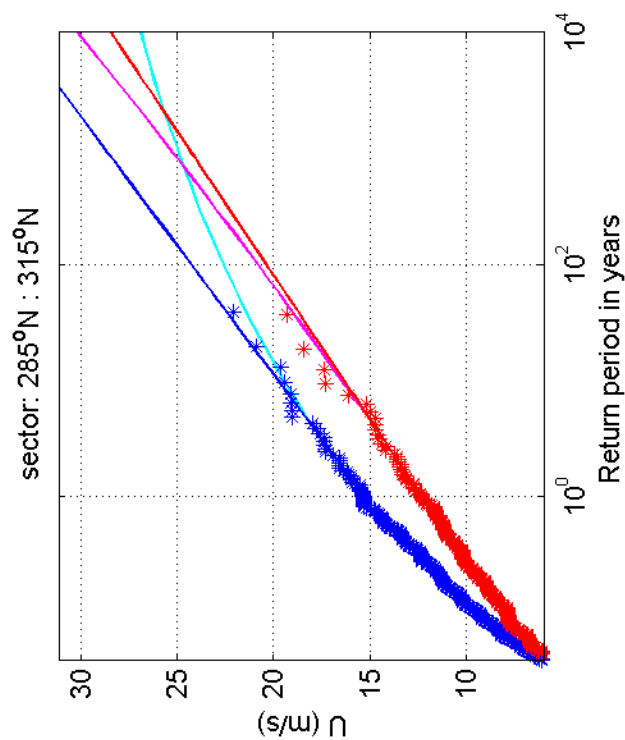
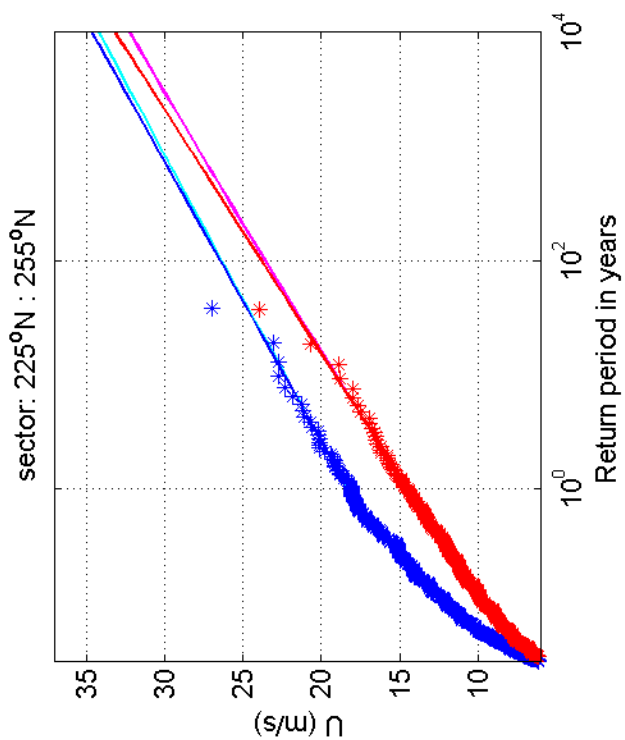
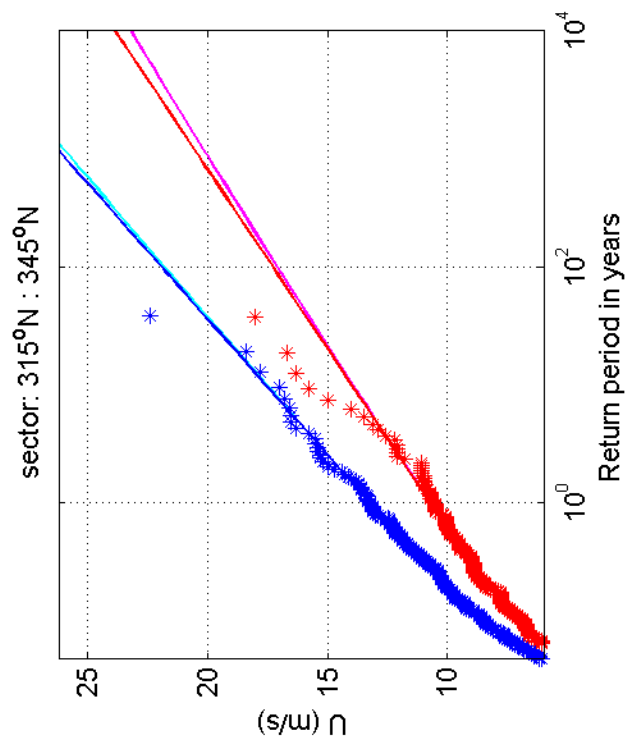
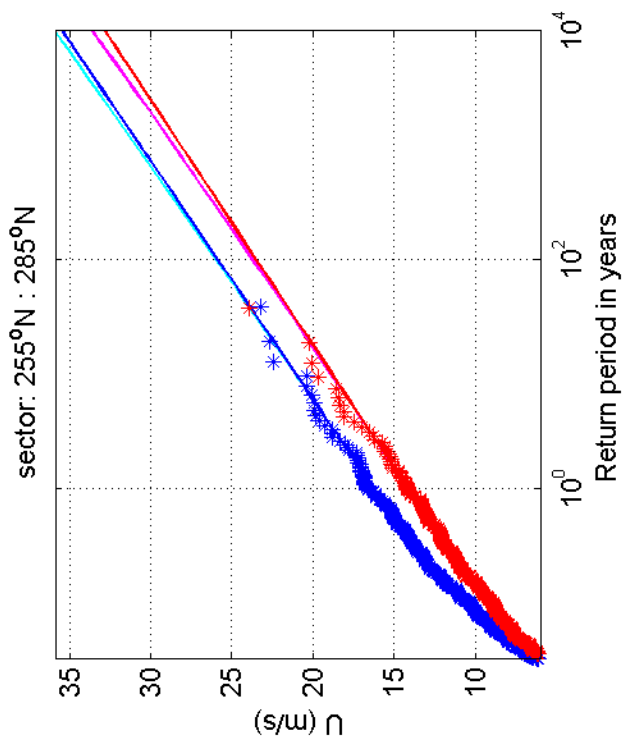
Return value plot per sector of Schiphol (blue) vs Soesterberg (red)
 Exponential (blue, red) and GPD (cyan, magenta) fits to U_p
 Plotting positions: x_i vs $(n+1)/(\lambda(n+1-i))$

1970-2008



Return value plot per sector of Schiphol (blue) vs Soesterberg (red)
 Exponential (blue, red) and GPD (cyan, magenta) fits to U_p
 Plotting positions: x_i vs $(n+1)/(\lambda(n+1-i))$

1970-2008



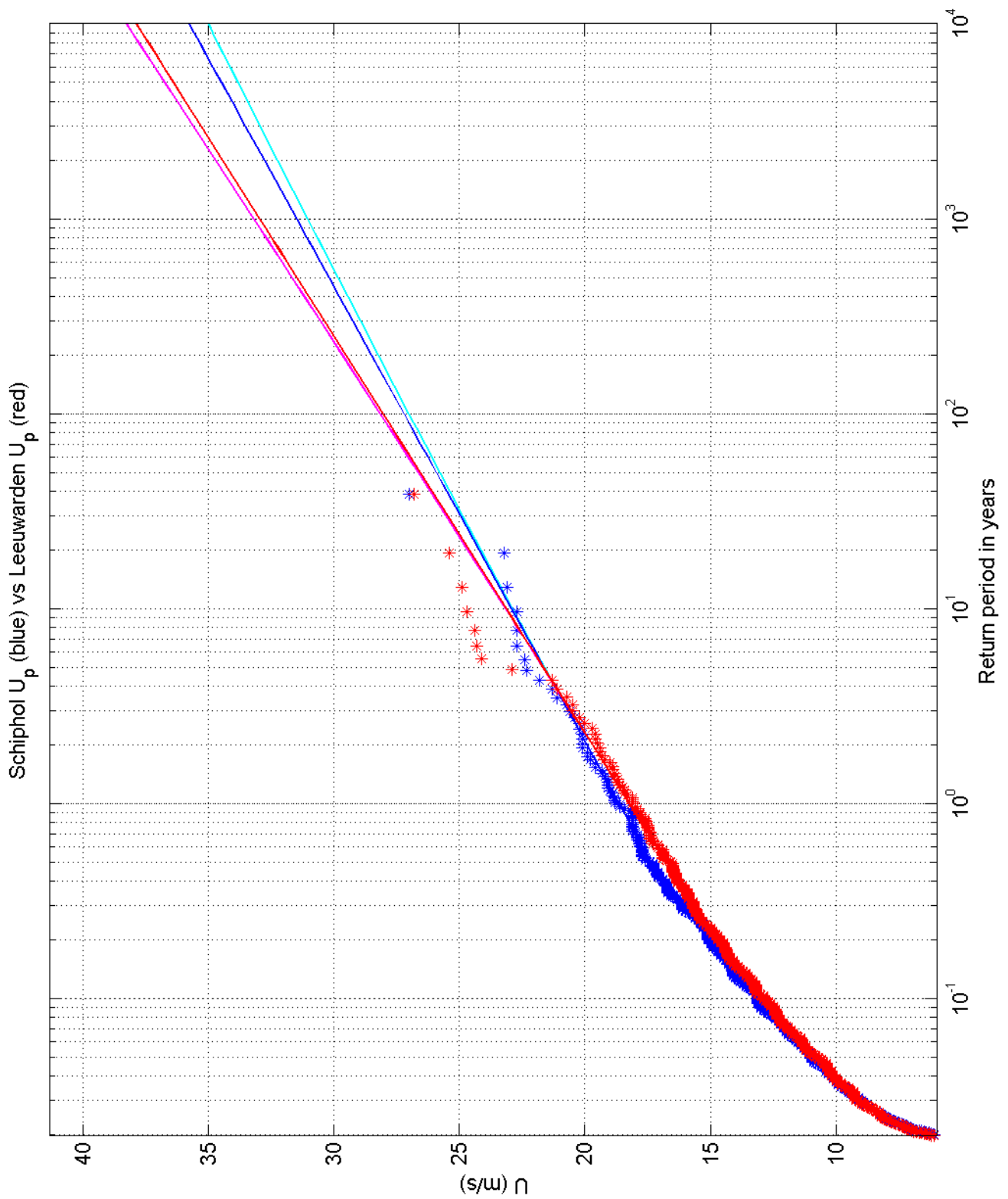
Return value plot per sector of Schiphol (blue) vs Soesterberg (red)
 Exponential (blue, red) and GPD (cyan, magenta) fits to U_p
 Plotting positions: x_i vs $(n+1)/(\lambda(n+1-i))$

1970-2008

Deltares

1200264-005

Fig. F.5d.5



Return value plot of Schiphol (blue) vs Leeuwarden (red)
 Exponential (blue, red) and GPD (cyan, magenta) fits to U_p
 Plotting positions: x_i vs $(n+1)/(\lambda(n+1-i))$

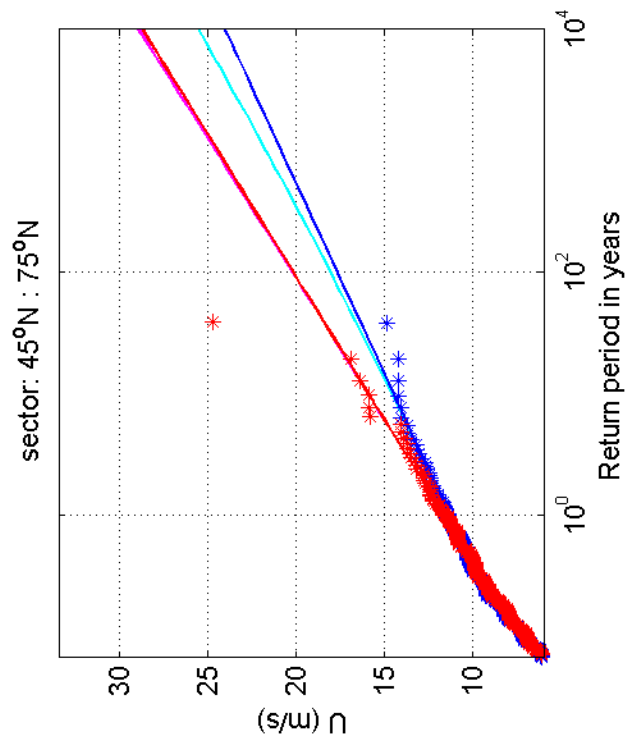
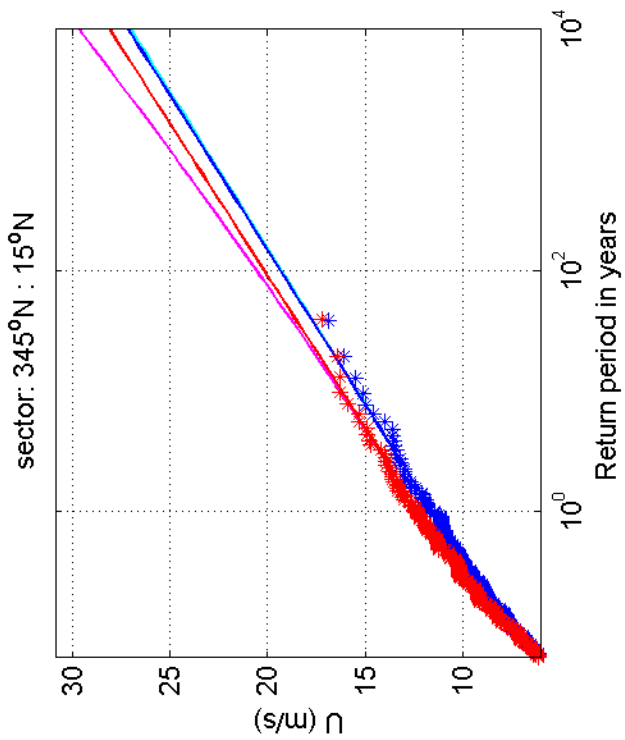
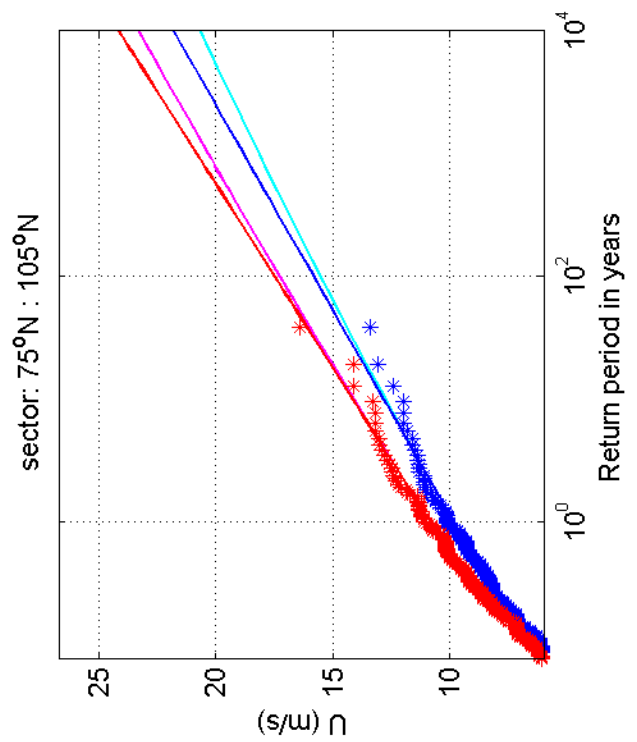
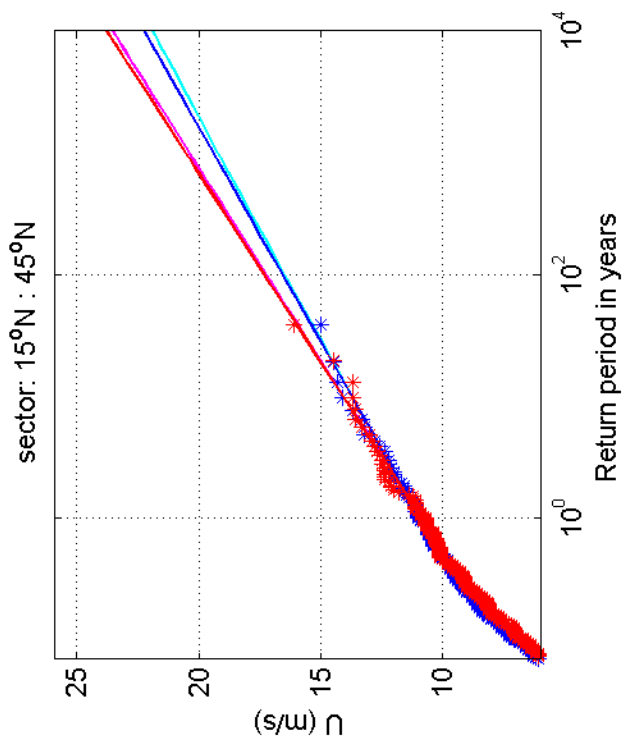
1970-2008

Schiphol vs Leeuwarden

Deltares

1200264-005

Fig. F.5a.6



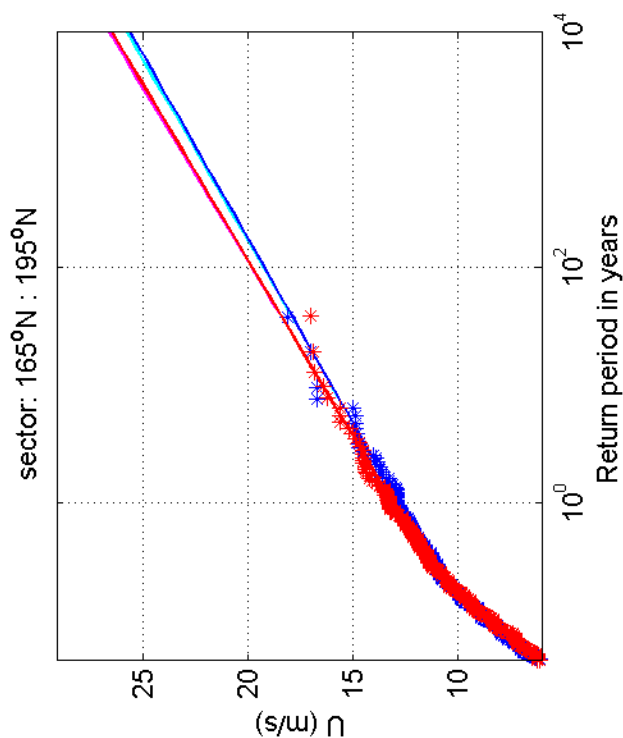
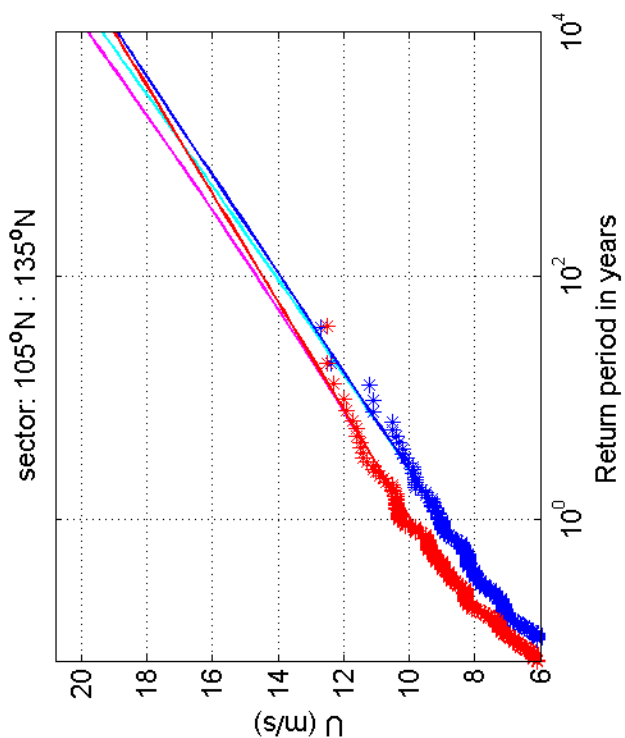
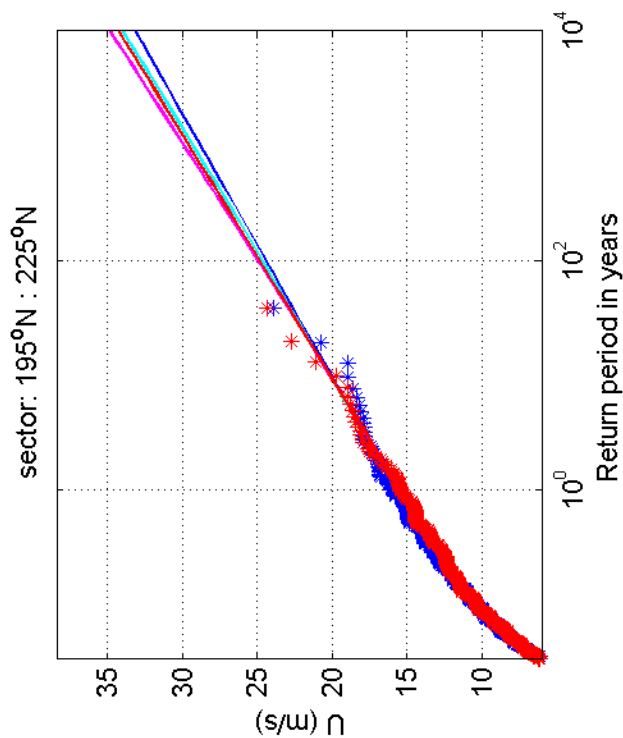
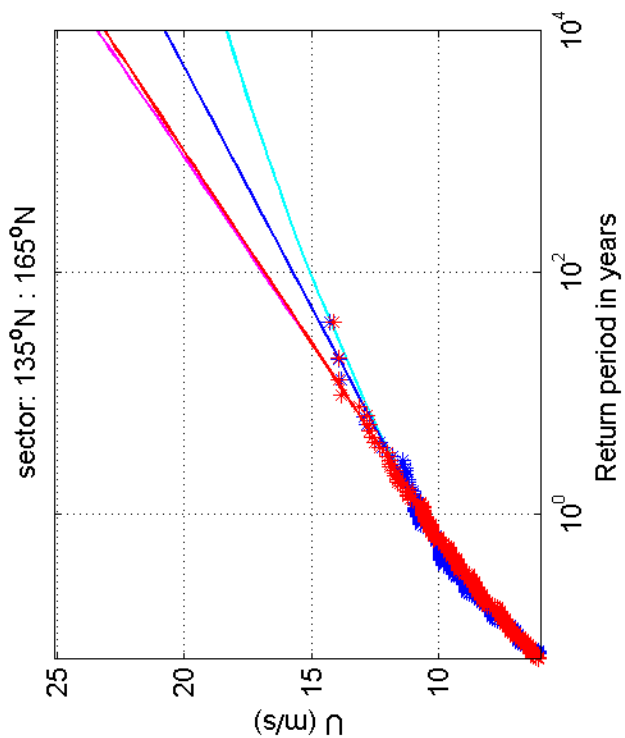
Return value plot per sector of Schiphol (blue) vs Leeuwarden (red)
 Exponential (blue, red) and GPD (cyan, magenta) fits to U_p
 Plotting positions: x_i vs $(n+1)/(\lambda(n+1-i))$

1970-2008

Deltares

1200264-005

Fig. F.5b.6



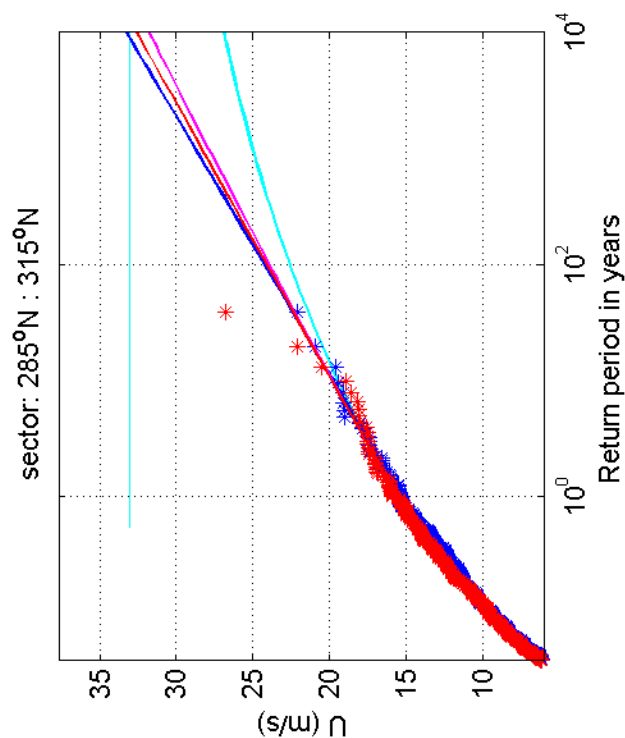
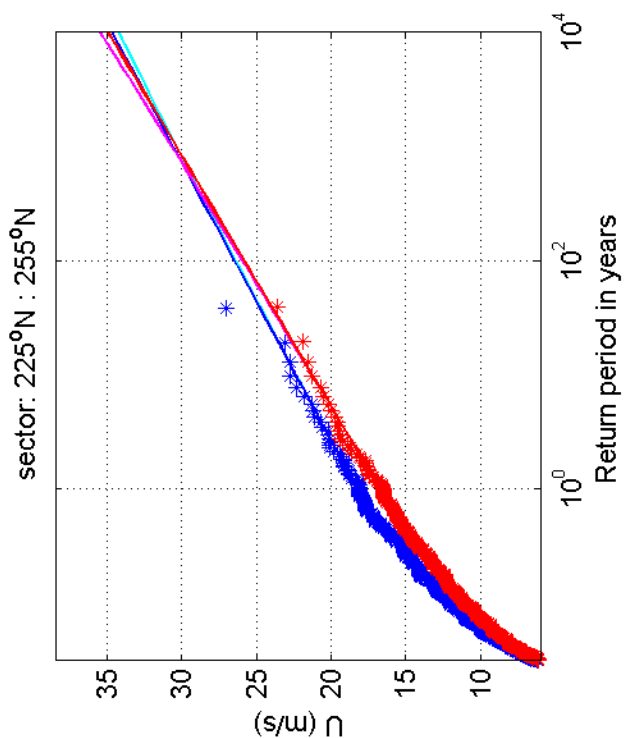
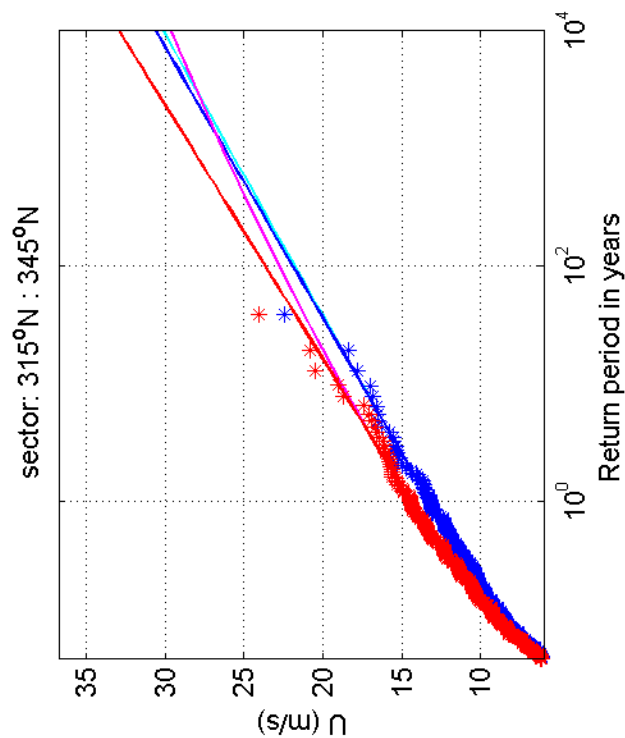
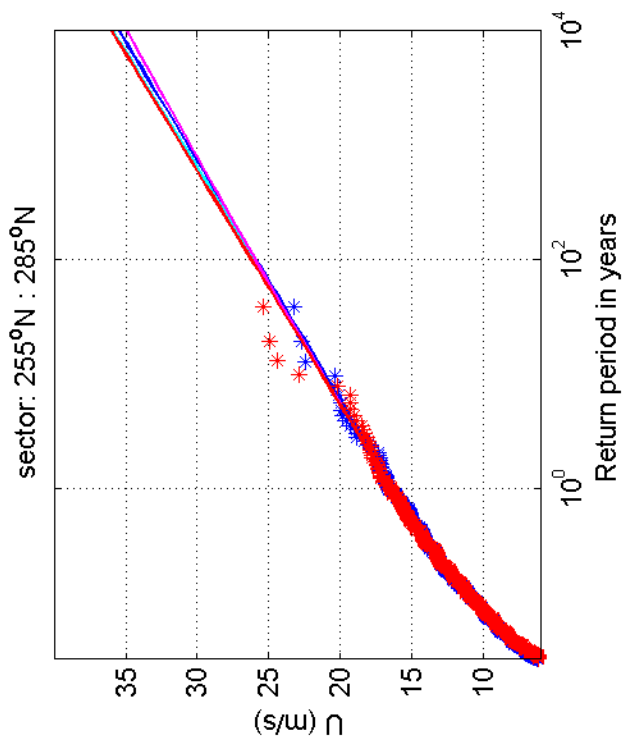
Return value plot per sector of Schiphol (blue) vs Leeuwarden (red)
 Exponential (blue, red) and GPD (cyan, magenta) fits to U_p
 Plotting positions: x_i vs $(n+1)/(\lambda(n+1-i))$

1970-2008

Deltares

1200264-005

Fig. F.5c.6



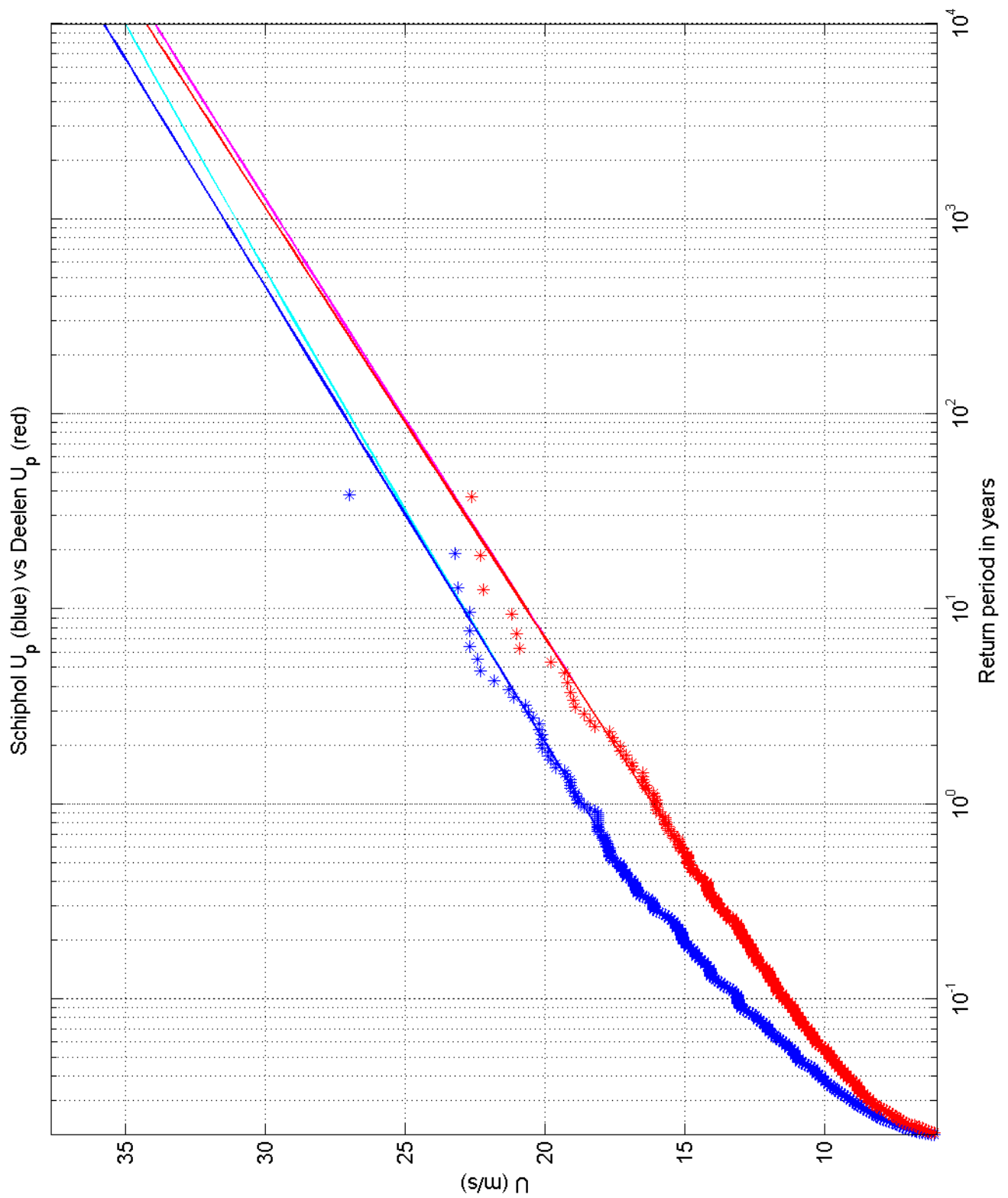
Return value plot per sector of Schiphol (blue) vs Leeuwarden (red)
 Exponential (blue, red) and GPD (cyan, magenta) fits to U_p
 Plotting positions: x_i vs $(n+1)/(\lambda(n+1-i))$

1970-2008

Deltares

1200264-005

Fig. F.5d.6



Return value plot of Schiphol (blue) vs Deelen (red)
 Exponential (blue, red) and GPD (cyan, magenta) fits to U_p
 Plotting positions: x_i vs $(n+1)/(\lambda(n+1-i))$

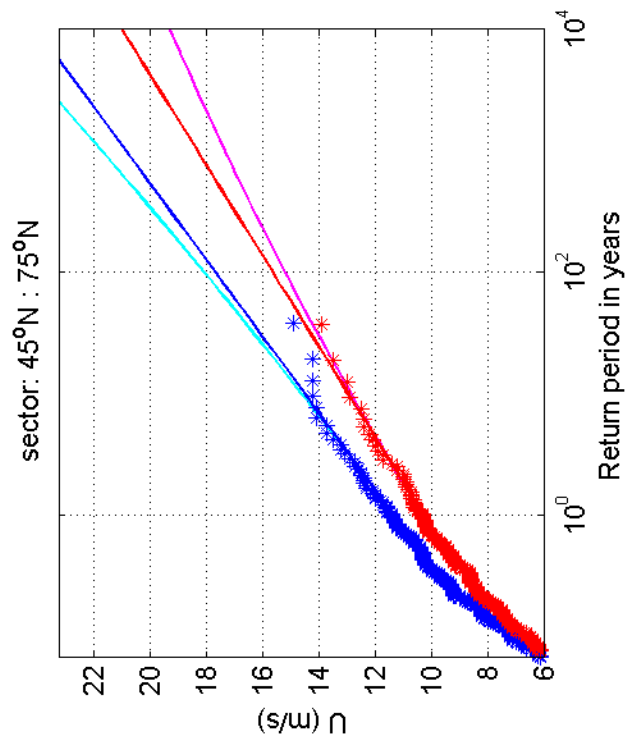
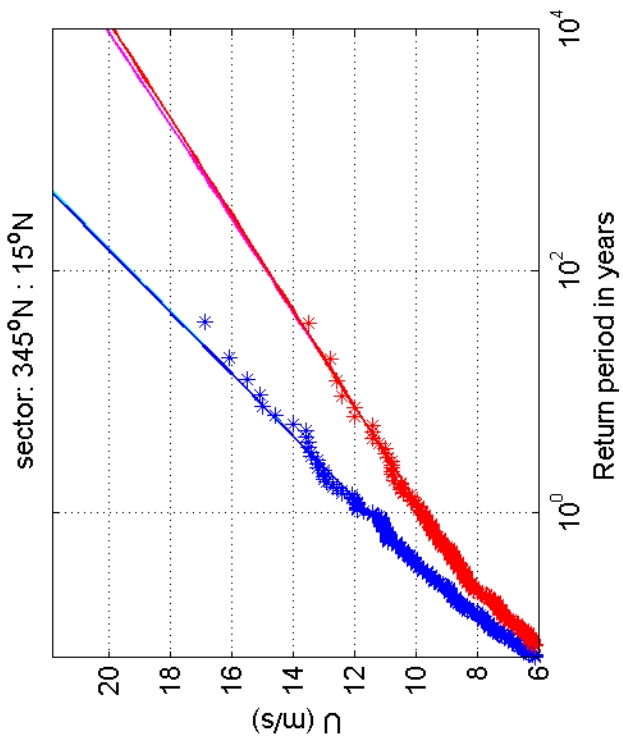
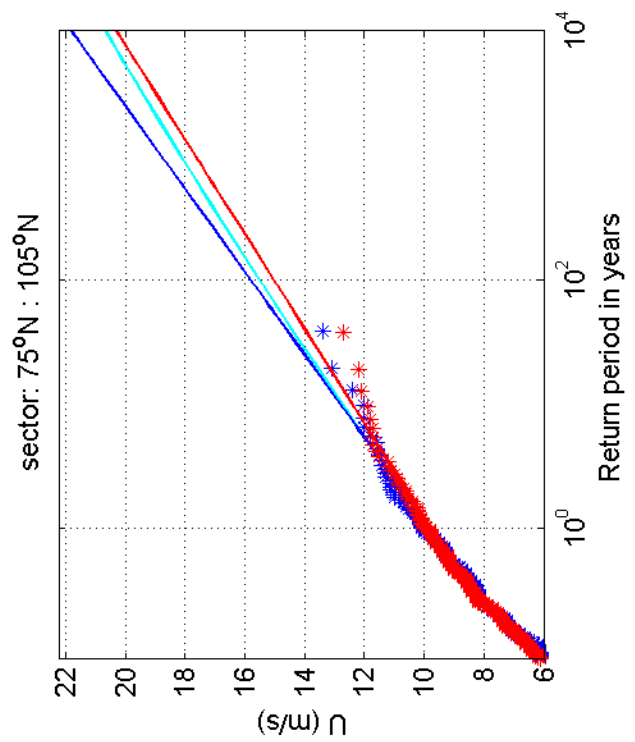
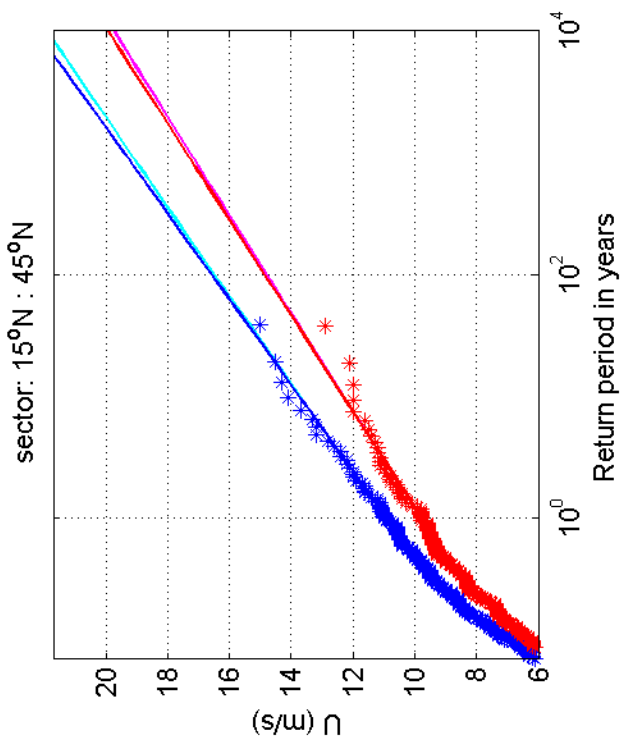
1970-2008

Schiphol vs Deelen

Deltares

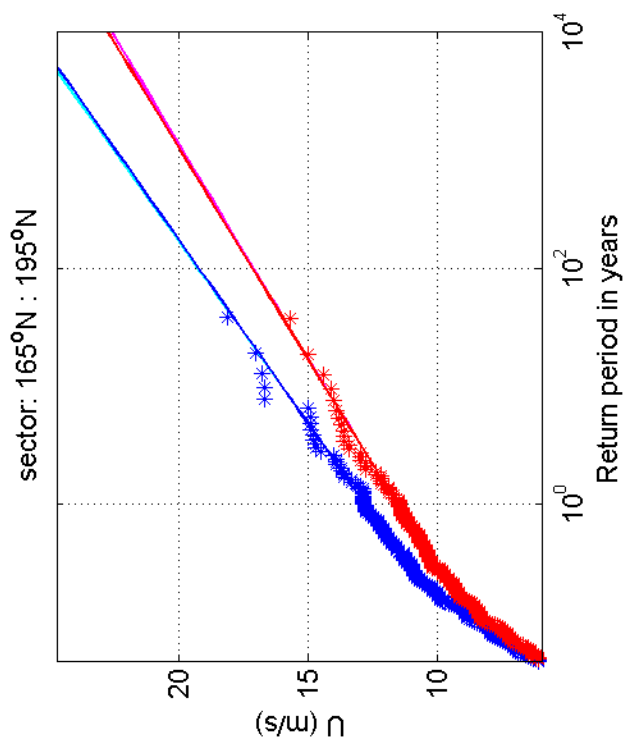
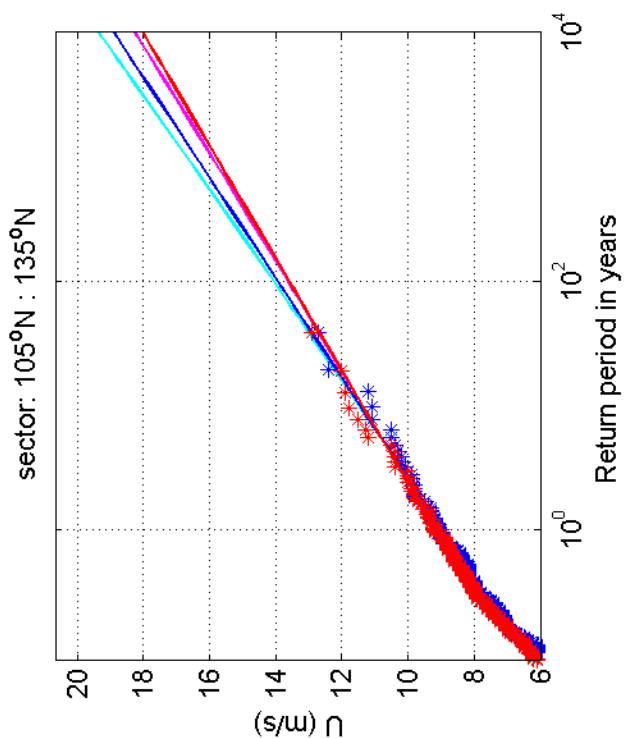
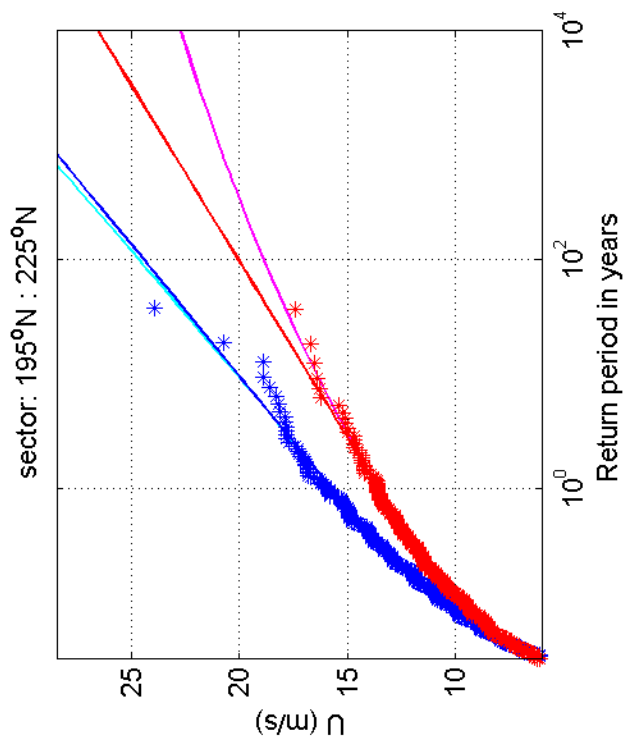
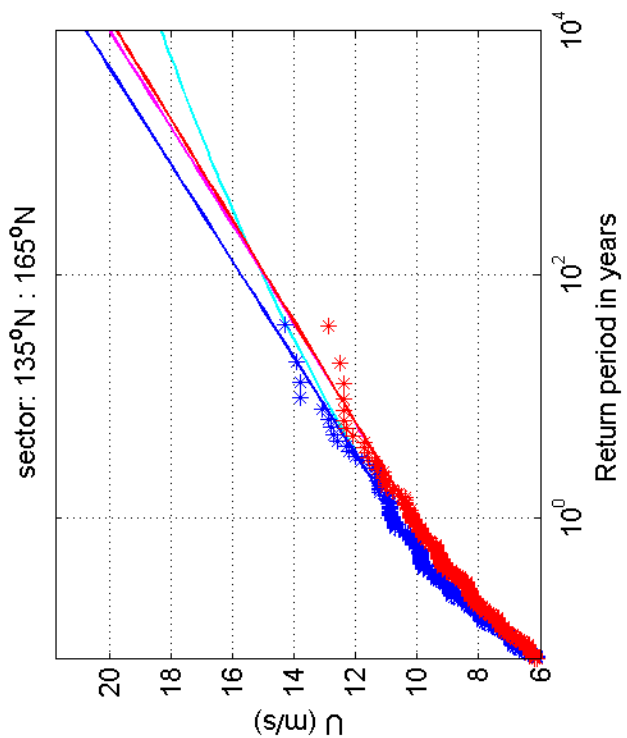
1200264-005

Fig. F.5a.7



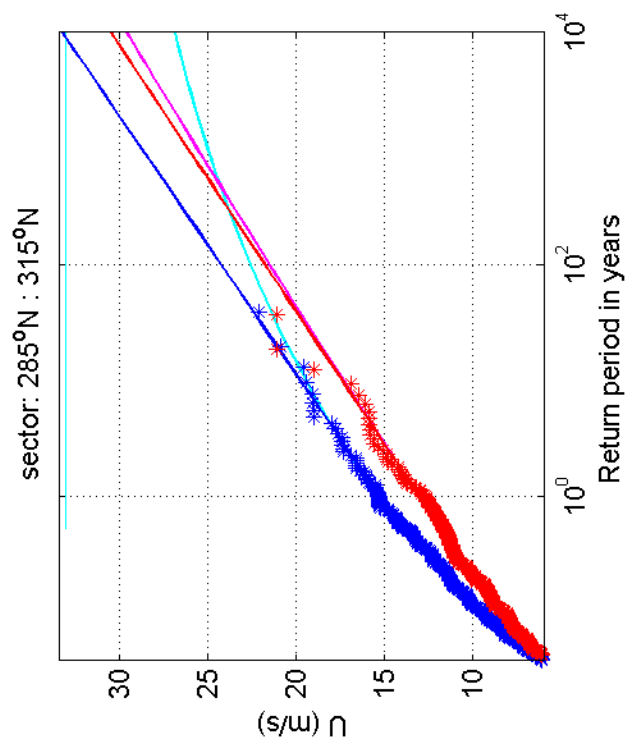
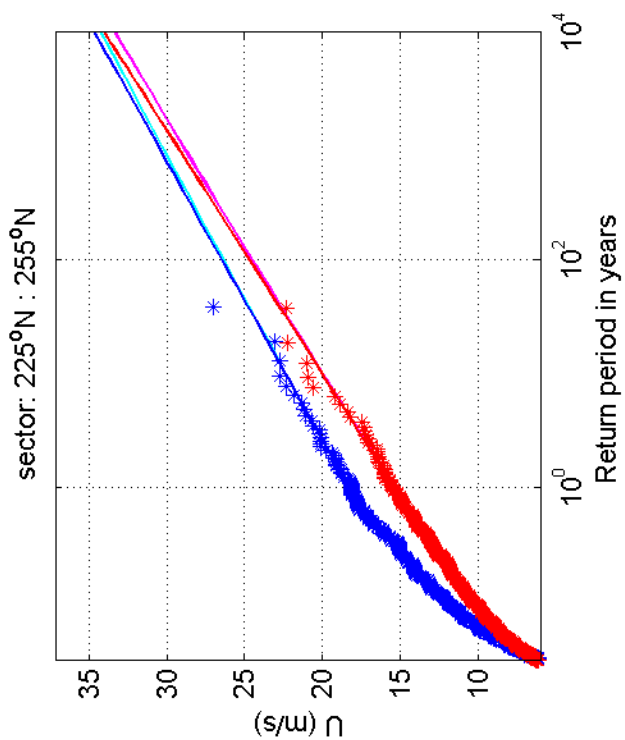
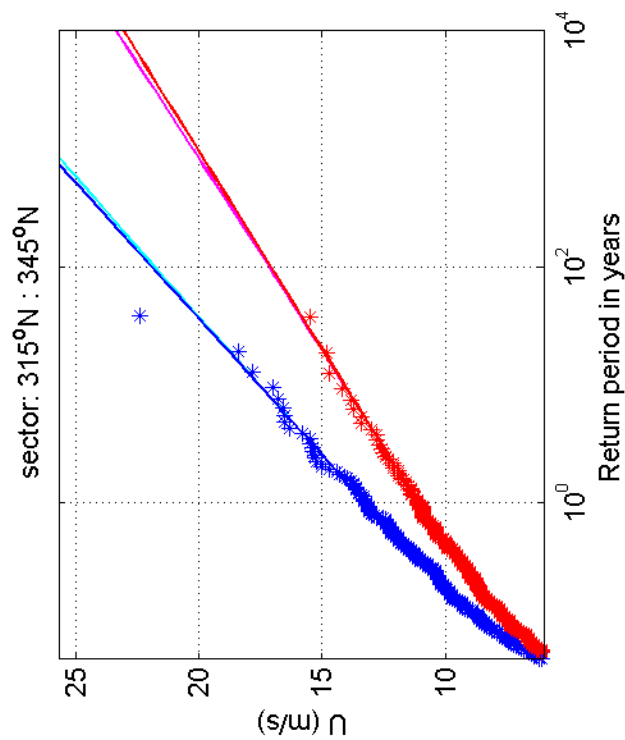
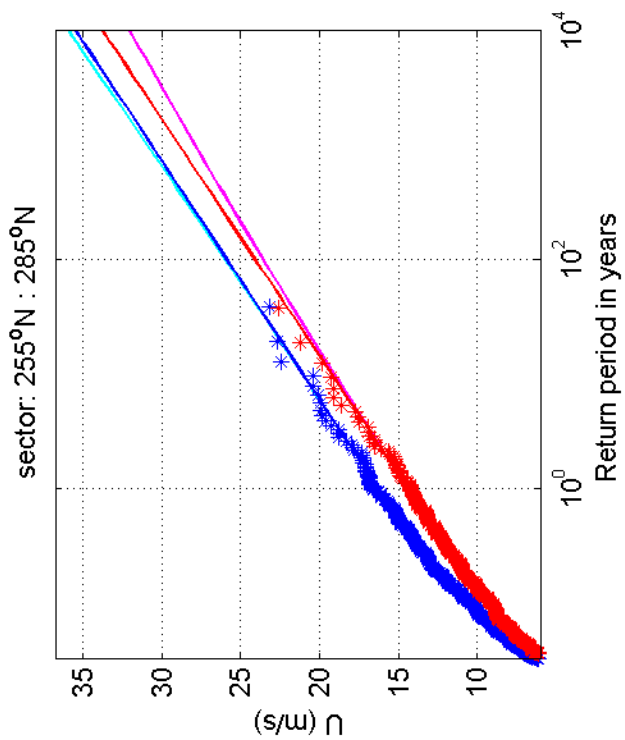
Return value plot per sector of Schiphol (blue) vs Deelen (red)
 Exponential (blue, red) and GPD (cyan, magenta) fits to U_p
 Plotting positions: x_i vs $(n+1)/(\lambda(n+1-i))$

1970-2008



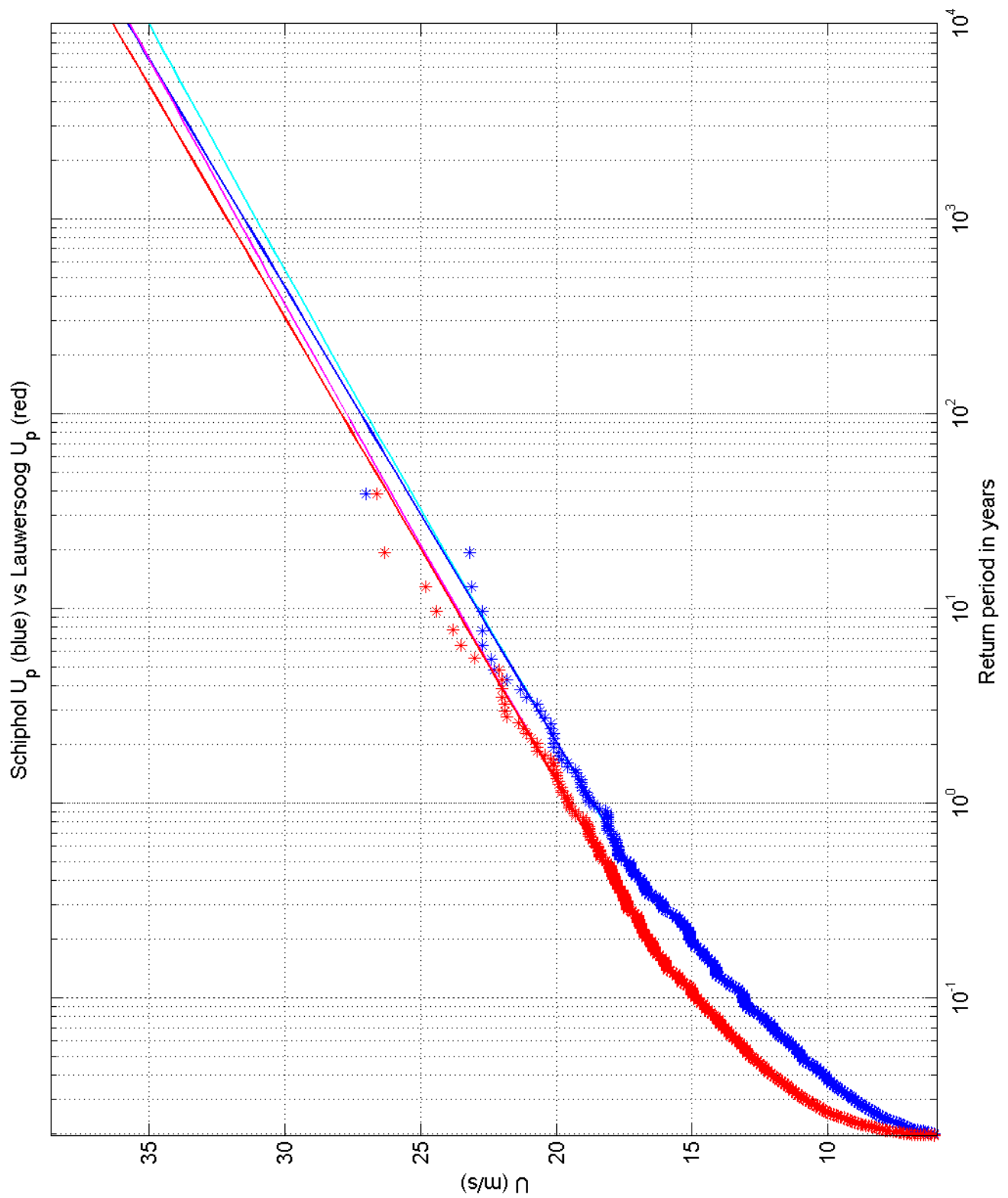
Return value plot per sector of Schiphol (blue) vs Deelen (red)
 Exponential (blue, red) and GPD (cyan, magenta) fits to U_p
 Plotting positions: x_i vs $(n+1)/(\lambda(n+1-i))$

1970-2008



Return value plot per sector of Schiphol (blue) vs Deelen (red)
 Exponential (blue, red) and GPD (cyan, magenta) fits to U_p
 Plotting positions: x_i vs $(n+1)/(\lambda(n+1-i))$

1970-2008



Return value plot of Schiphol (blue) vs Lauwersoog (red)
 Exponential (blue, red) and GPD (cyan, magenta) fits to U_p
 Plotting positions: x_i vs $(n+1)/(\lambda(n+1-i))$

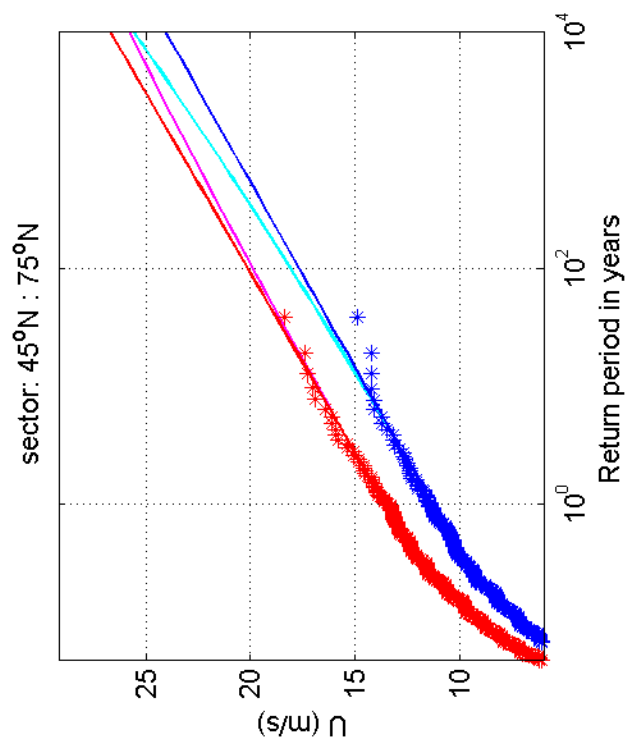
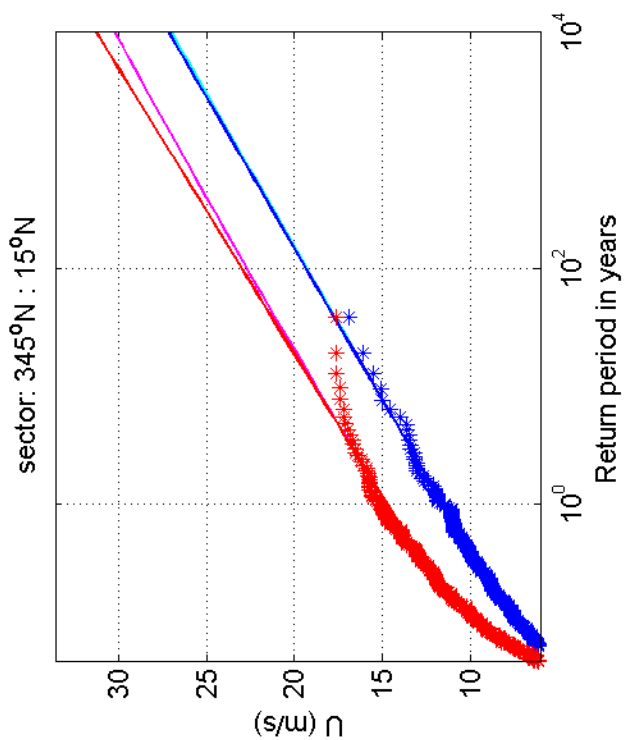
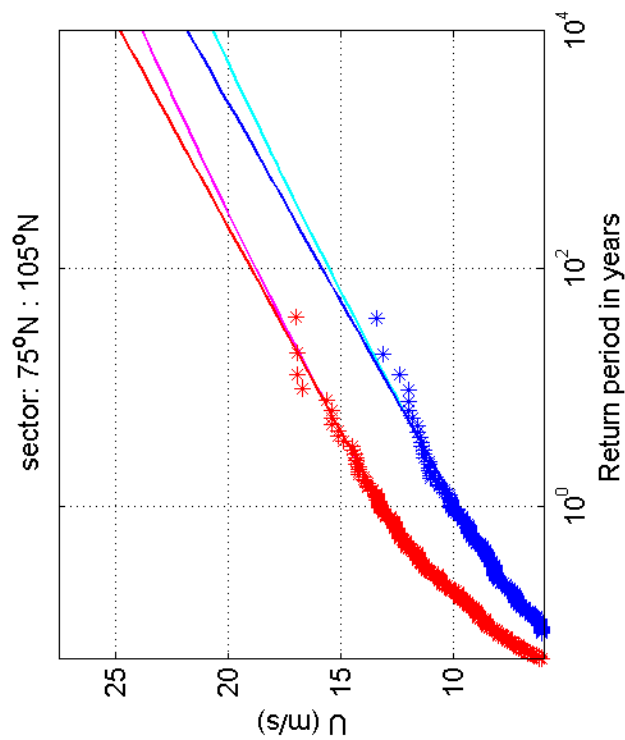
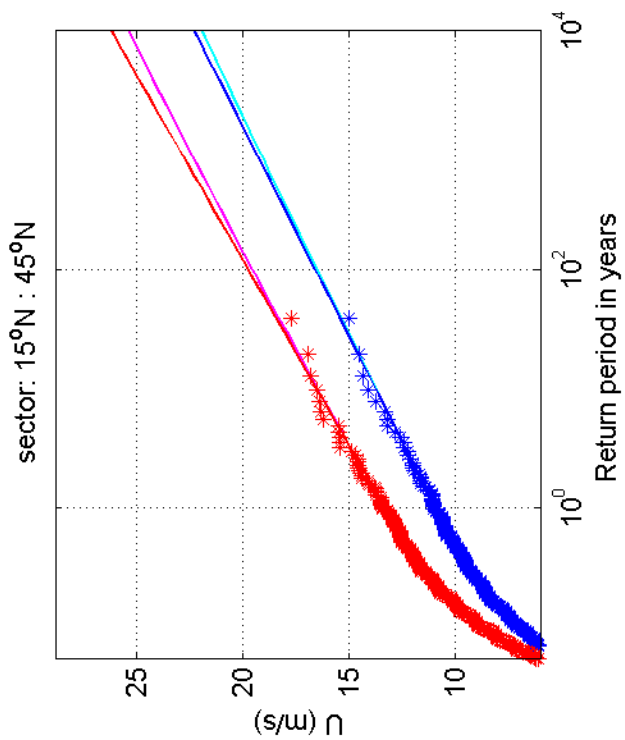
1970-2008

Schiphol vs Lauwersoog

Deltares

1200264-005

Fig. F.5a.8



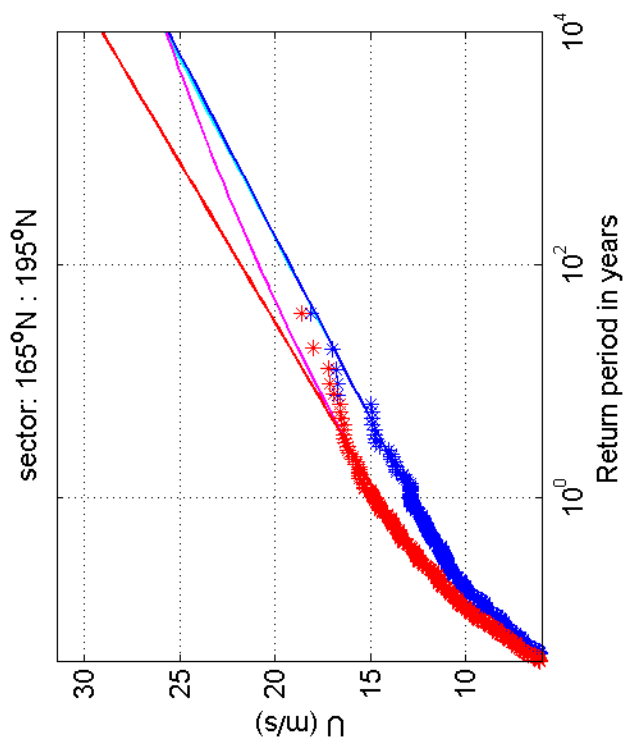
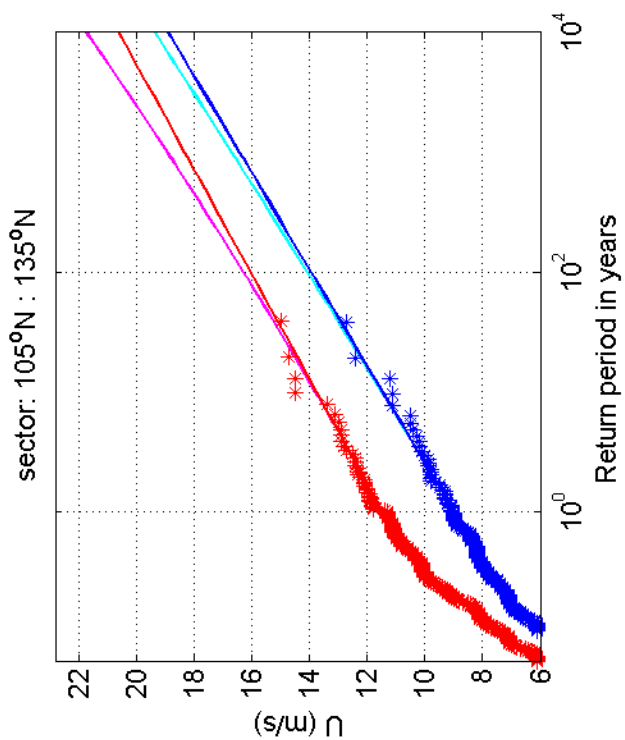
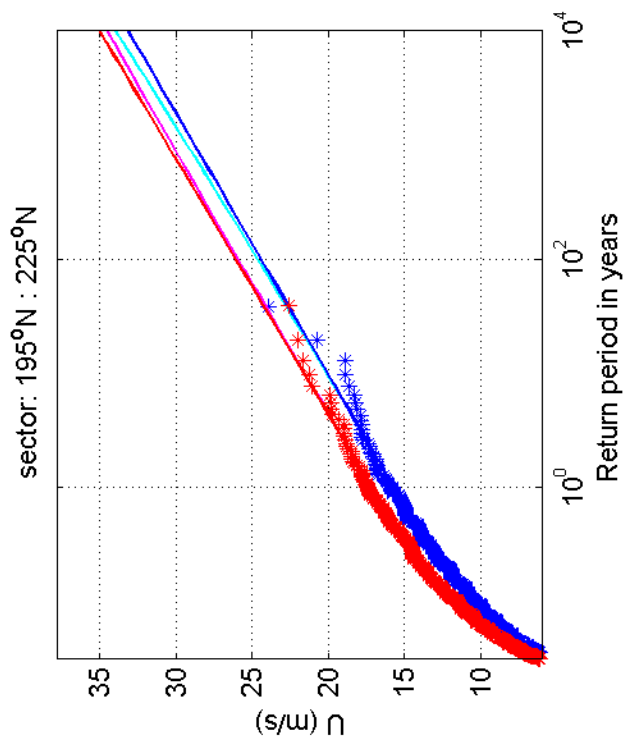
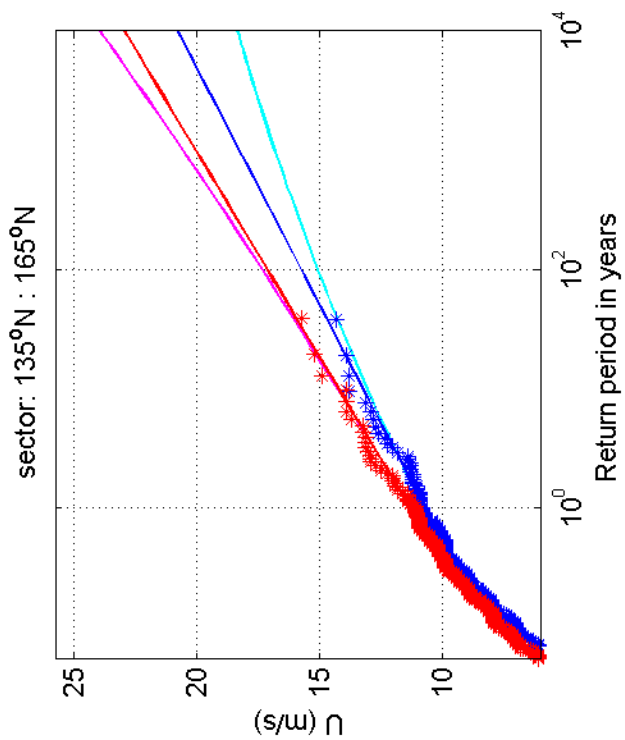
Return value plot per sector of Schiphol (blue) vs Lauwersoog (red)
 Exponential (blue, red) and GPD (cyan, magenta) fits to U_p
 Plotting positions: x_i vs $(n+1)/(\lambda(n+1-i))$

1970-2008

Deltares

1200264-005

Fig. F.5b.8



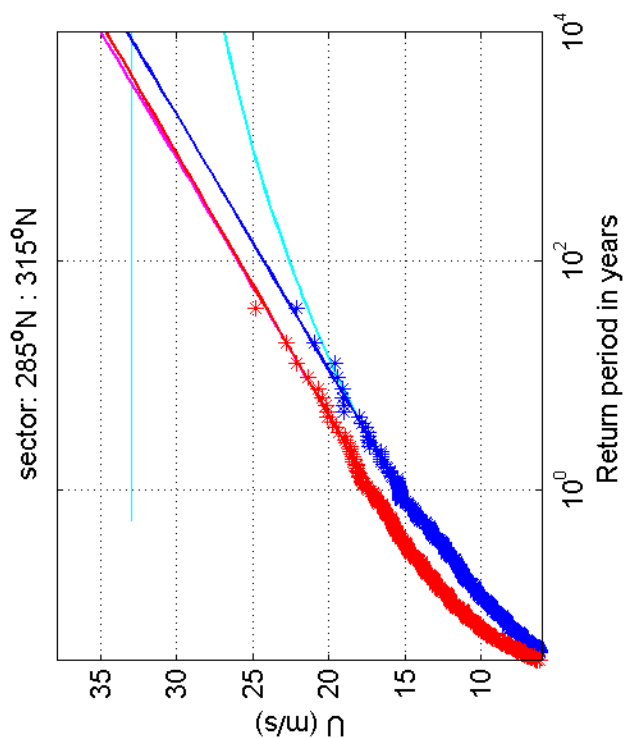
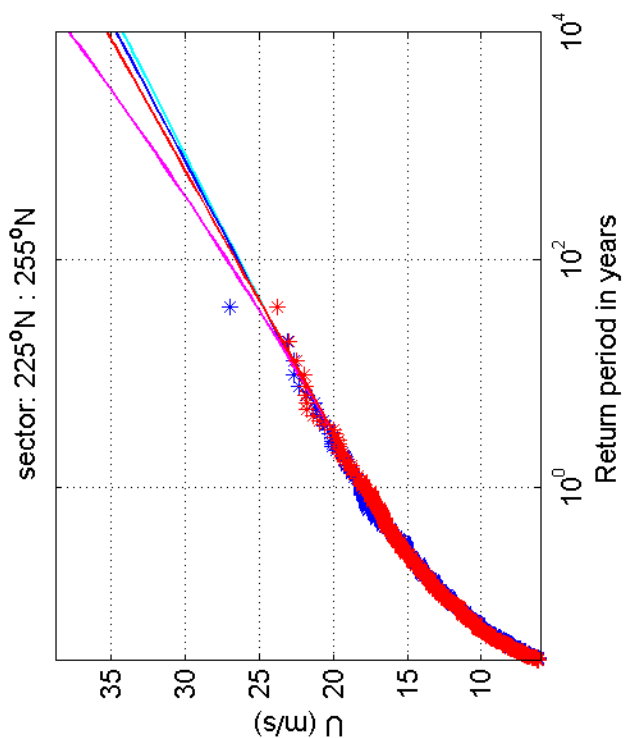
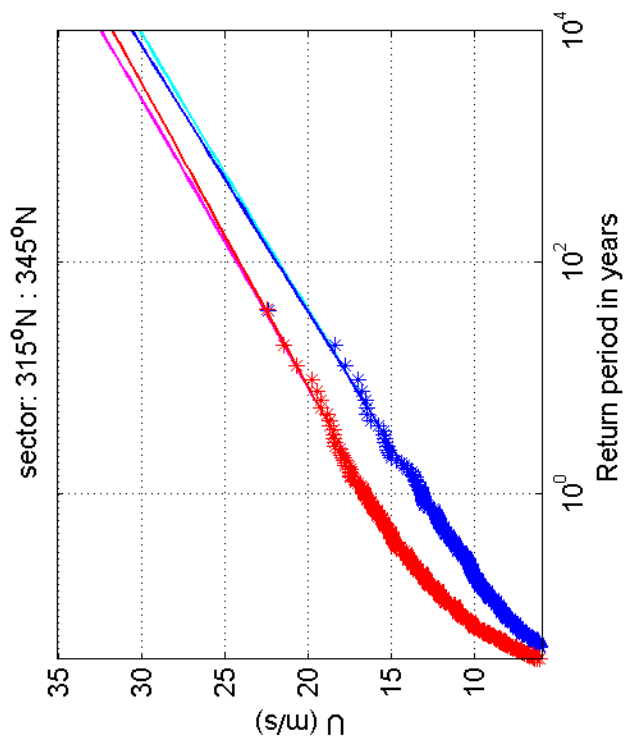
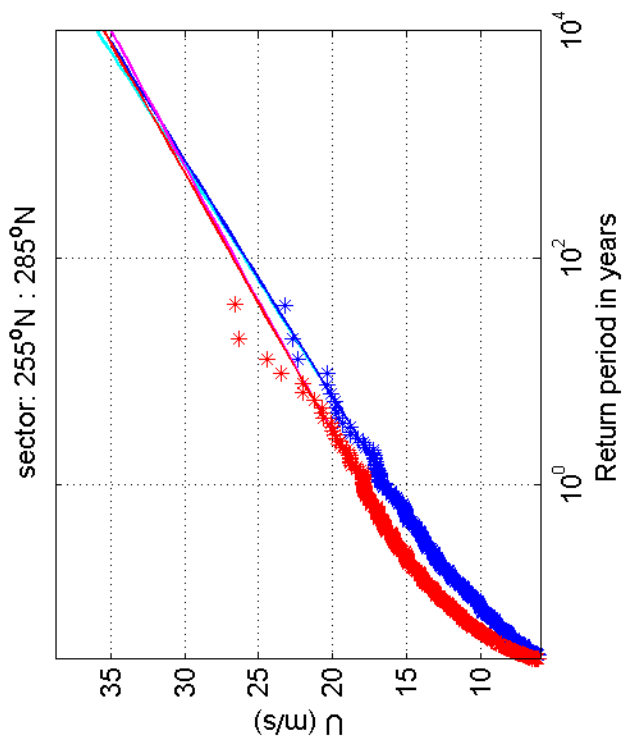
Return value plot per sector of Schiphol (blue) vs Lauwersoog (red)
 Exponential (blue, red) and GPD (cyan, magenta) fits to U_p
 Plotting positions: x_i vs $(n+1)/(\lambda(n+1-i))$

1970-2008

Deltares

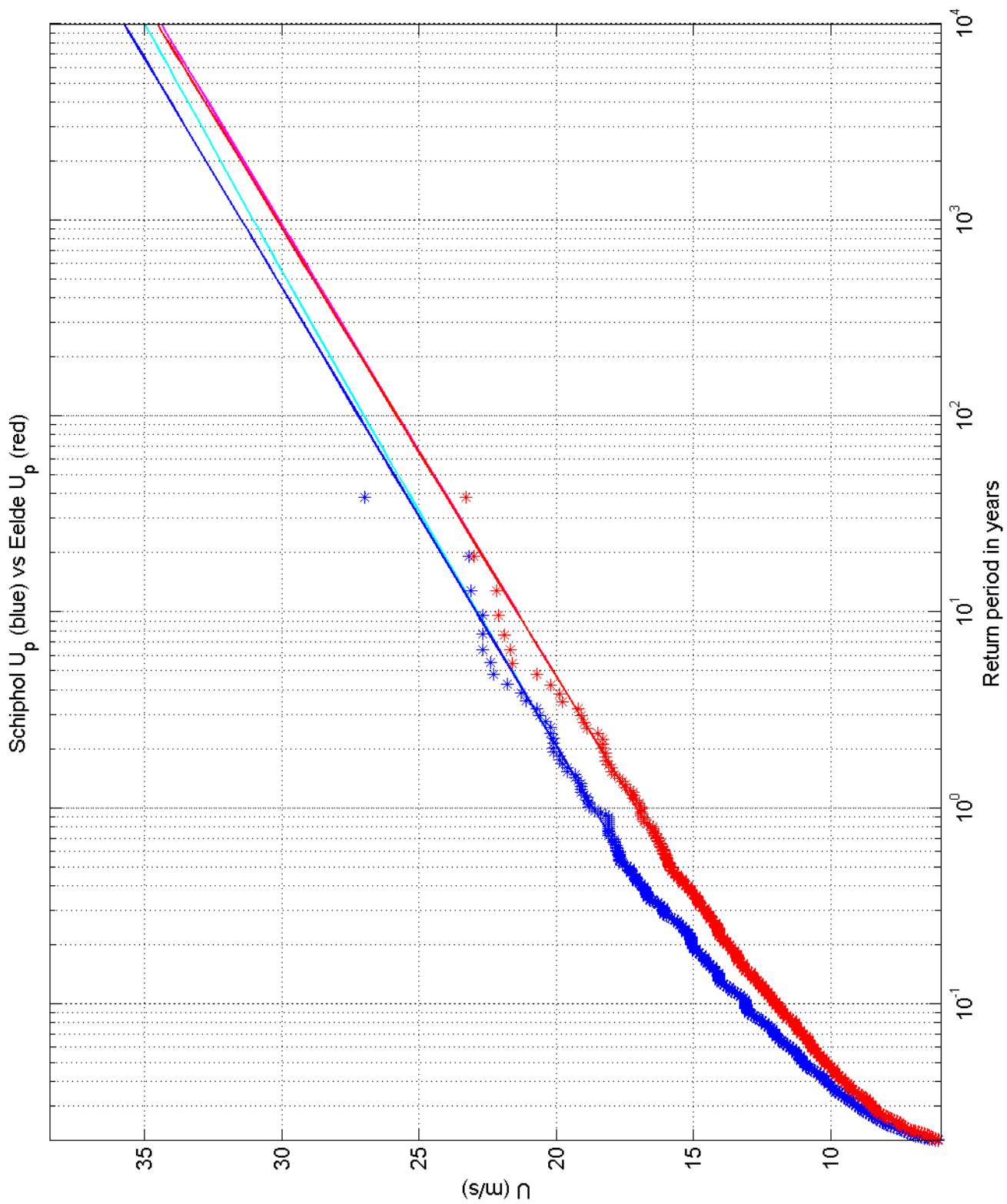
1200264-005

Fig. F.5c.8



Return value plot per sector of Schiphol (blue) vs Lauwersoog (red)
 Exponential (blue, red) and GPD (cyan, magenta) fits to U_p
 Plotting positions: x_i vs $(n+1)/(\lambda(n+1-i))$

1970-2008



Return value plot of Schiphol (blue) vs Eelde (red)
 Exponential (blue, red) and GPD (cyan, magenta) fits to U_p
 Plotting positions: x_i vs $(n+1)/(\lambda(n+1-i))$

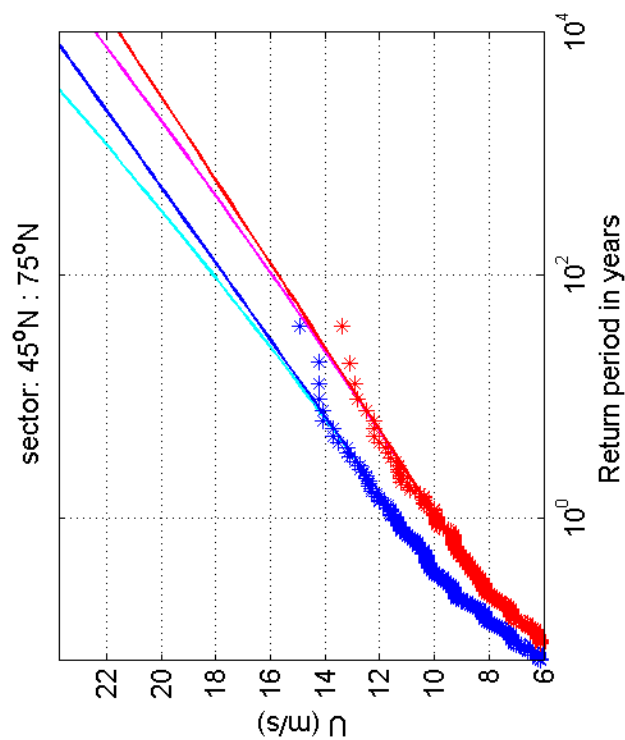
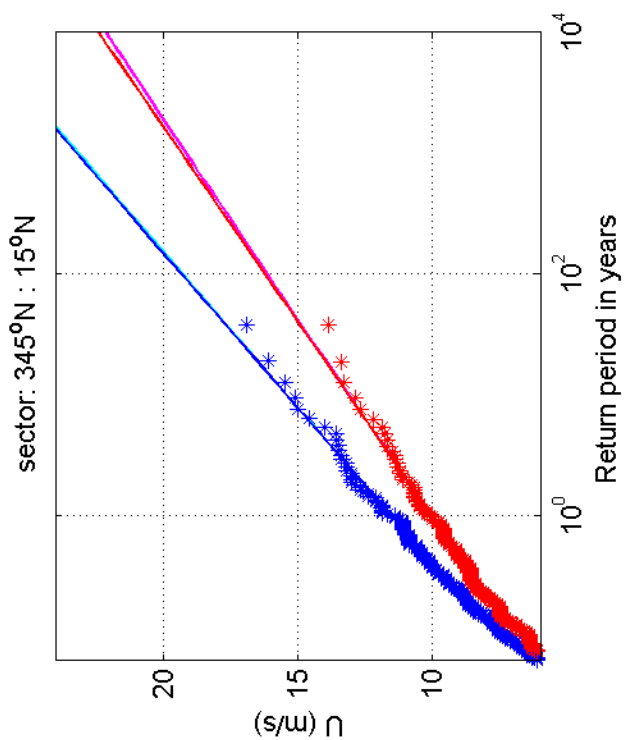
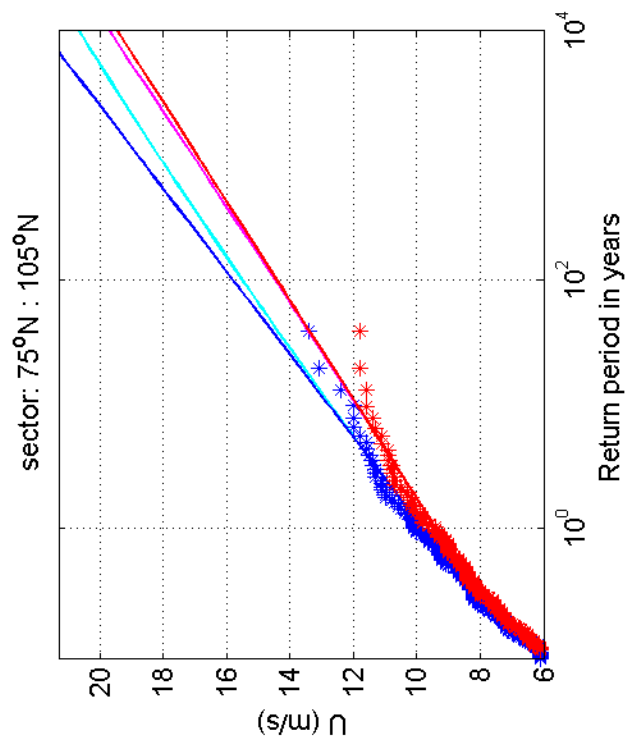
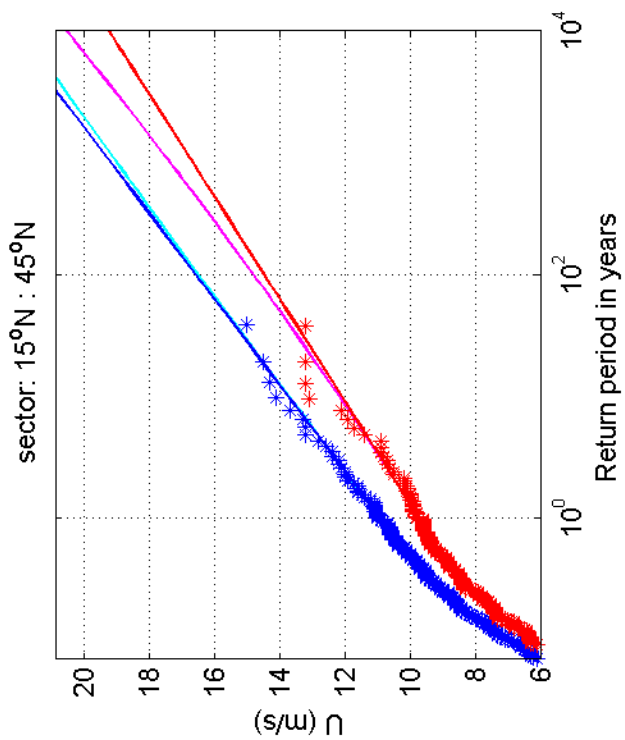
1970-2008

Schiphol vs Eelde

Deltares

1200264-005

Fig. F.5a.9



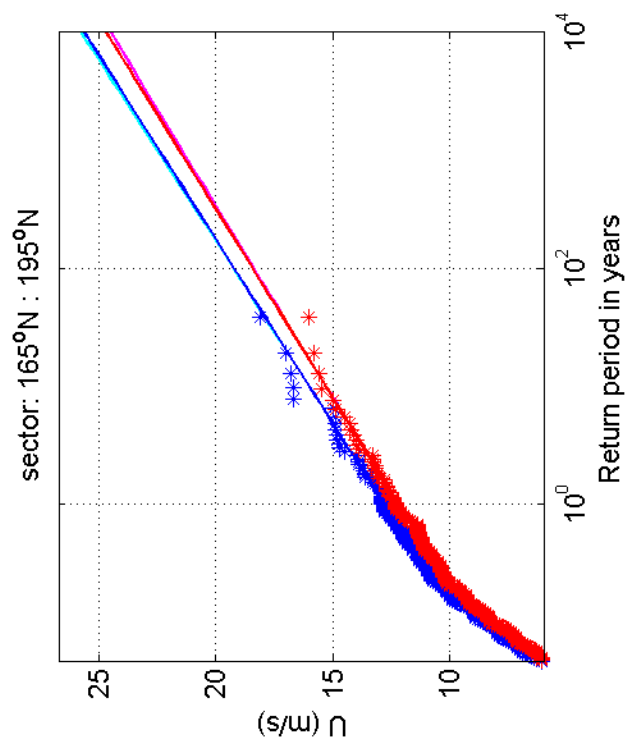
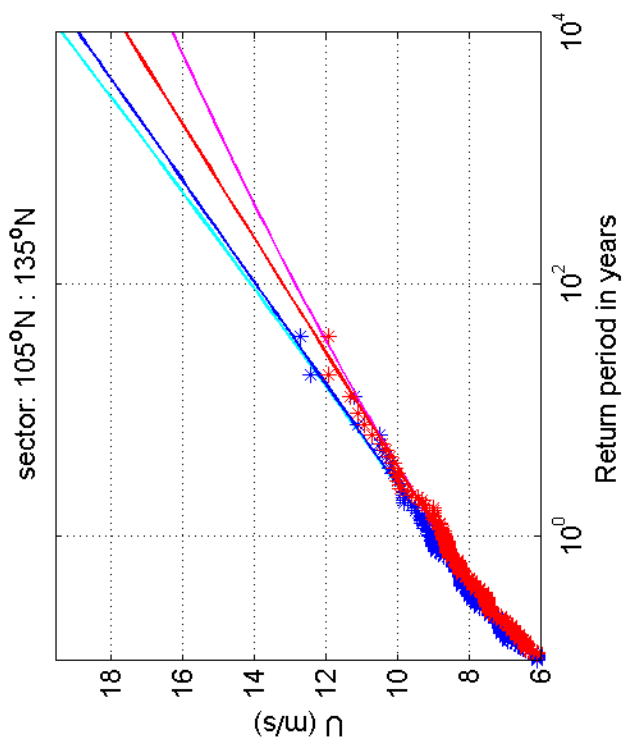
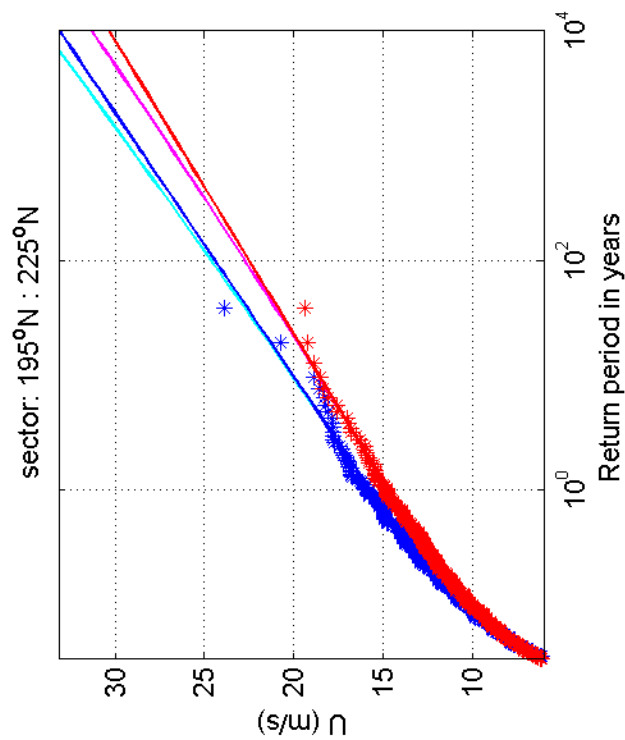
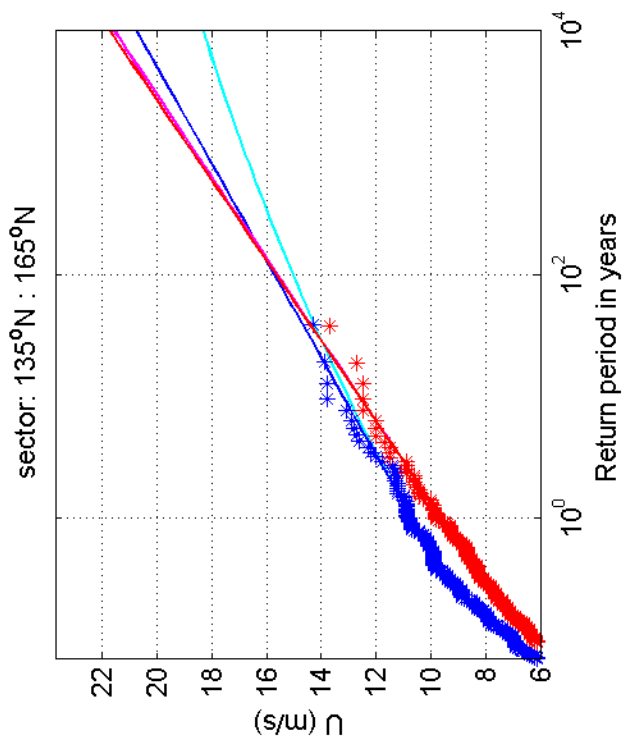
Return value plot per sector of Schiphol (blue) vs Eelde (red)
 Exponential (blue, red) and GPD (cyan, magenta) fits to U_p
 Plotting positions: x_i vs $(n+1)/(\lambda(n+1-i))$

1970-2008

Deltares

1200264-005

Fig. F.5b.9



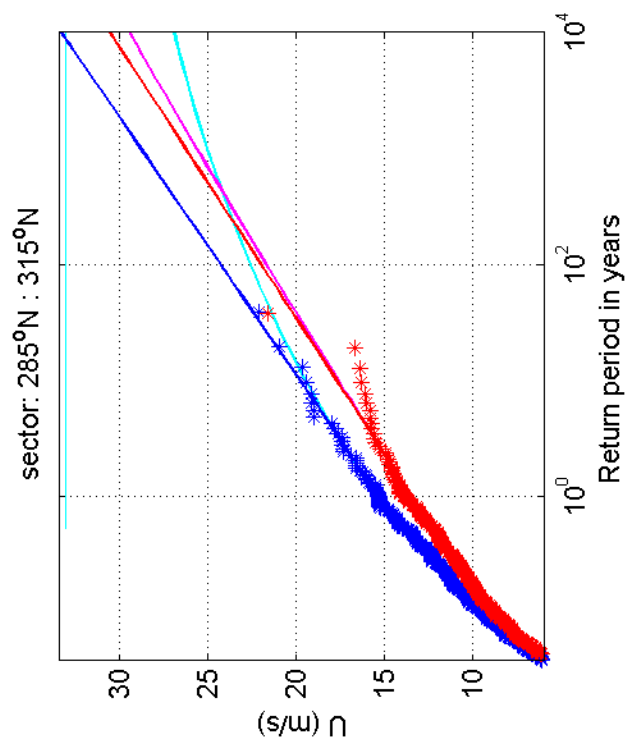
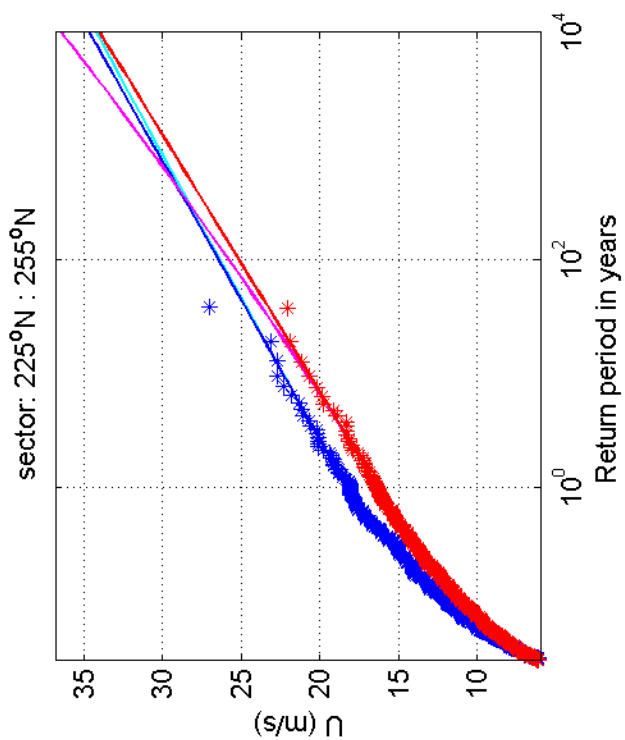
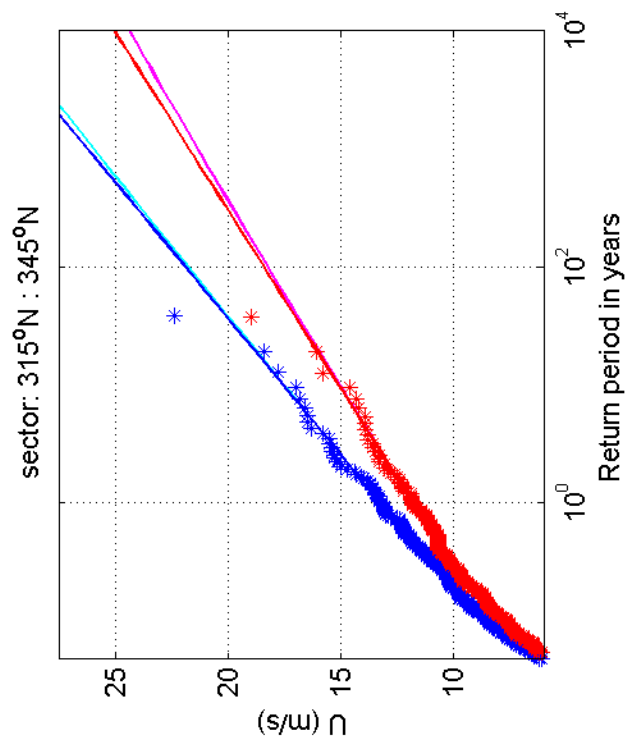
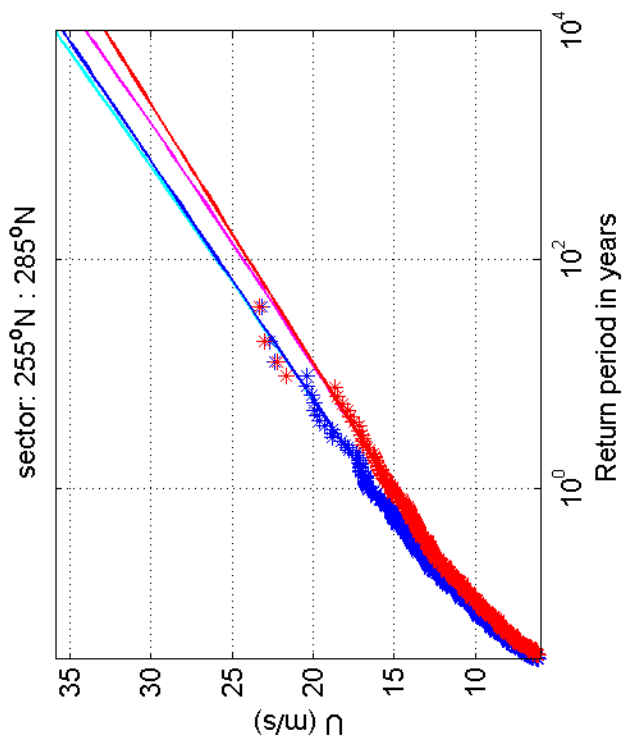
Return value plot per sector of Schiphol (blue) vs Eelde (red)
 Exponential (blue, red) and GPD (cyan, magenta) fits to U_p
 Plotting positions: x_i vs $(n+1)/(\lambda(n+1-i))$

1970-2008

Deltares

1200264-005

Fig. F.5c.9



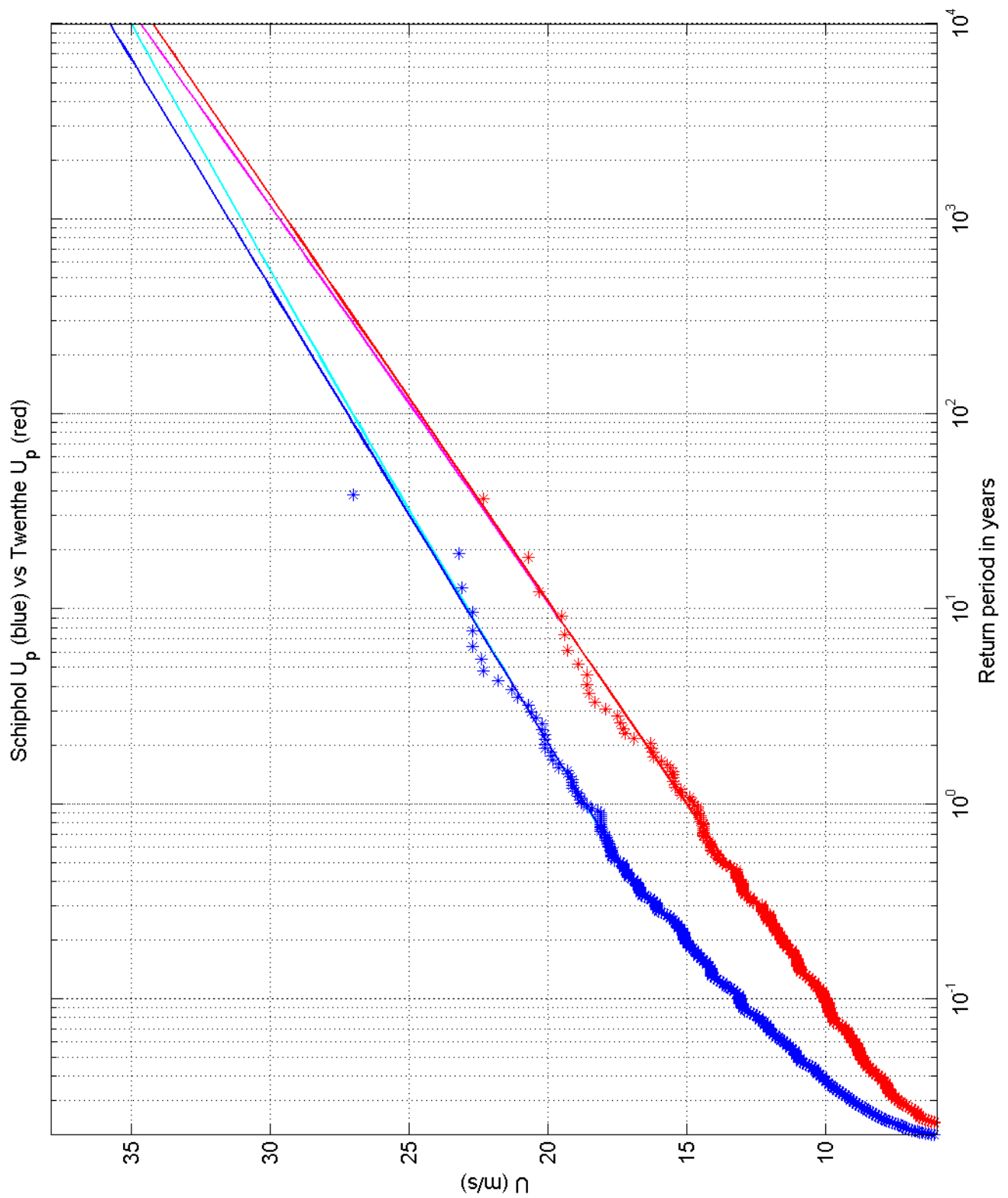
Return value plot per sector of Schiphol (blue) vs Eelde (red)
 Exponential (blue, red) and GPD (cyan, magenta) fits to U_p
 Plotting positions: x_i vs $(n+1)/(\lambda(n+1-i))$

1970-2008

Deltares

1200264-005

Fig. F.5d.9



Return value plot of Schiphol (blue) vs Twenthe (red)
 Exponential (blue, red) and GPD (cyan, magenta) fits to U_p
 Plotting positions: x_i vs $(n+1)/(\lambda(n+1-i))$

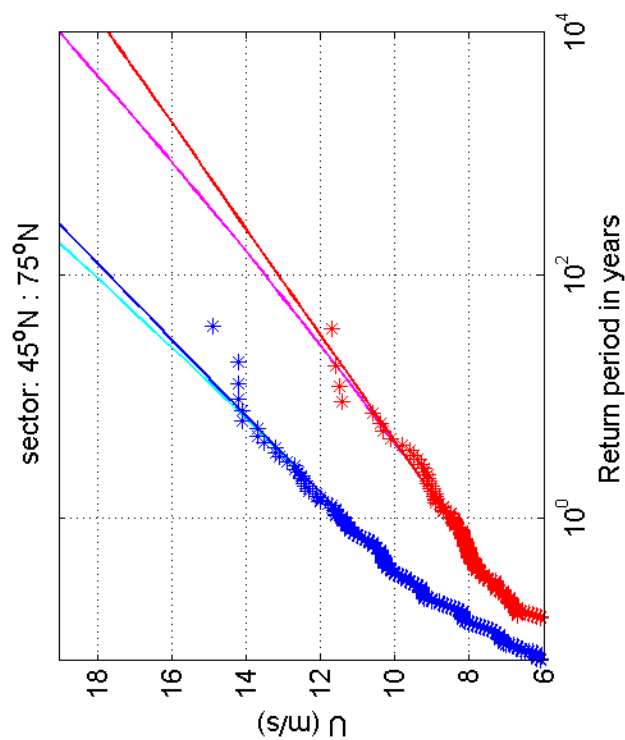
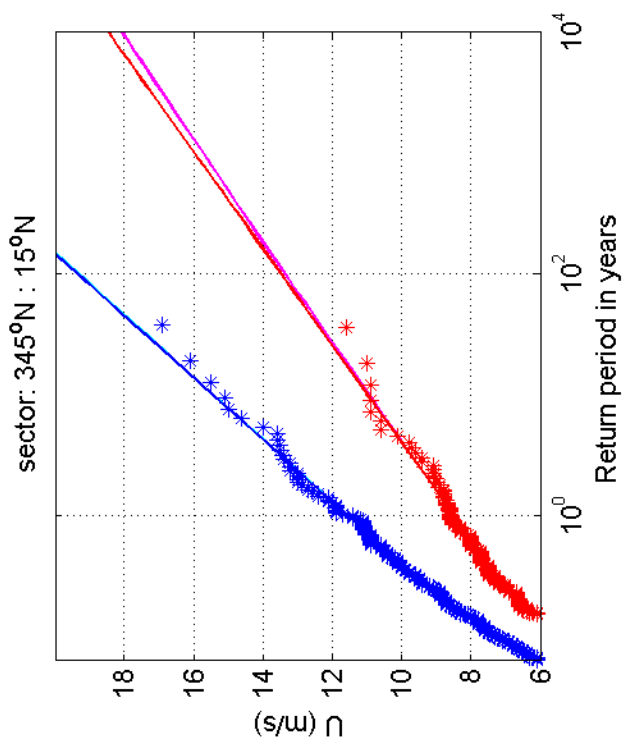
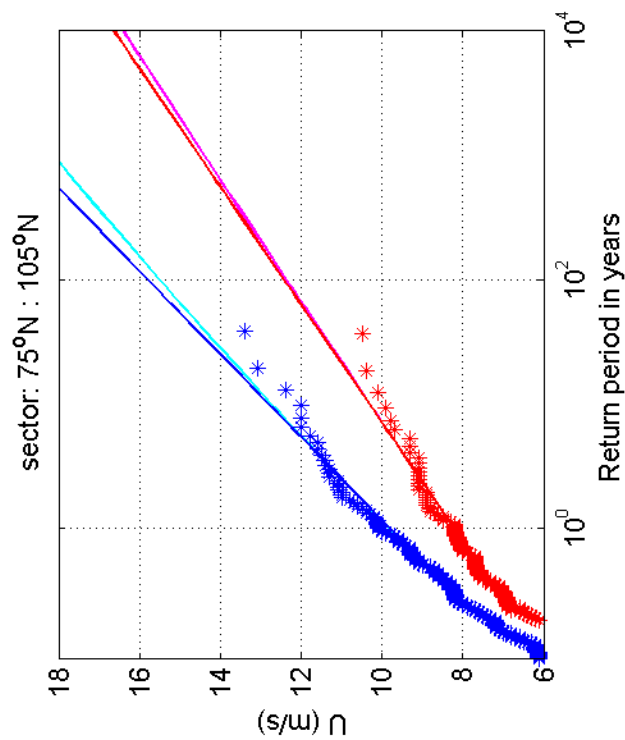
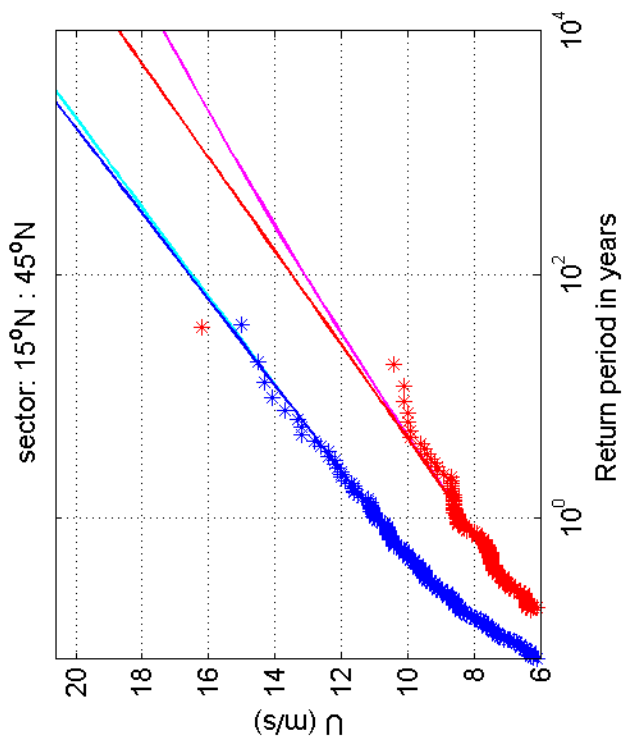
1970-2008

Schiphol vs Twenthe

Deltares

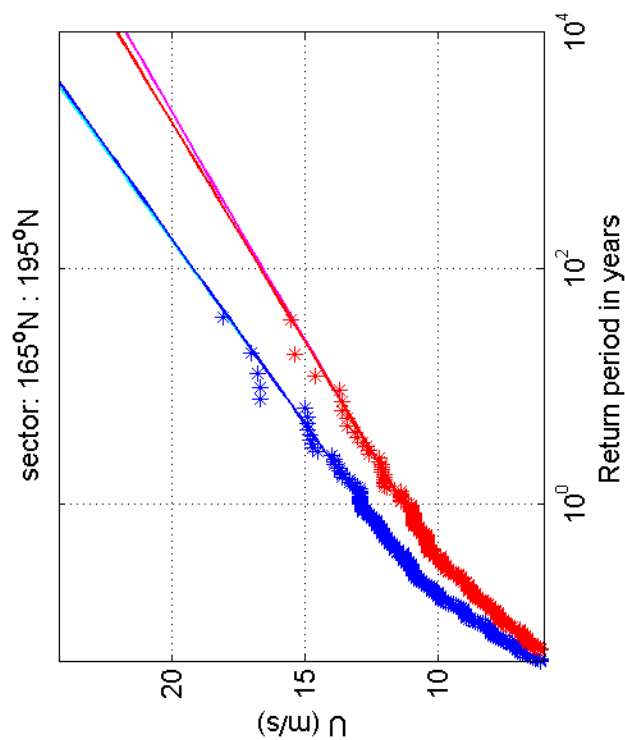
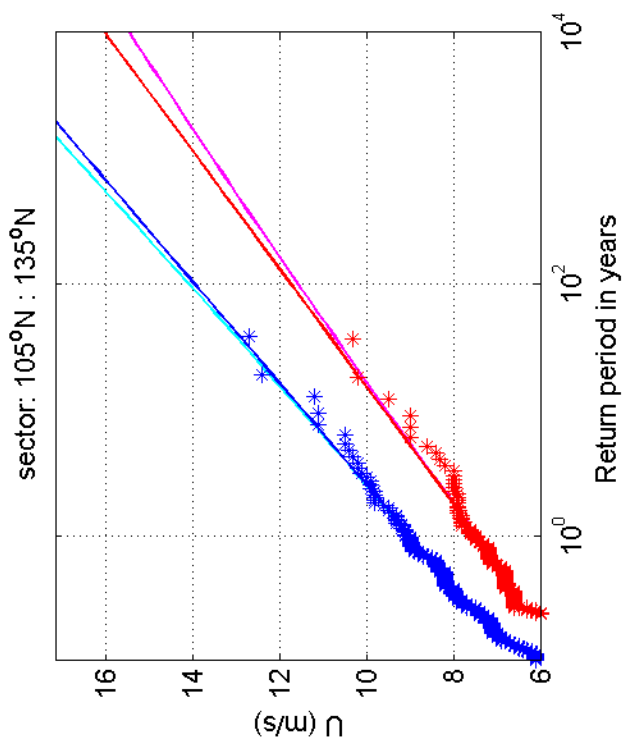
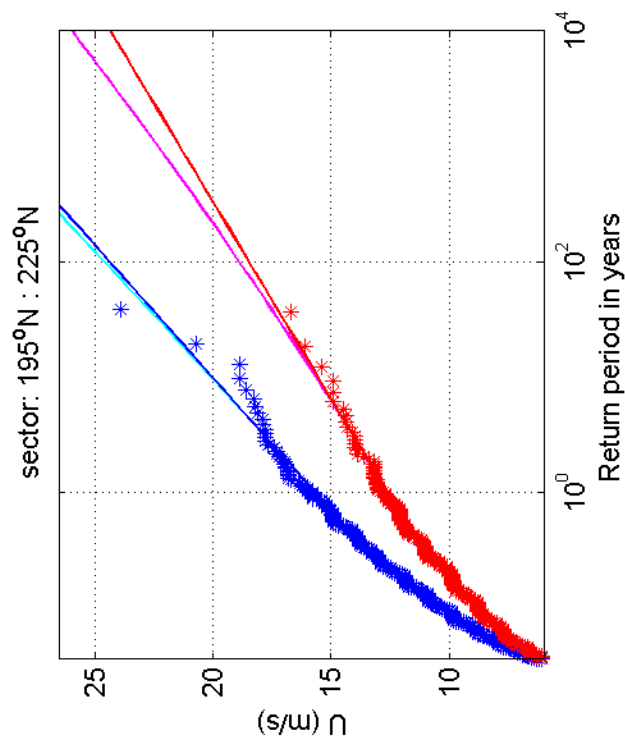
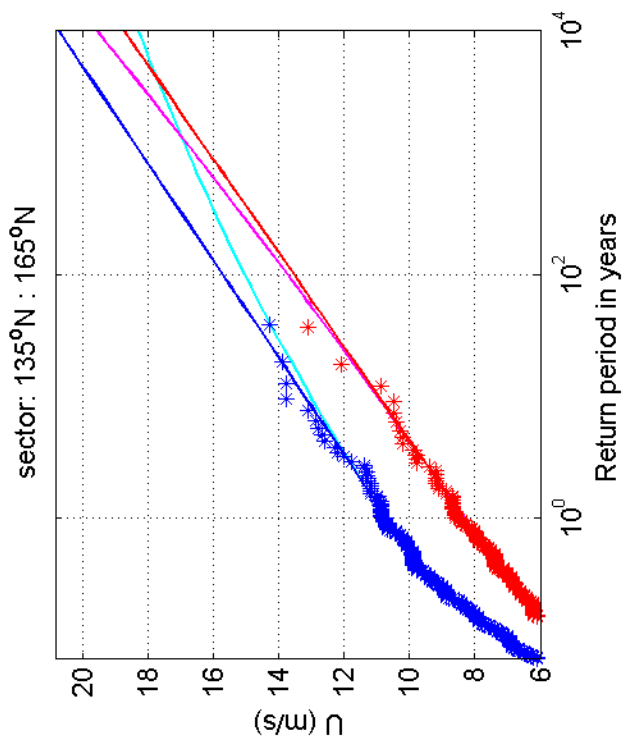
1200264-005

Fig. F.5a.10



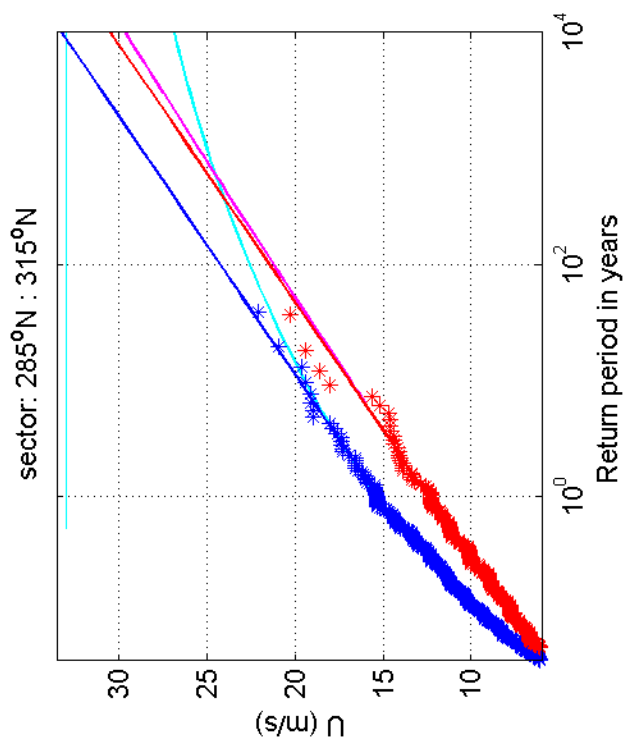
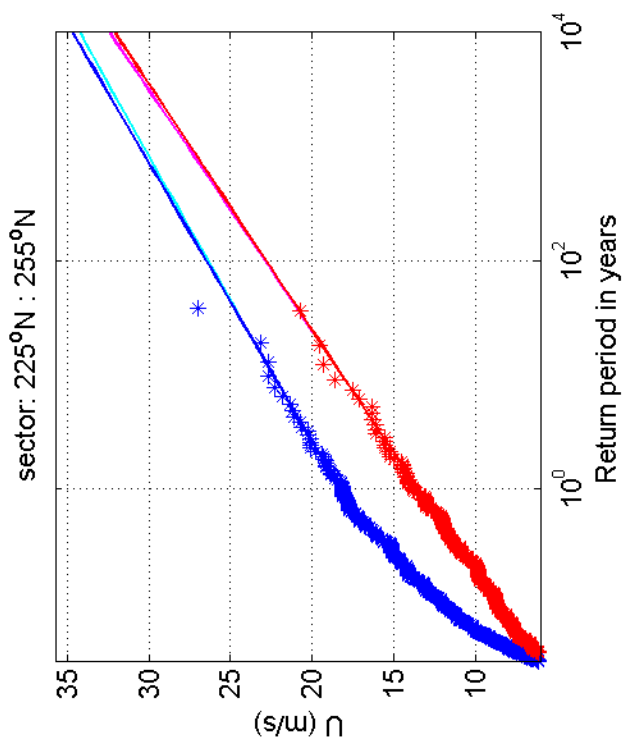
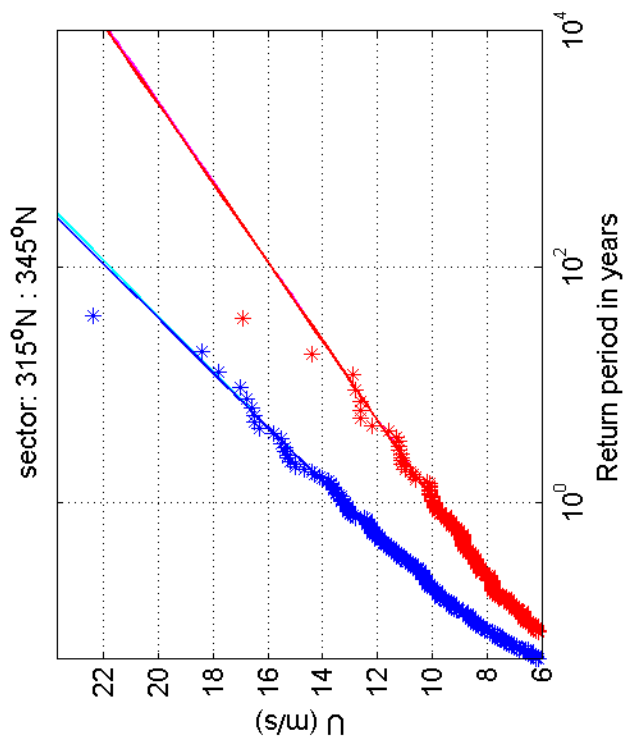
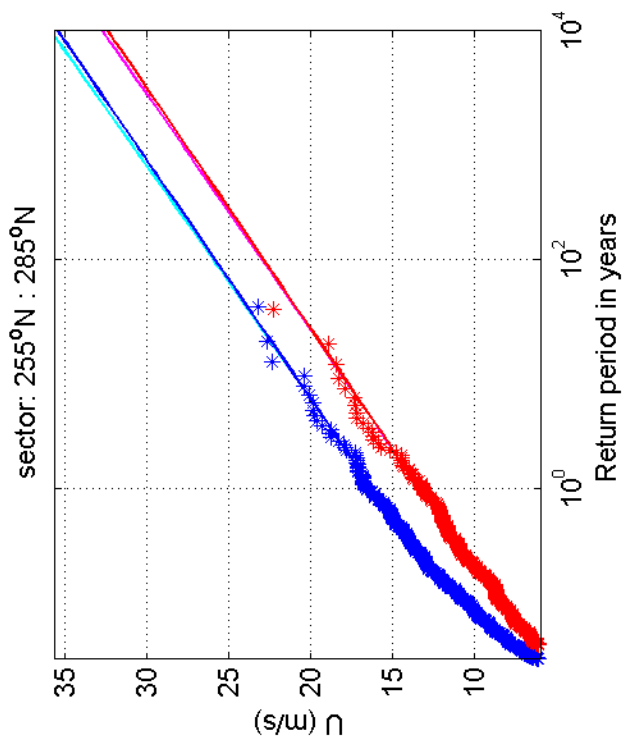
Return value plot per sector of Schiphol (blue) vs Twenthe (red)
 Exponential (blue, red) and GPD (cyan, magenta) fits to U_p
 Plotting positions: x_i vs $(n+1)/(\lambda(n+1-i))$

1970-2008



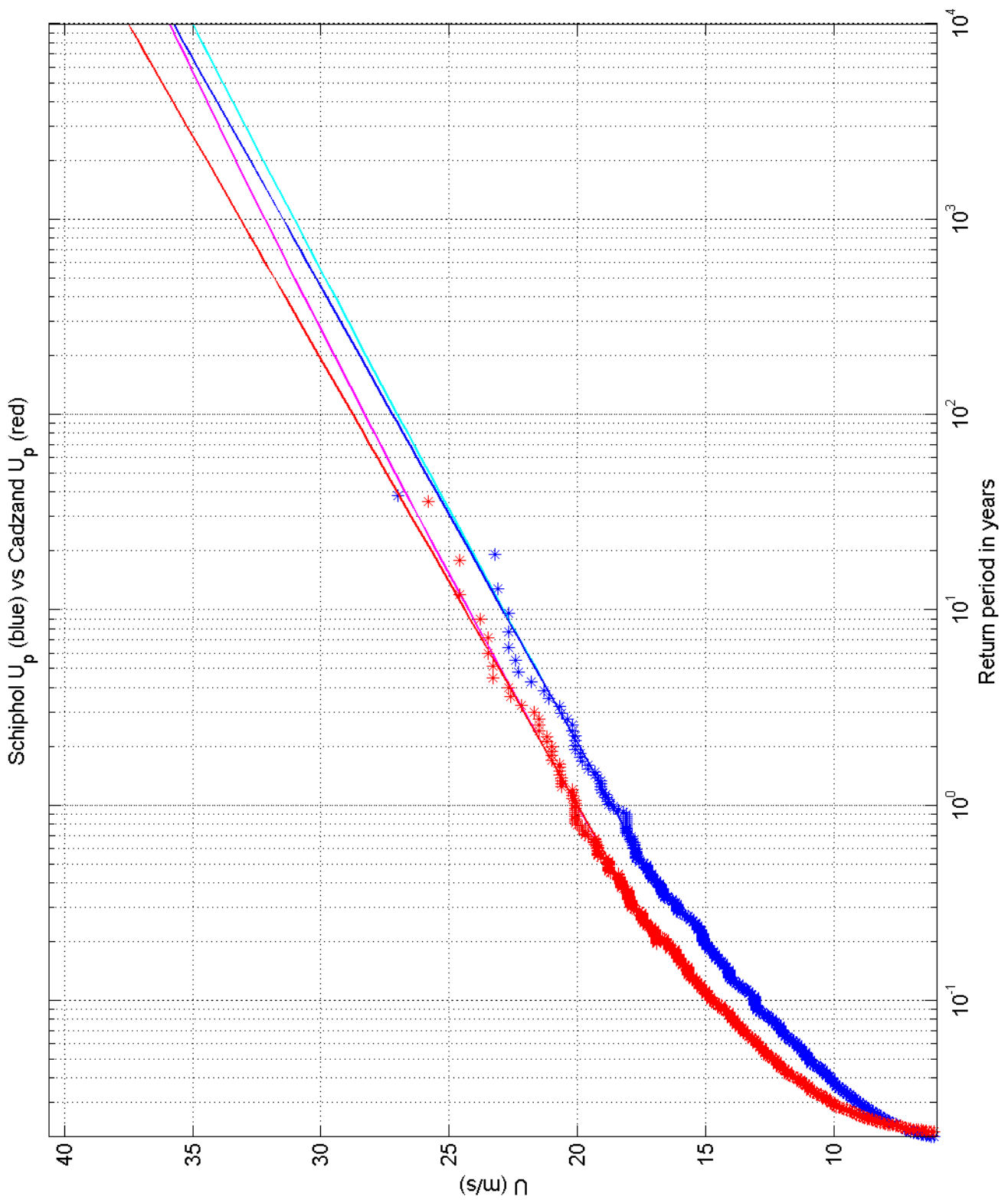
Return value plot per sector of Schiphol (blue) vs Twenthe (red)
 Exponential (blue, red) and GPD (cyan, magenta) fits to U_p
 Plotting positions: x_i vs $(n+1)/(\lambda(n+1-i))$

1970-2008



Return value plot per sector of Schiphol (blue) vs Twenthe (red)
 Exponential (blue, red) and GPD (cyan, magenta) fits to U_p
 Plotting positions: x_i vs $(n+1)/(\lambda(n+1-i))$

1970-2008



Return value plot of Schiphol (blue) vs Cadzand (red)
 Exponential (blue, red) and GPD (cyan, magenta) fits to U_p
 Plotting positions: x_i vs $(n+1)/(\lambda(n+1-i))$

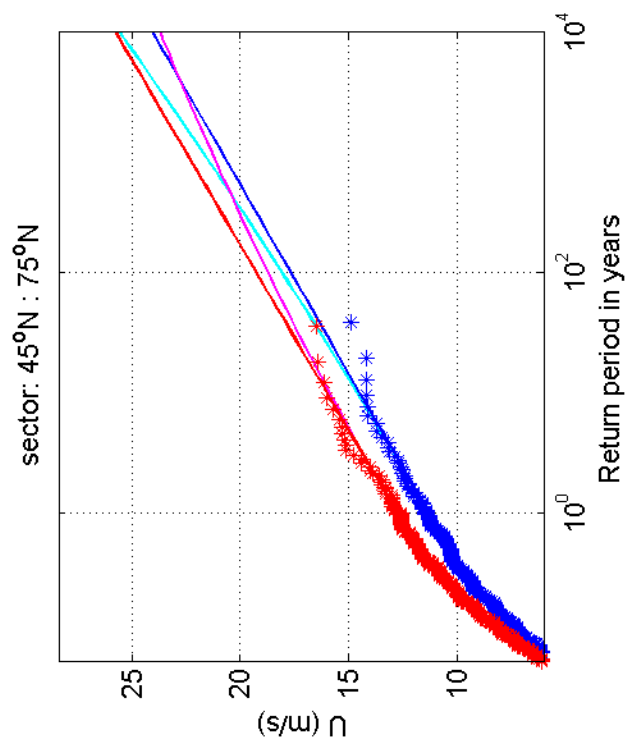
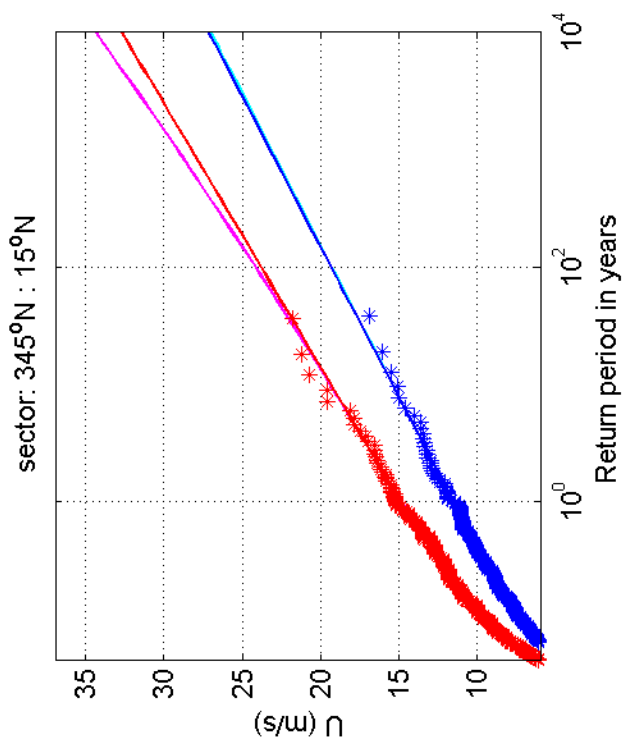
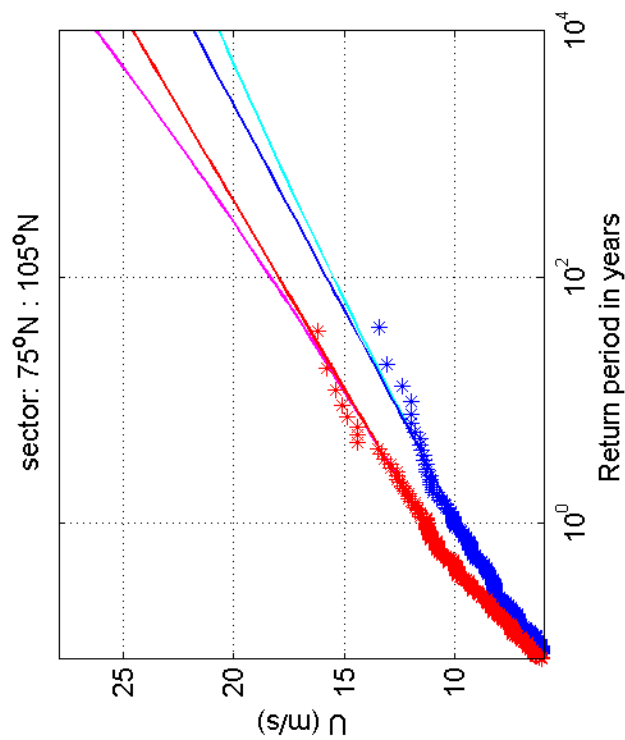
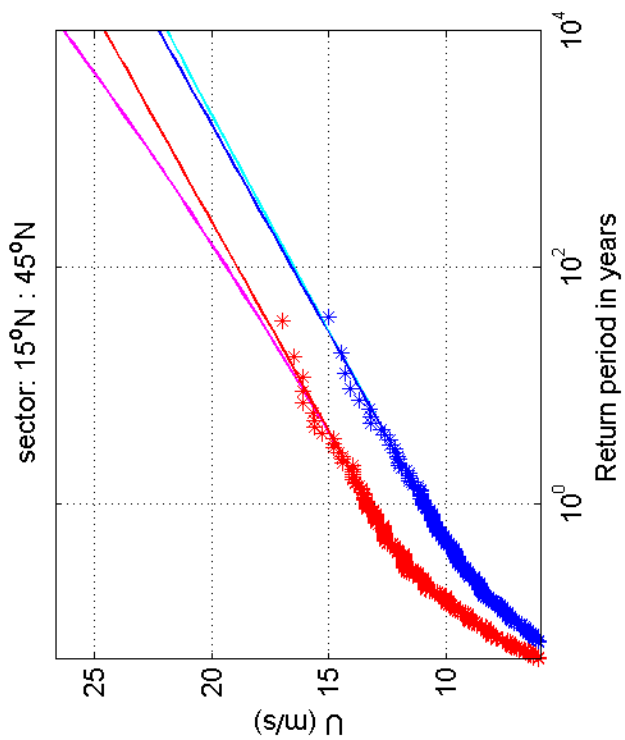
1970-2008

Schiphol vs Cadzand

Deltares

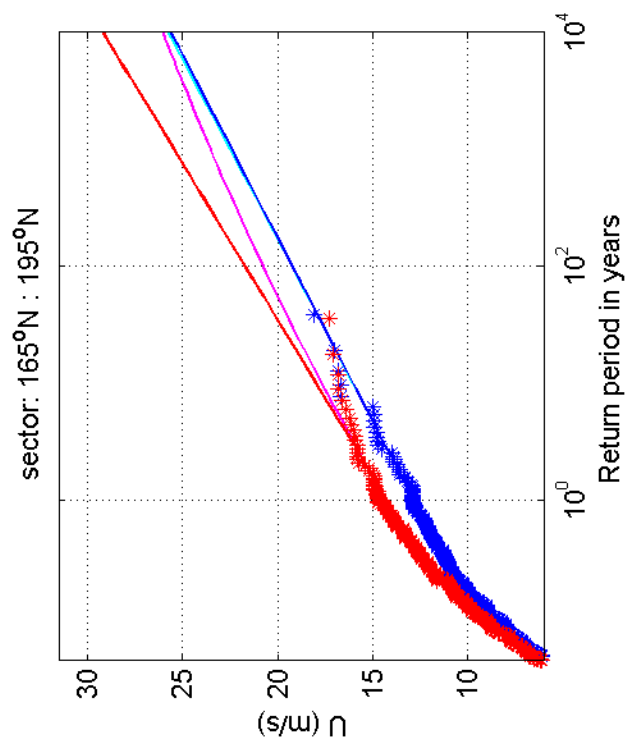
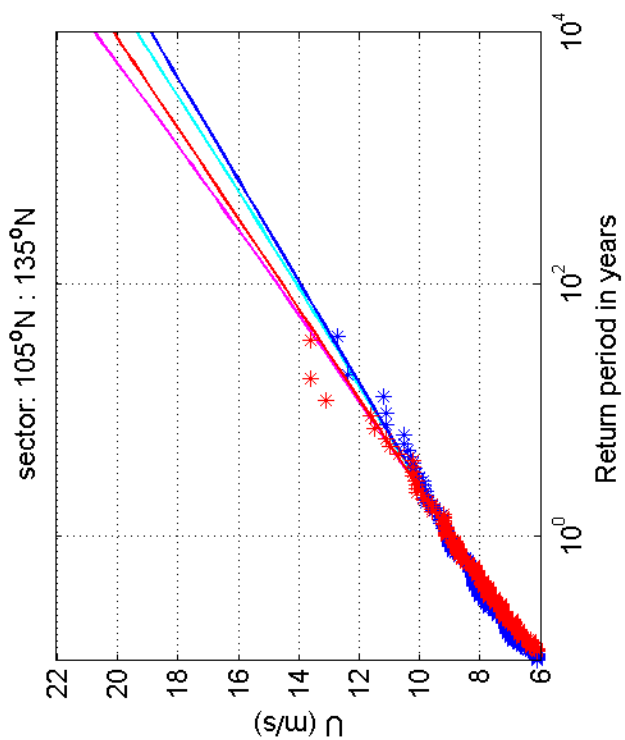
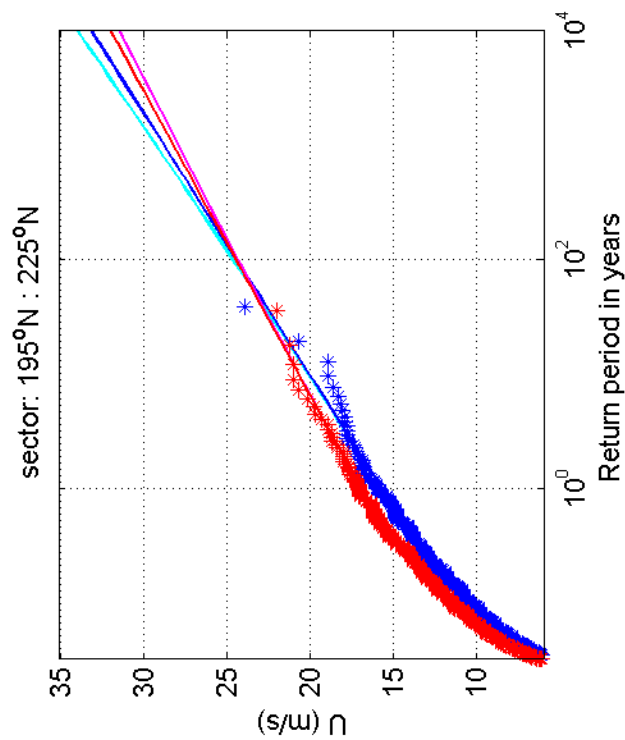
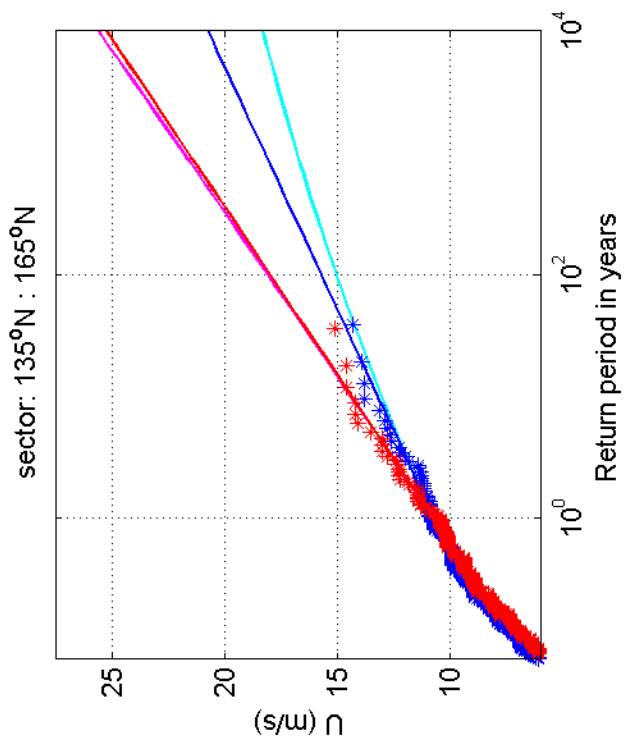
1200264-005

Fig. F.5a.11



Return value plot per sector of Schiphol (blue) vs Cadzand (red)
 Exponential (blue, red) and GPD (cyan, magenta) fits to U_p
 Plotting positions: x_i vs $(n+1)/(\lambda(n+1-i))$

1970-2008



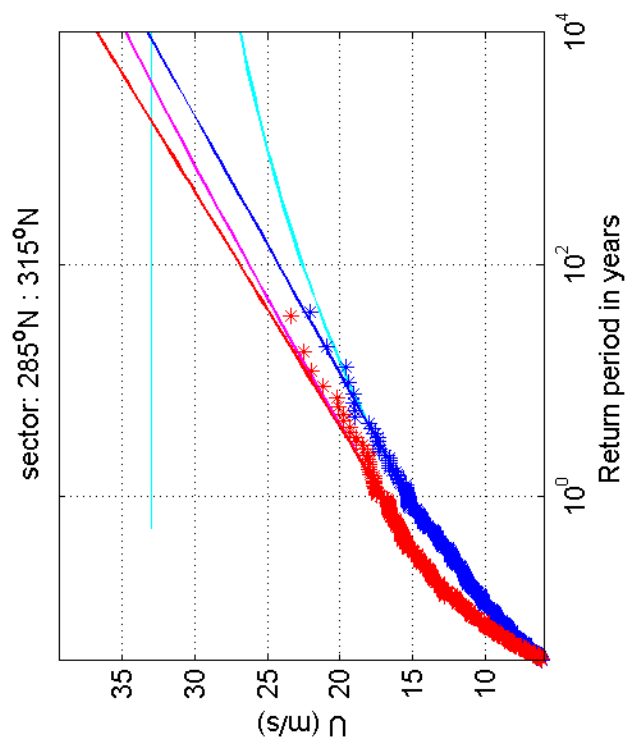
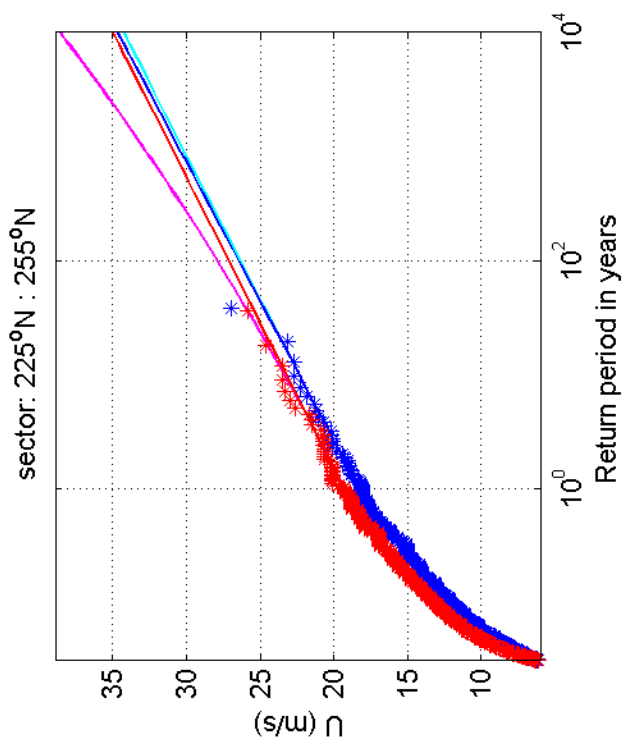
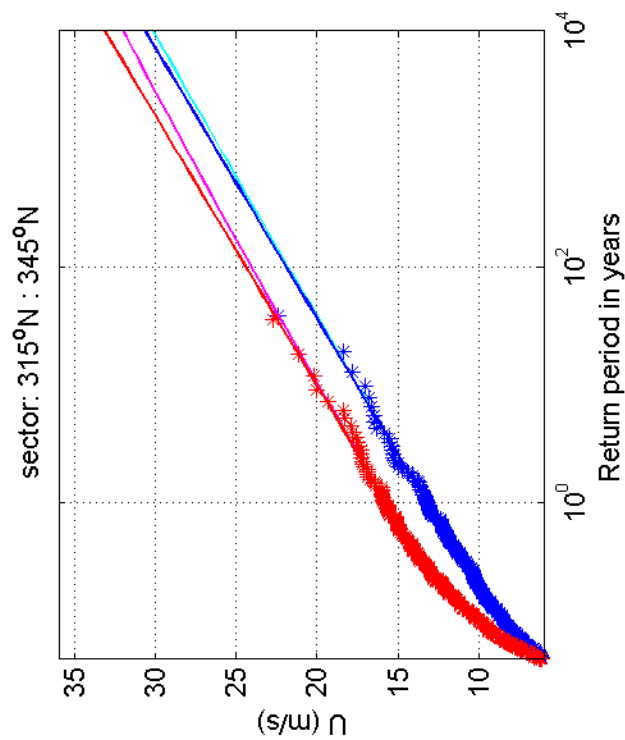
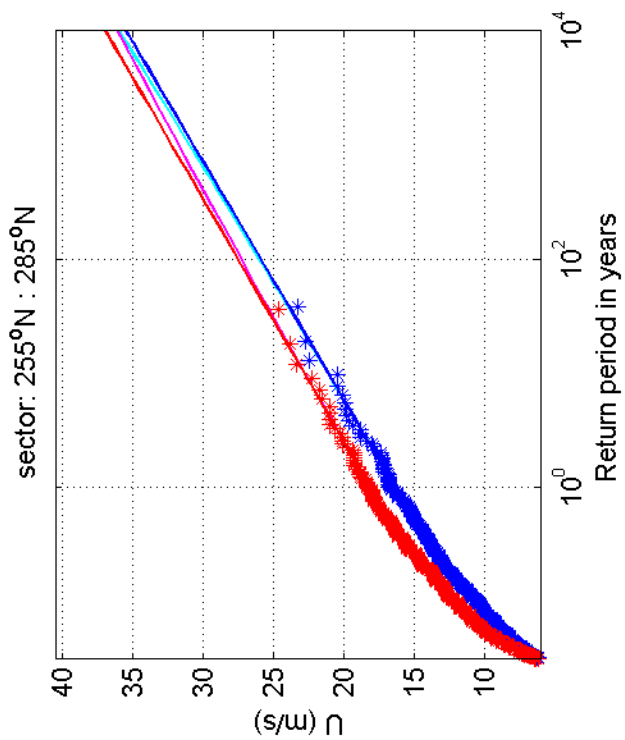
Return value plot per sector of Schiphol (blue) vs Cadzand (red)
 Exponential (blue, red) and GPD (cyan, magenta) fits to U_p
 Plotting positions: x_i vs $(n+1)/(\lambda(n+1-i))$

1970-2008

Deltares

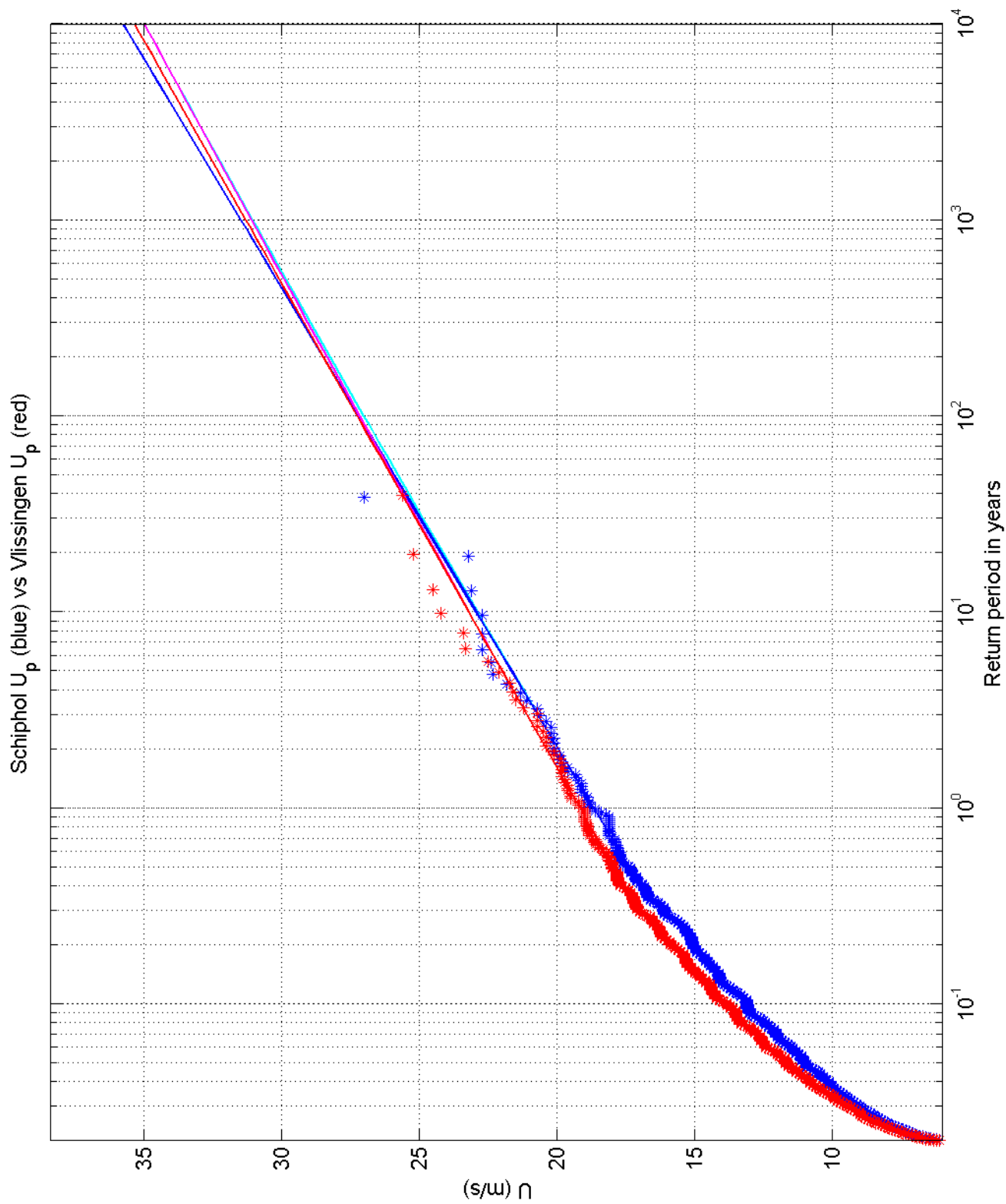
1200264-005

Fig. F.5c.11



Return value plot per sector of Schiphol (blue) vs Cadzand (red)
 Exponential (blue, red) and GPD (cyan, magenta) fits to U_p
 Plotting positions: x_i vs $(n+1)/(\lambda(n+1-i))$

1970-2008



Return value plot of Schiphol (blue) vs Vlissingen (red)
 Exponential (blue, red) and GPD (cyan, magenta) fits to U_p
 Plotting positions: x_i vs $(n+1)/(\lambda(n+1-i))$

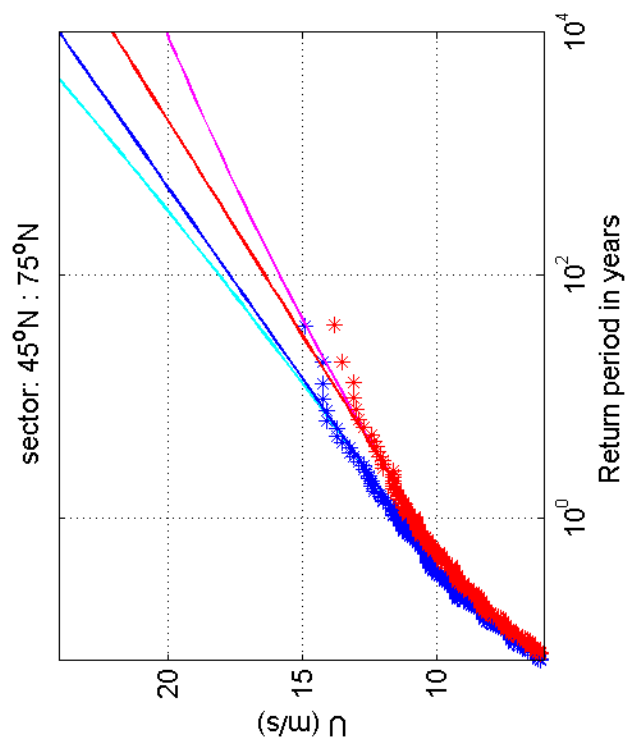
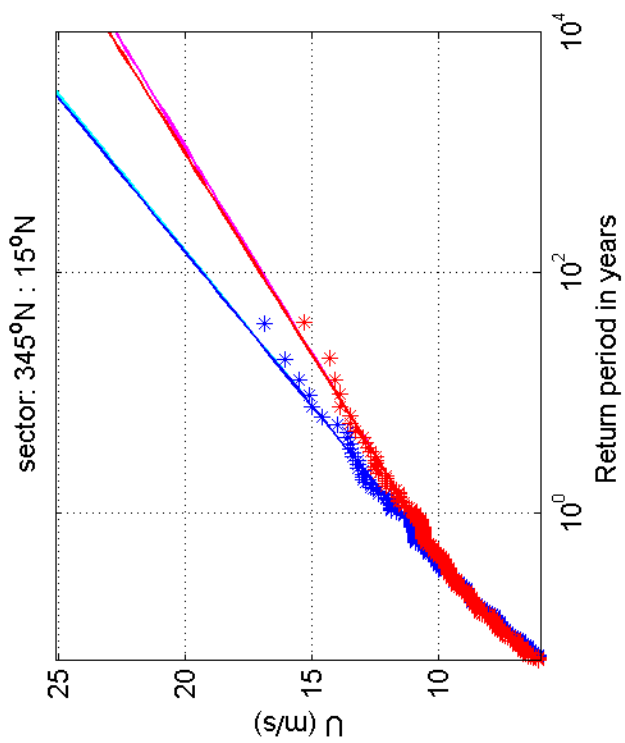
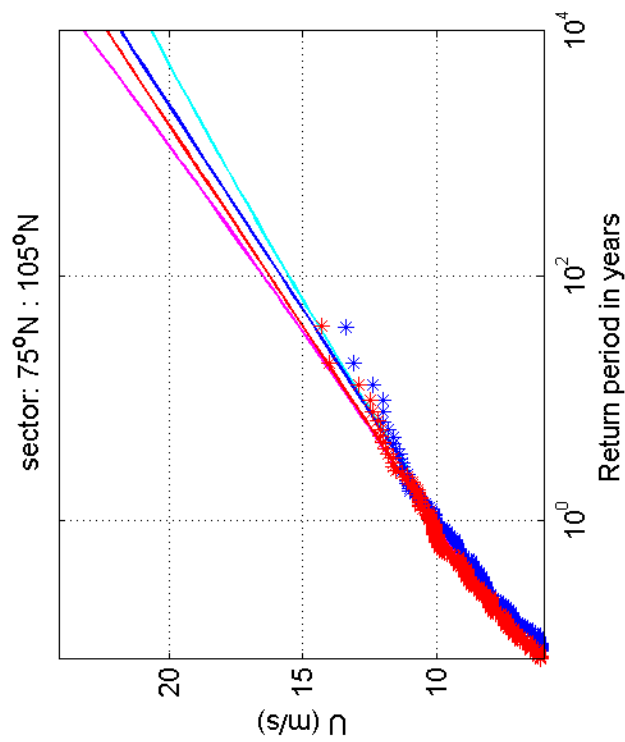
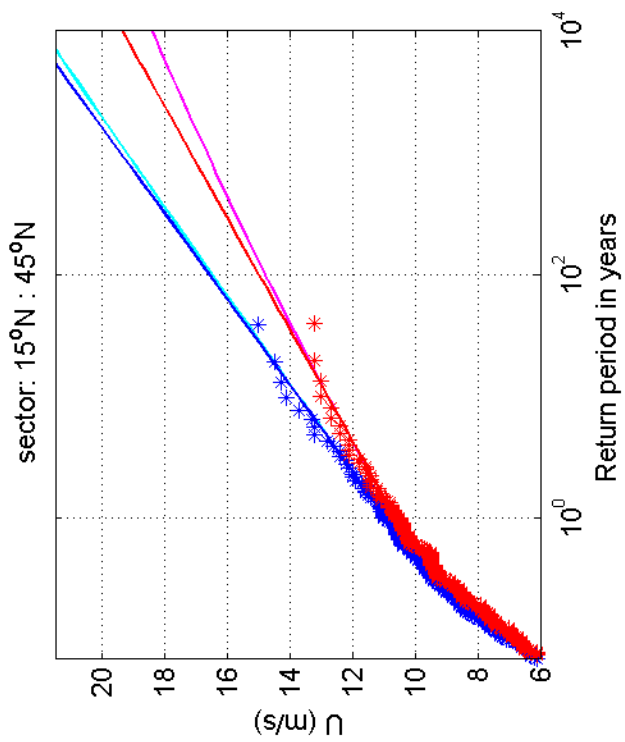
1970-2008

Schiphol vs Vlissingen

Deltares

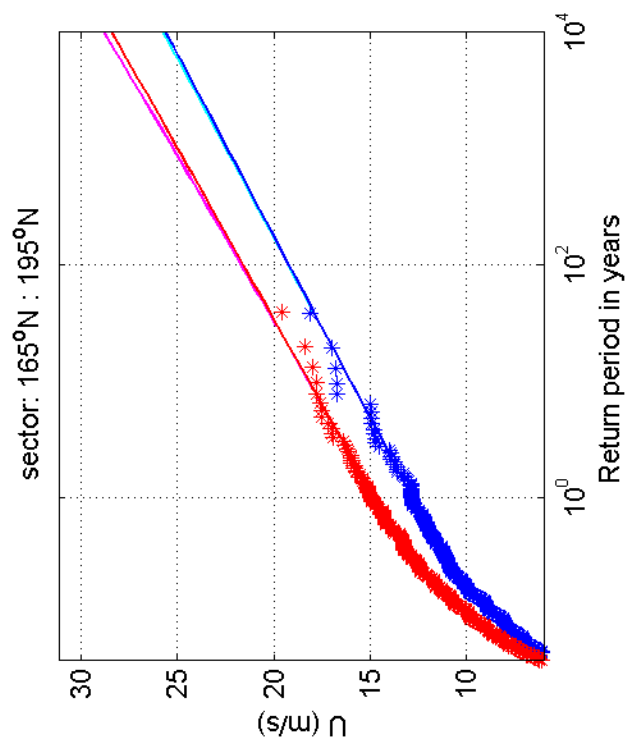
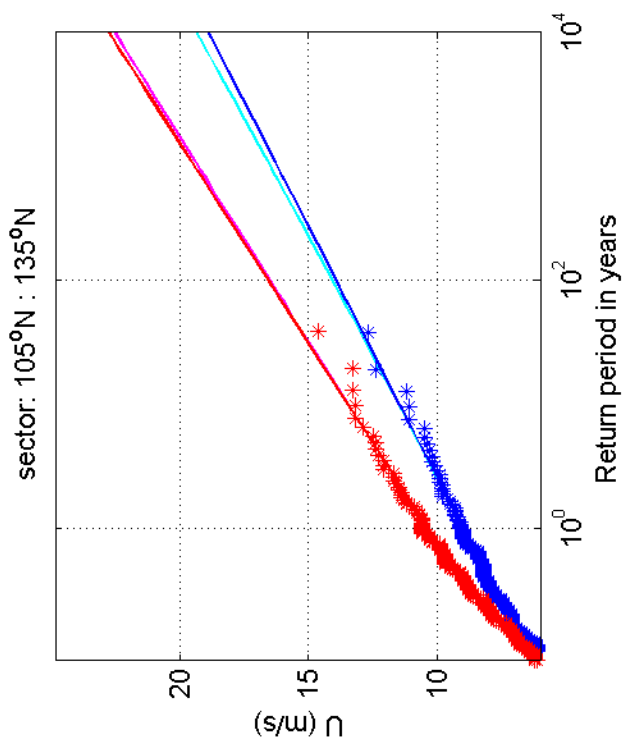
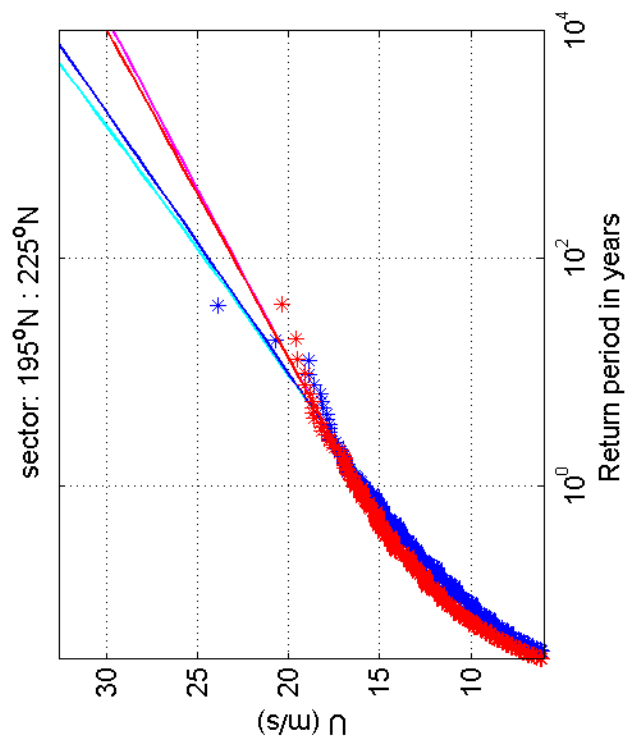
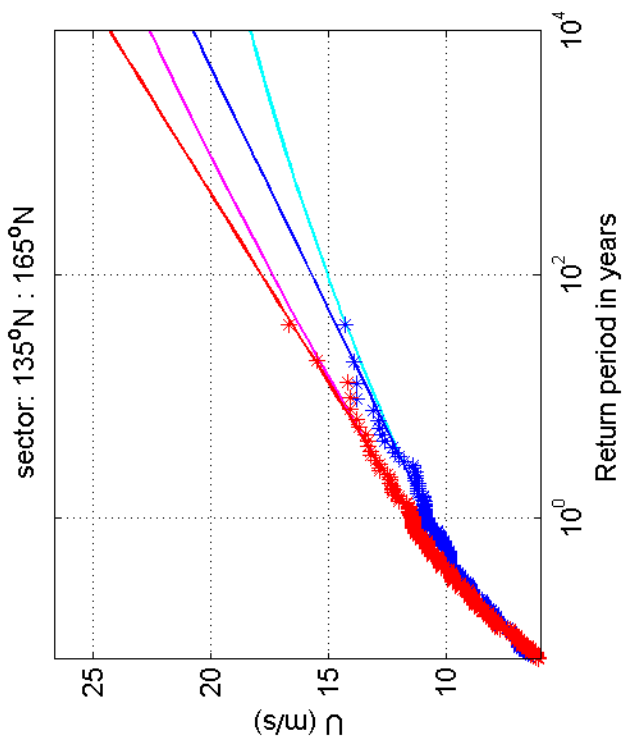
1200264-005

Fig. F.5a.12



Return value plot per sector of Schiphol (blue) vs Vlissingen (red)
 Exponential (blue, red) and GPD (cyan, magenta) fits to U_p
 Plotting positions: x_i vs $(n+1)/(\lambda(n+1-i))$

1970-2008



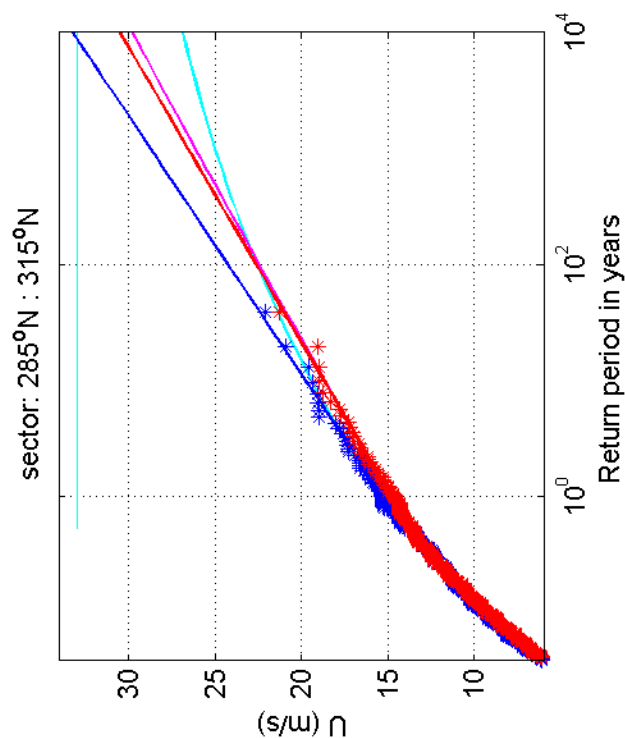
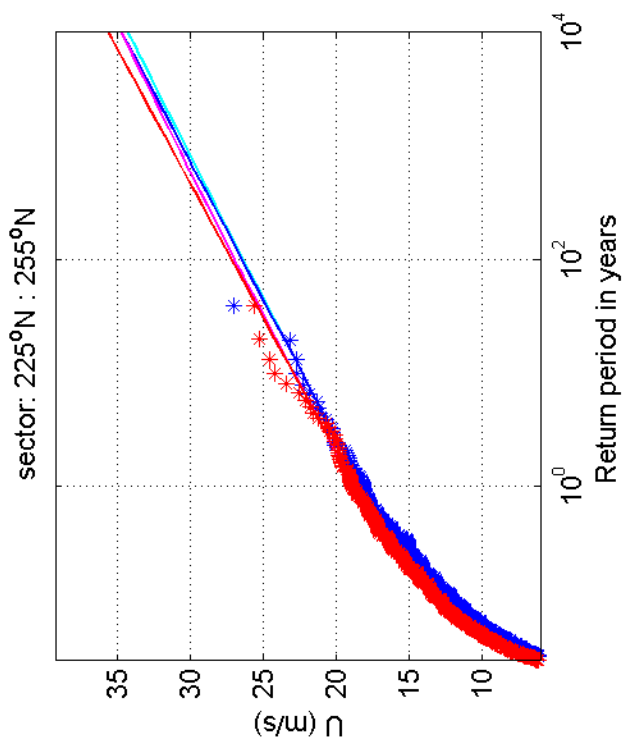
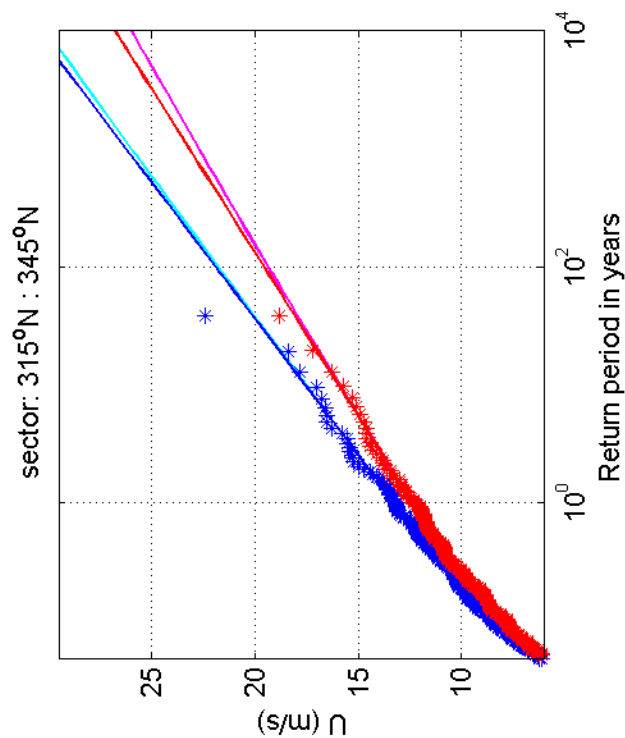
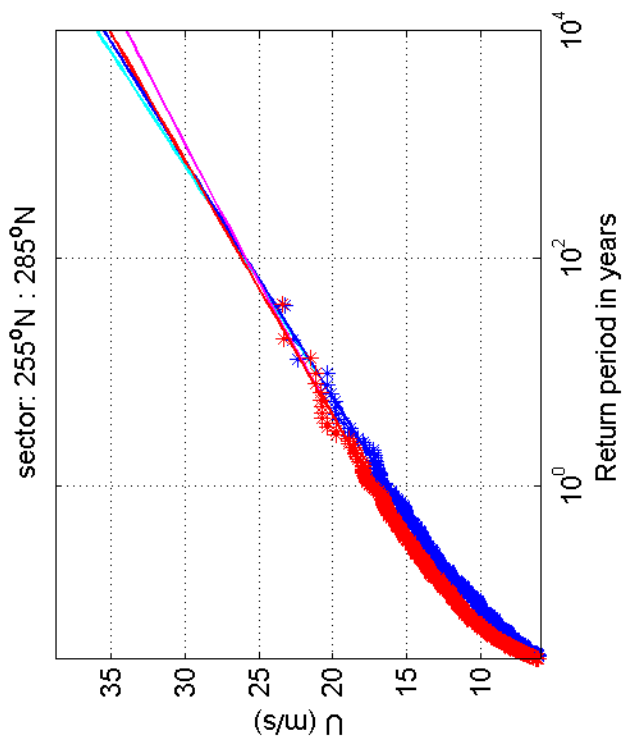
Return value plot per sector of Schiphol (blue) vs Vlissingen (red)
 Exponential (blue, red) and GPD (cyan, magenta) fits to U_p
 Plotting positions: x_i vs $(n+1)/(\lambda(n+1-i))$

1970-2008

Deltares

1200264-005

Fig. F.5c.12



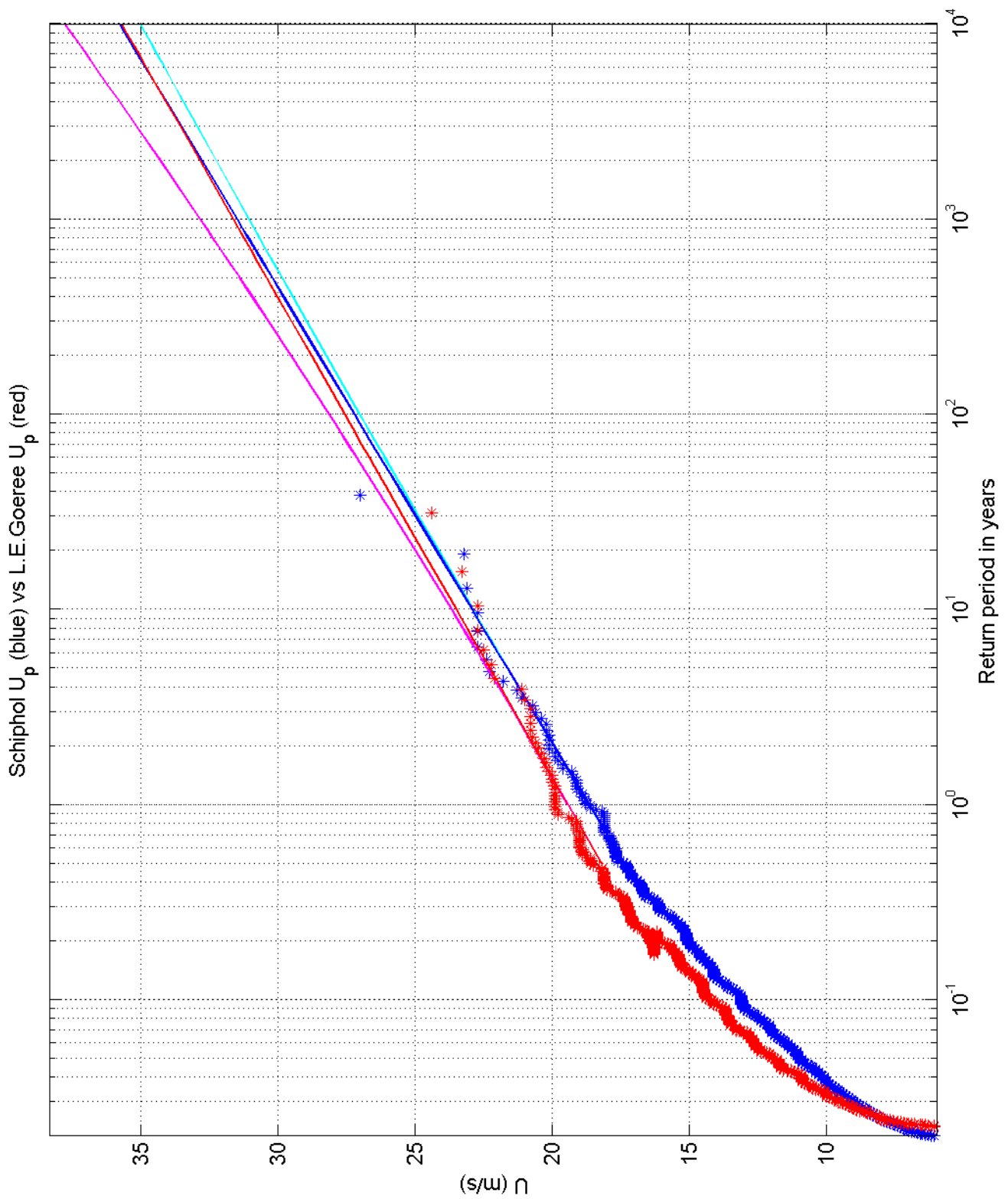
Return value plot per sector of Schiphol (blue) vs Vlissingen (red)
 Exponential (blue, red) and GPD (cyan, magenta) fits to U_p
 Plotting positions: x_i vs $(n+1)/(\lambda(n+1-i))$

1970-2008

Deltares

1200264-005

Fig. F.5d.12



Return value plot of Schiphol (blue) vs L.E.Goeree (red)
 Exponential (blue, red) and GPD (cyan, magenta) fits to U_p
 Plotting positions: x_i vs $(n+1)/(\lambda(n+1-i))$

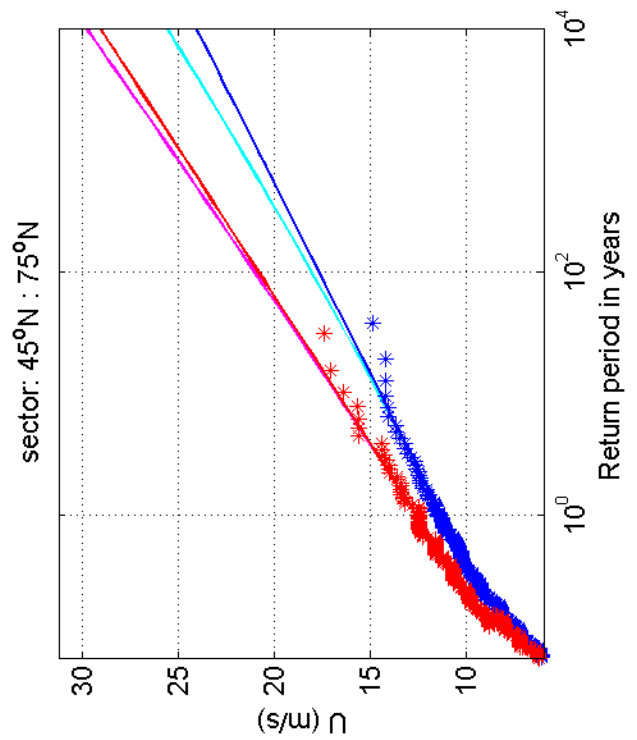
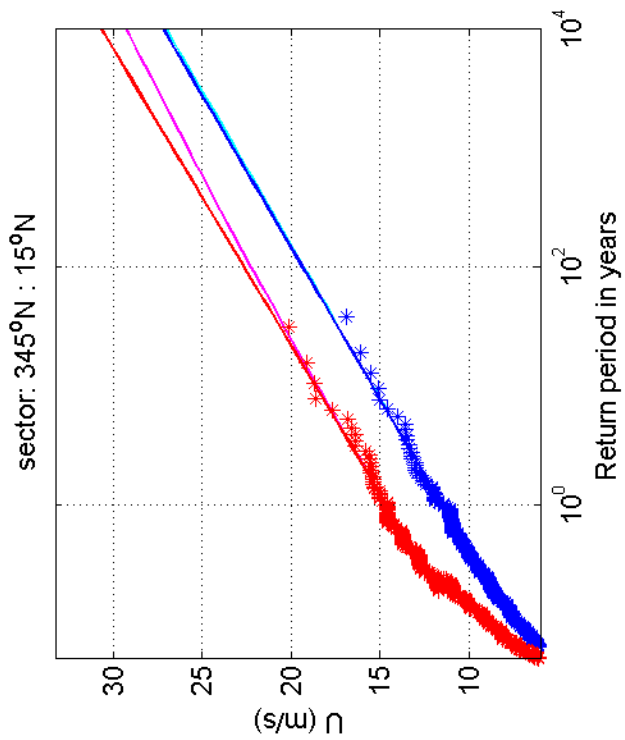
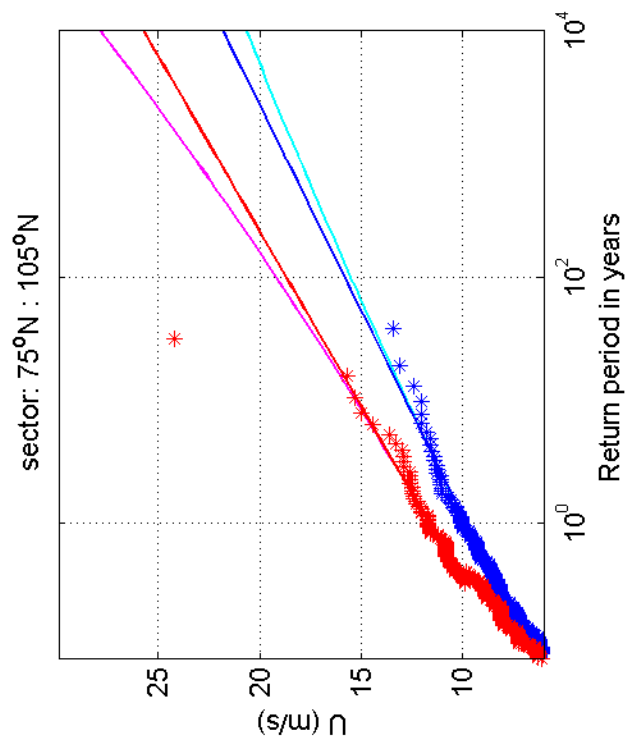
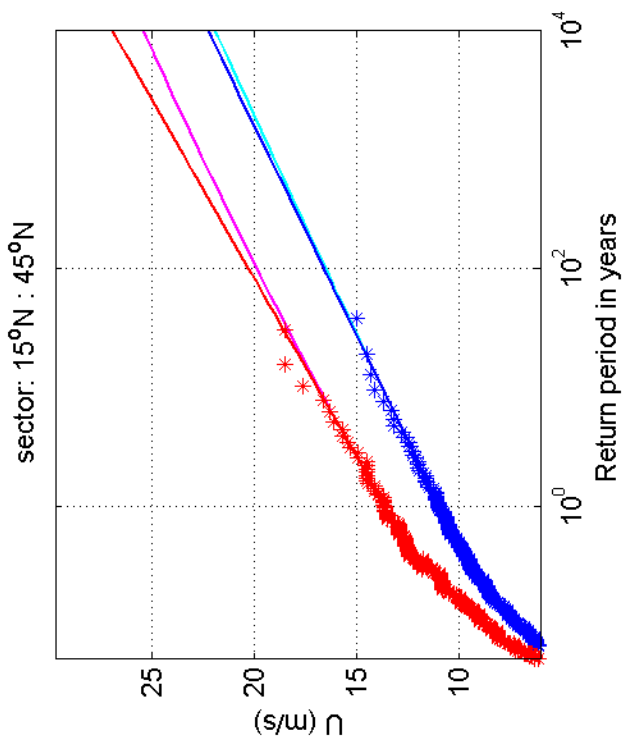
1970-2008

Schiphol vs L.E.Goeree

Deltares

1200264-005

Fig. F.5a.13



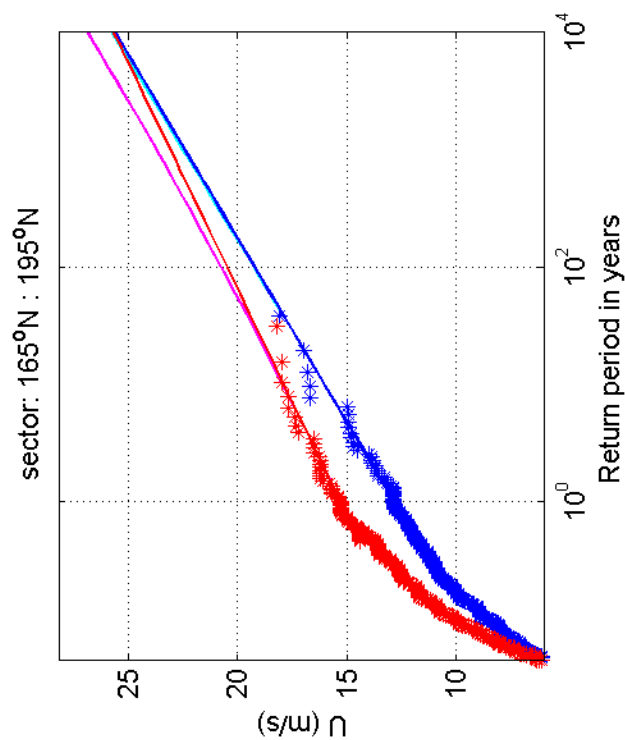
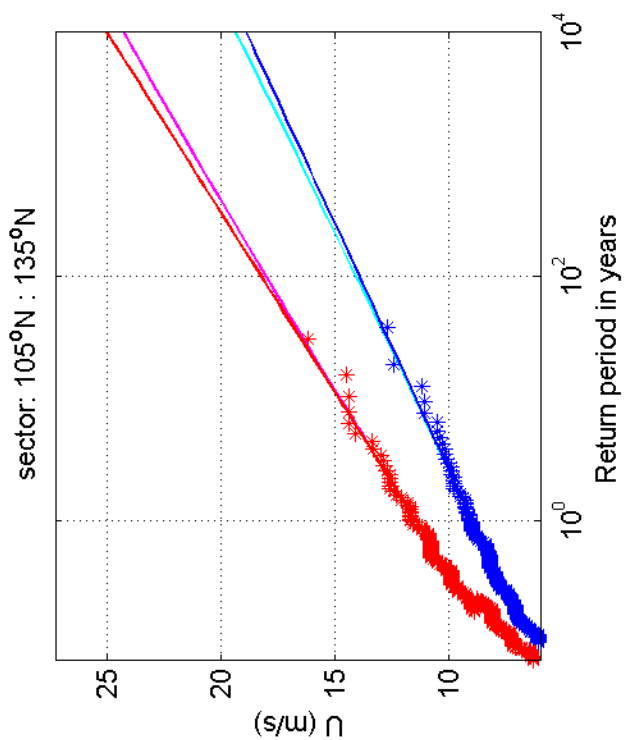
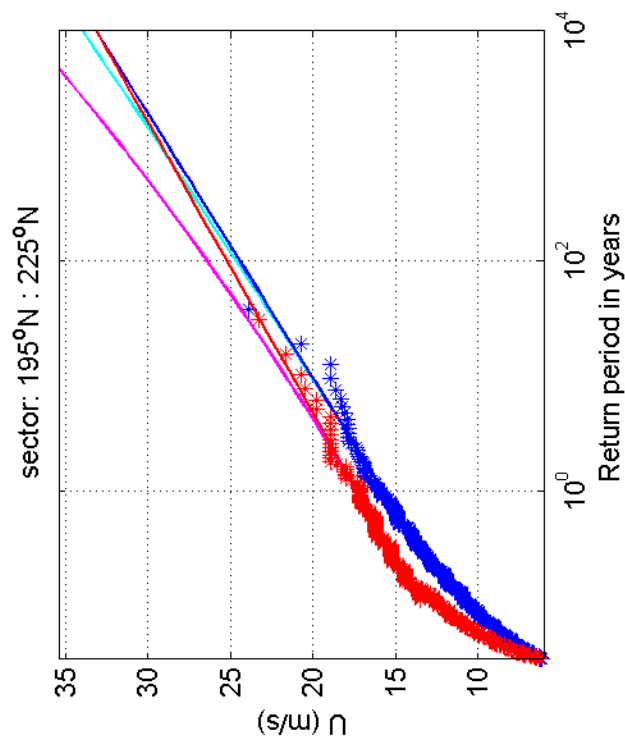
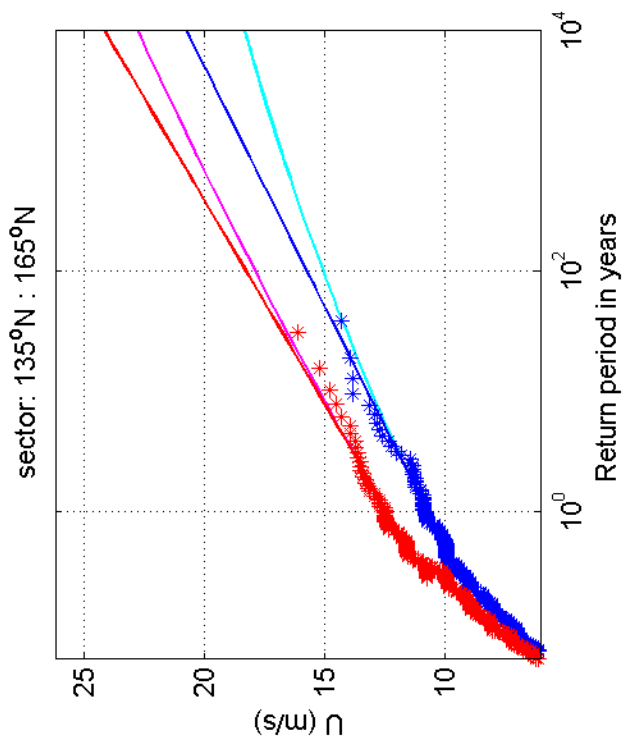
Return value plot per sector of Schiphol (blue) vs L.E. Goeree (red)
 Exponential (blue, red) and GPD (cyan, magenta) fits to U_p
 Plotting positions: x_i vs $(n+1)/(\lambda(n+1-i))$

1970-2008

Deltares

1200264-005

Fig. F.5b.13



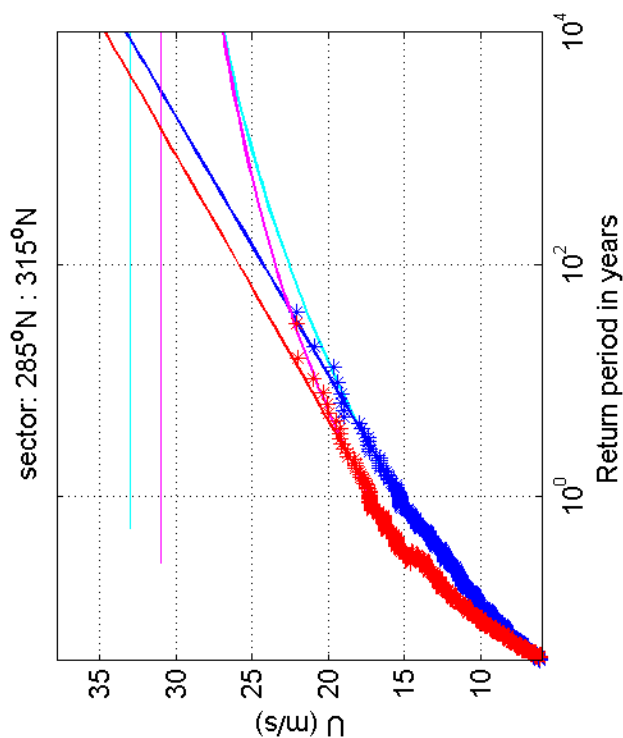
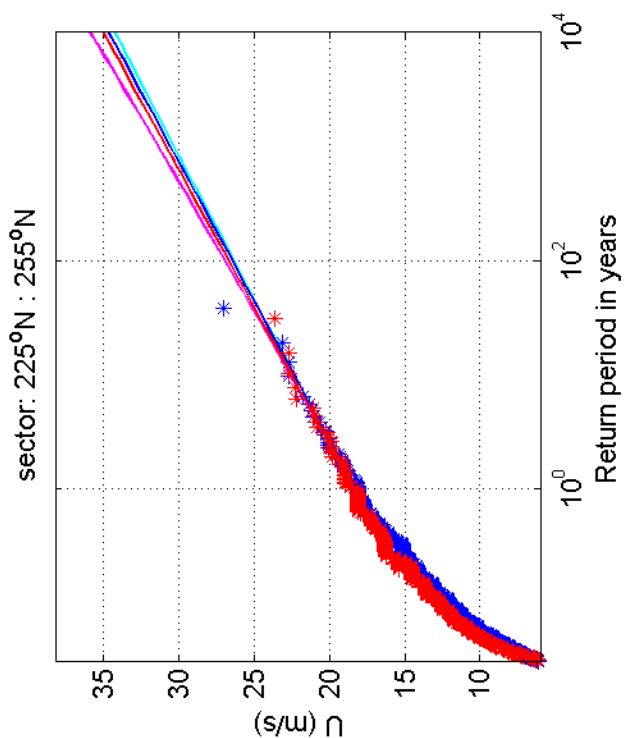
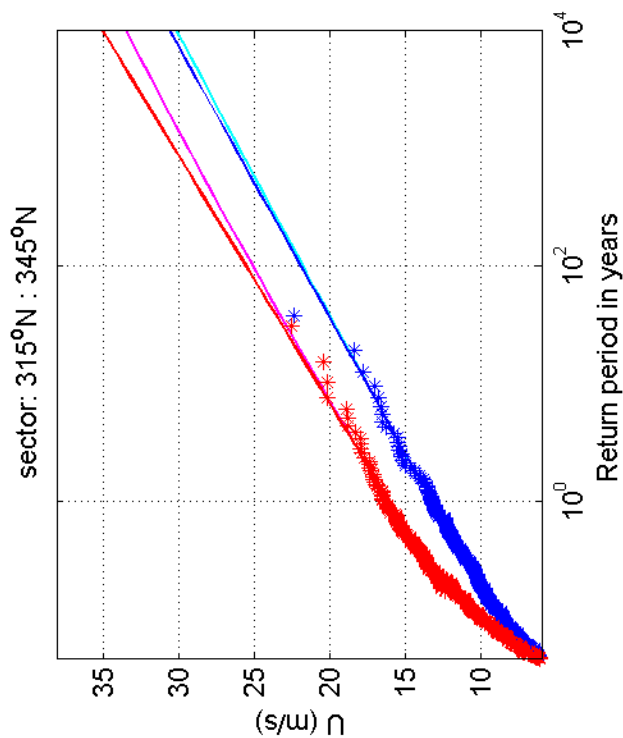
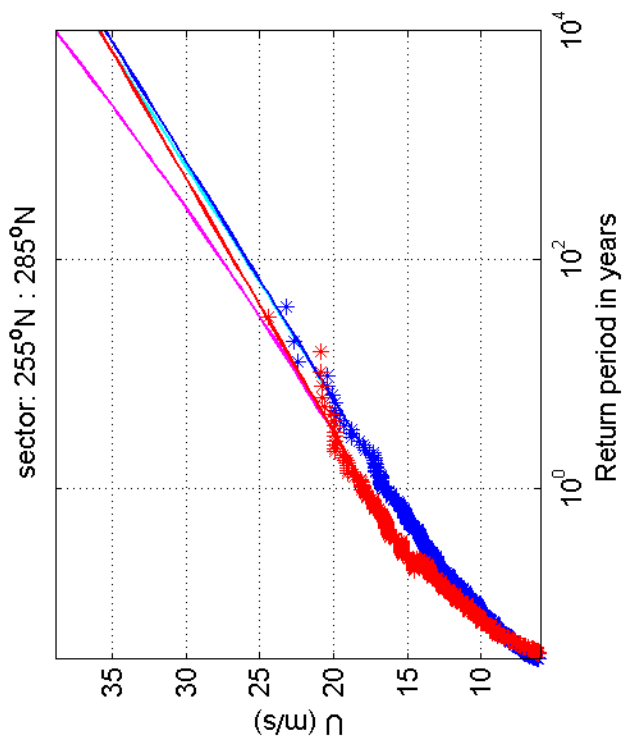
Return value plot per sector of Schiphol (blue) vs L.E. Goeree (red)
 Exponential (blue, red) and GPD (cyan, magenta) fits to U_p
 Plotting positions: x_i vs $(n+1)/(\lambda(n+1-i))$

1970-2008

Deltares

1200264-005

Fig. F.5c.13



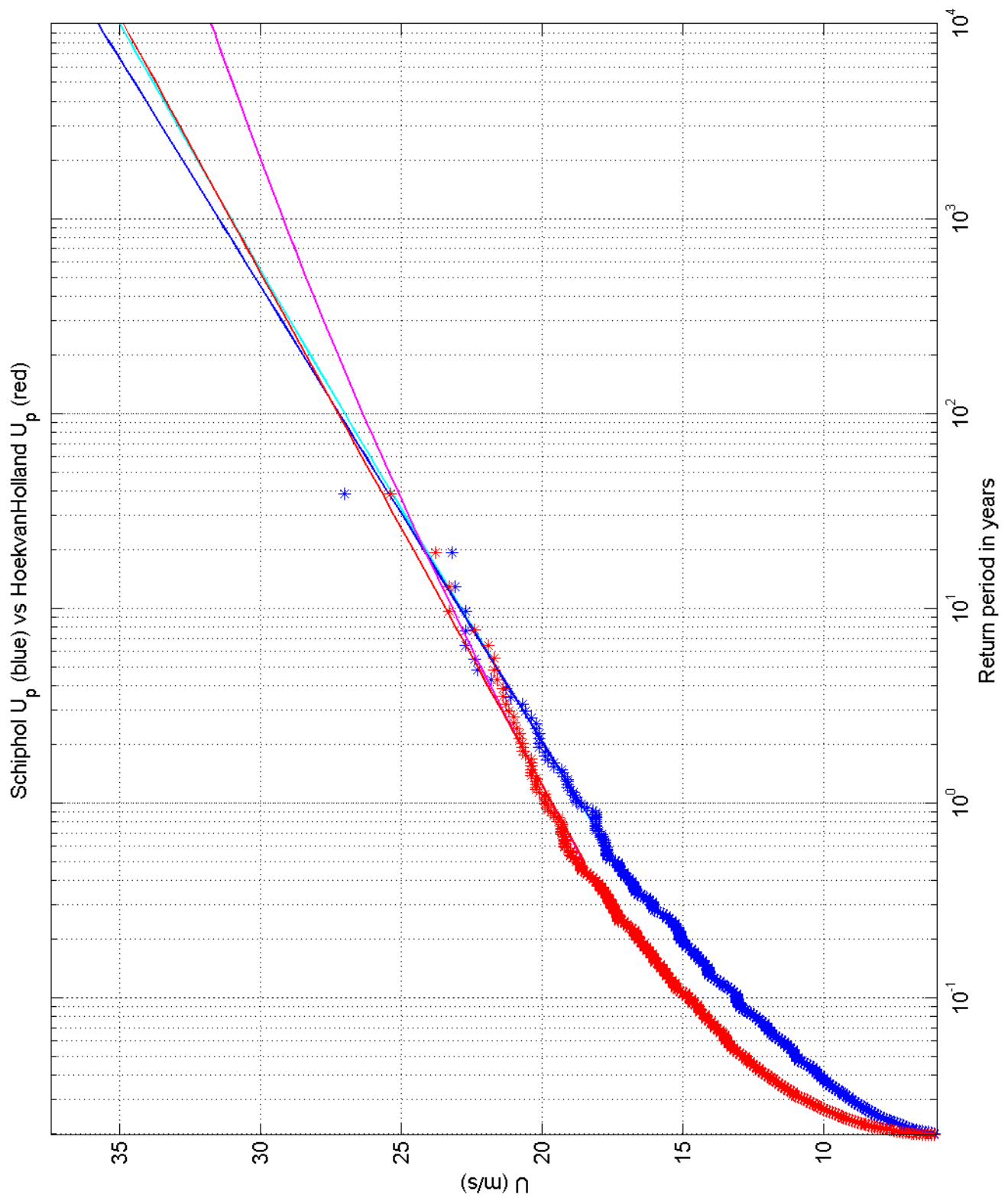
Return value plot per sector of Schiphol (blue) vs L.E. Goeree (red)
 Exponential (blue, red) and GPD (cyan, magenta) fits to U_p
 Plotting positions: x_i vs $(n+1)/(\lambda(n+1-i))$

1970-2008

Deltares

1200264-005

Fig. F.5d.13



Return value plot of Schiphol (blue) vs HoekvanHolland (red)
 Exponential (blue, red) and GPD (cyan, magenta) fits to U_p
 Plotting positions: x_i vs $(n+1)/(\lambda(n+1-i))$

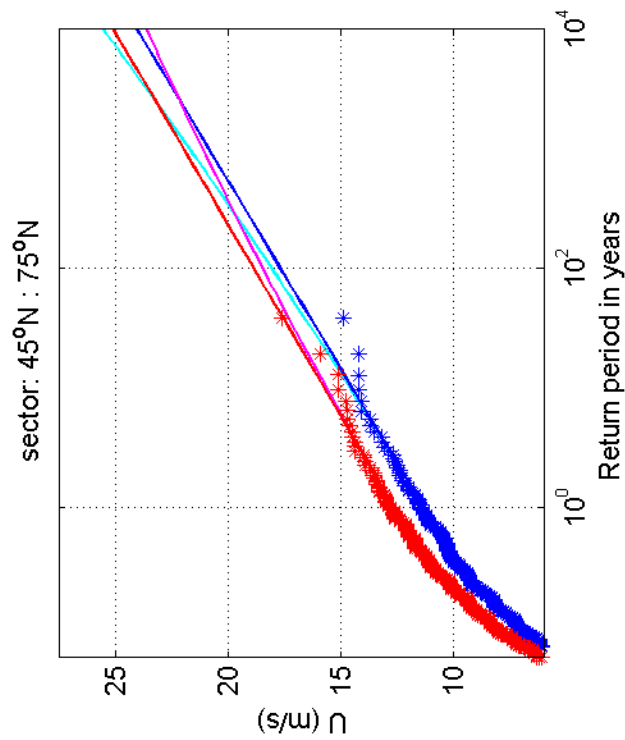
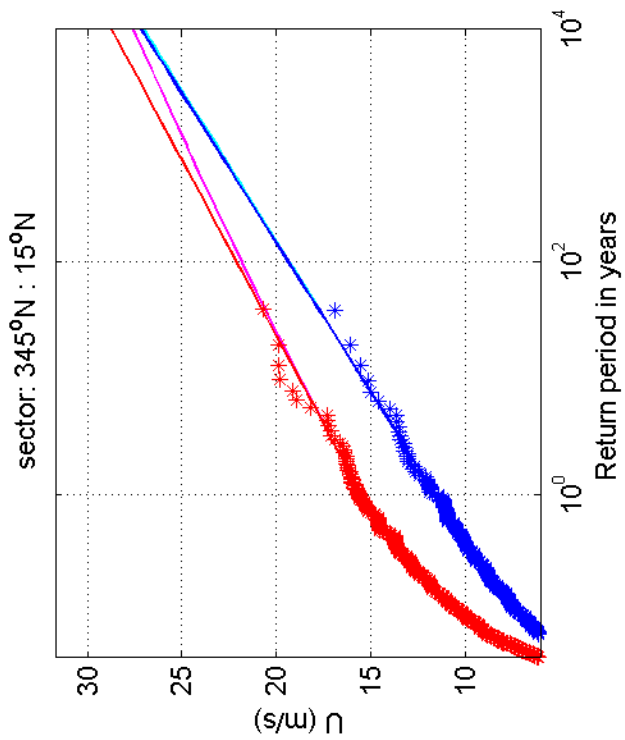
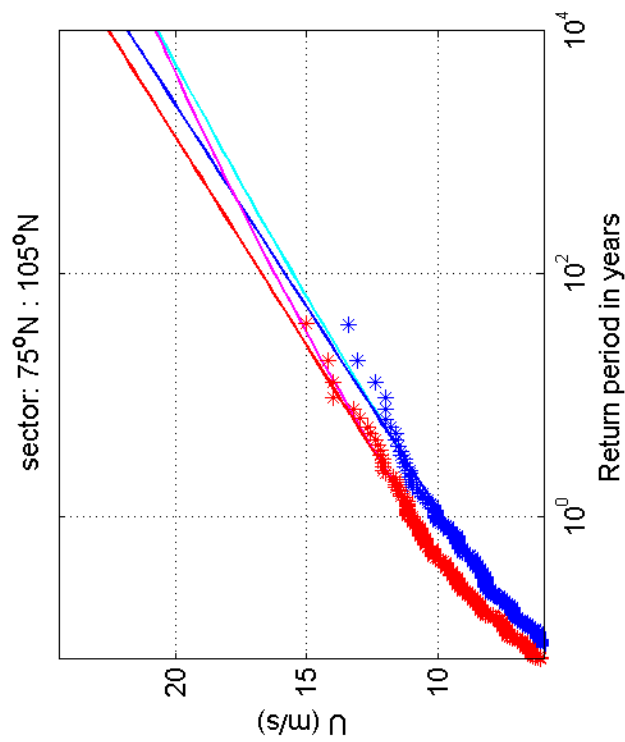
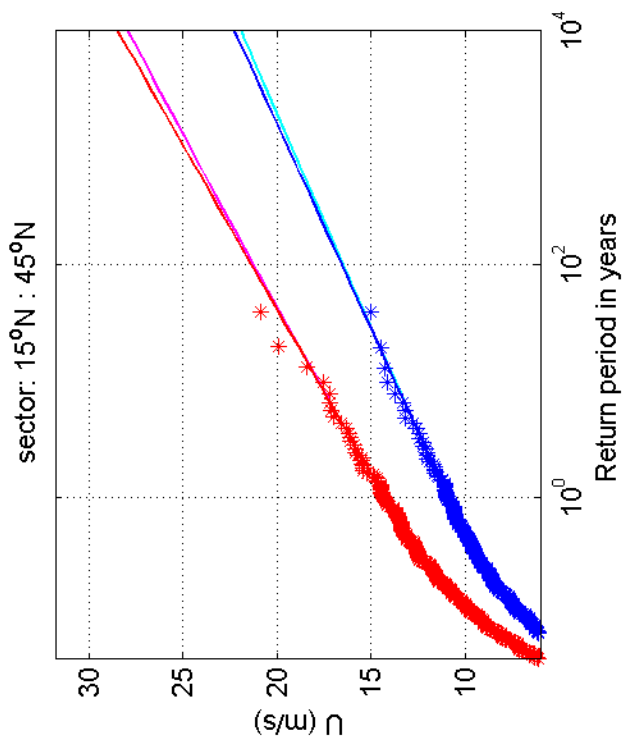
1970-2008

Schiphol vs HoekvanHolland

Deltares

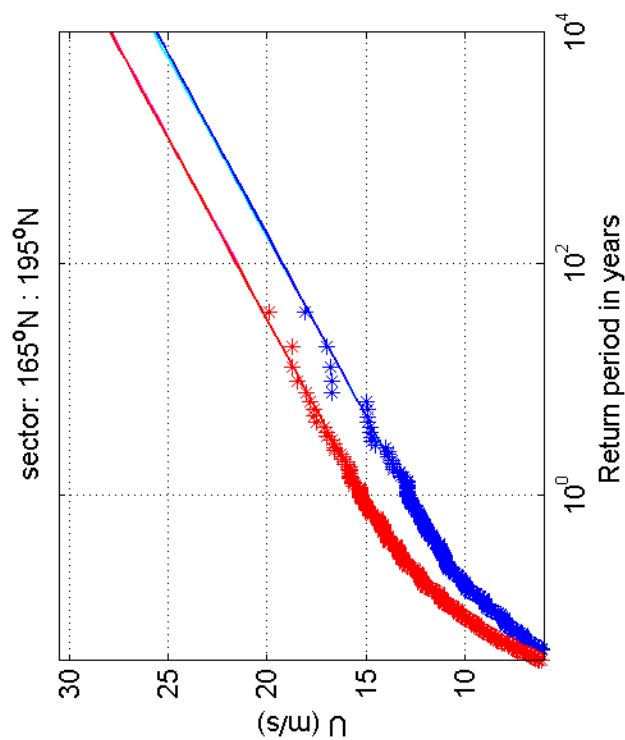
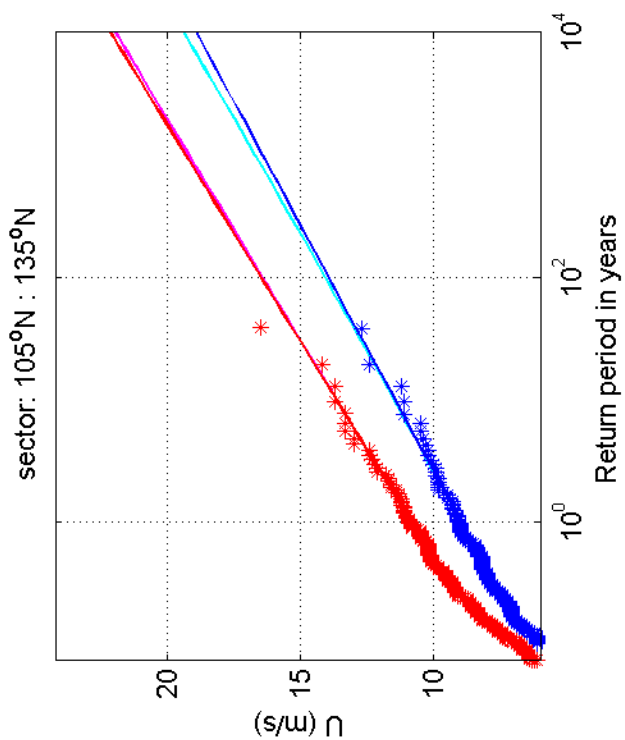
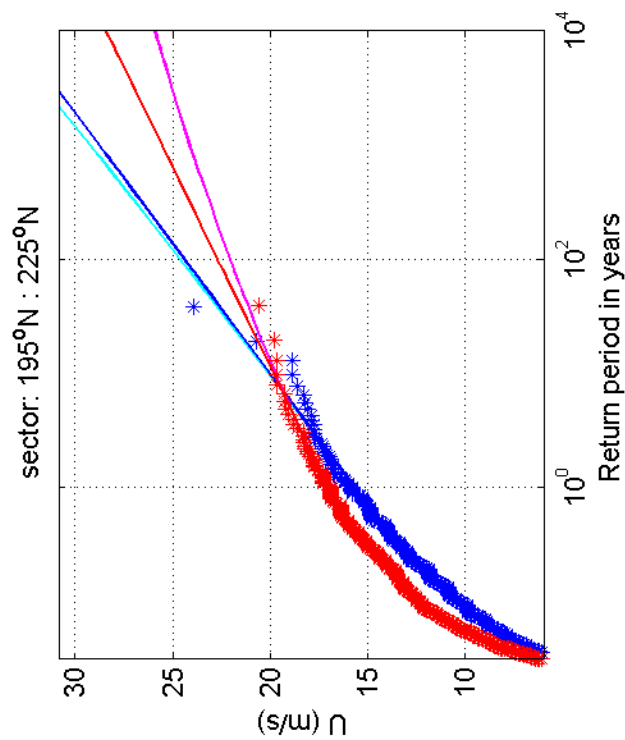
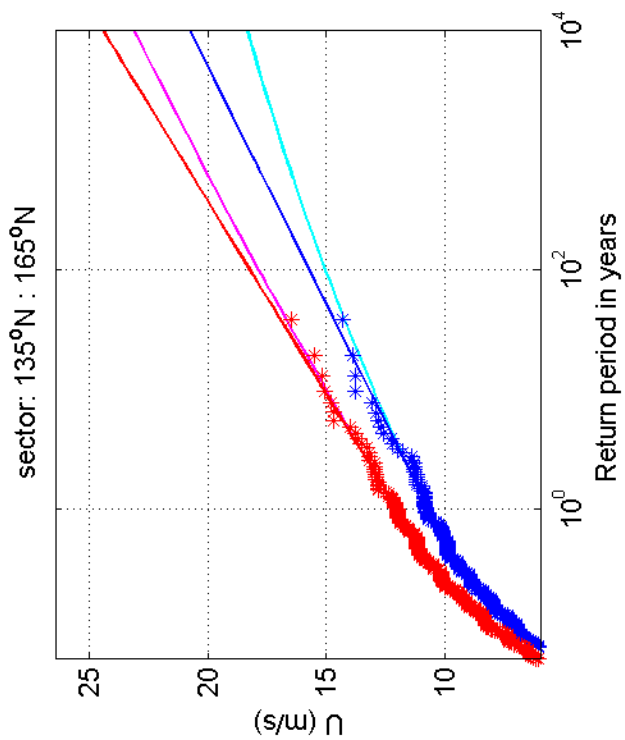
1200264-005

Fig. F.5a.14



Return value plot per sector of Schiphol (blue) vs HoekvanHolland (red)
 Exponential (blue, red) and GPD (cyan, magenta) fits to U_p
 Plotting positions: x_i vs $(n+1)/(\lambda(n+1-i))$

1970-2008



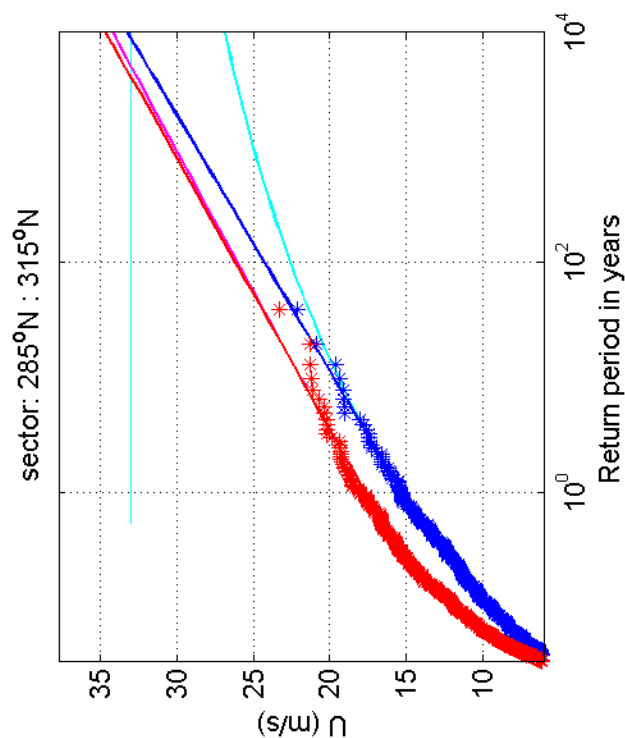
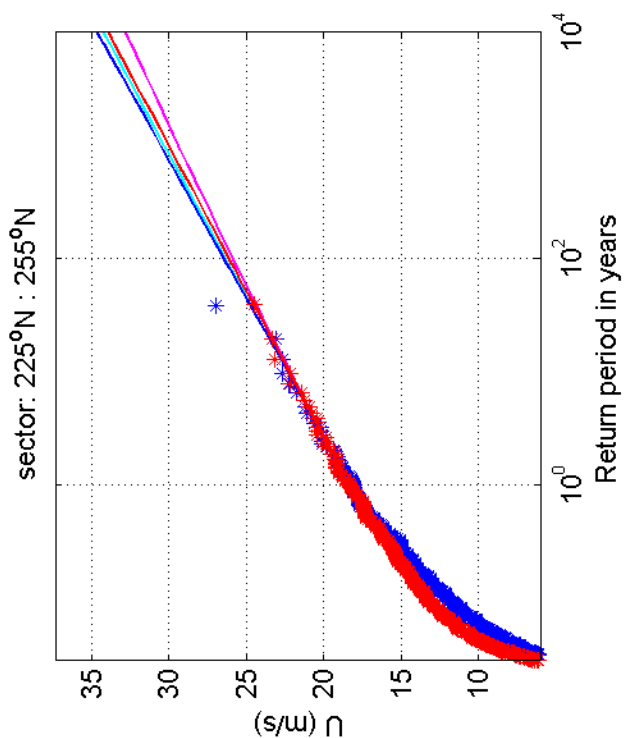
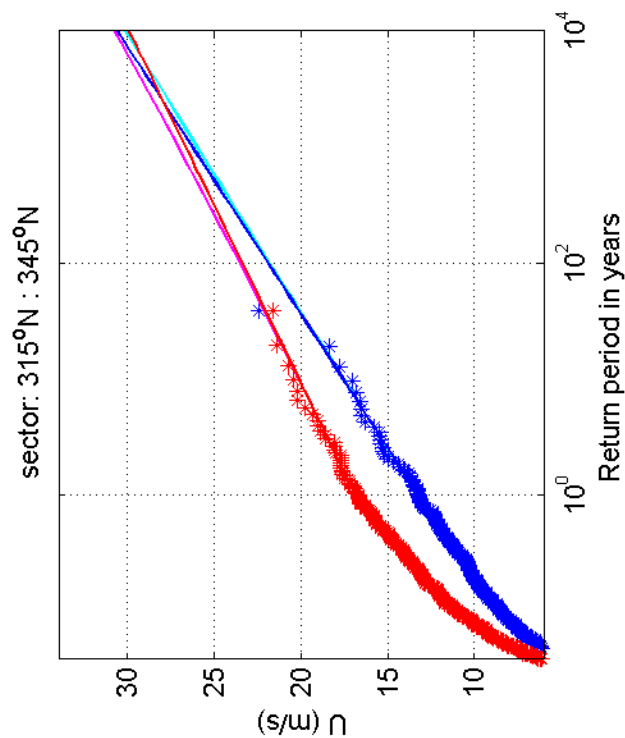
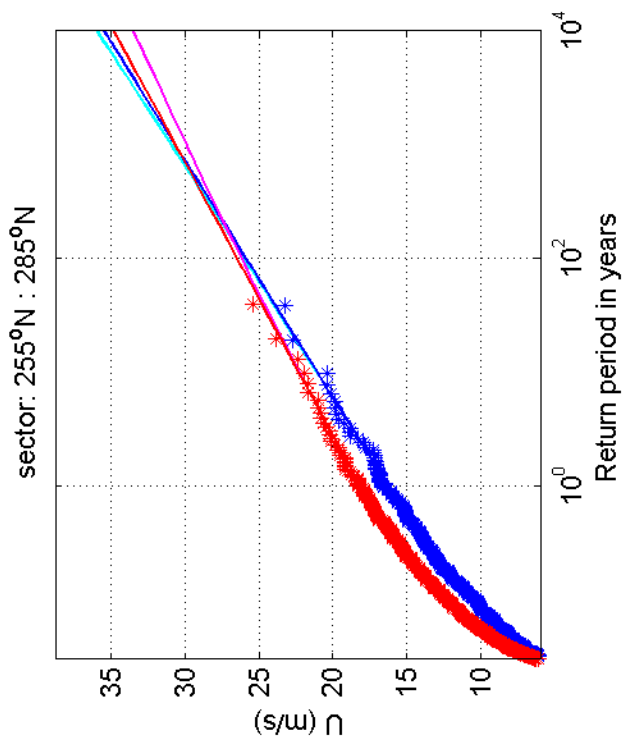
Return value plot per sector of Schiphol (blue) vs HoekvanHolland (red)
 Exponential (blue, red) and GPD (cyan, magenta) fits to U_p
 Plotting positions: x_i vs $(n+1)/(\lambda(n+1-i))$

1970-2008

Deltares

1200264-005

Fig. F.5c.14



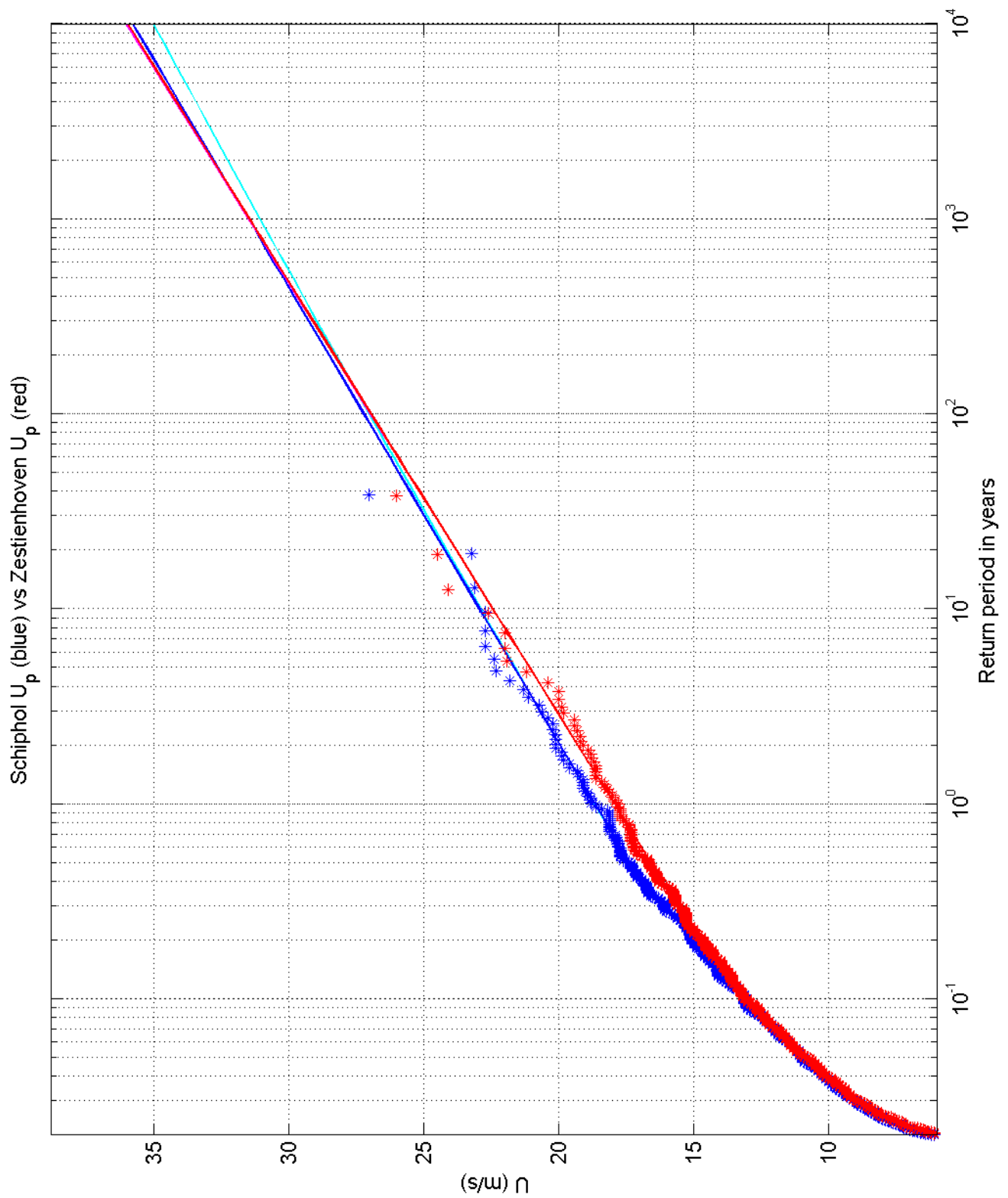
Return value plot per sector of Schiphol (blue) vs HoekvanHolland (red)
 Exponential (blue, red) and GPD (cyan, magenta) fits to U_p
 Plotting positions: x_i vs $(n+1)/(\lambda(n+1-i))$

1970-2008

Deltares

1200264-005

Fig. F.5d.14



Return value plot of Schiphol (blue) vs Zestienhoven (red)
 Exponential (blue, red) and GPD (cyan, magenta) fits to U_p
 Plotting positions: x_i vs $(n+1)/(\lambda(n+1-i))$

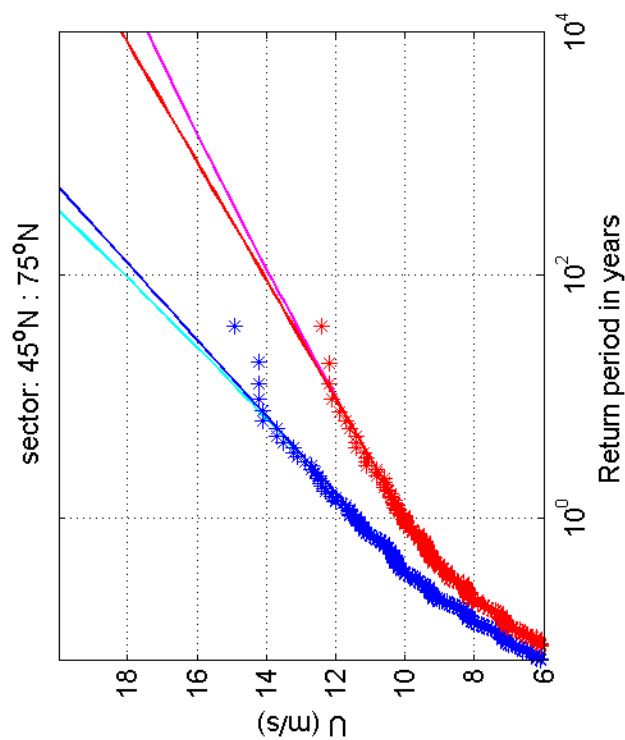
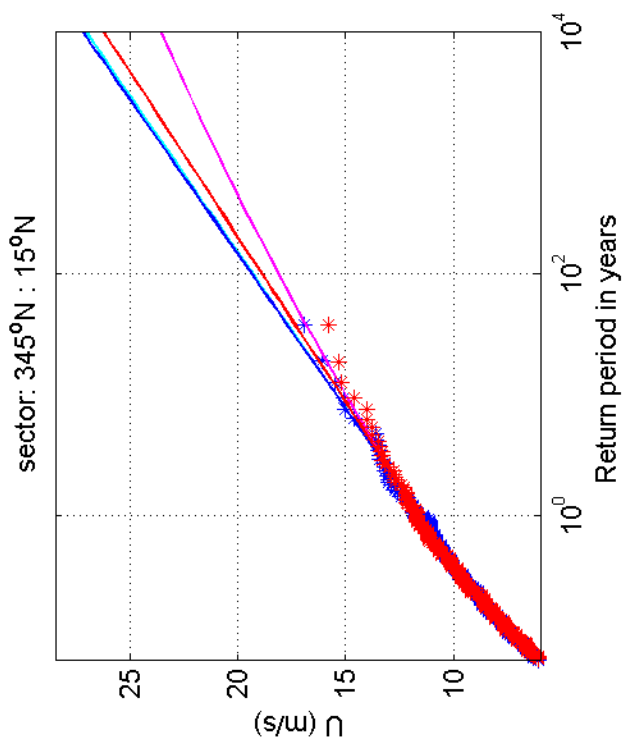
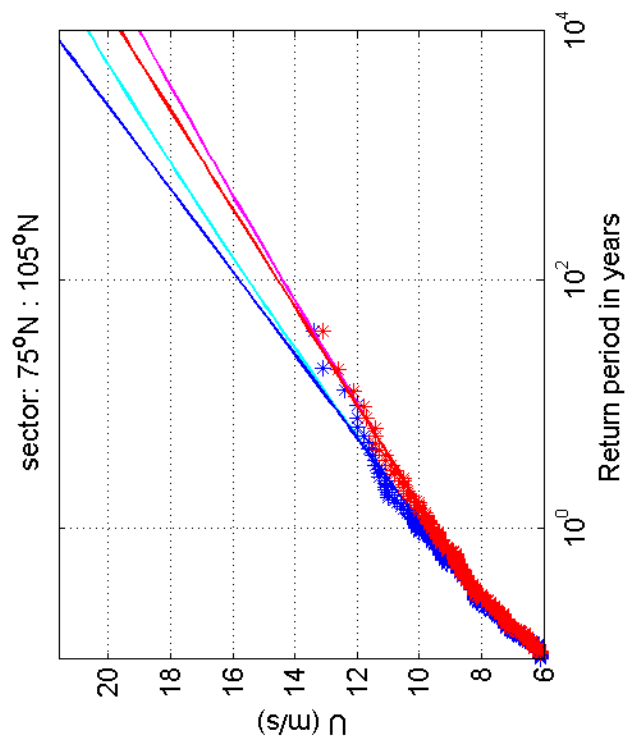
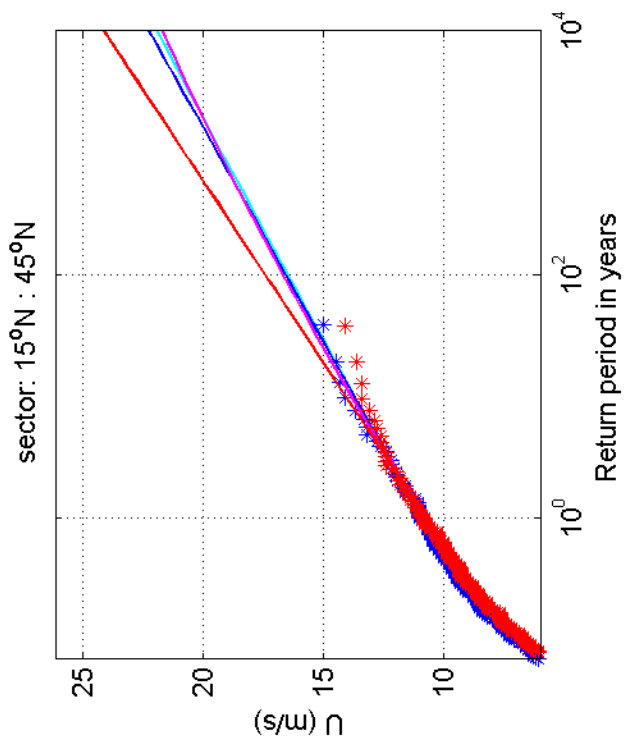
1970-2008

Schiphol vs Zestienhoven

Deltares

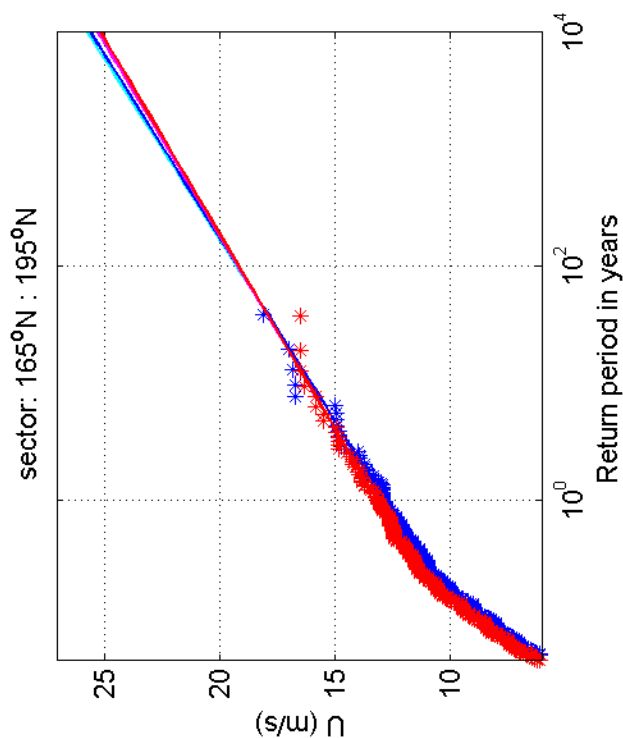
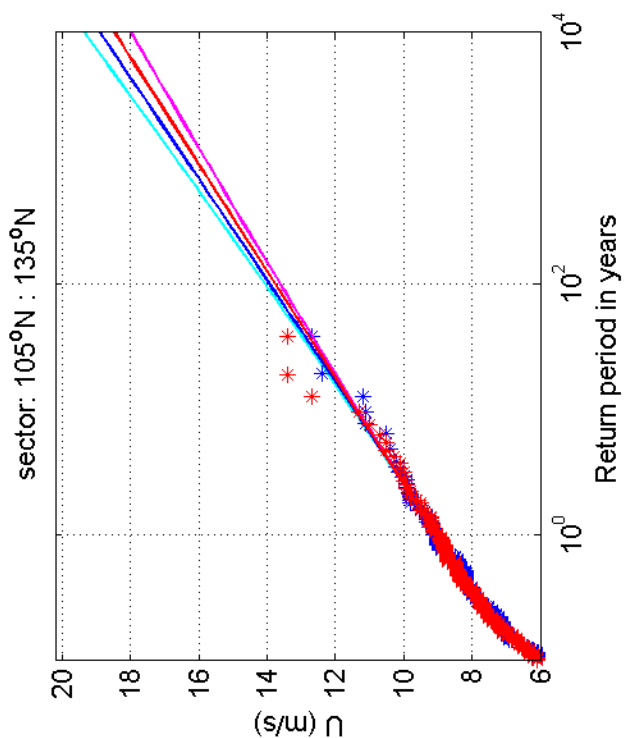
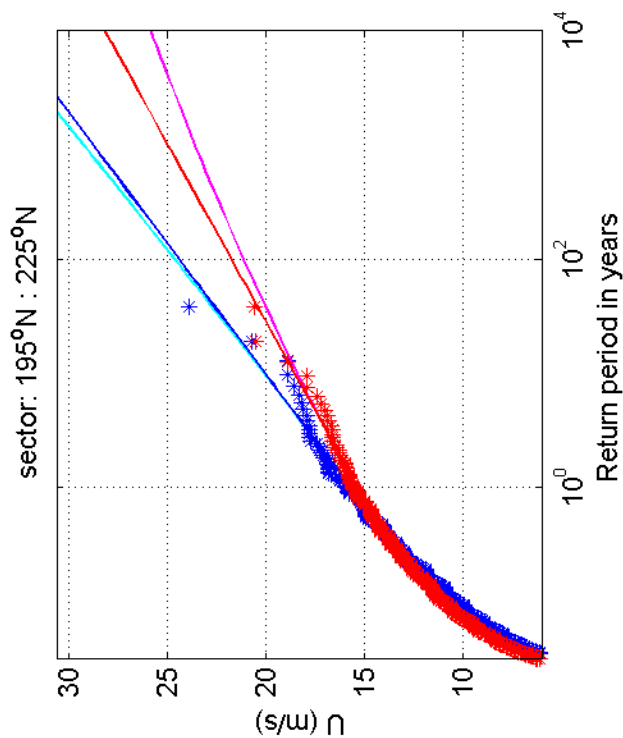
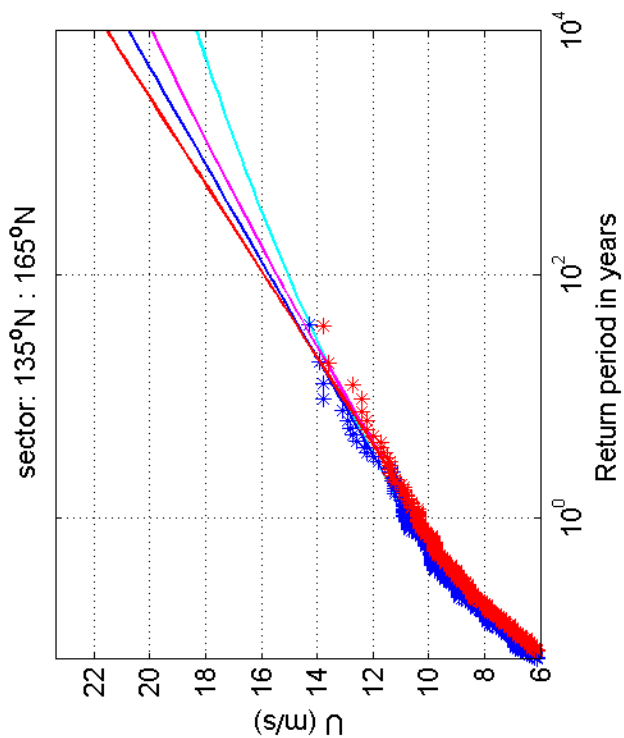
1200264-005

Fig. F.5a.15



Return value plot per sector of Schiphol (blue) vs Zestienhoven (red)
 Exponential (blue, red) and GPD (cyan, magenta) fits to U_p
 Plotting positions: x_i vs $(n+1)/(\lambda(n+1-i))$

1970-2008



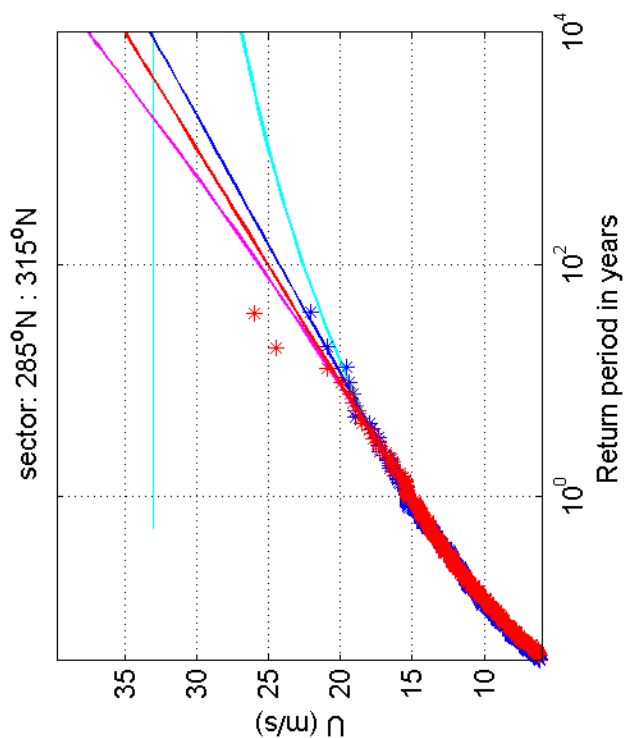
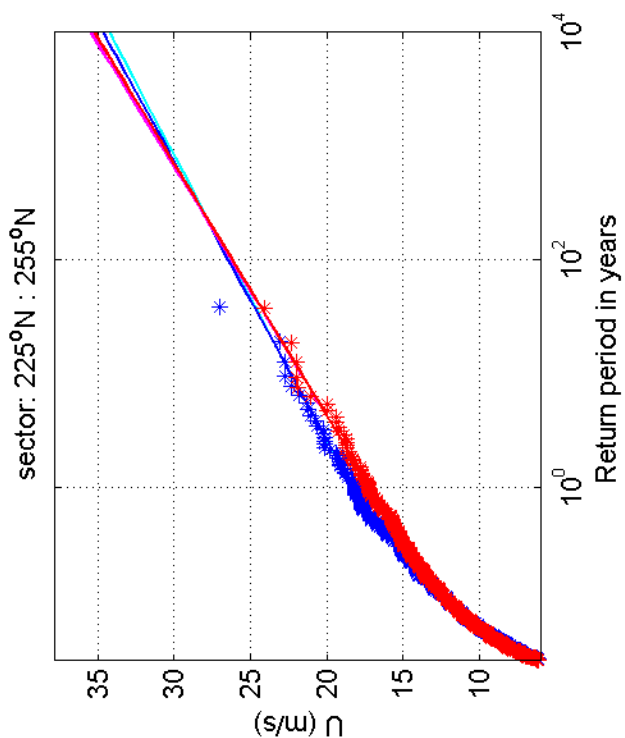
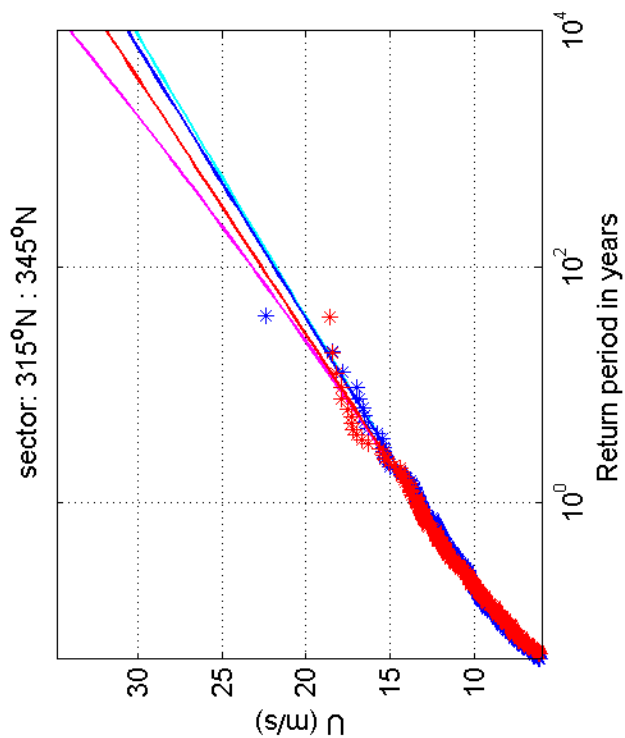
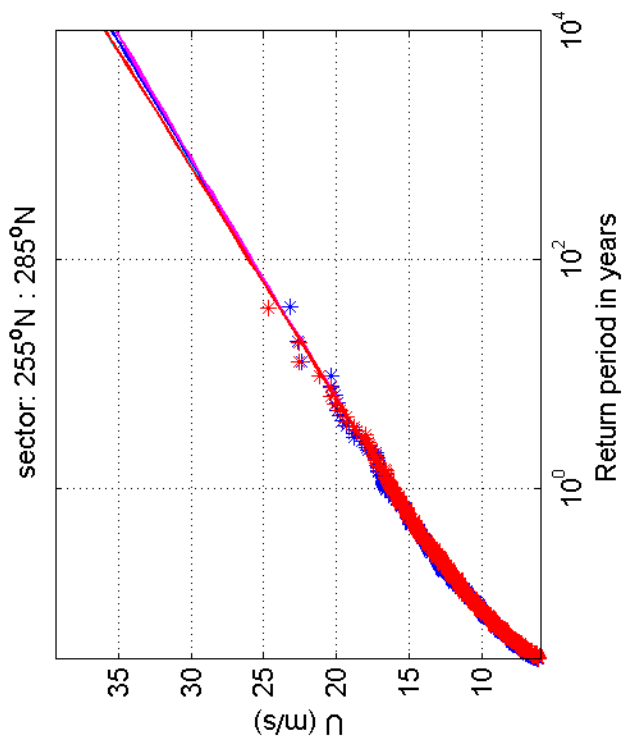
Return value plot per sector of Schiphol (blue) vs Zestienhoven (red)
 Exponential (blue, red) and GPD (cyan, magenta) fits to U_p
 Plotting positions: x_i vs $(n+1)/(\lambda(n+1-i))$

1970-2008

Deltares

1200264-005

Fig. F.5c.15



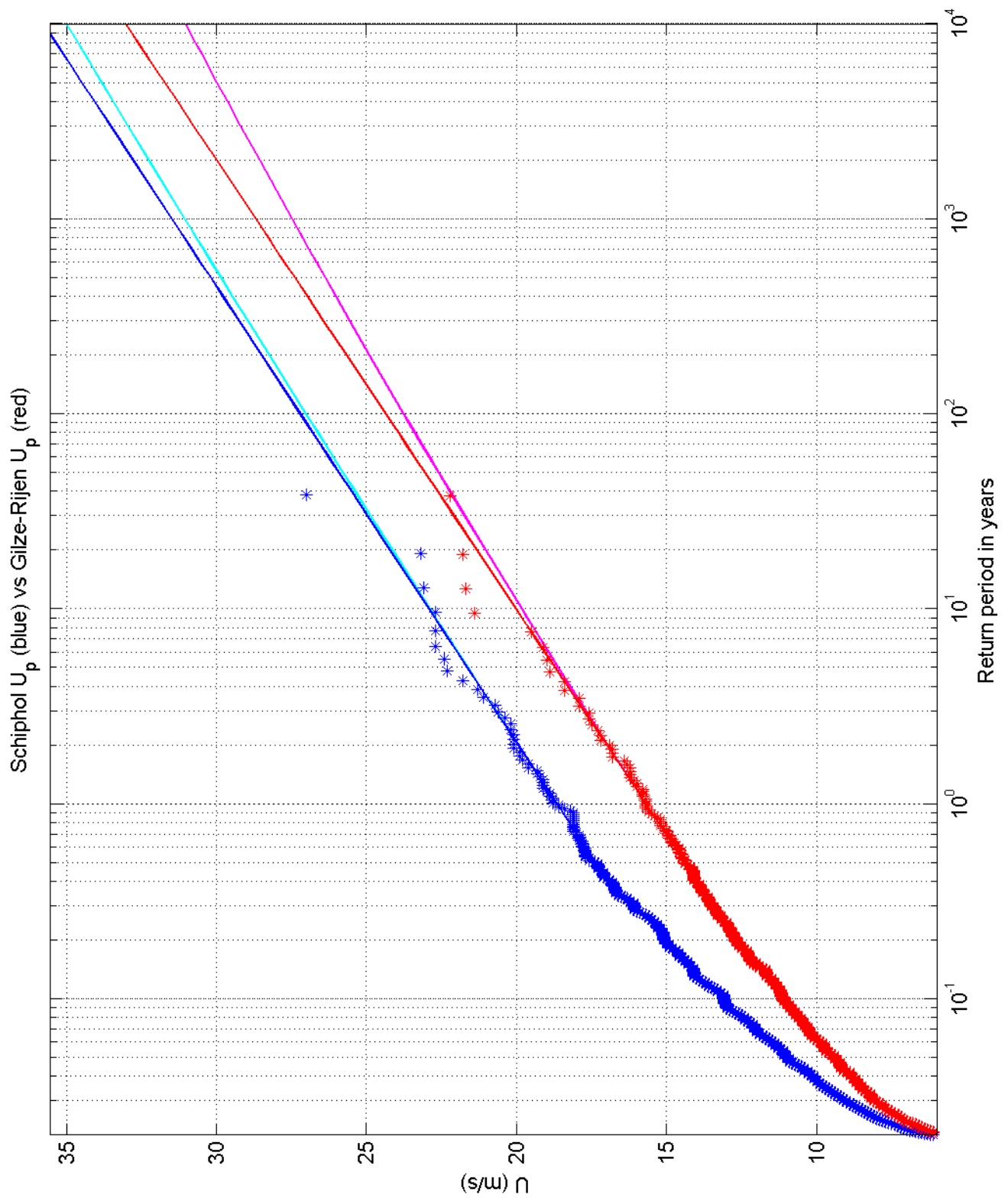
Return value plot per sector of Schiphol (blue) vs Zestienhoven (red)
 Exponential (blue, red) and GPD (cyan, magenta) fits to U_p
 Plotting positions: x_i vs $(n+1)/(\lambda(n+1-i))$

1970-2008

Deltares

1200264-005

Fig. F.5d.15



Return value plot of Schiphol (blue) vs Gilze-Rijen (red)
 Exponential (blue, red) and GPD (cyan, magenta) fits to U_p
 Plotting positions: x_i vs $(n+1)/(\lambda(n+1-i))$

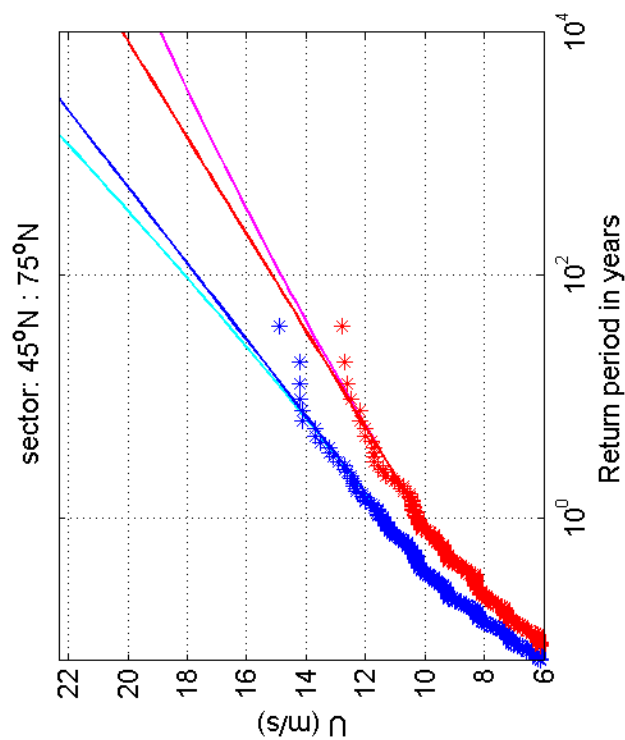
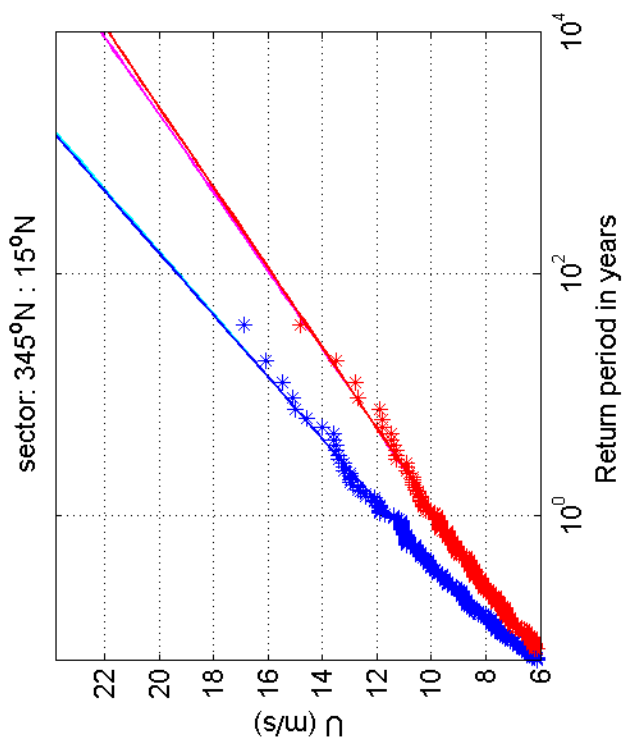
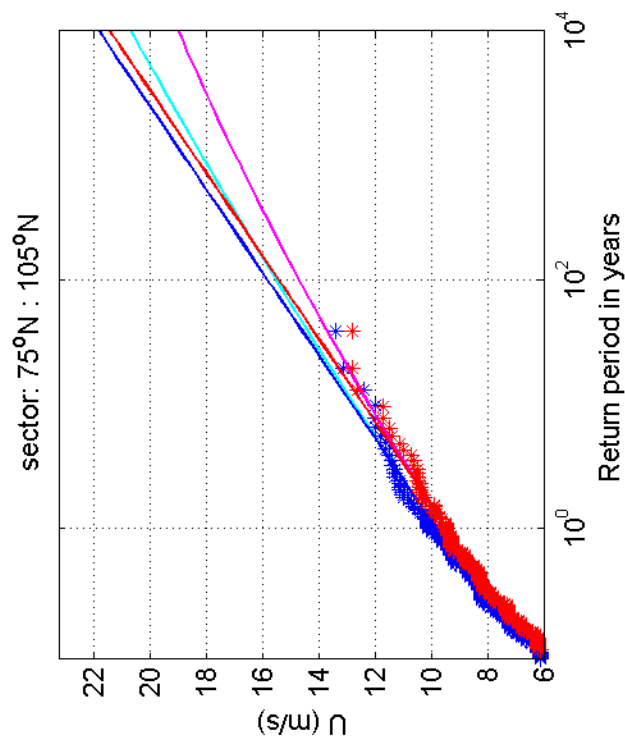
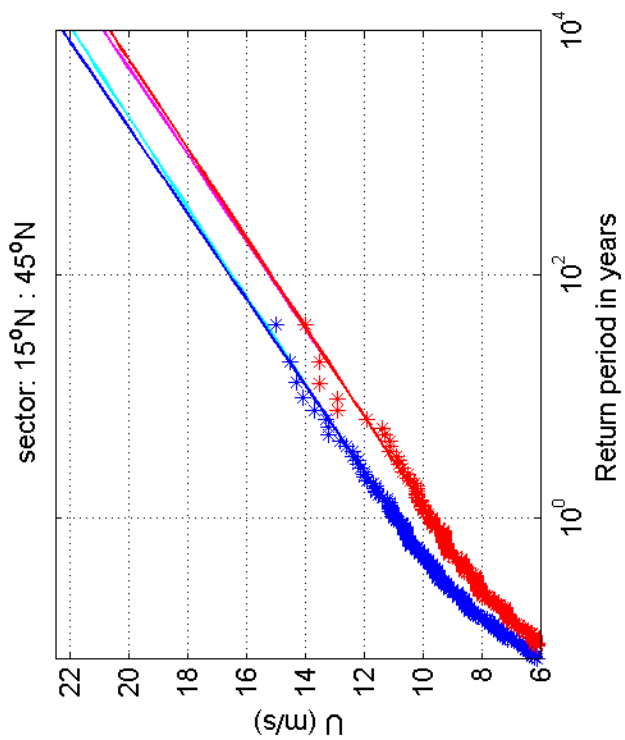
1970-2008

Schiphol vs Gilze-Rijen

Deltares

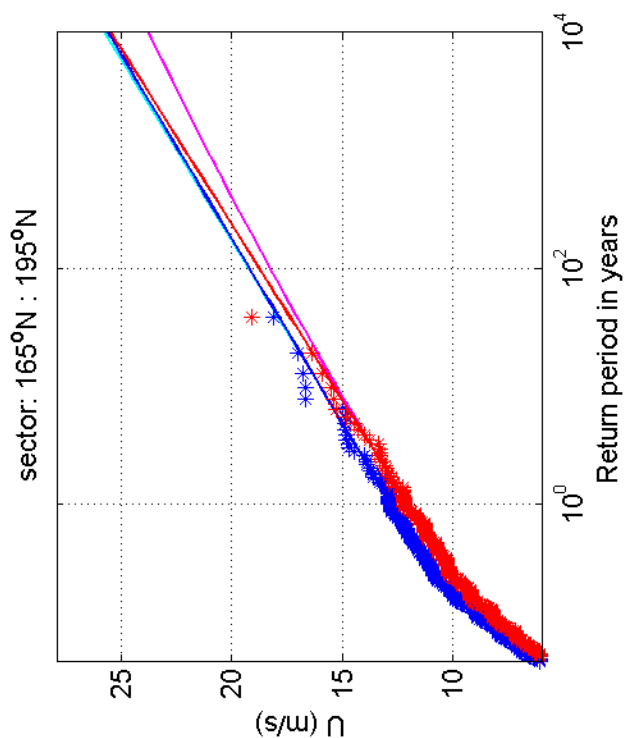
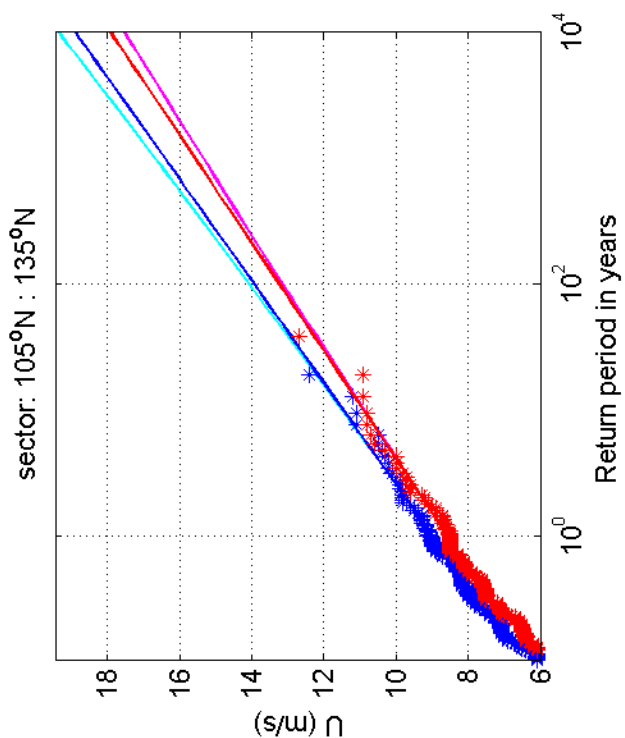
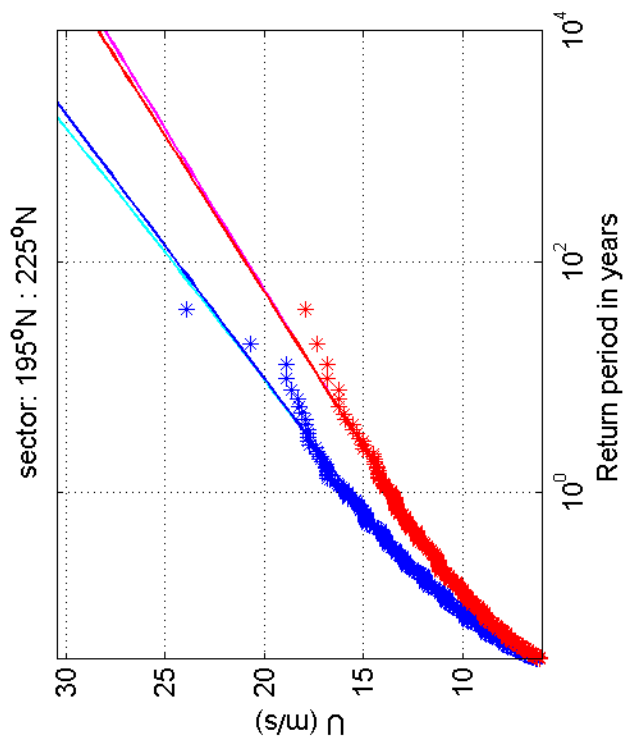
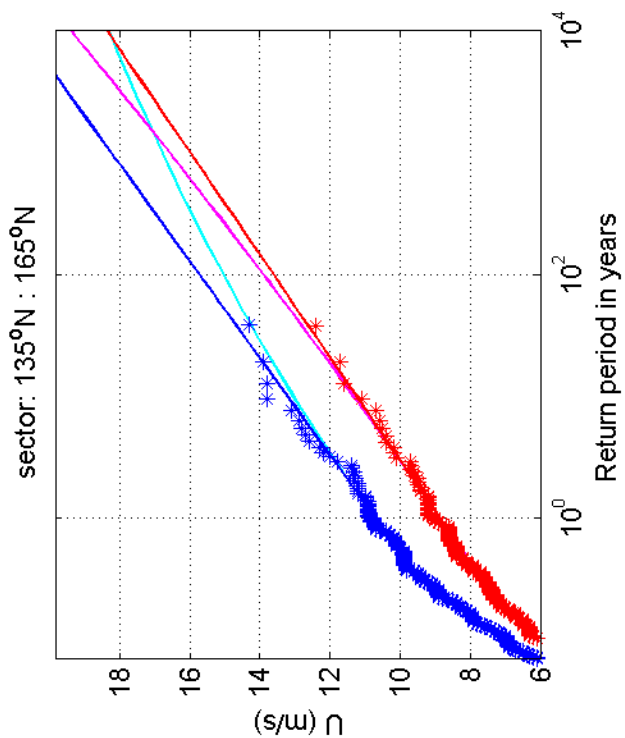
1200264-005

Fig. F.5a.16



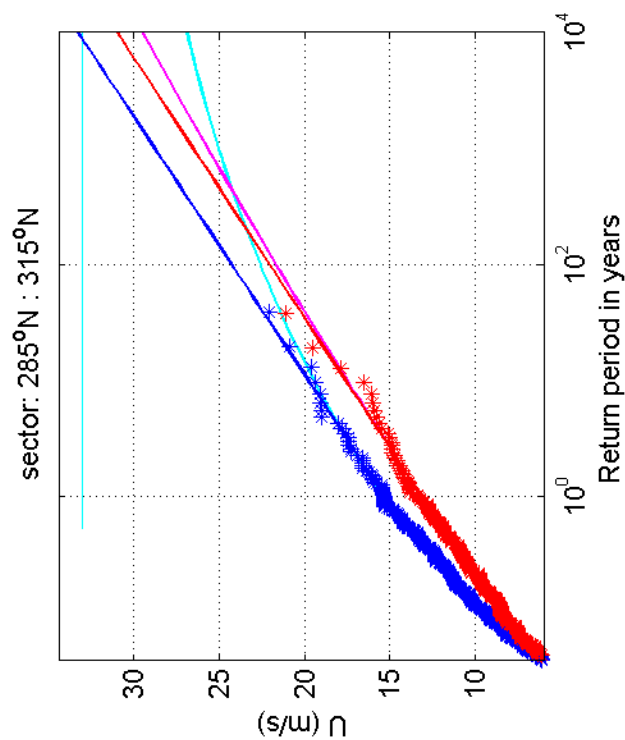
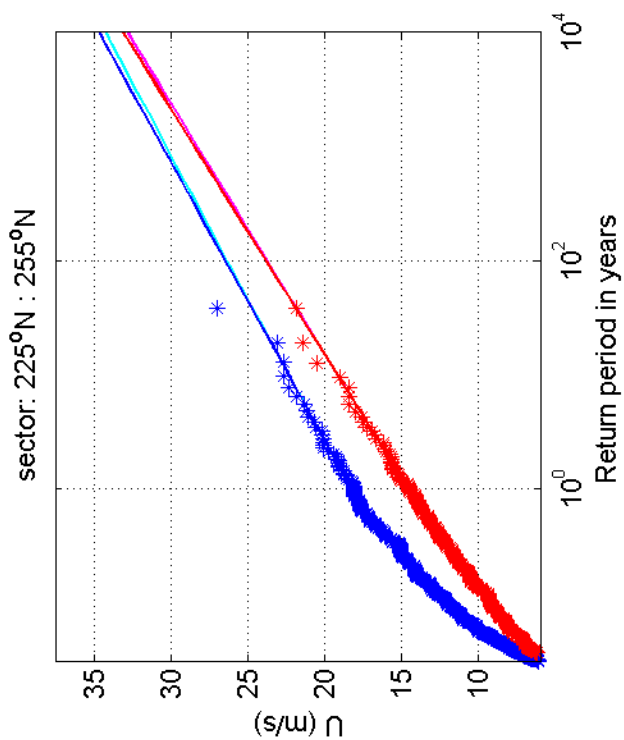
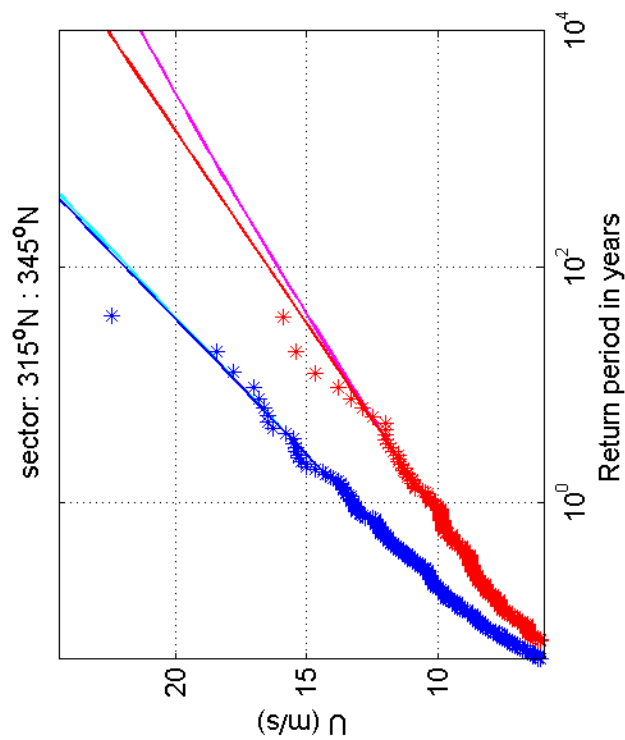
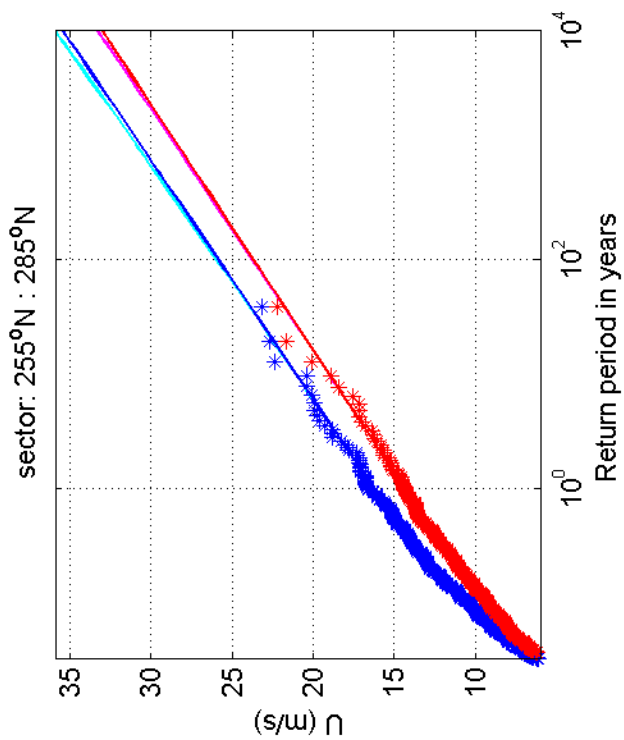
Return value plot per sector of Schiphol (blue) vs Gilze-Rijen (red)
 Exponential (blue, red) and GPD (cyan, magenta) fits to U_p
 Plotting positions: x_i vs $(n+1)/(\lambda(n+1-i))$

1970-2008



Return value plot per sector of Schiphol (blue) vs Gilze-Rijen (red)
 Exponential (blue, red) and GPD (cyan, magenta) fits to U_p
 Plotting positions: x_i vs $(n+1)/(\lambda(n+1-i))$

1970-2008



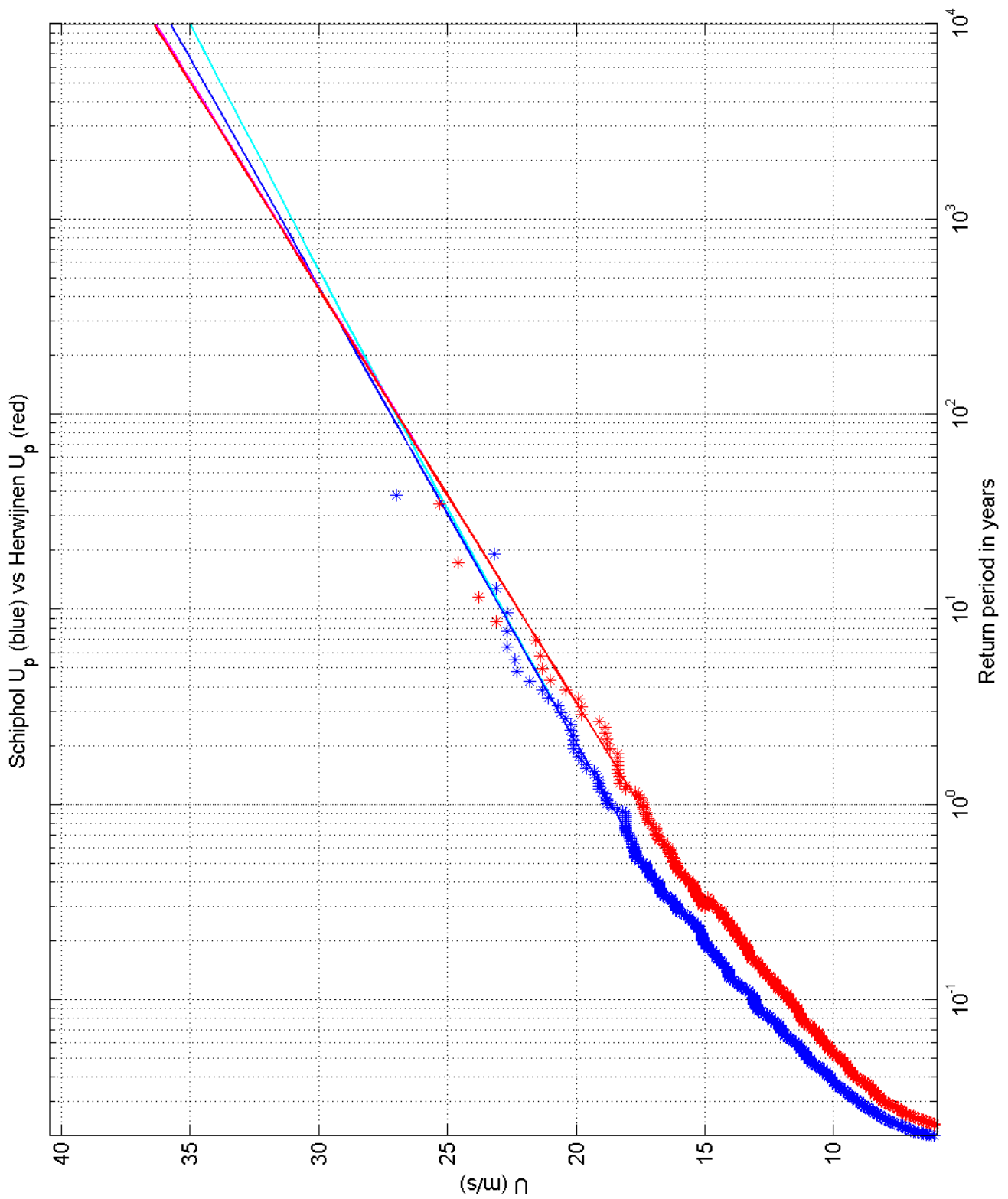
Return value plot per sector of Schiphol (blue) vs Gilze-Rijen (red)
 Exponential (blue, red) and GPD (cyan, magenta) fits to U_p
 Plotting positions: x_i vs $(n+1)/(\lambda(n+1-i))$

1970-2008

Deltares

1200264-005

Fig. F.5d.16



Return value plot of Schiphol (blue) vs Herwijnen (red)
 Exponential (blue, red) and GPD (cyan, magenta) fits to U_p
 Plotting positions: x_i vs $(n+1)/(\lambda(n+1-i))$

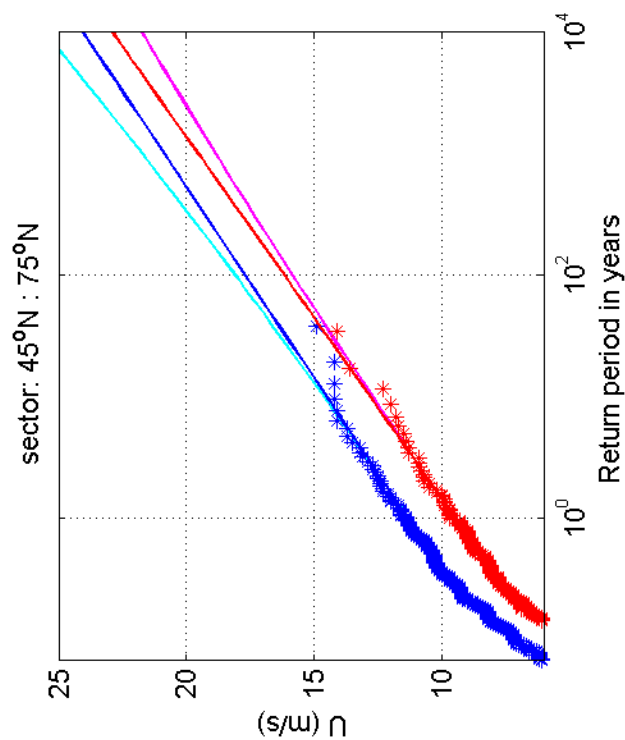
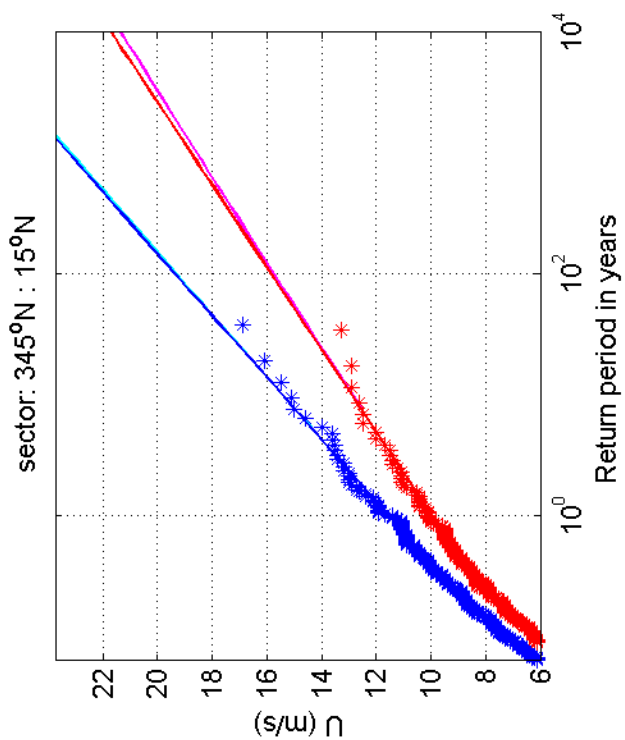
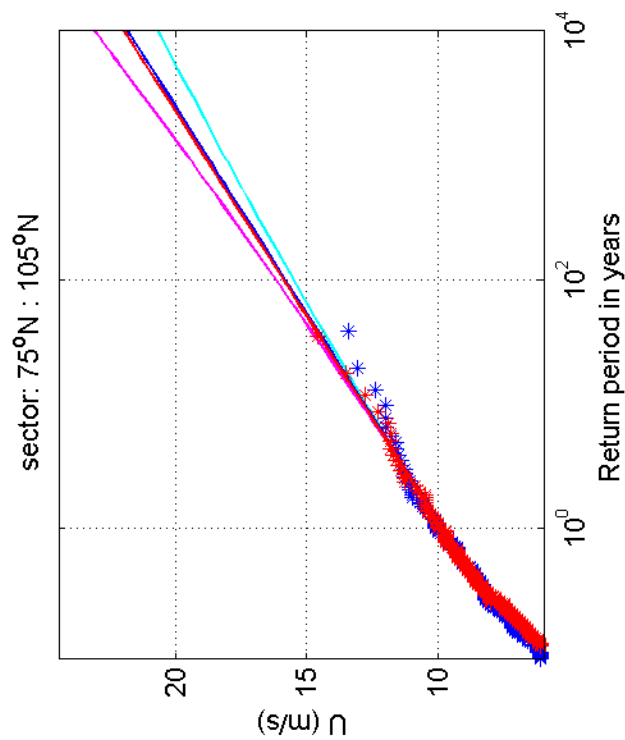
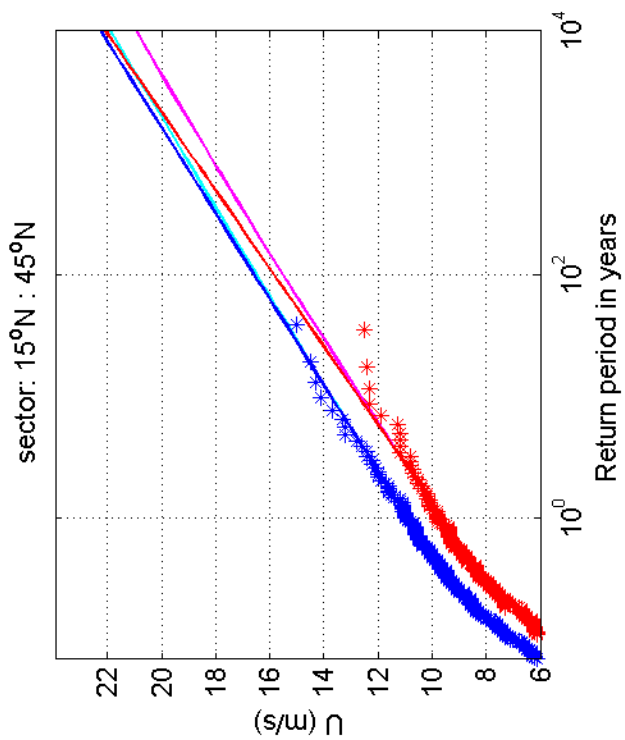
1970-2008

Schiphol vs Herwijnen

Deltares

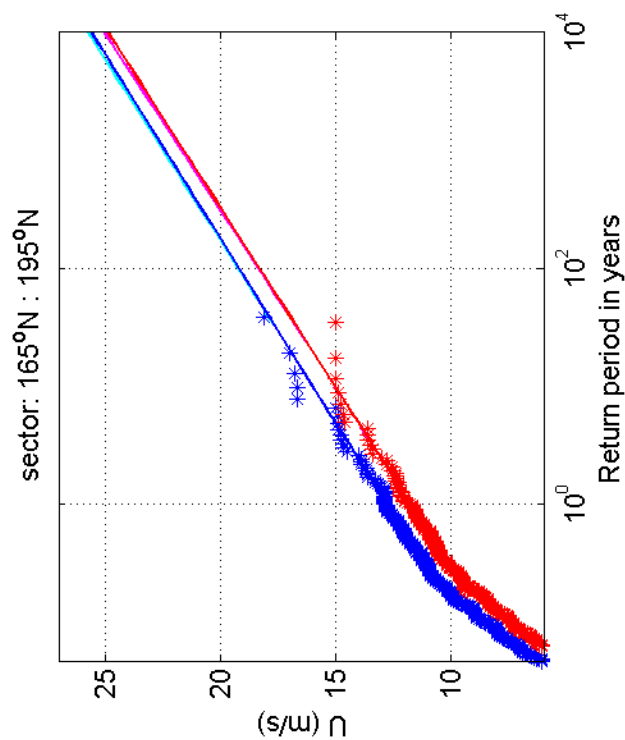
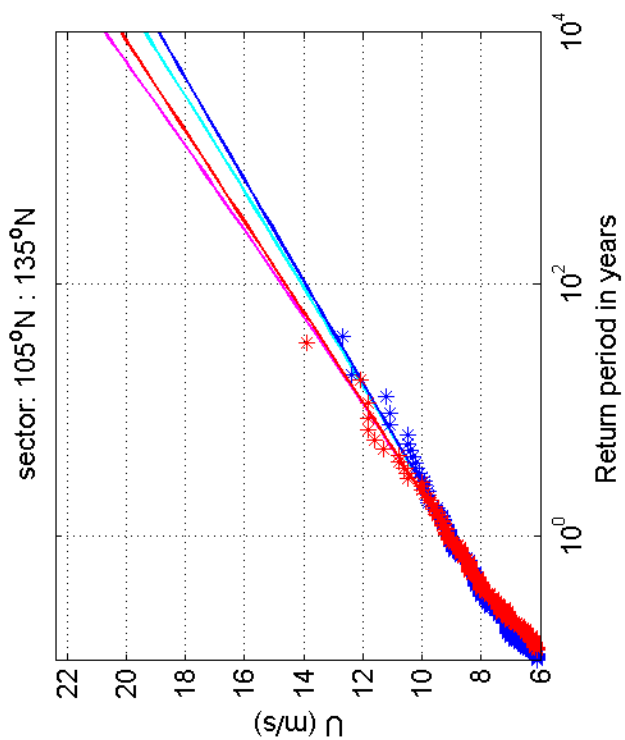
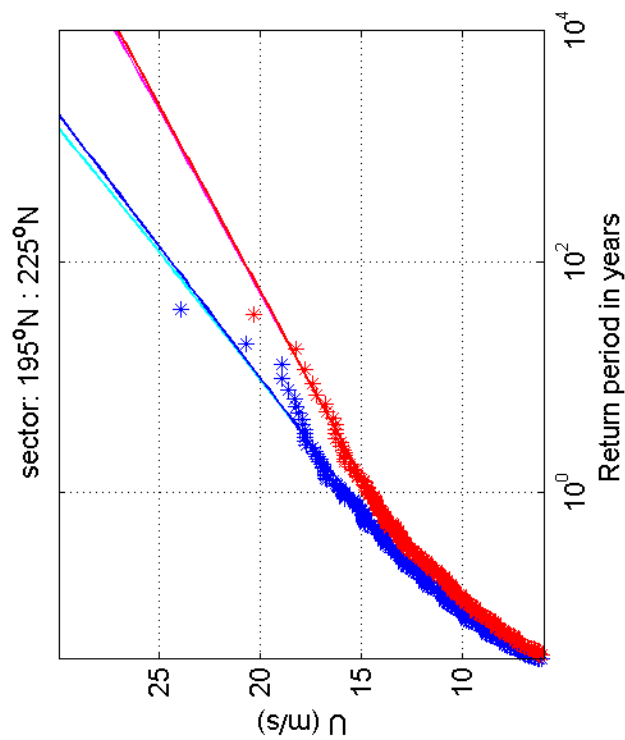
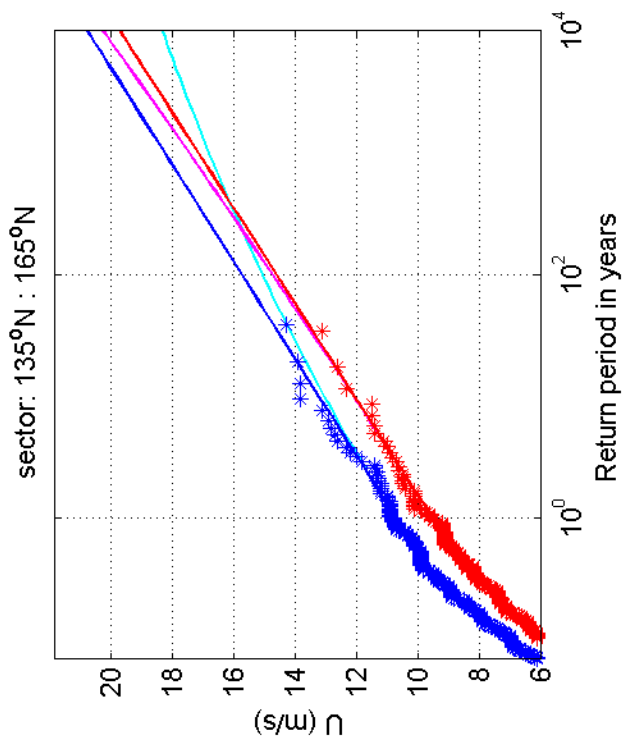
1200264-005

Fig. F.5a.17



Return value plot per sector of Schiphol (blue) vs Herwijnen (red)
 Exponential (blue, red) and GPD (cyan, magenta) fits to U_p
 Plotting positions: x_i vs $(n+1)/(\lambda(n+1-i))$

1970-2008



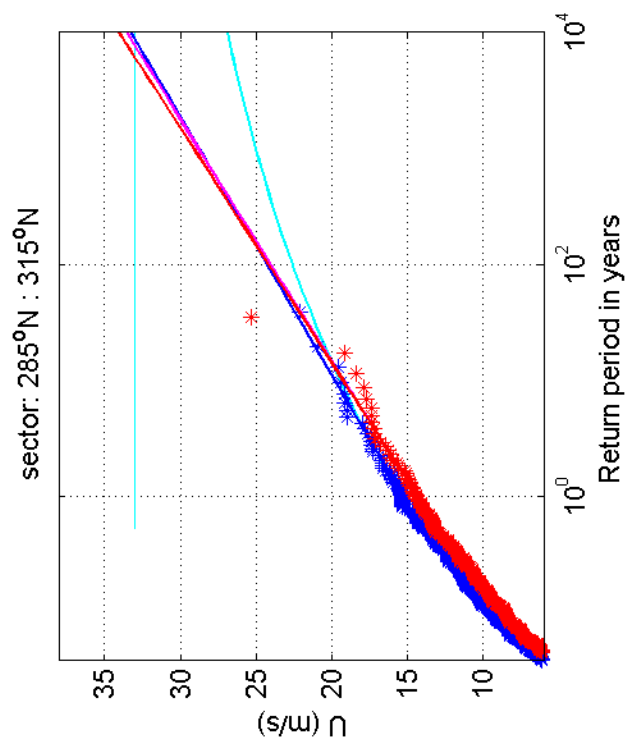
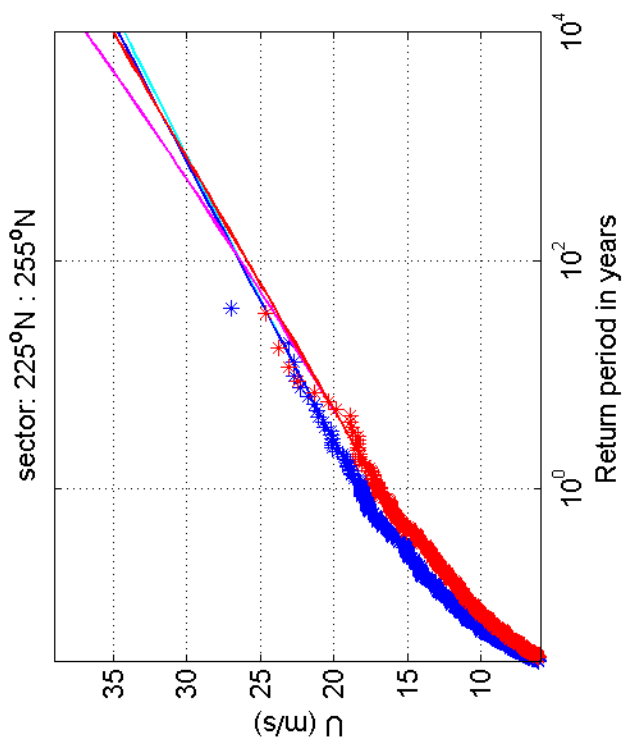
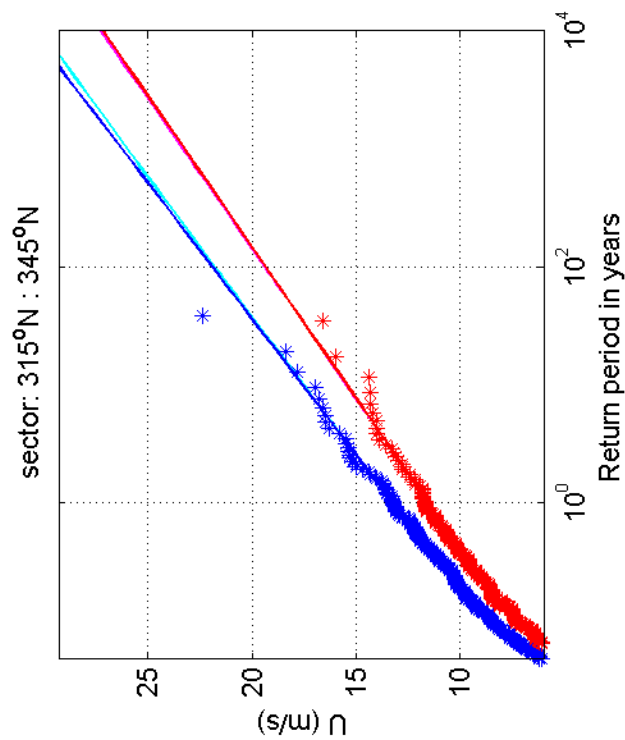
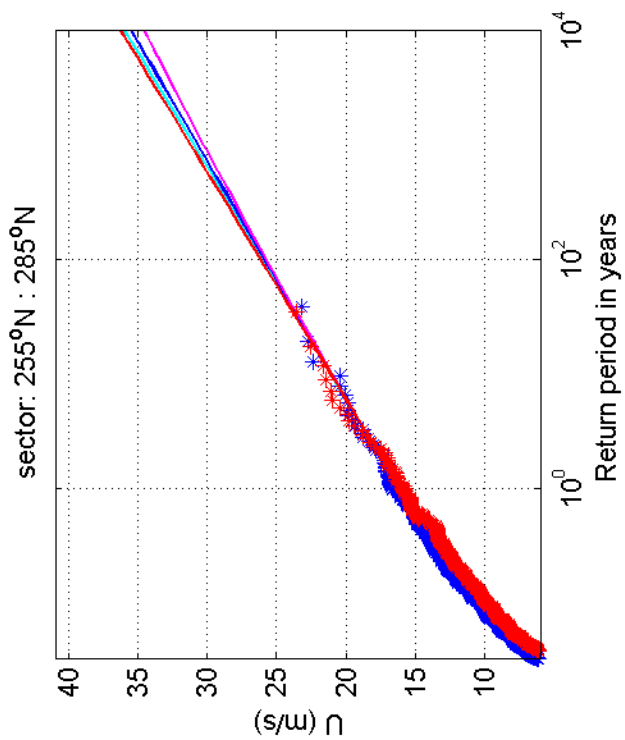
Return value plot per sector of Schiphol (blue) vs Herwijnen (red)
 Exponential (blue, red) and GPD (cyan, magenta) fits to U_p
 Plotting positions: x_i vs $(n+1)/(\lambda(n+1-i))$

1970-2008

Deltares

1200264-005

Fig. F.5c.17



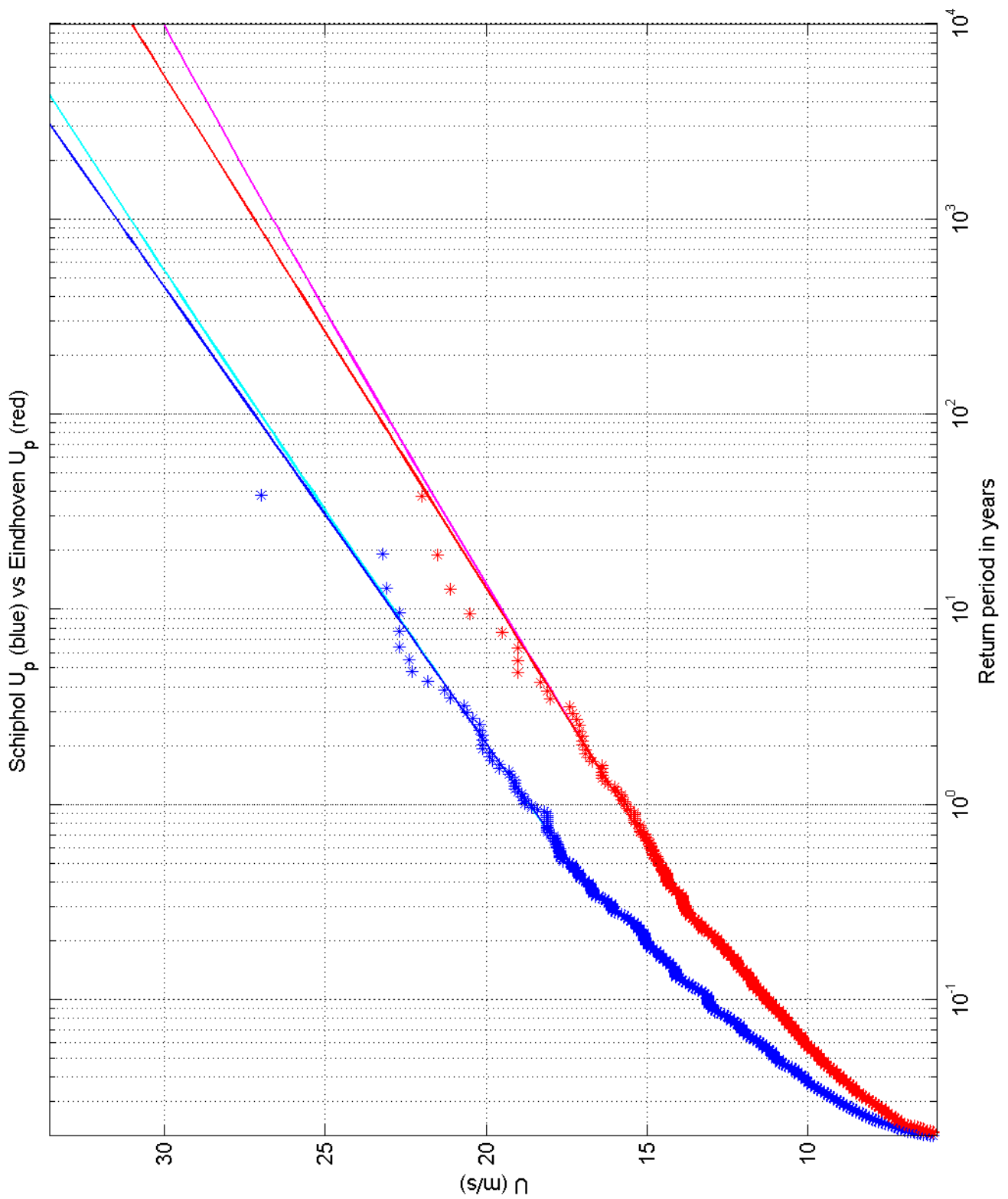
Return value plot per sector of Schiphol (blue) vs Herwijnen (red)
 Exponential (blue, red) and GPD (cyan, magenta) fits to U_p
 Plotting positions: x_i vs $(n+1)/(\lambda(n+1-i))$

1970-2008

Deltares

1200264-005

Fig. F.5d.17



Return value plot of Schiphol (blue) vs Eindhoven (red)
 Exponential (blue, red) and GPD (cyan, magenta) fits to U_p
 Plotting positions: x_i vs $(n+1)/(\lambda(n+1-i))$

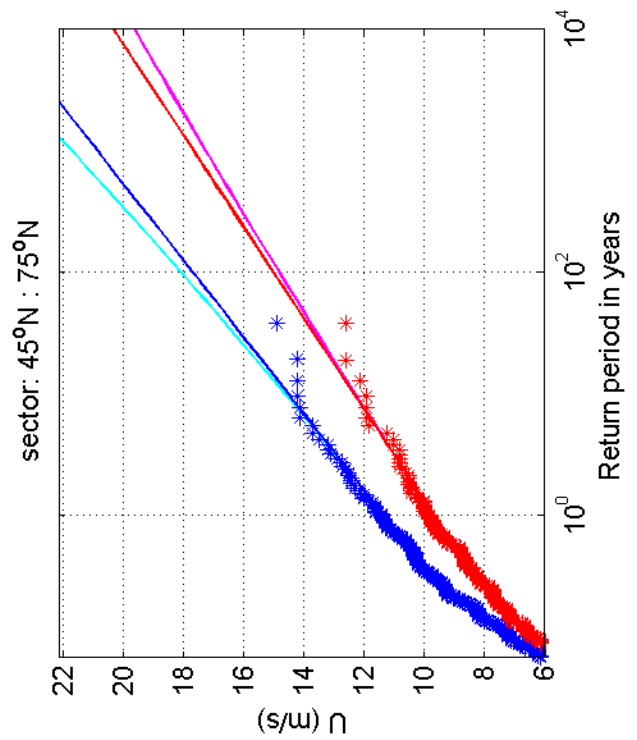
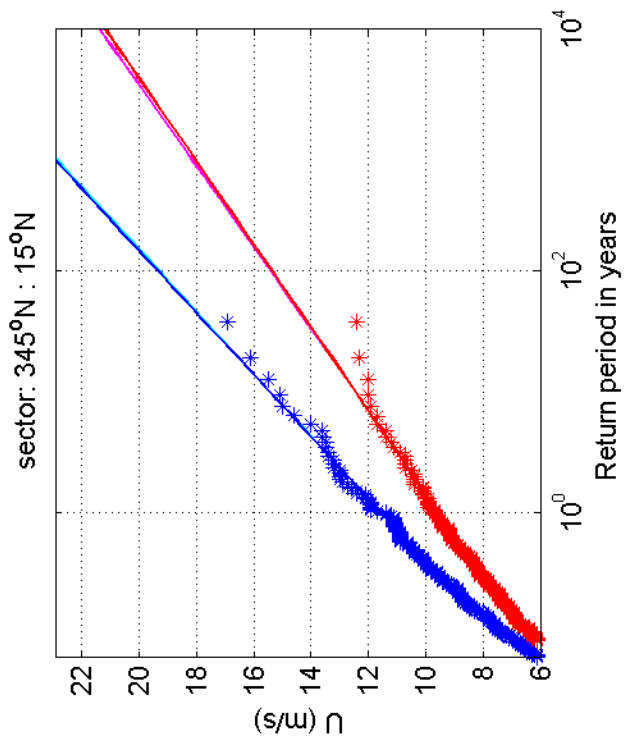
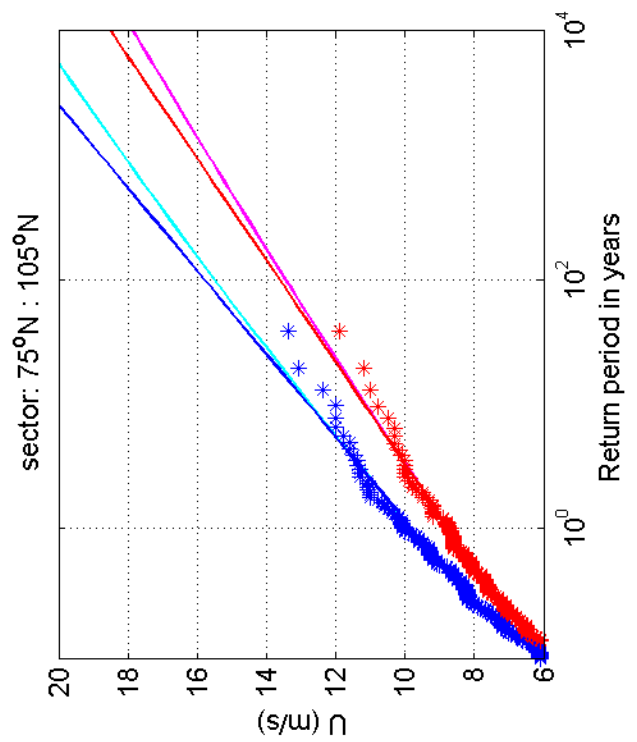
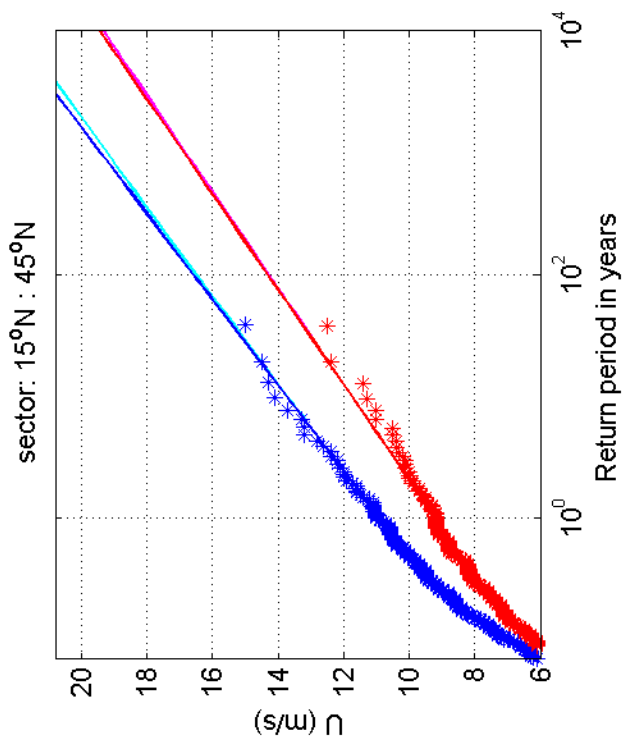
1970-2008

Schiphol vs Eindhoven

Deltares

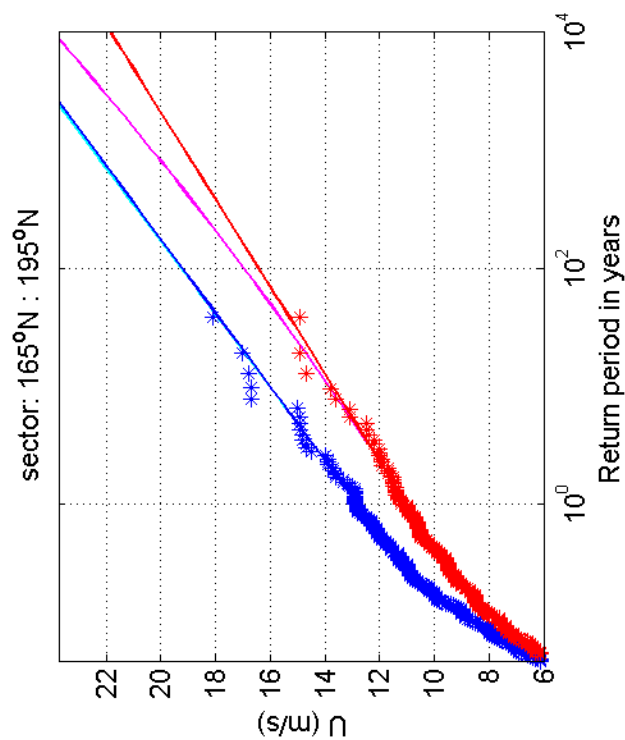
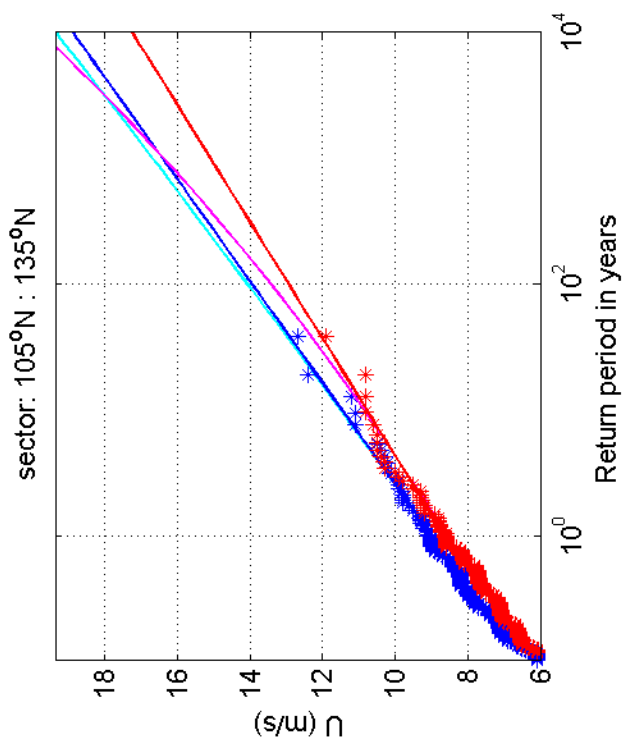
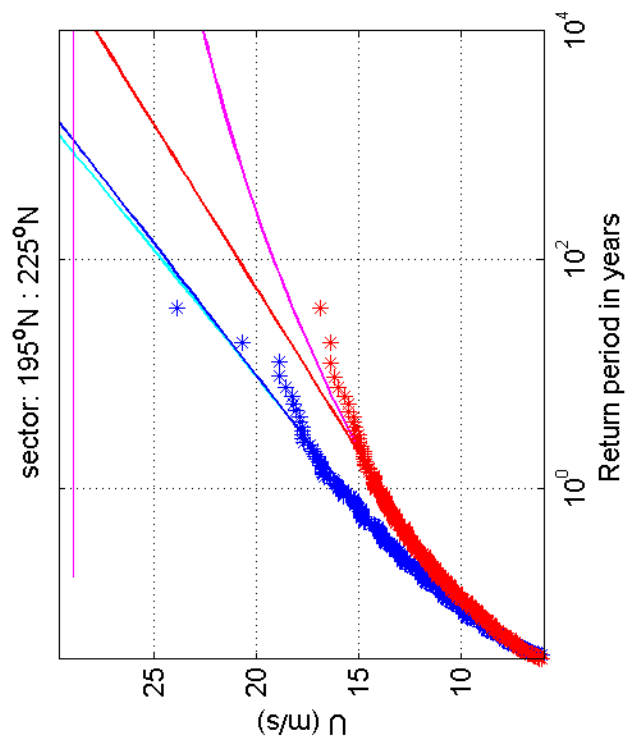
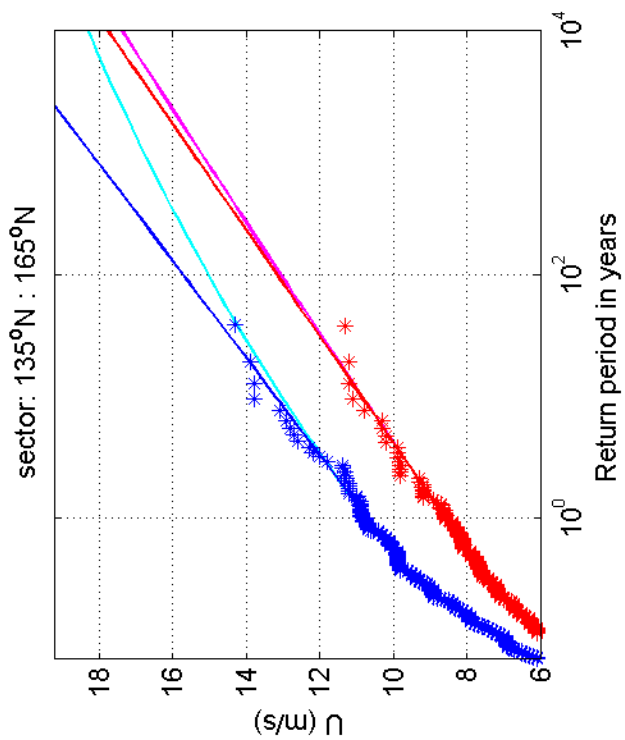
1200264-005

Fig. F.5a.18



Return value plot per sector of Schiphol (blue) vs Eindhoven (red)
 Exponential (blue, red) and GPD (cyan, magenta) fits to U_p
 Plotting positions: x_i vs $(n+1)/(\lambda(n+1-i))$

1970-2008



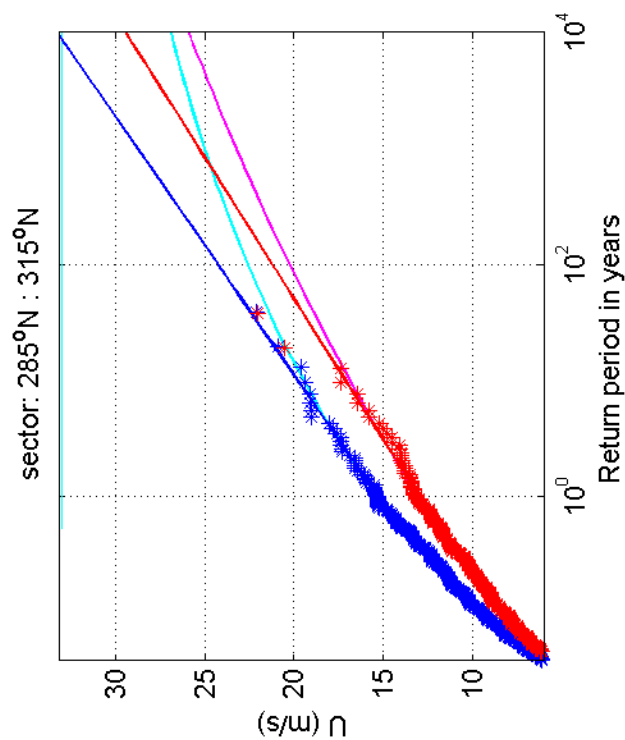
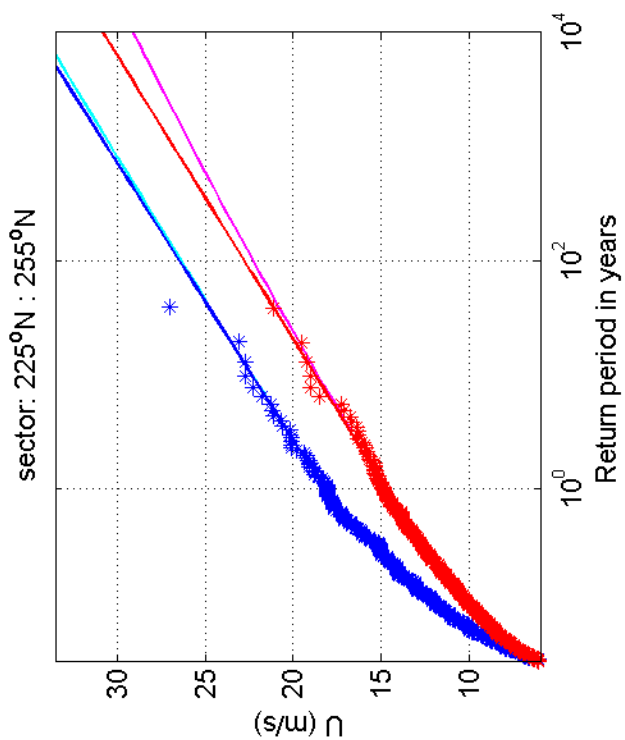
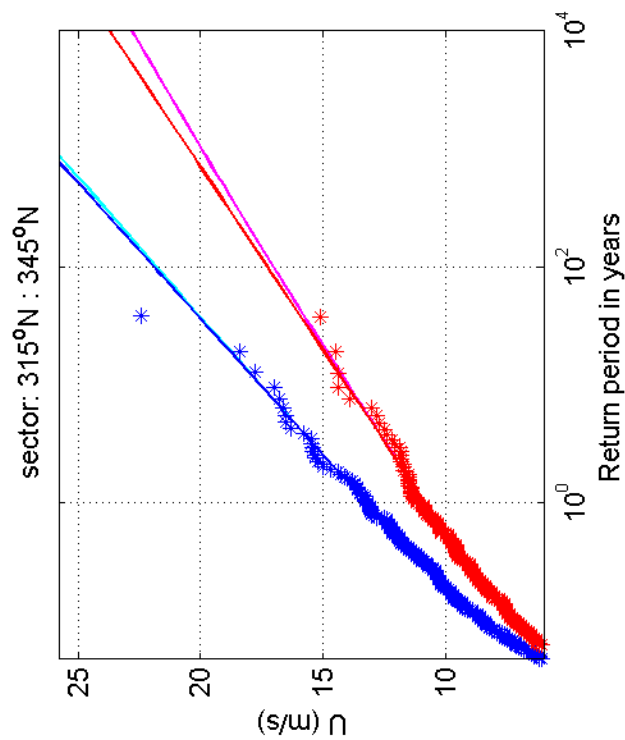
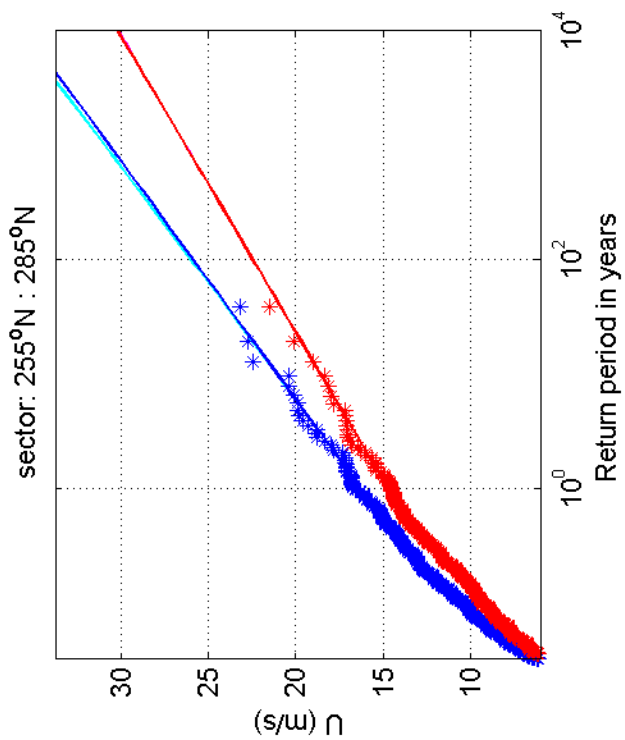
Return value plot per sector of Schiphol (blue) vs Eindhoven (red)
 Exponential (blue, red) and GPD (cyan, magenta) fits to U_p
 Plotting positions: x_i vs $(n+1)/(\lambda(n+1-i))$

1970-2008

Deltares

1200264-005

Fig. F.5c.18



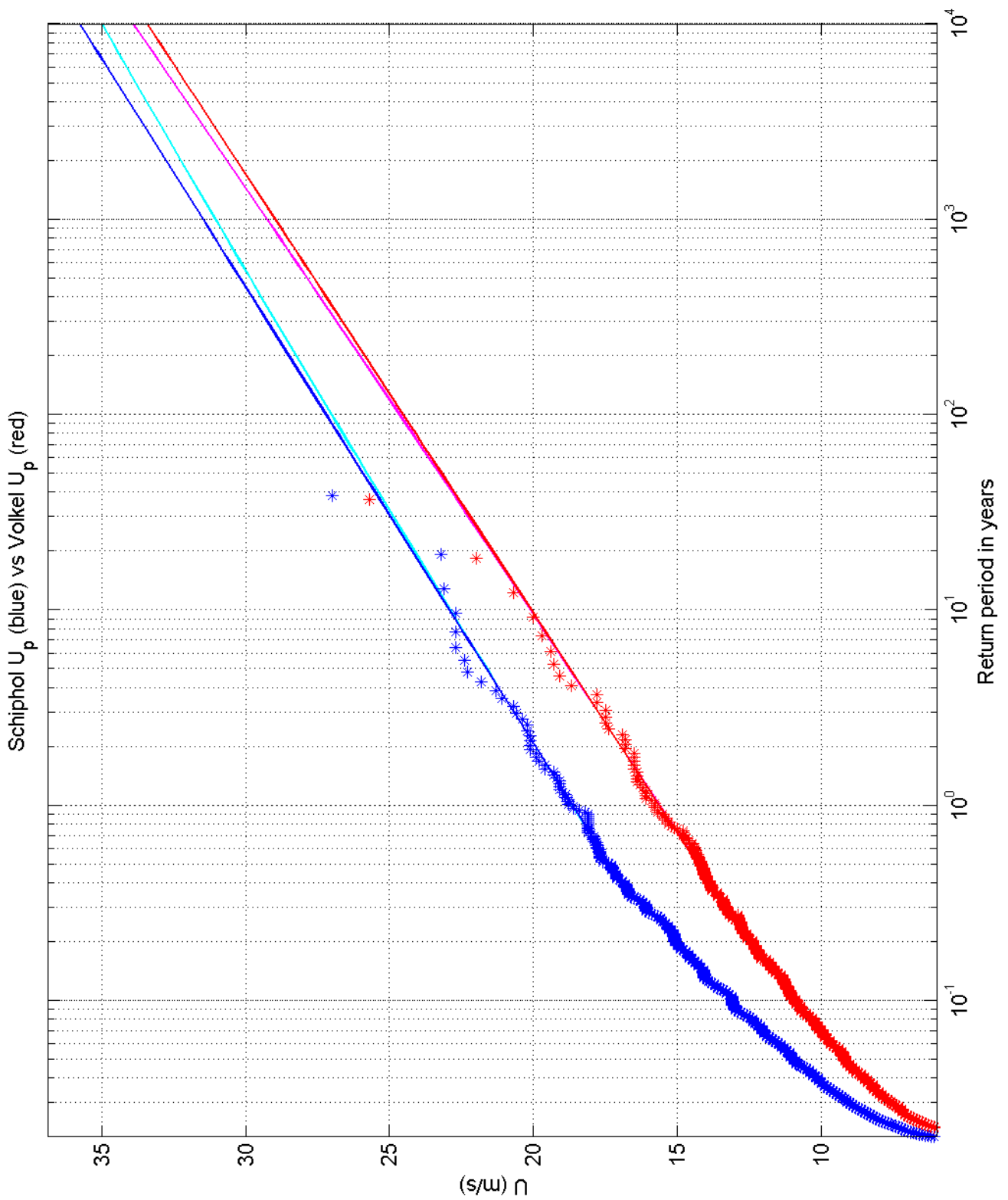
Return value plot per sector of Schiphol (blue) vs Eindhoven (red)
 Exponential (blue, red) and GPD (cyan, magenta) fits to U_p
 Plotting positions: x_i vs $(n+1)/(\lambda(n+1-i))$

1970-2008

Deltares

1200264-005

Fig. F.5d.18



Return value plot of Schiphol (blue) vs Volkel (red)
 Exponential (blue, red) and GPD (cyan, magenta) fits to U_p
 Plotting positions: x_i vs $(n+1)/(\lambda(n+1-i))$

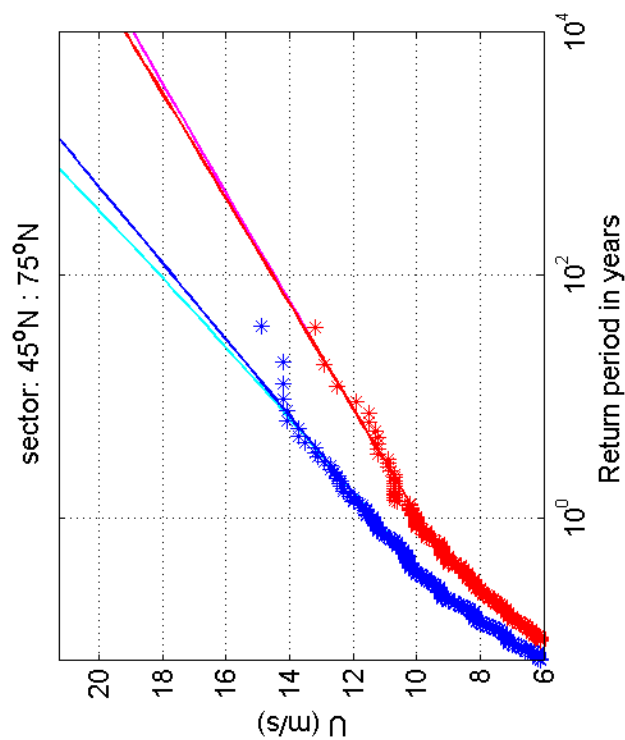
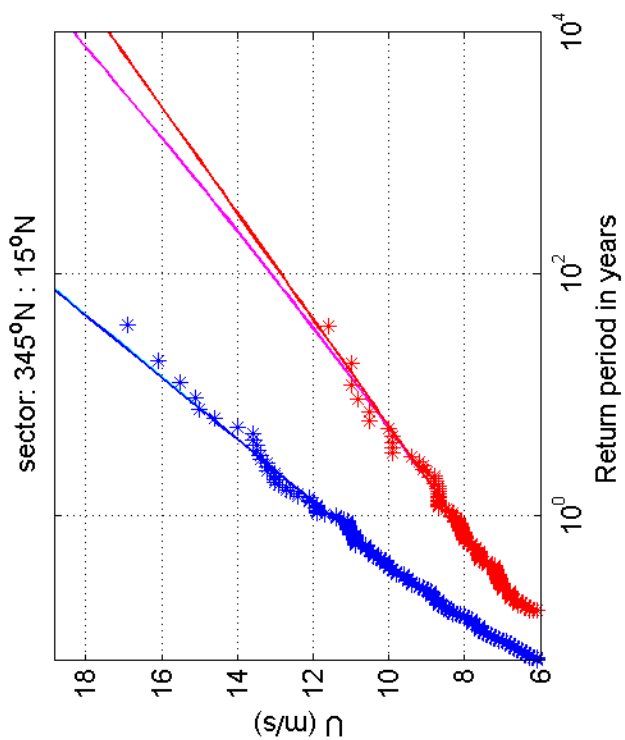
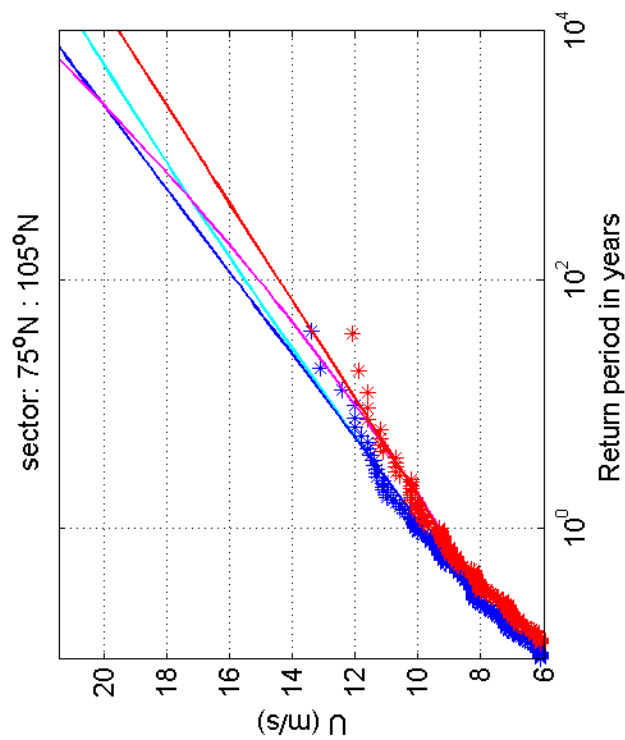
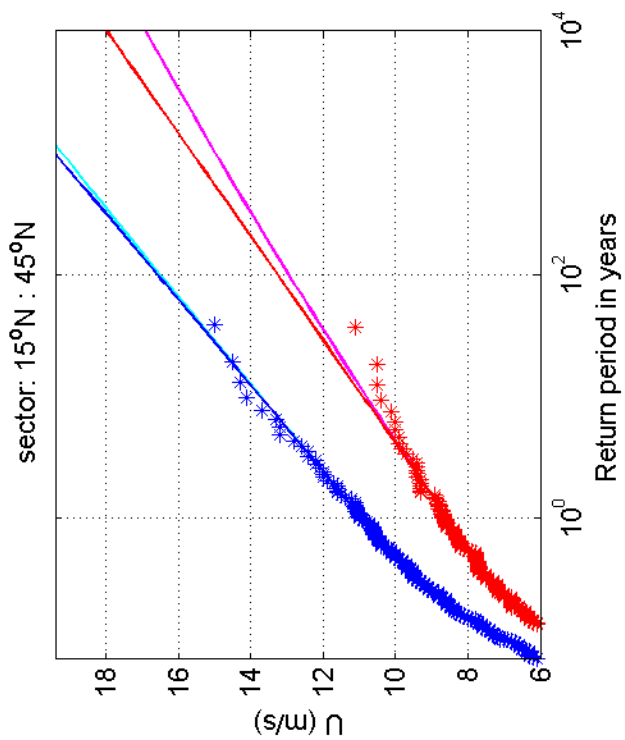
1970-2008

Schiphol vs Volkel

Deltares

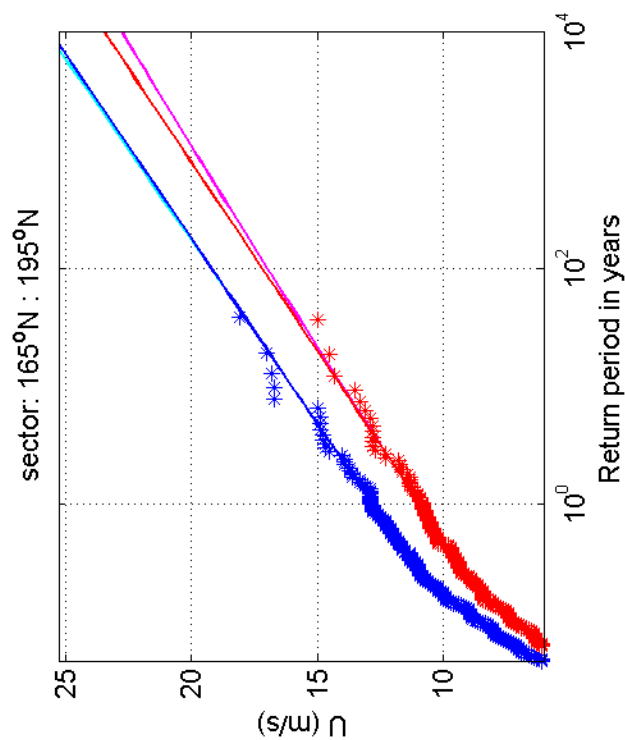
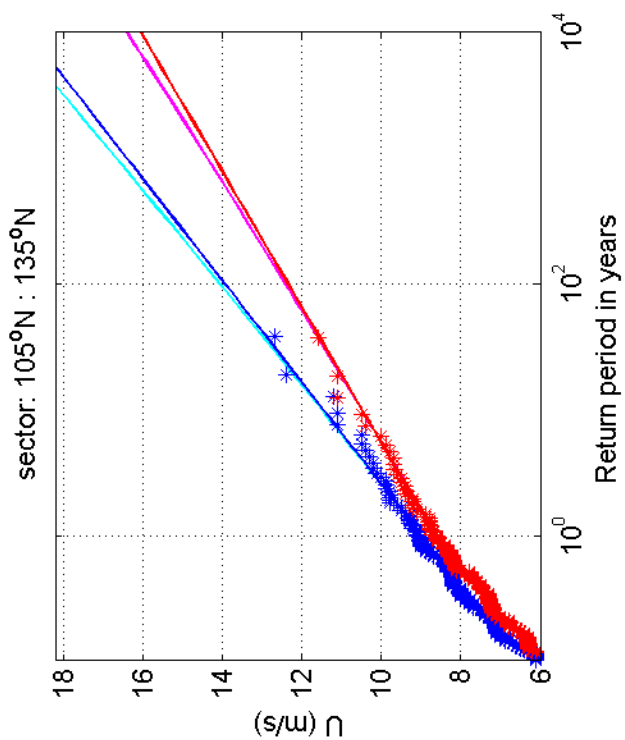
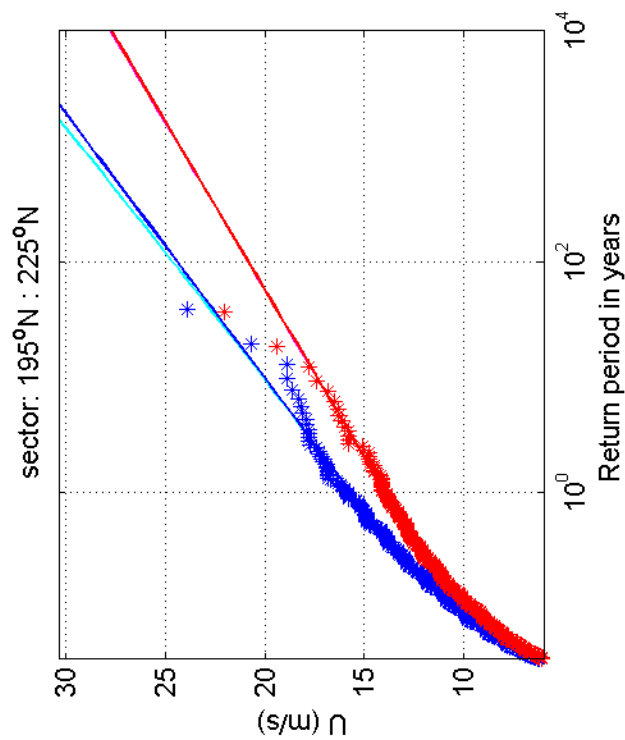
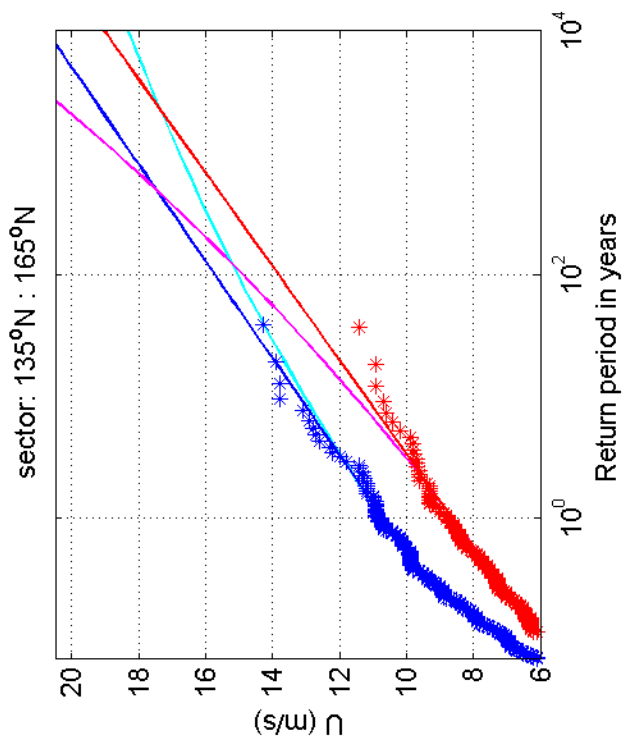
1200264-005

Fig. F.5a.19



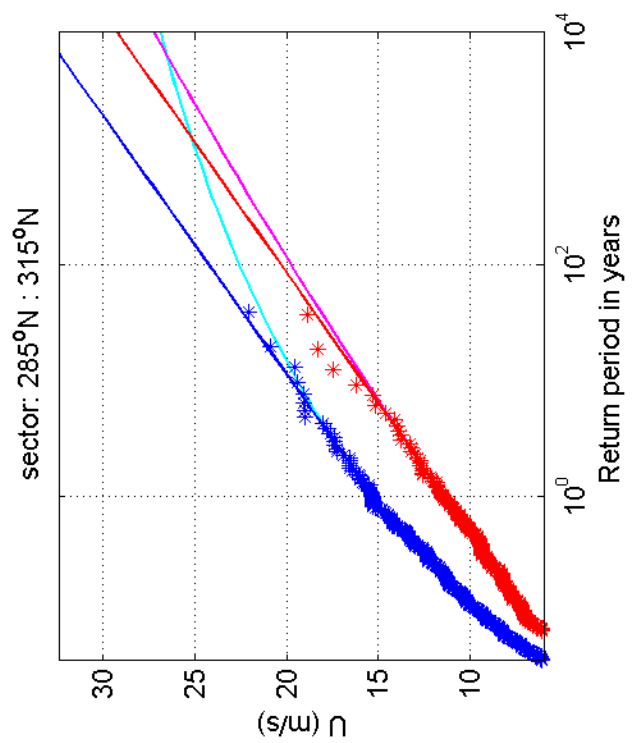
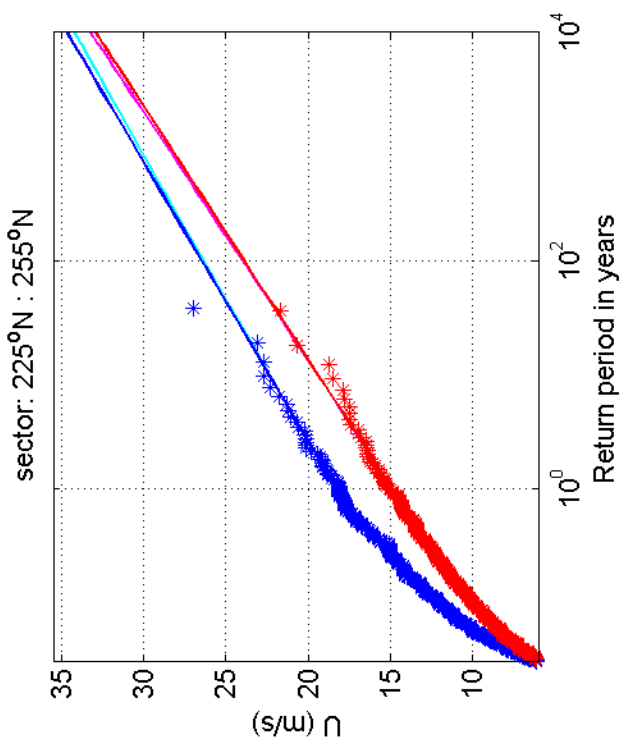
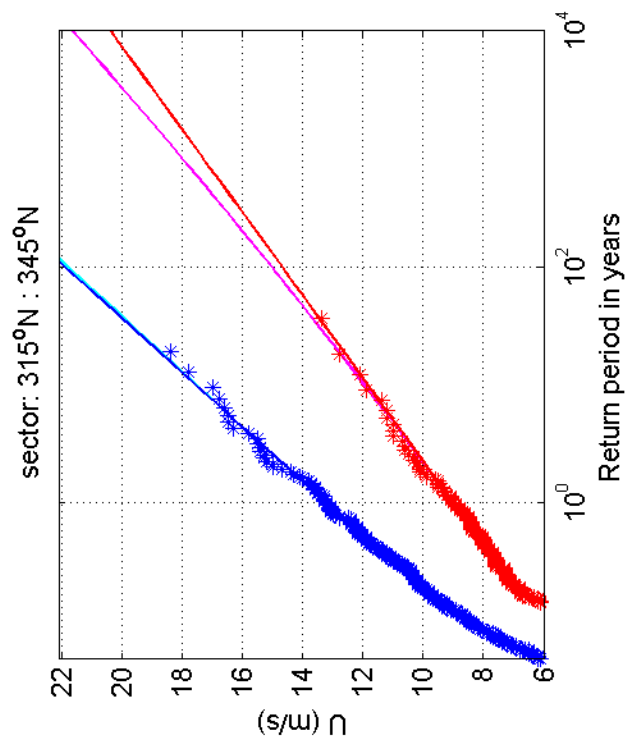
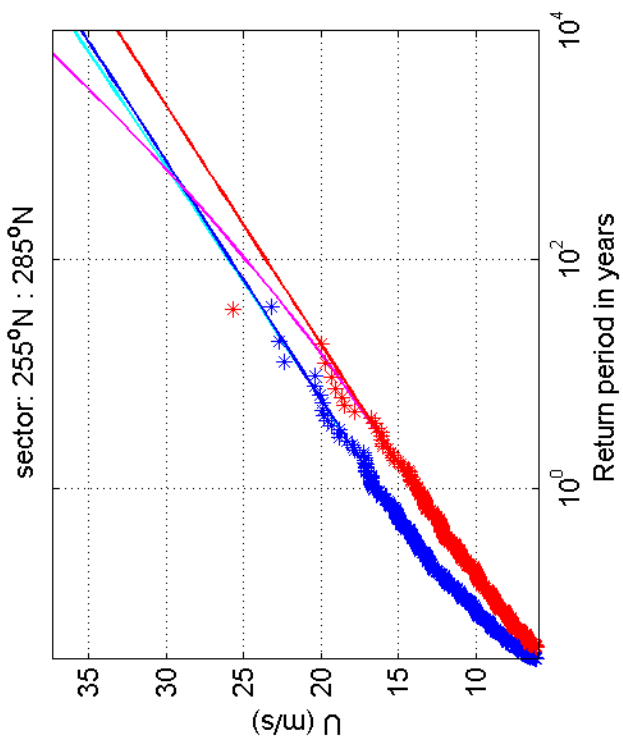
Return value plot per sector of Schiphol (blue) vs Volkel (red)
 Exponential (blue, red) and GPD (cyan, magenta) fits to U_p
 Plotting positions: x_i vs $(n+1)/(\lambda(n+1-i))$

1970-2008



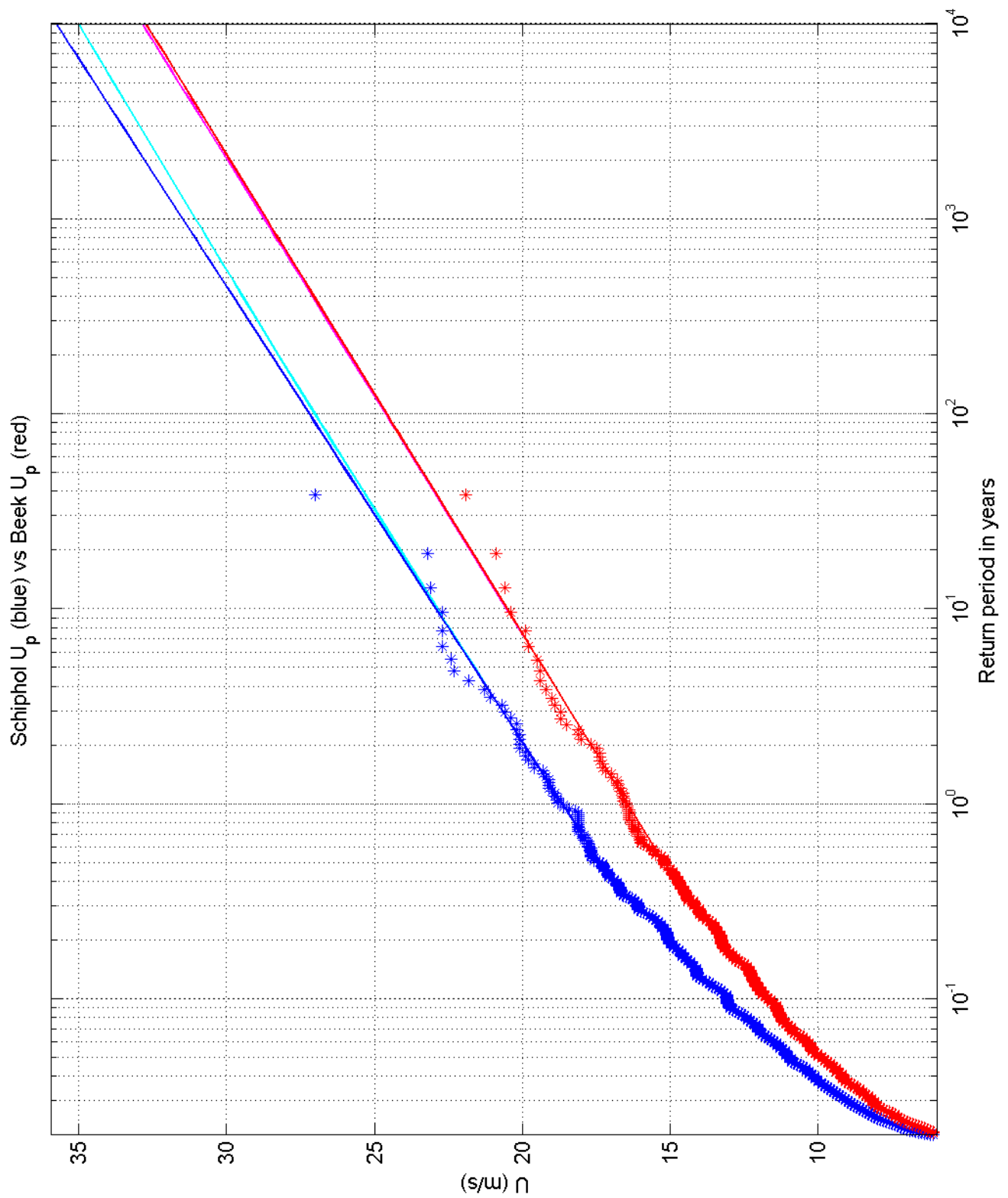
Return value plot per sector of Schiphol (blue) vs Volkel (red)
 Exponential (blue, red) and GPD (cyan, magenta) fits to U_p
 Plotting positions: x_i vs $(n+1)/(\lambda(n+1-i))$

1970-2008



Return value plot per sector of Schiphol (blue) vs Volkel (red)
 Exponential (blue, red) and GPD (cyan, magenta) fits to U_p
 Plotting positions: x_i vs $(n+1)/(\lambda(n+1-i))$

1970-2008



Return value plot of Schiphol (blue) vs Beek (red)
 Exponential (blue, red) and GPD (cyan, magenta) fits to U_p
 Plotting positions: x_i vs $(n+1)/(\lambda(n+1-i))$

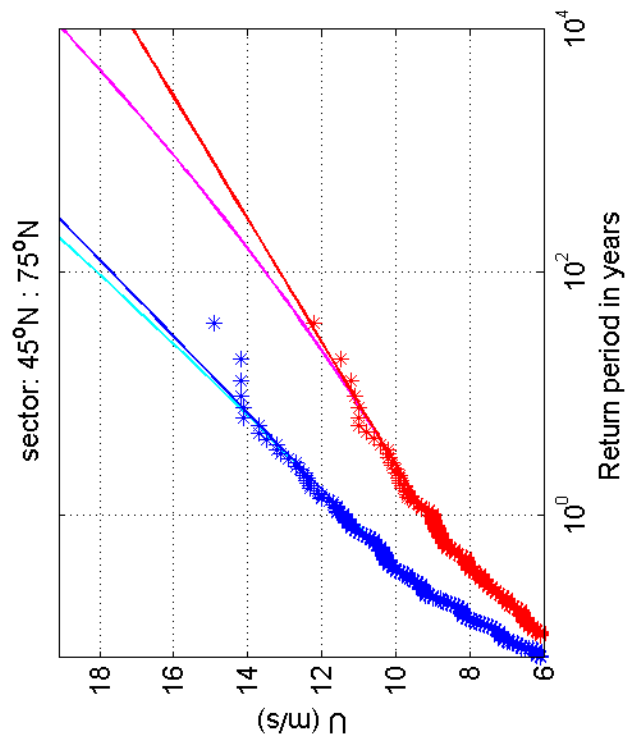
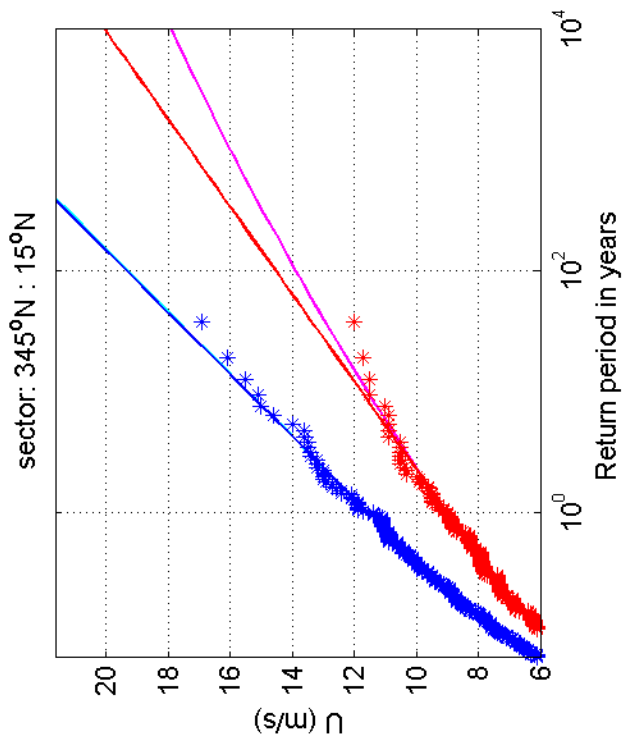
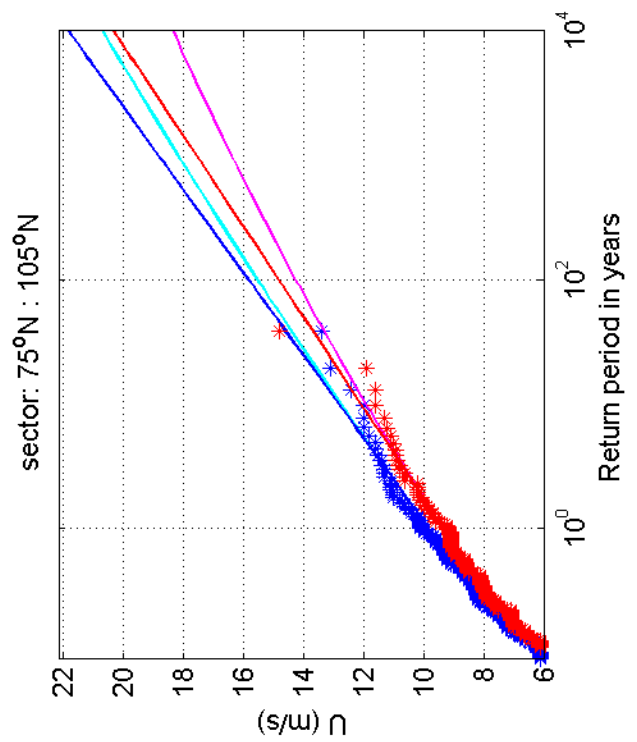
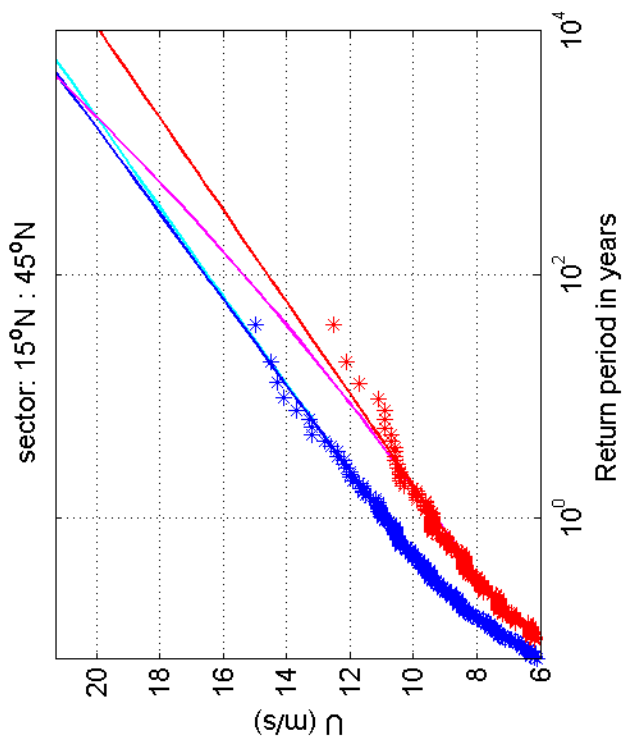
1970-2008

Schiphol vs Beek

Deltares

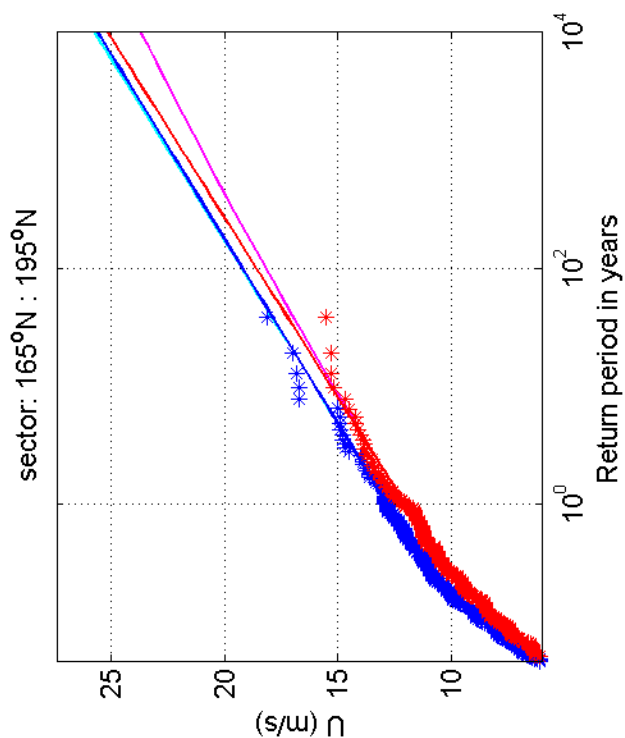
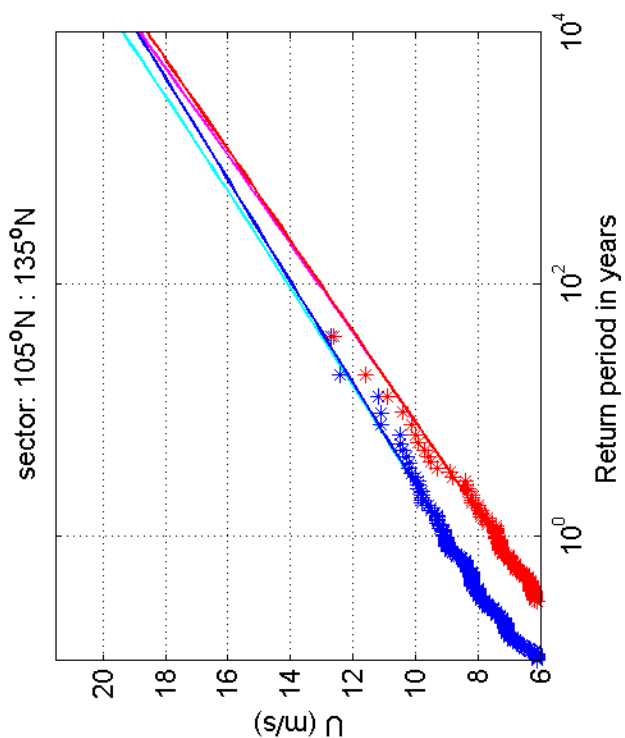
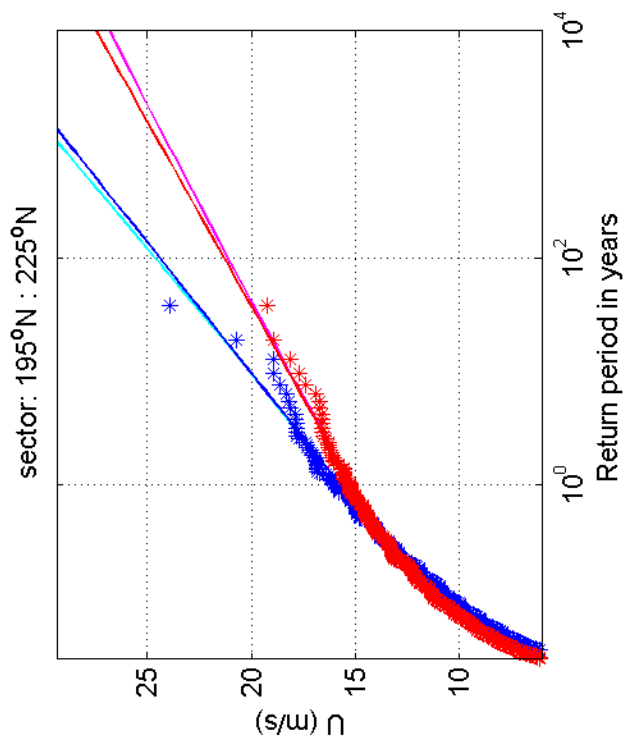
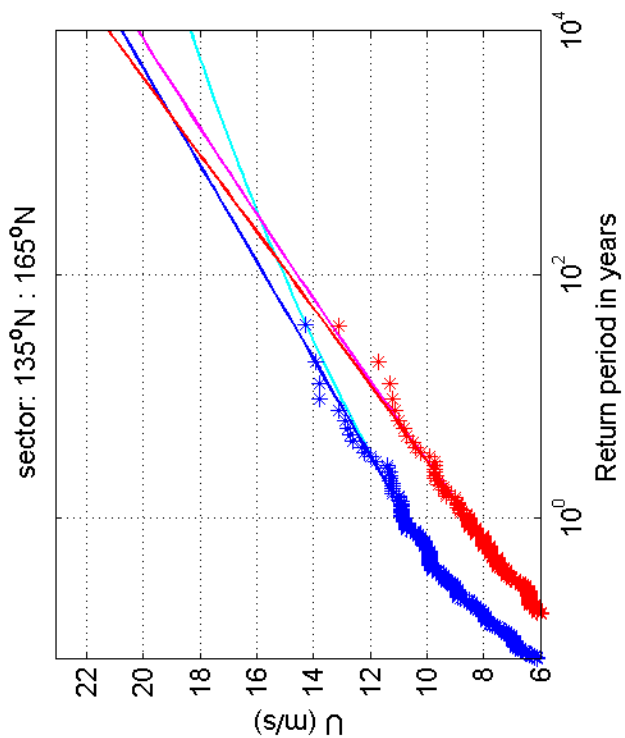
1200264-005

Fig. F.5a.20



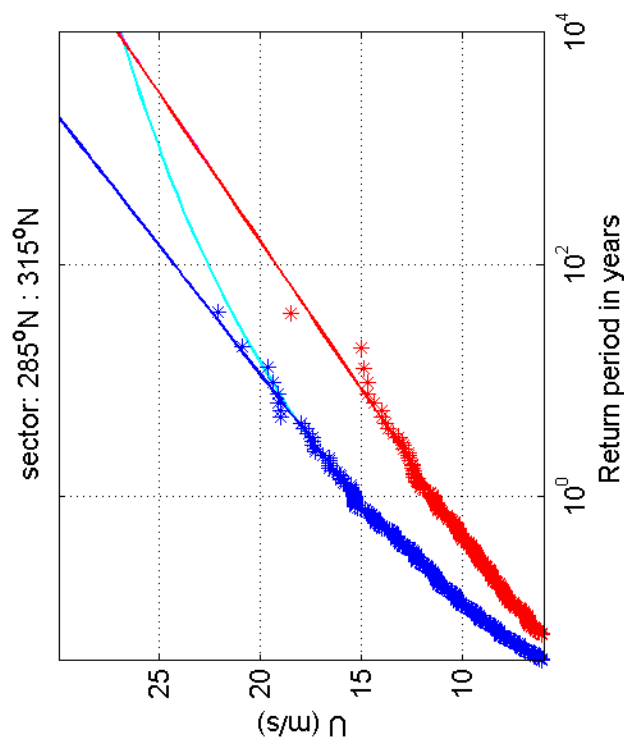
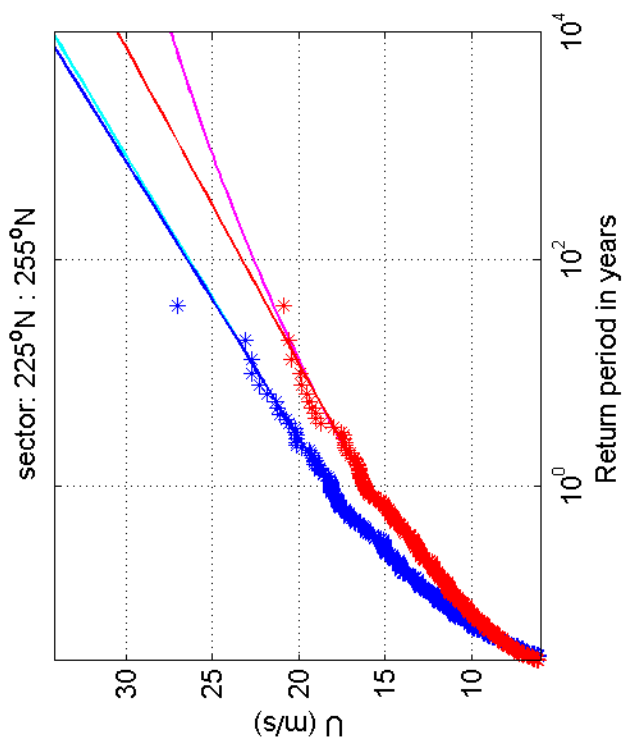
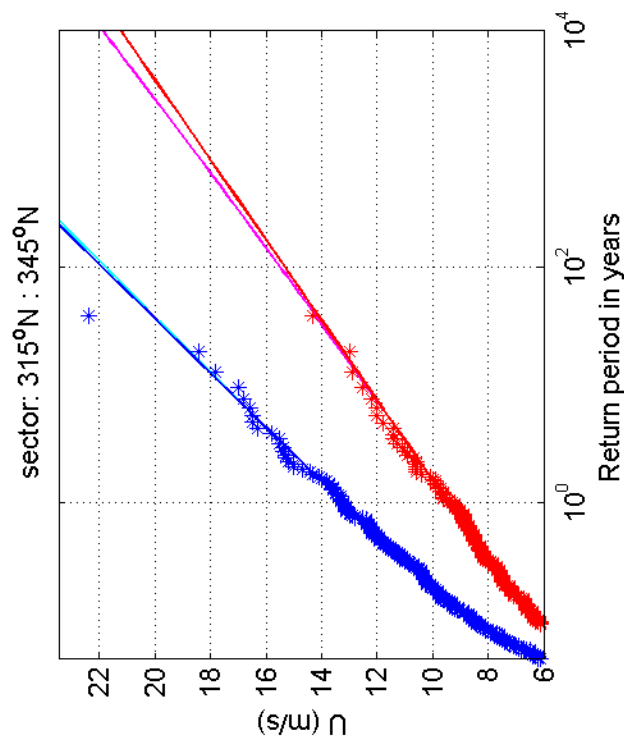
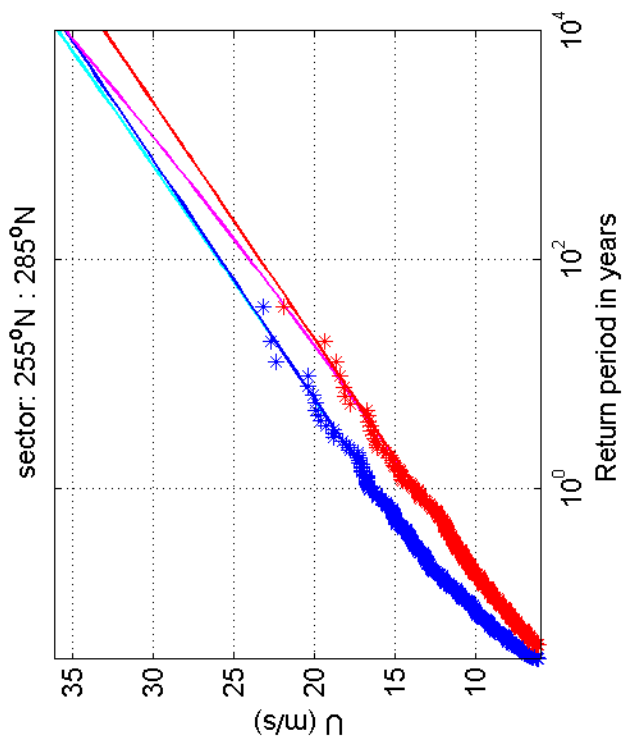
Return value plot per sector of Schiphol (blue) vs Beek (red)
 Exponential (blue, red) and GPD (cyan, magenta) fits to U_p
 Plotting positions: x_i vs $(n+1)/(\lambda(n+1-i))$

1970-2008



Return value plot per sector of Schiphol (blue) vs Beek (red)
 Exponential (blue, red) and GPD (cyan, magenta) fits to U_p
 Plotting positions: x_i vs $(n+1)/(\lambda(n+1-i))$

1970-2008



Return value plot per sector of Schiphol (blue) vs Beek (red)
 Exponential (blue, red) and GPD (cyan, magenta) fits to U_p
 Plotting positions: x_i vs $(n+1)/(\lambda(n+1-i))$

1970-2008

Deltares

1200264-005

Fig. F.5d.20